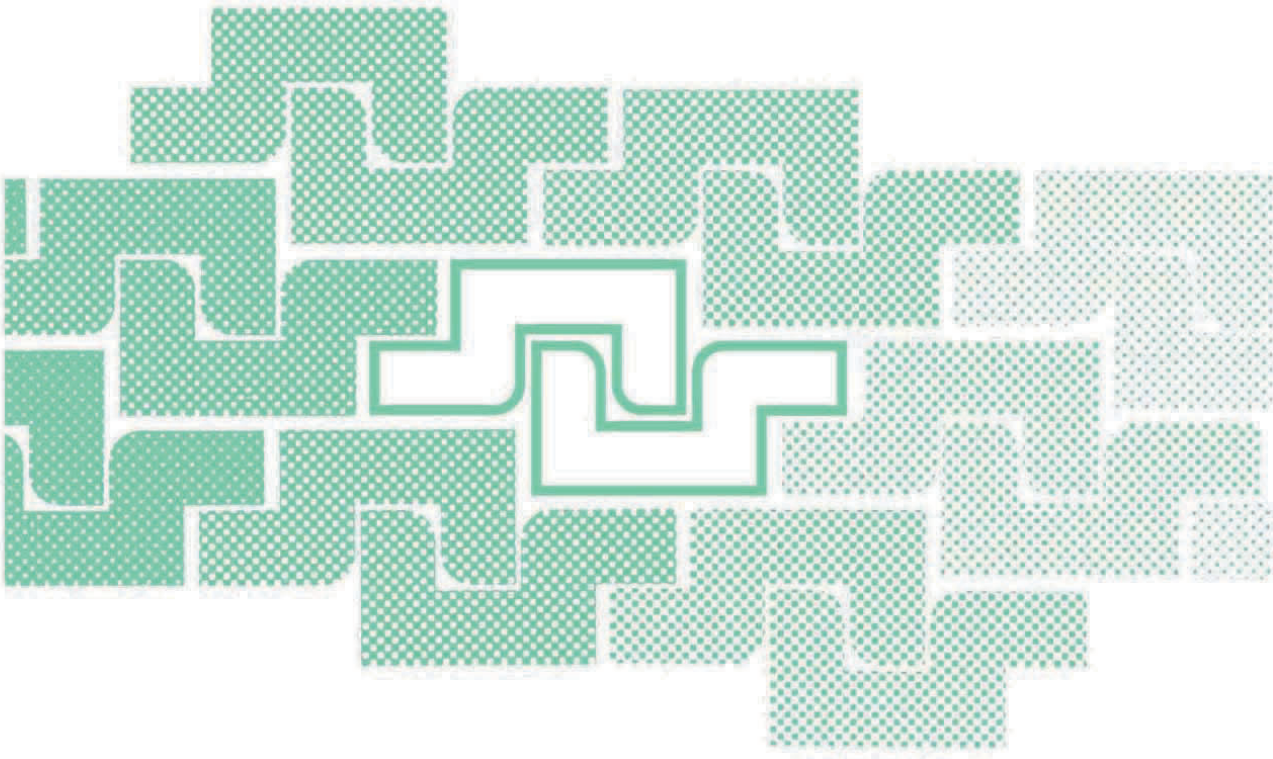

Past and Present Water Column Anoxia

Edited by

Lev N. Neretin

NATO Science Series

IV. Earth and Environmental Sciences – Vol. 64

Past and Present Water Column Anoxia

NATO Science Series

A Series presenting the results of scientific meetings supported under the NATO Science Programme.

The Series is published by IOS Press, Amsterdam, and Kluwer Academic Publishers in conjunction with the NATO Scientific Affairs Division

Sub-Series

I. Life and Behavioural Sciences	IOS Press
II. Mathematics, Physics and Chemistry	Kluwer Academic Publishers
III. Computer and Systems Science	IOS Press
IV. Earth and Environmental Sciences	Kluwer Academic Publishers

The NATO Science Series continues the series of books published formerly as the NATO ASI Series.

The NATO Science Programme offers support for collaboration in civil science between scientists of countries of the Euro-Atlantic Partnership Council. The types of scientific meeting generally supported are "Advanced Study Institutes" and "Advanced Research Workshops", and the NATO Science Series collects together the results of these meetings.The meetings are co-organized by scientists from NATO countries and scientists from NATO's Partner countries – countries of the CIS and Central and Eastern Europe.

Advanced Study Institutes are high-level tutorial courses offering in-depth study of latest advances in a field.
Advanced Research Workshops are expert meetings aimed at critical assessment of a field, and identification of directions for future action.

As a consequence of the restructuring of the NATO Science Programme in 1999, the NATO Science Series was re-organized to the four sub-series noted above. Please consult the following web sites for information on previous volumes published in the Series.

http://www.nato.int/science
http://www.wkap.nl
http://www.iospress.nl
http://www.wtv-books.de/nato-pco.htm

Series IV: Earth and Environmental Series – Vol. 64

Past and Present Water Column Anoxia

edited by

Lev N. Neretin
Max Planck Institute for Marine Microbiology,
Bremen, Germany
and
Federal Institute for Geosciences and Natural Resources,
Hannover, Germany

Published in cooperation with NATO Public Diplomacy Division

A C.I.P. Catalogue record for this book is available from the Library of Congress.

ISBN-10 1-4020-4263-9 (PB)
ISBN-13 978-1-4020-4263-8 (PB)
ISBN-10 1-4020-4262-0 (HB)
ISBN-13 978-1-4020-4262-1 (HB)
ISBN-10 1-4020-4297-3 (e-book)
ISBN-13 978-1-4020-4297-3 (e-book)

Published by Springer,
P.O. Box 17, 3300 AA Dordrecht, The Netherlands.

www.springer.com

Printed on acid-free paper

Contents

ARW Participants

Fuad Al-Horani P.O. Box 2446, 211-10 Irbid, Jordan

Volker Brüchert Max Planck Institute for Marine Microbiology, Celsiusstrasse 1, 28359 Bremen, Germany

Peter Burkill George Deacon Division for Ocean Sciences, Southampton Oceanography Centre, University of Southampton, Waterfront Campus, Southampton, SO14 3ZH, United Kingdom

Marco Coolen Royal Netherlands Institute for Sea Research, Landsdiep 4, 1797 SZ Den Hoorn (Texel), The Netherlands

Jaap Sinninghe Damsté Royal Netherlands Institute for Sea Research, P.O. Box 59, NL-1790 AB Den Burg Texel, The Netherlands

Tatyana Demidova Shirshov Institute of Oceanology RAS, 37 Nakhimovsky prosp., 117997 Moscow, Russia

Allan Devol School of Oceanography, University of Washington, Box 357940, Seattle WA 98195-7940, USA

Thomas DiChristina Georgia Institute of Technology, School of Biology, 311 Ferst Drive, Atlanta GA 30332, USA

Petko Dimitrov Department of Marine Geology and Archaeology Institute of Oceanology BAS P.O. Box 152 9000 Varna Bulgaria

Dimitar Dimitrov Department of Marine Geology and Archaeology, Institute of Oceanology BAS, P.O. Box 152, 9000 Varna, Bulgaria

Alexander Dubinin Shirshov Institute of Oceanology RAS, 37 Nakhimovsky prosp., 117997 Moscow, Russia

David Dyrssen Department of Analytical and Marine Chemistry, Göteborg University, S-412 96 Göteborg, Sweden

Alexander Egorov Shirshov Institute of Oceanology RAS, 36 Nakhimovsky prosp., 117997 Moscow, Russia

Roger Flood Marine Sciences Research Center, Endeavour Hall, Stony Brook University, Stony Brook, NY 11794-5000, USA

Maxim Gulin Kovalevsky Institute of Biology of the Southern Seas, Nakhimova prosp. 2, 335011 Sevastopol, Ukraine

Fumio Inagaki SUGAR Project, Japan Marine Science and Technology Center (JAMSTEC), 2-15 Natsushima-cho, Yokosuka 237-0061, Japan

Mikhail Ivanov Institute of Microbiology RAS, 60-letija Oktaybrya prosp. 7/2, 117312 Moscow, Russia

Bo Barker Jørgensen Max Planck Institute for Marine Microbiology, Celsiusstrasse 1, 28359 Bremen, Germany

Sergey Konovalov Marine Hydrophysical Institute, Kapitanskaya Str. 2, 99011 Sevastopol, Ukraine

Alexey Kouraev CESBIO, BPI 2801, Avenue Ed. 18 Belin, 31401 Toulouse Cedex 9, France

Marcel Kuypers Max Planck Institute for Marine Microbiology, Celsiusstrasse 1, 28359 Bremen, Germany

Gaute Lavik Max Planck Institute for Marine Microbiology, Celsiusstrasse 1, 28359 Bremen, Germany

Alexander Leonov Shirshov Institute of Oceanology RAS, Nakhimovsky prosp. 37, 117997 Moscow, Russia

George Luther III College of Marine Studies, University of Delaware, 700 Pilottown Rd., Lewes Delaware 19958, USA

Timothy Lyons Department of Geological Sciences, University of Missouri-Columbia, 101 Geological Sciences Building, Columbia MO 65211, USA

Ann Manske Institute for Genetics and Microbiology, Ludwig-Maximilians-University Munich, Maria-Ward-Str. 1a, Munich, Germany

Joseph Montoya School of Biology, Georgia Institute of Technology, 311 Ferst Dr., Atlanta GA 30332, USA

James Murray School of Oceanography, University of Washington, Box 355351, Seattle WA 98195-5351, USA

S. Wajih A. Naqvi Chemical Oceanography Dept., National Institute of Oceanography, 403004 Dona Paula Goa, India

Lev Neretin Max Planck Institute for Marine Microbiology, Celsiusstrasse 1, 28359 Bremen, Germany

Temel Oguz Institute of Marine Sciences, Middle East Technical University, P.O. Box 28, Erdemli 33731 Icel, Turkey

Naohiko Ohkouchi Institute for Frontier Research on Earth Evolution (IFREE), 2-15 Natsushima-cho, Yokosuka 237-0061, Japan

Jörg Overmann Institute for Genetics and Microbiology, Ludwig-Maximilians-University Munich, Maria-Ward-Str. 1a, Munich, Germany

Nikolay Pimenov Institute of Microbiology RAS, 60-letija Oktaybrya prosp. 7/2, 117312 Moscow, Russia

Oleg Podymov Shirshov Institute of Oceanology RAS Southern Branch, Okeanologiya 19-17, 353467 Gelendzhik 7, Golubaya Buchta, Russia

Igor Polikarpov Kovalevsky Institute of Biology of the Southern Seas, Nakhimova prosp. 2, 335011 Sevastopol, Ukraine

William Reeburgh Department of Earth System Science, 205 Physical Sciences Research Facility, University of California Irvine, CA 92067-3100, USA

Alexander Rozanov Shirshov Institute of Oceanology RAS, Nakhimovsky prosp. 37, 117997 Moscow, Russia

Maria Saburova Kovalevsky Institute of Biology of the Southern Seas, Nakhimova prosp. 2, 335011 Sevastopol, Ukraine

Axel Schippers Federal Institute for Geosciences and Natural Resources, Stilleweg 2, 30655 Hannover, Germany

Carsten Schubert EAWAG, Limnological Research Center, CH-6047 Kastanienbaum, Switzerland

Mary Scranton Marine Sciences Research Center, Endeavour Hall, Stony Brook University, Stony Brook NY 11794-5000, USA

Jens Skei Norwegian Institute for Water Research, P.O. Box 173, Brekkeveien 19, N-0411 Oslo, Norway

Yuriy Sorokin Shirshov Institute of Oceanology RAS Southern Branch, 353470 Gelendzhik 7, Golubaya Buchta, Russia

Gordon Taylor Marine Sciences Research Center, Endeavour Hall, Stony Brook University, Stony Brook NY 11794-5000, USA

Bradley Tebo Scripps Institution of Oceanography, University of California San Diego, 9500 Gilman Drive, La Jolla CA 92093-0202, USA

Bo Thamdrup Danish Center for Earth System Science, Institute of Biology, University of Southern Denmark, Campusvej 55, DK-5230 Odense, Denmark

Osvaldo Ulloa Centro de Investigacion Oceanografica (COPAS), Universidad de Concepcion, Cabina 7, Barrio Universitario, Casilla 160-C, Concepcion 3, Chile

Igor Volkov Shirshov Institute of Oceanology RAS, Nakhimovsky prosp. 37, 117997 Moscow, Russia

Stuart Wakeham Skidaway Institute of Oceanography, 10 Ocean Science Circle, Savannah GA 31411, USA

Josef Werne Large Lakes Observatory and Dept. of Chemistry, University of Minnesota Duluth, 10 University Dr. 109 RLB, Duluth MN 55812, USA

Evgeniy Yakushev Shirshov Institute of Oceanology RAS Southern Branch, 353470 Gelendzhik 7, Golubaya Buchta, Russia

Foreword

Life on Earth emerged under anaerobic conditions. Many fundamental biochemical and metabolic pathways evolved before the atmosphere contained oxygen. Today, anaerobic (anoxic) conditions in marine milieus are generally restricted to sediments and to basins isolated from oxygenated deep-sea circulation. Oxygen-deficient or hypoxic conditions are defined in operational terms. In speaking of the degree of O_2-deficiency, the term hypoxic is usually defined as ranging between 22 and 64 μM of O_2, while suboxic refers to a range below 10 μM, and anoxic is the complete absence of oxygen. Biologists commonly use the term hypoxia to describe the point at which animals suffocate. But the papers presented in this book deal with the whole range of oxygen-deficient conditions, and the definitions some authors have used here may vary.

Enhanced oxygen consumption by decomposition of organic matter and slow downward mixing and diffusion of dissolved oxygen from the surface waters can lead to oxygen deficiency in the water column in highly productive waters, forming the Oxygen Minimum Zone (OMZ). Bottom waters of coastal upwelling regions are frequently exposed to hypoxic (suboxic) or anaerobic conditions owing to extremely high primary productivity. The development of these conditions represents an acute perturbation to ecological dynamics and fisheries. In the past, anoxic conditions in the water column may have developed more readily. Oceanic anoxic events (OAE) were episodes of globally enhanced organic carbon burial that significantly affected global climate by reducing atmospheric CO_2. An excess of nutrient loading leads to eutrophication of coastal areas and enclosed seas, a wide-spread global problem. The imbalance of nutrient cycles is often directly linked to increased urbanization in coastal river drainage areas or to increased agricultural activities in watersheds.

About 60 scientists gathered in Sevastopol, Ukraine, on the Black Sea coast for a NATO Advanced Research Workshop (NATO ARW) devoted to improving knowledge of pelagic anoxic environments. The workshop aimed to facilitate exchange and communication among scientific groups from the nine participating European countries, Chile, India, Japan, Jordan, the Russian Federation, Turkey, and the United States; and to define and set future research directions. The research specialties of participants ranged from hard rock geology and

organic geochemistry, to mathematical modeling, and from microbiology and molecular biology, to biotechnology and bioremediation. The papers gathered in this volume reflect the interdisciplinary nature of the workshop and the complexity of the issues related to the formation and persistence of oxygen-deficient and anoxic conditions in the World Ocean though history. Not all chapters in this volume are based on presentations to the NATO ARW, however. This volume aims to bring together review-type papers by the most respected specialists in their fields, thus furthering discussion of the current state, and future directions, of research on pelagic suboxic and anoxic environments. The book is organized around several major topics such as (i) reconstructions of anoxic conditions during Earth's history, (ii) regional aspects of anoxia in the ocean and of eutrophication-induced hypoxia on the continental shelf, (iii) microbial ecology of the oxic/anoxic interface, (iv) the biogeochemistry of nitrogen and carbon, including methane cycling, and (v) the microbiology of the metal reduction. The studies presented here offer exceptional geographic coverage, including interdisciplinary research performed in almost all significant pelagic environments of the world ocean with permanent or transient anoxic conditions – such as the Black Sea, the Baltic Sea, the Cariaco Basin, the Arabian Sea, the Eastern South Pacific, Namibian upwelling area and others. Examples of human-induced hypoxia discussed in the book include seasonal oxygen deficiency over the north-western Black Sea shelf, the western continental shelf of India and in the Gulf of Mexico.

Multiple interdisciplinary approaches were obviously required to increase understanding of such systems. The combination of time-series studies with routine data collection, process studies on board larger ships, and new technologies (moorings, ARGO drifters, gliders and sensors) are advocated to improve our knowledge of temporal and spatial variability of anoxic environments. New data presented in the book highlight the importance of lateral ventilation processes in controlling the overall redox budget in many water column anoxic environments such as the Black Sea, the Cariaco Basin, and the Baltic Sea.

Nitrogen limits primary and secondary production in large parts of the ocean. Recent progress in the field suggests that the oceanic nitrogen cycle is more complex than we realized a few years ago. Existing global nitrogen budgets may be incorrect, because the rate of nitrogen loss was underestimated without considering the processes of anaerobic ammonium oxidation (anammox). Discovered first in a sewage plant, the anammox process appears to be widespread and important in natural environments. In view of the discovery of anammox, the observed deficit in the oceanic fixed nitrogen budget may be even larger. This suggests that either the oceanic nitrogen budget is far from being in a steady state, with a possible consequence for the CO_2 budget of the planet, or that oceanic nitrogen fixation is significantly underestimated. Our knowledge

of nitrogen fixation under oxic and anoxic conditions, in particular in OMZs, is obviously insufficient.

The process of anoxygenic photosynthesis mediated by green sulfur bacteria is widespread in present anoxic marine environments, including the Black Sea. As confirmed by molecular methods, it was a common process in the past ocean. It is to a large extent responsible for sulfide oxidation in settings where light reaches the oxic/anoxic interface. Recent findings show that the green sulfur bacteria that dominated the Black Sea interface are unique with respect to their extreme light adaptation. Similar bacteria using other light wavelengths may survive in environments far below the zone of photosynthesis; for example, in hydrothermal vents. Therefore the use of the energy of light supporting life may be distributed in a broader range of environmental settings than we knew earlier.

The Black Sea is a natural biogeochemical laboratory for studying methane cycling. The key process regulating the flux of methane into the atmosphere is the process of methane oxidation that may happen anaerobically. New data suggest that the process of anaerobic methane oxidation does occur in the Black Sea water column. However, we are still far from constructing a concise methane budget for the Black Sea, and therefore, the role of anoxic systems in controlling the global methane inventory needs to be studied further. Methane and sulfur cycles in the water column in some upwelling areas, for example, are more closely linked with sedimentary processes of methane and sulfide production and oxidation as we previously thought.

Although the interpretation of records in extant anoxic systems provides a key to understanding their contemporary counterparts, limited understanding of present anoxic environments also affects the growth in our knowledge about the past. New molecular biological techniques such as fossil DNA profiling combined with lipid biomarker studies have proven to be a successful approach for reconstructing ancient sedimentary biogeochemistry and aquatic microbial communities. Sometimes the pool of molecular information that can be retrieved from ancient environments is called "Paleome". This is a new and exciting area of research, extending the frontiers of our understanding of the biosphere.

We hope that the enormous spatial and temporal complexity of pelagic anoxic systems on display in this book will stimulate new interdisciplinary thinking. As such it should be fully implemented in future research planning and stimulate the establishment of international, long-term, ecological programs for studying anoxic environments.

The Editor
Bremen, 17 August 2005

Acknowledgments

The Organizing Committee of the NATO Advanced Research Workshop (ARW) on Past and Present Water Column Anoxia held on 4-8 October 2003 in Sevastopol, Ukraine acknowledge with thanks the financial support received from the NATO Science Programme and the U.S. National Science Foundation.

It is also a pleasure to express thanks to the Local Organizing Committee of the ARW in Sevastopol and especially to Igor Polikarpov (ARW Co-Director), Maria Saburova, Yury Burchenko and Nelly Gavrilova. The Editor wishes to thank Bo Barker Jørgensen, James Murray, Marcel Kuypers, Gaute Lavik, and Clarence Thomas Fernandez for helping with developing a concept of the book and the editorial assistance. Last but not least, the laborious text processing of the entire book typescript was done with devotion and care by Thomas Biegel, without whom the typescript would not have seen the light of day for submission to the publisher.

The Editor is indebted to the reviewers, whose constructive criticism helped ensure this book met the highest scientific standard:

Robert C. Aller, *Stony Brook University, U.S.A.*
Mark A. Altabet, *University of Massachusetts, U.S.A.*
Michael A. Arthur, *Pennsylvania State University, U.S.A.*
Robert E. Blankenship, *Arizona State University, U.S.A.*
Donald F. Boesch, *University of Maryland, U.S.A.*
Antje Boetius, *Max Planck Institute for Marine Microbiology, Germany*
Rizlan Bencheikh-Latmani, *Scripps Institution of Oceanography, U.S.A.*
Jochen J. Brocks, *Harvard University, U.S.A.*
Volker Brüchert, *Max Planck Institute for Marine Microbiology, Germany*
Peter Burkill, *University of Southampton, United Kingdom*
Louis A. Codispoti, *University of Maryland, U.S.A.*
Marco Coolen, *Woods Hole Oceanographic Institution, U.S.A.*
Tage Dalsgaard, *National Environmental Research Institute, Denmark*
Dirk De Beer, *Max Planck Institute for Marine Microbiology, Germany*

Timothy G. Ferdelman, *Max Planck Institute for Marine Microbiology, Germany*
Kirsten Habicht, *University of Southern Denmark, Denmark*
Fumio Inagaki, *Japan Marine Science and Technology Center, Japan*
Bo Barker Jørgensen, *Max Planck Institute for Marine Microbiology, Germany*
Michael W. Kemp, *University of Maryland, U.S.A.*
George W. Luther, III, *University of Delaware, U.S.A.*
Timothy W. Lyons, *University of California, Riverside, U.S.A.*
Frank E. Müller-Karger, *University of South Florida, U.S.A.*
Joseph P. Montoya, *Georgia Institute of Technology, U.S.A.*
James W. Murray, *University of Washington, U.S.A.*
S. Wajih A. Naqvi, *National Institute of Oceanography, India*
Lev N. Neretin, *Max Planck Institute for Marine Microbiology, Germany*
Nathaniel E. Ostrom, *Michigan State University, U.S.A.*
Hans W. Paerl, *University of North Carolina at Chapel Hill, U.S.A.*
Richard D. Pancost, *University of Bristol, United Kingdom*
Jakob Pernthaler, *Max Planck Institute for Marine Microbiology, Germany*
Falk Pollehne, *Baltic Sea Research Institute, Germany*
Nancy Rabalais, *Louisiana Universities Marine Consortium, U.S.A.*
William S. Reeburgh, *University of California Irvine, U.S.A.*
Axel Schippers, *Federal Institute for Geosciences and Natural Resources, Germany*
Andreas Schramm, *University of Aarhus, Denmark*
Dirk Schüler, *Max Planck Institute for Marine Microbiology, Germany*
Mary I. Scranton, *Stony Brook University, U.S.A.*
David C. Smith, *University of Rhode Island, U.S.A.*
Robin Sutka, *Michigan State University, U.S.A.*
Gordon T. Taylor, *Stony Brook University, U.S.A.*
Andreas Teske, *University of North Carolina at Chapel Hill, U.S.A.*
Maren Voss, *Baltic Sea Research Institute, Germany*
Bernhard Wehrli, *Limnogical Research Center EAWAG/ETH, Switzerland*
Evgeniy V. Yakushev, *Southern Branch of Shirshov Institute of Oceanology RAS, Russia*
Matthias Zabel, *University of Bremen, Germany*
Mike Zubkov, *University of Southampton, United Kingdom*

I

MARINE ANOXIA DURING EARTH HISTORY

ANOXIA THROUGH TIME

Harald Strauss[1]

[1] *Westfälische Wilhelms-Universität Münster, Geologisch-Paläontologisches Institut, Corrensstrasse 24, 48149 Münster, Germany*

Abstract The rock record provides unequivocal evidence for multiple times in Earth history during which the entire global ocean or parts of it were characterized by severe oxygen-deficiency. Evidence includes geological and paleontological observations but also diverse geochemical fingerprints such as trace element abundances, organic geochemical markers or various isotope records, all of which are diagnostic for water column anoxia. The duration of such episodes of oxygen-deficiency ranges from a few thousand to millions of years. In fact, considering the proposed temporal sequence of oxygenation of the atmosphere-ocean system during Earth's early history with the ventilation of the deep ocean not earlier than 1 Ga ago, it appears that the modern oxic world represents an exceptional state of the atmosphere-ocean system on our planet during its 4.5 Ga years history.

Keywords: Oceanic anoxic events, proxy signals, earth system evolution

1. INTRODUCTION

Earth scientists, specifically those studying the low temperature sedimentary realm, define the term "anoxia" as an environmental situation in which the abundance of free molecular oxygen is at (or very near) zero. Thereby, the attribute "anoxic" is applied to all scales, ranging from the interstitial water in porous sediments to parts of the oceanic or lacustrine water column and all the way up to the redox-state of the world's ocean-atmosphere system.

In contrast to anoxia, oxic conditions reflect the presence of free oxygen. Quantification of O_2-abundance for the geological past frequently refers to a percentage of the present day atmospheric level of oxygen (PAL O_2).

Somewhat more loosely defined in terms of its O_2-abundance are redox-states such as suboxic or dysoxic. However, common sense tells us that these attributes characterize an environmental situation between oxic and anoxic conditions.

Finally, the term "anoxia" is frequently utilized interchangeably with the term "euxinic". Euxinic conditions, however, refer to a water column, which contains dissolved hydrogen sulphide.

L. N. Neretin (ed.), Past and Present Water Column Anoxia, 3–19.

Following Berner's original classification of sediments [8], oxic sediments are deposited under an O_2-concentration greater than 30 μM, suboxic sediments are characterized by O_2-concentrations between 30 and 1 μM O_2. Anoxic sediments with less than 1 μM O_2 were differentiated into non-sulphidic (H_2S < 1 μM) and sulphidic (H_2S > 1 μM) deposits.

Any earth science text book contains ample descriptions of anoxia, even global anoxia. For example, we view the distant past, the early part of earth's history (the Archaean) as a world, in which the entire ocean-atmosphere system was anoxic, followed by a Great Oxygenation Event and subsequent oxygenation of atmospheric, surface and deep water environments [29, 30]. However, alternative views are also considered [51]. Prolonged deep ocean anoxia has also been proposed for the early Paleozoic [12]. Multiple levels of black shale deposition during the Cretaceous are described as oceanic anoxic events (OAEs) with global implications [3]. Large scale, possibly global anoxic conditions have been considered as cause for mass extinctions [88]. Finally, numerous modern oceanic settings show anoxic/euxinic water column conditions [21].

On a smaller scale, any sedimentary environment contains a transition from oxic to anoxic conditions as reflected by decreasing oxygen abundance with depth. Pertinent lithological (e.g., grain size) and biological (e.g., bioturbation, microbial activity) characteristics determine how steep this gradient is and how quickly the pore waters become anoxic.

Considering these examples, it is obvious that any discussion of anoxia, in particular with respect to the geobiological consequences, will strongly depend on the scale of observation. This contribution will focus on large scale anoxia, affecting the entire or at least large parts of the atmosphere-ocean-system. Following a previous comprehensive account of modern and ancient anoxia [5], it is the aim of this review to update and extend the temporal record of global anoxia.

2. MODERN ANOXIA

A long history of continuous research in modern anoxic environments has significantly improved our understanding of causes and consequences of water column anoxia. Based on differences in the oceanographic framework, three different types of marine anoxic environments have been suggested [21]: (a) silled basins, (b) upwelling zones and (c) stable oxygen minimum zones in the open ocean. Prominent examples include (a) the Black Sea, the Baltic Sea, the Cariaco Basin, the Framvaren Fjord, or the Saanich Inlet; (b) the South-West African shelf off Namibia, or the Peruvian/Chilean shelf, and (c) the Arabian Sea and northern Indian Ocean, or the Gulf of California, respectively. Results

for some of these settings will be presented in this volume, and will not be repeated here.

The central observation made in all studies of modern anoxic environments, however, should be emphasized here as well. Modern anoxic environments reflect the interplay between the two principal causes for anoxia: the delivery of large quantities of fresh organic matter to the deeper part of the water column, causing a high oxygen demand (aerobic respiration), and an oceanic circulation that is incapable of supplying sufficient quantities of dissolved oxygen to satisfy this demand.

Tracing anoxia through time can only be achieved on the basis of geological, biological and geochemical proxies that allow to differentiate anoxic from oxic conditions. These will be introduced in the following paragraph.

3. PROXIES FOR ANOXIA

Evidence for anoxic vs. oxic conditions, both in the atmosphere as well as the hydrosphere, includes geological and paleontological indicators that are entrained in the sedimentary rock record and readily available during field inspection. Equally important, however, are abundances or ratios of redox-sensitive elements such as C, S, Fe, Mo, U, Th, and others. Furthermore, the stable isotopic composition for some of these elements (C, S, N, Fe, Mo) provide evidence for (bio)geochemical cycling under changing redox conditions. Finally, organic geochemical evidence, specific biomarkers indicate biologically mediated processes in the water column and or the sediment.

It is beyond the scope of this contribution to fully evaluate the validity of every indicator listed above. Instead, all will be briefly introduced with the pertinent literature provided for further reference.

3.1 Geological and Paleontological Indicators

Already in the 1960s, a qualitative assessment of earth's oxygenation through Precambrian time was achieved [20], considering a variety of – now classical – sedimentary rocks and minerals (for review see [30]). All were deposited in surface or near-surface environments and would, thus, attest to the presence or absence of oxygen in the atmosphere-hydrosphere-system. Such proxies include detrital uraninite (UO_2) and detrital pyrite (FeS_2) in late Archaean sediments from the Witwatersrand Supergroup, South Africa (less-oxidizing atmosphere), Superior-type banded iron formations of late Archaean and Paleoproterozoic age in southern Africa, western Australia and North America (deep water anoxia overlain by oxic surface water), oxidized paleosols and red beds in Paleoproterozoic successions of southern Africa and North America (oxidized atmosphere), Meso- and Neoproterozoic sulphate occurrences

oxidized atmosphere and surface water) and Metazoan life during the terminal Neoproterozoic (oxidized atmosphere and surface water).

In more general terms and applicable throughout earth's history, the deposition of black shales, organic carbon and pyrite-rich siliciclastic sediments, is attributed to anoxic conditions in (larger) parts of the water column [89]. Such conditions of bottom water anoxia are further supported through the absence of bioturbation as indicated by the lack of trace fossils.

In addition, the size distribution of sedimentary pyrite is increasingly being utilized as a proxy signal for water column anoxia [91]. Microframboids formed in a necessarily anoxic water column are distinctly different in size and shape compared to diagenetic (even more so late diagenetic) pyrite formed in the sediment.

3.2 Geochemical Proxy Signals: C-S-Fe

The biogeochemical cycling of redox-sensitive elements in sedimentary environments results in characteristic changes in their abundances and ratios. One of the key processes in marine sediments is the anaerobic mineralization of sedimentary organic matter through fermenting and subsequently sulphate reducing bacteria. Sulphate is reduced at the expense of organic matter which is oxidized, thereby buffering the atmospheric oxygen abundance [9]. This is expressed in a positive correlation between the abundances of organic carbon and pyrite sulphur, a traditional proxy signal for normal marine, i.e. oxic bottom water [11, 43, 61, 62] vs. semi-euxinic and euxinic bottom water conditions [61]. Subsequently, it was realized that the availability of reactive iron was an additional important parameter in euxinic environments [63, 64]. No positive correlation between organic carbon and pyrite sulphur can be observed in such sediments.

Apart from C-S-Fe systematics described above, substantial effort has been devoted to a detailed quantification of different sedimentary iron species [60, 64]. Depending upon analytical data, two parameters were defined:

the degree of pyritization (DOP)

$$DOP = Fe_{PYR}/Fe_{PYR} + Fe_{HCl}$$

the degree of anoxicity (DOA)

$$DOA = (Fe_{PYR} + Fe_{MAG} + Fe_{OX} + Fe_{CARB})/Fe_{T}.$$

Both allow anoxic depositional conditions to be distinguished from oxic conditions. A DOP value less than 0.45 reflects deposition under normal marine, well-oxygenated bottom water conditions, whereas a DOP > 0.75 suggests anoxic bottom water conditions. Intermediate values are thought to reflect

dysaerobic or dysoxic conditions with low O_2, but no H_2S [63]. Alternatively, a DOA > 0.38 has been shown to reflect deposition beneath anoxic bottom water conditions [59].

3.3 Trace Element Abundances and Ratios

Abundances and ratios of redox-sensitive trace elements are frequently utilized to assess the redox conditions of modern and ancient sedimentary systems [37, 49, 76]. Classical examples include V, Cr, Ni, Co, Mo or U, all reacting differently under varying oxygen content, thus representing valuable proxy signals particularly in laminated sediments. A positive correlation with organic carbon abundances is further consistent with the aspect of enhanced preservation of organic matter and enrichment of numerous trace elements under anoxic conditions (for a recent review see [37]).

In addition to trace element abundances, the isotopic composition of selected redox-sensitive elements like molybdenum represents an equally powerful indicator for anoxia [1].

3.4 Biomarker Evidence

Biomarkers are molecular fossils which can be found in sediments/sedimentary organic matter and which reflect the former presence and metabolic activity of living organisms [24, 58]. Organic geochemical methods provide the means for identifying the precursor organisms but also for characterizing the depositional environment and/or bacterial and inorganic degradation during diagenesis. For the present discussion, the prevalence and extent of anoxic conditions in the water column of a sedimentary environment is the prime question. Undoubtedly, the anaerobic microbial reworking of sedimentary organic matter, either in the sediment or in anoxic bottom waters, is an important process in sedimentary environments. However, the ability to reconstruct photic-zone anoxia would indicate a possible contribution of anaerobic organisms to primary productivity via anoxygenic photosynthesis.

Unequivocal evidence for anoxic water conditions within the photic zone is provided by the presence of bacterial pigments (such as isorenieratene) which are uniquely biosynthesized by strictly anaerobic bacteria. The presence of isorenieratene and derivatives, together with their characteristic carbon isotopic composition, point to the (former) activities of photosynthetic green sulphur bacteria (Chlorobiaceae) which live under low light intensities and sulphide dissolved in the water column. Clear indications for anoxygenic photosynthesis exist in recent environments, such as the Black Sea (e.g. [67]), but evidence is growing also from ancient sedimentary environments, like the Mediterranean sapropels of Pliocene age (e.g. [14, 53]), Cretaceous sediments from the North

Atlantic (e.g. [81]), Jurassic black shales in Europe (e.g. [75, 77, 83]) or Devonian and Silurian rocks from Europe and North America (e.g. [36, 85]).

Additional biomarker evidence for paleoredox conditions during sedimentation includes the lycopane/C_{31} *n*-alkane ratio (e.g. [82]). Assumed to be derived from a photoautotrophic organism, high abundances of lycopane (with a characteristic carbon isotope signature) in modern and ancient sediments deposited from anoxic water column conditions attest to its preferential preservation under oxygen-deficient conditions. This selective preservation results in an increase of the lycopane/C_{31} *n*-alkane ratio, which provides a respective proxy signal for palaeoxicity.

4. ANOXIA IN THE GEOLOGICAL PAST

4.1 The Precambrian World

Qualitatively, the notion of an anoxic world during the early part of Earth's history (Fig. 1) is based in part on our understanding that the early atmosphere was largely reducing, containing CO, NH_3, H_2, all inorganic compounds from which the early building blocks of life could have been generated [47]. With regard to quantitative aspects, two strongly opposing models have been proposed in the past: a three stage model with the consecutive oxygenation of the atmosphere, surface water and deep water [29, 39] and an invariable abundance of atmospheric oxygen for the past 4 Ga, possibly within 10 % of the present days atmospheric level [51].

This longstanding controversial discussion whether or not the Archean and early Paleoproterozoic ocean-atmosphere-system contained substantial amounts of free oxygen has recently moved forward by a new "piece of evidence", notably the discovery of mass-independent sulphur isotope fractionation, recorded in sedimentary sulphide and sulphate. Independent of the precise mechanisms it appears that the photochemical dissolution of sulphur dioxide is the principal cause for mass-independent sulphur isotope fractionation. The fact that such signals have been measured in near-surface sedimentary sulphide and sulphate indicates an "oxygen free" atmosphere. Otherwise, oxidation of reduced atmospheric sulphur species, rainout of these as sulphate and subsequent homogenization of this signal in the ocean would have resulted in the loss of such a signature. However, a very distinct record of mass-independent sulphur isotopes exists [7, 26, 48, 52], thereby pointing to an atmospheric oxygen abundance of $<10^{-5}$ PAL [57]. Evidence for significant mass-independent sulphur isotope fractionation is absent in sedimentary rocks younger than 2.32 Ga, based on a sulphur isotope study of sedimentary pyrite from the Transvaal Supergroup, South Africa [7]. This in turn suggests, that the atmospheric oxygen abundance increased at 2.32 Ga, possibly from $<10^{-5}$ to 10^{-2} PAL O_2.

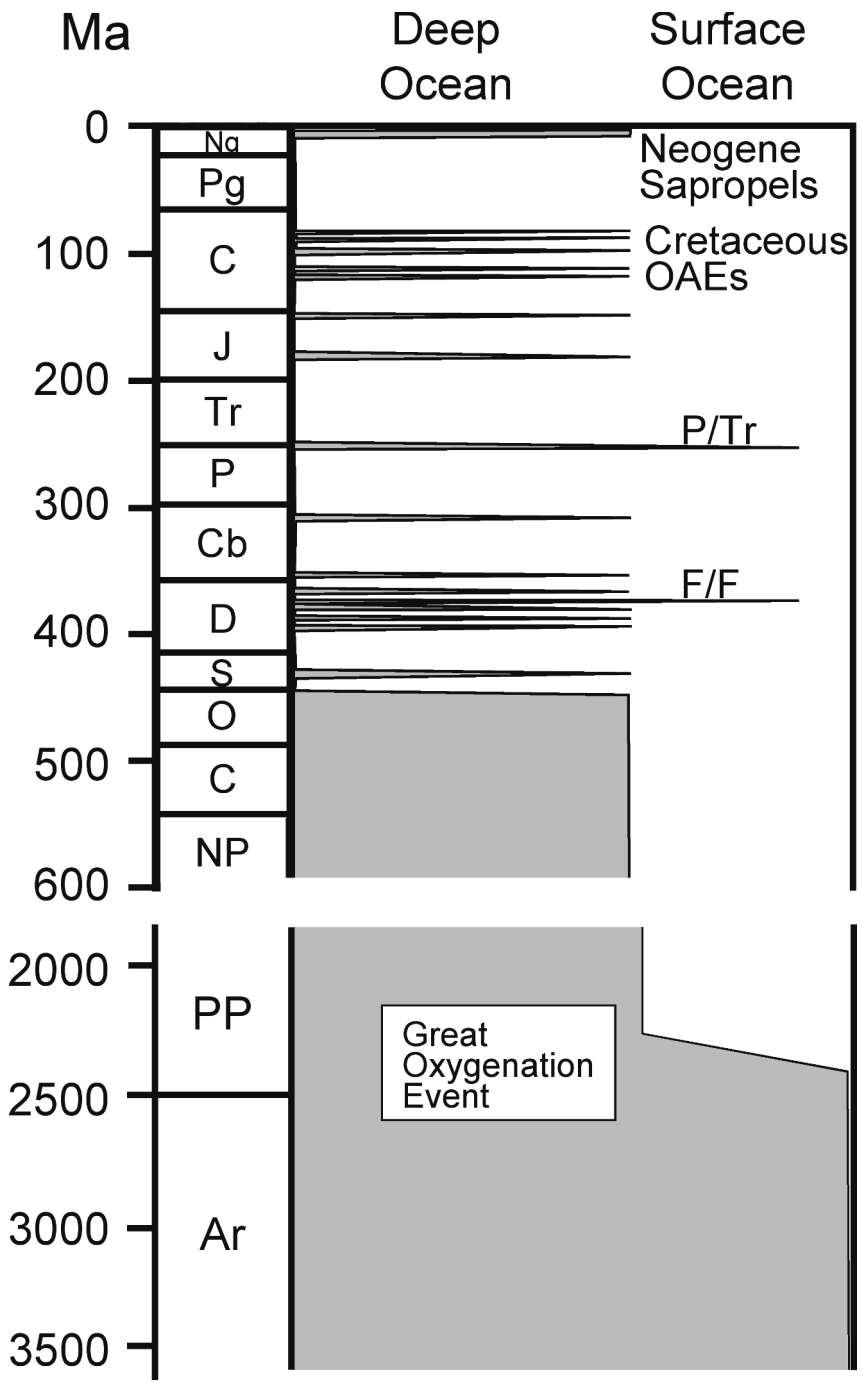

Figure 1. Temporal record of widespread anoxic conditions (grey shaded area) in the shallow and deep ocean (see text for source of data).

Evidence for a stepwise increase in the atmospheric oxygen abundance can be further obtained from long-term isotope records. Secular variations in the isotopic compositions of carbon, oxygen, strontium and sulphur in seawater are believed to faithfully reflect the evolution of the ocean-atmosphere system. While the strontium isotopic composition records temporal variations in the proportional inputs from continental weathering and high-temperature basalt-seawater reactions at mid-ocean ridges, carbon and sulphur isotopes react to biologically mediated redox reactions, resulting in changes of the fractional burial of reduced (organic C, pyrite S) vs. oxidized (carbonate C, sulphate S) compounds. Finally, oxygen isotopes are a proxy signal for climatic changes.

Respective isotope records have been determined with high temporal resolution for the Phanerozoic [38, 87] and with substantially less detail also for the Precambrian [45, 80, 84]. The seawater strontium isotopic evolution clearly displays two periods with a steep increase, between 3.0 and 2.0 Ga and between 0.8 and 0.55 Ga, respectively. Major tectonic rearrangements, resulting in an increasing contribution of radiogenic strontium, are the likely cause for this pattern [28]. The first time interval represents a period in Earth history of significant growth of continental crust whereas the Neoproterozoic shift in $^{87}Sr/^{86}Sr$ reflects the break-up of Rodinia. Both processes would result in a net increase of near-shore shelf habitats. Interestingly, the same time intervals also display an overall ^{13}C enriched carbonate carbon isotope signature [32, 46], sharply punctuated by shifts to negative $\delta^{13}C_{carbonate}$ values during intervals of glaciation. Mass-balance considerations suggest that these ^{13}C enriched values reflect an increase in the fractional burial of organic carbon [32] and/or alternatively a prolonged residence time of organic matter in the water column [70]. An increase in the fractional burial of organic carbon, however, translates into an increasing contribution of oxygen to the atmosphere, resulting in the proposed stepwise oxygenation of Earth's atmosphere [22]. Less well constrained, but still discernible, are shifts in the sulphur isotope record. In particular the terminal Neoproterozoic and early Cambrian display a strongly positive $\delta^{34}S$ signature of seawater sulphate [84]. Again, mass balance considerations suggest a higher fractional burial of reduced (biogenic) sulphur, and consequently less oxygen demand.

Recently, a new model for Proterozoic ocean chemistry [18], notably the drawdown of dissolved Fe from Proterozoic oceans as iron sulphide, has been proposed. Sulphide sulphur isotope data from Mesoproterozoic successions have been provided as evidence for a proposed anoxic if not sulphidic Paleo- and Mesoproterozoic deep ocean [60, 79]. It was suggested that oxygenation of deep ocean waters occurred not earlier than the early Neoproterozoic, consistent with earlier views on the emergence of sulfur disproportionation [19].

4.2 The Early Paleozoic

Following the break-up of Rodinia, the early Paleozoic world was characterized by a large continental area (Gondwana) above the South Pole and dispersed continents (such as Laurentia, Baltica, Siberia and others) in low and mid-latitudes [78]. An overall high sea level resulted in the flooding of large continental areas and the development of distinct facies variations including the deposition of extensive laminated non-bioturbated sediments (black shale deposits). Abundant occurrences, such as Cambrian varved black shales [94], the Ordovician and Silurian graptolite shales [12] or Devonian and Carboniferous black shales deposits [25] on many continents suggest deposition from an apparently oxygen deficient deeper part of the water column during much of early and middle Paleozoic times (Fig. 1). Combined sedimentological and paleontological evidence was utilized to propose a model for different facies developments and animal habitats in the early Paleozoic [13]. This shows the spatial distribution of proximal oxic, bioturbated sediments, termed shelly facies, followed by distal non-bioturbated, anoxic, pyritic black shales of the so called graptolite facies. Analogous to modern anoxic settings, the water column would have contained a chemocline and a distinct vertical sequence of primary productivity in the photic zone, followed downward by aerobic respiration, denitrification and sulphate reduction. The lateral extent of this facies distribution was dependent on the prevailing climatic conditions which were responsible for changes in sea level but more importantly for an initially sluggish oceanic circulation. Progressive ventilation of the early and mid-Paleozoic oceans with oxygen is viewed as a consequence of growing ice sheets in the high latitudes and a subsequent ocean circulation comparable to the modern world.

Additional evidence stems from temporal variations in the carbonate carbon [87] and sulphate sulphur [38] isotopic composition. Isotope mass balance calculations based on these records suggest enhanced anaerobic respiration of sedimentary organic matter via bacterial sulphate reduction, consistent with a view of oxygen-deficient bottom waters.

Apart from an overall appearance of (possibly) prolonged oxygen deficiency in the early and mid-Paleozoic deep ocean, evidence has been provided for a link between anoxia and extinction events during this time interval [35, 40, 90].

4.3 The Permian-Triassic Transition

Numerous causes have been proposed for the greatest mass extinction during Earth history at the Permian Triassic boundary (e.g. [6, 41, 42, 66, 71, 93]). Among them, widespread end-Permian oceanic anoxia (Fig. 1) is indicated by respective laminated organic and pyrite rich black shales from shallow and deep water environments [92].

Modeling results (general circulation model combined with oceanic biogeochemistry, specifically nutrient transport) suggest sluggish ocean circulation and the development of widespread anoxia in the deep ocean as a consequence of a low equator to pole temperature gradient and the enhanced export of phosphate to the deeper ocean [31]. However, nutrient limitation causing a reduced primary productivity prevents prolonged sulphidic deep water conditions.

In contrast, numerous sedimentary basins comprising pyritic black shale successions exhibit petrographic, geochemical and sulphur isotopic data in favor of sulphidic deep water during the late Permian and its transition into the Triassic (e.g. [50]). In fact, a significant drop in the atmospheric O_2 abundance has been attributed as a cause for a collapse of the marine ecosystem at this time boundary with an emphasis on reef communities [89].

Finally, perturbations of the global carbon cycle suggest a combination of a shift in magnitude and locality of organic carbon burial, from high burial of terrestrial and marine organic matter during late Paleozoic time to low and primarily marine organic carbon burial in the Triassic and thereafter [10]. A reduced level in atmospheric oxygen would be the predicted consequence. Superimposed on this is a proposed sudden release of methane [71], as indicated by a short-term, high-magnitude shift towards negative $\delta^{13}C$ values (e.g. [42]).

4.4 Jurassic and Cretaceous Black Shales (OAEs)

The widespread deposition of organic-rich black shales characterizes early Jurassic and Mid-Cretaceous times (Fig. 1), with numerous examples from present-day continental areas and in DSDP/ODP cores. The observation of an apparently time-equivalent deposition of this distinctive lithology during relatively short-term intervals on several continents suggested a global phenomenon and, hence, a common cause. Initially coined for the Mid-Cretaceous, these globally correlative short-term (less than 1 million years) levels of black shale deposition were termed "Oceanic Anoxic Event (OAE)" [73]. Extensive research over the past decades produced a wealth of information which centered on the following issues (e.g. [27, 33])::

Paleoceanography, Sea level changes, Paleoclimate

Organic and inorganic geochemistry

Implications for global geochemical cycles

A generally warm climate, relatively high sea level, a proposed high abundance of atmospheric carbon dioxide and climate induced oscillations in precipitation and continental run-off causing salinity stratification resulted in extended epicontinental seas characterized by sluggish deep water circulation and persistent deep water anoxia. One of the consequences was the enhanced deposition and preservation of organic matter, the latter visible on a global scale

by shifts to positive carbonate $\delta^{13}C$ values (e.g. [4, 34, 74]). Well preserved organic matter allows the detailed reconstruction of primary productivity and secondary mineralization of sedimentary organic matter. For the lower Jurassic Toarcian black shales of Europe for example, organic geochemical data (biomarker, compound-specific organic carbon isotope data) indicate oscillations in the depth of the chemocline suggesting recurring periods of anoxygenic photosynthesis (e.g. [75, 77]).

4.5 Neogene Mediterranean Sapropels

The Mediterranean Neogene sedimentary record contains abundant examples of centimeter to decimeter thick dark laminated layers containing up to 30% organic carbon (for review see e.g. [68]). These so called sapropels were deposited most prominently during Pliocene and Pleistocene time, predominantly but not exclusively in the eastern Mediterranean (Fig. 1). Sapropel formation is thought to be a consequence of sluggish deep water ventilation as a result of a stable pycnocline which affected much of the late Miocene to early Holocene Mediterranean Sea. The latter was induced by climate-driven enhanced river flow from Eurasia and Africa into the Mediterranean causing a strong salinity difference. Strongly contrasting views exist with respect to surface water nutrient availability and resulting levels of primary productivity (e.g. [16, 72]). Subsequent degradation of sinking organic matter, in addition to the salinity gradient, forced the establishment of a stagnant deep ocean. It has been proposed that climate-driven sapropel formation is ultimately linked to variations in the precession, which occur about every 21000 years (e.g. [69]).

Apart from the distinct lithology, ample biogeochemical and isotopic evidence exists for the sapropel formation (e.g. [15, 54–56]), but also extending into the photic zone [53].

5. SUMMARY

Multiple times in Earth history, anoxic conditions were prevailing in large parts of the ocean. The occurrence of widespread, possibly global oceanic anoxic conditions is a consequence of different factors interrelated with each other including the evolving oxygenation of Earth's surface environments, climate-induced differences in oceanic circulation and increased primary productivity causing an enhanced oxygen demand in the water column. The temporal record of water column anoxia is resolvable to different levels of detail, ranging from globally representative long-term seawater isotope records of carbon, sulphur, and to a lesser degree of nitrogen, to organism-specific molecular information and compound-specific organic carbon isotope work.

The temporal record of anoxia suggests a largely anoxic Precambrian world in which the oxygenation of the atmosphere and the surface ocean occurred

during the Paleoproterozoic, followed by the ventilation of the deep water probably as late as the Neoproterozoic. The early Paleozoic appears to be characterized by prolonged periods of deep water anoxia. In contrast, short-term oceanic anoxic events have been identified throughout the Mesozoic. The eastern Mediterranean sapropel layers represent a prominent example of Cenozoic anoxic sedimentation.

The temporal evolution of anoxia has been linked to the occurrences of redox sensitive sediments such as oolitic ironstones [86] or the deposition of stratiform sulphide deposits [23]. Finally, a causal relationship between oceanic anoxic events and biological evolution has been proposed, e.g. for the Permian-Triassic mass extinction.

Acknowledgements

Sincere thanks go to L. Neretin for inviting me to contribute to this volume and for his patience as an editor. Constructive reviews by Mike Arthur and an anonymous reviewer improved this manuscript.

References

[1] Anbar A.D. Molybdenum stable isotopes: observations, interpretations and directions. Reviews in Mineralogy and Geochemistry 2004; 55:429-54.

[2] Anderson T.F. and Raiswell R. Sources and mechanisms for the enrichment of highly reactive iron in euxinic Black Sea sediments. American Journal of Science 2004; 304:203-33.

[3] Arthur M.A. and Premoli Silva I. "Development of wide-spread organic-carbon rich strata in the Mediterranean Tethys." In *Nature of Cretaceous Carbon-Rich Facies*. S.O. Schlanger, M.B. Cita eds., Washington D.C., Academic Press, 1982.

[4] Arthur M.A., Dean W.E. and Pratt L.M. Geochemical and climatic effects of increased marine organic carbon burial at the Cenomanian/Turonian boundary. Nature 1988; 335:714-17.

[5] Arthur M.A. and Sageman B.B. Marine black shales: depositional mechanisms and environments of ancient deposits. Annual Reviews of Earth and Planetary Sciences 1994, 22:499-551.

[6] Becker L., Poreda R.J., Hunt A.G., Bunch T.B.E. and Rampino M.R. Impact event at the Permian-Triassic boundary: evidence from extraterrestrial noble gases in fullerenes. Science 2001; 291:1530-33.

[7] Bekker A., Holland H.D., Wang P.-L., Rumble III D., Stein H.J., Hannah J.L., Coetzee L.L. and Beukes N.J. Dating the rise of atmospheric oxygen. Nature 2004; 427:117-20.

[8] Berner R.A. A new geochemical classification of sedimentary environments. Journal of Sedimentary Petrology 1981; 51:359-65.

[9] Berner R.A. Biogeochemical cycles of carbon and sulfur and their effect on atmospheric oxygen over Phanerozoic time. Global and Planetary Change 1989; 1:97-122.

[10] Berner R.A. Examination of hypotheses for the Permian-Triassic boundary extinction by carbon cycle modeling. Proceedings National Academy of Sciences 2002; 99:4172-77.

[11] Berner R.A. and Raiswell R. Burial of organic carbon and pyrite sulfur in sediments over Phanerozoic time: a new theory. Geochimica et Cosmochimica Acta 1983; 47:855-62.

[12] Berry W.B.N. and Wilde P. Progressive ventilation of the oceans – an explanation for the distribution of the lower Paleozoic black shales. American Journal of Science 1978; 278:257-75.

[13] Berry W.B.N., Wilde P. and Quinby-Hunt M.S. Paleozoic (Cambrian through Devonian) anoxitrophic biotopes. Palaeogeography Palaeoclimatology Palaeoecology 1989; 74:3-13.

[14] Bosch H.-J., Sinninghe Damsté J.S. and de Leeuw J.W. Molecular palaeontology of Eastern Mediterranean sapropels: evidence for photic zone anoxia. Proceedings Ocean Drilling Program, Scientific Results 1998; 160:285-95.

[15] Böttcher M.E., Brumsack H.-J. and de Lange G.J. Sulfate reduction and related stable isotope (^{34}S, ^{18}O) variations in interstitial waters from the eastern Mediterranean (Leg 160). Proceedings Ocean Drilling Program, Scientific Results 1998.

[16] Calvert S.E., Nielsen B. and Fontugne M.R. Evidence from nitrogen isotope ratios for enhanced productivity during formation of eastern Mediterranean sapropels. Nature 1992; 359:223-22.

[17] Canfield D.E. Reactive iron in marine sediments. Geochimica et Cosmochimica Acta 1989; 53:619-32.

[18] Canfield D.E. A new model for Proterozoic ocean chemistry. Nature 1998; 396:450-53.

[19] Canfield D.E. and Teske A. Late Proterozoic rise in atmospheric oxygen concentration inferred from phylogenetic and sulphur-isotope studies. Nature 1996; 382:127-32.

[20] Cloud P. Atmospheric and hydrospheric evolution on the primitive earth. Science 1968; 160:729-36.

[21] Demaison G.J. and Moore G.T. Anoxic environments and oil source bed genesis. American Association of Petroleum Geologists Bulletin 1980; 64:1179-1209.

[22] Des Marais D.J., Strauss H., Summons R.E. and Hayes J.M. Carbon isotope evidence for the stepwise oxidation of the Proterozoic environment. Nature 1992; 359:605-9.

[23] Eastoe C.J. and Gustin M.M. Volcanogenic massive sulphide deposits and anoxia in the Phanerozoic oceans. Ore Geology Reviews 1996; 10:179-97.

[24] Eglinton G. and Calvin M. Chemical Fossils. Scientific American 1967; 261:32-43.

[25] Ettensohn F.R. "Compressional tectonic controls on epicontinental black-shale deposition: Devonian-Mississippian examples from North America." In *Shales and Mudstones*, Jürgen Schieber, Winfried Zimmerle, Parvinder S. Sethi eds., Stuttgart, Schweizerbart'sche Verlagsbuchhandlung, 1998.

[26] Farquhar J., Bao H. and Thiemens M. Atmospheric influence of earth's earliest sulfur cycle. Science 2000; 289:756-58.

[27] Ginsburg R.N. and Beaudoin B. Cretaceous Resources, Events and Rhythms. NATO ASI Series C: Mathematical and Physical Sciences Vol. 304, Dordrecht: Kluwer Academic Publishers, 1990.

[28] Goddéris Y. and Veizer J. Tectonic control of chemical and isotopic composition of ancient oceans and the impact of continental growth. American Journal of Science 2000; 300:434-61.

[29] Holland H.D. When did the Earth's atmosphere become oxic? A Reply. The Geochemical News 1999; 100:20-22.

[30] Holland H.D. Volcanic gases, black smokers, and the great oxidation event. Geochimica et Cosmochimica Acta 2002; 66:3811-26.

[31] Hotinski R.M., Bice K.L., Kump L.R., Najjar R.G. and Arthur M.A. Ocean stagnation and end-Permian anoxia. Geology 2001; 29:7-10.

[32] Jacobsen S.B. and Kaufman A.J. The Sr, C and O isotopic evolution of Neoproterozoic seawater. Chemical Geology 1999; 161:37-57.

[33] Jenkyns H.C. The early Toarcian (Jurassic) event: stratigraphy, sedimentary, and geochemical evidence. American Journal of Science 1988; 288:101-51.

[34] Jenkyns H.C. and Clayton C.J. Lower Jurassic epicontinental carbonates and mudstones from England and Wales: chemostratigraphic signals and the early Toarcian anoxic event. Sedimentology 1986; 44:687-706.

[35] Joachimski M.M. and Buggisch W. Anoxic events in the late Frasnian – causes of the Frasnian-Famennian faunal crisis? Geology 1993; 21:675-78.

[36] Joachimski M.M., Ostertag-Henning C., Pancost R.D., Strauss H., Freeman K.H., Littke R., Sinninghe Damsté J.S. and Racki G. Water column anoxia, enhanced productivity and concomitant changes in δ^{13}C and δ^{34}S across the Frasnian-Famennian boundary (Kowala – Holy Cross Mountains, Poland) Chemical Geology 2001; 175:109-31.

[37] Jones B. and Manning D.A.C. Comparison of geochemical indices used for the interpretation of paleoredox conditions in mudrocks. Chemical Geology 1994; 111:111-29.

[38] Kampschulte A. and Strauss H. The sulphur isotopic evolution of Phanerozoic seawater based on the analysis of structurally substituted sulphate in carbonates. Chemical Geology 2004; 204:255-86.

[39] Kasting J.F. Earth's early atmosphere. Science 1993; 259:920-26.

[40] Kimura H. and Watanabe Y. Oceanic anoxia at the Precambrian-Cambrian boundary. Geology 2001; 29:995-98.

[41] Knoll A.H., Bambach R.K., Canfield D.E. and Grotzinger J.P. Comparative Earth history and Late Permian mass extinction. Science 1996; 273:452-57.

[42] Krull E.S. and Retallack G.J. δ^{13}C depth profiles from paleosols across the Permian-Triassic boundary: evidence for methane release. Geological Society of America Bulletin 2000; 112:1459-72.

[43] Leventhal J.S. An interpretation of carbon and sulphur relationships in Black Sea sediments as indicators of environments of deposition. Geochimica et Cosmochimica Acta 1983; 47:133-37.

[44] Lyons T.W. and Berner R.A. Carbon-sulphur-iron systematics of the uppermost deep-water sediments of the Black Sea. Chemical Geology 1992; 99:1-28.

[45] Lyons T.W., Kah L.C. and Gellatly A.M. "The Precambrian sulfur isotope record of evolving atmospheric oxygen." In *The Precambrian Earth: Tempos and Events*, P.G. Eriksson et al. eds., Developments in Precambrian Geology Amsterdam, Elsevier, 2004.

[46] Melezhik V.A., Fallick A.E., Medvedev P.V. and Makarikhin V.V. Extreme $^{13}C_{carb}$ enrichment in ca. 2.0 Ga magnesite-stromatolite-dolomite-'red beds' association in a global context: a case for the world-wide signal enhanced by a local environment. Earth Science Reviews 1999; 48:71-120.

[47] Miller S.L. A production of amino acids under possible primitive earth conditions. Science 1953; 117:528-29.

[48] Mojszis S.J., Coath C.D., Greenwood J.P., McKeegan K.D. and Harrison T.M. Mass-independent isotope effects in Archean (2.5 to 3.8 Ga) sedimentary sulfides determined by ion microprobe analysis. Geochimica et Cosmochimica Acta 2003; 67:1635-58.

[49] Morfod J.L. and Emerson S. The geochemistry of redox sensitive trace elements in sediments. Geochimica et Cosmochimica Acta 1999; 63:1735-50.

[50] Nielsen J.K. and Shen Y. Evidence for sulfidic deep water during the Late Permian in the East Greenland Basin. Geology 2004; 32:1037-40.

[51] Ohmoto H. When did the Earth's atmosphere become oxic? The Geochemical News 1997; 93:12-13, 26-27.

[52] Ono S., Eigenbrode J.L., Pavlov A.A., Kharecha P., Rumble III D., Kasting J.F. and Freeman K.H. New insights into Archean sulfur cycle from mass-independent sulfur isotope records from the Hamersley Basin, Australia. Earth and Planetary Science Letters 2004; 213:15-30.

[53] Passier H.F., Bosch H.-J., Nijenhuis I.A., Lourens L.J., Böttcher M.E., Leenders A., Sinninghe Damsté J.S., de Lange G.J. and de Leeuw J.W. Sulphidic Mediterranean surface waters during Pliocene sapropel formation. Nature 1999b; 397:146-49.

[54] Passier H.F., Middelburg J.J., de Lange G.J. and Böttcher M.E. Modes of sapropel formation in the eastern Mediterranean: some constraints based on pyrite properties. Marine Geology 1999a; 153:199-219.

[55] Passier H.F., Middelburg J.J., de Lange G.J. and Böttcher M.E. Pyrite contents, microtextures, and sulfur isotopes in relation to formation of the youngest eastern Mediterranean sapropel. Geology 1997; 25:519-22.

[56] Passier H.F., Middelburg J.J., van Os B.J.H. and de Lange G.J. Diagenetic pyritization under eastern Mediterranean sapropels caused by downward sulphide diffusion. Geochimica et Cosmochimica Acta 1996; 60:751-63.

[57] Pavlov A. and Kasting J.F. Mass-independent fractionation of sulfur isotopes in Archean sediments: strong evidence for an anoxic Archean atmosphere. Astrobiology 2002; 2:27-41.

[58] Peters K.E. and Moldowan J.M. The Biomarker Guide: Interpreting Molecular Fossils in Petroleum and Ancient Sediments. Englewood Cliffs: Prentice Hall, 1993.

[59] Poulton S.W. and Raiswell R. The low-temperature geochemical cycle of iron: from continental fluxes to marine sediment deposition. American Journal of Science 2002; 302:774-805.

[60] Poulton S.W., Fralick P.W. and Canfield D.E. The transition to a sulphidic ocean ~1.84 billion years ago. Nature 2004; 431:173-77.

[61] Raiswell R. and Berner R.A. Pyrite formation in euxinic and semi-euxinic sediments. American Journal of Science 1985; 285:710-24.

[62] Raiswell R. and Berner R.A. Pyrite and organic matter in Phanerozoic normal marine shales. Geochimica et Cosmochimica Acta 1986: 50:1967-76.

[63] Raiswell R., Buckley F., Berner R.A. and Anderson T.F. Degree of pyritization of iron as a paleoenvironmental indicator of bottom-water oxygenation. Journal of Sedimentary Petrology 1988; 58:812-19.

[64] Raiswell R. and Canfield D.E. Sources of iron for pyrite formation in marine sediments. American Journal of Science 1998; 298:219-45.

[65] Raiswell R., Newton R. and Wignall P.B. An indicator of water-column anoxia: resolution of biofacies variations in the Kimmeridge Clay (Upper Jurassic, U.K.). Journal of Sedimentary Research 2001; 71:286-94.

[66] Reichow M.K., Saunders A.D., White R.V., Pringle M.S., Al'Mukhamedov A.I., Medvedev, A. and Kirda N.P. $^{40}Ar/^{39}Ar$ dates from the West Siberian Basin: Siberian flood basalt province doubled. Science 2002; 296:1846-49.

[67] Repeta D.J., Simpson D.J., Jorgensen B.B. and Jannasch H.W. Evidence for anoxygenic photosynthesis from the distribution of bacteriochlorophylls in the Black Sea. Nature 1989; 342:69-72.

[68] Rohling E.J. Review and new aspects concerning the formation of eastern Mediterranean sapropels. Marine Geology 1994; 122:1-28.

[69] Rohling E.J. and Hilgen F.J. The eastern Mediterranean climate at times of sapropel formation: a review. Geologie en Mijnbouw 1991; 70:253-64.

[70] Rothman D.H., Hayes J.M. and Summons R.E. Dynamics of the Neoproterozoic carbon cycle. Proceedings National Academy of Sciences 2003; 100:8124-29.

[71] Ryskin G. Methane-driven oceanic eruptions and mass extinctions. Geology 2003; 31:741-44.

[72] Sachs J.P. and Repeta D.J. Oligotrophy and nitrogen fixation during Eastern Mediterranean sapropel events. Science 1999, 286:2485-88.

[73] Schlanger S.O. and Jenkyns H.C. Cretaceous oceanic anoxic events: causes and consequences. Geologie en Mijnbouwe 1976; 55:179-84.

[74] Scholle P.A. and Arthur M.A. Carbon isotope fluctuations in Cretaceous pelagic limestones: potential stratigraphic and petroleum exploration tool. American Association of Petroleum Geologists Bulletin 1980, 64:67-87.

[75] Schouten S., van Kaam-Peters H.M.E., Schoell M. and Sinninghe Damsté J.S. Effects of an oceanic anoxic event on early Toarcian carbon. American Journal of Sciences 2000; 300:1-22.

[76] Schultz R.B. and Plimmer S.M. Geochemistry of organic-rich shales: new perspectives. Chemical Geology 2004; 206:1-426.

[77] Schwark L. and Frimmel A. Chemostratigraphy of the Posidonia Black Shale, SW Germany: II. Assessment of extent and persistence of photic-zone anoxia using aryl isoprenoid distributions. Chemical Geology 2004; 206:231-48.

[78] Scotese C.R. *Continental Drift*. 7th edition, PALEOMAP Project 1997. Arlington.

[79] Shen Y., Canfield D.E. and Knoll A.H. Middle Proterozoic ocean chemistry: evidence from the McArthur Basin, northern Australia. American Journal of Science 2002; 302:81-109.

[80] Shields G.A. and Veizer J. The Precambrian marine carbonate isotope database: version 1.1. Geochemistry, Geophysics, Geosystems 2002; 3:10.1029/2001GC000266.

[81] Sinninghe Damsté J.S. and Köster J. A euxinic southern North Atlantic Ocean during the Cenomanian/Turonian oceanic anoxic event. Earth and Planetary Sciences 1998; 158:165-73.

[82] Sinninghe Damsté J.S., Kuypers M.M.M., Schouten S., Schulte S. and Rullkötter J. The lycopane/C_{31} *n*-alkane ratio as a proxy to assess palaeoxicity during sediment deposition. Earth and Planetary Science Letters 2003, 209:215-26.

[83] Sinninghe Damsté J.S., Schouten S. and van Duin A.C.T. Isorenieratene derivatives in sediments: possible controls on their distribution. Geochimica et Cosmochimica Acta 2001; 65:1557-71.

[84] Strauss H. "4 Ga of seawater evolution: evidence from the sulfur isotopic composition of sulfate." In *Sulfur Biogeochemistry - Past and Present*, Jan P. Amend, Katrina J. Edwards, Timothy W. Lyons eds., Geological Society of America Special Paper 2004; 379:195-205.

[85] Summons R.E. and Powell T.G. Identification of aryl isoprenoids in source rocks and crude oils: biological markers for the green sulphur bacteria. Geochimica et Cosmochimica Acta 1987; 51:557-66.

[86] Van Houten F.B. and Arthur M.A. "Temporal patterns among Phanerozoic oolitic ironstones and oceanic anoxia." In *Phanerozoic Ironstones*. T.P. Young, W.E.G. Taylor eds., Geological Society of London Special Publication 1989; 46:33-49.

[87] Veizer J., Ala D., Azmy K., Bruckschen P., Buhl D., Bruhn F., Carden G.A.F., Diener A., Ebneth S., Godderis Y., Jasper T., Korte C., Pawellek F., Podlaha O.G. and Strauss H. ^{87}Sr / ^{86}Sr, $\delta^{13}C$ and $\delta^{18}O$ evolution of Phanerozoic seawater. Chemical Geology 1999; 161:59-88.

[88] Walliser O. *Global Events and Event Stratigraphy in the Phanerozoic.* New York, Springer-Verlag, 1986.

[89] Weidlich O., Kiessling W. and Flügel E. Permian-Triassic boundary interval as a model for forcing marine ecosystem collapse by long-term atmospheric oxygen drop. Geology 2003; 31:961-64.

[89] Wignall P.B. *Black Shales.* Oxford: Clarendon Press, 1994.

[90] Wignall P.B. and Hallam A. Anoxia as a cause of the Permian/Triassic extinction: facies evidence from northern Italy and the western United States. Palaeogeography Palaeoclimatology Palaeoecology 1992; 93:21-46.

[91] Wignall P.B. and Newton R. Pyrite framboid diameter as a measure of oxygen deficiency in ancient mudrocks. American Journal of Science 1998; 298:537-52.

[92] Wignall P.B. and Twitchett R.J. "Extent, duration, and nature of the Permian-Triassic superanoxic event." In *Catastrophic Events and Mass Extinctions: Impacts and beyond* Koeberl C. and Leod K.G. eds., Geological Society of America Special Paper 2002; 356:395-413.

[93] Wignall P.B. and Twitchett R.J. Oceanic anoxia and the end Permian mass extinction. Science 1996; 272:1155-58.

[94] Zhuravlev A. Yu. and Wood R.A. Anoxia as the cause of the mid-Early Cambrian (Botomian) extinction event. Geology 1996; 24:311-14.

THE PALEOME: LETTERS FROM ANCIENT EARTH

Fumio Inagaki[1] and Kenneth H. Nealson[1,2]

[1] *Japan Agency for Marine-Earth Science and Technology (JAMSTEC), Subground Animalcule Retrieval (SUGAR) Project, Extremobiosphere Research Center, 2-15 Natsushima-cho, Yokosuka 237-0061, Japan*

[2] *Department of Earth Sciences, University of Southern California, 3651 Trousdale Pkwy, Los Angeles, CA 90089-0740, USA*

Abstract Recent advances in molecular ecological techniques have led to the revelation that sedimentary environments contain molecular signals in the form of DNA sequences: signals that tend to be consistent with the in situ geochemical environment. However, as one moves to more ancient environments, the correlation of molecular signals with the in situ environment becomes more difficult. We have called the pool of molecular information that can be obtained from such ancient environments the 'Paleome'. This concept is controversial, in part because it demands that the molecular sequences be stable for long periods of time, and in part because the interpretation of such sequences in a geochemical context is often difficult, even for contemporary samples. We review results from a variety of environments, discussing the potential explanations for each, and focusing on the relationship of the molecular signals to the biological history of the sample. In almost every case, while molecular signals were abundant, viable cells were not cultivated. We posit here that the paleome is the genetic record of the biological past, a record that has been preserved on geologic timescales: a record that may well provide us with insights into both the paleoenvironment and the co-evolution of Earth and its biota.

Keywords: Paleome, Subsurface biosphere, 16S rRNA gene, Extremophiles

1. INTRODUCTION

Recent progress using culture-independent molecular (sequence-based) approaches has revealed the presence of ubiquitous and often abundant prokaryotes in many environments previously thought to be uninhabited. Because of the ability of the polymerase chain reaction (PCR) to amplify small signals, it is possible to interrogate very low levels of biomass in search of specific sequence information. Furthermore, because of the power of statistical analysis of the DNA sequences, it has been possible to define the remarkable systematic (i.e. taxonomic and phylogenetic) diversities within the prokaryotic communi-

L. N. Neretin (ed.), Past and Present Water Column Anoxia, 21–39.

ties. Our own work has utilized these approaches to investigate the microbial populations found in a variety of sedimentary and subsurface environments in both modern and ancient terrains. As a general rule, in the more ancient samples, the correlation between the microbial community and the present-day in situ geochemical environment is more difficult to establish. Many reasons may account for these discrepancies, including re-growth, deposition and storage of organisms from other ecosystems, as well as storage (i.e. preservation or degradation) of ancient relict DNA. We have called the composite nucleic acid signals from such ancient environments the paleome [20] to connote the idea that it may in some cases provide a taxonomic and phylogenetic window to the past microbial community that inhabited the environment under study. Here we review the results of community analyses of several environments and discuss these in terms of their possible role(s) as ancient molecular signals, or paleomes.

2. PALEOMES IN LOW-TEMPERATURE SUBSEAFLOOR ENVIRONMENTS

2.1 Extremophiles in Cold Marine Sediments at the West Philippine Basin

On the basis of the estimates of the prokaryotic biomass in core sediments obtained by the Ocean Drilling Program (ODP), the marine subsurface sediment is proposed to be the largest reservoir of biomass on Earth (Whitman et al., 1998). Marine sediments consistently harbor more than 10^5 prokaryotic cells/cm^3 even at a depth close to 1,000 m below the seafloor (mbsf) [39]. Perhaps the most intensively studied part of the marine subsurface, with regard to the phylogenetic diversity and distribution of the prokaryotic communities are the sediments at the continental margin associated with methane hydrates. Despite these efforts, however, only a few sediment samples at a few depths have been examined, and the role(s) of the microbiota in either formation or degradation of these important deposits remain elusive.

The situation with regard to subsurface sediments in the open Pacific, the locus of our studies, is even less well defined. In October 1999, we collected a 14 m piston core from the center of the West Philippine Basin at a water depth of 5719 m. The core was mainly composed of diatom ooze at the top, with pelagic clay beneath, and a magnetostratigraphic age of approximately 2.5 million years. Such sediments serve to demonstrate a major conundrum of sediment microbiology: surely microbes will be found, but are they merely today's microbes processing yesterday's nutrients, or are they a snapshot of the environmental conditions of the past?

With this question in mind, we extracted bulk DNA from the innermost part of the core samples collected at 14 different depth horizons, amplified the DNA

fragments of archaeal 16S rRNA genes, and used this material to investigate the vertical community structure of the Archaea in this environment, using a combination of molecular ecological techniques [14]. The T-RFLP fingerprint analysis showed that the archaeal community structure was clearly shifted at a point of 4 mbsf (Fig. 1). The phylogenetic analysis of clone libraries indicated that the archaeal community structures in shallow sediments were mainly composed of the members belonging to the Marine Crenarchaeota Group I (MGI) as they are called (Fig.1), a phylotype known to be the most abundant Crenarchaeota in marine benthic environments [8, 11, 25, 50]. These data are consistent with the notion of a continuous population of Crenarchaeota in ocean bottom waters and shallow sediments.

In contrast, the deeper core horizons below 4.8 mbsf were dominated by extremophilic Archaea. In the pelagic clay samples at depths of 4.8 and 5.8 mbsf, the archaeal 16S rRNA gene clone libraries were predominantly composed of sequences related to the genus *Thermococcus* and the Deep-Sea Hydrothermal Vent Euryarchaeotic (DHVE) Group. Both the *Thermococcus* group (known as hyperthermophilic fermenters) and the DHVE are ubiquitous inhabitants of hydrothermal vent environments [44]. At a depth range from 7.8 to 12.8 mbsf, in addition to *Thermococcus*, we found sequences related to the extreme halophilic Archaea in the genus *Haloarcula* (Fig. 1). *Haloarcula* species are known to be long-term survivors in various hyper-saline environments such as salt lakes, salt mines, salt firms, and salt deposits [24], with reports of 16S rRNA gene fragments detected from inside of a crystal halite formed over 200 million years ago [35]. These organisms are ubiquitously distributed in marine environments as well, with *Haloarcula* DNA reported from a deep-sea hydrothermal vent chimney structure obtained from the Manus Basin, Papua New Guinea [45]. In addition, the 16S rRNA fragments related to the genera *Sulfolobus* and *Sulfurisphaera* were found to be present in the deeper part of the piston core sediment (Fig. 1). These organisms are common in terrestrial acidic geothermal environments and characterized to be extreme thermophilic acidophiles; this was the first report of DNA of the order *Sulfolobales* from the marine environment. Attempts to cultivate these extremophilic Archaea from the marine sediments have so far yielded no growth. The DGGE analysis of the archaeal 16S rRNA using a different primer set from that used to establish the clone library showed almost the same results from the T-RFLP and clone library analyses (Fig. 1F).

These data pose a fundamental question related to the origin of the various cell types. A tempting hypothesis that we entertain here is that these unexpected DNA sequences represent paleomes of buried archaeal cells that were transferred from another terrains and preserved to the present time. Since the predicted growth characteristics of detected cells do not match the in situ cold, low-organic subseafloor environment and most of detected cells are known to

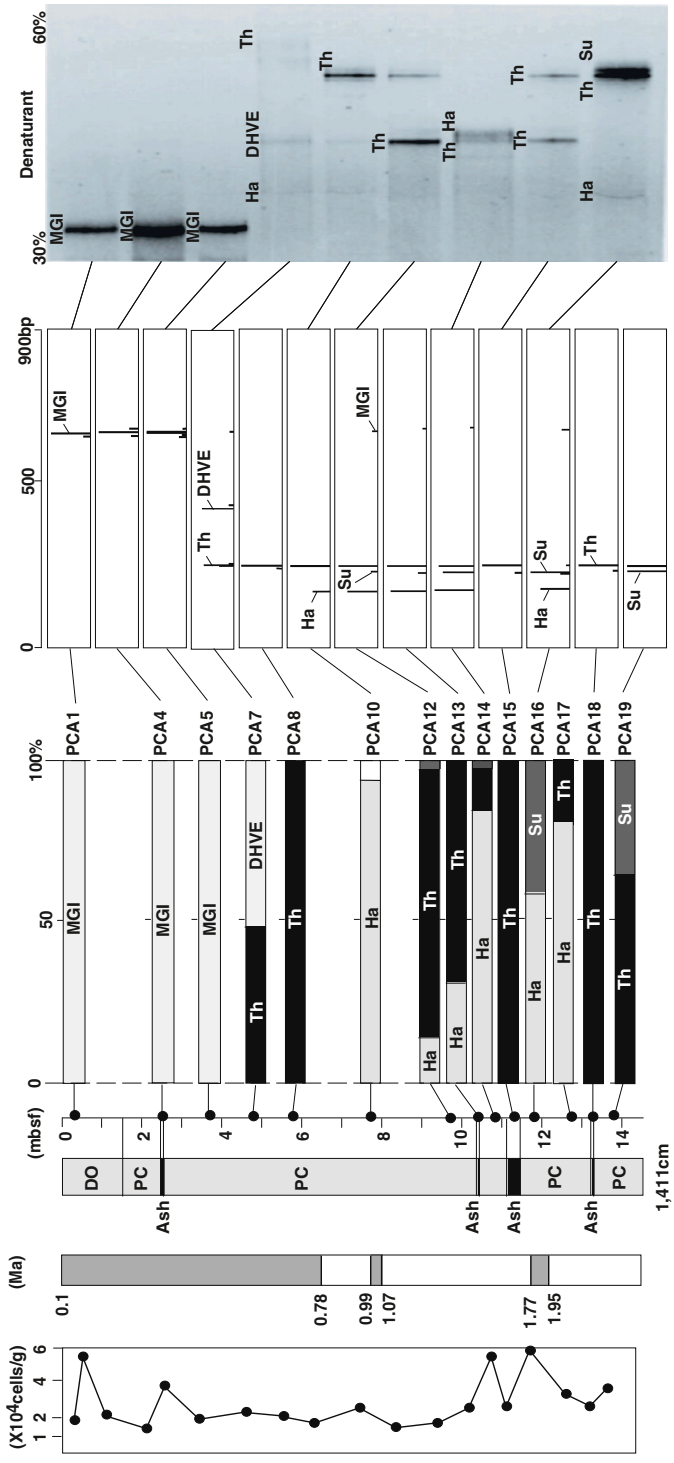

Figure 1. Detection of unexpected archaeal rRNA gene sequences from cold subseafloor sediments in the Philippine Sea. (A) Total cell counts in the sediments. (B) Age of the sediments evaluated by the magnetostratigraphic shift. (C) Lithology and depth of the sediment core. DO, diatom ooze; PC, pelagic clay; Ash, volcanic ash layer. (D) Phylotype structure of archaeal 16S rRNA gene clone libraries. MGI, marine Crenarchaeota group I; Th. *Thermococcus*; DHVE, deep-sea hydrothermal vent euryarchaeotic group; Ha,*Haloarcula*; Su, *Sulfolobus*. (E) T-RFLP profile of 16S rRNA gene digested with *Hha* I. (F) DGGE profile of archaeal 16S rRNA gene amplicons.

be the predominant archaeal components in habitats of deep-sea hydrothermal vent environments, we suggest that *Thermococcus*, DHVE and *Haloarcula* cells are most likely derived from the hydrothermally active environments surrounding the Philippine Sea such as the Izu-Bonin arc, Mariana arc, and Manus Basin (Fig. 2). Given the slow rate of ocean crust movement (a few cm/yr), the sediments themselves are still within 10-20 km of their location 2 million years ago, so other mechanisms must account for the results, such as sea-bottom currents, which might be one mode of transport of these cells. The extreme thermoacidophilic Archaea, *Sulfolobus-Sulfurisphaera*, might be derived from the terrestrial geothermal environments by the regional west wind (Fig. 2). Indeed, a representative sequence was closely related to the sequence of *Sufolobus yangmingensis* isolated from a hot spring in Taiwan [23]. Interestingly, these molecular signals were obtained from just beneath the volcanic ash layers. On the basis of these results, it may be possible to say that the molecular signals of terrestrial extremophiles are likely to be a good indicator of the geothermal activities before the volcanic eruptions.

Although the clonal frequency does not reflect the cell abundance because of the occurrence of bias during PCR and cloning steps and the copy number of 16S rRNA gene in genome, the results showed that the archaeal community structures were mixed with paleomes of extremophiles in marine and terrestrial environments and the compositions of these phylotypes changed with the age of the sediment horizons. For example, the sequences related to *Haloarcula* were only detected in a depth range from 7.8 to 12.8 mbsf deposited 1-2 million years ago. High numbers of the *Sulfolobales* clone sequences were found only just beneath the events of the volcanic eruption (Fig. 1). These facts suggest that the archaeal communities buried from the Pleistocene period, more than 2 million years, might reflect the past geologic thermal activities surrounding the sampling site in the Philippine Sea (Fig. 2). The paleomic signals may give us new insights as geomicrobiological evidences into paleo-proxies that have not been identified by conventional geologic surveys.

2.2 Unusual Endolithic Prokaryotes in a Deep-Sea Sedimentary Rock

While analysis of core samples is the usual approach for the investigation of sedimentary materials, there are other less obvious opportunities that occasionally arise. For example, the Japan Trench is recognized as a typical erosion-type subduction zone where frequent earthquakes occur. The associated seismic and subduction activities can lead to the movement of sedimentary rocks to the deep parts of the trench where they are found as dropstones. In May 1999, we collected such a rock sample from the Japan Trench at a depth of 6,337 m using the manned submersible Shinkai6500 and examined the microbial communities

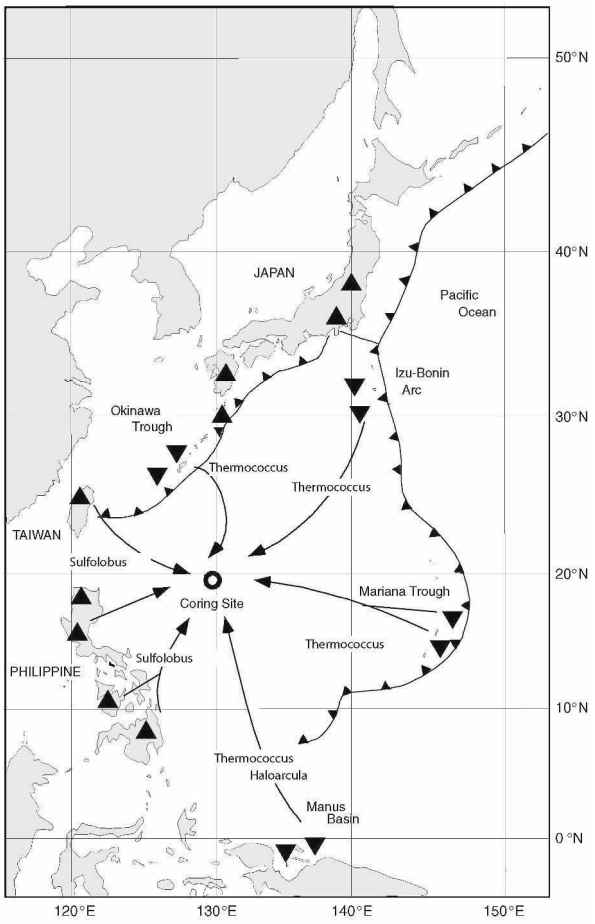

Figure 2. A schematic figure of the possible sources of archaeal 'Paleomes' that found in the cold subseafloor sediments.

on the outside and inside of the dropstone with an eye to the question: Could the community structures offer any insight into the environment from which the dropstones were derived – that is, can the surviving DNA be used as a paleome to reveal the history of the sample?

The rock (17 Kg) we examined was a sedimentary siltstone having a texture of horizontal layers [15]. The shape was sub-angular, indicating the rock probably dropped from outcrop recently. Based on the analysis of associated diatoms, the dropstones in this area were estimated to be of Miocene to Pliocene (5~20 Ma) in age [29]. Using a rock trimmer, subsamples were aseptically obtained at depth intervals of 5 cm in a horizontal direction. Bulk DNA was extracted from these four samples and analyzed for the presence of archaeal

and bacterial 16S rRNA gene using clone library sequence comparisons and T-RFLP analyses. The results showed that archaeal communities in the rock interior were different from those near the rock surface. In the surface sections, almost all archaeal 16S rRNA gene sequences were affiliated within the MGI, while the inner parts of the deep-sea rock were predominantly composed of hyperthermophilic Archaea, in the genus *Thermococcus* [15]. A similar transition was observed in the bacterial 16S rRNA genes, with the outermost samples being composed of three clusters; *Cytophaga-Flexibacter-Bacterioides* (CFB), alpha- and gamma-Proteobacteria, and the innermost samples being dominated by the gram-positive bacteria and the genus *Burkholderia* within the beta-Proteobacteria [15].

Rocks of the kind reported above offer a situation that is different from that seen in sediments that are examined via core analysis. In the case of the rock, the microbial populations have presumably been incorporated during the formation of the sediment, taken up residence, and then the rock transported to another environment where further sedimentation does not occur, but rather, an exchange with the exterior environment drives any population change that is seen. That is, the shift of the prokaryotic community structures we observed may be associated with the historical circumstances of the rock, with the outer communities (MGI and the gamma Proteobacteria) indicating the outer environment that slowly infiltrates the rock surface, and the *Thermococcus*, Gram positives, and *Burkholderia* representing organisms associated with the sedimentary history of the rock.

With regard to this notion, the outer regions of dropstone were more porous (13%) than the inner regions (7.5% approximately 15 cm from the rock surface) [15]. Thus, if communities were in place in the interior of the sedimentary stone, they would be expected to still be in place and detectable via our molecular approaches.

The existence of the *Thermococcus* signals in the interior of the dropstone is in keeping with a similar shift of the archaeal community structure reported above, and also described in deep subseafloor sediments recovered by ODP Leg 190 from the Nankai Trough [28]. As with the sediments described above, one imagines these organisms being transported to the sediments as they were forming. In contrast, the bacterial community in the innermost section is difficult to explain. Indeed, the genus *Burkholderia* is commonly found in soils and terrestrial subsurface environments [34]. If the rock interior represents a paleome, then one must invoke a transport event that brought a major input of terrestrial or soil microbes to the environment sometime in the distant past.

2.3 Are Viable Microbes in Deep Subseafloor Sediment Potentially Old?

For the most part, the large and varied efforts using culture-independent molecular genetics techniques to analyze subseafloor communities has not been accompanied by traditional cultivation efforts. Only a few species have been cultivated so far from deep subseafloor environments [2, 36]. In no case the population size, metabolic activity, or ecological significance of any of these isolates has been clearly delineated. A fair summary of the efforts to cultivate and evaluate the living microorganisms from the deep subseafloor core sediments, such as those of Smith [43] might be: (1) the activity of the cells appears to be extremely low, (2) the growth of the native populations may be extremely slow, (3) the cells may be very sensitive to oxygen and pressure, (4) most cells may require special cultivation techniques such as growth in mixed cultures; and, (5) most cells may be dormant or dead, constituting what we call here the 'Paleome'. Our own studies have involved both cultivation-independent, and, when possible cultivation-connected studies, thus raising the issue of whether there may be environments where truly ancient organisms are still surviving.

Viable cells in a subseafloor sediment core from the Sea of Okhotsk (IMAGES 2001). In August 2001, a sediment core, which extended 58.1 mbsf, was recovered from the southeastern Sea of Okhotsk by the International Global Environmental Change Study (IMAGES) Project [17]. The sediment core was found to be composed of pelagic clay with several volcanic ash layers containing pumice grains. The preliminary identification of the sedimentation age by the tephra analysis indicated that the bottom of the core sediment was approximately 130,000 years old, indicating a very high sedimentation rate. Culture-independent molecular analysis showed clear differences between the bacterial populations in the pelagic clay environments and the volcanic ash layers: the pelagic clays were dominated by members within the Green non-sulfur bacteria and the candidate OP9 division, while the ash layers harbored members of the genera *Halomonas*, *Psychrobacter* and type-I methanotrophs within the gamma-Proteobacteria and *Sulfitobacter* sp. within the alpha-Proteobacteria [17]. Cultivation-dependent analyses also showed clear differences: no growth was observed from the pelagic clay layers, while abundant populations of viable heterotrophs were obtained from the ash layers (Fig. 3). With the exception of a few spore formers and *Actinobacteria* that were recovered, there was a good agreement between the populations identified by culture dependent and culture independent methods [17]. The factors that account for the apparent good viability of the bacteria in this deep and old environment are not clear – it could be that small organic nutrients and electron acceptors are imported from the

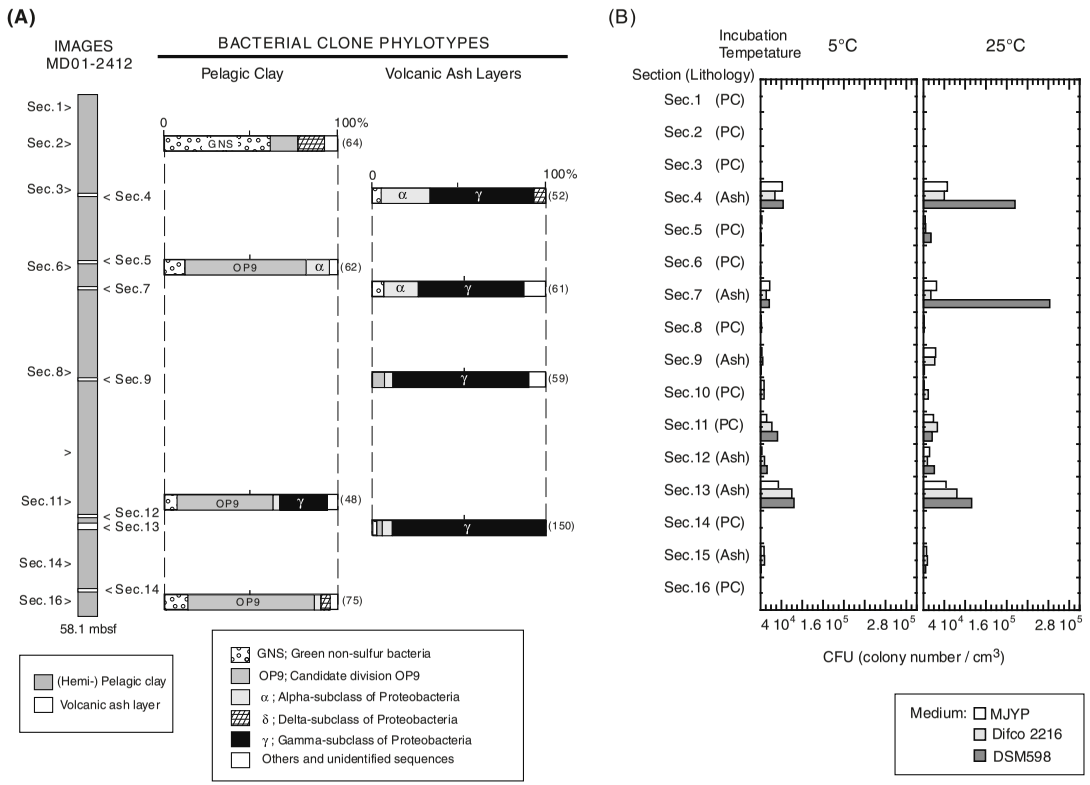

Figure 3. Lithology-dependent bacterial community structures in the subseafloor core sediments from the Sea of Okhotsk. (A) Culture-independent molecular analysis of bacterial 16S rRNA gene clone sequences. (B) Colony forming unit assay of cultivable bacterial population.

outcrop of the sampling site or squeezed from clay matrix with burial. Whatever the mechanism, our study suggests that the porous ash layers may provide horizontally distributed microbial habitats in the subseafloor environments that act as good reservoirs of potentially old viable microbial remnants.

Thermophilic Spore-Formers from the Sediments of the Peru Margin (ODP Leg 201). ODP Leg 201, which took place early in 2001 off the coast of Peru, represented the first ODP mission focused on the microbiology and biogeochemistry of the deep oceanic subsurface. As with the pelagic clay environment described for the Sea of Okhotsk, our attempts at cultivation yielded little in the way of viable cells, despite targeting a wide variety of physiological types of organisms under aerobic and anaerobic conditions at various temperatures [42]. Curiously, however, from several depths, we were able to cultivate thermophilic fermenters that grew at 55 °C (Table 1). Epifluorescence microscopic observation of the cells stained with DAPI and fluorescence in situ hybridization (FISH) with Archaea- and Bacteria-specific probes revealed that the cells were anaerobic thermophilic spore-forming fermentative bacteria (Fig. 4). Most probable number (MPN) method revealed that the viable population size of those thermophiles were below 10^2 cell per $1cm^3$ of the innermost core sediment sample (Table 1). Phylogenetic analysis of 16S rRNA gene revealed that isolates were closely related with *Anoxibacillus flavithermus* and *Bacillus licheniformis*. Since the growth temperature of isolates was clearly different from the in situ conditions and the sedimentation age of deep sediments was approximately 20,000,000 years, it would appear that these members are likely to be old microbial components that have been transported from either terrestrial geothermal or deep-sea hydrothermal fields and then buried in marine sediments, to be stored as spores for millions of years until clement conditions allow their germination and growth.

ODP Site	Core section	Depth (mbsf)	MPN population (cells/cm^3)
1227	Hole A12-3	102,4	33
1228	Hole A2-2	7,0	no growth
1229	Hole A2-2	7,0	no growth
	Hole A22-2	186,9	33
1230	Hole A1-2	1,8	66
	Hole C2-4	8,5	no growth
	Hole A9-2	66,5	83
	Hole A15-4	121,5	no growth
	Hole A21-3	160,6	14

Table 1. Population of anaerobic thermophilic heterotrophs in deep marine sediments of the Peru Margin (ODP Leg 201) estimated by three series of six-tubes MPN method.

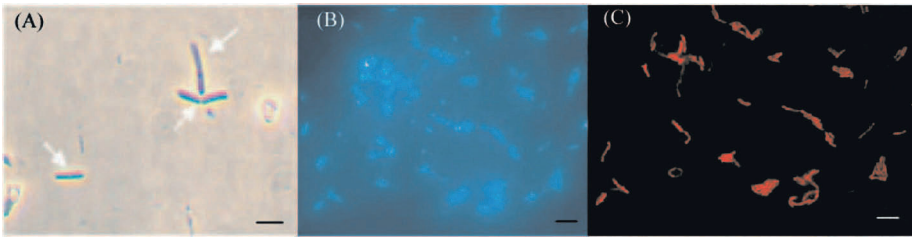

Figure 4. Onboard microscopic observations of anaerobic thermophilic spore-forming fermenters isolated from deep subseafloor sediments in the Peru Margin, ODP Leg 201. (A) Cell images on the optical microscopy. (B) DAPI-stained cells. (C) Cells hybridized by a specific probe for the domain Bacteria (BAC338) by FISH method. Bar=1 μm.

3. PALEOMES IN THE TERESTRIAL SUBSURFACE

The terrestrial subsurface offers an interesting and different environment from that seen in the marine subsurface. In general, these environments are older and more geologically "mature" than the young crustal environments of the marine system. Also, because of the nature of the hydrological cycle and groundwater flow, they are often impacted by subsurface water flowing from land to sea across the samples. Thus, while many of these environments originated with oceanic populations and processes, they are often strongly impacted by terrestrial contamination in the form of freshwater, nutrients, and biomass. Contamination that makes the interpretation of results even more problematic than the marine subsurface samples discussed above.

3.1 Molecular Signals from Terrestrial Tunneled Subsurface Environments

One of the prevalent examples of the terrestrial subsurface is that provided by deep subsurface tunnels drilled for various uses, usually mining for metals. Such mines provide easy access to the deep subsurface microbial habitat. In the past decade extensive surveys for microbial habitats in global deep subsurface environments beneath such tunneled environments have clearly demonstrated the existence of life in global deep subsurface was evidenced (e.g. [12, 26, 40, 46]). Most living microorganisms in deep subsurface environments are of course adapting to the ambient geochemical characteristics. For example, *Thermus* sp. found in a South African Gold mine was able to grow under anaerobic conditions using iron and manganese as electron acceptors for respiratory metabolism [26]. One of the most alkaliphilic microorganisms known, *Alkaliphilus transvaalensis* (optimum pH = 10.0, maximum pH = 12.5), was isolated from a deep subsurface environment of the South African gold mine at the depth of 3,200 m below land surface [47], a source that has many geological and geophysical similarities to the deep subsurface.

Our studies have focused on the distribution and phylogenetic diversities of microbial communities occurring at deep terrains in the Hishikari gold mine, located at the southern part of Kyushu Island in Japan. This mine is the epithermal type-gold mine associated with a geothermal activity of the Kirishima volcano and contains the most productive gold-silver deposits in the western Pacific Margin. The basement of the Hishikari gold mine is composed of shales of oceanic sediments formed at the Cretaceous period called 'Shimanto-Supergroup' [18]. The analyses of deuterium-oxygen isotopes suggested that the subground hot aquifer water was circulated meteoric water [33]. Thus, this environment is similar to many other mines: an ancient geologic setting impacted by modern aquifers and the organisms that adapt within them. Such an environment makes the concept of the "paleome" a difficult one to substantiate because of the opportunity for present day growth of microbial communities.

Using molecular genetic analyses, we determined that the predominant organisms were related to previously uncultivated bacteria of the order *Aquificales* [18]. Further work resulted in the cultivation of some of these bacteria [48], one of which was named *Sulfurihydrogenobium subterraneum* [49], and was found to be able to use various gases and geochemical components dissolved in the hot deep aquifer as electron donors and/or acceptors and to grow chemolithoautotrophically. In the same environment, we also isolated a variety of members related to known genera *Hydrogenophilus*, *Azoarcus*, *Thermus*, and to not-yet-known novel species. For example, *Thermus* sp. closely related to that of *T. scotoductus*, was found to be capable of anaerobic growth using nitrate and ferrihydrite as an electron acceptor. The physiological properties of *Thermus* and other isolates from the subsurface biosphere of the Hishikari gold mine leave us with a similar message from other tunneled environments, namely that the microbial population is adapting to and reflective of the surrounding geochemical settings.

Given these results, it is hard to consider the endemic populations in the deep mines as a paleome so much as active populations adapting to and growing in the subsurface. However, in addition to the above results, culture-independent molecular ecological surveys of subsurface terrestrial environments have revealed a variety of prokaryotes inhabiting the aquifers and rocks, including unexpected signatures that are not consistent with the current subsurface environment. For example, unusual archaeal phylotypes have been obtained from fissure water samples that were related to the hyperthermophilic Archaea *Pyrococcus* and other yet uncultivated, novel Archaea [46]. These results suggested that these molecular signatures might be derived from more deep anaerobic,

saline groundwater systems at depths of 5-6 km where temperatures are in the range of growth and/or survival of hyperthermophiles [46].

3.2 DNA from Mid-Cretaceous Black Shales (Ocean Anoxic Events)

One of the most enigmatic phenomena of the Cretaceous period is that of the episodic deposition of black shale layers. These occurrences, referred to as ocean anoxic events or OAEs, are thought to have occurred during warm anoxic periods during the Cretaceous, leaving clearly distinct organic-rich black layers. The OAEs are considered to have been caused by a complex combination of temporal warm temperature, high biological productivity and turnover, ocean current relaxation, methane hydrate explosion, and superplume activities (e.g. [10, 32, 51]). However, only limited fossils are found in these black shales, and the factors that led to their formation remain the objects of great debate. With regard to these issues, and because of the ability of microbes to survive a wide variety of conditions, we investigated some OAE layers to see whether or not microbial fossils might be left behind as indicators of their activities during the periods of shale formation.

In October 2000, in southwestern France, we collected a core from a depth of 338 cm below the surface [20] that contained a extremely black layer defined as the top of OAE1b formed at 108 million years ago [41]. The innermost part of the core was aseptically sampled at six vertical depths of the black shale core. No contamination occurred during drilling as judged by the use of fluorescence micro-beads [43]. Bacterial 16S rRNA genes were amplified from the six different horizons associated with an OAE stratum. Although the core was recovered from a terrestrial environment, the recovered sequences showed affinity to bacterial communities previously seen in deep-sea sedimentary environments (i.e., the sequence assemblage was easily recognizable as a marine community). At the non-OAE horizons, bacterial community structures were mainly composed of the gamma-Proteobacteria, similar to extant deep-sea genera such as *Shewanella*, *Moritella*, *Psychromonas*, *Halomonas*, and *Marinobacter*. Some of these sequence were closely related to the members of psychrophilic (cold-loving) or piezophilic (pressure-loving or tolerant) bacteria.

At the OAE horizons, the bacterial populations changed dramatically (Fig. 5), showing a shift towards sulfate-reducing bacteria (SRB) belonging to the delta-Proteobacteria. In particular, the predominant clone sequences within the delta-Proteobacteria were affiliated with the *Desulfosarcina/Desulfococcus* cluster and the *Desulfobulbus* cluster [20]. The members within these clusters are known to be the ‘putative anaerobic methane oxidation (AMO) syntrophic SRB group’ [37] and detected from global methane and cold seep environ-

ments [4, 13, 16, 22, 38]. In addition, the sequences indicative of the epsilon-Proteobacteria were also detected from the OAE horizon (Fig. 5). The prokaryotic rRNA genes in black shales were thus clearly distinguishable from those from other parts of the core, and from those seen in debris or circulation drilling waters. A likely explanation for these results is that the marine environments in the Cretaceous period were strongly affected by the large flux of methane and/or hydrocarbons from below (either biologically or abiotically produced). In these environments, prokaryotic communities might consume methane in the sediments, and the sulfur circulation mediated by SRB and sulfur-oxidizing bacteria (SOB) might occur at the oxic/anoxic-interface between the seawater and sediments.

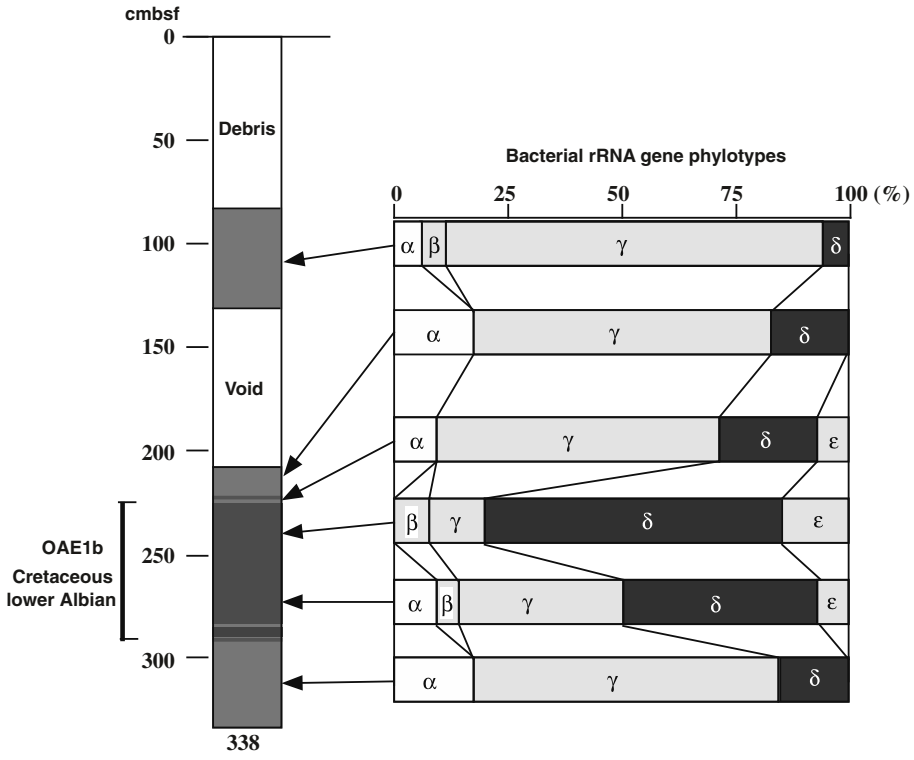

Figure 5. Profile of bacterial rRNA phylotype compositions in the black shale core containing a layer of OAE1b occurred at 108 million years ago. α, β, γ, δ, ϵ: alpha-, beta-, gamma-, delta-, and epsilon-Proteobacteria.

These data are in keeping with recent reports of modern communities of metabolically active bacterial in the deep-sea cold seep sediment at the Japan Trench, which were predominantly composed of a combination of the delta- and epsilon- Proteobacteria [16]. We isolated the most related species to those

environmental sequences, such as genera *Sulfurovum* and *Sulfurimonas,* which were found to be mesophilic chemolithoautotrophic SOB [19, 21].

Our results clearly indicate that these bacterial communities are quite similar to the extant communities occurring at the anaerobic cold and/or methane seep environments. The prokaryotic community on the seafloor might shift according to the environmental change. The OAE layers contain globular or framboidal metal sulfides thought to be produced by microbial activities of the SRB during sedimentation and diagenesis [5], which is consistent with our observation of the SRB dominance in the OAE black layer [20]. Although Kuypers [30] reported that archaeal lipids dominated in the OAE1b layer, we were not successful in obtaining archaeal DNA signals, even when using nested-PCR methods [20].

We had no success in cultivation efforts from any of the OAE samples. To some extent this is good news in terms of thinking about the paleome concept. It would appear that the samples were not tainted by contaminants (which grew readily from the drilling fluid and adjacent soils), and thus might be candidates for a paleome, whose signals in the form of amplifiable DNA fragments were still intact. While this is not truly ancient in geological terms, it is an interesting and hopeful start in terms of our search for useful 'paleomes'.

4. CONCLUSION: LETTERS FROM ANCIENT EARTH

In this chapter we have reviewed the evidence for the existence of unusual molecular signals retrieved from a variety of subsurface environments. Some of these cases would appear to be explained only by the long-term preservation of buried prokaryotic cells and/or their nucleic acids. In cases such as the terrestrial deep subsurface, where nutrient-containing groundwater flows through the environment, it may well be that active communities exist. However, in the marine subsurface, where nutrients arrive in much less abundance, the activities, as reported by D'Hondt [9] are extremely low. Thus we have the dilemma that the youngest sediments, i.e., those in the deep sea formed from the spreading centers, are those most likely to have the least input of nutrients and contamination. As they age, it is presumably a good place to "store" the genetic knowledge of the past. However, as these sediments are uplifted and become part of the continental mass, they become subject to the vagaries of nutrient and ground-water input, making it more difficult to substantiate just where the material arose that is being sampled. Thus it would appear that marine sediments might represent good reservoirs of prokaryotic biomass occurring at the shallow sediments near the seafloor. One might thus imagine that such sediments and the genetic records they contain could be used to gain insight into issues such as the co-evolution of Earth and microbial ecosystems. How-

ever, most of these sediments are geologically young, almost never exceeding 150 million years in age. The older sediments, where preservation is poorer and contamination more abundant reside in the terrestrial samples. Our search should thus be for well-preserved terrestrial samples where the paleomes are still able to communicate their message, and it is possible to understand it, even in the presence of the high noise level accompanying such samples.

In order to preserve DNA over long periods, it must be stored under specific conditions where degradation (by hydrolysis, oxidation, depurination, or other mechanisms) is minimized [1, 31]. Accumulating circumstantial evidence commonly implies that the anoxic organic-rich subseafloor conditions might effectively preserve the bio-molecules as well as enzymatic activities [6, 7] for long periods of time. On the basis of laboratory experiments for long-term survival of bacterial spores and bio-molecules, Kminek et al. argued that natural radiation might put an upper limit on viability of around 100 million years [27]. Another problem impacting this work is that we have to deal the paleome signals carefully, because the information in the geologic materials is strongly dependent on the ability to correlate it with past geological and ecological backgrounds [3]. During the preservation process, biases caused by differences in structural stability of the cell could also take place. It still remain strong arguments on this issue, however, if this can be established for a variety of ancient environments and consistent with other research results (e.g. biomarker, mineralogical feature, isotopic analysis), it may well be possible that the 'Paleome' could be used as a letter from the past prokaryotic community to infer the paleo-environmental proxies during the Earth's history.

Acknowledgements

We are grateful to K. Takai and K. Horikoshi for supporting our studies of Paleome and useful discussions. We thank A. Schippers for providing FISH photographs of thermophilic isolates from ODP Leg 201 core sediments. We thank all shipboard scientists and crews of JAMSTEC, IMAGES, and ODP cruises for their assistances of deep-sea and subseafloor core sampling.

References

[1] Bada J. L., Wang X. S. and Hamilton H. Preservation of key biomolecules in the fossil record: current knowledge and future challenges. Phil Trans R Soc Lond Bull 1999; 354:77-87.

[2] Bale S. J., Goodman K., Rochelle P. A., Marchesi J. R., Fry J. C., Weightman A. J. and Parkes R. J. *Desulfovibrio profundus* sp. nov., a novel barophilic sulfate-reducing bacterium from deep sediment layers in the Japan Sea. Int J Syst Bacteriol 1997; 47:515-21.

[3] Benner S. A., Caraco M. D., Thomson J. M. and Gaucher E. A. Planetary biology-Paleontological, geological, and molecular histories of life. Science 2002; 296:864-68

[4] Boetius A., Ravenschlag K., Schubert C. J., Rickert D., Widdel F., Gieseke A., Amann R., Jorgensen B. B., Witte U. and Pfannkuche O. A marine microbial consortium apparently mediating anaerobic oxidation of methane. Nature 2000; 407:623-26.

[5] Canfield D. E., Raiswell R. and Bottrell S. H. The reactivity of sedimentary iron minerals towards sulfide. Am J Sci 1992; 292:659-83.

[6] Coolen M. J. and Overmann J. Functional exoenzymes as indicators of metabolically active bacteria in 124,000-year-old sapropel layers of the eastern Mediterranean Sea. Appl Environ Microbiol 2000; 66:2589-98.

[7] Coolen M. J., Cypionka H., Sass A. M., Sass H. and Overmann J. Ongoing modification of Mediterranean Pleistocene sapropels mediated by prokaryotes. Science 2002; 296:2407-10.

[8] DeLong E. F. Archaea in coastal marine environments. Proc Natl Acad Sci USA 1992; 89:5685-89.

[9] D'Hondt S., Rutherford S. and Spivack A. J. Metabolic activity of subsurface life in deep-sea sediments. Science 2002; 295:2067-70.

[10] Erba E. Nannofossils and superplumes: The early Aptian 'nannoconid crisis'. Paleoceanography 1994; 9:483-501.

[11] Fuhrman J. A., McCallum K. and Davis A. A. Novel major archaebacterial group from marine plankton. Nature 1992; 356:148-49.

[12] Fredrickson J. K. and Onstott T. C. "Biogeochemical and geological significance of subsurface microbiology." In: *Subsurface Microbiology and Biogeochemistry*, Fredrickson J. K., Fletcher M. eds., Wiley-Liss, Inc., 2001.

[13] Hinrichs K. -U., Hayes J. M., Sylva S. P., Brewer P. G. and DeLong E. F. Methane-consuming archaebacteria in marine sediments. Nature 1999; 398:802-05.

[14] Inagaki F., Takai K., Komatsu T., Kanamatsu T., Fujioka K. and Horikoshi K. Archaeology of Archaea: geomicrobiological record of Pleistocene thermal events concealed in a deep-sea subseafloor environment. Extremophilies 2001; 5:385-92.

[15] Inagaki F., Takai K., Komatsu T., Sakihama Y., Inoue A. and Horikoshi K. Profile of microbial community structures and presence of endolithic microorganisms inside a deep-sea rock. Geomicrobiol J 2002a; 19:535-52.

[16] Inagaki F., Sakihama Y., Inoue A., Kato C. and Horikoshi K. Molecular phylogenetic analyses of reverse-transcribed bacterial rRNA obtained from deep-sea cold seep sediments. Environ Microbiol 2002b; 4:277-86.

[17] Inagaki F., Suzuki M., Takai K., Oida H., Sakamoto T., Aoki K., Nealson K. H. and Horikoshi K. Microbial community associated with geological horizons in coastal subseafloor sediments from the Sea of Okhotsk. Appl Environ Microbiol 2003a; 69:7224-35.

[18] Inagaki F., Takai K., Hirayama H., Yamato Y., Nealson K. H. and Horikoshi K. Distribution and phylogenetic diversity of the subsurface microbial community in a Japanese epithermal gold mine. Extremophiles 2003b; 7:307-17.

[19] Inagaki F., Takai K., Kobayashi H., Nealson K. H. and Horikoshi K. *Sulfurimonas autotrophica* gen. nov., sp. nov., a novel sulfur-oxidizing epsilon-proteobacterium isolated from hydrothermal sediments in the Mid-Okinawa Trough. Int J Syst Evol Microbiol 2003c; 53:1801-05.

[20] Inagaki F., Okada H., Tsapin A. I. and Nealson K. H. The Paleome: a sedimentary genetic record of past microbial communities. Astrobiology 2005; 5:141-53.

[21] Inagaki F., Takai K., Nealson K. H. and Horikoshi K. *Sulfurovum lithotrophicum* gen. nov., sp. nov., a novel sulfur-oxidizing chemolithoautotroph within the epsilon-Proteobacteria isolated from the Okinawa Trough hydrothermal sediments. Int J Syst Evol Microbiol 2004a; 54:1477-88.

[22] Inagaki F., Tsunogai U., Suzuki M., Kosaka A., Machiyama H., Takai K., Nunoura T., Nealson, K. H. and Horikoshi K. Characterization of C1-metabolizing prokaryotic communities in methane seep habitats at the Kuroshima Knoll, the southern Ryukyu arc, by analyzing *pmoA, mmoX, mxaF, mcrA, and* 16S rRNA genes. Appl Environ Microbiol 2004b; 70:7445-55.

[23] Jan R. L., Wu J., Chaw S. M., Tsal C. W. and Tsen S. D. A novel species of thermoacidophilic archaeon, *Sulfolobus yanmingensis* sp. nov. Int J. Syst Bacteriol 1999; 49:1809-16.

[24] Kamekura M. Diversity of extremely halophilic bacteria. Extremophiles 1998; 2:289-96.

[25] Karner N. B., DeLong E. F. and Karl D. M. Archaeal dominance in the mesopelagic zone of the Pacific Ocean. Nature 2001; 409:507-10.

[26] Kieft T. L., Fredrickson J. K., Onstott T. C., Gorby Y. A., Kostandarithes H. M., Bailey T. J., Kennedy D. W., Li S. W., Plymale A. E., Spadoni C. M. and Gray M. S. Dissimilatory reduction of Fe(III) and other electron acceptors by a *Thermus* isolate. Appl Environ Microbiol 1999; 65:1214-21.

[27] Kminek G., Bada J. L., Pogliano K. and Ward J. F. Radiation-dependent limit for the viability of bacterial spores in halite fluid inclusions and on Mars. Radiation Res 2003; 159:722-29.

[28] Kormas K. A., Smith D. C., Edgcomb V. and Teske A. Molecular analysis of deep subsurface microbial communities in Nankai Trough sediments (ODP Leg 190, Site 1176). FEMS Microbiol Ecol 2003; 45:115-25.

[29] Kuwano T., Ogawa Y., Koizumi I. and Oba T. Calcite-cemented Miocene to Pliocene breccia at the Sanriku Escarpment, Northern Japan Trench. JAMSTEC J Deep Sea Res 1997; 13:573-89. (in Japanese with English abstract)

[30] Kuypers M. M. M., Blokker P., Hopmans E. C., Kinkel H., Pancost R. D., Schouten S. and Damste J. S. S. Archaeal remains dominate marine organic matter from the early Albian oceanic anoxic event 1b. Palaeograph Palaeoclimatol Palaeoecol 2002; 185:211-34.

[31] Lindahl T. Instability and decay of the primary structure of DNA. Nature 1993; 362:709-15.

[32] Larson R. L. latest pulse of Earth: Evidence for a mid-Cretaceous superplume. Geology 1991; 19:547-50.

[33] Matsushima Y. and Aoki M. Temperature and oxygen isotope variations during formation of the Hishikari epithermal gold-silver veins, southern Kyushu, Japan. Ecol Geol 1994; 89:1608-13.

[34] McArthur J. V. D., Kovacic D. A. and Smith M. H. Genetic diversity in natural populations of a soil bacterium across a landscape gradient. Proc Natl Acad Sci USA 1988; 85:9621-24.

[35] McGenity T. J., Gemmell R. T., Grant W. D. and Stan-Lotter H. Origins of halophilic microorganisms in ancient salt deposits. Environ Microbiol 2000; 2:243-50.

[36] Mikucki J. A., Liu Y., Delwiche M., Colwell F. S. and Boone D. R. Isolation of a methanogen from deep marine sediments that contain methane hydrates, and description of *Methanoculleus submarines* sp. nov. Appl Environ Microbiol 2003; 69:3311-16.

[37] Orphan V. J., Hinrichs K. -U., Ussler III W., Paull C. K., Tayer L. T., Sylva S. P., Hayes, J. M. and DeLong E. F. Comparative analysis of methane-oxidizing archaea and sulfate-reducing bacteria in anoxic marine sediments. Appl Environ Microbiol 2001a; 67:1922-34.

[38] Orphan V. J., House C. H., Hinrichs K. -U., McKeegan K. D. and DeLong E. F. Methane-consuming archaea revealed by directory coupled isotopic and phylogenetic analysis. Science 2001b; 293:484-87.

[39] Parkes R. J., Cragg B. A. and Wellsbury P. Recent studies on bacterial populations and progresses in subseafloor sediments. Hydrogeol J 2000; 8:11-28.

[40] Pedersen K. Microbial life in deep granitic rock. FEMS Microbiol Rev 1997; 20:399-414.

[41] Schlanger S. O. and Jenkyns H. C. Cretaceous oceanic anoxic sediments: Causes and consequences. Geol Mijnbouw 1976; 66:3798-3806.

[42] Shipboard scientific party. Explanatory Notes. In D'Hondt S. L., Jorgensen B. B., Miller D. J., et al., Proc ODP Init Repts, 2003; 201:1-103 [CD-ROM]. Available from: Ocean Drilling Program, Texas A&M University, Colleague Station TX 77845-9547, USA.

[43] Smith D. C., Spivack A. J., Fisk M. R., Haveman S. A. and Staudigel H., ODP Leg 185 Shipboard Scientific Party. Tracer-based estimates of drilling-induced microbial contamination of deep sea crust. Geomicrobiol J 2000; 17:207-19.

[44] Takai K. and Horikoshi K. Genetic diversity of Archaea in deep-sea hydrothermal vent environments. Genetics 1999; 152:1285-97.

[45] Takai K., Komatsu T., Inagaki F. and Horikoshi K. Distribution of Archaea in a black smoker chimney structures. Appl Environ Microbiol 2001a; 67:3618-29.

[46] Takai K., Moser D. P., DeFlaun M., Onstott T. C. and Fredrickson J. K. Archaeal diversity in waters from deep South African gold mines. Appl Environ Microbiol 2001b; 67:5750-60.

[47] Takai K., Moser D. P., Onstott T. C., Spoelstra N., Pfiffner S. M., Dohnalkova A. and Fredrickson J. K. *Alkaliphilus transvaalensis* gen. nov., sp. nov., an extremely alkaliphilic bacterium isolated from a deep South Africa gold mine. Int J Syst vol Microbiol 2001c; 51:1245-56.

[48] Takai K., Hirayama H., Sakihama Y., Inagaki F., Yamato Y. and Horikoshi K. Isolation and metabolic characteristics of previously uncultured members of the orders *Aquificales* in a subsurface gold mine. Appl Environ Microbiol 2002; 68:3046-54.

[49] Takai K., Kobayashi H., Nealson K. H. and Horikoshi K. *Sulfurihydrogenobium subterraneum* gen. nov., sp. nov., from a subsurface hot aquifer. Int J Syst Evol Microbiol 2003; 53:823-27.

[50] Takai K., Oida H., Suzuki Y., Hirayama H., Nakagawa S., Nunoura T., Inagaki F., Nealson K. H. and Horikoshi K. Spatial distribution of marine Crenarchaeota I in the vicinity of deep-sea hydrothermal systems. Appl Environ Microbiol 2004; 70:2404-13.

[51] Wilson P. A. and Norris R. Warm tropical surface and global anoxia during the mid-Cretaceous period. Nature 2001; 412:425-29.

[52] Whitman W. B., Coleman D. C. and Wiebe W. J. Prokaryotes: the unseen majority. Proc Natl Acad Sci USA 1998; 95:6578-83.

SULFUR AND METHANE CYCLING DURING THE HOLOCENE IN ACE LAKE (ANTARCTICA) REVEALED BY LIPID AND DNA STRATIGRAPHY

Marco J. L. Coolen[1], Gerard Muyzer[2,3], Stefan Schouten[2], John K. Volkman[4], Jaap S. Sinninghe Damsté[2]

[1]*Woods Hole Oceanorgaphic Institution, 360 Woods Hole Rd., Woods Hole MA 02543, USA*

[2]*Royal Netherlands Institute for Sea Research, Department of Marine Biogeochemistry, P.O. Box 59, 1790 AB Den Burg, The Netherlands*

[3]*Department of Biotechnology, Delft University of Technology, Julianalaan 67, 2628 BC Delft, The Netherlands*

[4]*Antarctic CRC and CSIRO Marine Research, GPO Box 1538, Hobart, Tasmania 7001, Australia*

Abstract Postglacial Ace Lake (Vestfold Hills, Antarctica) was initially a freshwater lake, then an open marine system, and finally the present-day saline, stratified basin with anoxic, sulfidic, and methane-saturated bottom waters. Stratigraphic analysis of carotenoids and ancient 16S rDNA in sediment cores revealed that almost immediately after marine waters entered the palaeo freshwater lake as a result of post-glacial sea-level rise, Ace Lake became meromictic with the formation of sulfidic bottom waters and a chemocline colonized by obligate anoxygenic photolithotrophic green sulfur bacteria (Chlorobiaceae). Ancient 16S rDNA stratigraphy revealed that the fossil source of chlorobactene throughout the Holocene as well as in the present-day chemocline of Ace Lake was a species with 99.6% sequence similarity to the 16S rDNA sequence of *Chlorobium phaeovibrioides* DSMZ 269^T. Comparison of the ratio between rDNA and chlorobactene of the latter species in the water column and in Holocene sediment layers revealed that the degradation of DNA was mostly influenced by the preservation conditions of the ancient water column. Within the sulfidic Holocene sediments, the remaining ancient DNA of green sulfur bacteria was more stable than intact carotenoids. We showed the development of anoxygenic photosynthesis with our previous stratigraphic analysis of 16S rDNA and lipid biomarkers indicative for prokaryotes involved in the cycling of methane in order to get a more complete picture of anoxygenic processes in Ace Lake during the Holocene.

Keywords: Ace Lake, Ancient DNA, Antarctica, DNA stratigraphy, climate change, DGGE, fossil record, Holocene, green sulfur bacteria, lipid biomarkers, methane cycle

L. N. Neretin (ed.), Past and Present Water Column Anoxia, 41–65.

1. INTRODUCTION

Post-glacial Ace Lake (Fig. 1) is a permanently stratified (meromictic) saline lake with anoxic, sulfidic, sulfate-depleted and methane-saturated bottom waters [38]. The sulfidic chemocline at a depth of 12 m is colonized by obligate anoxygenic photolithotrophic green sulfur bacteria (GSB) of the family Chlorobiaceae [7], which play a major role in the cycling of carbon and sulfur. Therefore, Ace Lake may serve as a model system to study large stratified and anoxic systems such as the Black Sea. Ace Lake was originally a melt-water filled freshwater lake that became saline due to connection to the sea resulting from the Holocene deglaciation and sea-level rise. Isostatic rebound of the Antarctic continent caused the lake to become re-isolated from the ocean [53]. We expected that these climate-induced variations in the chemical and physical characteristics of the water column would have had a great impact on the diversity and abundance of species which thrived in the ancient water column of Ace Lake.

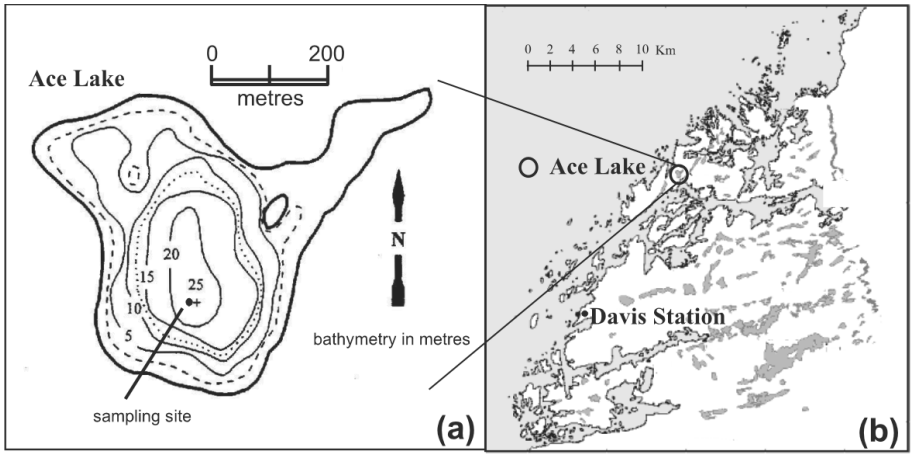

Figure 1. (a) The bathymetry of Ace Lake and location of sampling site (depocentre) and (b) the topographical setting of Ace Lake in the Vestfold Hills, eastern Antarctica (modified after Swadling [51]).

Preserved organic components provide an archive of ancient aquatic microbial communities and, hence, can be used to reconstruct variations in climate and its impacts on biodiversity. However, the interpretation of these data is complicated by the often limited specificity of traditional biomarkers, such as lipids and pigments. The ultimate biomarkers are ribosomal RNA genes (rDNA), the sequences of which can provide information on the species present by phylogenetic comparison. However, in order to identify microorganisms which

colonized the ancient water column, their 16S rDNA must be well preserved in the fossil sediments. During recent years, numerous reports have dealt with the successful retrieval of ancient DNA sequences from remains sequestered within aquatic sedimentary records including human skeletons [24], seagrass [39] and resting eggs of *Daphnia* (e.g. [30, 40]). In addition, remnants of fossil prokaryotes in ancient aquatic sediments were reported and the organisms were identified based on 16S rDNA analysis [10, 26, 27]. Most likely, these organisms were adapted to live within the sedimentary record for a substantial period of time. Other reports have dealt with ancient rDNA within Holocene lake sediments derived from Gram-negative obligate anoxygenic photosynthetic purple sulfur bacteria [13] as well as oxygenic photosynthetic algae [12]. The latter reports showed that ancient DNA derived from microorganisms from the photic zone could also survive in the sediments provided that preservation conditions were optimal. Optimal conditions for the preservation of DNA such as low temperatures and anoxic, sulfidic conditions prevail in the bottom waters and sediments of Ace Lake [12].

During the austral summer of 2000, we collected particulate organic matter (POM) from various positions in the oxygenated water column as well as the underlying anoxic, sulfidic waters. In addition, we obtained a 150-cm-long sediment core from the anoxic depocentre of Ace Lake, spanning the final 10450 calendar years of deposition. The oldest sediment layers were deposited during the freshwater lacustrine period, followed by the fjord period, and then the subsequent isolation of Ace Lake.

Our main objectives were to study the impact of climate-induced changes of the physical and chemical conditions of the ancient water column of Ace Lake on the presence and diversity of species involved in anaerobic processes during the Holocene. In this paper, the key-organisms involved in anoxygenic photosynthesis [green sulfur bacteria (GSB) of the family Chlorobiaceae] were identified based on a combined, high-resolution stratigraphic analysis of traditional lipid biomarkers (carotenoids) as well as 16S rDNA as a novel palaeoproxy. Since GSB of the family Chlorobiaceae are obligate anoxygenic photolithotrophic bacteria [36] they are restricted to the chemocline where both light and sulfide are present. The brown-coloured species such as *Chlorobium phaeovibrioides* and *Chlorobium phaeobacteroides* often have green coloured counterparts such as *C. limicola* and *C. vibrioforme* that, apart from pigment and carotenoid composition, are very similar in morphology and physiology [52] and can be closely phylogenetically related (i.e. similarity values > 90%) [35]. Chlorobactene is the predominant carotenoid in the green-coloured species, whereas brown-coloured Chlorobiaceae often contain small amounts of chlorobactene in addition to isorenieratene and β-isorenieratene [52].

Below the chemocline, light for photosynthesis is absent [6] and cells of Chlorobiaceae below the chemocline were assumed to be decaying. The ratio

between rDNA and chlorobactene of Chlorobiaceae measured in the photic chemocline, the dark stagnant bottom waters (monimolimnion), and the dark Holocene sediments, was therefore used to study the fate of ancient DNA in the sulfidic aquatic and sedimentary environment.

The cycling of methane during the Holocene in Ace Lake as well as the prokaryotes involved in methanogenesis and methanotrophy was reconstructed based on the combined stratigraphic analysis of lipids and 16S rDNA [11]. In this study we combined the latter lipid data with the data for carotenoids and 16S rDNA of GSB in order to get a more complete picture of the development of Holocene anaerobic processes as well as physical characteristics of the water column of Ace Lake.

2. EXPERIMENTAL

2.1 Setting

Ace Lake in the Vestfold Hills of eastern Antarctica (68°24'S, 78°11'E) is a shallow saline meromictic lake with a maximum depth of 25 m, and usually covered by ice for about 11 months of the year (Fig. 1). Salinity ranges from 6‰ at the surface to 43‰ in its bottom waters [8]. The water below 11.7 m of present-day Ace Lake is anoxic, and contains high sulfide concentrations (up to 8 mM towards the sediment; [18]), as a result of slow bacterial sulfate reduction. At present, the water below 20 m of Ace Lake is depleted in sulfate [9] (Fig. 2) and sulfate reduction rates are below the detection limit [19]. Methane occurs in the monimolimnion at depths greater than 11m, reaching its highest concentration (up to 5mM) at the bottom of the lake [18] (Fig. 2). Rates of methanogenesis in the water column of Ace Lake are slow reaching a maximum of 2.5 μmol $kg^{-1}day^{-1}$ at 20 m where sulfate is depleted [18].

During its post-glacial development, Ace Lake went through several climate-induced stages as deduced from stratigraphic analysis of diatom assemblages [15, 42], faunal microfossils [14, 51], as well as lipids and DNA of marine haptophytes [12]. The oldest sediment layers recovered were deposited when Ace Lake was a freshwater lacustrine basin filled with melt water (Unit III; 150-135 cm, 10450-9400 calendar years before the present). Deglaciation caused a world wide sea-level rise [53] and the introduction of surrounding seawater into the freshwater basin. Subsequently, the isostatic rebound of the Antarctic continent re-isolated Ace Lake from the ocean [2, 37, 53].

2.2 Sampling

Water samples were obtained in November 2000 using a Niskin bottle with a length of 50 cm and a volume of 5 L from various positions in the water column of Ace Lake. The sampling positions (measured from the ice sur-

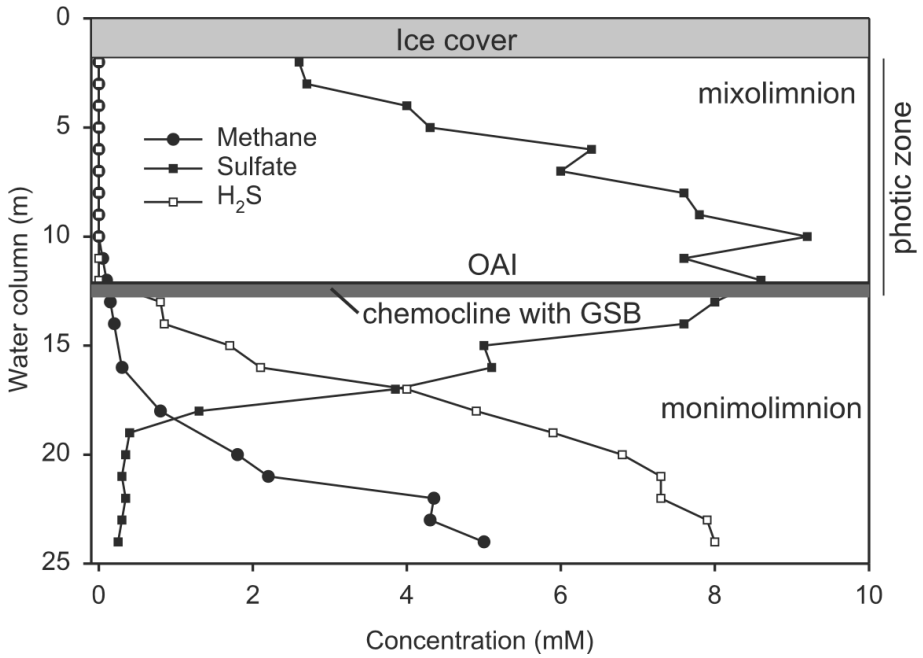

Figure 2. Vertical distribution of sulfate, hydrogen sulfide, and methane in Ace Lake (December 1987) (data from [18]). The position of the oxic/anoxic interface (OAI) was found to be at 11.7 m during our field work in November 2000 whereas the OAI was at 12.0 m in December 1987.

face) in the water column were: oxic mixolimnion (1.7–2.2 m; 6.7–7.2 m; 10.2–10.7 m), anoxic and sulfidic chemocline with dense accumulation of anoxygenic photosynthetic GSB (11.7–12.2 m), anoxic and sulfidic monimolimnion (14.7–15.2 m; 18.2–18.7 m; 21.5–22.0 m). In order to collect particulate organic matter (POM) from the water samples, a volume of 0.25–15 L, depending on particle densities, was filtered through 0.7 μm pore-size glass fibre filters (GFF) (Millipore). The particle density was highest in the chemocline and in the monimolimnion. The filtrate was then filtered through 0.2 μm pore-size polycarbonate (PC) filters (Millipore) in order to collect small prokaryotic cells that were not collected during the first filtration step. The filters were stored at –40°C prior to DNA or lipid extraction. The extracts from both the GFF and PC filters of each water depth were pooled.

Using a gravity corer, a 150-cm-long sediment core with a diameter of 5 cm was obtained from the depocentre (25 m; 68.47209°S, 78.18732°E) of Ace Lake. Immediately after sampling, the sediment core was kept in the dark and stored in the dark at –20°C at Davis Station and in the dark at –40°C at the Royal NIOZ. At the Royal NIOZ, the frozen sediment core was sliced in 2 cm

horizontal fragments and 41 out of 74 slices with 2 cm space intervals were used for lipid and 16S rDNA analysis.

2.3 Calibration of Sediment Ages

Accelerator mass spectrometry (AMS) radiocarbon (^{14}C) dating of selected bulk sediment from the sediment core (sections 1–3 cm, 17–19 cm, 33–35 cm, 63–65 cm, 89–91 cm, 117–119 cm, 133–135 cm, and 147–149 cm) was carried out at the R.J. Van der Graaff laboratory, University of Utrecht, The Netherlands. Standard techniques of calibration [49] were used to express the sediment ages in calendar years before the present (BP), assuming reservoir ages of 115 years (Unit I; closed saline lacustrine lake system), and 500 years for Unit II (marine inlet period) [11], and 0 years for the freshwater lacustrine period (Unit III) [53].

2.4 Carotenoid Analysis

Freeze-dried and ground sediment samples of 0.1 to 0.7 g were ultrasonically extracted with acetone (3×, 3 min). Samples were centrifuged at 3000 rpm for 5 min. The supernatants were decanted, combined and concentrated using rotary vacuum evaporation. The extracts were subsequently dried under a gentle flow of nitrogen. The residue was redissolved in dichloromethane and applied to a silica column and the apolar carotenoids eluted with dichloromethane, dried under nitrogen and the residue dissolved in acetone. Care was taken during the entire sample preparation procedure to avoid exposure of the samples to light and heat. This carotenoid fraction was then immediately analyzed on a HP 1100 series HPLC equipped with an auto-injector and photodiode array detector. Separation was achieved on a ZORBAX Eclipse XDB-C_{18} column (2.1 × 150 mm, 3.5 μm; Agilent Technologies, USA), maintained at 25°C, with a linear gradient from 65% solvent B to 80% solvent B in 45 min, with solvent A being methanol/water (4:1, v/v) and solvent B acetone/methanol/water (19:1:1, v/v/v). The flow rate was 0.3 ml/min. Detection was achieved by in-line UV-detection (250–700 nm). Chlorobactene and isorenieratene were quantified by comparing their UV responses at 462 nm (λ_{max} of chlorobactene in the mobile phase) and 454 nm (the λ_{max} of isorenieratene in the mobile phase) of known amounts of an authentic β-carotene standard (Aldrich) and correcting for the difference in extinction coefficients [5].

In order to examine whether chlorobactene was accompanied by its diagenetic products (e.g. partly hydrogenated chlorobactane), ca. 3 g of two sediment sections (37–39 cm and 85–87 cm) were ultrasonically extracted using mixtures of dichloromethane and methanol. An aliquot of the total lipid extract, with an internal standard (6,6-d_2-2-methylheneicosane) was hydrogenated for 1 h with PtO_2 and a few drops of acetic acid. The resulting fraction was chro-

matographed over a column packed with Al_2O_3 to obtain an apolar fraction using hexane/dichloromethane (9:1, v/v) as an eluent and analyzed by gas chromatography (GC) and GC-mass spectrometry (GC-MS) as described elsewhere [11].

2.5 Total Organic Carbon (TOC)

The total organic carbon content was determined by elemental analysis (EA) isotope ratio monitoring mass spectrometry (EA/irmMS) as described by Coolen [11].

2.6 Extraction of Total DNA

Total DNA was extracted from 0.25 g of sediment using the UltraClean Soil DNA Kit following the descriptions of the manufacturer (Mobio, Carlsbad, CA, USA). Because our study relied on the analysis of 16S rDNA by PCR amplification, it was of utmost importance to prevent any contamination of the sediment samples by foreign DNA. Extensive precautions against contamination of the samples were applied as described previously [10, 13]. As a control for contamination during DNA extraction, a parallel sample without sediment was subjected to the whole extraction and purification procedure (extraction control). All DNA extracts were tested for the presence of co-extracted impurities resulting in polymerase chain reaction (PCR) inhibition [11, 12].

The same extraction method was applied to the POM collected on the filters. Prior to extraction, the filters were sliced with a sterile scalpel. The total DNA-extract for each sediment sample and POM sample was quantified with the fluorescent dye PicoGreen (MoBiTec, Göttingen, Germany).

2.7 Amplification of 16S rDNA

Partial 16S rDNA of GSB within the POM and Holocene sediment layers of Ace Lake were amplified by PCR in a Geneamp PCR System 2400 (Perkin Elmer, Connecticut, USA). 16S rDNA solely found in GSB were selectively amplified using primer 341f (5'-cct acg gga ggc agc ag-3' [33]) in combination with gsb840r (5'-atg acc aac atc tag tat t-3' [34]). A 40-bp-long GC-clamp (5'-cgc ccg ccg cgc ccc gcg ccc ggc ccg ccg ccc ccg ccc c-3' [33]) was attached to the 5'-end of primer 341f to prevent complete melting of the PCR products during denaturing gradient gel electrophoresis (DGGE). The reaction mixtures were prepared according to Coolen [12]. The PCR conditions were: Initial denaturing at 96°C (4 min) followed by 35 cycles including denaturing at 94°C (30 sec), primer annealing at 57°C (40 sec), and primer extension at 72°C. A final extension step was performed at 72°C (10 min). Each PCR amplification series included one reaction without DNA template, which served as a control for contaminations during the pipetting of the reaction mixture components. A

second reaction with 1 μl of the extraction control was amplified by PCR as a control for contamination during the extraction of DNA from the sediment samples. A third reaction containing 15 ng of DNA of *Flavobacterium* sp. was used to monitor the specificity of the PCR reactions.

2.8 Denaturing Gradient Gel Electrophoresis (DGGE)

All PCR-products were separated by DGGE [33]. DGGE was carried out in a Bio-Rad D Code system (Bio-Rad). All PCR products were separated based on their variations in the nucleotide positions on 6% (wt/vol) polyacryl amide gels which contained a 20−70% linear gradient of denaturant. Electrophoresis proceeded for 5 h at 200 V and 60°C in 1× TAE pH 8.3. After ethidium bromide staining, DGGE-bands were cut out with a sterile scalpel and rinsed with ultra pure water (Sigma, USA). The DNA of each band was eluted [11, 12]. One μl of the eluted 16S rDNAs were re-amplified, using the primers for GSB, in order to generate template DNA for the subsequent cycle sequencing reactions.

2.9 Sequencing of DGGE Bands

Primers and dNTPs were removed from the re-amplified DGGE bands using the QIAquick PCR Purification Spin Kit (Qiagen) and 10 ng of DNA was subjected to cycle sequencing reactions using the conditions as described by Coolen [11, 12].

2.10 Phylogenetic Analysis

Sequence data were compiled using ARB software [31] and aligned with complete length sequences of closest relatives obtained from the databases of the ribosomal database project II (RDP-II, [32]) and GenBank [1] using the ARB FastAligner utility. Matrices of similarity, distance and phylogenetically corrected distance values were generated using the maximum parsimony option in ARB. Sequences obtained in this study have been deposited in the GenBank sequence database under accession numbers AY303358 and AY665401.

2.11 Real Time Quantitative PCR

Real time quantitative PCR was performed in an iCycler system (Biorad, Hercules, CA, USA) in order to quantify the amount of DNA derived from green sulfur bacteria in the POM samples of the extant water column as well as the 42 Holocene sediment layers of Ace Lake. The method was slightly modified after Coolen et al. (2004b). To quantify DNA of GSB, the PCR conditions and primers (without GC-clamp) were used as described above. Accumulation of newly amplified rDNA was followed online (80°C for 25 sec) as the increase

in fluorescence due to the binding of the fluorescent dye SYBR Green. Reaction mixtures (25 μl) contained 12.5 μl of iQ^{TM} SYBR Green Supermix (Biorad), 10 μg of BSA, 0.5 μM of primers, and ultra pure sterile water (Sigma). 15 ng of template DNA from each sample was added to each real time PCR reaction. Duplicate reactions of samples were run. For the calibration of samples, different amounts of genomic DNA of the GSB *Chlorobium phaeovibrioides* DSMZ 269^T (ranging between 0.1 and 1590 picogram) was subjected to real time PCR. Control reactions included: one reaction without template DNA as a control for contamination during pipetting, one control for contamination during the DNA extraction procedure, and three control reactions were performed with 15 ng of DNA from *Escherichia coli*, *Flavobacterium* sp., and *Mycobacterium interjectum* to monitor the specificity of the reactions. After the total amount of DNA of GSB per sample was determined by quantitative PCR, the amount of DNA from the phylotypes AL-GSB 1 and 2 was integrated from the intensities of the DGGE bands.

3. RESULTS

Carotenoids. The carotenoids chlorobactene, isorenieratene and β-isorenieratene of the obligate anoxygenic photolithotrophic GSB (members of the family Chlorobiaceae) were first detected just beneath the oxic-anoxic interface (OAI) located at a depth of 11.7 m in the water column of Ace Lake (Fig. 3a). Chlorobactene (structure I; Fig. 4) was the most predominant carotenoid of GSB with a concentration of up to 4.3 mg.L^{-1} in the euxinic chemocline. In water layers below the photic zone its concentration was a factor of two lower. Isorenieratene and β-isorenieratene (structures II, III; Fig. 4) concentrations were much lower throughout the anoxic water column with maximum concentrations of 0.3 mg.L^{-1} in the chemocline (Fig. 3a).

Within the Holocene sediment record of Ace Lake, carotenoids of GSB were absent in the ancient freshwater sediments of Unit III (Fig. 5d). Chlorobactene, isorenieratene and β-isorenieratene were first detected from the sediments which were deposited after seawater entered the lake (9400 years BP, Unit II). Chlorobactene concentrations were between 3 and 17 times higher than isorenieratene plus β-isorenieratene concentrations within the sediment layers of units I and II (Fig. 5d). The average concentration of chlorobactene in the older layers of Unit II (between 130 and 78 cm) was 6 mg.g^{-1} TOC. The chlorobactene concentration increased significantly in sediment layers shallower than 79 cm reaching a maximum concentration of 258 mg.g^{-1} TOC between 37 and 39 cm, but declined again at shallower depths (Unit I; saline, lacustrine, sulfate-depleted). These carotenoids were almost absent between 17 and 19 cm (Fig. 5d) with a chlorobactene content of only 0.2 mg.g^{-1} TOC.

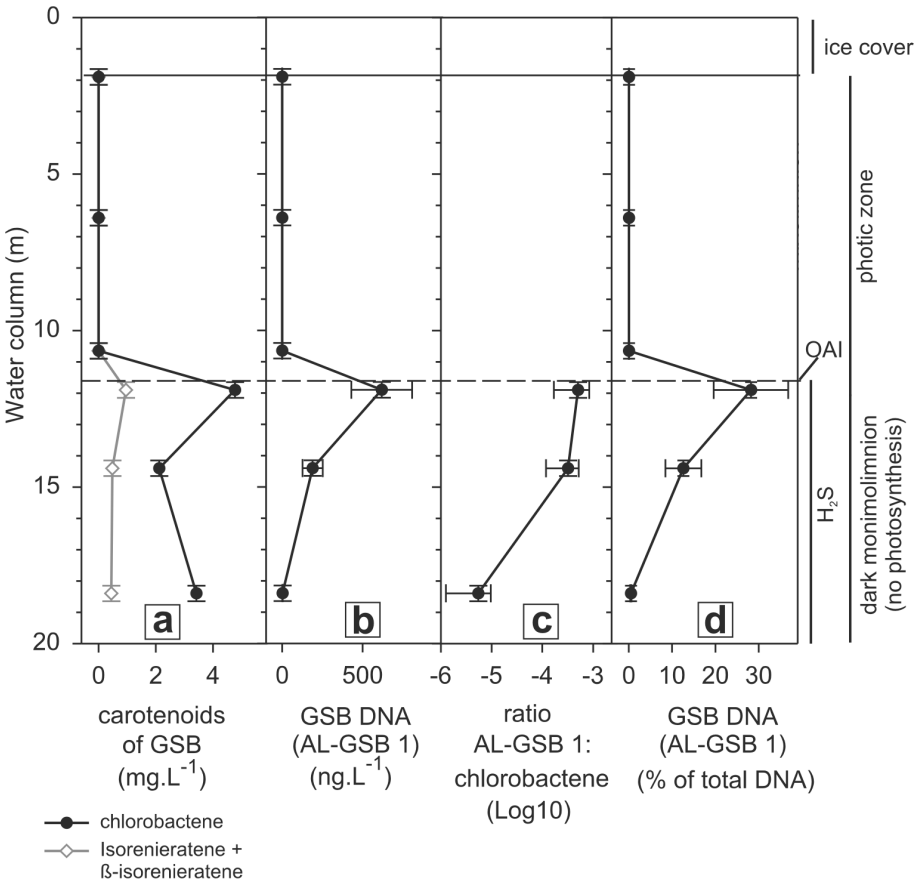

Figure 3. Depth profiles of biomarkers (carotenoids and 16S rDNA) of anoxygenic photolithotrophic green sulfur bacteria recovered from filtered particulate organic matter from the water column of Ace Lake. A dense population of green sulfur bacteria comprised of a species with 99.7% sequence similarity to *Chlorobium phaeovibrioides* (phylotype AL-GSB 1) is located just below the anoxic-oxic interface (OAI) where light and sulfide are available for anoxygenic photosynthesis. Below the bacterial plate, light for photosynthesis is absent [6].
(a) Concentration of chlorobactene and isorenieratene (mg.L^{-1}), (b) 16S rDNA of the predominant GSB [AL-GSB 1, (ng.L^{-1})]. This was the only GSB phylotype detected from the water column and the most likely source of the predominant carotenoid chlorobactene. (c) Ratio (Log_{10}) between phylotype AL-GSB 1 (ng.L^{-1}) to chlorobactene (mg.L^{-1}). (d) abundance of phylotype Al-GSB 1 as % of total DNA.

Diagenetic products of chlorobactene such as its hydrogenated form, chlorobactane, would be missed by UV detection during HPLC analysis. To allow the identification of chlorobactane, apolar fractions of total lipids were extracted from sediment layer 37–39 cm and 85–87 cm, hydrogenated, and analyzed by GC-MS. The amount of chlorobactene and chlorobactane in both sediment

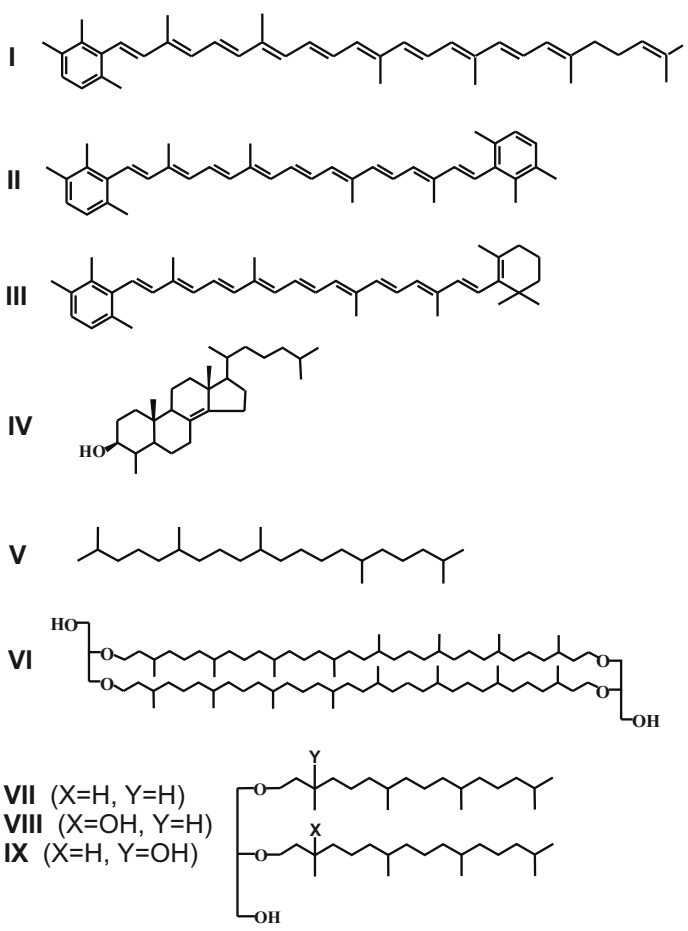

Figure 4. Structures of biomarkers analyzed from the Holocene sediment core. I: Chlorobactene [from green coloured species of Chlorobiaceae], II: Isorenieratene, III: β-isorenieratene [from brown-coloured species of Chlorobiaceae], IV: 4α-methyl-5α-cholest-8(14)-en-3β-ol [from aerobic methanotrophic bacteria of the family Methylococcaceae], V: 2,6,10,15,19-pentamethylicosane (PMI) [from methanogenic Archaea], VI: GDGT-0 [from (methanogenic) Archaea], VII: Archaeol (X=H, Y=H) [from (methanogenic) Archaea], VIII: *sn*2-hydroxyarchaeol (X=OH, Y=H), IX: *sn*3-hydroxyarchaeol (X=H, Y=OH) [from methanogens; Methanosarcinales, Methanococcales].

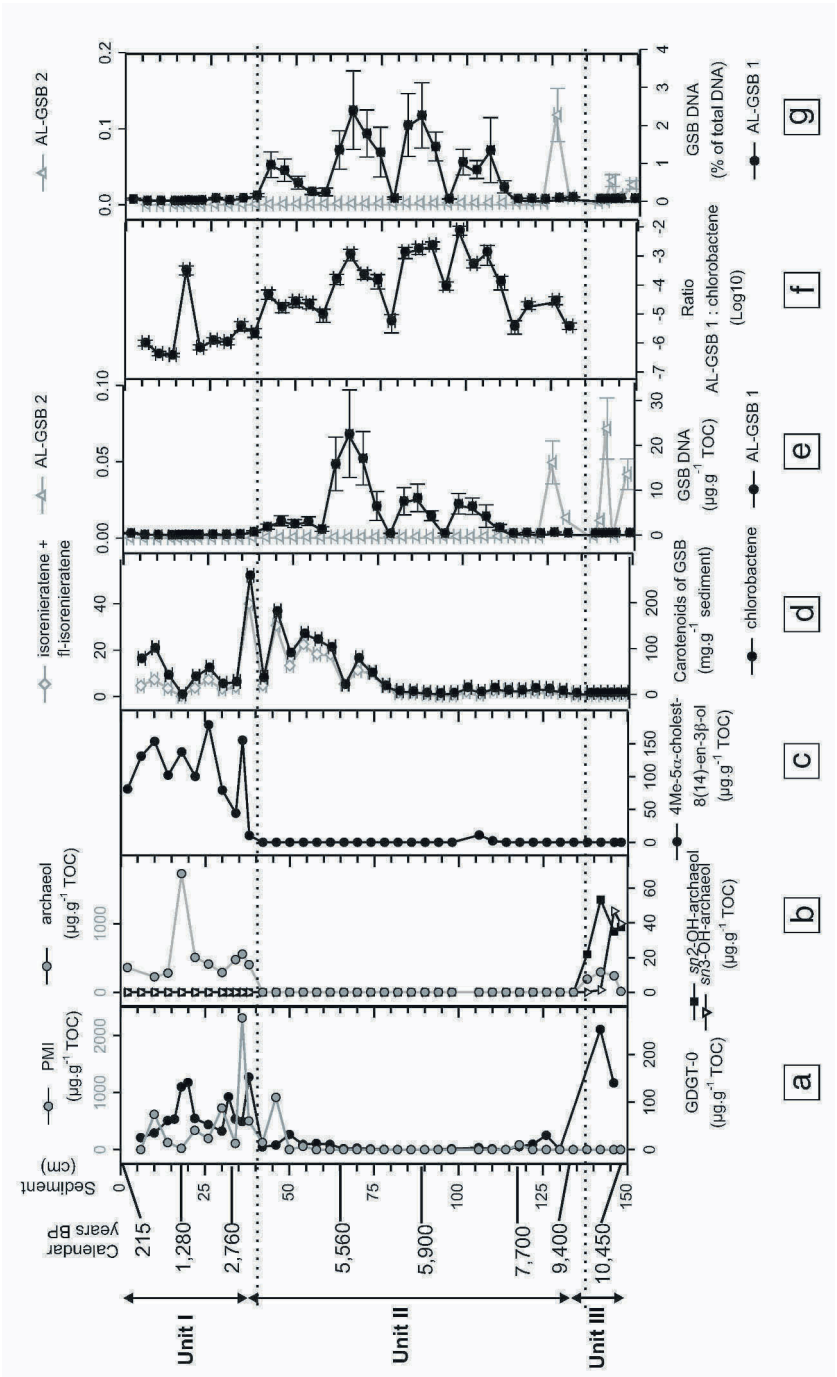

Figure 5. Lipid biomarkers indicative of a closed methane cycle (data from [111]) and carotenoids and 16S rDNA of green sulfur bacteria indicative of the fate of ancient DNA and stratification and anoxygenic photosynthesis during the Holocene history of Ace Lake.

Figure 5 (continued)
(a) glycerol dibiphytanyl glycerol tetraether (GDGT)-0 membrane lipid ubiquitous for Archaea, and 2,6,10,15,19-pentamethylicosane (PMI) of methanogenic Archaea ($\mu g.g^{-1}$ TOC). (b) Diether membrane lipids ($\mu g.g^{-1}$ TOC) ubiquitous in Archaea (i.e. archaeol), plus markers for methanogens of the orders Methanosarcinales and Methanococcales (i.e. *sn*-2-hydroxyarchaeol and *sn*-3-hydroxyarchaeol). (c) 4α-methyl-5α-cholest-8(14)-en-3β-ol ($\mu g.g^{-1}$ TOC) derived from group I aerobic methane oxidizing bacteria (Methylococcaceae). (d) Chlorobactene ($mg.g^{-1}$ TOC) indicative of fossil obligate photolithotrophic green sulfur bacteria derived from the ancient euxinic chemocline. (e) DNA of the two recovered phylotypes of GSB ($\mu g.g^{-1}$ TOC). (f) Ratio (Log_{10}) of phylotype AL-GSB 1 ($\mu g.g^{-1}$ TOC) to chlorobactene ($mg.g^{-1}$ TOC). Note that the partial 16S rDNA sequences of the fossil phylotype AL-GSB 1 and the phylotype AL-GSB 1 recovered from the extant chemocline of Ace Lake are identical. (g) Abundance of phylotypes AL-GSB 1 and 2 as % of total DNA. Dashed horizontal lines indicate sediments layers deposited at times when Ace Lake was a freshwater lacustrine basin (Unit III), a stratified, sulfidic fjord including an unknown substantial period in which Ace Lake became isolated from the ocean (Unit II), and the present day saline, sulfidic, methane saturated, stratified lacustrine basin with sulfate-depleted bottom waters (Unit I). Calendar years (BP) of selected sediment layers are denoted left of Fig. 5a.

layers as well as the ratio of chlorobactene or chlorobactane between both sediment layers are listed in Table 1.

Table 1. Concentration of intact chlorobactene and its hydrogenated form, chlorobactane, in two selected sediment layers.

Sediment (cm)	Chlorobactene ($mg.g^{-1}$ TOC)	Chlorobactane ($mg.g^{-1}$ TOC)
37-39	258	40
85-87	5	10
ratio	52	4

Extant and Ancient 16S rDNA of GSB. PCR amplified partial 16S rDNA of GSB recovered from the extant water column and the Holocene sediments were separated based on variations in the nucleotide positions on DGGE (Fig. 6). Sequences of GSB were not recovered from the oxygenated mixolimnion or the deepest analyzed water layer (21.5−22 m). Separation of the GSB amplicons of the chemocline and the water layers below the anoxyphotic zone (14.2−18.7 m) resulted in one DGGE band with identical melting position to the position marker (PM, Fig. 6). The PM represented 16S rDNA of GSB amplified from a sediment sample (5−7 cm) of Ace Lake. The same DGGE band was found in all analyzed sediment layers except for the sediments of freshwater Unit III (Fig. 6). The amplification of 16S rDNA of GSB resulted in a unique

DGGE band for the sediment layers of Unit III, but the band was no longer detected in sediment layers which were deposited shortly after marine waters first entered Ace Lake (Unit II, Fig. 6). Sequence analysis of the two unique DGGE bands revealed that sequence 1 (phylotype AL-GSB 1) recovered from the extant anoxic water column as well as from Unit I and II sediments was related to anoxygenic photolithotrophic species of the family Chlorobiaceae with *Chlorobium phaeovibrioides* DSMZ 269^T as the closest relative (99.6% sequence similarity, Fig. 7). Sequence 2 (phylotype AL-GSB 2) was affiliated with uncultivated, unclassified green sulfur bacteria which form a cluster separated from the anoxygenic photosynthetic members of the Chlorobiaceae (Fig. 7).

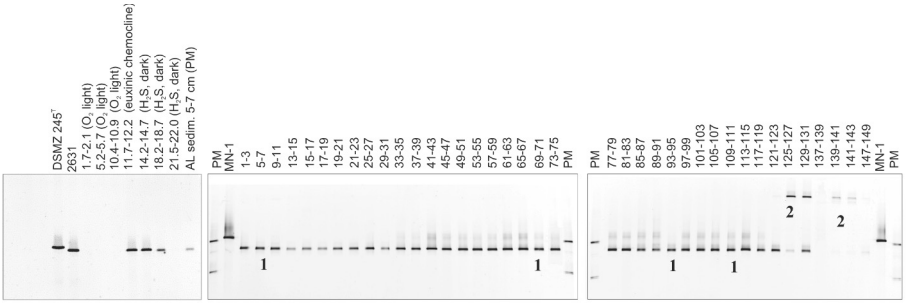

Figure 6. DGGE analysis of PCR-amplified partial 16S rDNA of green sulfur bacteria obtained from the water column as well as the Holocene sediments of Ace Lake. No amplicons were recovered from the oxygenated mixolimnion or the deepest analyzed water column sample. DGGE bands that were sliced from the gel and subsequently sequenced are indicated with numbers.

The amount of rDNA of GSB was quantified by means of real time PCR. No rDNA of GSB was detected within the oxygenated mixolimnion. The highest concentration of GSB DNA was found in the chemocline of the lake (600 ng.L^{-1} filtered water) and its concentration declined sharply in the deeper and dark monimolimnion (Fig. 3b). The ratio between rDNA and chlorobactene of GSB was 2 orders of magnitude lower at 18 m depth compared to the euxinic chemocline (Fig. 3c). GSB rDNA comprised up to 30% of the total rDNA content within the chemocline, but only 0.1% at a depth of 18 m (Fig. 3d).

Within the Holocene sediment core, rDNA concentrations of AL-GSB 1 were up to 3 μg per gram of total organic carbon (TOC) within the upper 50 cm, but increased significantly up to 23 μg.g^{-1} TOC in older Unit II deposits (Fig. 5e). The phylotype Al-GSB 1 was not detected from the Unit III sediment layers. Instead, up to 0.08 μg.g^{-1} TOC of rDNA of AL-GSB 2 was detected from Unit III sediments and this phylotype was below the detection limit from sediment layers above 121 cm (Fig. 5e). The ratio between DNA and chlorobactene

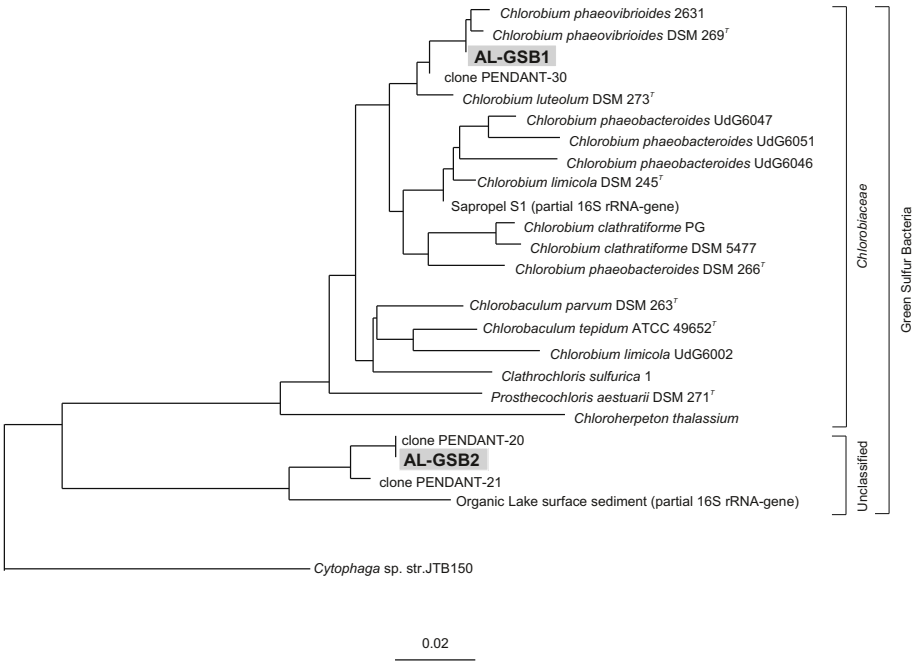

Figure 7. Phylogenetic tree showing the relationship of 16S rDNA sequences of green sulfur bacteria retrieved from particulate organic matter (POM) of the water column and Holocene sediment layers of Ace Lake (bold text) to reference sequences obtained from the GenBank and RDP-II databases. The GSB sequences from Ace Lake were determined from the DGGE represented in Fig. 6. DGGE-bands with identical melting positions within the gel appeared to contain identical sequences. As a result, phylotype AL-GSB 1 was recovered from the extant water column and Holocene sediment layers of Unit I and II, whereas phylotype AL-GSB 2 was unique to Unit III.

of AL-GSB 1 in the top layers of sediment (Fig. 5f) was comparable to this ratio observed in the deepest analyzed water layer (Fig. 3d). This ratio was 2 to 3 orders of magnitude higher in the deeper Unit II sediments and varied significantly between alternating layers (Fig. 5f). The percentage of DNA of AL-GSB 1 was only around 0.1% within the top 39 cm of sediment (Unit I) and reached up to 2.5% of the total rDNA pool in sediment layers of Unit II (Fig. 5g). The amount of DNA of AL-GSB 2 comprised only 0.02% of the total DNA pool (Fig. 5g).

4. DISCUSSION

4.1 Fate of Ancient DNA and Carotenoids of Chlorobiaceae

All known species of the Chlorobiaceae are obligate anoxygenic photolitho-

trophic bacteria [36] and their ecological niche is therefore restricted to just below the oxic-anoxic interface where both light and sulfide are present. Since no light penetrates the bacterial plate in the chemocline of Ace Lake [6], their biomarkers (carotenoids and 16S rDNA) in the sedimentary record are therefore expected to be of fossil origin and serve as indicators for past anoxic conditions.

The phylogenetic affiliation of phylotype AL-GSB1 to a brown species (*Chlorobium phaeovibrioides*) (Fig. 7) would seem to imply that it was the fossil source of isorenieratene and β-isorenieratene and not the source of chlorobactene. However, the comparable concentration profiles of the predominant carotenoid chlorobactene with isorenieratene plus β-isorenieratene in both the water column and in the sediment (Figs. 3a and 5d) implies the same GSB-source for the three carotenoids. Within the upper 25 cm of Ace Lake sediments, these carotenoids were found to be 10–15‰ enriched in ^{13}C compared to phytoplankton biomarkers, indicating that GSB are their biological source [46]. Although we identified only AL-GSB 1 using the sensitive and selective PCR approach, two green-coloured species of Chlorobiaceae, *C. vibrioforme* and *C. limicola* (for which no 16S rDNA sequences are available) were enriched from the chemocline of Ace Lake in 1988 [7]. In order to see whether additional GSB-phylotypes were present in the extant chemocline and Holocene sediments, we identified the predominant bacterial 16S rDNA by PCR/DGGE using non-selective primers for the domain Bacteria (data not shown). Also using this non-selective PCR/DGGE approach, only one phylotype with *C. phaeovibrioides* DSMZ 269T as its closest relative was detected from the water column and the Holocene sediment layers. This indicated that if additional phylotypes of GSB would have been present, they comprised less than 1% of the total bacterial community [33]. Therefore, AL-GSB 1 was the predominant *Chlorobium* phylotype during the history of Ace Lake and the most likely source of the predominant carotenoid chlorobactene as well as the less abundant carotenoids isorenieratene and β-isorenieratene.

The highest concentration of DNA of GSB (600 $ng.L^{-1}$ filtered water) was measured at the chemocline (Fig. 3b), as were the highest concentration of chlorobactene. Whereas chlorobactene concentrations varied only by a factor of two with increasing water depth (Fig. 3a), the concentration of GSB DNA declined significantly with depth. As a result, the ratio between DNA and the carotenoid chlorobactene within the cells of GSB at a depth of 18 m, where light for anoxygenic photosynthesis was absent, was 2 orders of magnitude lower compared to the cells thriving within the photic, sulfidic chemocline (Fig. 3c). This showed that a substantial part of the DNA was degraded in dead cells settling towards the sediment. The DNA:chlorobactene ratio measured from the deeper part of the water column (10^{-5}) did not further decline in the Holocene sediments (Fig. 5f). This indicated that the DNA which became buried within

the sedimentary record was very well protected from further degradation. This is in agreement with the results of fossil remains of anoxygenic photosynthetic purple sulfur bacteria in Holocene sulfidic sediments of the meromictic Canadian Mahoney Lake [13]. Within these sediments, the ratio between rDNA and the carotenoid okenone of the predominant purple sulfur bacterium, *Amoebobacter purpureus*, was 6 orders of magnitude lower compared to the ratio in intact cells of *Amoebobacter*. This ratio also did not further decline in deeper and older sediment layers [13]. Since we used a 0.5-m-long Niskin bottle to collect water from the chemocline, the collected POM contained a mixture of *Chlorobium* cells which were exposed to optimal and sub-optimal light conditions. It can, therefore, be expected that the DNA to chlorobactene ratio in a pure *Chlorobium* culture under excellent light conditions would be higher compared to this ratio measured at the chemocline.

Interestingly, the ratio DNA:chlorobactene was 2 to 3 orders of magnitude higher in the deeper sediment layers of the core (59-105cm) (Fig. 5f), perhaps suggesting that at certain times of the lake history the DNA of the *Chlorobium* was relatively better preserved than in the present day situation. However, it is difficult to envisage how the preservation conditions of present-day Ace Lake can be substantially improved since the waters below the chemocline are anoxic, sulfide-rich, cold and characterized by the absence of light. Alternatively, the increase in the DNA:chlorobactene ratio may be caused by carotenoid diagenesis. In reducing organic carbon-rich sediments, intact chlorobactene is known to be prone to diagenetic processes such as (partial) hydrogenation to chlorobactane as well as the incorporation via sulfurization into macromolecular organic matter ([47] and references therein). Schaeffer et al. [43] have shown that these processes already occur in the upper sediments of the meromictic Lake Cadagno. The relatively high abundance of DNA of GSB between 59 and 105 cm (Figs. 5f and 5g) may thus indicate that diagenetic products of chlorobactene were formed which would not have been detected via UV detection during HPLC analysis. Analysis for (partially) hydrogenated counterparts of chlorobactene indicated indeed a much higher relative contribution of such diagenetic products in the sediment section at 85-87 cm (high GSB-DNA:chlorobactene ratio) than in the section at 37-39 cm (low GSB-DNA:chlorobactene ratio) (Table 1). This revealed that a substantial part of the chlorobactene had become partially hydrogenated in the deeper sediments resulting in substantially increased GSB-DNA:chlorobactene ratios. These results showed that the degradation of DNA compared to chlorobactene is substantially higher in the water column but that within the sediments chlorobactene concentrations were affected by diagenesis whereas the GSB DNA remained unaltered. In good agreement with these findings is that in the same sediment core, the quantitative comparison of alkenones and 18S rDNA of their biological sources (haptophytes of the order Isochrysidales) showed a good correlation

and resulted in the identification of fossil biological sources of alkenones at the species-level [12]. Alkenones are not as sensitive for diagenetic alteration as carotenoids. Due to the diagenesis of chlorobactene, the stratigraphic profiles of chlorobactene or DNA of AL-GSB 1 were not significantly correlated (Figs. 5d, 5e). The correlation would most likely improve if all diagenetic products of chlorobactene could also be identified and quantified. Next to hydrogenated forms, also sulfurized diagenetic products of chlorobactene are likely to occur in the sediments of Ace Lake.

4.2 Anoxygenic Photosynthesis in Ace Lake During the Holocene

The coinciding presence of carotenoids and 16S rDNA of a *Chlorobium* species in 9400-year-old and shallower sediments showed that Ace Lake became stratified and sulfidic within ca. 100 years after marine waters first entered Ace Lake. Moreover, an active cycling of sulfur between anaerobic sulfate reducing bacteria and sulfide oxidizing GSB must have occurred during most of the lake's history.

During deposition of Unit III when Ace Lake was a freshwater-filled melt water lake, conditions for anoxygenic photolithotrophic growth such as an anoxic, sulfidic chemocline were most likely absent. Carotenoids as well as 16S rDNA specific for Chlorobiaceae were indeed below the detection limit in Unit III sediments. Phylotype AL-GSB 2 (Figs. 6, 7) which was detected from Unit III by means of the GSB-specific PCR approach, was not affiliated with anoxygenic photosynthetic Chlorobiaceae but to a cluster of 'unclassified GSB'. Sequences related to AL-GSB 2 were, for example, recovered from nearby meromictic, sulfidic Pendant Lake [4] as well as the hypersaline Organic Lake (Coolen, unpublished data) with anoxic, but non-sulfidic bottom waters [16, 22]. The affiliation of AL-GSB 2 with the sequence of the non-sulfidic hypersaline Organic Lake points towards a physiology different from anoxygenic photosynthesis.

4.3 Evolution of the Holocene Methane Cycle in Relation to the Cycling of Sulfur

To date, two methanogenic Archaea have been isolated from the extant monimolimnion of Ace Lake [17, 20] and low rates of methanogenesis using radiolabelled bicarbonate were measured below a water depth of 20 m [18]. *Methanococcoides burtonii* is a methylotrophic methanogen with an optimum growth temperature of 23°C [20]. Since this organism catabolizes non-competitive substrates, its presence should not be restricted to sulfate-depleted regions within the anoxic monimolimnion. However, methanogenesis does not occur in other non-sulfate-depleted, anoxic lake monimolimnia,

which have been examined throughout the Vestfold Hills [18]. Therefore, this type of methanogenesis is likely to be of minor importance in Ace Lake. *Methanogenium frigidum*, on the other hand, is a true psychrotroph growing on H_2 plus CO_2 or formate and has been isolated from the sulfate-depleted part of the monimolimnion of Ace Lake [17] where CO_2 is the next favorable electron acceptor remaining for the oxidation of organic matter [23]. At least a part of the released methane is consumed aerobically since strains of the group I aerobic methanotrophic bacteria of the family Methylococcaceae (γ-Proteobacteria) were isolated from the micro-aerophilic part of the water column of Ace Lake, and their carbon-substrate range was found to be limited to methane and methanol [3]. The type strain *Methylosphaera hansonii* ACAM 549 [3] was found to biosynthesize relatively large amounts of the specific sterol 4α-methyl-5α-cholest-8(14)-en-3β-ol (Fig. 5c; structure IV in Fig. 4) [44]. Its structure and $\delta^{13}C$ value of ca. –57‰ [44] is diagnostic for methanotrophy [50].

In previous work, we described the cycling of methane during the Holocene in Ace Lake, as well as the prokaryotes involved in methanogenesis and methanotrophy, based on the combined stratigraphic analysis of lipids and 16S rDNA [11]. In the present study we combined the latter lipid data (Fig. 5a-c) with the data on carotenoids and 16S rDNA of green sulfur bacteria (Fig. 5d-g) in order to obtain a more complete picture of the development of Holocene anaerobic processes as well as physical characteristics of the water column of Ace Lake.

Lipids characteristic for Archaea such as archaeol and 2,6,10,15,19-pentamethylicosane (PMI) (e.g. [41, 45]), were first detected in a shorter core comprising the upper 25 cm of Ace Lake sediments. Those compounds' isotopic values fell in the range –17‰ to –28‰ which is indicative of an origin from methanogens [46]. In that same short core of Ace Lake, the isotopically depleted sterol 4α-methyl-5α-cholest-8(14)-en-3β-ol and diagenetic derivatives were found [46]. From the 150-cm-long core that was used in this study, the relative abundance of lipid biomarkers indicative of methanogens (Fig. 5a,b; structures V-VII in Fig. 4) as well as the specific sterol 4α-methyl-5α-cholest-8(14)-en-3β-ol within the upper 39 cm of sediment showed that an active methane cycle occurred during the last 3000 calendar years [11]. Fossil 16S rDNA analysis revealed that the sterol was biosynthesized by a member of the aerobic methane-consuming bacteria of the family Methylococcaceae [11].

Since methanogenesis is restricted to the sulfate-depleted waters of present-day Ace Lake, and methanogenesis does not occur in other sulfate-rich anoxic lakes of the Vestfold Hills [18], we assumed that the onset of the formation of an active methane cycle is indicative of sulfate-depleted ancient bottom waters. These data suggest that Ace Lake became completely isolated from the sulfate-containing ocean at least 3000 cal years BP. An analysis of the ionic composition of the marine-derived waters of present-day Ace Lake indeed shows a nearly

80% loss of total S during the history of the lake [9]. Sulfate-depletion was most likely a result of destabilization of meromixis, resulting in turnover of the water column and subsequent venting of gaseous H_2S, the product of bacterial sulfate reduction, to the atmosphere [14]. There are several indications that these events occurred in the ancient water column of Ace Lake: A diatom-inferred salinity record showed that the salinity of the photic zone of Ace Lake was significantly increased as a result of increased evaporation during deposition of sediments between 10 and 30 cm [42]. Interestingly, in a parallel combined lipid and 18S rDNA stratigraphy study on the Holocene sediments of Ace Lake, we found that a haptophyte species initially recovered from sediment layers of Unit II, re-colonized the photic zone during deposition of sediments between 15 and 21 cm (Unit I) [12]. Our carotenoid stratigraphy (Fig. 5d) provides evidence that the increase in photic zone salinity caused at least one event of destabilization and turn-over of the water column. For example, in the sediment layer between 17 and 19 cm, the chlorobactene concentration was 195 to 215 times lower compared to adjacent sediment layers.

Biomarkers indicative of methanogens were also predominant within Unit III, the oldest sediment layers studied. Two hydroxyarchaeol isomers were only identified in Unit III (Fig. 5b; structures VIII, IX in Fig. 4). Both compounds are known to occur only in methanogenic Archaea and, specifically, in the orders Methanosarcinales and Methanococcales [28, 48]. In good agreement with the observed shift in the archaeal community towards phylotypes with 99.5-100% sequence similarity with cultivated *Methanosarcina* species and their predominance in Unit III [11], these Archaea most likely represented methanogens, and were the sources of both hydroxyarchaeol isomers. Since the hydroxyarchaeols and their sources were clearly restricted to the freshwater sediment deposits of Unit III, it is likely that these phylotypes represented remnants of archaeal species that thrived in the anoxic freshwater sediments at the time of deposition [11]. Soon after sulfate-containing marine waters entered Ace Lake, the hydroxyarchaeols as well as the sequences of methanogenic *Methanosarcina* species became undetectable and a shift towards archaeal phylotypes related to uncultured Archaea from various marine settings occurred [11]. Ace Lake was not likely to be sulfate-depleted during the marine phase. Bacterial sulfate reduction to sulfide must have occurred soon after marine waters entered Ace Lake since the occurrence of fossil carotenoids and a sequence of the *Chlorobium* species indicated that at least part of the sulfide was oxidized via anoxygenic photosynthesis.

5. CONCLUSIONS

The combined absence of carotenoids and 16S rDNA of Chlorobiaceae and the presence of hydroxyarchaeols of Archaea related to methanogenic

Methanosarcinales species within Unit III sediments are indicative for the non-sulfidic freshwater palaeo-Ace Lake. About 9400 calendar years BP, the post-glacial sea-level rise resulted in the introduction of sulfate-containing marine waters into Ace Lake. Low levels of carotenoids and a 16S rDNA of a *Chlorobium* species (99.6% sequence similarity to *C. phaeovibrioides* DSMZ 269^T) were detected. This proves that anoxygenic photosynthesis by Chlorobiaceae, which oxidize sulfide to sulfate, developed soon after Ace Lake became a fjord system. Lipids indicative for methanogenic Archaea disappeared and anaerobic bacterial sulfate reduction to sulfide became involved in the active cycling of sulfur.

The reappearance of lipid biomarkers of methanogenic Archaea and the concomitant presence of a sterol of ancient aerobic methanotrophic bacteria of the family Methylococcaceae in the upper 39 cm of the core indicate that an active methane cycle developed 3000 years BP. The onset of methanogenesis most likely reflects a concomitant depletion in bottom water sulfate. Sulfate depletion was most likely a result of turn-over events and the venting of gaseous H_2S to the atmosphere, indicated by the marked decrease in carotenoid content in the top sediment layers.

The ratio between DNA to chlorobactene of the predominant *Chlorobium* species revealed that a substantial part of the DNA of dead but intact cells was degraded before burial in the sediment. Within the anoxic, sulfidic, Holocene sediments of Ace Lake, the remaining DNA is well preserved and forms a species-specific molecular record of microorganisms which colonized the ancient water column. In contrast, within the Unit II sediment layers older than 5,700 years, a substantial part of the intact carotenoid chlorobactene of GSB was reduced to chlorobactane and was therefore less stable than DNA. Since anoxic settings with potential preserving conditions for ancient DNA can be found throughout the world, the combined stratigraphic analysis of lipid biomarkers and ancient 16S rDNA is a promising and powerful tool for reconstructing the palaeomicrobiology of aquatic systems as well as to refine the reconstruction of palaeoenvironments and important biogeochemical processes. Nevertheless, a more detailed analysis on the impact of H_2S concentration and residence time of cells within the water column is still needed to improve our knowledge of the preservation of ancient fossil DNA.

References

[1] Benson D.A., Karsch-Mizrachi I., Lipman D.J., Ostell J., Rapp B.A. and Wheeler D.L. GenBank. Nucl Acids Res 2000; 28:15-18.

[2] Bird M.I., Chivas A.R., Radnell C.J. and Burton H.R. Sedimentological and stable-isotope evolution of Ace Lake in the Vestfold Hills, Antarctica. Palaeogeo Palaeoclimatol Palaeoecol 1991; 84:109-130.

[3] Bowman J.P., McCammon S.A. and Skerratt J.H. Methylosphaera hansonii gen. nov., sp. nov., a psychrophilic, group I methanotroph from Antarctic marine-salinity, meromictic lakes. Microbiol 1997; 143:1451-1459.

[4] Bowman J.P., Rea S.M., McCammon S.A. and McMeekin T.A. Diversity and community structure within anoxic sediment from marine salinity meromictic lakes and a coastal meromictic marine basin, Vestfold Hills, Eastern Antarctica. Env Microbiol 2000; 2:227-237.

[5] Britton G. UV/Visible Spectroscopy. In: *Carotenoids*, vol. 1B: Spectroscopy, Britton G., Liaaen-Jensen S. and Pfande H., eds., Basel, Birkhäuser Verlag, 1995.

[6] Burch M.D. Annual cycle of phytoplankton in Ace Lake, an ice covered, saline meromictic lake. Hydrobiol 1988; 165:59-75.

[7] Burke C.M. and Burton H.R. Photosynthetic bacteria in meromictic lakes and stratified fjords of the Vestfold Hills, Antarctica. Hydrobiol 1988; 165:13-23.

[8] Burton H.R. Methane in a saline Antarctic lake. In: *Biogeochemistry of ancient and modern environments*, Trudinger P.A. and Walter M.R., eds., Canberra, Australian Academy of Science, 1980.

[9] Burton H.R. and Barker R.J. Sulfur chemistry and microbiological fractionation of sulfur isotopes in a saline Antarctic lake. Geomicrobiol J 1979; 1:329-340.

[10] Coolen M.J.L., Cypionka H., Sass A.M., Sass H. and Overmann J. Ongoing modification of Mediterranean Pleistocene sapropels mediated by prokaryotes. Science 2002; 296:2407-2410.

[11] Coolen M.J.L., Hopmans E.C., Rijpstra W.I.C., Muyzer G., Schouten S., Volkman J.K. and Sinninghe Damsté J.S. Evolution of the methane cycle in Ace Lake (Antarctica) during the Holocene: Response of methanogens and methanotrophs to environmental changes. Org Geochem 2004a; 35:1151-1167.

[12] Coolen M.J.L., Muyzer G., Rijpstra W.I.C., Schouten S., Volkman J.K. and Sinninghe Damsté J.S. Combined DNA and lipid analysis of sediments reveal changes in Holocene haptophyte and diatom populations in an Antarctic lake. Earth Planet Sci Lett 2004b; 223:225-239.

[13] Coolen, M.J.L. and Overmann, J. Analysis of subfossil remains of purple sulfur bacteria in a lake sediment. Appl Environm Microbiol 1998; 64:4513-4521.

[14] Cromer L., Gibson J.A.E., Swadling K.M. and Ritz D.A. Faunal indicators of Holocene ecological change in a Antarctic Lake. Palaeogeo Palaeoclimatol Palaeoecol 2005; 221:83-97.

[15] Fulford-Smith S.P. and Sikes E.L. The evolution of Ace Lake, Antarctica, determined from sedimentary diatom assemblages. Palaeogeo Palaeoclimatol Palaeoecol 1996; 124:73-86.

[16] Franzmann P.D., Deprez P.P., Burton H.R. and van den Hoff J. Limnology of Organic Lake, Antarctica, a meromictic lake that contains high concentrations of dimethyl sulfide. Austral J Mar Freshw Res 1987; 38:409-417.

[17] Franzmann P.D., Liu Y., Balkwill D.L., Aldrich H.C., Conway de Macario E. and Boone D.R. Methanogenium frigidum sp. nov., a psychrophylic H_2-using methanogen from Ace Lake, Antarctica. Intern J System Bact 1997; 47:1068-1072.

[18] Franzmann P.D., Roberts N.J., Mancuso C.A., Burton H.R. and McMeekin T.A. Methane production in meromictic Ace Lake, Antarctica. Hydrobiol 1991; 210:191-201.

[19] Franzmann P.D., Skyring G.W., Burton H.R. and Deprez P.P. Sulfate reduction rates and some aspects of the limnology of four lakes and a fjord in the Vestfold Hills, Antarctica. Hydrobiol 1988; 165:25-33.

[20] Franzmann, P.D., Springer, N., Ludwig, W., Conway de Macario, E. and Rhode, M. A methanogenic archaeon from Ace Lake, Antarctica: Methanococcoides burtonii sp. nov. System Appl Microbiol 1992; 15:573-581.

[21] Gibson J.A.E. The meromictic lakes and stratified marine basins of the Vestfold Hills, East Antarctica. Antarctic Sci 1999; 11:175-192.

[22] Gibson J.A.E., Garrick R.C., Franzmann P.D., Deprez P.P. and Burton H.R. Reduced sulfur gases in saline lakes of the Vestfold Hills, Antarctica. Palaeogeogr Palaeoclimatol Palaeoecol 1991; 84:131-140.

[23] Hanselmann, K.W. Microbially mediated processes in environmental chemistry. Chimia 1986; 40:146-159.

[24] Hauswirth W.W., Dickel C.D. and Lawlor D. DNA analysis of the Windover population. In: *Ancient DNA*, Herrmann B. and Hummel S. eds., New York, Springer, 1994.

[25] Inagaki F., Okada H., Tsapin A.I. and Nealson K.H. The paleome: A sedimentary record of past microbial communities. Astrobiol 2005; 5:141-53.

[26] Inagaki F., Sakihama, Y., Takai K., Komatsu T., Inoue A. and Horikoshi K. Profile of microbial community structure and presence of endolithic microorganisms inside a deep-sea rock. Geomicrobiol J 2002; 19:535-552.

[27] Inagaki F., Takai K., Komatsu T., Kanamatsu T., Fujioka K. and Horikoshi K. Archaeology of Archaea: Geomicrobiological record of Pleistocene thermal events concealed in a deep-sea subseafloor environment. Extremophiles 2001; 5:385-392.

[28] Koga Y., Morii H., Akagawa-Matsushita M. and Ohga M. Correlation of polar lipid composition with 16S rRNA phylogeny in methanogens. Further analysis of lipid component parts. Biosci Biotech Biochem 1998; 62:230-236.

[29] de Leeuw J.W. and Largeau, G. A review of macromolecular organic compounds that comprise living organisms and their role in kerogen, coal and petroleum formation. In: *Organic Geochemistry*, Engel M.H. and Macko S.A. eds., New York, Plenum Press, 1993.

[30] Limburg P.A. and Weider L.J. 'Ancient' DNA in the resting egg bank of a microcrustacean can serve as a palaeolimnological database. Proc Roy Soc London Ser B-Biol Sci 2002; 269:281-287.

[31] Ludwig W., Strunk O., Westram R., Richter L., Meier H., Yadhukumar, Buchner A., Lai T., Steppi S., Jobb G., Förster W., Brettske I., Gerber S., Ginhart A.W., Gross O., Grumann S., Hermann S., Jost R., König A., Liss T., Lüßmann R., May M., Nonhoff B., Reichel B., Strehlow R., Stamatakis A., Stuckmann N., Vilbig A., Lenke M., Ludwig T., Bode A. and Schleifer K.-H. ARB: a software environment for sequence data. Nucl Acids Res 2004; 32:1363-1371.

[32] Maidak B.L., Cole J.R., Lilburn T.G., Parker Jr. C.T., Saxman P.R., Farris R.J., Garrity G.M., Olsen G.J., Schmidt T.M. and Tiedje J.M. The RDP-II (Ribosomal Database Project). Nucl Acids Res 2001; 29:173-174.

[33] Muyzer G., de Waal E.C., Uitterlinden A.G. Profiling of complex microbial populations by denaturing gradient gel electrophoresis analysis of polymerase chain reaction-amplified genes coding for 16S rRNA. Appl Environm Microbiol 1993; 59:695-700.

[34] Overmann J., Coolen M.J.L. and Tuschak C. Specific detection of different phylogenetic groups of chemocline bacteria based on PCR and denaturing gradient gel electrophoresis of 16S rRNA gene fragments. Archiv Microbiol 1999; 172:83-94.

[35] Overmann J. and Tuschak C. Phylogeny and molecular fingerprinting of green sulfur bacteria. Arch Microbiol 1997; 167:302-309.

[36] Pfennig N. and Trüper H.G. Anoxygenic phototrophic bacteria In: *Bergey's Manual of Systematic Bacteriology*, vol. 3, Staley J.T., Bryant M.P., Pfennig N. and Holt J.C. eds. Baltimore, Williams and Wilkins, 1989.

[37] Pickard J. Antarctic oases. Davis Station and the Vestfold Hills. In: *Antarctic oases*. Pickard J. ed., Sydney, Academic Press, 1986.

[38] Rankin L.M., Gibson J.A.E., Franzmann P.D. and Burton H.R. The chemical stratification and microbial communities of Ace Lake, Antarctica: A review of the characteristics of a marine-derived meromictic lake. Polarforschung 1999; 66:33-52.

[39] Raniello R. and Procaccini G. Ancient DNA in the seagrass Posidonia oceanica. Mar Ecol Prog Ser 2002; 227:269-273.

[40] Reid V.A., Carvalho G.R. and George D.G. Molecular genetic analysis of Daphnia in the English Lake District: Species identity, hybridization and resting egg banks. Freshw Biol 2000; 44:247-253.

[41] Risatti J.B., Rowland S.J., Yon D.A. and Maxwell, J.R. Stereochemical studies of acyclic isoprenoids-XII. Lipids of methanogenic bacteria and possible contributions to sediments. In: *Advances in Organic Geochemistry 1983*, Schenck P.A., de Leeuw J.W. and Lijmbach G.W.M. eds., Oxford, Pergamon Press Ltd, 1984.

[42] Roberts D. and McMinn A. A diatom-based palaeosalinity history of Ace Lake, Vestfold Hills, Antarctica. The Holocene 1999; 9:401-408.

[43] Schaeffer P., Adam P., Wehrung P. and Albrecht P. Novel aromatic carotenoid derivatives from sulfur photosynthetic bacteria in sediments. Tetrahedron Lett 1997; 38:8413-8416.

[44] Schouten S., Bowman J.P., Rijpstra W.I.C. and Sinninghe Damsté J.S. Sterols in a psychrophylic methanotroph, Methylosphaera hansonii. FEMS Microbiol Lett 2000; 186:193-195.

[45] Schouten, S., van der Maarel M.J.E.C., Hubert R. and Sinninghe Damsté J.S. 2,6,10,15,19-pentamethylicosenes in Methanolobus bombayensis, a marine methanogenic archaeon and Methanosarcina mazei. Org Geochem 1997; 26:409-414.

[46] Schouten S., Rijpstra W.I.C., Kok M., Hopmans E.C., Summons R.E., Volkman J.K. and Sinninghe Damsté J.S. Molecular organic tracers of biogeochemical processes in a saline meromictic lake (Ace Lake). Geochim Cosmochim Acta 2001; 65:1629-1640.

[47] Sinninghe Damsté J.S. and Koopmans M.P. The fate of carotenoids in sediments: An overview. Pure Appl Chem 1997; 89:2067-2074.

[48] Sprott G.D., Dicaire C.J., Choquet C.G., Patel G.B. and Ekiel I. Hydroxy diether lipid structures in Methanosarcina spp. and Methanococcus voltae. Appl Environm Microbiol 1993; 59:912-914.

[49] Stuiver M., Reimer P.J. and Braziunas T.F. High-precision radiocarbon age calibration for terrestrial and marine samples. Radiocarbon 1998; 40:1127-1151.

[50] Summons R. E., Jahnke L.J. and Roksandic Z. Carbon isotope fractionation in lipids from methanotrophic bacteria: relevance for the interpretation of the geochemical record of biomarkers. Geochim Cosmochim Acta 1994; 58:2853-2863.

[51] Swadling K.M., Dartnall H.J.G., Gibson J.A.E., Saulnier-Talbot E. and Vincent W.F. Fossil rotifers and the early colonization of an Antarctic Lake Quat Res 2001; 55:380-384.

[52] de Wit R. and Caumette P. An overview of the brown-coloured isorenieratene-containing green sulphur bacteria (*Chlorobiaceae*). In: *Organic Geochemistry: Developments and applications to energy, climate, environment and human history*, Grimalt J.O. and Dorronsoro C. eds., A.I.G.O.A, Donostia-San Sebastian, 1995.

[53] Zwartz D., Bird M., Stone J. and Lambeck K. Holocene sea-level change and ice-sheet history in the Vestfold Hills, East Antarctica. Earth Planet Sci Lett 1998; 155:131-145.

II

ANOXIA AND OXYGEN DEFICIENCY OF THE PRESENT WORLD OCEAN

BIOGEOCHEMISTRY OF THE BLACK SEA ANOXIC ZONE WITH A REFERENCE TO SULPHUR CYCLE

Lev N. Neretin[1,2], Igor I. Volkov[3], Alexander G. Rozanov[3], Tatyana P. Demidova[3], Anastasiya S. Falina[3]

[1] *Max Planck Institute for Marine Microbiology, Celsiusstrasse 1, 28359 Bremen, Germany*

[2] *Federal Institute for Geosciences and Natural Resources, Stilleweg 2, 30655 Hannover, Germany*

[3] *P.P.Shirshov Institute of Oceanology of Russian Academy of Sciences, 37 Nakhimovsky prosp., 117997 Moscow, Russia*

Abstract The Black Sea is the largest anoxic basin on earth. Hydrogen sulphide inventory in the sea is about 4,600 Tg. This review discusses the evolution and contemporary physical and chemical characteristics of the Black Sea anoxic zone. We present hydrogen sulphide concentrations at different depths in the sea and discuss mechanisms of physical mixing in the anoxic interior. Special emphasis is given to recently discovered bottom convective layer located at depths below 1700-1750 m and concentrations of dissolved sulphide and other chemical species in this zone. The mechanism of double diffusion driven by geothermal heat flux is the main mixing process there. Mesoscale physical dynamics associated with the Main Rim Current has important imlications for the dissolved sulphide spatial distribution and, in general, for ventilation of the anoxic interior. We suggest that, together with the Bosporus influx, the nearshore convergence zone supplies dissolved oxygen into the anoxic zone and leads to the formation of inorganic sulphur intermediates. A detailed analysis of total alkalinity and its components in the Black Sea and other euxinic basins shows unambigously that sulfate reduction is the main process of organic matter anaerobic mineralization in the water column. This result is confirmed by the sulphur budget, whose components are discussed at the end.

Keywords: Black Sea, anoxic zone, evolution, sulphur cycling, alkalinity

1. HISTORY OF THE BLACK SEA ANOXIA

During the past three million years, the Black Sea experienced at least eight marine flooding events with the last Pleistocene/Holocene transition of the highest magnitude [78]. During the Last Glacial Maximum, also called Neoeuxinian epoch, which lasted from ca. 17 to 11 and possibly 9 ka BP (Before Present) [87], the Black Sea was a freshwater lake with a minimum water levels

L. N. Neretin (ed.), Past and Present Water Column Anoxia, 69–104.

estimated between 20 and 110 m below the present sea level (Fig. 1; reviewed by [35]). Air temperatures were 8-10°C lower than today [25] and salinity was in the range 5-7‰ [11, 16, 65]. The inflow of glacial meltwaters from rivers and the Caspian Sea contributed significantly to permanent seawater rise over the entire Neoeuxinian epoch [87]. Accumulated paleontological, geological and geomorphological data suggest that during most of this time a unidirectional outflow from the Black Sea to the Sea of Marmara and the Mediterranean Sea existed [1, 2, 40, 57]. There were probably short periods of 200-300 yrs when the Black Sea level dropped below 80 m compared to the current sea level and the Black Sea outflow ceased. Terraces observed on the Black Sea shelf are indicative for these low sea level stands (A. Aksenov, personal communication).

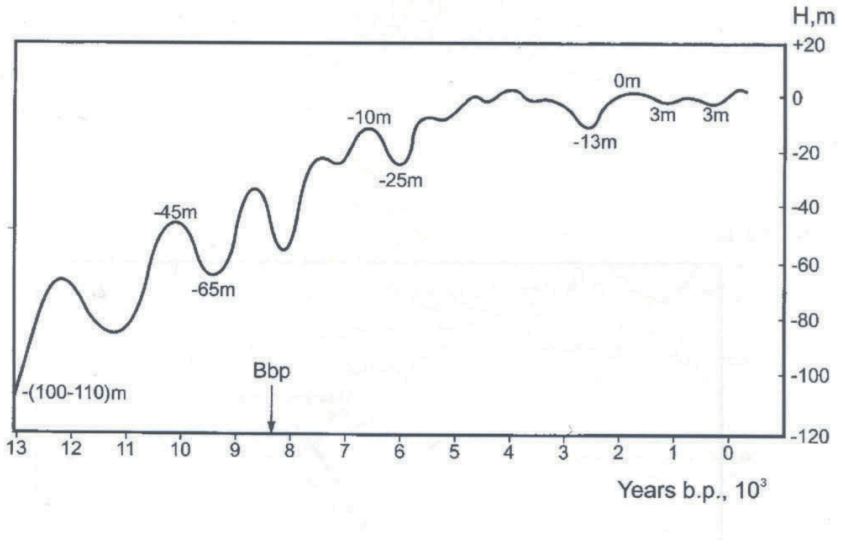

Figure 1. Changes of the Black Sea level during Late Pleistocene-Holocene. The arrow indicates the timing of the Bosporus breakthrough [6].

Two layered flow across the Bosporus connected with melting of glaciers on the northern Eurasian continent and the post-glacial rise of the global sea level. However, the timing and the intensity of this process are disputed. Dating of this event varies from 10 ka BP [72] to 7.15 ka B.P. [79]. Ryan and his colleagues [79] suggested that the influx of Bosporus waters in the Black Sea occurred on a catastrophic scale of some 100 meters in just a few years. The authors hypothesized in a popular book that the event was associated with a Noah's flood described in the Bible [77]. The hypothesis was recently supported by computer modelling [81]. In contrast, the sedimentary record for the post-glacial sea-level

rise along the southwestern Black Sea shelf does not support the catastrophic refilling of the Black Sea [2]. Studies by Gorur et al. [26] around the mouth of the Sakarya River demonstrated that there was a gradual rise in the level of the Black Sea from some time before 8,0 ka BP until it attained a surface level of 18 m below present sea-level around 7,2 ka BP, when the most recent Mediterranean influx occured. Recent sedimentological and palaeontological studies in the Bosporus Strait suggest that the sill depth was probably not the critical factor in the exchange between the Black Sea and Mediterranean Sea at the Holocene/Pleistocene transition. Other alternative routes such as the Gulf of Izmit-Sapanca and Lake-Sakarya Valley may have existed at that time [40].

The evolution of the Black Sea anoxic zone is closely connected with the evolution of the Black Sea stratification pattern, that is presently characterized by the existence of a strong pycnocline separating the upper freshwater influenced surface layer with a salinity of 17.5-18.5‰ and the deep water mass below ca. 150-200 m with a salinity of 22.3‰ at the bottom. Models for evolving Black Sea salinity after the opening of Bosporus show that salinity in bottom waters reached 90% of present-day values about 3,000 yrs or less after the Bosporus opening [5, 10, 36, 54] or indicate that the freshwater content of the Black Sea became depleted over a period of about 3,700 yrs after the opening [46]. Due to the stable stratification, anoxia developed below the pycnocline, which corresponded to the deposition of an organic-rich sapropel after 7,800 yrs [94] or 7,540 yrs B.P. [34] through the entire Black Sea area. Since that time bottom waters in the Black Sea have remained anoxic. Development of anoxic conditions over time after the Bosporus inflow was modelled by Dueser [18], who suggested that present anoxic conditions were achieved within 2.0-4.0 ka after Mediterranean waters reached the Black Sea. These data are in correspondence with the evolution of the T-S structure of the Black Sea waters discussed earlier and residence time of main seawater anions such as chloride, bromide, and sulphate [82].

Our knowledge about the anoxic zone is of great importance for understanding the functioning of the Black Sea ecosystem. The goal of this review is to present an overview of the processes occurring in the anoxic zone of the Black Sea with an emphasis on the sulphur cycle using data obtained during the last ten years. Hydrogen sulphide, ΣH_2S[1], is the key chemical compound, which defines the direction and origin of many biogeochemical cycles in the anoxic zone. The chapter starts with describing the inventory of hydrogen sulphide, its vertical and spatial dynamics, and the distribution of sulphur intermediates. It is followed by the discussion of the Black Sea alkalinity, which is a cu-

[1] $\Sigma H_2S=[H_2S] + [HS^-]+[S^{2-}]$, where $[HS^-]$ represents ca. 80% under pH=7.5-7.65 in the Black Sea anoxic interior

mulative result of the ongoing organic mineralization processes in the anoxic zone dominated by sulphate reduction. We finally present the sulphur budget of the Black Sea. Physiochemical dynamics of the oxic/anoxic interface and the sulphur isotopic composition of hydrogen sulphide are discussed elsewhere in this volume (Ivanov and Lein; Murray and Yakushev).

2. H_2S INVENTORY

The total sulphide inventory of the contemporary Black Sea is about 4.6 x 10^3 Tg, the main part residing between 500 and 2000 m [61]. The average dissolved sulphide concentrations at different depths are given in Table 1. The H_2S concentrations below 30 μM for the period after 1989 given in Table 1 were obtained using methylene blue photometric method [13]. Iodometric titrations were used for higher concentrations. The averaged data for the period before 1996 represent basin-wide averages, whereas more recent data were obtained in the north-eastern part of the sea only (Fig. 2). The lower sulphide concentrations given by Skopintsev [82] are explained by the underestimation of sulphide concentrations determined from water samples collected with metal bottles routinely used before 1980s [66].

The H_2S vertical distribution is quasi-linear above 500-600 m. Dissolved sulphide concentration increases gradually with depth for every station in the Black Sea (Fig. 3). The vertical gradient above 500 m is about 0.5 mmol m^{-4} and decreases with depth (Table 1). The vertical sulphide gradient at the boundary between the entire anoxic water mass and the bottom convective layer (ca. 1700-1750 m) increases sharply and is only two times less the vertical gradient in the upper 500 m. The H_2S distribution in this zone is controlled by the density gradient and can be twice as large as the average gradient of 0.24 mmol m^{-4} given in Table 1. H_2S concentrations do not change with depth in the bottom convective layer.

The average H_2S concentration in the Black Sea water column is about 270 μM. The H_2S concentration in bottom waters changes between 367 and 400 μM, the average is 376 μM.

3. H_2S VERTICAL DISTRIBUTION AND MIXING PROCESSES IN THE ANOXIC ZONE

Vertical distributions of temperature, salinity, and density in the Black Sea correlate with the sulphide vertical distribution. As a consequence, the H_2S vertical distribution versus salinity (Fig. 4a) and temperature (Fig. 4b) is consistent with the θ-S curve (Fig. 4a) for deep waters. The evidence suggests that thermohaline structure of the water column controls the vertical distribution of hydrogen sulphide in the sea [62]. Identifiable on the both, θ-H_2S and S-H_2S diagrams, the boundaries of three water masses in the anoxic water column

Table 1. The average $\sum H_2S$ concentrations in the Black Sea water column.

Depth, m	*H_2S concentration, μM*					*Vertical gradient, mmol m^{-4}*
	Skopintsev (1975) 1950-60s	*Bezborodov and Eremeev (1993) 1984-1992*	*Neretin (1996) 1989-1995*	*Shirshov Institute data 1999-2002*	*Average concentrations 1989-2002*	
150	5.6 (135)	10	13 ± 12 (91) 0 – 38 (92%)	11.5 ± 10.9 (34) 0 – 39 (94%)	12.5 (125)	0.6
175				27.4±11.2 (27) 4.1 – 42.2 (41%)	27.4 (27)	0.5
200	24 (156)		40 ± 15 (82) 3.8 – 73 (38%)	39.8 ± 9.6 (27) 18.9 – 59 (24%)	40 (109)	0.47
250			63 ± 15 (60) 24 – 93 (24%)	64.0 ± 9.1 (28) 43.0 – 81.2 (14%)	63.3 (88)	0.47
300	69 ± 18 (158) (26%)	80	87 ± 16 (62) 49 – 133 (18%)	86.4 ± 8.3 (35) 68 – 101 (10%)	86.8 (97)	0.43
400			130 ± 14 (58) 96 – 159 (11%)	129 ± 12 (35) 85 – 144 (9%)	130 (93)	0.46
500	148 ± 29 (156) (20%)	166	176 ± (58) 142 – 205 (7%)	176 ± 8 (33) 160 – 196 (4%)	176 (91)	0.41
600			216 ± 12 (14) 192 – 232 (6%)	217 ± 8 (19) 206 – 240 (4%)	217 (33)	0.41

700				258 ± 8 (7) 249 – 269 (3%)	258 (7)	0.33
800			291 ± 9 (5) 276 – 299 (3%)		291 (5)	
900			309 ± 9 (5) 294 – 317 (3%)		309 (5)	0.05
1000	249 ± 28 (155) (11%)	298	314 ± 13 (18) 294 – 334 (4%)	314 ± 8 (31) 297 – 331 (2.4%)	314 (49)	0.10
1250			344 ± 16 (6) 313 – 354 (5%)	339 ± 7 (32) 326 – 351 (1.9%)	340 (38)	0.05
1500	281 ± 26 (115) (9%)	336	351 ± 11 (8) 334 – 369 (3%)	354 ± 5 (27) 344 – 364 (1.5%)	353 (35)	0.08
1700				369 ± 8 (19) 358 – 390 (2.1%)	369 (19)	0.24
1750			381 ± 14 (10) 360 – 399 (4%)		381 (10)	-0.14
1800				374 ± 4 (15) 367 – 383 (1.2%)	374 (15)	0.03

1900				377 ± 4 (16) 370 – 382 (1.0%)	377 (16)	-0.02
2000	282 ± 42 (65) (15%)	360	369 ± 19 (5) 354 – 401 (5%)	376 ± 4 (23) 369 – 384 (1.0%)	375 (28)	0.03
2100				378 ± 6 (18) 372 – 400 (1.6%)	378 (18)	

Note:
369 ± 19 (5) – numerator: mean ± standard deviation (number of measurements)
354 – 401 (5%) – denominator: range (coefficient of variability)

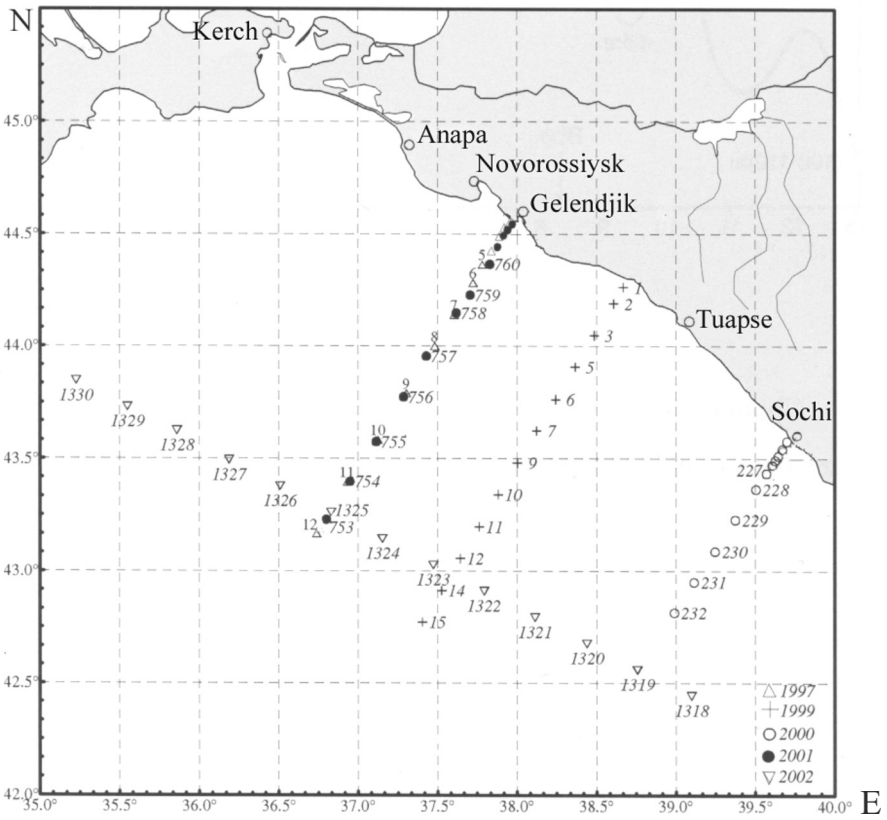

Figure 2. The location of stations sampled during *R/V Akvanavt* cruises in 1997, 1999-2002.

correspond strictly to the boundaries on θ-S diagram (Fig. 4a). Temperature-salinity relationship in the Black Sea is a result of large-scale external factors such as water and heat balance of the basin. Physical mixing processes dominate over the *in situ* sulphide production by sulphate-reducing bacteria. Therefore the depth distribution of dissolved sulphide corresponds strictly to the existing θ-S structure of the water column.

Our 605 simultaneous measurements of H_2S concentrations and density (451 data points in summer and 148 data points in winter) show the following regression curve between H_2S (mM) and relative density $\sigma_\theta=\sigma_{insitu}-1000$ (kg m^{-3}) [61]:

$$H_2S = 0.261\sigma_\theta^3 - 12.716\sigma_\theta^2 + 206.573\sigma_\theta - 1119.01$$

In the upper part of the sulphide zone the correlation between H_2S and σ_θ is smaller due to a larger hydrophysical inhomogeneity of the upper 300 m (Fig. 5). The location of the upper sulphide boundary and distribution of

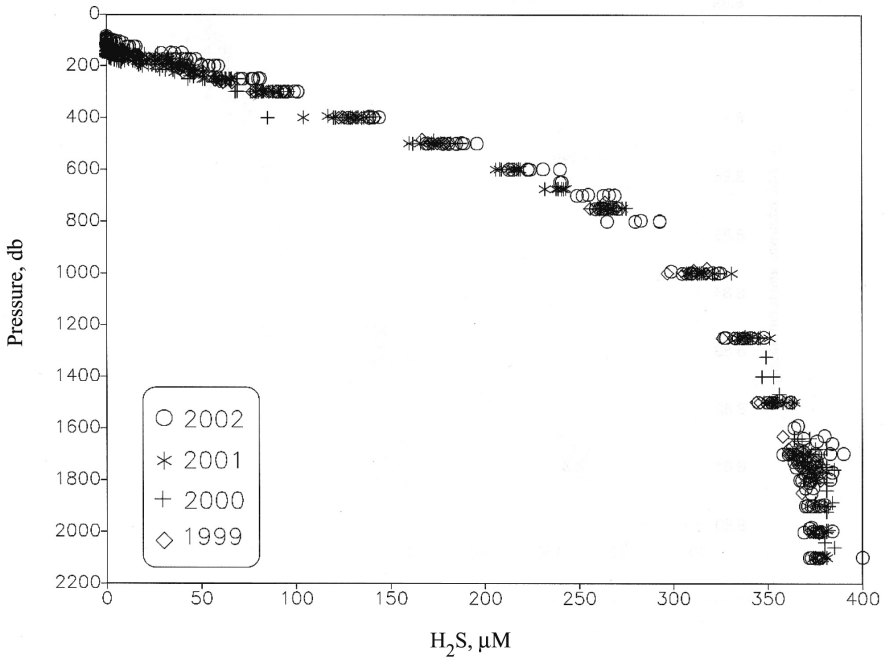

Figure 3. Combined depth distributions of dissolved hydrogen sulphide in the Black Sea water column from data collected in the period from 1999 to 2002 in the north-eastern Black Sea (stations are shown in Fig. 2).

other chemical parameters in the Black Sea water column are also density dependent [59, 76, 95, 105; Murray and Yakushev, this volume]. On average, the upper sulphide boundary corresponds to a density surface of about 16.2 kg m^{-3} independent of geographical position and season. This density surface corresponds to the lower pycnocline and was used as an independent estimate for the location of the sulphide onset in many studies. Our studies have shown that the upper sulphide boundary shoaled from σ_θ=16.2 kg m^{-3} to σ_θ = 16.09-16.15 kg m^{-3} in 1999-2002 (see also Murray and Yakushev, this volume). The observed tendency is a result of several warm winters during this period, which led to a weakening of winter convection process in the upper water column and increased temperature in the core of Cold Intermediate Layer and decreased dissolved oxygen content. The reverse trend has been observed after 2002 [74].

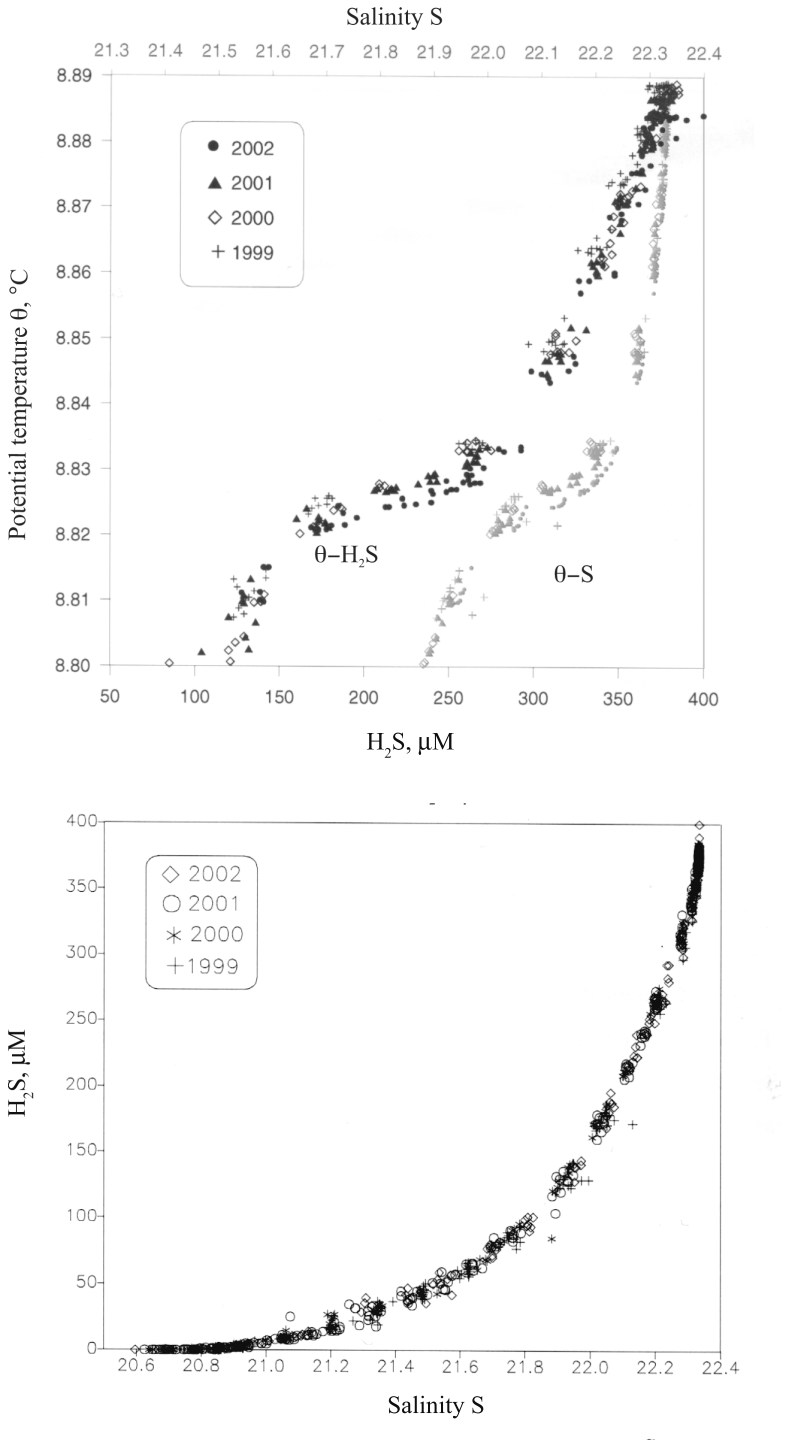

Figure 4. θ-S and θ-H_2S (upper panel) and S-H_2S (lower panel) diagrams for the Black Sea anoxic zone (stations are shown in Fig. 2).

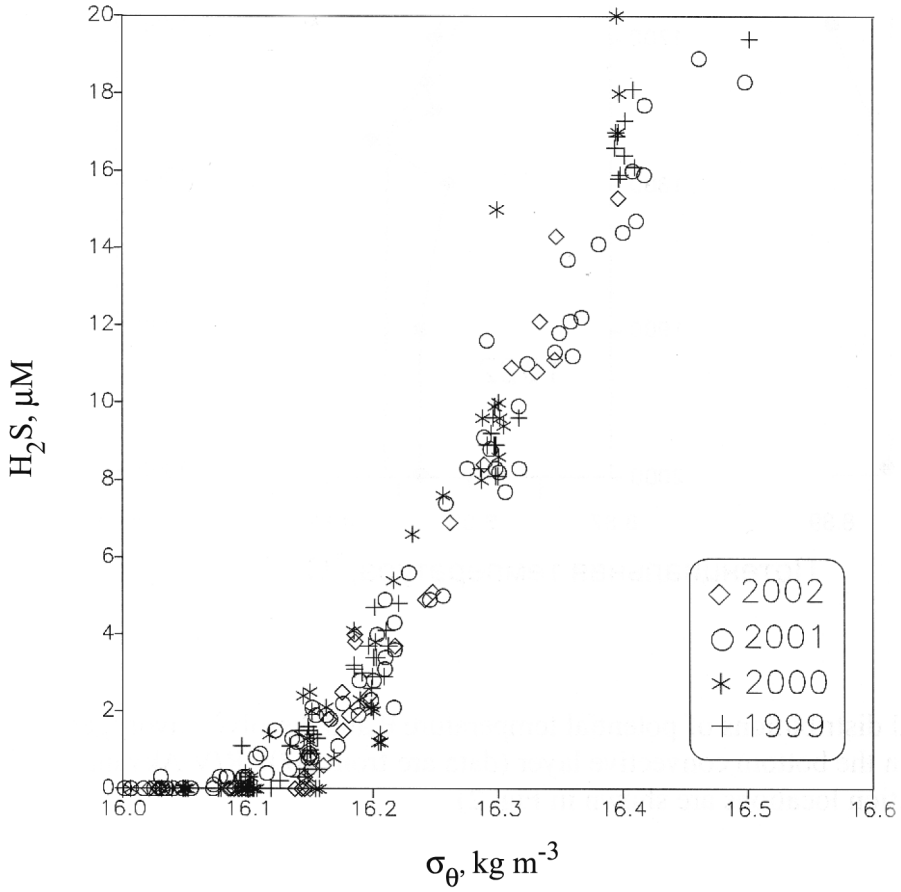

Figure 5. σ_θ-H_2S diagram in the Black Sea upper anoxic zone (stations are shown in Fig. 2).

4. BLACK SEA BOTTOM CONVECTIVE LAYER

The existence of homogeneous bottom water mass (bottom convective layer) at water depths below 1740-1800 m is first reported based on detailed CTD profiling by Murray et al. [60], and since then it has been intensively studied [22–24, 30, 37, 55, 67, 106, 107]. Based on our data obtained in 1999-2002 in the north-eastern Black Sea, the bottom water mass was characterized by the following parameters: potential temperature θ=8.883-8.888°C, salinity S=22.330-22.334, and potential density σ_θ=17.233-17.236 kg m^{-3}. Murray et al. [60] gives the following characteristics of the bottom convective layer in the western Black Sea: θ=8.895-8.897°C, S=22.336-22.338, and σ_θ=17.235-17.236 kg m^{-3}. Volkov and Falina [24] have concluded that on average the water column below 500 m is about 0.01°C warmer and 0.003-0.005 saltier in

the western part than in the eastern part. Recent detailed studies have shown that not only the thermohaline characteristics, but also concentrations of several chemical species in bottom waters below 1670 m are uniform, and like thermohaline characteristics independent of a geographical location. The average concentrations of some chemical species and alkalinity in the bottom convective layer measured in the period from 1999 to 2002 are given in Table 2.

Table 2. Hydrochemical characteristics of the bottom convective layer of the Black Sea during 1999-2002.

	1999: Depth ≥ 1750 m 7 stations	*2000: Depth ≥ 1750 m 5 stations*	*2001: Depth ≥ 1750 m 7 stations*	*2002: Depth ≥ 1650-1800 m 7 stations*
pH	n.d.	n.d.	7.42 – 7.67 (34) / 7.52 ± 0.06 (0.8%)	n.d.
Alk, μM	4419 – 4530 (19) / 4478 ± 33 (0.7%)	4400 – 4529 (18) / 4485 ± 44 (1.0%)	4375 – 4551 (32) / 4450 ± 45 (1.0%)	n.d.
H_2S, μM	367–379 (26)* / 376 ± 3 (0.9%)	375-385 (18) / 380 ± 3 (0.7%)	369-381 (34) / 376 ± 3 (0.9%)	368-400 (36) / 376 ± 6 (1.7%)
NH_4^+, μM	n.d.	n.d.	85.8 – 100.6 (24) / 94.4 ± 4.0 (4.3%)	n.d.
SiO_3^{2-}, μM	n.d.	n.d.	321 – 335 (35) / 330 ± 3 (1.0%)	n.d.
Mn^{2+}, μM	n.d.	n.d.	4.0 – 4.3 (27) / 4.1 ± 0.1 (2.0%)	n.d.
CH_4, μM	n.d.	n.d.	11.8 – 13.4 (29) / 12.5 ± 0.4 (3.4%)	n.d.

Note:
*367 – 379 (26) – numerator: range (number of measurements)
376 ± 3 (0.9%) – denominator: mean ± standard deviation (coefficient of variability)

A transport between the bottom convective layer and the overlying waters occurs via a single diffusive interface. A destabilizing geothermal heat flux at the bottom acts against stable salinity stratification resulting in double diffusion [60, 67]. It is the main mixing mechanism in bottom waters of the Black Sea. Mixing inside the bottom convective layer occurs on a scale of about 40 yrs [69]. Interestingly enough, the bottom convective layer in the Black Sea covering

the entire abyssal plain, is the largest known example of bottom convection in the world ocean [67].

Distribution of dissolved sulphide in the bottom layer varies between different parts of the sea as shown in Fig. 7 and can be explained by spatial differences in the bottom heat flux [45]. Eremeev and Kushnir [22] have found that the width of the bottom convective layer is directly proportional to the intensity of heat flux from the bottom. Transects covering the area opposite to Sochi show higher dissolved sulphide concentrations in water layers below 1650 m (Fig. 7a, c) compared to other transects (Fig. 7b, d). The upper boundary of the bottom convective layer at the terminal stations of the Sochi transect shoal up to 1650-1680 compared to its location at 1750-1800 m close to Sochi, which corresponds to the local maximum of the surface heat flow observed in this region [45].

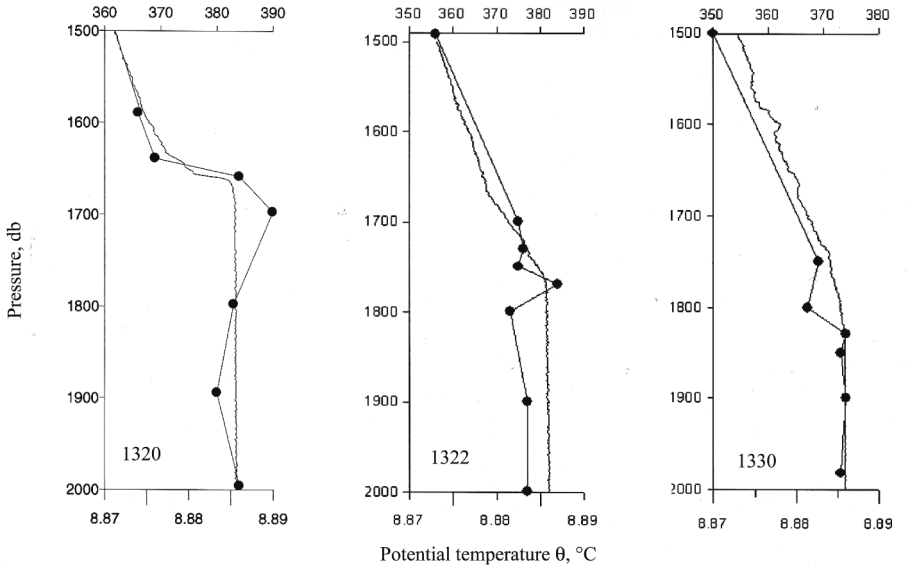

Figure 6. Vertical distributions of potential temperature θ (continuous line) and dissolved hydrogen sulphide ($\sum H_2S$) (circles) in the bottom convective layer (data are from 2002 *R/V Akvanavt* expedition, station locations are shown in Fig. 2).

A relative increase in the H_2S vertical gradient is observed at the boundary between the intermediate water mass and bottom waters below 1640-1750 m in the zone of 20-50 m (Fig. 6 and Table 1 last column; 106, 107]. Higher vertical gradients of thermohaline and chemical parameters are typical in this zone. The H_2S concentrations in bottom waters increase with the increased heat flux at the bottom and with larger volume of the bottom convective layer. The existence of the bottom homogeneous layer has important implications

for the physical and chemical exchange at the sediment/water interface and at the interface between intermediate and bottom water masses. These mixing processes at the interface between deep and bottom waters are particularly important for hydrogen sulphide dynamics and its balance in the sea, because about 30% of the Black Sea sulphide is concentrated in the layer below 1500 m.

There exist data indicating that the average concentrations of sulphide in the upper 1000 m of the anoxic zone have increased by 0.6-0.8 % a year from 1985 to 1995 [41, 42]. The authors argued that the Black Sea anoxic zone is not presently at a steady-state as it was in 1960-1970s. These data however should be interpreted with a caution, since most chemical data on sulphide concentrations obtained before 1980s using metal bottles are about 20% lower than the data obtained using plastic bottles [66]. In addition, significant spatial and temporal variability of physical and chemical parameters in the basin (Table 1, particularly in the upper 500-1000 m of the anoxic layer, compare variation coefficients of sulphide concentrations given in the first column) and the absence of basin-wide monitoring in previous years, make comparative assessments of sulphide concentrations over time for the entire basin difficult.

The possibility that dissolved sulphide concentration may be increasing in the bottom waters of the Black Sea however cannot be ruled out. Mathematical model of Ayzatullin et al. [5] suggests ongoing salination of the Black Sea bottom waters with a rate of 0.0005‰ per yr, which may result in sulphide annual increase of 0.003 μM. If such trend does exist it can be detected after 10-20 yrs from now given the accuracy of routine dissolved sulphide measurements.

5. THE H_2S SPATIAL DISTRIBUTION AND COASTAL DYNAMICS

Close correlation between sulphide vertical distribution and density is also reflected in the whole-basin hydrogen sulphide spatial distribution. Main circulation structures of the Black Sea (Main Rim Current (MRC), Eastern and Western Gyres, and anticyclonic eddies around Crimea and Batumi) are visible on the H_2S map. In the centers of cyclonic gyres, the location of the H_2S upper boundary decreases to 90-110 m, whereas at the periphery of the basin and in the centers of anticyclonic gyres it can deepen to depths 160-240 m. The spatial differences of the H_2S topography recognizable at the oxic/anoxic interface can be traced to depths below to 1000 m [61].

Recent advances in our understanding of the Black Sea coastal zone, and in particular, of the Rim Current and transverse water transport have revealed the crucial role of mesoscale eddies in the ventilation of the suboxic and the upper anoxic zone [70, 73]. Oguz et al. [71] conclude that about nine mesoscale nearshore anticyclonic eddies (NAE) propagate cyclonically around the basin at a given time. Usually mesoscale cyclonic eddies (CE) occur at the inner

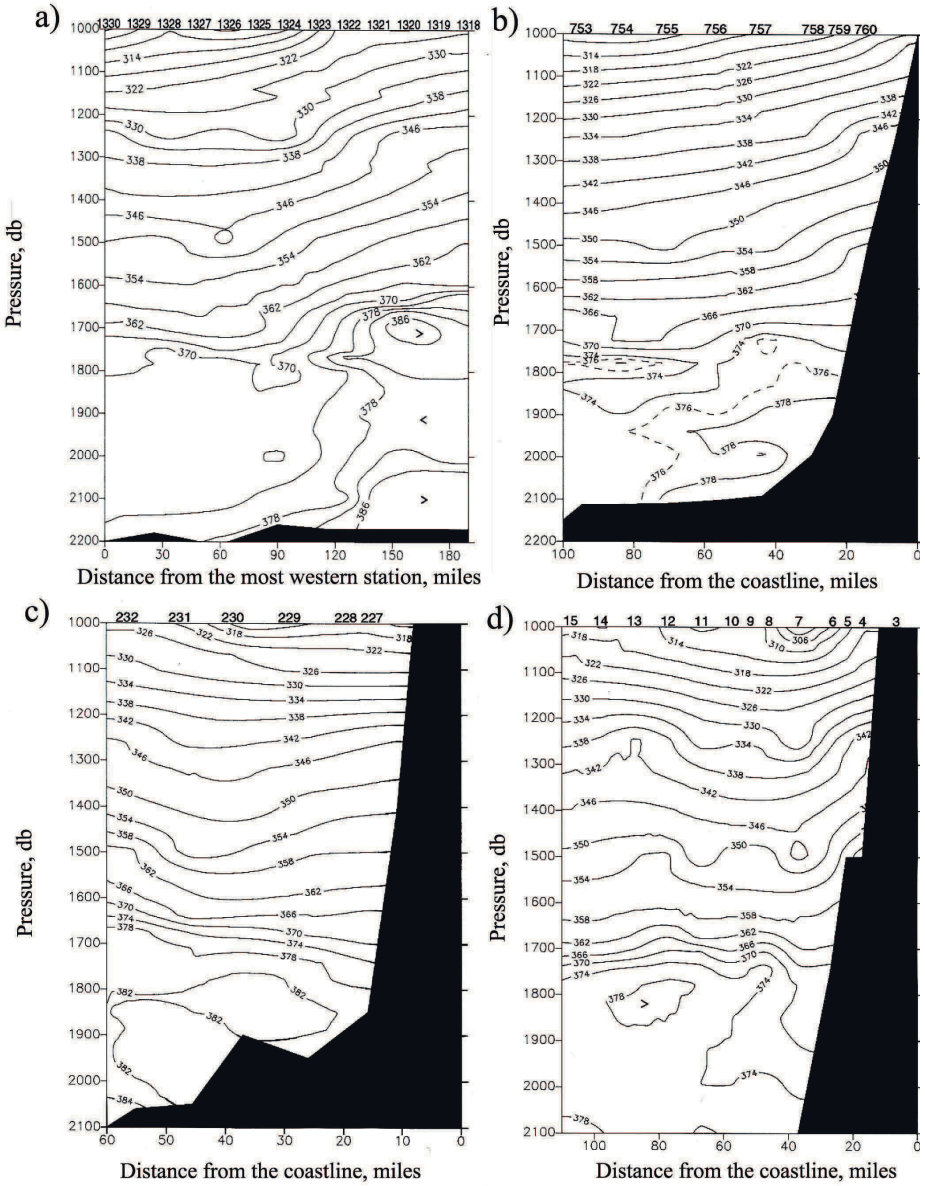

Figure 7. Hydrogen sulphide spatial distribution in deep waters (1000 m). Data are from different years: a) 2002; b) 2001; c)2000; d) 1999. Stations are shown in Fig. 2.

periphery of the Rim Current (Fig. 8A). In some of the very deep anticyclonic gyres, downwelling of the Cold Intermediate Waters can be traced to depths up to 1000-1200 m [4]. The diameter of large anticyclonic eddies can attain 50-100 miles with the current velocity of 30-40 cm s^{-1} at their peripheries. They can persist for about three to six months [71]. The anticyclonic eddies form a joint hydrodynamic convergence zone along the periphery of the basin that represent a natural physiochemical barrier between warm and less saline coastal waters and the open sea waters over the slope edge [73].

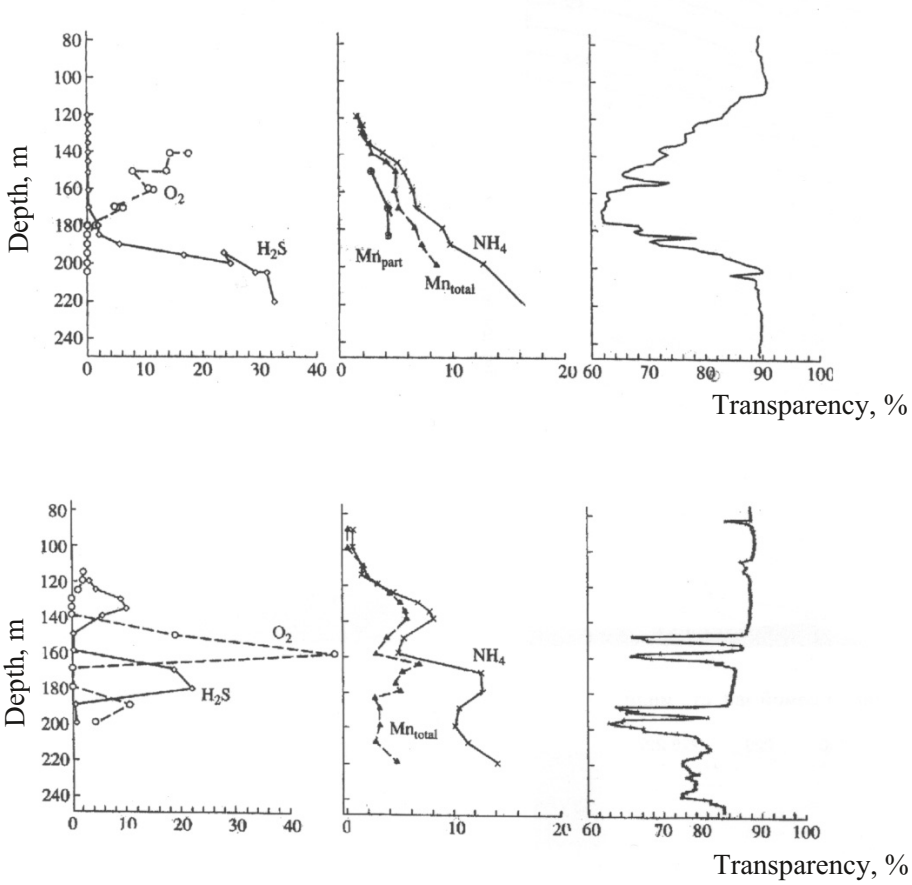

Figure 8. Depth distributions of dissolved O_2, H_2S, NH_4^+, and total Mn (all in μM), and transparency (%) at stations L29M46 (upper panel) and L34M46 (lower panel) of Sakarya Canyon [7].

The role of mesoscale dynamics on the H_2S spatial and vertical distributions has been underestimated in previous years. Descending water in the centers of anticyclonic eddies influences not only thermohaline characteristics of the

water column, but also the H_2S spatial field. H_2S boundary deepens 10-20 m in the centers of these structures compared to the adjacent waters (Fig. 8B). The isopycnal analysis of the H_2S distribution on several transects across the coastal zone show that an intensified exchange between oxic and anoxic waters may happen down to 500 m in the convergence zone between the MRC and propagating anticyclonic gyres [61]. Such mesoscale mixing processes can significantly enhance sulphide oxidation at the interface and contribute in ventilation of the anoxic zone as a whole. The difference between the sulphur isotopic composition of sulfate and sulphide is about 60 ‰ in the anoxic zone of the Black Sea. Neretin et al. [63] hypothesized that a combination of very low sulfate reduction rates throughout most of the water column (<< 1 nM d^{-1}, [3]) and efficient mixing mechanisms below the chemocline producing sulphur intermediates are the factors that cause high isotope depletion in sulphide. A range of physical processes such as intensified winter mixing and coastal dynamics together with oxygen intrusions carried by the modified Mediterranean Water may facilitate the formation and transport of intermediate sulphur species into the anoxic interior.

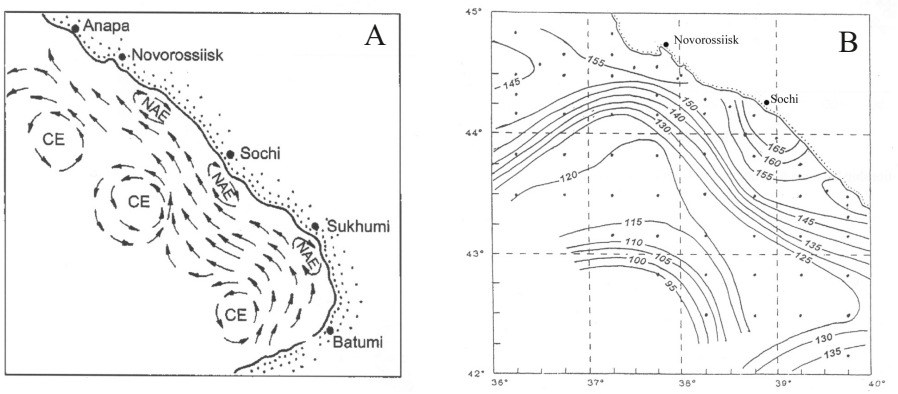

Figure 9. Geostrophic circulation [73] (A) and topography of the H_2S upper boundary [61] (B) in the north-eastern part of the Black Sea in September 1994; NAE stands for nearshore anticyclonic eddy, CE stands for cyclonic eddy.

6. "IRREGULAR" VERTICAL SULPHIDE DISTRIBUTIONS CAUSED BY LATERAL OXYGEN INTRUSIONS

Overall, the average H_2S vertical profiles look rather similar over the entire Black Sea area. However, there are exceptions caused by intense perturbations to the hydrodynamics along the Main Rim Current. Such an 'irregular' H_2S vertical distribution has been observed in the water column in the area adjacent to Sakarya Canyon (Fig. 8). Results of the RV "Bilim" expedition conclusively

show the presence of oxygen intrusions at depths 158 and 190 m, well below the sulphide onset. Hydrogen sulphide disappearance at these depths is accompanied by decreased ammonium and Mn(II) concentrations and increased turbidity values [7]. The authors attribute the presence of oxygen intrusions below the upper H_2S boundary to the existence of strong vertical and horizontal water mixing caused by the meandering of the MRC along the steep and complicated topography of the Sakarya Canyon.

The presence of modified saline Mediterranean waters below to 500-600 m (from T/S analysis) was first reported in 1960s [9], although no evidence of oxygen intrusions was discussed. Detailed studies in the western Black Sea have shown that a dense Mediterranean water after passage over a Bosporus sill flows over a wide continental shelf and entrains ambient Black Sea water. The Mediterranean effluent follows along the canyon and the shelf and produces a delta-like structure on the shelf region. The vertical spread in the interface region between shelf and continental slope is the result of mixing of Bosporus waters with CIL [15, 68]. Upon passage over the shelf, Mediterranean Water (MW) is altered to "shelf-modified MW" (SMMW) (terminology suggested by Özsoy et al. [68]) resulting in a T-S signature distinctly different from the initially warm, saline characteristics of MW. Cascades of dense SMMW sink down to 500-600 m on the continental slope where they are distinguishable from the ambient waters as a cold anomaly [68].

The role of oxygen intrusions below the upper sulphide boundary on depth profiles of chemical parameters in the western Black Sea is discussed in details by Murray and Yakushev (this volume). Recently Schippers et al. [80] explained the observed Mn(II) oxidation rates in the western Black Sea as a result of lateral oxygen intrusions with the modified Bosporus waters. The authors reported that intrusions were observed far below the oxic/anoxic interface up to the density surface of 18.4 kg m^{-3}. In Section 9.3 we discuss quantitatively the possible maximum impact of oxygen carried by Bosporus intrusions on the sulphide inventory in the Black Sea.

7. INTERMEDIATE SULPHUR SPECIES IN THE BLACK SEA WATER COLUMN

Inorganic sulphur species are important intermediates in the sulphur cycle. In euxinic environments, the most commonly detected S species are elemental sulphur, S^0, and thiosulphate, $S_2O_3^{2-}$. Sulphite, SO_3^{2-}, is usually of minor importance. Polythionates, $S_nO_6^{2-}$ (n=2-5), have not been reliably determined in the anoxic water due to analytical difficulties. Furthermore, polythionates are not stable in the presence of H_2S yielding $S_2O_3^{2-}$ and polysulphides [111]. In the presence of hydrogen sulphide, elemental sulphur usually reacts with HS^- and S^{2-} to form polysulphides, S_n^{2-} (n=2-6). In the presence of iron and

dissolved sulphur species, a range of insoluble iron sulphides, such as iron monosulphide (FeS), greigite (Fe_3S_4), and pyrite (FeS_2), are formed. Insoluble iron sulphides have been detected in water columns of the Black Sea and Framvaren Fjord [14, 58, 88]. Organic sulphur in the suspended phase and thiols have been measured in several anoxic marine basins [14, 20].

The origin of sulphur intermediate species under anoxic conditions is a controversial issue and the details of their transformations are poorly understood (for review see Zopfi et al. [111]). The formation of these species occurs via both chemical and biological reactions. Oxidation of hydrogen sulphide with oxygen and Fe(Mn) oxyhydroxides and sulfate reduction are the main processes responsible for sulphur intermediates formation in the euxinic water columns except of the elemental sulphur, which is formed only during hydrogen sulphide oxidation. Biological sulphide oxidation is described elsewhere in this volume (e.g., Overmann and Manske; Pimenov). Chemically mediated reactions of thiosulphate formation are elemental sulphur(polysulphides) hydrolysis, polythionate disproportionation, and the reaction between elemental sulphur and sulphite (e.g., [96]).

A number of different analytical techniques including voltammetry, reverse-phase high pressure liquid chromatography (RP-HPLC), colorimetry, ion chromatography have been used to measure concentrations of sulphur intermediates in euxinic environments (reviewed by Zopfi et al. [112]).

The occurrence of inorganic sulphur species in the oxic water is discussed elsewhere [99]. Data on sulphur intermediates using colorimetry method were obtained by Volkov [99] and by Volkov et al. [102]. The precision of the original method is ±3-5% and the detection limit is 0.03 μM [100]. The average concentrations of reduced inorganic sulphur species in the anoxic zone of the Black Sea are summarized in Table 3. Elemental sulphur data refer to the sum of elemental sulphur allotropes (zero-valent sulphur) and the zero-valent sulphur derived from some fraction (n-1) of the original polysulphide S_n^{2-}. Thiosulphate data in the table represent the total amount of thiosulphate, sulphite and polythionates.

Elemental sulphur concentrations in the Black Sea anoxic zone varied between zero and 5.4 μM and increased with depth. At some stations there was a concentration maximum observed at the oxic/anoxic interface. The latter is likely to be associated with sulphide oxidation by dissolved oxygen and/or Mn oxyhydroxides. [97] suggested that concentrations increasing with depth reflect ongoing process of polysulphide formation by the reaction between zero-valent sulphur and ΣH_2S. The vertical distribution of thiosulphate had similar shape as that of the elemental sulphur. The concentration range was from 0 to 5.9 μM. In contrast, Luther [50] using a cathodic stripping square wave voltammetry (CSSWV) method did not detect all, thiosulphate, sulphite and tetrathionate, in the Black Sea anoxic zone (method's detection limit is 50 nM). Zero-valent

Table 3. The mean and range of concentrations of sulphur intermediates in the Black Sea anoxic zone (from [97]).

Depth, m	*Number of samples*	H_2S, μM		S^0, μM		$S_2O_3^{2-}$, μM	
		Range	*Average*	*Range*	*Average*	*Range*	*Average*
115-150	16	0.5-22.1	8.1	0.06-5.4	0.66	0-1.7	0.45
150	7	13.5-28.8	15.3	0-1.2	0.38	0.05-1.5	0.54
160	8	16.5-34.6	20.1	0-2.2	0.53	0-3.4	1.1
170	5	3.7-36.9	23.5	0-1.0	0.41	0-1.6	0.60
180	4	11.4-42.1	24.5	0.13-0.63	0.44	0.04-3.7	1.3
200	5	n.d.		0.38-3.1	1.1	0.5-3.1	1.3
250	7	n.d.		0.34-5.1	1.3	0.26-5.9	1.6
300	5	n.d.		0.75-1.6	1.2	0.42-4.5	1.7
400	1	n.d.		n.d.	1.4	n.d.	1.6
500	4	n.d.		1.0-5.0	2.4	0.11-1.7	1.0
750	3	n.d.		0.59-1.4	0.91	1.3-2.7	2.1
1000	4	n.d.		1.5-2.5	2.1	1.0-4.2	2.1
1500	2	n.d.		2.3-2.9	2.6	1.7-2.7	2.2
2000	3	n.d.		2.1-4.6	3.4	1.5-3.5	2.8

elemental sulphur was collected on 0.2 μm filters. The maximum concentration measured at two central Black Sea stations in the anoxic zone was 61 nM (with a minimum detection limit between 5 and 10 nM). In contrast with Volkov [97], the concentration of S^0 did not change with depth. Luther [50] suspected that very low concentrations of elemental sulphur and probably even lower of polysulphides indicate that these species once formed can undergo rapid uptake or disproportionation by microorganisms. Luther [50] data for elemental sulphur are in the same order of magnitude as the data presented by Jørgensen et al. [32]. Vairavamurthy and Mopper [92] have detected maximum concentrations of sulphite and thiosulphate of 2.1 and 2.9 μM, respectively, in the Black Sea bottom waters using a derivatization method with a high-pressure liquid chromatography (HPLC) separation and quantification.

This brief overview of the existing data on the distribution of inorganic sulphur intermediates in the Black Sea anoxic zone shows a confused picture that may reflect both the non-equilibrium kinetics of chemical transformations within the sulphur cycle, and differences in methods employed. The origin of zero-valent elemental sulphur in the anoxic zone needs further investigation. This is particularly relevant to studies addressing ventilation of the anoxic zone by entrained modified Bosporus waters carrying dissolved oxygen and the existence of sulphur disproportionation reactions in the anoxic interior. Future progress in the field will depend on the advance in analytical techniques

capable to produce reliable data for individual sulphur intermediates in natural waters at low concentrations and on sampling and preparation methods without oxidation artefacts.

8. ALKALINITY AND C/S RATIOS

Alkalinity usually increases in the anoxic zone and in the pore water of marine sediments [19, 21, 27, 38, 52, 82, 101]. Total alkalinity A_T is a sum of several components such as hydrocarbonate (or carbonate) A_C and borate A_B alkalinities, both typical for anoxic and oxic waters. Silicate A_{Si}, hydrosulfide (sulfide) A_S, phosphate A_P, and ammonium A_N alkalinities add to the total alkalinity A_T in the anoxic water:

$$A_T = A_C + A_S + A_B + A_{Si} + A_P + A_N \text{ or}$$
$$A_T = [HCO_3^-] + 2[CO_3^{2-}] + [HS^-] + 2[S^{2-}] + [B(OH)_4^-] + [Si(OH)_3^-] + [HPO_4^{2-}] + 2[PO_4^{3-}] + [NH_3] + [OH^-] - [H^+] \quad (1)$$

Total alkalinity is calculated using in situ pH and dissociation constants for particular species in the equation (1) [21, 56]. Here we have used new alkalinity data obtained by Makkaveev (Shirshov Institute of Oceanology RAS, Moscow) in the north-eastern Black Sea during several cruises of *R/V Akvanavt* in 1999-2001. Close relationships between A_T and hydrogen sulphide $S_T = \Sigma$ (H_2S + HS^- + S^{2-}) have been observed during several years in the Black Sea anoxic water (Fig. 10):

In 1999: $A_T = 3304 + 3.11\ S_T$ (n = 134)
In 2000: $A_T = 3312 + 3.05\ S_T$ (n = 145)
In 2001: $A_T = 3302 + 3.04\ S_T$ (n = 180)
Average: $A_T = 3306 + 3.06\ S_T$ (n = 459).

The average A_T of 4457 μM and total hydrogen sulphide S_T of 376 μM in the bottom layer of 1700-2200 m were used to calculate the increase of total alkalinity (ΔA_T) and its components in the layer from 100 to 2000 m (Table 4). The contribution of different components in the total alkalinity changes with depth. The sulfide component is responsible for up to 312 μM (or 27%) of the total alkalinity increase ΔA_T in the anoxic zone. Silicate, phosphate and ammonium components increase with depth too, but their relative contribution is insignificant compared to A_S. The role of borate alkalinity decreases insignificantly with depth.

The stoichiometry of the organic matter decomposition suggested by Richards [75] is closely connected with the alkalinity concept:

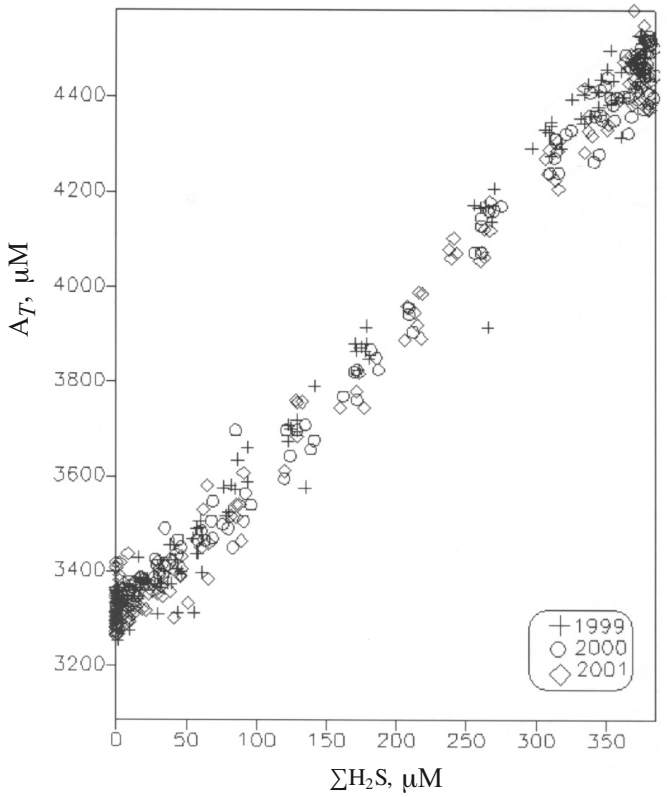

Figure 10. The relationship between total alkalinity A_T and dissolved sulphide $\sum H_2S$ in the Black Sea water column.

$$(CH_2O)_{106}(NH_3)_{16}MeHPO_4 + 53SO_4^{2-} \rightarrow 106HCO_3^- + 16NH_4^+ + 37H_2S + 16HS^- + MeHPO_4 \quad (2)$$

Where $\Delta A_T = 123$, $\Delta A_T / \Delta C_T = 1.16$, $\Delta A_T / S_T = 2.32$, e.g. when $\Delta C_T / S_T = 2$ then $\Delta A_T / S_T = 2\ \Delta A_T / \Delta C_T$. The "Richard's" equation is usually used to derive theoretical ratios of nutrients formed during mineralization of the organic matter. The 'theoretical ratios' can be compared with the observed in situ ratios. Deviations in the observed $\Delta C_T / S_T$ ratios in the Black Sea anoxic zone have been explained either by the non-stoichiometric mineralization of the organic matter or by a relative increase(decrease) in the total inorganic carbon due to $CaCO_3$ dissolution(precipitation) reactions [19, 27, 108, 110].

The stoichiometry of the organic matter composition and its anaerobic mineralization (C:S:N:P = 106:53:16:1) is only the first approximation of the

Table 4. Total alkalinity (A_T) and the increases over depth of total alkalinity (ΔA_T) and its components in the anoxic zone of the Black Sea (see text for details).

Depth or depth interval, m	Total alkalinity and its components (μM)						
	A_T	A_C	A_S	A_N	A_P	A_{Si}	A_B
100	3306	3283	0	0.21	1.26	2.10	19
200	4457	4117	312	1.10	7.64	5.00	14
				ΔA_T			
100-2000	**1151**	**834**	**312**	**0.89**	**6.38**	**2.90**	**-5.0**
				% of A_T			
100	100	99.30	0	<0.01	0.04	0.06	0.57
2000	100	92.37	7.00	0.02	0.17	0.11	0.31
				% of ΔA_T			
100-2000	**100**	**72.46**	**27.11**	**0.08**	**0.55**	**0.25**	**-0.43**

ongoing complex biogeochemical and physiochemical mineralization processes in seawater [101]. Among factors that complicate the application of "Richard's stoichiometry" for describing the aerobic and anaerobic mineralization of organic matter are seasonal changes in the composition of plankton communities and non-stoichiometric composition of the total organic carbon and its components.

Given that $\Delta A_T \approx \Delta A_C + \Delta A_S$ and pH changes with depth, the ratios $\Delta A_C/\Delta C_T$, $\Delta A_S/\Delta C_T$, and $\Delta A_T/\Delta C_T$ cannot be constant with depth according to Richards' equation. If $C_T = 1$ and $C_T/S_T = 2$ in the pH range of 6.6-8.2, $\Delta A_C/C_T$ must increase from 0.8 to 1.08, $\Delta A_S/C_T$ from 0.21 to 0.48. $\Delta A_T/C_T$ and $\Delta A_T/S_T$ ratios must change from 1.01 to 1.56 and from 2.02 to 3.12, respectively [103]. Theoretical Richardsian $\Delta A_T/C_T = 1.16$ and $\Delta A_T/S_T = 2.32$ will occur when pH is 6.8-6.9, which is the pH range observed in the bottom water of the Framvaren Fjord below 100 m. In the Black Sea anoxic zone with pH=7.5-7.7, $\Delta A_T/C_T$ is in the range of 1.40-1.46, whereas it is equal to 1.48-1.50 in the anoxic water of the Cariaco Trench with pH=7.8-7.9. In sum, fixed Richards' stoichiometry in equation (2) can not be used to describe alkalinity changes during anaerobic mineralization of the organic matter under different pH conditions.

Volkov et al. [103] have undertaken a systematic analysis of the alkalinity variations and its composition in different anoxic basins using own and published data [109, 110]. These results showed that the increase in total alkalinity with depth and its compositional changes in anoxic waters are determined by the scale (depth) of the organic matter mineralization process and pH that is itself a function of the anaerobic mineralization. Carbonate and sulfide alkalinities are

the predominant alkalinity forms and serve as a buffer system determining pH. Other alkalinities such as ammonium, silicate, and phosphate alkalinities are formed in response to pH conditions. Depending on the total H_2S concentration, the role of sulfide alkalinity in the total alkalinity increases from 2% in the Cariaco Trench and 7% in the Black Sea to 24% in the Framvaren Fjord. The total alkalinity increase ΔA_T with depth in the Black Sea is supported by 27% increase in the sulfide component (ΔA_S). Overall the total alkalinity increase in the anoxic zone of the Black Sea (ΔA_T) is explained by 99.6% increase in the carbonate (ΔA_C) and sulfide (ΔA_S) alkalinities.

The $\Delta C_T/S_T$ ratio of 2.09-2.17 and $C_T = 3240 + 2.13S_T$ calculated using new alkalinity and sulphide data show that bacterial sulfate reduction is the only significant process of the anaerobic mineralization of organic matter in the anoxic zone of the Black Sea. Insignificant deviations of 10-15% from the "theoretical" C/S ratio of 2.0 can be explained by methodological problems with alkalinity and sulphide measurements or by fermentation reactions resulting in CO_2 generation in addition to sulfate reduction. The conclusion that sulfate reduction is the dominant process of organic matter mineralization in the anoxic water column is valid not only for the Black Sea, but also for Cariaco Trench and Framvaren Fjord, where C/S ratios are in the range of 2.00-2.19 [103].

9. SULPHIDE BUDGET IN THE BLACK SEA

The sulphur budget for the Black Sea has been considered in several papers [3, 8, 48, 49, 64, 82]. The main budget components to be considered are: sulphide production in sediments and sulphide flux at the sediment/water interface, sulphide production in the water column, sulphide oxidation at the oxic/anoxic interface and in the basin interior by dissolved oxygen of the modified Mediterranean water, and iron sulphide formation in the water column.

9.1 Sulphide Production in Deep-Sea Sediments

Based on measurements by Sorokin [83], Deuser [17] calculated an average annual sulphide production in Black Sea sediments of 3.6 Tg. No sulfate reduction was measured below the uppermost 5 cm of sediment [83]. Sulphate reduction presence throughout the whole Holocene and upper Pleistocene sedimentary sequences was challenged by Vainshtein and co-authors [91]. Recent data on the presence of the anaerobic methane oxidation have shown that sulphate-reducing bacteria can be active in deep sediments of the Black Sea [33]. Lein et al. [49] calculated the average hydrogen sulphide production in the anoxic sediments of the Black Sea of about 560 mmol m^{-2} yr^{-1}, or 5.9 Tg yr^{-1}. This estimate is higher than Deuser's because the whole Holocene sequence was considered. Recent measurements by Albert and co-authors [3] gave an average sulphide production in the upper 20 cm (including 2 cm fluffy layer)

of about 5.2 Tg yr^{-1}. Lein and Ivanov [47] have estimated the total sulphide burial in the Black Sea of 2.4 Tg yr^{-1} including about 1 Tg yr^{-1} that is buried in the anoxic zone. Using these data and integrated over the upper 20 cm of sediments sulfate reduction rates, Neretin et al. [63] concluded that the annual sulphide flux into the water column from sediments of the anoxic zone is in the range between 3 and 5 Tg per year. The value is likely to be overestimated due to spatial differences in pyrite burial rates and possible sulphide diffusion downward into the deeper sediment layers [33]. The limnic Late Pleistocene clays with high reactive iron and low dissolved sulphide concentrations are often exposed to the surface on continental slopes of the Black Sea bordering the Caucasus and Anatolia [104]. These sediments may serve as a sink for hydrogen sulphide formed in the deep sea.

9.2 Hydrogen Sulphide Production in the Black Sea Water Column

Measurements of SRRs in Black Sea water column are summarized in Table 5 [64]. Generally, a maximum in sulfate reduction rates is observed in the upper (200-300 m down to 600-700 m) part of anoxic column and in the layers adjacent to the bottom. The highest rate measured for the upper anoxic zone so far was 1569 nmol l^{-1} day^{-1} [29]. The lowest SRRs in the water column are reported by Albert et al. [3] and do not exceed 3.5 nmol l^{-1} day^{-1}. With a sensitivity of the radiotracer method of about 0.2-0.6 nmol l^{-1} day^{-1} [3, 49], reduction of sulfate in the intermediate zone (600(700)-2000 m) comprising the main part of the Black Sea hydrogen sulphide pool has not been detected [49, 83]. SRRs in these layers are 1-2 orders of magnitude lower than in the proximity to the upper anoxic boundary [3, 28].

Seasonal variability of sulfate reduction in the water column is still unresolved. The only data acquired in wintertime show measurable SRR in the upper 200-300 m only at three of nine sampling stations [86]. The authors attributed the absence of SR at the other stations during this season to the disappearance of anaerobic bacterial community in the central parts of the basin due to intense mixing at the chemocline during winter convection. Careful examination of the published data and methods suggests that the variability in the SRR is not an analytical artifact. Existing data sets are characterized by significant seasonal variations and yield the average sulphide production in the water column of 41±31 (95%CI) Tg yr^{-1}.

Sulfate reduction in the deeper parts of the anoxic zone is probably particle-associated. Vertical distribution of this process is related to sinking rate and size of the particles, and can have a seasonal pattern and spatial patchiness. Concentrations and turnover times of potentially important substrates for sulfate-reducers (acetate, lactate, formate) in the anaerobic layers are well above the

Table 5. Hydrogen sulphide production in the Black Sea water column from experimental measurements with $^{35}SO_4^{2-}$ (from [64]).

Season	Number of stations	Maximum SRR (nmol day^{-1})	Mean (range) sulphide production (Tg yr^{-1})	Reference	Remarks
Winter	9	309	17 (0-105)	[86]	data below to 300-400 m
Spring	7	117	109 (11-207)	[28]	data below 300 m
Spring	2	3.5	2.7 (0.9-4.6)	[3, 32]	whole water depth
summer	9	1569	61 (8-190)	[29]	data below to 1000 m
Summer	3	86	34 (25-44)	[83]	with temperature correction factor 2.5; whole water depth
autumn	2	129	20 (15-24)	[49]	whole water depth
Mean			41 ± 31 (95%CL)		

threshold levels and could also support particle-associated processes. Competition with acetoclastic methanogens or iron limitation could also limit active growth of sulfate reducers in anoxic layers [3, 93].

Modeling data [64] combined with median data from experimentally determined SRRs yield SR rates in the water column in the range of 30 to 50 Tg yr^{-1}. This is one order of magnitude higher than the potential flux of hydrogen sulphide from bottom sediments. Despite the fact that the gross SR activity is highest close to the interface and in general concentrated in the upper 500 m, most of the net water column sulphide production occurs in the middle and lower parts of the sulfidic zone.

9.3 Sulphide Oxidation at the Oxic/Anoxic Interface and Sulphide Removal with Dissolved Oxygen of the Lower Bosporus Current

Integration of the measured using $H_2{}^{35}S$ oxidation rates in the Black Sea chemocline yielded values between 53 and 125 Tg yr^{-1} [32, 84, 85], which

are probably overestimated. Rate measurements and modeling data give the median sulfide oxidation rates in the range from 20 to 50 Tg yr^{-1} [64].

The role of dissolved oxygen intrusions in sulphide removal is a subject of intensive scientific debate. The annual Bosporus flux into the Black Sea is estimated to be 120-312 km^3 [90]. In regard of the significant variability in the magnitude and direction of water exchange through the Bosporus, and the absence of quantitative information on the volumes of entrained waters during the cascade-like intrusions to the anoxic zone, satisfactory estimates of the sulphide removal rates by the Lower Bosporus Current are impossible at the moment. Qualitatively, the significant role of the modified Bosporus waters in the entrainment of the Black Sea interior was confirmed by direct in situ measurements of physiochemical parameters in the areas adjacent to the Bosporus (reviewed by Murray and Yakushev, this volume).

Sulphide oxidation in the anoxic interior was estimated using reported in the literature entrainment ratios and simple chemistry of the sulphide oxidation by Neretin et al. [64]. The authors have found that sulphide consumption with Bosporus intrusions may vary in the range 4.4-9.2 Tg yr^{-1}, which roughly represents 10-20% of the sulphide oxidation at the oxic/anoxic interface. The modeling approach has shown that the oxygen flux below the anoxic interface may be responsible for as much as 50-70% of the total sulphide consumption in the Black Sea water column [42].

Apart from oxygen intrusions with the entrained modified Bosporus waters, other lateral sources of oxygen were discussed in the literature. Mesoscale dynamics characterized by the existence of anticyclonic gyres described in the Sections 4 and 5 may provide an efficient mechanism for the ventilation of the anoxic zone. In addition, in some years intensified density convention in winter superimposed by internal wave forcing may cause the erosion of the upper pycnocline and ventilate the upper anoxic layers [44, 89]. Lateral intrusions of oxygen are not specific for the Black Sea only and have been reported in other anoxic marine basins such as the Cariaco Basin (Scranton et al., this volume), Framvaren Fjord [109], and the Mariager Fjord [112]. At the moment, without extensive temporal and special studies, the contribution of these processes in sulphide removal below the oxic/anoxic interface for the whole basin is difficult to estimate. The cumulative effect of the modified Bosporus waters together with mesoscale eddies providing dissolved oxygen laterally may have significant impact on the total sulphide oxidation in the basin and need to be addressed by future studies.

9.4 Fe Sulphide Formation in the Black Sea Water Column

Pyrite formation in the water column of the Black Sea is the subject of several studies [14, 58, 88, 98]. Some authors suggested that that most syngenetic

pyrite forms in the upper part of the anoxic zone (below to 200 m) [12, 51, 58], whereas others have argued that the zone of pyrite formation in the water column is wider and may take place down to 1000-1500 m water depth [88]. Mass-balance calculation by Neretin et al. [64] suggested that only about 10-50% of the sulphur buried in sediments may come from the syngenetic component. The magnitude of the particulate sulphur flux in the Black Sea water column is in the range of 0.1-0.5 Tg yr^{-1} [58, 88].

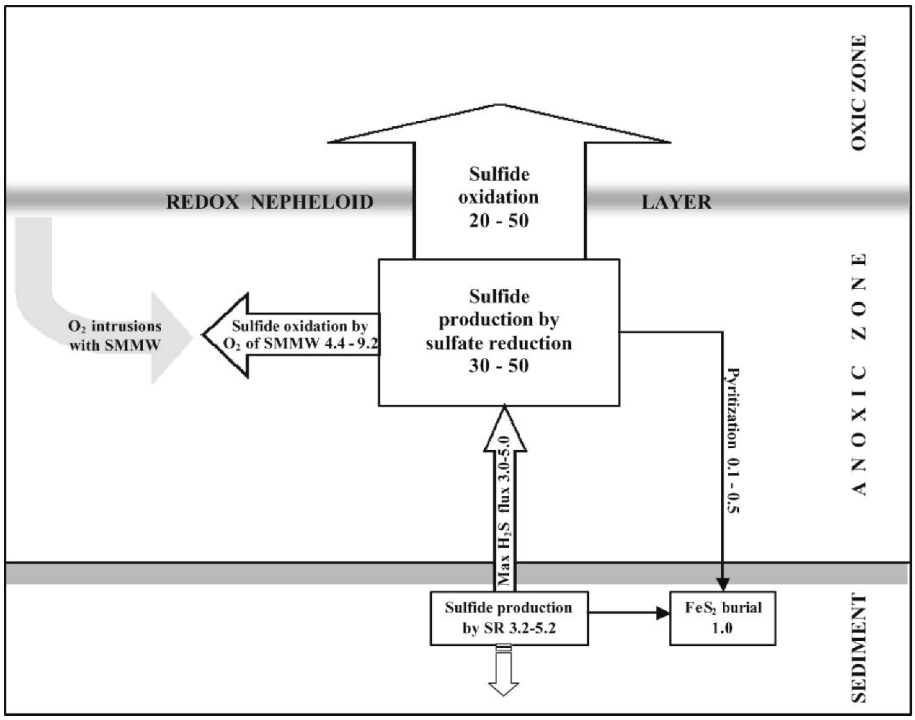

Figure 11. Sulphur budget for the Black Sea anoxic zone. The width of arrows and dimension of boxes represent the relative magnitudes of respective processes. SMMW stands for "Shelf Modified Mediterranean Water". Processes rates are in Tg yr^{-1} [64].

10. CONCLUSIONS

A general scheme of the processes within the sulphur cycle as discussed above and with their assigned annual fluxes is presented in Fig. 11. Hydrogen sulphide inventory and the location of the upper sulphide boundary is a delicate balance between complex physical and biological processes. Among them are ventilation of the Cold Intermediate Layer (CIL), the entrainment ratio between CIL and the Modified Lower Bosporus waters, and the rates of organic matter respiration processes, specifically oxygen consumption in the oxic zone. If the

average sulphide production in the Black Sea is 30-50 Tg yr^{-1} and represents an average annual figure, and the total sulphide inventory is about 4.6×10^3 Tg, then the residence time of hydrogen sulphide in the water column would is about 90-150 yr. This value compares well with the water exchange rate between oxic and anoxic layers (e.g., [82]).

Temporal variations in the average depth of the chemocline in the Black Sea and particularly in the sulphide boundary are mainly the result of climatic changes in the density structure of the water column. The upper anoxic boundary location versus density for this basin has not changed over the period from 1910 to 1995 [8]. However, recent data have shown a prominent increase in sulphide concentrations, as well as nutrient levels, within the anoxic zone (at 1000-2000 m) supposedly due to anthropogenic impact [43] or climatic variations. Future research is needed to reveal how significant this fact or it does reflect statistical artifacts and measurements bias.

In this review we emphasize the importance of ventilation processes in the Black Sea anoxic zone. The sulphide budget demonstrates that the Bosporus flux cannot be considered a main factor for deep basin ventilation. More attention in future studies should be paid to near-shore mesoscale dynamics and their influence on chemocline processes and transversal exchange between shore and open waters [39, 76]. Severe winter conditions accompanied by strong horizontal and vertical mixing can initiate pronounced erosion of the pycnocline. The propagation of anticyclonic gyres along the Rim Current may serve as an additional source of dissolved oxygen into the upper anoxic layers (e.g., Ovchinnikov et al. [73]). Field data for the winter season are critical to progress in our understanding of the Black Sea ecosystem. These processes are important for the specific biogeochemical pathways within the sulphur cycle in the Black Sea, particularly for the production of sulphur intermediate species. The regular monitoring of mesoscale physical and chemical dynamics should be implemented in order to understand ventilation processes in the anoxic interior.

Acknowledgements

The authors wish to thank N.N. Zhabina (P.P. Shirshov Institute of Oceanology, Moscow) for invaluable analytical help and crews of RV *Akvanavt*, *Yantar* and *Petr Kotzov* for collaboration. We are grateful to T. Ferdelman (MPI MM) for review and editorial assistance. This work was financially supported by the Russian Fund for Basic Research (grant 05-05-65092), Project 14.4.3. "World Ocean" of the Russian Academy of Sciences, and Project "Black Sea" of the Russian Ministry of Science to IIV and the German Science Foundation and Max-Planck-Society for LLN.

References

[1] Aksu A.E., Hiscott R.N. and Yasar D. Oscillating Quaternary water levels of the Marmara Sea and vigorous outflow into the Aegean Sea from the Marmara Sea-Black Sea drainage corridors. Mar Geol 1999; 153:275-302.

[2] Aksu A.E., Mudie P.J., Rochon A., Kaminski M., Abrajano T. and Yasar D. Persistent Holocene outflow from the Black Sea to the eastern Mediterranean contradicts Noah's Flood hypothesis. GSA Today 2002; May 2002 Issue:1-9.

[3] Albert D.B., Taylor G. and Martens C. Sulfate reduction rates and low molecular weight fatty acid concentrations in the water column and surficial sediments of the Black Sea. Deep-Sea Res I 1995; 42:1239-1260.

[4] Andrianova O.P. and Ovchinnikov I.M., 1991. Transformation of fresh waters in the western Black Sea. Meteorologiya i Gidrologiya 7, 74-79. (In Russian)

[5] Ayzatullin T.A., Leonov A.V. and Shaporenko S.N. "Mathematical modelling of the formation and evolution of the Black Sea anoxic zone". In *Current problems in oceanography.* Moscow, Nauka, 2003. (In Russian)

[6] Balabanov I.P., Kwirelia B.D. and Ostrovskiy A.B. Recent formation of geological features of the Pitzunda peninsula zone. Tbilisi, 1981. (In Russian).

[7] Bastürk Ö., Volkov I.I., Gökmen S., Gungor H., Romanov A.S. and Yakushev E.V. International expedition RV "Bilim" in July 1997 in the Black Sea. Okeanologiya 1998; 38:473-76 (In Russian).

[8] Bezborodov A.A. and Eremeev V.N. The Black Sea: oxic/anoxic interface zone. Marine Hydrophysical Institute AS of the Ukraine, Sevastopol, Ukraine, 1993. (In Russian)

[9] Bogdanova A.K. On the distribution of Mediterranean waters in the Black Sea. Okeanologiya 1961; 1:983-91 (in Russian).

[10] Boudreau B.P. and LeBlond P.H. A simple evolutionary model for water and salt in the Black Sea. Paleoceanogr 1989; 4:157-66.

[11] Bruevich S.V. Buried freshened pore waters under modern Black Sea sediments. Dokl Akad Nauk SSSR 1952; 84:575-77. (In Russian)

[12] Calvert S.E., Thode H.G., Yeung D. and Karlin R.E. A stable isotope study of pyrite formation in the Late Pleistocene and Holocene sediments of the Black Sea. Geochem Cosmochim Ac 1996; 60:1261-70.

[13] Cline J.D. Spectrophotometric determination of hydrogen sulphide in natural waters. Limnol Oceanogr 1969; 14:454-58.

[14] Cutter G.A. and Kluckhohn R.S. The cycling of particulate carbon, nitrogen, sulphur, and sulphur species (iron monosulphide, greigite, pyrite, and organic sulphur) in the water columns of Framvaren Fjord and the Black Sea. Mar Chem 1999; 67: 149-60.

[15] Di Iorio, D., Yüce, H. Observations of Mediterranean flow into the Black Sea. J Geophys Res 1999; 104(C2): 3091-3108.

[16] Degens E.T. and Ross D.A. Chronology of the Black Sea over the last 25,000 years. Chem Geol 1972; 10:116.

[17] Deuser W.G. Organic carbon budget of the Black Sea. Deep-Sea Res I 1971; 18: 995-1004.

[18] Deuser W.G. "Evolution of anoxic conditions in the Black Sea during Holocene". In *The Black Sea–Geology, Chemistry and Biology.* Degens E.T. and Ross D.A., eds., AAPG Tulsa, Oklahoma, 1974.

[19] Dyrssen D. Some calculations on the Black Sea chemical data. Chemica Scripta 1985; 25:199-205.

[20] Dyrssen D., Haraldsson K., Westerlund S, and Ären K. Indication of thiols in Black Sea water. Mar Chem 1985; 17:323-27.

[21] Dyrssen D., Haraldsson K., Westerlund S, and Ären K. Report XXXII on the chemistry of seawater. Dept. of Anal. Chem. Marine Chem 1986, Chalmers University of Technology, Göteborg University, Göteborg, Sweden, 1986.

[22] Eremeev V.N. and Kushnir V.M. The bottom convective layer in the Black Sea: current results and future studies. Marine Hydrophysical Journal 1998; 1:50-70. (In Russian)

[23] Falina A.S. and Volkov I.I. About fine structure and thermohaline stability of the deep Black Sea waters. Okeanologiya 2003; 43(4):516-23. (In Russian)

[24] Falina A.S. and Volkov I.I. The role of double diffusion in general hydrological structure of the Black Sea deep waters. Okeanologiya 2005; 45(1):21-31. (In Russian)

[25] Frenzel B. "European Climate Reconstructed from Historical Documents: Methods and Results". In *Paleoclimate Research*, Fischer Verlag, Stuttgart, Special Issue 7, 1992.

[26] Görur N., Cagatay M.N., Emre Ö., Alpar B., Sakinc M., Islamoglu Y., Algan O., Erkal T., Keser M., Akkok R. and Karlik G. Is the abrupt drowning of the Black Sea shelf at 7150 yr. BP a myth? Mar Geol 2001; 176:65-73.

[27] Goyet C.A., Bradshwa L. and Brewer P.G. The carbonate system in the Black Sea. Deep Sea Res II 1991; 38:S1049-S1068.

[28] Gulin, M.B. The investigation of bacteria mediated sulfate reduction and chemosynthesis in the Black Sea water column. Ph.D. thesis abstract, Institute of biology of the southern seas, Sevastopol, Ukraine, 1991. (In Russian)

[29] Il'chenko, S.V., Sorokin Yu.I. "To the estimate of hydrogen sulphide production in the Black Sea". In *The Black Sea ecosystem variability: natural and anthropogenic factors.* Vinogradov M.E., ed., Nauka, Moscow, 1991. (In Russian)

[30] Ivanov L.I. and Samodurov A.S. The role of lateral fluxes in ventialtion of the Black Sea. J Mar Syst 2001; 31:159-174.

[31] Ivanov L.I. and Shkvorets I.Yu. Thermohaline structure of the Black Sea deep and bottom waters. Marine Hydrophysical Journal 1995; 6:53-61. (In Russian)

[32] Jørgensen B.B., Fossing H., Wirsen C.O. and Jannasch, H.W. Sulphide oxidation in the anoxic Black sea chemocline. Deep-Sea Res II 1991; 38(2A):S1083-S1103.

[33] Jørgensen B.B., Böttcher M.E., Lüschen H., Neretin L.N. and Volkov I.I. Anaerobic methane oxidation and a deep H_2S sink generate isotopically heavy sulphides in Black Sea sediments. Geochem Cosmochim Ac 2004; 68(9):2095-2118.

[34] Jones G. and Gagnon A. AMS radiocarbon dating of sediments in the Black Sea. Deep-Sea Research I 1994; 41: 531-557.

[35] Kaplin P.A. and Selivanov A.O. Late glacial and Holocene sea level changes in semi-enclosed seas of North Eurasia: Examples from the contrasting Black and White Seas. Paleogeogr Paleoclimat Paleoecol 2004; 209:19-36.

[36] Karaca M., Wirth A., Ghil M. A box model for the paleoceanography of the Black Sea. Geophys Res Lett 1999; 26:497-500.

[37] Kelley D.E., Fernando H.J., Yargett A.E., Tanny J. and Özsoy E. The diffusive regime of double-convection. Progr Oceanogr 2003; 56(3-4):461-81.

[38] Kempe S. Alkalinity: the link between anaerobic basins and shallow water carbonates? Naturwissenschaften 1990; 77:426-27.

[39] Kempe S., Diercks A.R., Liebezeit G. and Prange A. "Geochemical and structural aspects of the pycnocline in the Black Sea (R/V Knorr 134-8 Leg 1, 1988)". In *Black Sea Oceanography,* Izdar E. and Murray J.M., eds. NATO ASI Series C, Vol. 351, Kluwer Academic Publishers, 1991.

[40] Kerey I.E., Meric M., Tunoglu C., Kelling G., Brenner R.L. and Dogan A.U. Black Sea-Marmara Sea Quaternary connections: New data from the Bosporus, Istanbul, Turkey. Paleogeogr Paleoclimat Paleoecol 2004; 204:277-95.

[41] Konovalov S.K. and Murray J.W. Variations in the chemistry of the Black Sea on a time scale of decades (1960-1995). J Mar Sys 2001; 31:217-43.

[42] Konovalov S.K., Ivanov L.I. and Samodurov A.S. Fluxes and budget of sulphide and ammonia in the Black Sea. J Mar Syst 2001; 31:203-16.

[43] Konovalov S.K., Eremeev V.N., Suvorov A.M., Khaliulin A.Kh. and Godin, E.A. Climatic and anthropogenic variations in the sulphide distribution in the Black Sea. Aquat Geochem 1999; 5:13-27.

[44] Krivosheya V.G., Titov V.B., Ovchinnikov I.M., Kos'yan R.D. and A.Yu. Skirta. Influence of circulation and mesoscale eddies on the deep water location of the upper sulphide boundary of the hydrogen sulphide zone and ventilation of the anaerobic zone of the Black Sea. Okeanologiya 2000; 40(6):816-25. (In Russian)

[45] Kutas R.I., Paliy S.I. and Rusakov O.M. Deep faults, heat flow and gas leakage in the northern Black Sea. Geo-Mar Lett 2004; 24:163-168.

[46] Lane-Serff G.F., Rohling E.J., Bryden H.L. and Charnock H. Postglacial connection of the Black Sea to the Mediterranean and its relation to the timing of sapropel formation. Paleoceanogr 1997; 12:169-74.

[47] Lein A.Yu. and Ivanov M.V. "Reduced sulphur accumulation in sediments of marine basins with high rates of sulphate reduction". In *The Global Biogeochemical Sulphur Cycle.* SCOPE 19, Wiley & Sons, Chichester, UK, 1983.

[48] Lein A.Yu. and Ivanov M.V. "On the sulphur and carbon balances in the Black Sea". In *The Black Sea oceanography* Izdar E. and Murray J.W .,eds. Kluwer Acad Publ, Amsterdam, 1991.

[49] Lein A.Yu., Ivanov M.V., Vaynshtein M.B. Hydrogen sulphide balance in the deep water zone of the Black Sea. Microbiologiya 1990; 59:656-64. (In Russian)

[50] Luther III G.W. Sulphur and iodine speciation in the water column of the Black Sea. In Black Sea Oceanography, E. Izdar and J.W. Murray, eds. Kluwer Acad Publ, 1991.

[51] Lyons T. Sulphur isotopic trends and pathways of iron sulphide formation in upper Holocene sediments of the anoxic Black Sea. Geochem Cosmochim Ac 1997; 61:3367-3382.

[52] Makkaveev P.N. Dissolved inorganic carbon and total alkalinity in the anaerobic water of the Black Sea. Okeanologiya 1995; 35(4):537-43. (In Russian)

[53] Makkaveev P.N. "Calculation of the total alkalinity components in the Black Sea water". In *Interdisciplinary studies of the north-western BlackSea.* Zatsepin A.G. and Flint M.V., eds. Nauka, Moscow, 2002. (In Russian)

[54] Mamaev O.I. Primitive model for the Black Sea salinization. Oceanologiya 1995; 34(6):756-59. (In Russian)

[55] Mamaev O.I. Double diffusion in the analytical theory of T-S curve. Okeanologiya 1995; 35(2):168-77. (In Russian)

[56] Millero F.J. Thermodynamics of the carbon dioxide system in the oceans. Geochim Cosmochim Ac 1995; 59(4):661-77.

[57] Mudie P.J., Rochon A. and Aksu A.E. Pollen stratigraphy of Late Quaternary cores from Marmara Sea: land–sea correlation and paleoclimatic history. Mar Geol 2002; 190(1-2):233-60.

[58] Muramoto J., Honjo S., Fry B., Hay B.J., Howarth R.W. and Cisne J.L. Sulphur, iron and organic carbon fluxes in the Black Sea: sulphur isotopic evidence for origin of sulphur fluxes. Deep-Sea Res II 1991; 38(2A):S1151-S1189.

[59] Murray J.W., Codispoti L.A. and Friederich G.E. "Oxidation-reduction environments: The suboxic zone in the Black Sea". In *Aquatic Chemistry.* Huang C., O' Melia C.R., Morgan J.J. eds., Kluwer Acad Publ, Amsterdam, 1995.

[60] Murray J.W., Top Z. and Özsoy E. Hydrographic properties and ventilation of the Black Sea. Deep-Sea Research II 1991; 38(2A):S663-S689.

[61] Neretin L.N. Contemporary state of the hydrogen sulphide zone in the Black Sea, Ph.D. thesis abstract, P.P.Shirshov Institute of Oceanology RAS, Moscow, 1996. (In Russian)

[62] Neretin L.N. and Volkov I.I. On the vertical distribution of hydrogen sulphide in deep waters of the Black Sea. Okeanologiya 1995; 35:60-65.

[63] Neretin, L.N., Böttcher M.E. and Grinenko V.A. Sulphur isotope geochemistry of the Black Sea water column. Chem Geol 2003; 200:59-69.

[64] Neretin L.N., Volkov I.I., Böttcher, M.E. and Grinenko, V.A. A sulphur budget for the Black Sea anoxic zone. Deep Sea Res I 2001; 48:2569-93.

[65] Nevesskaya L.A. *Late Quaternary Bivalvia of the Black Sea: Their Systematics and Ecology.* Nauka, Moscow, 1965. (In Russian)

[66] Novoselov A.A. and Romanov A.S. "Present state of the Black Sea anoxic zone". In *The origin and seasonal variability of hydrophysical and hydrochemical parameters in the Black Sea.* MHI, Sevastopol, 1988. (in Russian)

[67] Özsoy E., Rank D. and Salihoglu I. Pycnocline and deep mixing in the Black Sea: stable isotope and transient tracer measurements. Estuar Coast Shelf Sci 2002; 54:621-29.

[68] Özsoy E., Ünlüata U. and Top Z. The Mediterranean water evolution, material transport by double diffusion intrusions, and interior mixing in the Black Sea. Progr Oceanogr 1993; 31:275-320.

[69] Özsoy E., Top Z., White G. and Murray J.W "Double diffusive intrusions, mixing and deep sea convection processes in the Black Sea". In *The Black Sea Oceanography.* Izdar E. and Murray J.W., eds., NATO/ASI Series. Kluwer Acad Publ, Dordrecht, 1991.

[70] Oguz T. and Besiktepe S. Observations on the Rim Current structure, CIW formation and transport in the western Black Sea. Deep Sea Res I 1999; 46:1733-53.

[71] Oguz T., Latun V.S., Latif M.A., Vladimirov V.V., Sur H.I., Markov A.A., Ozsoy E., Kotovshchikov B.B., Eremeev V.V. and Unluata U. Circulation in the surface and intermediate layers of the Black Sea. Deep-Sea Res I 1993; 40:1597-1612.

[72] Ostrovskii A.B., Izmailov Ya.A., Shcheglov A.P. and Arslanov Kh.A. "New data on Pleistocene stratigraphy and geochronology from marine terraces of the Caucasus Black Sea coast and Kerch-Taman region". In *Paleogeography and sediments of Pleistocene in Southern Seas of USSR*. Nauka, Moscow, 1977.

[73] Ovchinnikov,I.M., Titov V.B., Krivosheya V.G. and Popov Yu.I. Principal hydrophysical processes and their role in the ecology of the Black Sea. Okeanologiya 1993; 33:801-807. (In Russian)

[74] Podymov O.I. Quantitative characteristics of the redox layer of the Black Sea assessed with problem-oriented database. Ph.D. thesis abstract. Shirshov Institute of Oceanology RAS, Moscow, Russia, 2005. (In Russian)

[75] Richards F.A. *Anoxic basins and fjords. Chemical Oceanography.* Vol. 1. NY Acad. Press. NY, 1965.

[76] Rozanov A.G., Neretin L.N. and Volkov I.I. "Redox nepheloid layer (RNL) of the Black Sea: its location, composition and origin". In *Ecosystem modeling as a management tool for the Black Sea.* Ivanov L.I. and Oguz T., eds. Kluwer Acad Publ, Amsterdam, 1998.

[77] Ryan W.B.F. and Pitman W. Noah's Flood: The new scientific discoveries about the event that changed history. Simon and Schuster, NY, 1998.

[78] Ryan W.B.F., Major C.O., Lericolais G. and Goldstein S.L. Catastrophic flooding of the Black Sea. Ann Rev Earth Planet Sci 2003; 31:525-54.

[79] Ryan W.B.F., Pitman W.C.I., Major C.O., Shimkus K. and Moskalenko V., Jones G.A., Dimitrov P., Gorur N., Sakinc M. and Yuce H. Abrupt drowning of the Black Sea shelf. Mar Geol 1997; 138:119-26.

[80] Schippers A., Neretin L.N., Lavik G., Leipe Th. and Pollehne F. Manganese (II) oxidation driven by lateral oxygen intrusions in the western Black Sea. Geochim Cosmochim Ac 2005; 69:2241-52.

[81] Siddall M., Pratt L.J., Helfrich K.R. and Giosan L. Testing the physical oceanographic implications of the suggested sudden Black Sea infill 8400 years ago. Palaeoceanogr 2004; 19:PA1024.

[82] Skopintsev B.A., 1975. Formation of contemporary chemical composition of the Black Sea waters. Hidrometeoizdat, Leningrad, 1975. (In Russian)

[83] Sorokin Yu.I. Experimental investigation of bacterial sulfate reduction in the Black Sea using ^{35}S. Microbiologiya 1962; 31:329-35. (In Russian)

[84] Sorokin Yu.I. The bacterial population and the processes of hydrogen sulphide oxidation in the Black Sea. Journal du Conseil International pour l'Exploration de la Mer 1972; 34:423-54.

[85] Sorokin Yu.I. "The Black Sea". In *Ecosystems of the world.* Vol. 26. Estuaries and enclosed seas, Ketchum B.H., ed. Elsevier, Amsterdam, 1983.

[86] Sorokin Yu.I., Sorokin P.Yu., Sorokina O.V., Sorokin D.Yu. and Sukhomlin A.V. "The distribution and functional activity of bacteria in the Black Sea water column during winter-beginning spring 1991". In *The open Black Sea ecosystem during wintertime.* Vinogradov M.E., ed. P.P.Shirshov Institute of Oceanology, Moscow, 1992. (In Russian)

[87] Svitoch A.A., Selivanov A.O. and Yanina T.A. Pleistocene Palaeogeographic events in the Ponto-Caspian and Mediterranean Basins. Moscow State University Press, Moscow, 1998. (In Russian)

[88] Tambiev S.B. and Zhabina N.N. Pyritization in the Black Sea anoxic water: its scale and influence on recent sediments. Dokl Akad Nauk SSSR 1988; 299:1216-21. (In Russian)

[89] Titov V.B. Formation of the winter hydrological situation in the Black Sea depending on the severity of winter. Okeanologiya 2000; 40:826-32. (In Russian)

[90] Ünlüata Ü., Oguz T., Latif M.A. and Özsöy, E. "On the physical oceanography of the Turkish straits". In *The physical oceanography of sea straits.* Pratt L.G. ed. Kluwer Acad Publ, Amsterdam, 1990.

[91] Vainshteyn M.B., Tokarev V.G., Shakola V.A., Lein A.Yu. and Ivanov M.V. The geochemical activity of sulfate-reducing bacteria in sediments in the western part of the Black Sea. Geochem Intern 1986; 1:110-22.

[92] Vairamamurphy A. and Mopper K. Determination of sulphite and thiosulphate in aqueous samples including anoxic water by liquid chromatography after derivatization with 2,2'-Dithiodis(5'-nitropyridine). Env Sci Technol 1990; 24:333-337.

[93] Vetriani C., Tran H.V. and Kerkhof L.J. Fingerprinting microbial assemblages from the oxic/anoxic chemocline of the Black Sea. Appl Environ Microbiol 2003; 69:6481-88.

[94] Vinogradov A.P., Grinenko V.A. and Ustinov V.I. Isotopic compositions of sulphur compounds in the Black Sea. Geochem Intern 1962; 10:973-97.

[95] Vinogradov M.E. and Nalbandov Yu.R. Effect of changes in water density on the profiles of phisiochemical and biological characteristics in the pelagic ecosystem of the Black Sea. Okeanologiya 1990; 30:567-73. (In Russian)

[96] Volkov I.I. *Sulphur geochemistry in ocean sediments.* Nauka, Moscow, 1984. (In Russian)

[97] Volkov I.I. "Reduced sulphur species in the Black Sea water". In *Variability of the Black Sea ecosystem: natural and anthropogenic factors.* Vinogradov M.E. ed., Nauka, Moscow, 1991. (In Russian)

[98] Volkov I.I. "Hydrogen sulphide and reduced sulphur species in the Black Sea: comparative analysis". In *The chemistry of seas and oceans.* Bordovsky O.K., ed. Nauka, Moscow, 1995. (In Russian)

[99] Volkov I.I. and Demidova T.P. Inorganic reduced sulphur species in the oxic zone of the Black Sea. Dokl Akad Nauk 1991; 320(4):977-81. (In Russian)

[100] Volkov I.I. and Zhabina N.N. The method of determination of inorganic sulfur species in sea water. Okeanologiya 1990; 30(5):778-782. (In Russian)

[101] Volkov I.I., Dyrssen D. and Rozanov A.G. Alkalinity problem and anaerobic mineralization of organic matter in the Black Sea. Geokhimiya 1998; 1:78-87. (In Russian).

[102] Volkov I.I., Rozanov A.G. and Demidova T.P. "Inorganic reduced sulfur species and dissolved manganese in the Black Sea water column". In *Black Sea ecosystem during wintertime.* Nauka, Moscow, 1992. (In Russian)

[103] Volkov I.I., Rozanov A.G. and Dyrssen D. Principles of hydrochemistry of the anoxic basins. NATO TU-Black Sea Project: Symposium of Scientific Results, Crimea, Ukraine, June 15-19, 1997.

[104] Volkov I.I., Rozanov A.G. and Yagodinskaya T.A. Pyrite micro-nodules in the Black Sea sediments. Dokl Akad Nauk SSSR 1971; 197:195-98. (In Russian)

[105] Volkov I.I., Kontar E.A., Lukashev Yu.F., Neretin L.N., Nyffeler F. and Rozanov A.G. The upper hydrogen sulphide boundary and the origin of the redox nepheloid layer (RNL) in waters of the Caucasus continental slope of the Black Sea. Geokhimiya 1997; 6:618-629. (In Russian)

[106] Volkov I.I., Skirta A.Yu., Makkaveev P.N., Demidova T.P., Rozanov A.G. and Yakushev E.V. "On physical and chemical homogeneity of bottom waters in the Black Sea". In *Multidisciplinary investigations of the northeastern part of the Black Sea.* Nauka, Moscow, 2002. (In Russian)

[107] Volkov I.I., Falina A.S., Skirta A.Yu. and Yakubenko V.G. "Hydrophysical and hydrochemical structure of the Black Sea deep waters". In *Current problems in oceanology.* Nauka, Moscow, 2003. (In Russian)

[108] Yao W. and Millero F.J. "Oxidation of hydrogen sulphide by Mn(IV) and Fe(III) (hydr)oxides in seawater". In *Geochemical transformations of sedimentary sulphur.* Vairavamurthy M.A. and Schoonen M.A.A., eds. ACS Symposium Series 1995; 612:260-79.

[109] Yao W. and Millero F.J. The chemistry of anoxic waters in the Framvaren Fjord, Norway. Aquatic Chem 1995; 1:53-88.

[110] Zhang J.Z. and Millero F.J. The chemistry of anoxic waters in the Cariaco Trench. Deep Sea Res I 1993; 40:1023-41.

[111] Zopfi J, Ferdelman T.G. and Fossing H. "Distribution and fate of sulfur intermediates - sulfite, tetrathionate, thiosulfate, and elemental sulfur - in marine sediments". In *Sulfur Biogeochemistry - past and present.* Amend J.P., Edwards K.J. and Lyons T.W., eds. Boulder Co., GSA Special Paper 379, 2004.

[112] Zopfi J., Ferdelman T.G., Jørgensen B.B., Teske A. and Thamdrup B. Influence of water column dynamics on sulphide oxidation and other major biogeochemical processes in the chemocline of Mariager Fjord (Denmark). Mar Chem 2001; 74:29-51.

THE SUBOXIC TRANSITION ZONE IN THE BLACK SEA

James W. Murray[1], Evgeniy Yakushev[2]

[1] *University of Washington, School of Oceanography, Box 355351, Seattle WA 98195-5351, USA*

[2] *Russian Academy of Sciences, P.P. Shirshov Institute of Oceanology, Okeanologiya, Gelendzhik-7, 353470, Russia*

Abstract The Black Sea is a classic marine anoxic basin. It has an oxygenated surface layer overlying a sulfide containing (anoxic) deep layer. At the interface between these layers there is a suboxic layer in which both oxygen and sulfide are extremely low and have no perceptible vertical gradients. This condition has evolved because of the superposition of the flux of organic matter which consumes oxygen during respiration on the strong density stratification on the water column. The density stratification is strong because water with high salinity enters the Black Sea from the Bosporus Strait and mixes with overlying cold intermediate layer (CIL) water that forms in the winter on the northwest shelf and in the center of the western and eastern gyres. The rate of CIL formation is also variable over 5 to 10 year periods in response to climate variability on that same time interval. This variability appears to be driven by the North Atlantic Oscillation. This mixture of Bosporus outflow and entrained cold intermediate layer water results in formation the Bosporus Plume which ventilates the layers of the Black Sea deeper than the CIL. New data about the biogeochemical distributions (oxygen, sulfide, nitrate and ammonium) were obtained during R/V Knorr research cruises in 2001 and 2003. The distributions in the upper layers reflect a classic example of the connection between climate forcing, physical regime, chemical fluxes and biological response.

1. INTRODUCTION

The Black Sea, Pontus Euxinus to the Greeks because of its stormy weather, is an inland marine water body with a peculiar layering of oxic, suboxic and anoxic or sulfidic water that has been of great interest to geochemists and microbiologists [9, 62]. In this overview we will describe the physical and chemical distributions and summarize new ideas about how variability in regional climate modulates the physical forcing and circulation, nutrient fluxes and biological response.

L. N. Neretin (ed.), Past and Present Water Column Anoxia, 105–138.

The bathymetry of the Black Sea and the topography of the surrounding land masses are shown in Fig. 1. The narrow (0.76 – 3.60 km) and shallow (<93 m) Bosporus Strait provides the only pathway of water exchange between the Black Sea and the Mediterranean. The sill depths of the Bosporus are 32-34 m at the southern end and 60 m at the northern end [18, 29] The seawater that flows into the Black Sea from the Mediterranean along the bottom of the Bosporus Strait is the only source of salty water to the basin. Deep-water salinity values increase to S = 22.33. Freshwater inflow from several European rivers (especially the Danube, Dniester, Dnieper, Don and Kuban) keeps the salinity low in the surface layer (S $\approx$ 18.0 to 18.5 in the central region). As a result, the water column is strongly stratified with respect to salinity, which is the main control of density. The main water fluxes are summarized in Table 1. These values show that evaporation exceeds precipitation and that the surface outflow is about twice as large as the deep inflow through the Bosporus. The currents in both directions are very strong (ms^{-1}).

Table 1. Present-day water fluxes of the Black Sea.

River input (Total)	350 km^3 y^{-1}
Danube River	250 km^3 y^{-1}
Dniester	8
Dnieper	51
Don	28
Kuban	12
Precipitation	303 km^3 y^{-1}
Evaporation	350 km^3 y^{-1}
Bosporus outflow to Black Sea	313 km^3 y^{-1}
average Bosporus deep salinity	= 34.9
average Bosporus deep temperature	= 14.5° C - 15.0° C in summer
	= 12.5° C - 13.5° C in winter
Bosporus outflow to Marmara Sea	610 km^3 y^{-1}
Slope of water surface along the Bosporus from north to south	35 cm
Current Velocities (surface)	~ 2 m s^{-1}
(deep)	~0.5 m s^{-1} (but reaching ~1.5 m s^{-1} over sills)

A consequence of the vertical stratification is that the surface layer (about 0 to 50 m) is well oxygenated while the deep layer (100 m to 2000 m) is anoxic and contains high concentrations of hydrogen sulfide. At the boundary between the oxic surface and anoxic deep layers, there is a suboxic zone (between approximately 50 to 100 m depth) where the concentrations of both O_2 and H_2S are extremely low (< 3 μM) and do not exhibit significant vertical or horizontal gradients in the central gyre regions on a given density surface in

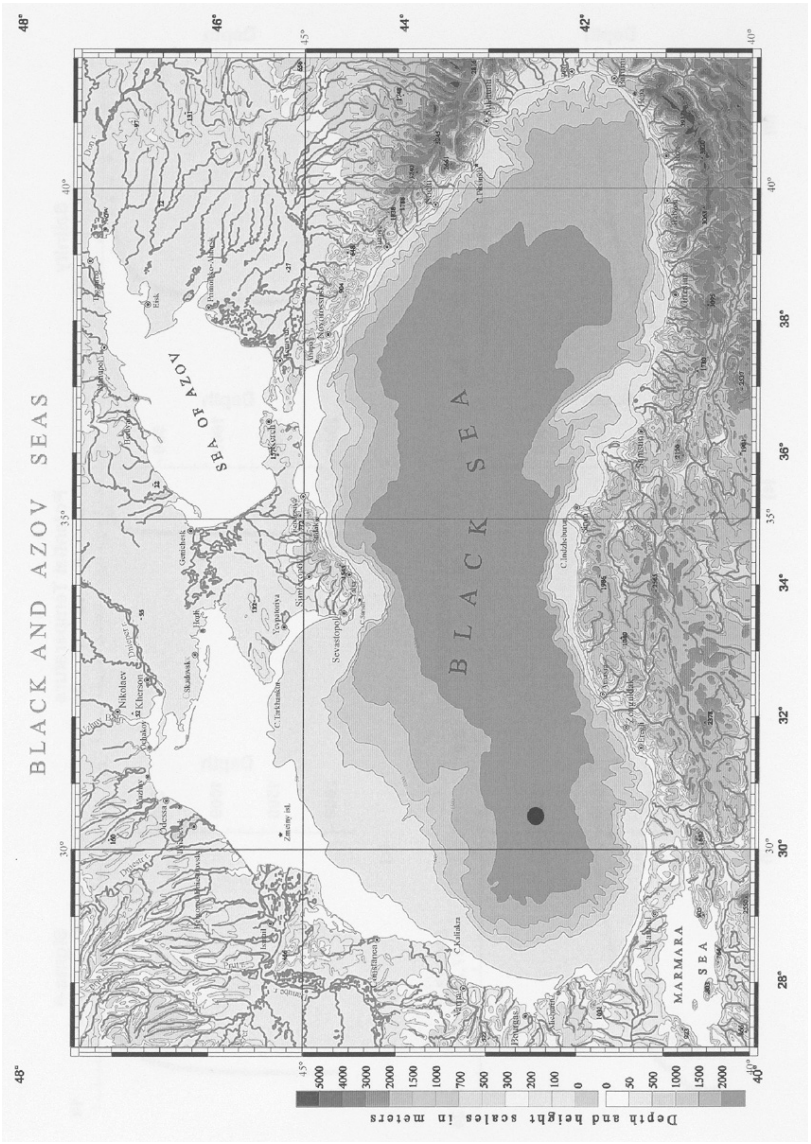

Figure 1. Bathymetry of the Black Sea and topography of the surrounding land areas. Prepared by S. Stanichny (MHI, Sevastopol, Ukraine). The circle represents the approximate location of the data in Figures 2, 4, 5, 7, 8, 9, 10.

any given year [10, 36]. An excellent example of the vertical profiles of O_2 and H_2S in the center of the western gyre is shown plotted versus depth and density in Fig. 2.

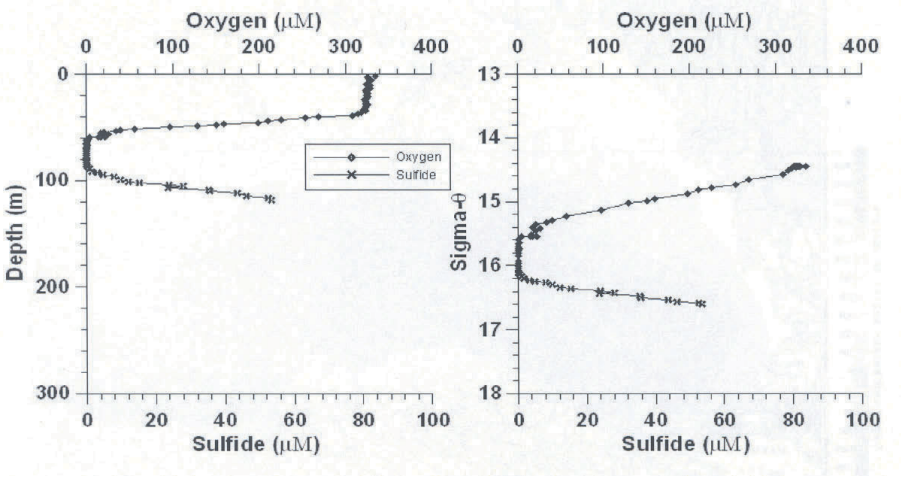

Figure 2. Oxygen and sulfide data from the center of the western gyre (Leg 7; Stn 12; Pump Cast #10) during R/V Knorr 2003. The data are courtesy of G. Luther (U. Delaware) and S. Konovalov (MHI, Sevastopol, Ukraine). The vertical scales are depth on the left and density on the right. Depth is the traditional scale but density is frequently used in the Black Sea to facilitate comparisons of different locations.

The suboxic zone in the Black Sea [10, 22, 36, 40] is an important biogeochemical transition zone between the oxic surface layer and sulfidic deep waters. This layer, where O_2 and H_2S do not overlap, was first observed during the 1988 Knorr Black Sea Expedition [35, 38]. Its boundaries were chosen from the vertical distribution of oxygen and sulfide observed in the central gyre. It was defined as the region between the depth where oxygen decreases to near zero ($O_2 < 10\,\mu M$) and the depth where sulfide first appears ($H_2S > 0.3\,\mu M$) [36, 40]. After its discovery, these distributions were confirmed by others [2, 57, 72] and the processes controlling its origin and variability have been extensively discussed.

When the suboxic zone was first observed, Murray et al, [36] suggested that it might be a new feature resulting from reduced fresh water input from rivers and a resulting change in the ventilation of the shallow Black Sea. Subsequent research has demonstrated that the suboxic zone is most likely a permanent feature of the Black Sea (at least since the early 1960s) [8, 40]. The balance between oxygen injected due to ventilation of the thermocline with surface water and oxygen consumed by oxidation of organic matter governs the depth of the upper boundary of the suboxic zone [25]. The injection of oxygen into the

upper part of the sulfide zone by water of Bosporus origin (the Bosporus Plume) is also an important control for the depth of the first appearance of sulfide [25]. Redox processes involving nitrogen-manganese-iron-sulfur are important for cycling of those elements in the lower part of the suboxic zone and they also play a role in determining the depth of the lower boundary [49].

There are several reasons why the Black Sea is an important location for geochemists to study.

1. It is a classic anoxic ocean basin and is considered a possible analog for the earth's ancient ocean. The ocean was initially totally anoxic. As atmospheric oxygen increased during the Proterozoic, the ocean contained an oxic surface layer and anoxic deep water from about 2.5 billion yrs. to 0.6 billion yrs. [3, 19]. After 0.6 b.y. the ocean was mostly oxic as it is today.
2. It has a well developed suboxic zone at the interface between the oxic and sulfidic layers where many important redox reactions involving Fe, Mn, N and other intermediate redox trace elements (e.g. Co, As, Sb, I, Ce) occur. Similar redox reactions take place in organic rich sediments throughout the world's oceans but they are easier to study in the Black Sea because they are spread out over a depth scale of 10s of meters (rather than cm or mm scales as in sediments).
3. The chemical distributions have been shown to occur on similar density (or depth) horizons from year to year, making the chemical reactions and the sequence of microbes that mediate them easy to study in a predictable way on repeated cruises.
4. The Black Sea is an ideal site to study how variability in climate affects air-sea physical forcing and resulting changes in chemical fluxes and resulting biological distributions.

2. HOW DOES THE BLACK SEA WORK?

In order to understand the suboxic zone it is necessary to describe the physical framework where it exists. Like the open oceans the Black Sea has wind driven circulation with gyres, eddies, deep water thermohaline circulation and shallower ventilation into the thermocline. Neuman [42] described the surface circulation of the Black Sea as consisting of two large cyclonic (counterclockwise) central gyres that define the eastern and western basins (Fig. 3). These gyres are bounded by the wind-driven Rim Current [47] which flows along the abruptly varying continental slope all the way around the basin. The Rim Current exhibits large meanders and filaments that protrude into the regions of the central gyres. The geostrophically calculated currents along the axis of the Rim Current typically have speeds of 25 cm s^{-1}. Inshore or coastal of the Rim Current there are several anticyclonic (clockwise currents) eddies [43]. Some of these eddies are permanently controlled by topography (e.g. the Sakarya Eddy

located over the Sakaraya submarine canyon) while others are more temporally and spatially variable (e.g. the Sevastopol Eddy) [46]. Mesoscale coastal anticyclonic eddies that move with the Rim Current are usually observed along the Caucasus coast in the NE region of the Sea.

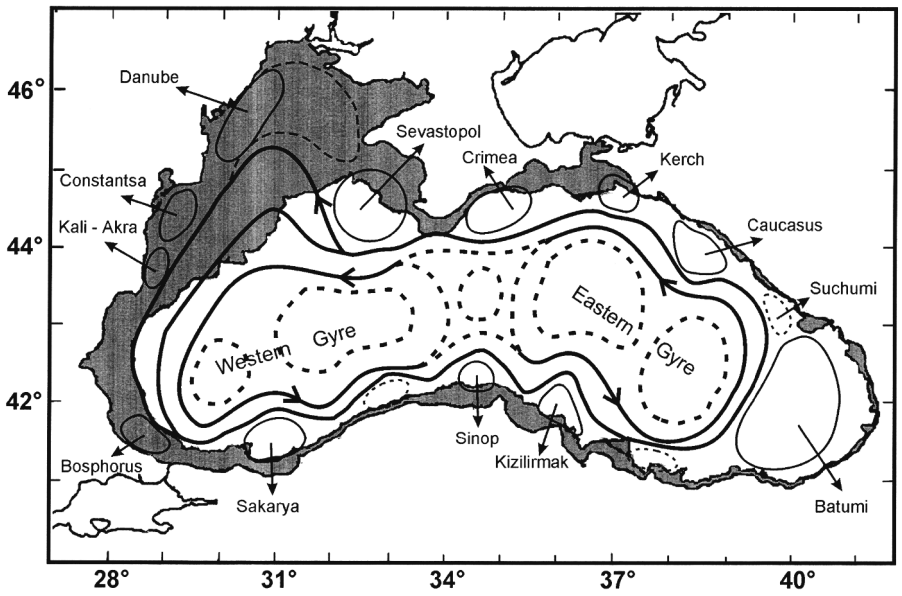

Figure 3. Chart of the Black Sea showing the wind-driven Rim Current which flows in a cyclonic or counterclockwise direction and several of the main anticyclonic gyres that are located between the Rim Current and the coast. The shelf area (<300 m) is shaded dark [from 27].

As a result of this surface circulation individual subsurface density surfaces are deeper around the margins and shallower in the central regions. All characteristic features tend to be deeper near the margins and shallower in the central gyres but they almost always fall on the same density levels. Thus, density is usually used as a depth coordinate in the Black Sea. Plotting properties against depth in the Black Sea produces a scatter of data, but when plotted against density, the same data shows much less variability [10].

The Black Sea has an estuarine type circulation. Water flows in at depth and out at the surface. The high salinity water (S = 35) that flows through the Bosporus is also relatively warm (~15°C). The rivers are the main source of fresh water (300 km^3 y^{-1}) and they mostly drain onto the NW shelf where the surface water can get relatively cold (5.5° C) in the winter. On average the lower layer inflow through the Bosporus to the Black Sea is about 313 km^3 y^{-1}

and the upper layer outflow is about 610 $km^3\ y^{-1}$ which gives 303 $km^3 y^{-1}$ for the vertically integrated net transport out through the Bosporus [52]. The value of 303 $km^3\ y^{-1}$ reflects the balance between river inflow (350 $km^3\ y^{-1}$) plus precipitation (~303 $km^3\ y^{-1}$) minus evaporation (350 $km^3\ y^{-1}$) (Table 1).

These inputs result in strong vertical stratification with a fresh, lower density layer at the surface and a salty higher density layer in the deep water. Full scale (0-2200 m) salinity, potential temperature and density (sigma-theta) are shown in Figs. 4a, b, c. These CTD data were obtained during a research cruise on the R/V Knorr in the center of the western gyre in May 1988 [39]. Salinity increases continuously from low values of about S = 18 at the surface to deepwater values of over S = 22.3. Density (σ_θ), which is controlled primarily by the salinity, increases similarly. Temperature is seasonally variable at the surface and decreases with depth to a feature with a temperature minimum called the cold-intermediate layer (CIL) located at about 50 m. This layer forms in the winter on both the NW shelf and in the center of the eastern and western gyres. Its extent of replenishment varies from year to year depending on the climate [44]. Below the CIL the temperature increases continuously all the way to the bottom. The values of S, T and density are extremely uniform in the deep water from about 1750 m to the bottom and form a homogeneous bottom boundary layer (Fig. 4d, e, f) [39]. This layer appears to be formed due to bottom heating of the Black Sea by the upward flux of geothermal heat flow (which destabilizes density) superimposed on the downward increasing salinity (which stabilizes density).

A temperature-salinity diagram can be used to illustrate the relationships between the distributions of temperature and salinity. The data from Fig. 4a are shown as a T-S plot in Fig. 5. The high temperature and low salinity data on the left are near the surface. Temperature decreases to a minimum of about 7.6°C in the Cold Intermediate Layer (CIL) and then both salinity and temperature increase continuously into the deep water.

When the T-S data from the Black Sea is plotted with data from the Bosporus (which reaches T = 15°C and S = 36) it is apparent that, to a first approximation, the deep water of the Black Sea forms from linear two-end member mixing of the Bosporus inflow with the CIL. The magnitude of the Bosporus outflow averages 313 $km^3\ y^{-1}$ but is variable in response to changing local wind conditions. This implies that local synoptic meteorological conditions exert strong controls on the magnitude of transport. Numerical model results have been used to estimate short term [45] and longer term, decadal time scale [66] variability. The net transport varies from 200 to 350 $km^3\ y^{-1}$ over the decadal time scale. The CIL has two sources that are highly variable in intensity depending on climate. The first is the shallow northwest shelf where the water gets very cold in the winter [70]. The second site is in the eastern and western gyres where surface water can become sufficiently cold to rejuvenate the CIL during some

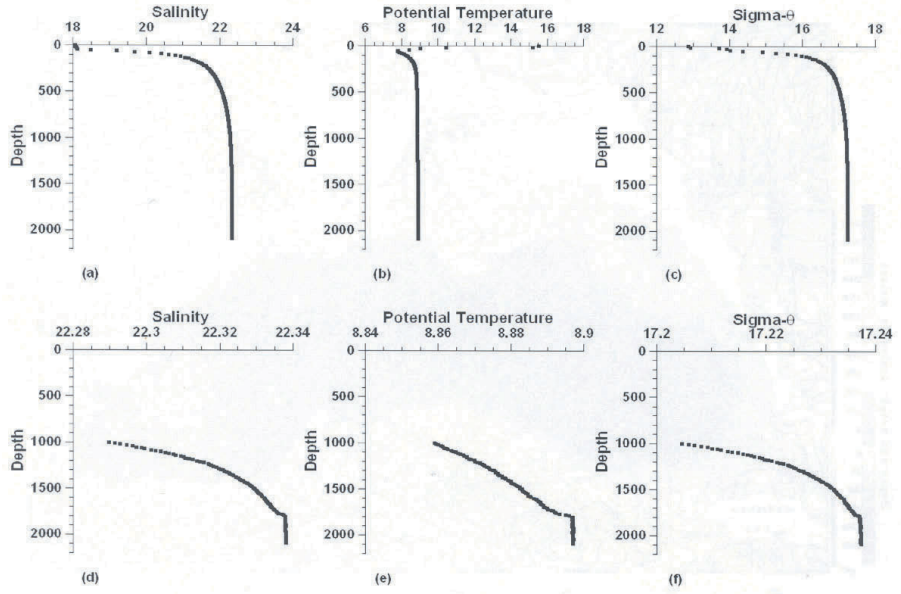

Figure 4. Salinity, potential temperature and density (sigma-theta) from the 1988 R/V Knorr Expedition [39]. The location is Station BS3-2 HC-20 in the center of the western gyre. a, b, c are full water column. d, e, f show a blow up of the bottom 1000 m.

winter storms [45]. Gregg and Yakushev [17] observed in March 2003 that the surface water had uniformly cold temperature (T = 6.1°C) from the surface to the depth (density σ_θ = 14.5) of the CIL. The intensity and relative importance of these two sources are probably variable on a year to year basis depending on climatic conditions.

Most of the mixing between the Bosporus outflow and the CIL occurs on the continental shelf just north of the Bosporus [71]. The bottom layer of high salinity water from the Marmara Sea comes in from the south and thins as it enters the Black Sea. Salinity gradients are sharp at its upper boundary indicating mixing with overlying water. The overlying water is characterized by the temperature minimum characteristic of the CIL. This mixing results in the linear, two end-member mixing characteristics for T and S seen in Fig. 5. Most mixing occurs before the Bosporus outflow reaches the shelf break at 200 m. The resulting Bosporus plume ventilates the interior of the Black Sea at the depth represented by its density when it reaches the shelf break [51, 67]. The most common entrainment conditions result in ventilation of the upper 500 m but evidence suggests there must be occasionally rare ventilation events that reach the bottom. We know this because the only source for relatively warm

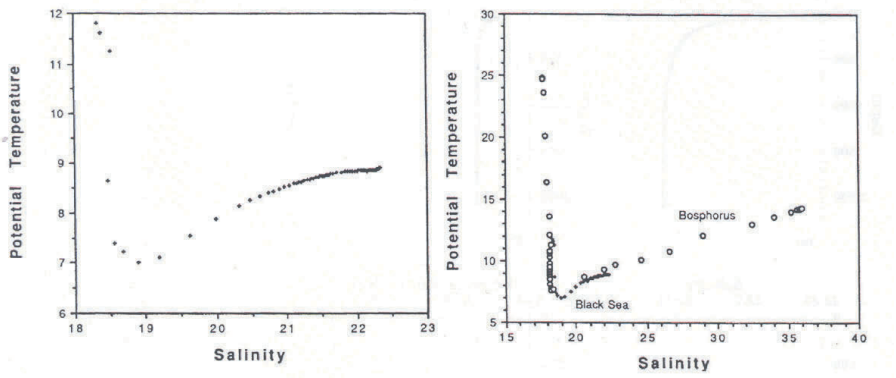

Figure 5. Left panel. Potential temperature-salinity diagram for the data shown in Figure 4a, b. (from Knorr 2001; Leg 1 Stn 1 (Bosporus) and Stn 6 (Central Western Gyre); Right panel. Combined temperature-salinity for Black Sea and Bosporus. The Bosporus data are open circles and the densest water has S = 36 and T = 14 °C.

and salty water is the Bosporus Plume and S and T increase all the way to the bottom. Based on the salinity balance for the deep Black Sea (50 m to 2200 m) the ventilating water is composed of an average CIL to Bosporus entrainment ratio of ~ 4:1 [39]. Thus, on average the composition of the Bosporus Plume resembles a mixture of 4 parts CIL with 1 part high salinity Bosporus inflow from the Mediterranean.

In detail this ratio is higher in the upper few 100 m and lower in the deeper water. Buesseler et al. [7] used Cs isotope data to estimate an entrainment ratio of 10 for depths shallower than 200 m. Lee et al. [30] used chlorofluorocarbon (CFC) data to model the decrease in ventilation and increase in residence time with depth over the upper 500 m. The entrainment ratio of CIL to Bosporus inflow decreases from ~10 in the suboxic layer to 3.8 for depths near 500 m. The residence time of water increases from 4.8 yr in the suboxic zone to 625 yr at 500 m over the same interval.

Microstructure profiles have been used to study mixing in the Black Sea. Diapycnal diffusivities (K_ρ) calculated from microstructure measurements of turbulent dissipation were only (1-4) x 10^{-6} m^2 s^{-1} in the lower part of the CIL and in the suboxic zone with no apparent dependence on (the density gradient or N) [17]. Consequently, turbulent fluxes are too slow to replace the oxygen consumed by respiration. Thus the Black Sea has an oxygen containing surface layer and a sulfide containing deep layer.

3. HISTORY OF STUDY OF THE SUBOXIC LAYER (SOL)

The presence of hydrogen sulfide in the deep waters of the Black Sea was first described by Andrusov [1] in his report of the scientific expedition to the Black Sea on the Russian gunboat "Chernomorets" in 1890. He proposed that the reason for this occurrence is that the Bosporus restricts the exchange of deep waters between the Black and Mediterranean Seas. He also proposed that the hydrogen sulfide originated due to reaction of non-mineralized organic matter with sulfurous salts of the sea water.

A layer of co-existence of oxygen and hydrogen sulfide (C-layer or S-layer) was observed in some of the earliest hydrochemical studies in the Black Sea. The origin of this term is that C is the Cyrillic letter for S and is the first letter of the Russian word for overlap. It was assumed that oxidation of hydrogen sulfide took place mainly by direct reaction with oxygen within this layer [4, 60, 61]. Sorokin [61] devised a special analytical technique to determine oxygen in the presence of sulfide. During the 1988 RV "Knorr" Expedition it was found that when special care was taken to avoid contamination the oxygen concentrations measured with the standard and micro Winkler techniques were significantly lower than found earlier [10, 36] . Bezborodov and Eremeev [4] and Broenkow and Cline [6] showed that the error connected with contamination of reagents with oxygen and consumption of oxygen during the standard sampling procedure can reach 0.15 ml^{-1} (6.6 μM), and after this correction the C-layer practically disappears. This absence of oxygen at the hydrogen sulfide boundary was subsequently confirmed by [2, 32, 72].

The disappearance of oxygen above the hydrogen sulfide zone was also confirmed by Stunzhas [68] who used a specially designed membrane-less oxygen sensor for studies of the Black Sea suboxic layer.

4. DISTRIBUTIONS

Here we describe the distributions of the key biogeochemical species in the region of the suboxic zone. The density values that were characteristic of many water column features during the 1988 Knorr Expedition are shown in Table 2. These values have served as a benchmark for subsequent cruises to evaluate the stability of the characteristic features. Since 1988 there has been some spatial and temporal variability but the general picture of the distributions has remained the same.

4.1 OXYGEN - SULFIDE

An example of the oxygen and sulfide distributions versus depth (left) and density (right) in the center of the western gyre is shown in Fig. 2 (R/V Knorr 2003 Leg 7, Stn 12). Oxygen is close to atmospheric saturation (~330 μM) in

Table 2. Characteristic density values of biogeochemical features biogeochemistry of the Black Sea as observed during the Knorr 1988 Research Cruise. Based on data from both the eastern and western basins. Stations in the SW region influenced by the Bosporus Plume were omitted. The uncertainty of each value is about 0.05 density units.

Feature	Density (σ_θ)
PO_4 shallow maximum	15.50
O_2 < 10 μM	15.70
NO_3 maximum	15.40
Mn_d < 200 nM	15.85
Mn_p maximum	15.85
PO_4 minimum	15.85
NO_2 maximum	15.85
NO_3 < 0.2 μM	15.95
NH_4 > 0.2 μM	15.95
Fe_d < 10 nM	16.00
H_2S > 1 μM	16.15
PO_4 deep maximum	16.20

the upper 40 m (down to a density of about $\sigma_\theta \approx 14.5$) due to gas exchange and biological production. It then decreases linearly with depth in the main pycnocline (halocline) to $\leq$10 μM at the density level of 15.50-15.60 kg/m^3 (about 60 m). Below this depth there is usually no detectable vertical gradient of oxygen.

The first appearance of sulfide occurs at about 90 m or σ_θ = 16.15 (Fig. 2) and then sulfide increases continuously with depth to maximum values up to 400 μM by 2200 m [33]. One of the intriguing questions about the Black Sea is what is the sink for the upward flux of sulfide [5]? Sulfide decreases to zero before the first appearance of oxygen thus sulfide is apparently not oxidized by the downward flux of oxygen. Several hypotheses have been made to explain the removal of sulfide. Millero [34], Luther et al. [33] and Debolskaya and Yakushev [11] suggested that Mn cycling plays an important role and that the upward flux of sulfide is oxidized by a downward flux of oxidized species of Mn (III, IV). Konovalov and Murray [25] estimated that a significant amount of upward flux of sulfide is oxidized by O_2 injected horizontally by the Bosporus Plume. The Bosporus Plume results in a complicated interleaving of water that can be best seen in the high resolution *in situ* profiling data. Oxygen containing intrusions from the Bosporus plume (deeper than σ_θ = 15.0) are easily seen in the *in situ* voltammetric O_2 and H_2S profiles from the stations of the 2001 and 2003 KNORR cruises in the southwestern part of the sea, close to the Bosporus [26] (Fig. 6). Whenever there is a temperature maximum (a tracer for the Bosporus Plume) there is an oxygen maximum and sulfide minimum

(for $\sigma_\theta > 16.15$). The Winkler O_2 data in this Fig. 6 are from a different rosette bottle cast at the same location and don't have the same detail of resolution.

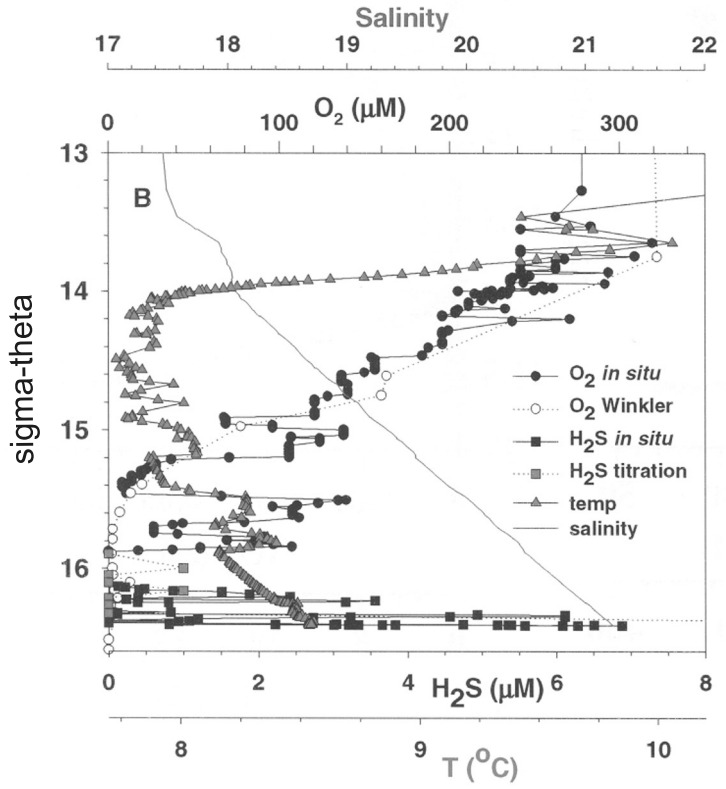

Figure 6. High resolution in situ voltammetric O_2 and H_2S data coupled with temperature and salinity from the CTD on the pump profiler from Station 9 on Leg 1 of the Knorr 2001 Black Sea cruise. Winkler O_2 and iodometric H_2S data are also shown. The location is in the southwest region of the Black Sea under the influence of the Bosporus Plume. The data are courtesy of G. Luther (U. Delaware) and S. Konovalov (MHI, Sevastopol, Ukraine) [from 26].

4.2 Nitrogen Species

The vertical profiles of nitrate, nitrite and ammonium in the center of the western gyre (Knorr 2003; April 2003; Leg 8; Stn 7) are shown versus density in Fig. 7. Oxygen and sulfide are shown on the left for ease of comparison with boundaries of the suboxic zone. Nitrate is depleted at the surface due to

biological uptake. It starts to increase at 40 m and reaches a maximum at 65m (σ_θ = 15.5) (approximately where O_2 decreases to 0). Nitrate then decreases to zero at 75m (σ_θ = 15.95) which is well above the first appearance of sulfide at 90 m or σ_θ = 16.15. After oxygen has decreased to zero, nitrification of ammonium released from organic matter no longer occurs, yet ammonium still does not accumulate. There are often two NO_2^- maxima located near the upper and lower boundaries of the NO_3^- maximum corresponding to zones of nitrification (shallow maximum) and denitrification (deep maximum) [73]. NO_2^- is an intermediate in both reactions. Ammonium starts to increase at σ_θ = 15.95 and increases progressively into the deep water. The disappearance of NO_3 and NH_4 at the same depth is consistent with a downward flux of NO_3 and an upward flux of NH_4 that are consumed over a narrow depth interval by the anammox reaction ($NO_2^- + NH_4^+ = N_2 + 2H_2O$). Anammox stands for anaerobic ammonium oxidation. Note that the anammox reaction reduces NO_2^-, not NO_3^-, so there must also be some heterotrophic denitrification that occurs that reduces NO_3^- to NO_2^- or nitrification that makes NO_2^- from NH_4^+ (from PON) in order for anammox to occur. The fact that there is a NO_2^- maximum implies that the rate of denitrification may be faster than anammox. So far these rates are unknown. The lack of ammonium accumulation between 15.5 and 15.95 suggests that anammox may be occuring throughout the suboxic zone. An additional sink for ammonium is consumption by microbial chemosynthesis, but this rate is hard to estimate.

N_2 has been measured in the Black Sea as the N_2/Ar ratio [15]. The N_2/Ar ratios in the center of the western gyre are shown versus density for three different cruises in 2000, 2001 and 2003 in Fig. 8. The vertical dashed line indicates the ratio expected when the water is at atmospheric equilibrium. The horizontal dashed line shows the density of the CIL, the deepest layer ventilated directly from the surface. Most of the water column is supersaturated with N_2 with a maximum centered at $\sigma_\theta \approx 16.0$. This is the density where NO_3^- and NH_4^+ decrease to zero. These data from three different years suggest that N_2 concentrations vary significantly on interannual scales suggesting that its production is sensitive to small perturbations in the vertical gradients and fluxes of NO_2^- and NH_4^+ driven by variability in ventilation. The maximum in N_2/Ar was largest in 2000 which was a period when the CIL was relatively warm and less ventilated.

Kuypers et al. [28] used 16S RNA gene sequences, RNA probes, ^{15}N label experiments and ladderane membrane lipids to show that anammox bacteria are indeed present at this level in the Black Sea. This reaction where ammonium is oxidized anaerobically to N_2 is important in the nitrogen cycle of the Black Sea [15] and results in a prominent maximum in N_2 gas concentration (Fig. 8). The anammox reaction had long been inferred from chemical distributions [5, 55] and has now been confirmed. The relative importance of anammox

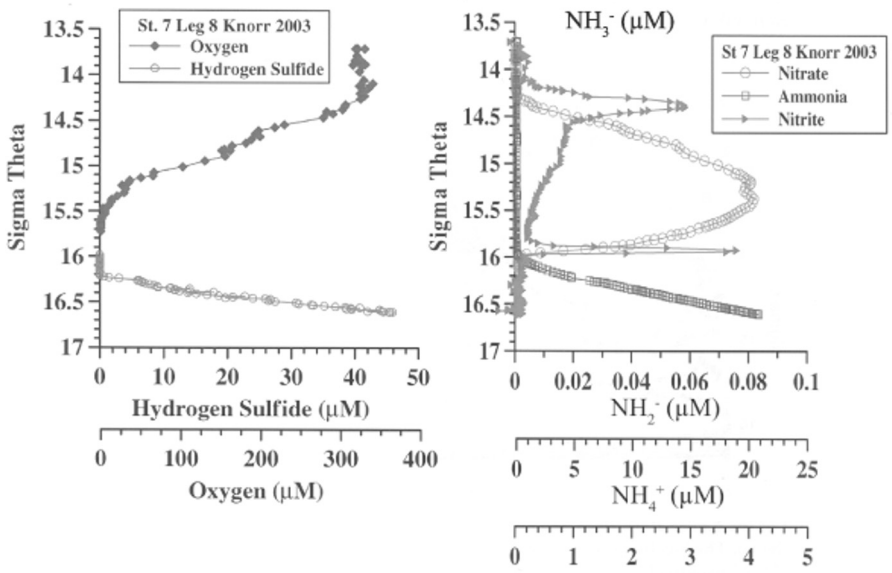

Figure 7. Dissolved oxygen and hydrogen sulfate (left panel), and nitrate and ammonium (right panel) versus density from the center of the western gyre (Leg 7; Stn 12) during R/V Knorr April 2003.

versus heterotrophic denitrification and how this varies with depth relative to the distribution of nitrogen species still needs to be determined.

4.3 Phosphate

Phosphate only has one oxidation state but its distributions in the Black Sea are clearly influenced by changes in the redox environment. The vertical profile of phosphate has the most complicated structure of all the profiles of basic chemical properties. The profiles in the central Black Sea are characterized by two maxima and two minima [5, 14]. A representative profile from the center of the western gyre is shown plotted versus depth and density in Fig. 9 (R/V Knorr 172-05; March 2003; Stn 7, E.Yakushev, unpublished data). The typical profile shows that PO_4 concentrations are low (~0.15 μM) in the euphotic zone. They increase to a maximum that coincides approximately with the NO_3 maximum at about $\sigma_\theta \approx$15.50 kg m^{-3}. Phosphate then decreases to low concentrations ranging from zero to 2.5 μM at $\sigma_\theta \approx$ 15.80 to 15.95 kg m^{-3}. This minimum is well above the first appearance of sulfide. Finally, it increases to a maximum (5 to 7.7 μM) in the upper part of the sulfide zone at $\sigma_\theta \approx$ 16.20 kg m^{-3}. The density values of these maximums appear to be are very stable but profiles do display distinct spatial and temporal variations [24] which are probably caused

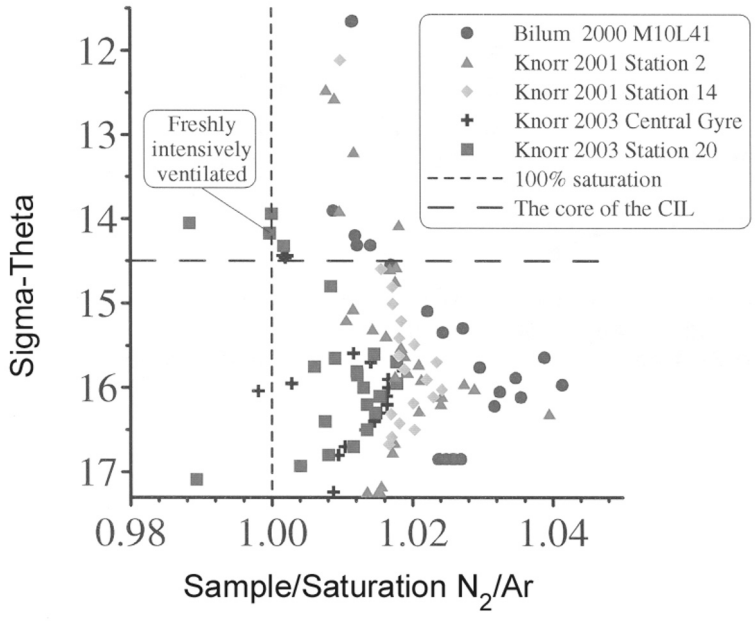

Figure 8. N_2/Ar solubility ratios versus density from Bilim 2000, Knorr 2001 and Knorr 2003. From [15]. The vertically dashed line shows what the ratio would be if the gases were at atmospheric equilibrium. The surface values during Knorr 2003 Stn 20 were at this value. The horizontal dashed line shows the characteristic density of the CIL.

by variable seasonal biological fluxes and meso-scale physical processes. This structure described above is mainly observed in the central parts of the Black Sea. Near the margins the maximums are often less well developed due to stronger mixing.

It is generally assumed that the called "phosphate pumps and shuttles" processes involving Mn and Fe cycling between oxidized and reduced forms [59], are responsible for the extremes in the phosphate profile. In this process phosphate is adsorbed by iron and manganese oxyhydroxides in the suboxic zone that form due to upward transport (vertical diffusion is more important than upwelling) of reduced Fe (II) and Mn (II) from the anoxic layer. The maximum in the sulfide layer is due to reduction of these oxides as they sink into the sulfide layer. The adsorbed PO_4 is released to solution where it can then be transported upward to be scavenged again in the suboxic zone. Shaffer [59] argued that both manganese and iron cycling contribute about equally to this phosphate pump. Yao and Millero [75] found that sorption of phosphate by MnO_2 was weaker than by iron hydroxides and that the content of MnO_2 in

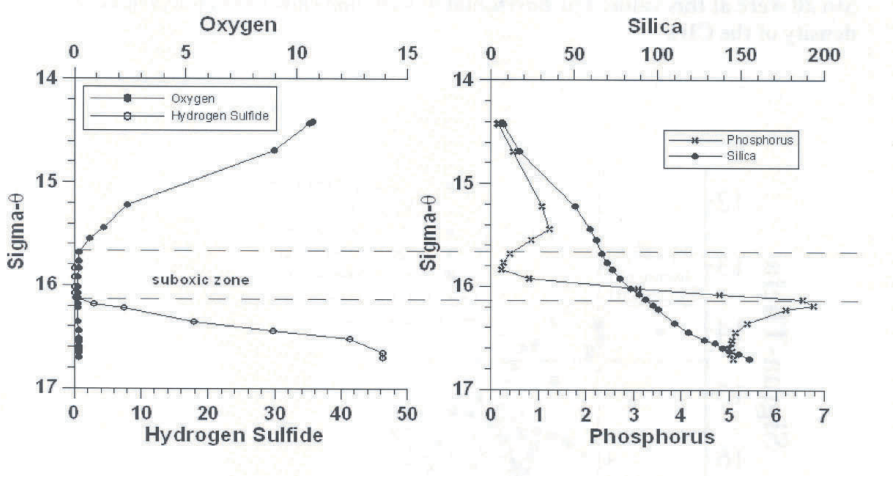

Figure 9. Representative profiles for oxygen, sulfide (left) and for Si and PO_4 (right) from the center of the western gyre during R/V Knorr 172-05, March 2003, Station 7, CTD 7.

the suboxic layer was insufficient to explain the phosphate minimum. Based on sorption experiments conducted by [63] it may be difficult to explain the PO_4 minimum as due to sorption because the concentrations of the Fe/Mn oxides are too low (on the order of 0.01-0.1 μM).

Another hypothesis suggested is that the decrease in phosphate in the suboxic zone is due to its consumption by microbial chemosynthesis [63]. A maximum of chemosynthesis occurs between the layers of the phosphate minimum and maximum. The deeper maximum of phosphate could be explained by the remineralization of organic phosphorus. Yakushev et al. [74] observed an increase of organic phosphorus (total phosphorus minus total phosphate) in this layer that supported this explanation. In the deeper sulfidic layers sorption of phosphate can occur on biogenic $CaCO_3$ particles [63].

Finally, there is spatial variability in the distribution of phosphate. New data from the northeastern Black Sea (Yakushev, unpublished data) at the coastal boundaries of the Rim current and at the marine sides of anticyclonic eddies showed that the structure of the phosphate profile is different when the hydrophysical dynamics are more intensive [11]. In these coastal regions (where there are stronger currents and eddies) the upper phosphate minimum was more pronounced in summer period but was not present during the winter. The deep maximum was always present.

Thus, there are multiple mechanisms for the origin of the PO_4 minima and maxima. The details of the processes that form the phosphate anomalies are still uncertain.

4.4 Silicate

A representative profile for Si is shown in Fig. 9 (R/V Knorr 172-05 Stn 7, E. Yakushev, unpublished data). Silica concentrations are low in the surface (~5 μM) and increase smoothly from 50 μM to 100 μM across the suboxic zone. The highest values in the deep water reach 400 μM (not shown but data are on Knorr 2003 web site).

Tugrul et al. [72] and Humborg et al. [20] demonstrated that the silicate concentrations in the wintertime surface waters of the Black Sea decreased by 60% from 1969 (R.V. ATLANTIS cruise) to 1988 (R.V. KNORR cruise). They suggested that these changes were due to a two-thirds reduction in the input of silicate from the Danube due to dam construction in the early 1970s. The observed decrease in silicate inventory in the oxic layer may have been responsible for dramatic shifts in phytoplankton species composition from diatoms to coccolithophores and flagellates [20]. Temporal changes in the distribution of silicate in the anoxic zone have not been discussed much because only there are only a few time points available.

Comparison of the Atlantis II 1969 and Knorr 1988 data sets suggest that the concentration of silicate in the deep water increased by a factor of two between those two cruises [25]. This increase in the inventory of silicate appears to be too high to reflect real changes in the inventory of dissolved silicate. However, no analytical or methodological problems appear to exist. Data since 1991 has been obtained by the same analytical procedures which were inter-calibrated during the CoMSBlack and NATO "TU-Black Sea" International Programs [21]. The opposing temporal trends in the silica concentrations of the oxic and anoxic layers may represent real variations in the downward flux of biogenic silica.

4.5 Carbonate System Parameters

The carbonate system properties undergo large changes with depth reflecting the oxidation reduction reactions that influence the magnitude of total CO_2 (DIC) and alkalinity [16]. An example of data obtained during the 2001 R/V Knorr cruise is shown in Fig. 10 versus density (Hiscock and Millero, unpublished data). DIC is slightly less than 3000 μmol kg^{-1} at the surface. It increases with depth to the top of the suboxic zone where it is relatively constant. It then starts to increase again after the appearance of sulfide. Total Alkalinity is fairly uniform at 3550 μmol kg^{-1} until the sulfide zone where it starts to increase. pH (which reflects the relative magnitudes of DIC and alkalinity) starts at 8.2 at the surface and then decreases to about 7.45 in the suboxic zone. It then increases slightly in the sulfide zone.

Total CO_2 and alkalinity are key parameters because they reflect the net effect of all the oxidation-reduction reactions on the carbon and proton balances. In

the oxic euphotic zone, total CO_2 increases with depth while alkalinity stays approximately constant. This indicates a source of CO_2, probably due to aerobic respiration of organic matter. Both increase with depth below the suboxic zone into the deep anoxic water. There must be significant production of alkalinity within the Black Sea [12, 13, 16]. In the sulfide containing deep waters, total CO_2 and alkalinity are dominated by sulfate reduction. Each mole of sulfide produced is matched by two equivalents of alkalinity:

$$106\,CH_2O + 53\,SO_4^{2-} = 106\,HCO_3^- + 53\,H_2S$$

Goyet et al. [16] observed that dissolution of $CaCO_3$ caused both total CO_2 and alkalinity to increase faster than expected based on sequential oxidation of Redfield organic matter by O_2, NO_3 and SO_4. Thus, total alkalinity needs to be corrected for the minor bases: borate, ammonia, phosphate, silicate, bisulfide and with Ca^{2+} representing $CaCO_3$ dissolution. Both calcite and aragonite are undersaturated at depth in the Black Sea.

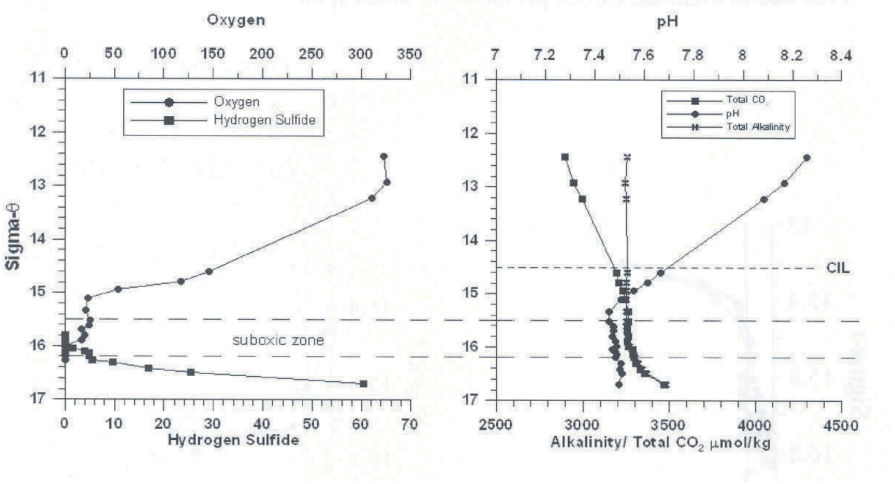

Figure 10. Dissolved oxygen and hydrogen sulfide (left panel) and carbonate system â^ pH, Alkalinity and Total CO_2 (right panel) - versus density from Knorr 2001; April 2001; leg 1, Stn 5 (Hiscock and Millero, unpublished data).

4.6 Manganese-Iron

The Black Sea has long been an important site for investigating the biogeochemical cycling of Fe and Mn across redox boundaries. The studies of Mn cycling by Spencer and Brewer [64] and Spencer et al. [65] are considered classics. Typical profiles for dissolved and particulate manganese (together

with oxygen and sulfide) in the western central gyre (Knorr2001; Stn 6) are compared in Fig. 11. Dissolved Mn is low in the surface layer (~5 nM) and increases rapidly below σ_θ = 16.0. It increases to a maximum of about 8 to 9 μM in the upper part of the sulfide zone (~200 m). The concentrations at this maximum appear controlled by $MnCO_3$ saturation [64]. Mn then decreases slowly with depth to approximately 4.5 μM at 2000 m. The deep water Mn concentrations appear controlled by MnS_2 (haurite) solubility, rather than MnS (alabandite) or $MnCO_3$ (rhodochrosite) solubility [31].

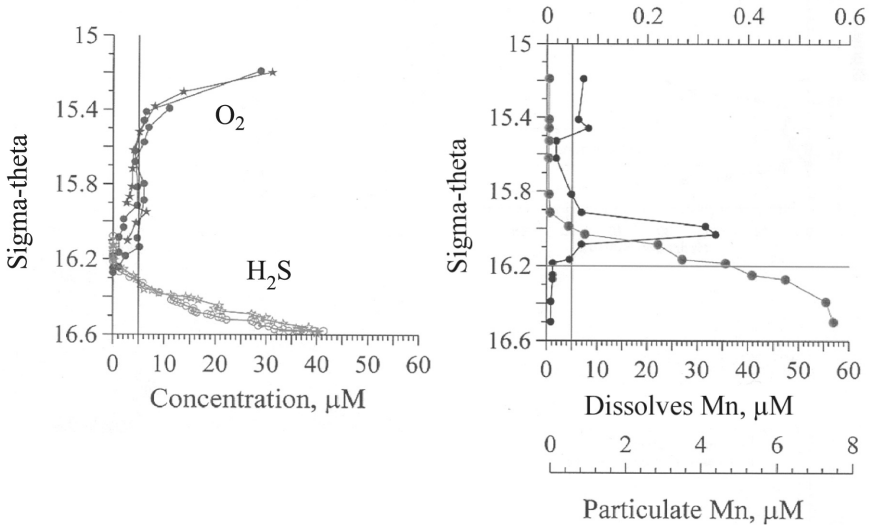

Figure 11. Vertical distributions versus density of oxygen, sulfide (left) and dissolved and particulate manganese (right) in the central gyre of the western basin of the Black Sea. From Knorr 2001 Leg 1 Station 6 and Leg 2 Station 2. Data from B. Tebo and B. Clement, UCSD, personal communication.

There is an upward flux of dissolved reduced Mn (as Mn (II)) that is oxidized in the suboxic zone. Mn-oxidizing bacteria are active in this layer [69]. Particulate Mn has a well formed maximum centered at ~ σ_θ = 16.0 (Fig. 11). There are significant spatial variations in the distributions of particulate Mn [69]. There are sometimes two maxima where the shallower maximum corresponds to the maximum specific oxidation rates of Mn but appears to consist of adsorbed Mn (II) rather than oxidized Mn. The deeper maximum is composed of Mn (III, IV) manganate material. Tebo [69] hypothesized that particulate oxidized Mn is transported laterally from coastal sites where Mn cycling is

faster than in the interior. This appears to be especially important in the SW region influenced by oxygen injected by the Bosporus Plume.

The distribution and cycling of Fe is similar to Mn but the concentrations are lower. Dissolved Fe increases to a maximum of 200-300 nM between 130 to 200 m then decreases to 14 – 40 nM in the deep water. The oxidative removal is also bacterially mediated. The deep concentrations appear to be controlled by solubility with FeS (mackinawite) or Fe_3S_4 (greigite), even though FeS_2 (pyrite) is more insoluble and is present in the water column [53]. In general the "iron interface" is slightly deeper than the "Mn interface", though both are shallower than the first appearance of sulfide [31].

4.7 Phototrophic Reactions

Most of the redox reactions in the suboxic zone are mediated by bacteria resulting in *in situ* consumption of CO_2 [5]. Chemosynthetic bacteria grow on carbon dioxide and water and get their energy from reduced compounds like H_2S, NH_4, Mn (II), Fe (II) and CH_4. High rates of chemosynthesis have been measured (Yilmaz et al., in press). In addition, the discovery by Repeta et al. [54] of high concentrations of bacteriochlorophyll BChl e in the suboxic zone suggests that anoxygenic photosynthesis occurs [22]. This is surprising because the light availability at these depths (<4 μEinst m^{-2} s^{-1}) is equal to between 0.0005% to 0.00005% of the surface irradiance [50]. The BChl e is associated with brown phototrophic *Chlorobium* bacteria. These bacteria are obligate phototrophs and compete with other bacteria under conditions of severe light limitation. They require light and sulfur. Their growth rates are extremely slow and their calculated doubling times are on the order of 2.8 yrs but somehow they maintain their existence. The role these bacteria play in elemental cycling is still unclear.

5. SPATIAL VARIABILITY

At any given time there are not any significant differences in the thickness of the suboxic zone in most of the Black Sea. Representative profiles from the central gyre, NW margin (both from Knorr 2001) and NE margin (by SBSIO) are shown in Fig. 12. These profiles were all collected about the same time of year. These data show that the density values of the upper and lower boundaries of the suboxic zone vary only slightly from the western central gyre to the NW and NE regions. Variations in the density of the lower boundary of the suboxic zone (the first appearance of sulfide) are typically small. The changes that are seen are at the upper boundary of the suboxic zone where small changes in the shape of the oxygen profile have a big impact. In any given region the vertical profiles of oxygen are very similar but they vary slightly on a sub-basin scale. The thickness of the oxic surface layer and the Cold Intermediate Layer (CIL) is

smaller in the central part of the Black Sea because of the dome shape structure of the pycnocline. As a result there is a smaller total inventory of oxygen in the upper water column. Thus, an equal flux of sinking organic matter moves the oxycline and the upper boundary of the suboxic zone upward more effectively in the central part of the sea. In addition, the central part of the Black Sea is considered to be more biologically productive, as compared to the periphery of the deep part of the sea, especially in the early spring when blooms occur [48, 76]. This is another factor that results in a thicker suboxic zone in the central gyre area. The thickness of the suboxic zone is larger in the central area because the exported carbon flux has a greater impact in that region.

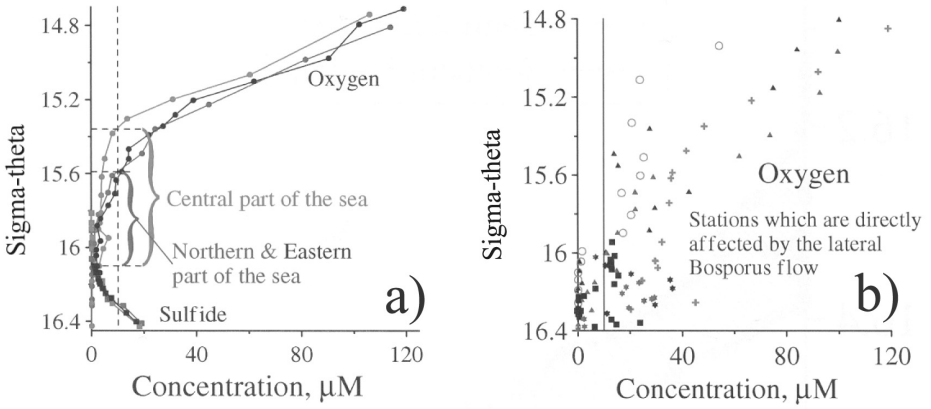

Figure 12. Regional variability of the oxygen and sulfide distributions. a) distributions in the central gyre, NW and NE regions b) distributions in the SW region influenced by the Bosporus Plume.

More dramatic differences are observed in the southwestern part of the Black Sea. This is the region influenced by the Bosporus Plume and is an area of intensive redox processes in a multi-layered oxic/anoxic transition zone. The suboxic zone cannot be traced into this region because of the intrusion of the oxygenated Bosporus plume waters. In this region, dissolved manganese is actively oxidized by the injected oxygen [58]. Maximum particulate manganese concentrations are 3 to 7 times larger than those in the central and northwestern parts of the sea. The onset of dissolved manganese in the SW region is moved deeper from its usual density of σ_θ = 15.8 – 15.9 to a density of about σ_θ = 16.2. The onset of sulfide is moved deeper from σ_θ = 16.1 – 16.2 to about σ_θ = 16.4 and it usually exhibits an interleaved, multi-layered oxic-suboxic-sulfidic structure.

By comparison the suboxic layer of the central part of the sea suggests an example of a stagnant biogeochemical structure. The oxygen concentration remains at the level of 5 μM throughout the upper and middle part of the suboxic zone and decreases to the analytical detection limit below σ_θ = 15.9. The maximum of particulate manganese is smaller than observed in the NW and SW parts of the sea, and seems to be disconnected from the onset of sulfide. The onset of dissolved manganese starts far below the upper boundary of the suboxic zone suggesting that redox transformations of manganese cannot generate a significant flux of electron-acceptors through the suboxic zone.

As a result of the Bosporus Plume there are significant lateral gradients along density surfaces in the SW region. An example for sulfide is shown in Fig. 13 where we compare sulfide versus density for the western central gyre and the SW region. In the SW region sulfide is consumed by direct reaction with the injected O_2 or indirectly by reacting with Mn (III, IV) formed from Mn (II) by the O_2 injection. As a result there are significant horizontal gradients for sulfide on densities from about 16.2 to 16.5. Thus, there must also be significant lateral fluxes of sulfide to the SW region driven by mixing along isopycnal surfaces. This has yet to be modeled in detail but Konovalov and Murray [25] and Neretin et al. [41] calculated that as much as 50% of the sulfide production in the Black Sea appears to be oxidized by oxygen injected laterally by the Bosporus Plume.

6. TEMPORAL VARIABILITY

The thickness of the suboxic zone varies temporally (Fig. 14) mostly on time scales of 5 to 10 years [25]. The vertical distribution of O_2 is determined by a balance between oxygen consumption due to respiration of sinking particulate organic matter (enhanced by increasing eutrophication during the 1970s and 1980s) and the input of O_2 by ventilation of the CIL and layers below [25]. Ventilation of the CIL sets the upper oxygen concentration and fundamentally determines the steepness of the vertical gradient and thus the downward flux of oxygen. Thus, the upper boundary of the suboxic zone varies with time. The first appearance of sulfide has been much less variable. It may be that sulfate reduction is less susceptible to changes in POC flux, which may not be as large at this depth. In addition, the first appearance of sulfide may not be as dependent on changes in ventilation because it is deeper. During the 1980s the suboxic zone thickened and then the oxycline moved deeper in the late 1980's and early 1990's (Fig. 14). These changes corresponded to a series of warmer winters when there was probably less ventilation of the CIL followed by a series of severe winters that produced favorable colder climate conditions for ventilating the CIL. The thickness of the suboxic zone decreased as the input of oxygen increased. During this period the temperature minimum (T_{min}) of the CIL was

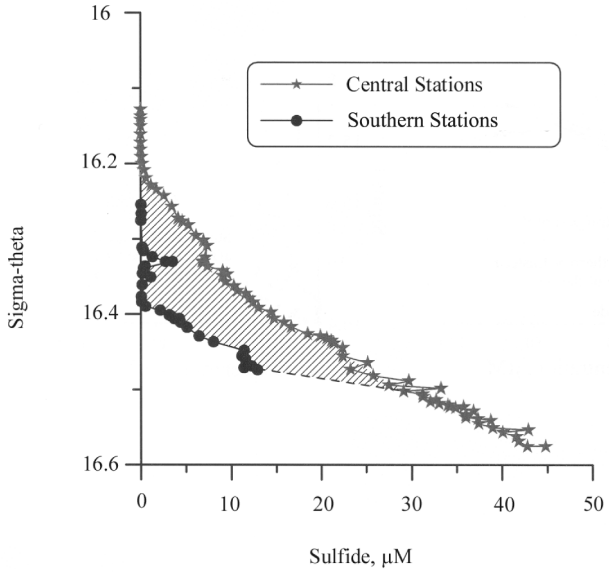

Figure 13. Horizontal gradients of sulfide from σ_θ = 16.2 to 16.6 from the central western gyre to the southwest region near the Bosporus Plume [from 26].

low and it moved to deeper density layers. Ventilation of the CIL from the surface was enhanced and oxygen concentrations on σ_θ = 15.4 were higher. This density surface was chosen because it is just above the upper boundary of the suboxic zone. The years 1987 and 2001 had lower oxygen concentrations on σ_θ = 15.4 and followed warm periods with less CIL formation and resulted in higher temperatures. As a result the suboxic layer became thicker. The increased ventilation resulting from the cold winters of 2002 and 2003 resulted in a thinner suboxic zone.

The temporal variation of O_2 and temperature on σ_θ = 15.4 is shown in Fig. 15. In the 1960s and early 1970s the temperature – oxygen data varied along an inverse trend (lower temperature had higher oxygen). The dashed lines are visual fits to the data. Starting in the late 1970s there was a shift to a new trend with a similar slope but at lower oxygen values. The nutrient concentrations and inventories (especially nitrate) in the euphotic zone of the Black Sea increased during this period [25]. We interpret this shift as resulting from increased eutrophication in the Black Sea due to increased nutrient fluxes from rivers. The eutrophication probably resulted in an increased flux of organic matter that resulted in increased oxygen consumption.

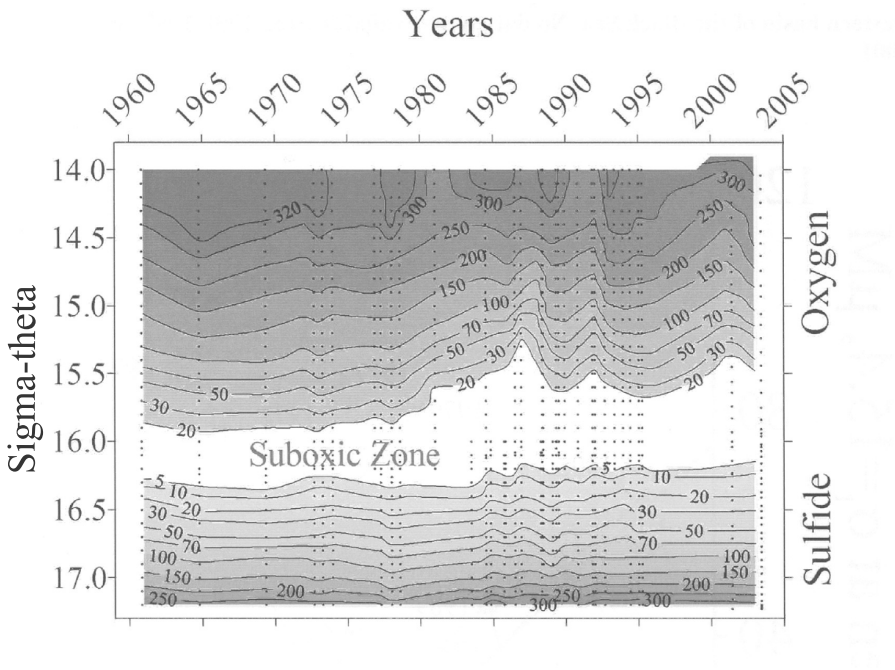

Figure 14. Temporal variability of the suboxic zone from 1962 to 2003. The data were complied from the central areas of the Black Sea (updated from [25]).

Unfortunately, with the exception of Karl and Knauer [23], there is almost no data for sinking fluxes of particulate organic matter at these depths in the Black Sea.

Distributions of properties in the Black Sea are influenced by climate related forcing. These fluctuations are superimposed on the anthropogenic eutrophication that occurred after the mid 1970s. Oguz and Dippner [44] have synthesized historical data from the Black Sea. Their historical time series of winter sea surface temperature (SST) averaged over the interior basin of the Black Sea is shown in Fig. 16a. The SST varied from 9.25 °C to 7.25 °C from 1875 to the present. The warm periods (labeled W) and cold periods (labeled C) vary on time scales of 5 to 10 years. Oguz and Dippner [44] showed that the warm periods are highly correlated with the negative phase of the North Atlantic Oscillation and the cold periods correlate with the positive NAO. The North Atlantic Oscillation is a large scale weather system that controls the atmospheric circulation over the North Atlantic and Eurasia. A positive NAO corresponds to a strong pressure gradient between the Azores high and Iceland low. Interestingly, positive NAO is associated with warm, wet conditions in northern Europe but cold, windy and dry conditions in the Black Sea region.

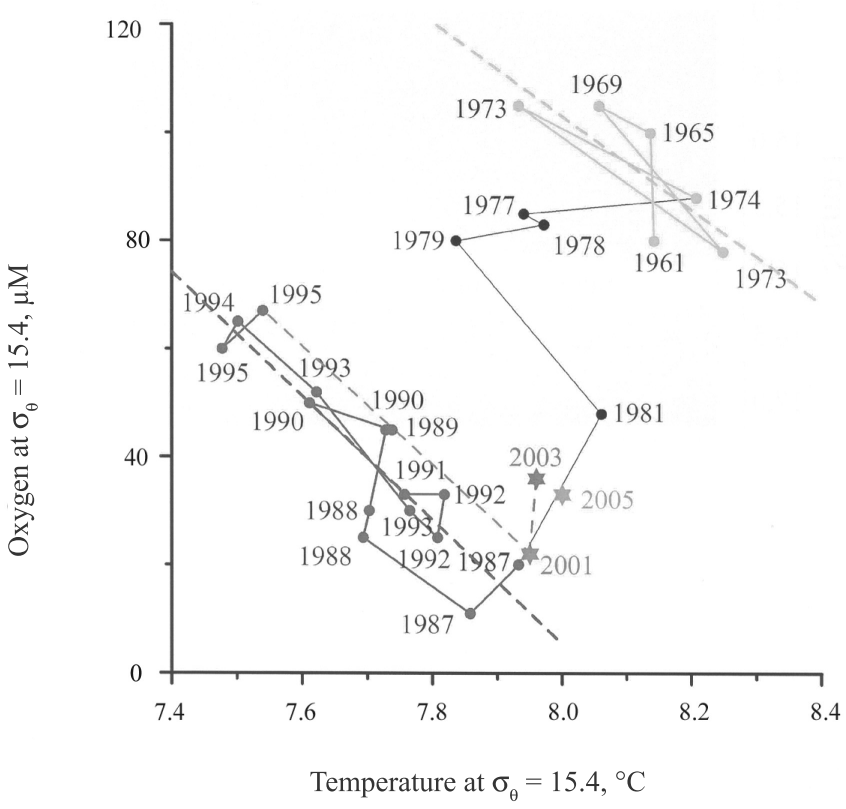

Figure 15. Time history of oxygen and temperature from 1961 to 2001 on the density surface σ_θ = 15.4 which is at the top of the suboxic zone. Most data are from the western basin of the Black Sea. No data were available from 1981-1987 and 1995-2001 [updated from 25].

Low surface air temperatures are associated with each cold interval and evaporation exceeds precipitation thus surface salinity increases. The time series is not as long but mean temperature of the CIL (Fig. 16 b) also has a minimum when SST is low. The complete Oguz and Dippner [44] analysis showed that, in general, there are significant positive correlations between positive NAO, cold air temperature, cold SST, stronger winds, colder CIL, higher surface nutrients, higher chlorophyll and plankton biomass and high sprat stock and recruitment but low anchovy (hamsa) stock and recruitment. According to this reasoning some of the variability is Black Sea fisheries may be determined by large scale climate patterns.

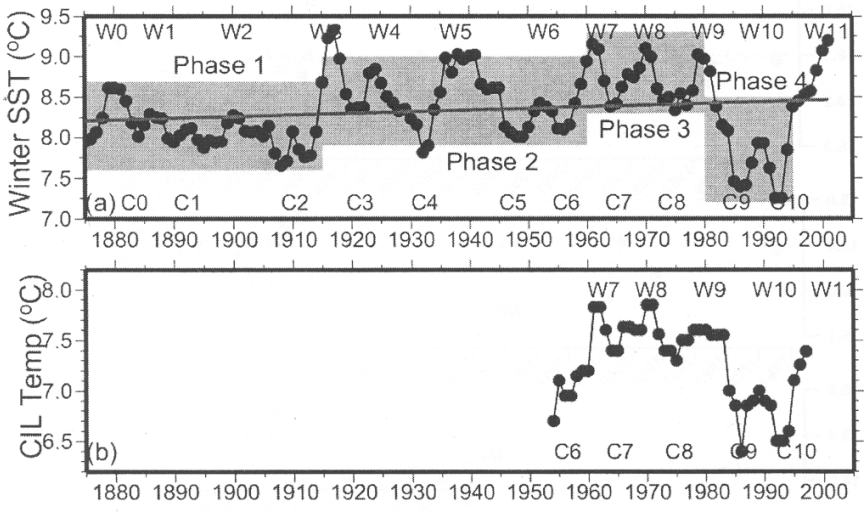

Figure 16. Long term variations in a) winter sea surface temperature (SST) (°C) averaged over the interior basin of the Black Sea, and b) the mean temperature (°C) of the Cold Intermediate Layer for the May-November period. The Cold (C) and Warm (W) periods since 1880 are indicated. Positive periods of the North Atlantic Oscillation (NAO) correspond to colder, dryer climate in the Black Sea region (C periods). Negative NAO periods are warmer and wetter (W periods). Modified from Oguz and Dippner [44].

Recently Podymov (O.I. Podymov, Ph.D. Thesis Abstract, Shirshov Institute of Oceanology RAS, Moscow, Russia, 2005) identified similar changes in the boundary of the anoxic zone in the northeastern part of the Black Sea near Gelendzhik. This part of the Sea is far from the influence of the inputs of the Bosporus plume and Danube River. Therefore the vertical structure in this region reflects "integrated", rather than local, forcing.

Data from individual stations from 1989 to the present are shown in Fig. 17. The results show that the density of first appearance of hydrogen sulfide occurred from σ_θ =16.15-16.25 kg/m^3 from 1991 - 1998 (Fig. 17a). In 1999-2000 this boundary appeared to shoal by about σ_θ = 0.05-0.15 kg/m^3 (corresponding to about 5-15 m). After 2000 the density was more stable. The same tendency can be seen for the increase of ammonium, total manganese and methane (Fig. 17 b, c, d). These changes appear related to the two warm winters that occurred in 1998-1999. This probably affected the balance between the input of fresh water from rivers and saline water from the Bosporus and the winter formation of the oxygen-rich CIL. In these same years there was an increase in sea surface temperature, an increase of temperature of the CIL [44], and shoaling of CIL in

the density field [37]. All these events appear to be connected with the weather conditions associated with the North Atlantic Oscillation (NAO) [44].

The decrease of intensity of CIL formation should lead to an increase in its core temperature and a decrease in its oxygen content. We calculated the average concentrations of dissolved oxygen in the CIL (for the layer σ_θ = 14.45-14.60 kg/m^3) (Fig. 17e). After 1999-2000 the integrated oxygen content decreased significantly. Minimum concentrations were observed in 2001-2002. In 2003-2004 the oxygen content in this layer increased back to values typical for the early 1990s.

These results give some hints for how the Black Sea may respond to future global climate change. Increases in sea surface temperature may lead to reductions in ventilation of the CIL and lack of replenishment of its oxygen content. The oxygen inventory in the CIL acts as a buffer for the consumption of oxygen due to organic matter respiration and controls the boundary condition for the downward diffusive flux of oxygen into the suboxic zone. Variations in the oxygen content of the CIL should lead to changes in the structure of the suboxic layer [25]. Following the distributions of physical and chemical parameters in the density field in the Black Sea should be an excellent approach for monitoring variations due to global climate change.

7. CONCLUSIONS AND FUTURE RESEARCH

The suboxic zone is a feature that exists at the boundary between the aerobic surface layer and sulfidic deep layer of the Black Sea. It is a region where both oxygen and sulfide have extremely low concentrations with no perceptible vertical gradients. In most of the Black Sea its upper and lower boundaries are at reasonably similar density values. In the southwest region of the Black Sea this structure is disrupted by ventilation by the Bosporus Plume which injects dissolved oxygen and results in enhanced sulfide oxidation, probably coupled with Mn oxidation and reduction. A complex interleaving of water layers exists in that region and there is no resolved suboxic layer.

The processes controlling the origin and variability of the suboxic zone include:

1. The source of oxygen by ventilation from the surface. Surface ventilation occurs down to the depth of the cold intermediate layer (CIL) (σ_θ = 14.5). This ventilation occurs in the winter on both the NW shelf and the center of the western and eastern gyre. The intensity of ventilation is determined by climate forcing which may be determined by large scale climate patterns like the North Atlantic Oscillation (NAO). This ventilation sets the upper boundary conditions for the downward transport of O_2.

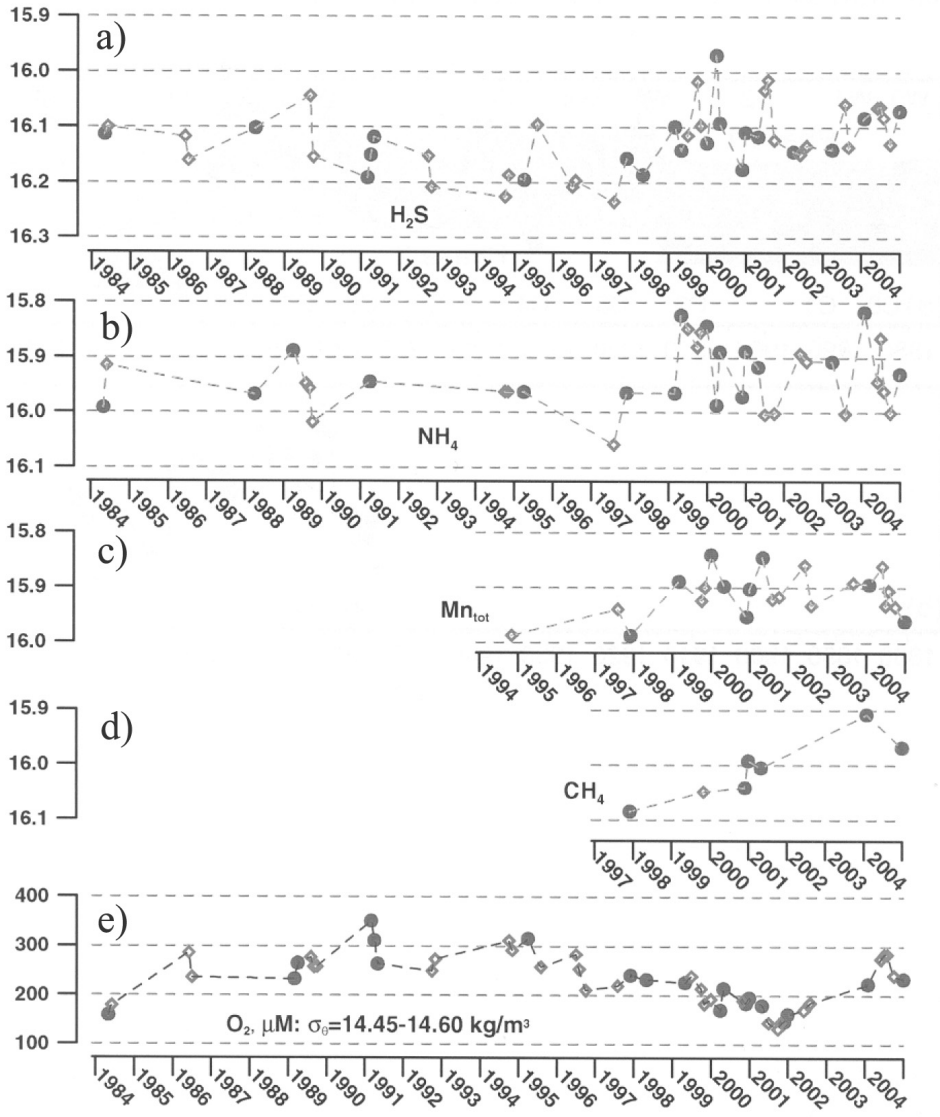

Figure 17. Interdecadal variability of the density (σ_θ, kg/m3) of first onsets of hydrogen sulfide, total manganese, ammonia, methane and averaged content of oxygen in the CIL (σ_θ=14.45-14.60 kg/m^3).

2. The main sink for oxygen is respiration of sinking particulate organic carbon (POC). Dissolved organic carbon (DOC) may also be important but much less is known about its distributions. Variability in the flux of POC (export production) is probably influenced by nutrient concentrations and food web structure (which are not unrelated). The late 1970s were a period of increased nutrient levels in the Black Sea (eutrophication) and this appeared to result in a thicker suboxic zone resulting from enhanced respiration.

In the near future it will be important to initiate and maintain time series of biogeochemical distributions in the Black Sea at several locations. Much is learned about the oceanography of a system when you can watch its response to a perturbation. Two important perturbations we want to continue to watch are climatic forcing (both natural and anthropogenic) and eutrophication. Process studies should be conducted of 1) the ventilation of the CIL and suboxic zone and 2) the flux and respiration of particulate organic matter and its relation to food web structure.

Acknowledgements

Tolga Uysal and Emre Pamukcu (both at Bogazici University), Amy Callahan, Clara Fuchsman, John Kirkpatrick (all in the School of Oceanography at University of Washington), Valery Chasovnikov, Oleg Podymov and Svetlana Pachomova (Shirshov Institute of Oceanology, Gelendjik and Moscow) helped with the nutrient analyses, collection and interpretation of hydrographic data and interpretation microbial distributions. Doug DiJulio and Keith Stewart, Steven Kassakian and Marta Krynytzky (UW undergraduates) helped with data analysis. George Luther (Delaware) and Brad Tebo (SIO) helped organize and conduct the research cruises and have allowed their data to be shown. The lab groups of Steve Emerson and Paul Quay (both at UW) assisted with the N_2 and isotope analyses. We acknowledge NSF Grants OCE 0081118 and MCB 0132101; NATO Collaborative Linkage Grant # EST-CLG-979141 and CRDF Awards RG1-2388-GE-02. F. Muller-Karger, L. Neretin and an anonymous reviewer provided constructive reviews.

References

[1] Andrusov N.I. Predvaritelnii otchyot ob uchastii v Chernomorskoi glubomernoi ekspiditsii 1890 g. (Preliminary report on participation in the 1890 Black Sea fathometer expedition) *Izvestiya Russkogo Geograficheskogo Obschestva (Proceedings of the Russian Geographical Society* 1890; 26(5):398-409.

[2] Basturk O., Saydam C., Salihoglu I. , Eremeeva L.V., Konovalov SK., Stoyanov A., Dimitrov A., Cociasu A., Dorogan L. and Altabet M. Vertical variations in the principle chemical properties of the Black Sea in the autumn of 1991. Journal of Mar Chem 1994; 45:149-65.

[3] Berner R.A. and Canfield D.E. A model for atmospheric oxygen over phanerozoic time. Am J Sci 1989; 289: 333-61.

[4] Bezborodov A.A. and Eremeev V.N. *Chernoe more. Zona vzaimodeistviya aerobnikh I anaerobnikh vod. (Black Sea. The oxic/anoxic interface)*, Sevastopol, MHI ASU, 1993. (in Russian)

[5] Brewer P.G. and Murray J.W. Carbon, nitrogen and phosphorus in the Black Sea. Deep-Sea Res 1973; 20:803-18.

[6] Broenkow W.W. and Cline J.D. Colorimetric determination of dissolved oxygen at low concentrations. Limnol Oceanogr 1969; 14(3):450-54.

[7] Buesseler K.O., Livingston H.D. and Casso S.A. Mixing between oxic and anoxic waters of the Black Sea as traced by Chernobyl cesium isotopes. Deep-Sea Res 1991; 38:725-46.

[8] Buesseler K.O., Livingston H.D., Ivanov L. and Romanov A. Stability of the oxic-anoxic interface in the Black Sea. Deep-Sea Res I 1994; 41(2):283-96.

[9] Caspers H. "Black Sea and Sea of Azov". In *Treatise on marine ecology and paleoecology*. Hedgpeth J.W. ed., Geological Society of America Memoirs, 1957.

[10] Codispoti L.A., Friederich G.E., Murray J.W. and Sakamoto C.M. Chemical variability in the Black Sea: implication of continuous vertical profiles that penetrated oxic/anoxic interface. Deep-Sea Res 1991; 38(2):691-710.

[11] Debol'skaya E.I. and Yakushev E.V. The role of suspended manganese in hydrogen sulfide oxidation in the Black Sea redox-zone. Water Resources 2002; 29:72-77. (In Russian)

[12] Dyrssen D. Metal complex formation in sulphidic seawater. Mar Chem 1985; 15:285-93.

[13] Dyrssen D., Haraldsson C., Westerlund S. and Aren K. *Report on the Chemistry of seawater, XXXII. Department of Analytical and Marine Chemistry*, Chalmers University of Technology and university of Goteborg, Goteborg, Sweden, 1986.

[14] Fonselius S.H. "Phosphorus in the Black Sea." In *The Black Sea – Geology, Chemistry and Biology.* Degens E.J., Koss D.A. eds., Amer Ass of Petrol Geologists Tulsa, 1974.

[15] Fuchsman C.A. and Murray J.W. Nitrogen species concentration and natural stable isotope profiles of the Black Sea. Deep-Sea Res Pt II, submitted.

[16] Goyet C., Bradshaw A.L. and Brewer P.G. The carbonate system in the Black Sea. Deep-Sea Res 1991; 38:1049-68.

[17] Gregg M.C. and Yakushev E. Surface ventilation of the Black Sea's cold intermediate layer in the middle of the western gyre. Geophys Res Lett 2005; 32:L03604, doi:10.1029/2004GL021580.

[18] Gunnerson C.G. and Ozturgut E. "The Bosporus." In *The Black Sea-geology, chemistry and biology.* Degens E.T. and Ross D.A. eds., AAPG, Memoir 20, 1974.

[19] Holland H.D. *The Chemical Evolution of the Atmosphere and Oceans.* Princeton Univ. Press, Princeton, 1984.

[20] Humborg C., Ittekkot V., Cociasu A. and v.Bodungen B. Effect of Danube River dam on Black Sea biogeochemistry. Nature 1997; 386:385-88.

[21] Ivanov L.I., Konovalov S.K., Belokopytov V. and Ozsoy E. "Regional peculiarities of physical and chemical responses to changes in external conditions within the Black Sea pycnocline: cooling phase." In *NATO ASI Series. NATO TU-Black Sea project: Ecosystem modeling as a management tool for the Black Sea. Symposium on scientific results.* Ivanov L. and Oguz T. eds., Kluwer Academic Publishers, The Netherlands, 1998.

[22] Jørgenson B.B., Fossing H., Wirsen C.O. and Jannasch H.W. Sulfide oxidation in the anoxic Black Sea chemocline. Deep-Sea Res 1991; 38:1083-1104.

[23] Karl D.M. and Knauer G.A. Microbial production and particle flux in the upper 350 m of the Black Sea. Deep-Sea Res 1991; 38:921-42.

[24] Konovalov S.K., Tugrul S., Basturk O. and Salihoglu I. "Spatial isopycnal analysis of the main pycnocline chemistry of the Black Sea: Seasonal and interannual variations." In *Sensitivity to change: Black Sea, Baltic Sea and North Sea.* Ozsoy E. and Mikaelyan A. eds., Kluwer Academic Publishes, Dordrecht, NATO ASI, 1997.

[25] Konovalov S.K. and Murray J.W. Variations in the chemistry of the Black Sea on a time scale of decades (1960-1995). J Marine Syst 2001; 31:217-43.

[26] Konovalov S.R., Luther G.W. III, Friederich G.E., Nuzzio D.B, Tebo B.M., Murray J.W., Oguz T., Glazer B., Trouwborst R.E., Clement B., Murray K.J. and Romanov A Lateral injection of oxygen with the Bosporus plume – fingers of oxidizing potential in the Black Sea. Limnol Oceanogr 2003; 48:2369-76.

[27] Korotaev G., Oguz T., Nikiforov A. and Koblinksy C. Seasonal, imterannual and mesoscale variability of the Black Sea upper layer circulation derived from altimeter data. J Geophys Res 2003; 108:19-1 to 19-15.

[28] Kuypers M.M.M., Sliekers A.O., Lavik G., Schmid M., Jorgensen B.B., Kuenen J.G., Damsté J.S.S., Strous M. and Jetten M.S.M. Anaerobic ammonium oxidation by anammox bacteria in the Black Sea. Nature 2003; 422:608-11.

[29] Latif M.A., Özsoy E., Oguz T. and Ünlüata U. (1991) Observations of the Mediterranean inflow into the Black Sea. Deep-Sea Res 1991; 38: S711-S724.

[30] Lee B-S, Bullister J.L., Murray J.W., Sonnerup R.E. Anthropogenic chlorofluorocarbons in the Black sea and the Sea of Marmara. Deep-Sea Res 2002; 49:895-913.

[31] Lewis B.L. and Landing W.M. The biogeochemistry of manganese and iron in the Black Sea. Deep-Sea Res 1991; 38:773-804.

[32] Lukashev Yu.F., Yakushev E.V. "Dissolved oxygen content measurements on the border of the sulfide zone of the Black Sea." In *PACON-99 Symposium.* Abstracts, Russian Academy of Sciences, Moscow, Russia, 1999.

[33] Luther G.W. III, Church T.M. and Powell D. Sulfur speciation and possible sulfide oxidation in the water column of the Black Sea. Deep-Sea Res 1991; 38:1121-37.

[34] Millero F.J. The oxidation of H_2S in Black Sea waters. Deep-Sea Res 1991; 38:1139-50.

[35] Murray J.W. and Izdar E. The 1988 Black Sea Oceanographic Expedition: Overview and new discoveries. Oceanography 1989; 2:15-21.

[36] Murray J. W., Jannasch H.W., Honjo S., Anderson R.F., Reeburgh W.S., Top Z., Friederich G.E., Codispoti L.A. and Izdar E. Unexpected changes in the oxic/anoxic interface in the Black Sea. Nature 1989; 338:411-13.

[37] Murray J.W., Konovalov S.K., Romanov A., Luther G., Friederich G., Tebo B., Oguz T., Besiktepe S., Tugrul S. and Yakushev E. "R/V Knorr Cruise: New Observations and variations in the structure of the suboxic zone." In *Oceanography of Eastern Mediterranean and Black Sea*. Yilmaz A. ed., Tubitak Press, 2003.

[38] Murray J.W. "Hydrographic variability in the Black Sea." In *Black Sea Oceanography,* Izdar E. and Murray J.W. eds., Kluwer Academic Publishers, 1991.

[39] Murray J.W., Top Z. and Ozsoy E. Hydrographic properties and ventilation of the Black Sea. Deep-Sea Res 1991; 38:663-89.

[40] Murray J.W., Codispoti L.A. and Friederich G.E. "Oxidation-reduction environments: the suboxic zone in the Black Sea." In *Aquatic Chemistry: Interfacial and Interspecies Processes.* Huang C.P., O'Melia C.R. and Morgan J.J. eds., Adv Chem Ser, No. 224, 1995.

[41] Neretin L.N., Volkov I.I., Bottcher M.E. and Grinenko V.A. A sulfur budget for the Black Sea anoxic zone. Deep-Sea Res Pt I 2001; 48:2569-93.

[42] Neuman G. Die absolute Topographie des physikalischen Meeresniveaus und die Oberflächenströmungen des Schwarzen Meeres. Annalen der Hydrographie und Maritimen Meteorologie 1942; 70:265-82.

[43] Oguz T. Role of physical processes controlling oxycline and suboxic layer structures in the Black Sea. Global Biogeochem Cy 2002; 16:3-1 to 3-13.

[44] Oguz T. and Dippner J.W. Regulation of the Black Sea physical and ecosystem structure by climate variability and anthropogenic forcing. Deep-Sea Res Pt II, in press.

[45] Oguz T., Latif M.A., Sur H.I., Ozsoy E. and Unluata U. "On the dynamics of the southern Black Sea." In *Black Sea Oceanography*, Izdar E. and Murray J.W. eds., Kluwer Academic Publishers, 1991.

[46] Oguz T., Malanotte-Rizzoli P. and Aubrey D. Wind and thermohaline circulation of the Black Sea driven by yearly mean climatological forcing. J Geophys Res 1995; 100:6845-63.

[47] Oguz T., Ivanov L.I. and Besiktepe S. "Circulation and hydrographic characteristics of the Black Sea during July 1992." In *Ecosystem Modeling as a Management Tool for the Black Sea.* Ivanov L.I. and Oguz T. eds., NATO Science Series, Vol. 2, 1998.

[48] Oguz T., Tugrul S., Kideys A.E., Ediger V. and Kubilay N. Physical and biogeochemical characteristics of the Black Sea. Chpt. 33 in The Sea Volume 14. Eds. Robinson A.R. and Brink K.H. Harvard University Press, 2004; 1331-69.

[49] Oguz T., Murray J.W. and Callahan A. Modeling redox cycling across the suboxic-anoxic interface zone in the Black Sea. Deep-Sea Res 2001; 48:761-87.

[50] Overmann J., Cypionka H and Pfennig N. An extremely low-light-adapted phototrophic sulfur bacterium from the Black Sea. Limnol Oceanogr 1992; 37:150-55.

[51] Ozsoy E., Unluata U., Top Z. The evolution of Mediterranean water in the Black Sea: interior mixing and material transport by double diffusive intrusions. Prog Oceanogr 1993; 31:275-320.

[52] Peneva E., Stanev E., Belokopytov V. and Le Traon P.Y. Water transport in the Bosporus Strait estimated from hydro-meteorological and altimeter data: seasonal and decadal variability. J Marine Syst 2001; 31:21-33.

[53] Pilskaln C.H. "Biogenic aggregate sedimentation in the Black Sea Basin." In *Black Sea Oceanography*, Izdar E. and Murray J.W. eds., Kluwer, 1991.

[54] Repeta D.J., Simpson D.J., Jorgensen B.B. and Jannasch H.W. Evidence of anoxygenic photosynthesis from the distribution of bacteriochlorophylls in the Black Sea. Nature 1989; 342:69-72.

[55] Richards F.A. "Anoxic basins and fjords." In *Chemical Oceanography*, Riley J.P. and Skirrow G. eds., Academic Press 1, 1965.

[56] Savenko A. V. Precipitation of phosphate with iron hydroxide forming by mixing of submarine hydrothermal solutions and the sea water (on the base of experimental data). Geochem Int 1995; 9:1383-89.

[57] Saydam C., Tugrul S., Basturk O. and Oguz T. Identification of the oxic/anoxic interface by isopycnal surfaces in the Black Sea. Deep-Sea Res 1993; 40:1405.

[58] Schippers A., Neretin L.N, Lavik G., Leipe T. and Pollehne F. Manganese (II) oxidation driven by lateral oxygen intrusions in the western Black Sea. Geochim Cosmochim Ac 2005; 69:2241-52.

[59] Shaffer G. Phosphorus pumps and shuttles in the Black Sea. Nature 1986; 321:515-17.

[60] Skopintsev B.A. *Formirovanie sovemennogo khimicheskogo sostava Chyornogo moray (Formation of the modern chemical composition of the Black Sea)*, Ed. Hydrometeoizdat, Leningrad, 1975. (In Russian).

[61] Sorokin Yu.I. The bacterial population and the processes of hydrogen sulfide oxidation in the black Sea. Journal du Conseil International Exploration de la Mer 1972; 34:423-54.

[62] Sorokin Y.I. "The Black Sea." In *Ecosystems of the world 26: estuaries and enclosed seas*, Ketchum B.H. ed., Amsterdam: Elsevier, 1983.

[63] Sorokin Yu. I. *The Black Sea. Ecology and Oceanography.* Backhuys Publishers, Leiden, 2002.

[64] Spencer D.W. and Brewer P.G. Vertical advection diffusion and redox potentials as controls on the distribution of manganese and other trace metals dissolved in waters of the Black Sea. J Geophys Res 1971; 76:5877-92.

[65] Spencer D.W., Brewer P.G. and Sachs P.L. Aspects of the distribution and trace element composition of suspended matter in the Black Sea. Geochim Cosmochim Ac 1972; 36:71-86.

[66] Stanev E.V. and Peneva E.L. Regional sea level response to global climatic change: Black Sea examples. Global Planet Change 2002; 32:33-47.

[67] Stanev E.V., Staneva J., Bullister J.L. and Murray J.W. Ventilation of the Black Sea Pycnocline. Parameterization of convection, model simulations and validations against observed chlorofluorocarbon data. Deep-Sea Res Pt I 2005; 51:2137-69.

[68] Stunzhas P.A. "Fine structure of vertical oxygen distribution in the Black Sea." In *Complex investigation of the Northeastern Black Sea*, Zatsepin A.G., Flint M.V. eds., Nauka, Moscow, 2002. (In Russian)

[69] Tebo B.M. Manganese (II) oxidation in the suboxic zone of the Black Sea. Deep-Sea Res 1991; 38:883-906.

[70] Tolmazin D. Changing coastal oceanography of the Black Sea. I. Northwestern shelf. Prog Oceanogr 1985a; 15:217-76.

[71] Tolmazin D. Changing Coastal Oceanography of the Black Sea. II: Mediterranean Effluent. Prog Oceanogr 1985b; 15:277-316.

[72] Tugrul S., Basturk O., Saydam C. and Yilmaz A. Changes in the hydrochemistry of the Black Sea inferred from water density profiles. Nature 1992; 359:137-39.

[73] Ward B.B. and Kilpatrick K.A. "Nitrogen transformations in the oxic layer of permanent anoxic basins: The Black Sea and Cariaco Trench." In *Black Sea Oceanography*, Izdar E. and Murray J.W. eds., Kluwer Academic Publishers, 1990.

[74] Yakushev E.V., Lukashev Yu.F., Chasovnikov V.K. and Chzhu V.P. "Modern notion of the vertical hydrochemical structure of the Black Sea redox zone." In *Complex investigation of the Northeastern Black Sea*, Zatsepin A.G., Flint M.V. eds., Nauka, Moscow, 2002. (In Russian)

[75] Yao W. and Millero F.J. Adsorption of phosphate on manganese dioxide in seawater. Environ Sci Technol 1996; 30:536-41.

[76] Yilmaz A., Coban-Yildiz Y., Morkoc E. and Bologa A. Surface and mid-water sources of organic carbon by phyto- and chemo-autotrophic production in the Black Sea. Deep-Sea Res Pt II, submitted.

TEMPORAL VARIABILITY IN THE NUTRIENT CHEMISTRY OF THE CARIACO BASIN

Mary I. Scranton[1], Michelle McIntyre[2], Yrene Astor[3], Gordon T. Taylor[1], Frank Müller-Karger[2], Kent Fanning[2]

[1] *Stony Brook University, Marine Sciences Research Center, Stony Brook, NY 11794-5000, USA*

[2] *University of South Florida, College of Marine Science, 140 7th Avenue South, St. Petersburg, FL 33701, USA*

[3] *Fundación La Salle de Ciencias Naturales, Estacion de Investigaciones Marinas de Margarita, Apartado 144 Porlamar, Isla de Margarita, Venezuela*

Abstract Nutrient data have been collected monthly at the CARIACO time series site in the Cariaco Basin since 1995, providing a unique picture of the cycling of NO_3^-, NO_2^-, NH_4^+, PO_4^{3-} and SiO_2 in this permanently anoxic system underlying a major coastal upwelling zone. Our data indicate that nutrients for phytoplankton growth are primarily supplied by upwelling of subsurface water on a seasonal basis. In addition, coastal runoff seems to supply important amounts of silica and ammonium to surface waters. We saw no indication of local nitrogen fixation in the Cariaco surface waters. In the suboxic zone, our data to date are not of sufficiently high enough resolution to resolve all important features. However, at least partial phosphate removal appears to occur in a zone above the first appearance of sulfide, and associated with intermittent intrusions of oxygenated water. In the suboxic zone, there appear to be thin layers where ammonium and nitrite coexist, potentially permitting anaerobic ammonium oxidation (anammox) to take place. In the deep waters, concentrations of ammonium, phosphate and silica continue to increase at a rate consistent with prior studies. However, in the upper part of the anoxic zone, there is evidence for sulfide removal, probably associated with oxygen intrusions.

Keywords: Cariaco Basin, upwelling, nutrients, time series

1. INTRODUCTION

The Cariaco Basin has been known since the mid-1950s to be the world's largest fully marine system which is permanently sulfidic [28]. As such, it has been the site of a variety of studies focused on the products of remineralization of organic matter [13, 27, 28, 30, 31, 37]. This fifty year time series has recently been greatly enhanced by the establishment of the international (Venezuela and

L. N. Neretin (ed.), Past and Present Water Column Anoxia, 139–160.

United States) CARIACO program. CARIACO (Carbon Retention in a Colored Ocean) consists of a monthly time series station in the eastern basin of the Cariaco at which hydrographic, nutrient and primary productivity measurements have been made since November 1995. A suite of other measurements, including a sediment trap mooring, roughly semiannual microbiological studies and current meter measurements are also available from this site [24]. Although early studies typically assumed that the chemistry of the Cariaco Basin was in steady state or changed very slowly [27, 31], more recent work, including that from the CARIACO program, has demonstrated that the system is quite dynamic [29].

The location of the CARIACO station in the tropics, in an area of strong seasonal upwelling, means that the chemistry of the water column and sediments of this system are potentially very sensitive to climatic shifts as well as episodic events. In this paper we present evidence of the seasonal and interannual variability of nutrients (nitrate, nitrite, phosphate, and silicate) and other species in the Cariaco Basin between 1998 and 2004, as well as some information on long-term trends in the deep water. We also discuss the factors that control both the vertical and temporal variability of these parameters.

2. STUDY SITE

The Cariaco Basin is a pull-apart basin located on the continental shelf of Venezuela in the trade wind belt. It is about 1400 m deep, is divided into two subbasins separated by a saddle rising up to about 900 m, and is nearly 150 km long (E-W), but only about 50 km wide (N-S). It is located between the mainland of Venezuela and a series of small islands (Isla Margarita, Tortuga) near the edge of the continental shelf. The regional sill in this area is approximately 75-100 meters deep, but there are two deeper channels of about 135-150 m in the east and west allowing exchange of Caribbean water to depth. Very little is known about the exchange process, although Astor [3] have speculated that intrusions over the eastern sill may be caused in part by impingement of Caribbean eddies along the continental margin. The CARIACO time series site is located on the northern side of the deepest part of the Eastern Basin at 10^o30'N 64^o40'W in about 1400 m of water. Sampling is carried out monthly at this site using the Venezuelan research vessel R/V Hermano Gines, operated by the Fundación La Salle from Punta de Piedras, Isla de Margarita.

Because of the limited connection of the deep basin to the open Caribbean, and because of the location of the basin within the core of seasonal upwelling which occurs along the South American coast from Guiana to Columbia, the waters of the Cariaco are oxygen depleted, and below about 300 m are sulfidic. Primary production rates peak during the windy, upwelling season (roughly January to April) and are relatively low during the rest of the year (although

a secondary upwelling tends to occur in July). Previous studies [17, 18, 33] have demonstrated that there are two maxima in microbial activity, one in the surface euphotic layer and one bracketing the oxic/anoxic interface.

3. METHODS

Hydrographic data were collected using a SeaBird rosette with a coupled SBE-19 or SBE-25 Conductivity-Temperature-Depth (CTD) and YSI-23-Y oxygen sensor. In January 2003, the oxygen sensor was replaced with a Seabird model SBE-43. Discrete oxygen samples were collected in duplicate using glass-stoppered bottles and analyzed by Winkler titration ([32] as modified by [1]). The analytical precision for oxygen is about 1.5 μM, and the limit of detection is estimated to be about 5 μM [29].

Water samples for nutrients (ammonium, nitrite, nitrate, phosphate and silicate) were collected from Niskin bottles into 1-L plastic bottles. These samples were filtered through a 0.8 μm glass fiber filter into clear 60mL polycarbonate bottles and frozen within minutes of collection. Beginning in September 2001 the samples were filtered through a 0.8 μm Nuclepore filter and a separate sample was collected, filtered, and stored unfrozen for silicate analysis. All samples were transported within 1 to 4 months to the University of South Florida, where samples were analyzed following the recommendations of Gordon [15] for the WOCE WHP project for nitrate, nitrite, phosphate and silicate analysis and the standard techniques described by Strickland and Parsons [32]. For ammonium analyses, we employed a method based on modifications (developed by Alpkem (now Astoria-Pacific International, Inc.) and L. Gordon at Oregon State University allowing the manual method to be used in an automated manner) of published methods [22] and described at: `http://chemoc.coas.oregonstate.edu:16080/~lgordon/cfamanual/WHPMANw_nh4_web.htm#_6.5._Ammonia`.

Detection limits for the nutrients were determined by calculating the concentrations in triplicate standards, averaging the results within each triplicate group, averaging those standard deviations, and finally doubling the averages to get the detection limits. Through April 2000 samples were analyzed on an ALPKEM RFA II. For this RFA equipment the detection limits were: for phosphate 0.03 μM, for ammonium 0.07 μM, for nitrite 0.02 μM, for nitrate 0.06 μM, and for silicate 0.04 μM. Beginning in May 2000 analyses were performed on a Technicon Analyzer II. Detection limits for this equipment are: for phosphate 0.02 μM, for ammonium 0.1 μM, for nitrite 0.01 μM, for nitrate 0.04 μM, and for silicate 0.4 μM.

Sulfide was measured on triplicate samples preserved with $ZnCl_2$ using a modification of the Cline method [8, 29]. Precision of triplicate measurements were about ±5% for concentrations greater than 1 μM. The detection

limit for sulfide is estimated to be about 1-2 μM [29]. TCO_2 was calculated from measurements of alkalinity and pH determined as described by Astor [4]. Chlorophyll was extracted in methanol and read on a Turner Designs fluorometer using standard methods [12, 19]. Primary production was measured using in situ incubations of samples enriched with $^{14}CO_2$ as described by Muller-Karger [25].

4. RESULTS

Nutrient and oxygen data have been collected at the CARIACO time series site every month since November 1995 from 19 to 20 depths. However, the above estimates of precision and accuracy are only applicable for data obtained since 1998 by the USF laboratory of Kent Fanning. We restrict our time series presentations to data collected since that date. Silicate samples were frozen prior to cruise 70, so silicate data for the Cariaco prior to September 2001 have not been used. All data used in this report are available from the Cariaco web site at `http://imars.usf.edu/cariaco/sdmt.html` or from the authors.

4.1 Vertical Profiles

To demonstrate the distribution of nutrients at the CARIACO station, vertical profiles are presented in Fig. 1 for cruise 96 from January 2004 (upwelling period) for the nutrient species nitrate, nitrite, ammonium, phosphate and silicate, together with oxygen, hydrogen sulfide, chlorophyll a, primary production, and beam attenuation (light scattering) which in this system near the interface seems to reflect bacterial abundance [33]. This date was chosen because samples for nutrients were taken both at the standard depths used for all monthly cruises, and at additional depths across the interface (on a separate cruise one week later). The basic features of the system can clearly be seen. Nitrate, nitrite and silica values all were extremely low in the upper 15-25 m, while chlorophyll a and primary production were high. For this date, the chlorophyll maximum was at 25 m and the maximum in primary productivity was observed at 1 m (Varela, personal communication). At 35 m, which was the base of the surface warm layer, nutrient values increased noticeably, with a marked primary nitrite maximum. The nitrate concentrations reached a maximum at 200 m and a small secondary nitrite maximum was found immediately above the depth where sulfide could first be detected. Ammonium was detectable within the suboxic zone, but started to increase rapidly only after the onset of sulfide. Throughout this paper, we empirically define the suboxic zone as the layer where oxygen and sulfide concentrations were both less than about 2 μM. Based on the oxygen sensor on the CTD, oxygen concentrations less than 2 μM were present below depths of about 250 m, and colorimetric analysis showed that sulfide concentrations exceeded 2 μM below about 300 m resulting in a 50 m suboxic layer on

this date. Phosphate concentrations increase relatively steadily below the euphotic zone although there are some features near the interface in the suboxic zone. Silicate concentrations increased monotonically through the interface.

4.2 Temporal Variability

Upwelling. One of the strengths of a study which emphasizes reoccupation of a single site is that temporal variability in parameters can be examined. In Fig. 2, we present contours of the concentrations of nitrate, nitrite, ammonium, phosphate and silicate in the upper 400 m of the Cariaco water column between 1998 and early 2004. We have chosen this depth range because our sampling resolution is relatively high and because, based on other studies [3], we believe that the primary variability due to climatological factors occurs in this portion of the water column. The time series data (Fig. 2) show an annual pattern of shoaling nutrient isopleths in the early part of the year (January through May) and a deepening in summer and fall. Fig. 3 presents a plot representing the variation over time of the integrated primary production, the depth of mixed layer inside the Cariaco Basin, the depth at which nitrate begins to increase (nitracline), and the estimated speed of upwelling. In this figure we have approximated the depth of the nitricline as the depth at which the increase in nitrate concentrations between adjacent depths is greater than 0.1 μM and the depth of the mixed layer by the depth at which sigma-t difference between the surface and a particular depth exceeds 0.125 kg m^{-3}. Rates of upwelling are calculated by computing the change of depth of the 25.6 isopycnal between two cruises. Since the cruises are approximately one month apart, the rates of upwelling are not exact and may not reflect short term upwelling events

The variation of the integrated primary production with time (Fig. 3, bottom panel) is important to the entire Cariaco ecosystem, and the analysis of the effects of other parameters on that variation is therefore of particular interest. Out of 69 cruises between 1998 and mid-2004, 18 had primary production above 2 g C m^{-2} d^{-1} and 22 had productivities above 1.5 g C m^{-2} d^{-1}, representing high values compared to the average production value of 1.4 g C m^{-2} d^{-1}. For 15 of these cruises, the nitricline was located within the mixed layer (above the solid line in Figure 3, middle panel). For several other dates (December 2000 and 2002 and July 2000), production increased above 1.5 g C m^{-2} d^{-1} even though the nitricline was deeper than the base of the mixed layer. On these dates, however, upwelling was strong enough to have raised the nutricline (by 20 m between November and December of 2000, by 30 m between November and December 2002, and by 20 m between June and July of 2000). In these cases, although the nitricline did not reach the mixed layer, upward displacement of water probably injected nutrients into the surface. Although we may not have

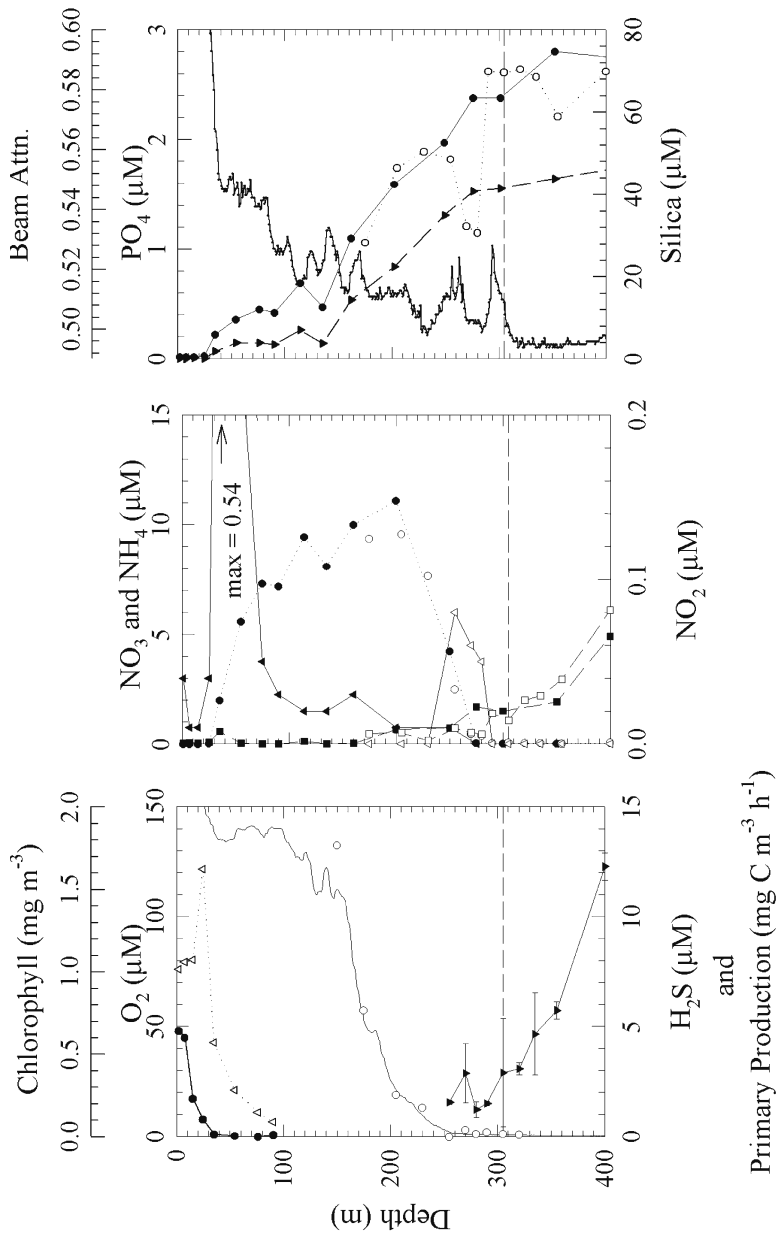

Figure 1. Profiles from Cariaco 96 (January 2004). Left panel: ●, primary production; △, chl a; ○, discrete oxygen samples; solid thin line, CTD oxygen values; ▼, H_2S. Center panel: open symbols from monthly Cariaco cruise, closed symbols from geochemistry cruise 7 d later; △, ▲, NO_2^-; ○, ● NO_3^-; □, ■ NH_4^+. Right panel: ▽, ▼ SiO_2; ○, ● PO_4^{3-}; solid line, beam attenuation coefficient.

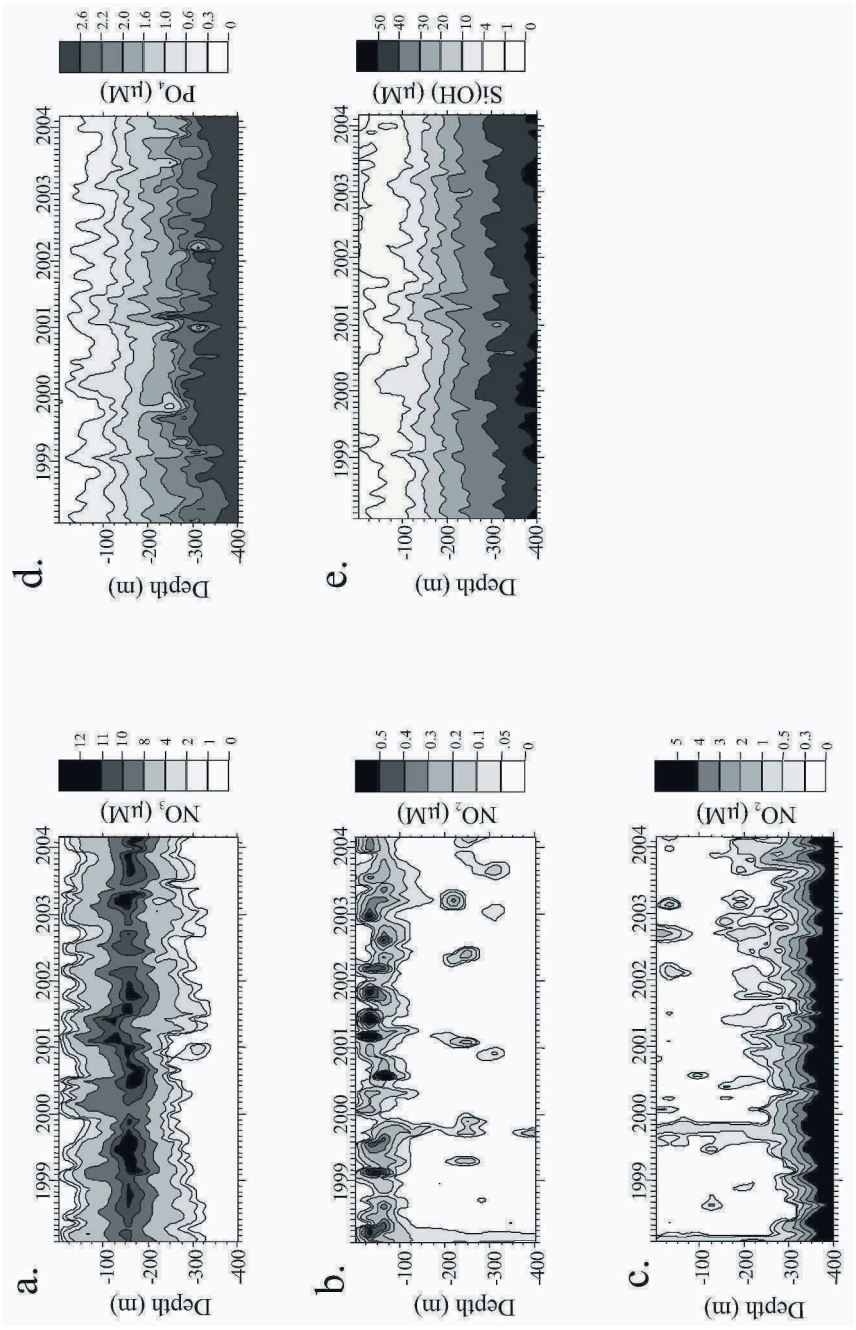

Figure 2. Time series plots of nutrient species in the top 400 m at the CARIACO site.

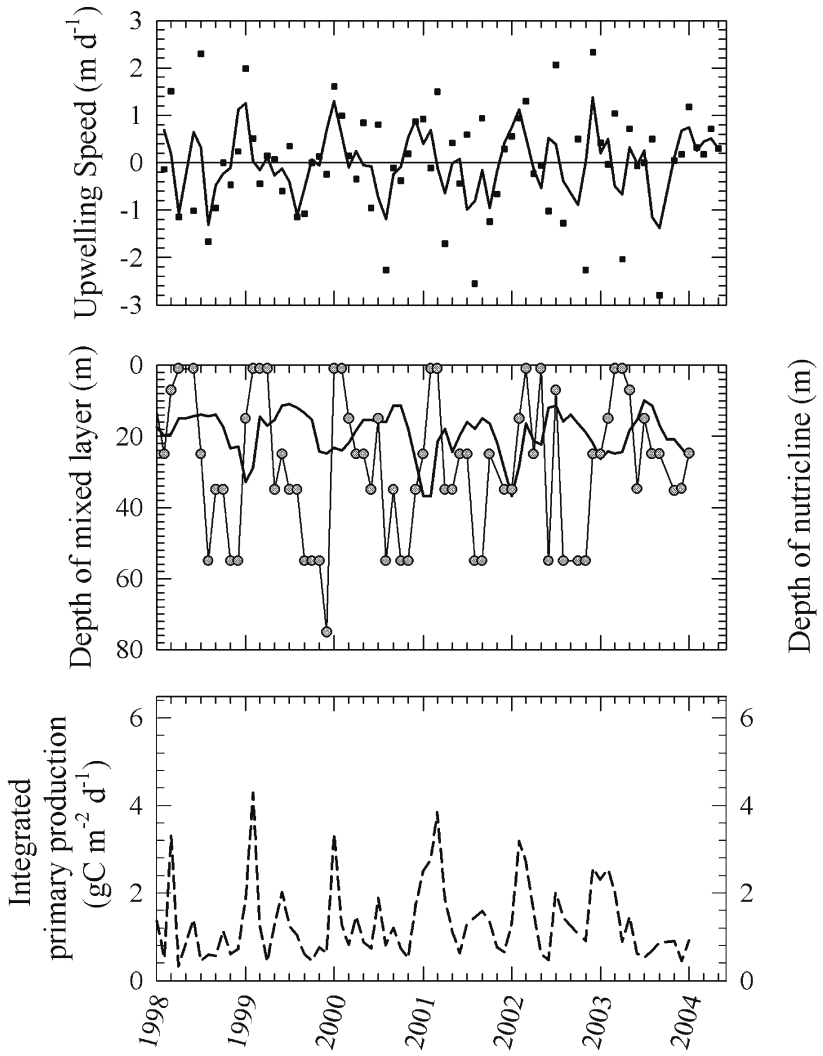

Figure 3. Upper panel: Upwelling speed (squares) and two month running average of upwelling speed (solid line) where upwelling speed is calculated as the rate of change of depth of the 25.6 isopycnal. Middle panel: depth of mixed layer (upper solid line plotted as two month running average) and depth of nitricline (circles and grey line). Bottom panel: Integrated primary production (dashed line).

measured nutrients in the surface waters, they may have been promptly removed by a sudden increase in production.

Another factor which may be important in whether a bloom is maintained is whether upwelling rates exceed the sinking rate of phytoplankton, which would enable cells to remain longer in the mixed layer, thus increasing production. Estimated upwelling rates ≥ 0.5 m d^{-1} were observed for 23 cruises, of which 16 exhibited high productivity. We conclude that the presence of strong upwelling, and the upward transport of nutrients (including nitrite and nitrate) through a mixed layer, results in conditions suitable for a bloom, especially when the wind increases the turbulence and deepens the mixed layer. Fig. 2 (a, b) suggests that high nitrite levels, as well as high nitrate levels, also contributed to the occurrences of higher primary production.

Oxygen. Fig. 4 shows the contoured oxygen probe data for the period 1998 to early 2004. Oxygen concentrations decrease immediately below the euphotic zone (top 35 to 50 m) and reach values of less than 20 μM at depths of 200 to 250 m. The steepest gradient in oxygen concentration is typically between 100 and 200 m, but there is considerable annual and interannual variability. Upwelling causes shoaling of oxygen isopleths (compare Fig. 3 and 4). We have observed multiple occasions where small oxygen maxima were seen at depths as great as 400 m, representing intrusions of oxygenated water from outside the basin [3] and these maxima have been confirmed by discrete samples in some cases. Some years (1997; 1998; 2001, 2002, late 2003) experienced much more intense ventilation of deep layers than other years (1999-2000).

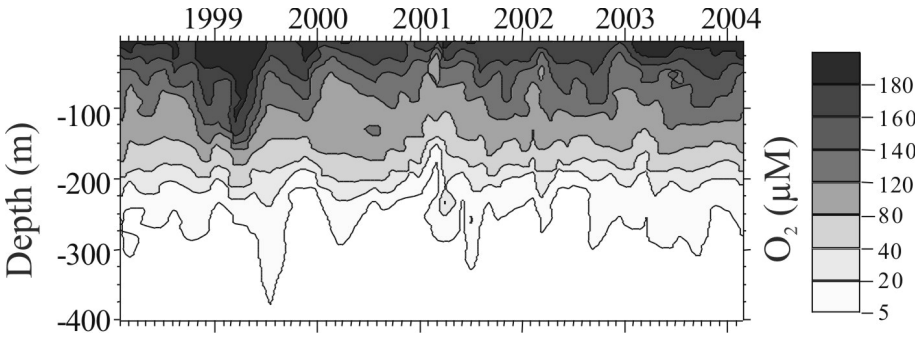

Figure 4. Contours of oxygen from the continuous probe on the CTD at the CARIACO time series site over time.

Nitrate. In surface waters, nitrate concentrations are consistently low in the upper 35-55 m, although occasionally during upwelling events, surface waters contained more than 1 μM nitrate (Fig. 2a). During upwelling season, nitrate contours move toward the surface. Nitrate concentrations increase rapidly below the surface, reaching a maximum of up to 12 μM at about 160 m. Below this depth, nitrate decreases to zero at about same depth oxygen reaches values

less than 5 μM. Measurable nitrate was seen as deep as 300 m in 1998, rising to about 250 m in late 2000. In January 2001, a deep intrusion occurred (see oxygen plot) and maximum depths of nitrate penetration increased, but have subsequently decreased again with time.

Nitrite. Nitrite concentrations in the Cariaco Basin are always very low, although there is frequently evidence for a primary nitrite maximum at the base of the euphotic zone (Fig. 2b). Sampling resolution (with depth) for the time series is not adequate to consistently see a secondary nitrite maximum at the base of the suboxic zone, although this feature has been observed on several occasions, and is clear in the detailed profile taken during the Jan 2004 microbiology cruise (Fig. 1). Deep nitrite maxima in Fig. 2b tend to be present on dates when deep penetration of oxygen is apparent in Fig. 4.

Ammonium. In oxic portions of the water column, ammonium concentrations are usually quite low (Fig. 2c). Most times when ammonium is detected at the surface are times when nitrate data suggest that upwelling is bringing subsurface water into the mixed layer and when productivity is high. High concentrations of ammonium from September to December 1999 were associated with a period of heavy rains. River discharge during this period was elevated well above typical levels and these months show the lowest salinity for the whole time series, with a salinity having been observed for December of 36.080 in the top 25 m. During this period the heavy coastal runoff may have influenced ammonium supply to the basin. However, in Oct/Nov 1999, high ammonium levels were seen throughout the water column which also might reflect problems with sample contamination. The depth of the 0.5 μM ammonium isopleth roughly coincides with the base of the suboxic zone or the upper part of the anoxic layer. Based on contour plots for ammonium and nitrite, there frequently are depths where low but measurable amounts of ammonium and nitrite coexist (see below).

Phosphate. Phosphate concentrations are always low in the upper 35-55 m. Surface waters depleted in phosphate typically deepen late in the fall, while shoaling of high phosphate water occurs between November and April (Fig. 2d). Concentrations tend to increase relatively monotonically with depth, although the contour plot shows a series of small deep minima between 250 and 350 m, usually in winter. In contrast to patterns reported for the Black Sea where phosphate concentrations decrease almost to zero [6, 10, 21], deep minima usually are relatively modest. However, we have coarse sample spacing below 250 m, so we may have missed sampling the depths of maximum phosphate removal.

Silica. Silica concentrations in surface waters (1-7 m) were generally low but measurable (Fig. 2e). Fig. 5 shows a plot of silica values at 1 and 7 m for 1998-2004. In 1999, persistently high surface values were likely attributable to enhanced terrestrial supply from land during the period of unusually high precipitation and runoff mentioned above in the discussion of ammonium. Other, shorter periods of high surface silica values may be due to other periods of runoff, or with upwelling and deep mixing. However, silica concentrations seldom were below 1 μM for extended periods, except in 1999 and 2001. In contrast, phosphate and nitrate concentrations are often at or below the detection limit in surface water. Previously, Ferraz-Reyes [14] reported that diatoms are most abundant during the upwelling season (November to April), and that cyanobacteria and dinoflagellates are more important during periods of low winds. The CARIACO silica data suggest that silica is almost never limiting at the CARIACO site.

N:P Ratios. Fig. 6 shows contour plots of the ratio of total inorganic N ($NO_2^- + NO_3^- + NH_4^+$) to PO_4. In the surface layers, this ratio is very low, but is strongly influenced by the fact that both inorganic nitrogen and phosphate concentrations are frequently at or near blank levels. At depths immediately below the euphotic zone, the N:P ratio seldom falls below 14:1. At depths below about 100 m the ratio decreases again, due to nitrate and nitrite removal by denitrification.

5. DISCUSSION

5.1 Oxic Waters

Some of the nutrient time series data have already been published. Astor [2] described the temporal variability of nitrate, nitrite, ammonium and phosphate between November 1995 and October 2001. Thunell [35] reported on the temporal variability of nitrogen isotopes as well as of nitrate and phosphate in the surface layers of the Cariaco Basin for 1998 and 1999, finding that the sinking flux of nitrogen in the Cariaco has an isotopic signature which was controlled by the isotopic composition of nitrate in the thermocline, indicative of complete consumption of nitrate in the surface. The longer time series reported in the present study confirms the patterns seen over the shorter periods.

Water column data are consistent with this picture. In Fig. 5 we present data for the top two depths sampled (1 and 7 m) during the time series. This graph shows clearly the times at which nutrients are elevated in the surface waters, usually during the first few months of the year. The vertical axes in the plots are in the ratio 16 SiO_2: 16 NO_3: 1 PO_4 or roughly in the ratio that organisms take up these compounds when nutrient concentrations are not limiting [7, 26]. From

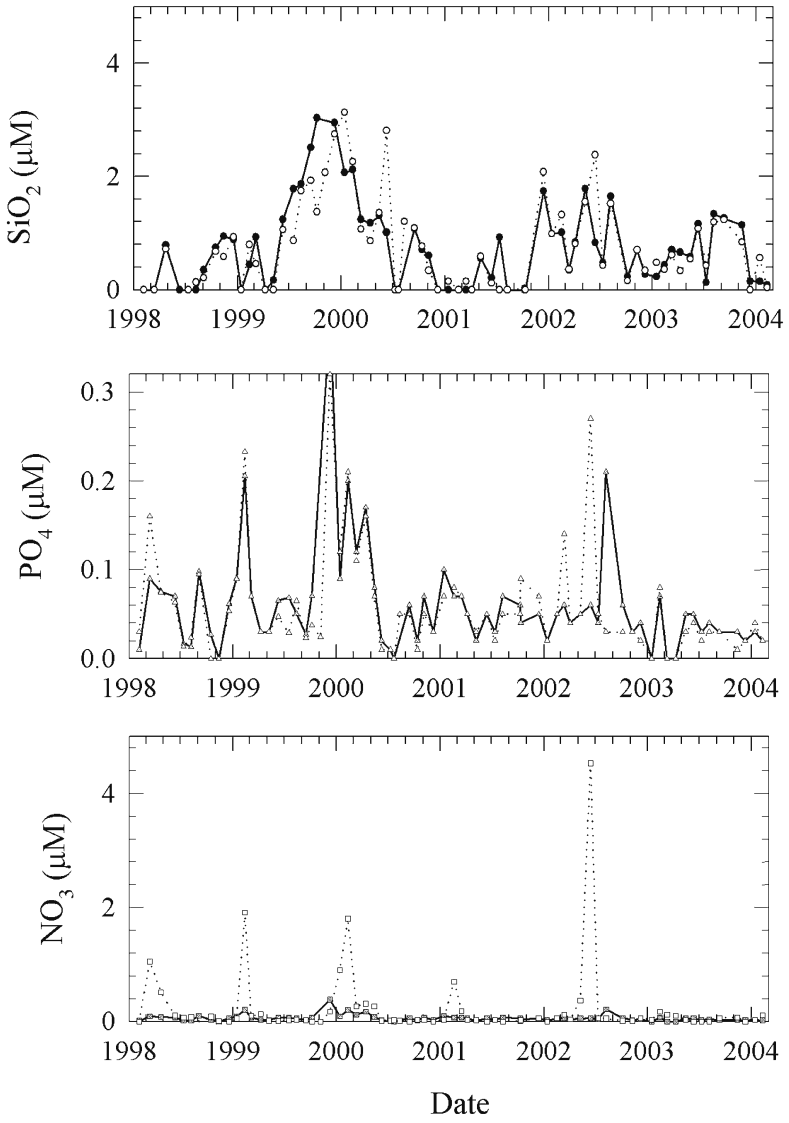

Figure 5. Silica, phosphate and nitrate at 1 m (closed symbols) and 7 m (open symbols) at the Cariaco site. The scales on the different panels are in the ratio 16 SiO_2: 1 PO_4: 16 NO_3.

these data, nitrate appears to be relatively more limiting than either phosphate or silicate.

However, it is unclear that the surface waters are sufficiently nitrogen depleted to result in local nitrogen fixation. At times when nitrate and phosphate were detectable in the surface 50 m, N^*, defined as $[NO_3^-] + [NO_2^-] - 16[PO_4^{3-}] + 2.9$ and representing the deviation of the inorganic nitrogen/-phosphate ratio from the Redfield ratio, was always greater than 1.0 μM and was frequently above 2.0 μM, suggesting the possible importance of nitrogen fixation [16]. However, the waters at the base of the euphotic zone are rich in both inorganic nitrogen and phosphorus ([35]; Fig. 2). The ratio of total inorganic nitrogen (nitrate + nitrite + ammonium) to phosphate for our study period is shown in Fig. 6. At essentially all times, at the base of the mixed layer, this ratio is at the theoretical Redfield ratio of 15 or 16:1. This water is likely to be the major source of supply of nutrients to the surface waters, which would mean that the phytoplankton populations receive N and P in the ratio at which they use these elements. While the nitrogen isotope and N^* data [35] suggest that nitrogen fixation may be at least regionally important, the high levels of nitrate typically found at 35 to 50 m, together with the N:P ratio of 15:1 in this water suggests that nitrogen fixation within the waters of the Cariaco Basin itself is unlikely to be an important source of fixed nitrogen. Consistent with this, *Trichodesmium*, a nitrogen fixer commonly found in the open Caribbean, is relatively rare in the Cariaco surface waters (Varela, personal communication).

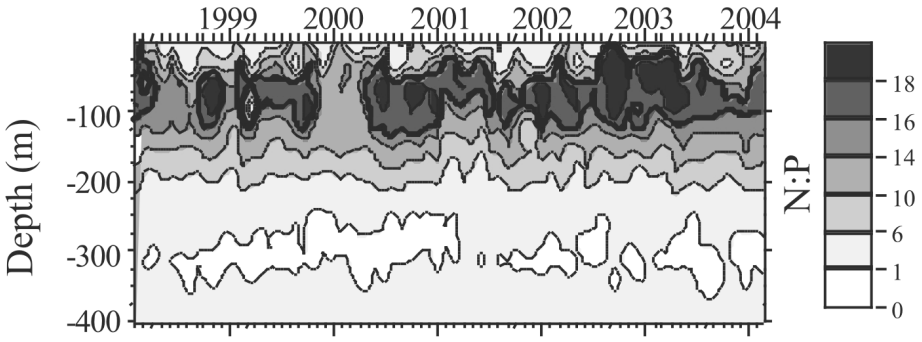

Figure 6. Temporal variability of Total Inorganic N:P ratio at the CARIACO site. The heavy line represents an N:P ratio of 16:1.

Surprisingly, N:P ratios in both the sinking flux and in plankton tows collected in a 200 μm mesh net between the surface and 200 m are much higher than Redfield ratios would predict. Benitez-Nelson [5] report POC:PON ratios in plankton tows between 2001 and 2002 of 5.6 ± 0.5 and N:P ratios of 53 ± 9 indicating a P deficit rather than an N deficit in the particulate organic matter. Sinking particulate matter collected in sediment traps is also depleted in phosphorus relative to both C and N. We do not have N:P data for phyto-

plankton samples, and so far have no explanation of why the sinking material is so depleted in P in a situation where denitrification is active and where the upwelled waters appear to contain nutrients in relatively balanced ratios.

5.2 Suboxic/Transition Zone

Phosphate distributions in the Cariaco Basin differ from the "classic" patterns typically reported for the Black Sea and often assumed to hold for other anoxic basins. The contour plot shows little sign of the pattern seen in the Black Sea of a strong minimum immediately above the onset of sulfide and a phosphate maximum in the upper portions of the anoxic zone. However, in the one cruise for which we have detailed samples across the interface (Fig. 1), we did see a minimum in phosphate just above the depth sulfide was first detected. In the Black Sea such features have been attributed to phosphate scavenging above the interface onto iron oxides and phosphate release as the iron oxides dissolve after settling into the anoxic zone [6]. The Cariaco minimum, although present, is much less pronounced than in the Black Sea where concentrations have been reported to be as low as 0.1 μM. The absence of clear minima in the contour plot (Fig. 2) suggests any such feature in the Cariaco Basin must be fairly thin. Even though phosphate scavenging in the suboxic zone of the Cariaco Basin seems to be much less intense in the Cariaco than in the Black Sea, it may occur. On a number of occasions, small phosphate minima are seen in the vicinity of the interface and these could be due to scavenging onto a metal oxide phase, perhaps formed during intrusions. In addition, biologically mediated phosphate removal may occur at depths where chemoautotrophy is active. Coarse sample spacing above the interface for most cruises suggests we may have missed the most intense minimum as well. Comparison of the oxygen and phosphate time series plots shows that phosphate minima tend to occur at times when deep oxygen maxima are present. The Cariaco Basin water column has similar or higher levels of dissolved iron compared with the Black Sea (250-500 nM in the Cariaco [18], compared to 300 nM in the Black Sea [23]), but oxygen injection occurs over a much thicker layer in the Cariaco due to a much more gradual density gradient. Recently, Konovalov has suggested that Mn-oxides (> 8 μM in the Black Sea; [23]; maximum of 600 nM in the Cariaco; [18]) may be more important in scavenging phosphate in the Black Sea (Konovalov personal communication).

Another major question about nutrients in the Cariaco is whether nitrite and ammonium co-occur. A number of recent studies ([9], [11] among others) have suggested that the anammox reaction ($NO_2^- + NH_4^+ \rightarrow 2\ N_2 + 2\ H_2O$) may be very important in suboxic regions in systems ranging from the Arabian Sea to the Black Sea. However, the possibility of anammox in the Cariaco has not yet been examined. In Fig. 1 we present the nutrient distributions for two cruises

taken about one week apart in January 2004 (cruise 96). On the regular monthly cruise (solid symbols in figure), nitrite values are very low below 250 m, nitrate is at blank values, but ammonium begins to increase at about 200 or 250 m. No sulfide measurements were made, so we do not know exactly where the interface was on the regular monthly cruise, but continuous oxygen data from that cruise indicated that oxygen values were less than 2 μM at about 250 m. In contrast, during a second cruise taken about one week later, a secondary nitrite maximum was observed in the deepest samples containing nitrate (270-290 m). Ammonium was also present in these samples, although at relatively low levels. Based on these profiles it appears that nitrite and ammonium may coexist just above the first appearance of sulfide, but that this coexistence may not occur at all times.

5.3 Anoxic Waters

The previous discussion has emphasized relatively short-term (annual to interannual) variability at a single site. Data are also available to examine longer trends in the deep water. Previous studies, over almost 50 years, have shown that conditions at the bottom of the Basin (water depths greater than 1200 m) are fairly (but not completely) stable. Scranton [29, 30], and Zhang and Millero [37] reported steady changes in the chemistry of the bottom few hundred meters. Scranton [29] demonstrated that these long term trends continued through the next decade, until an earthquake in July of 1997 apparently resulted in sulfide scavenging from deep water.

With the current data set we can look at the bottom waters from several additional perspectives. As in the previous long term studies for the Cariaco, we are restricting our discussion to samples taken below 1200 m. We have also limited this analysis to dates between 1998 to present (and for silicate, after December 2001) for reasons of analytical quality. We now have a long enough data set to directly examine trends at one site for parameters measured by a single lab. Fig. 7 shows increases in ammonium, phosphate and silica over the course of the Cariaco program. Trends are highly significant (at the $p<0.01$ level) because of the large number of observations (68 for phosphate and ammonium; 20 for silica) being plotted. In spite of some cruise-to-cruise variability, the trends are clear. Phosphate increases at a rate of 0.035 μM y^{-1}, ammonium increases at 0.62 μM y^{-1} and silicate increases at 1.3 μM y^{-1}. The time series for high quality silicate data is quite short, and it is most difficult to distinguish trends in this data. However, the observed rates are very similar to estimates by Zhang and Millero [37] who, using the quite small historical data set available at that time, found increases of 0.0372 ± 0.0069 μM y^{-1} for phosphate, 0.28 ± 0.061 μM y^{-1} for ammonium and 0.85 ±0.096 μM y^{-1} for silicate. If we merge all data, we obtain overall rates of increase of 0.034

μM y^{-1} for phosphate, 0.34 μM y^{-1} for ammonium, and 1.06 μM y^{-1} for silica, which is quite consistent with the earlier estimates of Zhang and Millero [37].

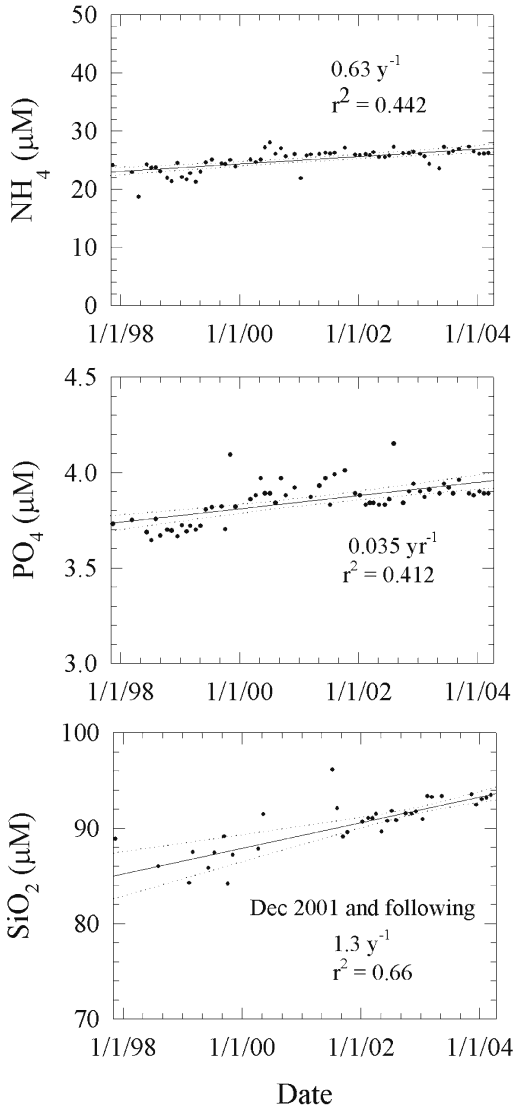

Figure 7. Trend in concentrations for waters deeper than 1200 m over the CARIACO program.

Another chemical species for which temporal trends have been assessed is sulfide. Scranton [30] reported an increase in sulfide of 14 μM in 9 years (1.56 μM y^{-1}). Zhang and Millero updated this number based on additional field work and obtained a value of about 1.5 μM y^{-1}. As reported in Scranton [29] the rate of increase of sulfide consistent with the literature and the first few CARIACO cruises was about 1.58 μM y^{-1}. However, following the earthquake in 1997, sulfide concentrations at the bottom of the basin water suddenly decreased by about 20-40 μM [29]. Sulfide values measured for deep water since 1997 have all been much lower than the previously predicted trend line, although recently, sulfide concentrations in the bottom water have started to increase again. We are unsure whether the large cruise-to-cruise variability is natural (perhaps due to heterogeneity in deep basin sulfide accompanied by circulation at depth in the basin) or whether it is related to the fact that our sulfide analyses are made on preserved samples run weeks to occasionally months following the cruise. We run sulfides on triplicate samples taken without bubbles into VICI Precision gas tight syringes and preserved immediately by addition directly to a solution of zinc chloride in a sample vial. Samples are stored in a cooler until return to the lab, and then refrigerated except during shipping until analysis by a modification of the Cline method [8]. The time between sample collection and mixture with the preservative is less than 1 minute. The "within cruise" variation is much smaller than the cruise-to-cruise variability. The most recent data (cruises in January and May 2004) indicate that sulfide is again increasing, with values below 1200 m of 54 μM in January and about 68 μM in May (Meredith Hayes, unpublished data). One possibility is that there may be more spatial variability in the deep water than has been reported in the past and that the mixing time of the basin is on the order of a few years. Unfortunately, we do not yet have data from the western basin to assess this question.

In addition to long term trends in bottom water, there is information in the ratios of the different nutrient species as a function of depth. Zhang and Millero [37] made this comparison and concluded that the products of organic matter remineralization were those predicted by sulfate reduction coupled to oxidation of organic matter containing the Redfield ratio amounts of N and P. Based on our detailed nutrient profile from January 2004, ratios of ammonium to sulfide (0.374), phosphate to sulfide (0.0216) and silica to sulfide (0.788) are all 13% higher than previously reported by Zhang and Millero [37] (Fig. 8). This is qualitatively consistent with the fact that maximum sulfide decreased at the time of the earthquake from 75 to about 50 μM. We have previously attributed this decrease to formation of FeS solids [29], which would remove sulfide without removing CH_4, N or P. Other possible removal mechanisms could include conversion of sulfide to elemental sulfur as has been seen in the Black Sea (for example, [20]) or conversion to sulfite and thiosulfate as seen in

Mariager Fjord [38]. Unfortunately, we do not have high quality nutrient data from before the earthquake to determine whether ratios were the same as those observed by [37].

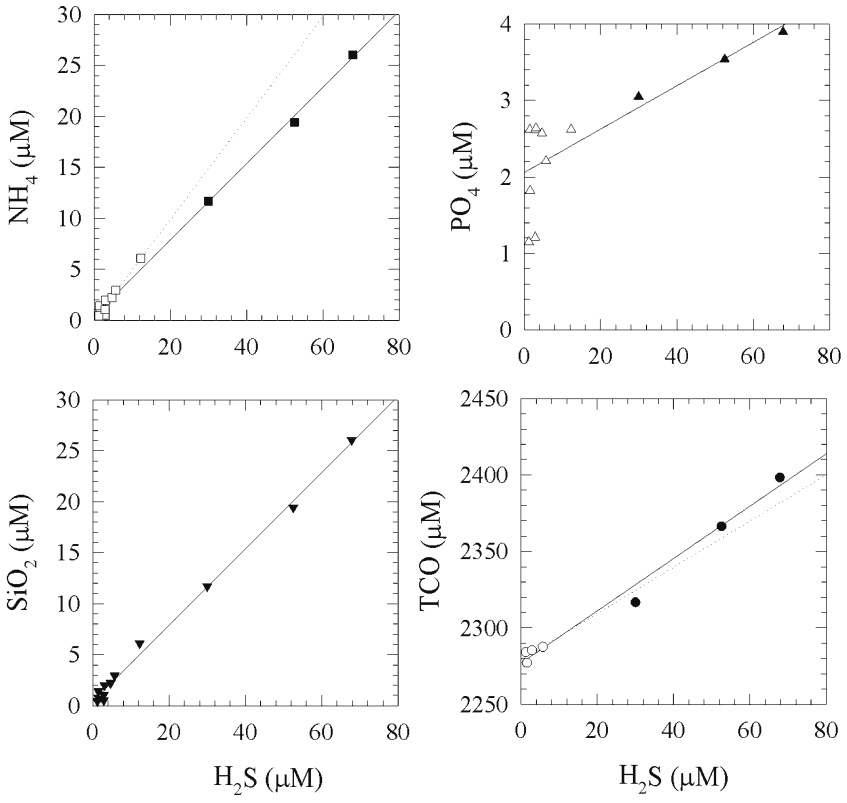

Figure 8. For data collected on January 2004, the relationship between nutrient species and sulfide. Open symbols are from depths between the suboxic zone and 400 m.

Finally, a plot of alkalinity vs. TCO_2 (Fig. 9) can provide information on the type of metabolic processes responsible for organic carbon mineralization. If the dominant process were sulfate reduction coupled with organic matter remineralization, as predicted by Zhang and Millero [37], the slope of a plot of alkalinity versus TCO_2 should be 1. In fact, the observed slope is 0.76 ($r^2 = 0.976$). Sulfide oxidation, producing elemental sulfur, thiosulfate and/or sulfite, will decrease alkalinity without affecting TCO_2, so the fact that our observed slope is less than one is consistent with our hypothesis that sulfide oxidation is an important sink for sulfide in the Cariaco. It also is consistent with our observations of fluctuation in the depth of the oxycline, with the phosphate

minima seen in the region 250-350 m and peaks in chemoautotrophic production within the redox gradient as discussed above and in [34] (this volume).

6. CONCLUSIONS

Nutrient distributions in oxic waters of the Cariaco Basin vary seasonally with fluctuations in rates of upwelling and primary productivity as well as in variations in the intensity of intrusions. In the suboxic zone, there appears to be at least occasional overlap of ammonium and nitrite, which could allow the growth of anammox bacteria. Although our sample spacing has not been sufficiently fine to always resolve these features, we also have evidence for phosphate removal above the sulfidic layer as is seen in the Black Sea. Intrusions of oxygenated water into deep, sulfidic layers occur intermittently but not infrequently, also influencing distributions of nitrite and phosphate. In the upper part of the anoxic zone, sulfide concentrations are lower than would be predicted by the amounts of inorganic nitrogen and phosphorous present. This is likely due to sulfide removal during intrusions of water containing oxidant. The deepest waters of the Cariaco Basin continue to have nutrient concentrations, which have increased at a roughly constant rate for the past 50 years.

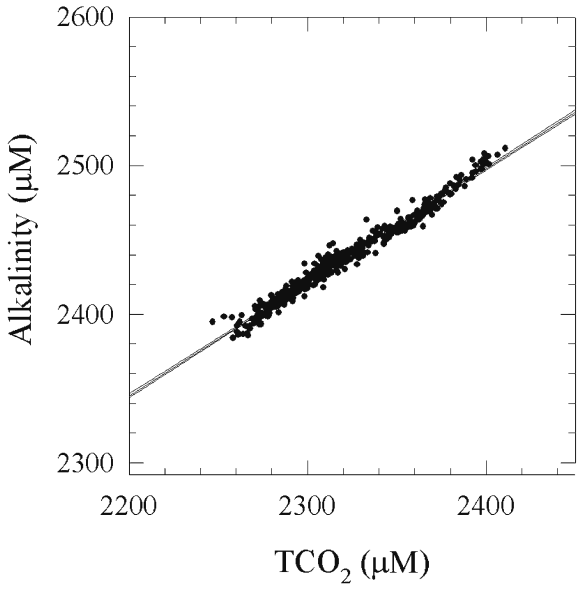

Figure 9. Alk/TCO_2 plot for CARIACO cruises between Dec 1995 and May 2003 for depths greater than 250 m. The equation of the line is Alk = 0.76 TCO_2 + 664 and the r^2 = 0.976.

Acknowledgements

The National Science Foundation (through multiple grants to FMK and MIS), and Proyecto Cariaco of the Consejo Nacional de Investigaciones Cientificas y Tecnológicas (CONICIT) and Fondo Nacional de Ciencia, Tecnologia e Innovacion (FONACIT) in Venezuela supported this work. We are indebted to the personnel of the Fundacion La Salle de Ciencias Naturales, Estacion de Investigaciones Marinas Isla Margarita (FLASA/EDIMAR) and the crew of the R/V *Hermano* Ginés for their enthusiasm and professional support. Richard Bohrer provided great assistance in early assessment of CARIACO data quality. Ramon Varela provided unwavering leadership in coordinating and carrying out field expeditions. We particularly thank Dr. Pablo Mandazen (Hermano Gines, Director, FLASA) for his confidence in our activities. This is contribution number 1299 from the Marine Sciences Research Center, Stony Brook University.

References

[1] Aminot A. "Dosage de l'oxygène dissous." In: *Manuel des analyses chimiques en milieu marin*, Aminot A. and Chaussepied M. eds., France: Centre National pour L'Exploitation des Oceans, 1983.

[2] Astor Y., Muller-Karger F., Bohrer R., Scranton M.I., Troccoli L. and Garcia J. Variabilidad interanual y estactional del CO_2 y los nutrientes en la Fosa de Cariaco. Memorias de la Sociedad de Ciencias Naturales La Salle. In press.

[3] Astor Y., Muller-Karger F. and Scranton M.I. Seasonal and interannual variation in the hydrography of the Cariaco Basin, Venezuela: Implications for basin ventilation. Cont Shelf Res 2003; 23:125-44.

[4] Astor Y.M., Scranton M.I., Muller-Karger F., Bohrer R. and García J. Seasonal and interannual variations for TCO_2 and fCO_2 in an upwelling tropical continental margin. Mar Chem accepted.

[5] Benitez-Nelson C.R., O?Neill L. Phosphonates and particulate organic phosphorus cycling in an anoxic marine basin. Limnol Oceanogr 2004; 49:1593-1604.

[6] Brewer P.G. and Murray J.W. Carbon, nitrogen and phosphorus in the Black Sea. Deep-Sea Res 1973; 20:803-18.

[7] Brzezinski M.A. The Si:C:N ratio of marine diatoms: interspecific variability and the effect of some environmental variables. J Phycol 1985; 2:347-57.

[8] Cline J.D. Spectrophotometric determination of hydrogen sulfide in natural waters. Limnol Oceanogr 1969; 14:454-58.

[9] Codispoti L.A., Brandes J.A., Christensen J.P., Devol A.H., Naqvi S.W.A., Paerl H.W. and Yoshinari T. The oceanic fixed nitrogen and nitrous oxide budgets: Moving targets as we enter the anthropocene? Sci Mar 2001; 65 Suppl. 2:85-101.

[10] Codispoti L.A., Friederich G.E., Murray J.W. and Sakamoto C.M. Chemical variability in the Black Sea: implications of continuous vertical profiles that penetrated the oxic/anoxic interface. Deep-Sea Res 1991; 38 (suppl. 2):691-710.

[11] Dalsgaard T. and Thamdrup B. Factors controlling anaerobic ammonium oxidation with nitrite in marine sediments. Appl Environ Microbiol 2002; 68:3802-08.

[12] Falkowski P. and Kiefer D.A. Chlorophyll fluorescence in phytoplankton: Relationship to photosynthesis and biomass. J Plankton Res 1985; 7:715-31.

[13] Fanning K.A. and Pilson M.E.Q. A model for the anoxic zone of the Cariaco Trench. Deep-Sea Res 1972; 19:847-63.

[14] Ferraz-Reyes E. Estudio del fitoplankton en la cuenta Tuy-Cariaco, Venezuela. Bol Inst Oceanog Univ Oriente 1983; 22:111-24.

[15] Gordon L.I., Jennings J.C. Jr., Ross A.A. and Krest J.M. "A Suggested Protocol For Continuous Flow Automated Analysis of Seawater Nutrients." In: *WOCE Operation Manual.* WHP Office Report 90-1, 1993. WOCE Report 77, No. 68/91:1-52.

[16] Gruber N. and Sarmiento J.L. Global patterns of marine nitrogen fixation and denitrification. Global Biogeochem Cy 1997; 11:235-66.

[17] Ho T.-Y., Scranton M.I., Taylor G.T., Thunell R.C., Varela R. and Muller-Karger F. Acetate cycling in the water column of the Cariaco Basin: Seasonal and vertical variability and implication for carbon cycling. Limnol Oceanogr 2002; 47:1119-28.

[18] Ho T.-Y., Scranton M.I., Taylor G.T., Thunell R.C., Varela R. and Muller-Karger F. Redox zonation and carbon oxidation pathways in the water column of the Cariaco Basin. Mar Chem 2003; 86:89-104

[19] Holm-Hansen O., Lorenzen C.J., Holmes R.W. and Strickland J.D.H. Fluorometric determination of chlorophyll. J Cons Int Explor Mer 1965; 30:3-15.

[20] Konovalov S.K., Luther G.W., Friederich G.E., Nuzzio D.B., Tebo B.M., Murray J.W., Oguz T., Glazer B., Trouwborst R.E., Clement B., Murray K.J. and Romanov A.S. Lateral injection of oxygen with the Bosporus plume - fingers of oxidizing potential in the Black Sea. Limnol Oceanogr 2003; 48:2369-76.

[21] Konovalov S.K. and Murray J.W. Variations in the chemistry of the Black Sea on a time scale of decades (1960-1995). J Marine Syst 2001; 31 (1-3):217-43.

[22] Koroleff F. "Determination of nutrients." In: *Methods of Seawater Analysis*, Grasshoff K. ed., Weinheim Germany and New York NY, Verlag Chemie, 1976.

[23] Lewis B.L. and Landing W.M. The biogeochemistry of manganese and iron in the Black Sea. Deep-Sea Res 1991; 38:773-803.

[24] Muller-Karger F., Varela R., Thunell R., Scranton M., Bohrer R., Taylor G., Capelo J., Astor Y., Tappa E., Ho T.-Y., Iabichella M., Walsh J.J. and Diaz J.R. The CARIACO Project: Understanding the link between the ocean surface and the sinking flux of particulate carbon in the Cariaco Basin. EOS (Transactions of the American Geophysical Union) 2000; 81:529 & 534-35.

[25] Muller-Karger F., Varela R., Thunell R., Scranton M., Bohrer R., Taylor G., Capelo J., Astor Y., Tappa E., Ho T.-Y. and Walsh J.J. The annual cycle of primary production in the Cariaco Basin: Implications for vertical export of carbon along a continental margin. J Geophys Res 2001; 106:4527-42.

[26] Redfield A.C., Ketchum B.H and Richards F.A. "The influence of organisms on the composition of sea water." In: *The Sea*, Hill N.M. ed., New York: Wiley, 1963.

[27] Richards F.A. Cariaco Basin (Trench). Oceanography and Marine Biology Annual Reviews 1975; 13:11-67.

[28] Richards F.A. and Vaccaro R. The Cariaco Trench, an anaerobic basin in the Caribbean Sea. Deep-Sea Res 1956; 3:214-28.

[29] Scranton M.I., Astor Y., Bohrer R., Ho T.-H. and Muller-Karger F. Controls on temporal variability of the geochemistry of the deep Cariaco Basin. Deep-Sea Res 2001; 48:1605-25.

[30] Scranton M.I., Sayles F.L., Bacon M.P. and Brewer P.G. Temporal changes in the hydrography and chemistry of the Cariaco Trench. Deep-Sea Res 1987; 34:945-63.

[31] Spencer D.W. and Brewer P.G. The distribution of some chemical elements between dissolved and particulate phases in the ocean. USAEC Report No. C00-3566-3, 1972.

[32] Strickland J.D.H. and Parsons T.R. *A practical handbook of seawater analysis,* 2nd ed., Bulletin Fisheries Research Board Canada, 1972.

[33] Taylor G.T., Scranton M.I., Iabichella M., Ho T.-Y., Thunell R.C. and Varela R. Chemoautotrophy in the redox transition zone of the Cariaco Basin: A significant source of midwater organic carbon production. Limnol Oceanogr 2001; 46:148-63.

[34] Taylor G.T., Iabichella-Armas M., Varela R., Muller-Karger F., Lin X. and Scranton M.I. Microbial ecology of the Cariaco Basin's redoxcline: the U.S.-Venezuela CARIACO time seriesprogram, In: *Past and Present Water Column Anoxia,* L.N Neretin, ed. Dordrecht: Springer 2006.

[35] Thunell R.C., Sigman D.M., Muller-Karger F., Astor Y. and Varela R. Nitrogen isotope dynamics of the Cariaco Basin, Venezuela. Global Biogeochem Cy 2004; 18: GB3001. doi: 10.1029/2003GB002185.

[36] Tuttle J.H. and Jannasch H.W. Thiosulfate stimulation of microbial dark assimilation of carbon dioxide in shallow marine waters. Microb Ecol 1977; 4:9-25.

[37] Zhang J.-Z. and Millero F.J. The chemistry of the anoxic waters in the Cariaco Trench. Deep-Sea Res 1993; 40:1023-41.

[38] Zopfi J., Ferdelman T.G., Jørgensen B.B., Teske A. and Thamdrup B. Influence of water column dynamics on sulfide oxidation and other major biogeochemical processes n the chemocline of Mariager Fjord (Denmark). Mar Chem 2001; 74:29-51.

BIOGEOCHEMICAL AND PHYSICAL CONTROL ON SHELF ANOXIA AND WATER COLUMN HYDROGEN SULPHIDE IN THE BENGUEL A COASTAL UPWELLING SYSTEM OFF NAMIBIA

Volker Brüchert[1], Bronwen Currie[2], Kathleen R. Peard[3], Ulrich Lass[4], Rudolf Endler[4], Arne Dübecke[1], Elsabé Julies[1,5], Thomas Leipe[4] and Sybille Zitzmann[1]

[1]*Max-Planck Institute for Marine Microbiology, Celsiusstrasse 1, 28359 Bremen, Germany*

[2]*Ministry of Fisheries, National Marine Information and Research Centre, Strand Street, P.O. Box 912, Swakopmund, Namibia*

[3]*Ministry of Fisheries, Marine Research Station, 357 Lüderitz, Namibia*

[4]*Baltic Sea Research Institute Warnemünde, Seestrasse 15, 18119 Rostock, Germany*

[5]*University of Namibia, Department of Biology, Private Bag 13301, Windhoek, Namibia*

Abstract Shelf anoxia and recurring sulphidic water column conditions are characteristic features of the coastal upwelling system off Namibia. The development of oxygen-depleted water column conditions is linked to the relative dominance of South Atlantic Central Water, which flows southward from the Angolan Dome over Eastern South Atlantic Central Water. Inter- and intra-annual variations in the strength of upwelling influence the thickness and stability of the relatively stagnant boundary layer. Hydrogen sulphide accumulation in this boundary layer is mainly driven by the diffusive flux of hydrogen sulphide from the sediment. The hydrogen sulphide derives from the rapid degradation of organic material by bacterial sulphate reduction in the topmost 20 cm of sediment. Low reactive iron contents in the diatomaceous mud belt limit iron sulphide precipitation and sulphide oxidation by oxidized iron. In the absence of oxygen, iron, and manganese as important electron acceptors, sulphide oxidation proceeds largely by the reduction of nitrate by the large sulphur bacteria *Beggiatoa* and *Thiomargarita*, which cover large areas of the shelf. Regional differences in the distribution of these bacteria affect the development of sulphidic bottom waters. While hydrogen sulphide is quantitatively oxidized in sediments covered by *Beggiatoa* mats, only a fraction of the sulphide is removed by *Thiomargarita*. Areal estimations of aerobic water column respiration, diffusive fluxes of hydrogen sulphide from the sediment, and rates of bacterial sulphate reduction indicate that oxidation of sulphide at the sediment-water interface and oxidation of water column sulphide may comprise up to 25 % of the total oxygen consumption in the coastal

L. N. Neretin (ed.), Past and Present Water Column Anoxia, 161–193.

upwelling system. Advective transport of methane and hydrogen sulphide from gas-charged sediments has an intermittent and locally restricted impact on water column sulphide.

Keywords: Benguela, coastal upwelling, Namibia, bottom water sulphide

1. INTRODUCTION

Many coastal upwelling systems are characterized by year-round low-oxygen conditions in the water column and seasonal water column anoxia [17, 26, 39]. In contrast, the regular occurrence of wide spread sulphidic waters on open-ocean shelves is rare. One example is the Namibian shelf between 22°S and 27°S. Continuous upwelling between 25°30'S and 27°S in the Lüderitz cell feeds high primary production, which contributes to extreme water column oxygen depletion and episodically occurring sulphidic bottom water in the area between 25°30'S and 20°S [2, 6, 7, 11]. Turquoise discolorations of the near-shore surface waters are a regular phenomenon during the austral summer and spring. These discolorations were traditionally interpreted as coccolithophore blooms, but more recent interpretations suggest that some of these patches reflect the presence of dispersed colloidal sulphur – an oxidation product of hydrogen sulphide [40]. During the occurrence of these patches, the water column is severely oxygen-depleted and sulphidic up to the photic zone, with severe repercussions for the living resources (fish and crustaceans) in one of the largest marine ecosystems on earth [15].

A characteristic bathymetric feature of the central Benguela coastal upwelling region is a 50 to 150 km broad shelf with two edges, one at 150 m depth, and the second between 300 and 350 m water depth. Due to the high productivity and relatively shallow water depth, large amounts of phytoplankton debris reach the sea bottom before they are consumed in the water column. The large flux of organic matter permits high rates of carbon mineralization in the sediment. Since oxygen is already largely consumed in the water column, bacterial sulphate reduction becomes the dominant sediment mineralization process [7]. Ultimately, even sulphate availability is limited in these sediments, and methanogenesis starts a few centimetres below the sediment surface, which leads to the accumulation of free methane gas [14].

It is clear that the high productivity in this upwelling system is ultimately responsible for the development of free water column hydrogen sulphide. However, the pattern of hydrogen sulphide occurrence suggests very specific interactions between the dynamic oceanographic conditions, the biogeochemical processes in the sediment and water column, and the physical processes occurring within the sediment. Emeis et al. [14] suggested a close relationship between anoxia and eruptions of biogenic methane. Weeks et al. [40] also observed a sudden development of near-shore water column hydrogen sul-

phide followed by turquoise discolouration and suggested an abrupt injection of hydrogen sulphide-containing water triggered by methane eruptions from the sediment. According to Emeis et al. [14], methane gas and hydrogen sulphide in the unconsolidated sediments may be released following changes in the physical regime of the overlying water or the sediment. So far, studies have been largely descriptive and only qualitative assessments have been possible. For a quantitative analysis of the various potential sources of hydrogen sulphide – sediment or water column – regional and temporal distribution patterns of fluxes, concentrations, and budgets of hydrogen sulphide and oxygen are required. In this respect leading questions are:

1. What is the oceanic circulation pattern over the shelf and how does the chemistry of the water masses entrained in the upwelling affect overall oxygen levels on the shelf?

2. What is the rate of oxygen consumption in the water column and how does this rate compare to oxygen consumption rates at the sediment-water interface?

3. What is the regional and temporal variation in hydrogen sulphide flux in the upwelling zone and what regulates the flux from the sediments?

4. How does the gas distribution in the shelf sediment affect the flux of hydrogen sulphide from the sediment?

2. DATA AND METHODS

Water column and sediment data were acquired between May 1997 and May 2004 on cruises with the research vessel of the Namibian Ministry of Fisheries *RV Welwitchia* and during expeditions of the research vessels *RV Meteor, cruises M48-2 and M57-3, RV Poseidon, cruise 250/2, RV Petr Kottsov, Benefit cruise* and *RV Alexander von Humboldt, cruise legs AHAB-3 and AHAB-4.* Station locations on the different cruises and water depths are shown on Fig. 1. A summary of the measurements is listed in Table 1. A complete table of sample locations, sampling times, and types of measurement is available from the senior author upon request. Altogether, sediment and water column data were acquired from over 130 stations.

In addition, over the course of a period of three years (May 2001 until May 2004) sediment and water column data were obtained from a shallow-water station (Station 1) at 22°50.9' S, 14°28.4' E (27 m water depth).

Continuous data records on water column physics and chemistry were obtained from a mooring that was deployed at 22°59.7'S, 14°02.8'E (131 m water depth) from December 12, 2002 until April 1, 2003 and again from January 7, 2004 until May 5, 2004.

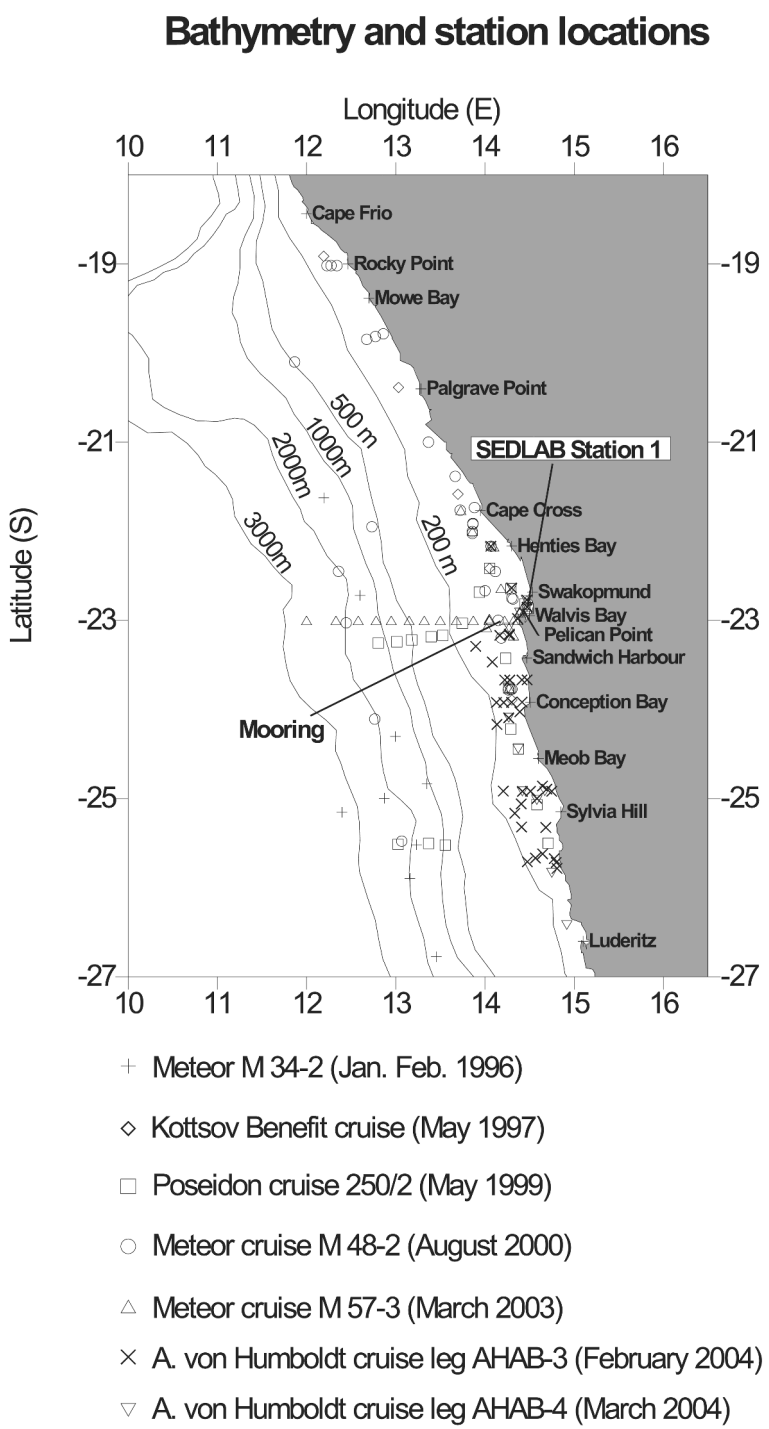

Figure 1. Bathymetry of Namibian shelf and station locations. Symbols indicate the locations of stations on the different cruises.

Table 1. Summary of biogeochemical measurements on cruises included in this survey.

	Period	*Bottom water* O_2 *(μM)*	*Bottom water* $NO_3^- + NO_2^-$ *(μM)*	^{35}*S-Sulphate reduction rates*	*Biomass large sulphur bacteria* *Thiomargarita*	*Beggiatoa*
Meteor M 34-2 cruise[1]	Jan-Feb 1996	+	n.d.	+	n.d.	n.d.
RV Petr Kottsov	cruise May 1997	+	n.d.	+	+	+
Poseidon 250/2 cruise	May 1999	+	+	+	+	+
Meteor M 48-2 cruise [2]	August 2000	+	n.d.	+	+	+
Meteor M 57-3 cruise [3]	March 2003	+	+	+	+	+
A. V. Humboldt cruise	Jan-March 2004	+	+	+	+	+
RV Welwitschia cruises	May 2001-May 2004	+	+	+	+	+

	Period	*Oxygen*	Hydrogen sulphide			
		Water column	*Water column*	*Sediment*	*Water column*	*Sediment*
Meteor M 34-2 cruise[1]	Jan-Feb 1996	+	n.d.	+	n.d.	n.d.
RV Petr Kottsov cruise	May 1997	+	+	+	n.d.	n.d.
Poseidon 250/2 cruise	May 1999	+	+	+	n.d.	n.d.
Meteor M 48-2 cruise[2]	August 2000	+	+	+	n.d.	+
Meteor M 57-3 cruise[3]	March 2003	+	+	+	+	+
A. V. Humboldt cruise	Jan-March 2004	+	+	+	+	+
RV Welwitschia cruises	May 2001-May 2004	+	+	+	+	+

+ : analyzed n.d.: not determined
[1] Bleil et al. (1996)
[2] Emeis et al. (2002)
[3] Zabel et al. (2004)

2.1 Water Column

During the research cruises with the German vessels and RV Welwitchia, water column data were obtained with a CTD SBE 911+ with SBE 43 oxygen sensors, 2-channel Haardt fluorometer, a Datasonics PSA-900 altimeter with a 300 m range for bottom finding together with a rosette sampler equipped with 12 five-litre free-flow HydroBios water sample bottles. Attached to the CTD frame was an Acoustic Doppler Current Profiler (ADCP) consisting of a coupled upward- and downward-looking Workhorse ADCP 300 kHz in a 3000 dbar pressure case. Water from the HydroBios bottles was directly transferred to 120 ml Winkler bottles for duplicate determination of dissolved oxygen and sulphide. Dissolved oxygen and sulphide were determined immediately after retrieval of the rosette sampler. Dissolved oxygen was determined by Winkler titration and dissolved sulphide was determined by the method of Cline [12]. The dissolved oxygen concentrations determined by Winkler were used for calibration of the CTD SBE oxygen probe. The mooring was equipped with an upward looking 300 kHz Workhorse ADCP, four Seacat SBE 16 recorders and three Seamon temperature recorders.

2.2 Sediment

Sediments were collected to determine ^{35}S-sulphate reduction rates, methane concentrations, fluxes of hydrogen sulphide, and abundances of the large sulphur bacteria *Beggiatoa* and *Thiomargarita*. At each station, several casts were made until sufficient material was obtained. Methods are described in detail in [7, 14]. Fluxes of hydrogen sulphide and methane were calculated from porewater profiles using the fitting procedure described by Berg et al [3]. Fluxes were calculated across the sediment-water interface. These procedures are described in detail in [7]. Distribution maps of sulphate reduction rates, sulphide fluxes, large sulphur bacteria, and bottom water oxygen and hydrogen sulphide were created with the Surfer software package using Kriging with linear interpolation as the gridding method.

Morphology, distribution, and layering of shelf sediments were investigated using the multibeam echosounder HYDROSWEEP and the PARASOUND sub-bottom profiling system on R/V Meteor. Detailed technical descriptions of the acoustic systems are given in [4, 36, 42]. A frequency of 4 kHz and a pulse length of two periods were used during the cruises. Additional measurements with different frequencies (2.5-5.5 kHz) and pulse durations of 1 to 6 periods were performed at coring stations in order to study the influence of frequency and length of the source signal on the reflection pattern. PARASOUND data were recorded continuously. High-resolution sub-bottom profiling in shallow water (up to 400 m) was performed using the parametric sediment echosounder SES96-Standard in addition to the PARASOUND device. The parametric SES96

Standard sediment echosounder is designed for operation in water depths down to 400 m. The main advantages of the SES96 echosounder are its high spatial resolution and the information contained in raw data of both HF and LF channels. This is particularly important for acoustic sediment classification in connection with the results of sediment physical property measurements.

3. HYDROGRAPHIC EFFECTS ON OXYGEN LEVELS IN THE COASTAL UPWELLING ZONE

The general hydrography of the Benguela Current system has been reviewed in [16, 34, 35]. More recent on-board and moored measurements have provided detailed insight into the dynamics of the regional hydrography. Two advection processes are involved in the ventilation of the subsurface water on the Namibian shelf. South Atlantic Central Water (SACW) is transported southward by the poleward undercurrent (Fig. 3a). This water originates from the area of the Angola gyre along the Namibian shelf and carries water of low oxygen (< 45 μM) and high nutrient concentrations [25]. The intensity of the poleward undercurrent appears to be controlled by remote forcing in the eastern tropical Atlantic and to a lesser extent by the local wind. The second water mass is the East South Atlantic Central Water (ESACW), which is transported by the Benguela current from the area of the Agulhas retroflection zone to the north [31]. The ESACW is well-ventilated and has a lower nutrient concentration than the SACW. Sub-thermocline cross-shelf circulation advects ESACW in depths between 20 and 70 m from the area off the shelf break onto the shelf (Fig. 3b). This transport is mainly driven by the local alongshore wind stress and compensates for the Ekman offshore transport in the surface layer (Fig. 3b). Since the oxygen concentration of the ESACW water is higher, advection by cross-shelf circulation ventilates the intermediate waters on the shelf much more efficiently than the advection by the poleward undercurrent. The oxygen concentration of the subsurface water on the shelf is very sensitive to the local balance of consumption and ventilation processes, which both shape the pattern of oxygen concentration and its variation in space and time.

Upwelling-favourable winds on the Namibian shelf are strong in the Cape Frio and Lüderitz upwelling cells and weak in the area between the upwelling cells. While the northern part of the Benguela is strongly affected by the advection of SACW with the poleward undercurrent, with increasing distance from the Angola-Benguela front, the cross-shelf circulation in the subsurface shelf water gradually increases the proportion of ESACW. Cross shelf circulation intensifies in the Lüderitz upwelling cell such that well-ventilated ESACW becomes the dominating water mass on the shelf and limits the southward extension of SACW to the latitude of Lüderitz, where the subsurface shelf waters consist entirely of ESACW. Upwelled water of the Lüderitz cell is also ad-

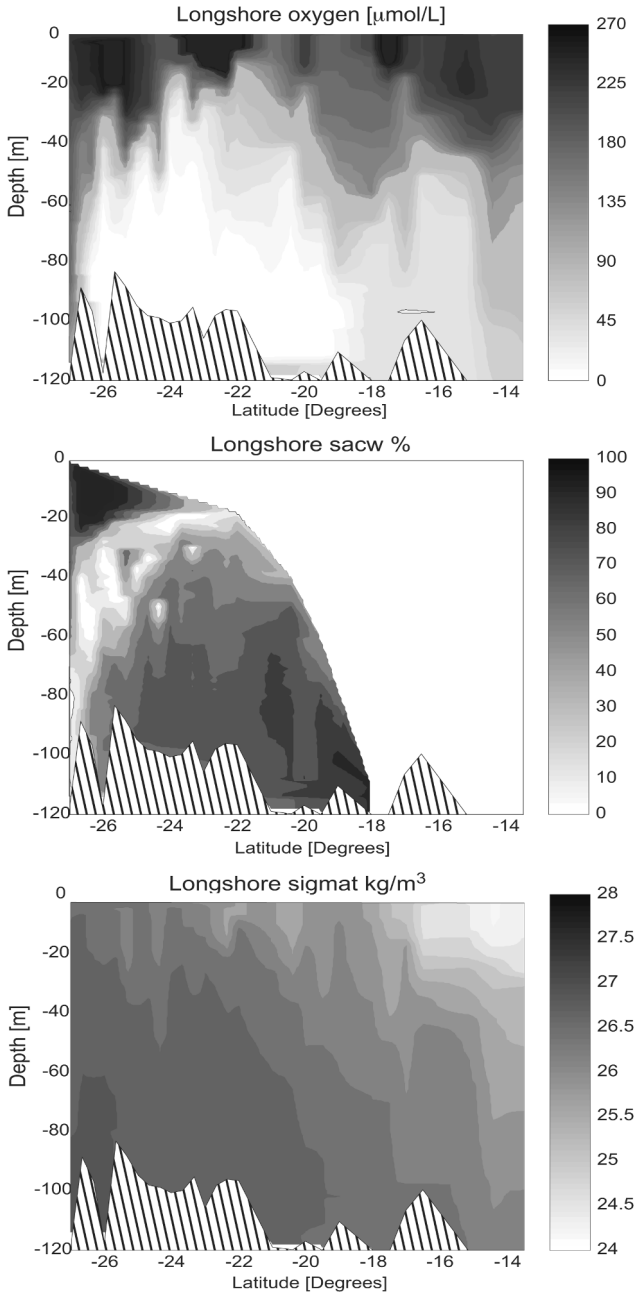

Figure 2. Density, oxygen, and percentage of SACW in a alongshore transect from 13°S to 27°S based on volumetric temperature-salinity (T-S) analysis. Water masses outside the definition of the ESACW-SACW T-S field are not shown.

vected northward by the surface current and causes a northward displacement of the most productive area by a few degrees latitude. This displacement is associated with a northward shift of the area of the most extreme subsurface oxygen depletion produced by the respiration of sinking organic matter to the area around 24°S (Fig. 2).

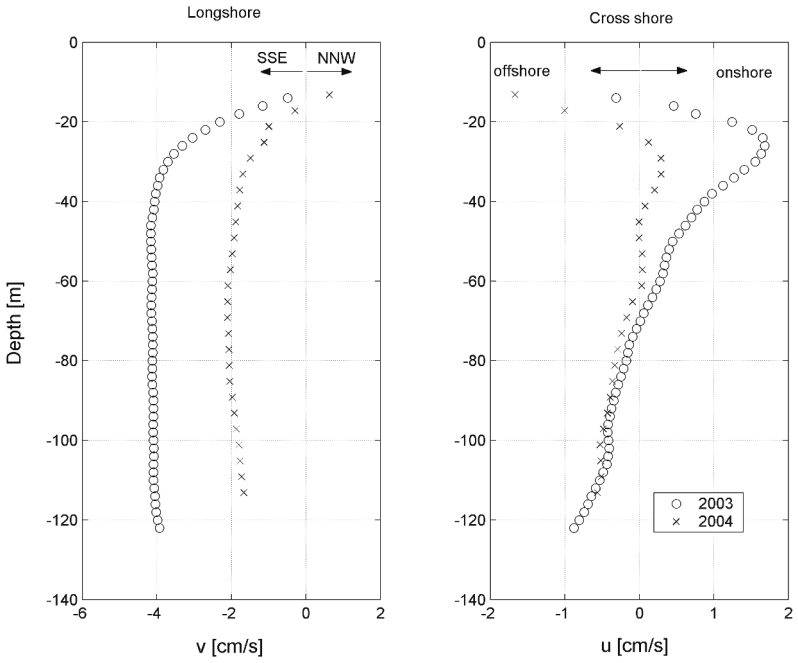

Figure 3. Averaged alongshore (a) and cross-shore (b) current velocity at the mooring (22° 59.7' S, 14° 02.8' E, 131 m water depth) located in the mud belt off Walvis Bay. The mooring was deployed from December 9, 2002 until April 1, 2003, and from January 7, 2004 until May 5, 2004.

Data from the mooring in 130 m water depth at 23°S indicate interannual variations in the strength of the poleward undercurrent located below 20 m water depth (Fig. 3a, b). In the period December 2002 until April 2003, the meridional (southward) component had average current speeds of 4 cm s^{-1}, but for the period January 2004 until May 2004, the current speed was averaging only 2 cm s^{-1} (Fig. 3a). Similarly, the cross-shelf circulation represented by the zonal component of the current varied between the two observation periods (Fig. 3b). On-shore transport was weaker in 2004 compared to 2003 indicating that the ventilation by ESACW in the intermediate layer was weaker in the austral fall of 2004.

The mooring data indicate a transient, sluggish bottom water layer of up to 30 m thickness. This layer appears to be stable for months. The slower the meridional current component, the longer the residence time on the shelf, the more this layer becomes oxygen- and nitrate-depleted, and ultimately sulphidic. At coast-parallel bottom current speeds of 2 and 4 cm s^{-1}, water is transported within approximately 600 and 300 days, respectively, from the Angola-Benguela front to 26°S. Hence, this period can be taken as an approximate residence time for shelf bottom water reaching 26°S.

4. PATHWAYS, RATES, AND AMOUNT OF WATER COLUMN RESPIRATION

4.1 Aerobic Water Column Respiration

Generally, oxygen concentrations decrease rapidly below the thermocline on the shelf as a result of the aerobic respiration of sinking organic material. Video observations from a remotely operated vehicle during RV METEOR Expedition M57-3 in March 2003 suggest that particulate organic material in the water column over the shelf consists mostly of aggregates [42]. We have used a new approach to estimate the rate of oxygen consumption in the water column by combining volume-specific oxygen consumption rates of diatom aggregates with abundances and size spectra of aggregates determined by in-situ video observation during a diatom bloom in the southern Benguela system [20]. Size-dependent rates of diffusive oxygen uptake in diatom aggregates have been determined by [30]. Diffusive oxygen uptake varied as a function of aggregate size, and was described by the relationship $Q_{tot,vol} = 65.8(\mathrm{vol})^{0.67}$, where $Q_{tot,vol}$ is the total oxygen consumption (nmol agg^{-1} h^{-1}) as a function of aggregate volume (vol) [30]. The above equation can be recast as a function of aggregate radius, which yields the expression

$$Q_{tot,r} = 171r^{2.0} \tag{1}$$

where $Q_{tot,r}$ has the unit nmol O_2 cm^{-3} h^{-1}. Extrapolation of the aggregate radius-specific respiration rate to a respiration rate per volume seawater requires that the aggregate size spectrum in the water column is known. We used the empirical relationship reported in Kiørboe and co-workers [20] for a diatom bloom in the southern Benguela. The aggregate size spectrum was described by the power function

$$n_r = b_3 r^{-b_4} \tag{2}$$

where n_r represents the volume-normalized number of aggregates, the subscript r is the aggregate radius, b_3 is a particle concentration coefficient and b_4 describes the slope of the spectrum [19]. The larger b_4, the smaller are the

particles. The total respiration by aggregates (Total R_{agg} across a complete size spectrum was determined by integrating equations (1) and (2) to yield the expression

$$Total\,R_{agg} = \int_{r_1}^{r_2} n_r\, Q_{tot,r}\, dr = \frac{b_3 * 171}{2.0 - b_4 + 1} r^{2.0-b_4+1} \tag{3}$$

We used published values of b_3 and b_4 for the diatom bloom reported in Kiørboe and Jackson [19]. These values are 1 x 10^{-4} and 1.3 x 10^{-3} for b_3, and 1.6 and 2.6 for b_4, respectively. Mean values for b_3 and b_4 are 7.5 x 10^{-4} and 2.1, respectively. The reported aggregate size spectrum ranged from 0.225 mm to 5 mm [20]. The calculated respiration rates vary between 0.1 and 7.7 μM O_2 day^{-1} with a mean of 1.7 μM day^1. These average oxygen consumption rates translate into depth-integrated oxygen consumption rates of 52, 96, 172 mmol O_2 m^{-2} day^{-1} for water depths of 30, 50, and 100 m depth, respectively. Decreasing particle abundances with depth and variations in the intensity and the temporal and spatial extent of blooms in the Benguela current [10, 16] introduce uncertainties to our method that are difficult to quantify at the moment. Yet, this method for the calculation of oxygen consumption is superior over other approaches such as the apparent oxygen utilization in that it is independent of variations in the oxygen concentration of the source waters feeding the upwelling system.

4.2 Anaerobic Water Column Processes

Nitrate is a potential electron acceptor for the respiration of organic matter in the absence of oxygen and may serve as electron acceptor for the oxidation of dissolved sulphide, when oxygen is depleted. Thus, the development of sulphidic bottom waters may require the complete consumption not only of oxygen, but also of dissolved nitrate. Long-term records of bottom water nitrate and hydrogen sulphide indicated highly variable nitrate concentrations in the bottom water of the Namibian shelf. Hydrogen sulphide was detected in the coastal inshore bottom waters (25m depth) in May 2001 and 2004, and during these periods, nitrate was absent from the shelf bottom waters (Fig. 4). However, there were also periods when sulphide was absent and nitrate was very low, e.g., January 2003, and when sulphide and nitrate co-existed, albeit at very low concentrations, e.g. September 2003 (Fig. 4). One possible explanation is that the bottom water was in a transitional stage during these sampling times.

An extensive data set of the Sea Fisheries Institute of South Africa and the Ministry of Fisheries, Namibia indicates a permanent deficit of nitrate relative to phosphate and silicate in the coastal upwelling waters. The nitrate deficit

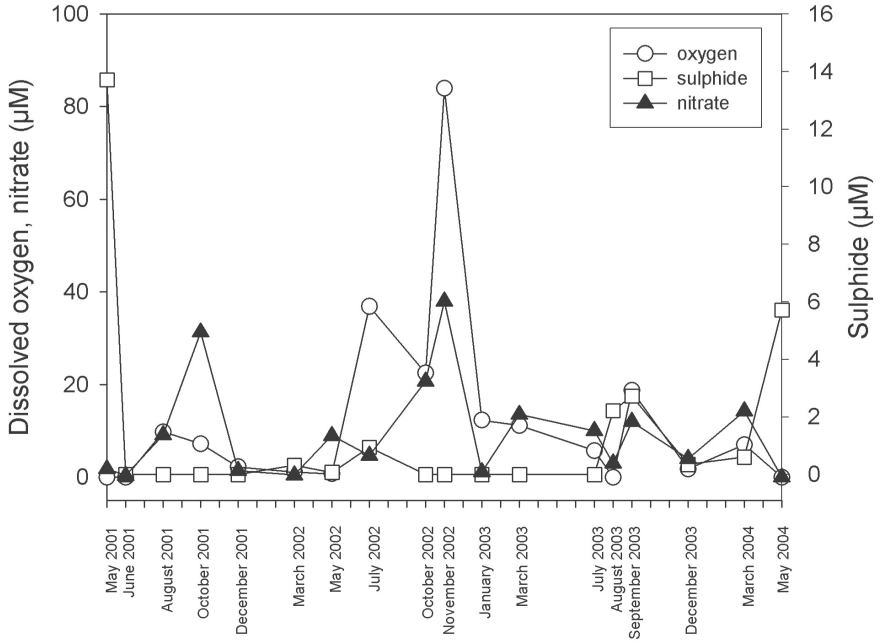

Figure 4. Time series of bottom water oxygen, nitrate, and hydrogen sulphide at SEDLAB Station 1 from May 2001 until May 2004.

defined as $\Delta N = 16[PO_4^{3-}] - [NO_3^-]$ is most extreme in the in-shore areas in the Northern Benguela near 23°S [38]. Tyrell and Lucas [38] interpreted this deficit as the anaerobic respiration of organic matter with nitrate as electron acceptor, i.e., denitrification. However, direct tracer measurements using ^{15}N-labelled nitrate and ammonium do not support this interpretation. Anammox, a recently discovered anaerobic bacterial process in anoxic water columns, which catalyzes the consumption of nitrate/nitrite together with ammonium to form N_2, appears to be the main process for nitrogen removal in the oxygen deficient water column of the Namibian shelf [21]. Irrespective of which bacterial process is ultimately responsible for nitrogen removal, our current data suggest that complete bottom water nitrate depletion is a common corollary of sulphidic bottom waters.

The only direct measurements of bacterial sulphate reduction with radiolabelled $^{35}S\text{-}SO_4^{2-}$ in bottom waters (3 m above ground) were performed at four shelf stations in March 2004. During this period, bottom waters were anoxic, but did not contain hydrogen sulphide. The experimental rates ranged from 0.2 to 6.8 nmol l^1 day^{-1}. At the highest rates, it would require 147 days to

reach a concentration of 1μM hydrogen sulphide, the detection limit for the methylene blue method [12]. Measured hydrogen sulphide concentrations in the water column have been as high as 40 μM, but have been observed to rise and disappear much faster than 147 days (see section 5.3).

5. BACTERIAL SULPHATE REDUCTION, METHANOGENESIS, FLUXES, AND RECYCLING OF SULPHIDE AT THE SEABED

5.1 Carbon Oxidation Processes and Methanogenesis

Sediments on the Namibian shelf generally contain less than 20 percent clastic material, which is transported mainly as dust from the Namibian desert. Minerals containing reactive iron and manganese oxide are minor components of the sediment, with the consequence that these two anaerobic electron acceptors are quantitatively unimportant for carbon oxidation [5]. Rates of nitrogen removal including denitrification in the shelf sediments range from 0.2 to 2.7 mmol m^2 day^{-1}, averaging 2 mmol m^{-2} day^{-1} (Zitzmann and Brüchert, unpubl. data). This leaves bacterial sulphate reduction as the dominant terminal organic carbon oxidation process. Areal rates of bacterial sulphate reduction on the shelf (28 m to 200 m water depth) vary between 3.1 and 62.7 mmol m^{-2} day^{-1} [7].

On average, more than 90 % of bacterial sulphate reduction takes place in the top 10 cm of sediment indicating a very reactive pool of organic material (Fig. 5). However, the amount of remaining organic material below 10 cm sediment depth is still very large. Sulphate reduction continues below 10 cm depth at low rates until all sulphate is consumed and methanogenesis starts. Rapid increases in methane concentration lead to methane saturation only centimetres below the sediment-water interface (Fig. 6). Steep opposing gradients of porewater methane and sulphate indicate anaerobic oxidation of methane coupled to sulphate reduction [14]. In the absence of reactive iron oxides, the capacity for precipitation of dissolved sulphide as iron sulphides is limited, and slowly forming organic sulphides remain as the only significant sediment sink for hydrogen sulphide [5, 8]. These conditions explain, why concentrations of dissolved sulphide in porewaters from Namibian shelf sediments can be as high as 22 mM at only 10 cm sediment depth (Fig. 6), and consistently exceed 2 mM at 6 cm depth in all currently analyzed sediments between 19°S and 27°S on the shelf.

5.2 Sulphide Oxidation

In most marine sediments, a significant amount of hydrogen sulphide can be oxidized with iron and manganese oxides [1, 32, 37]. Low concentrations of reactive iron and manganese in the Namibian shelf sediments limit the

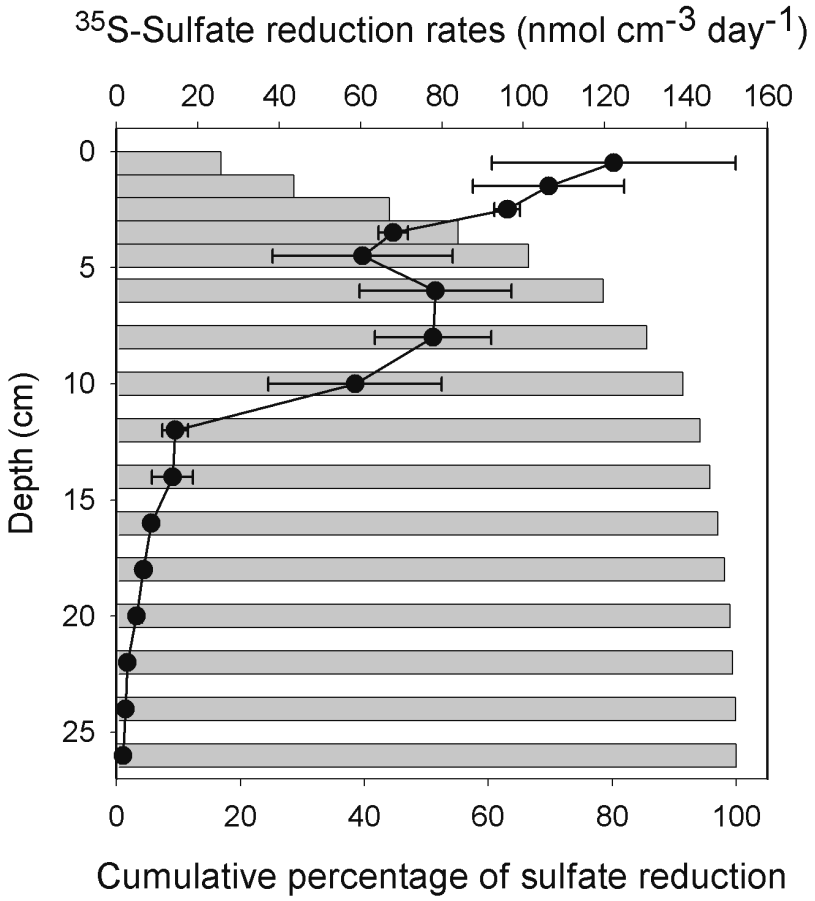

Figure 5. Representative depth profile of ^{35}S-sulphate reduction rates and cumulative percentage of sulphate reduction, here shown for M57-3 Station 178, March 2003.

oxidation of hydrogen sulphide to dissolved oxygen and nitrate. Since oxygen concentrations are already very low near the sediment-water interface, the major amount of hydrogen sulphide oxidation must take place by the reduction with nitrate. Studies of the large sulphur bacteria *Thioploca*, *Beggiatoa*, and *Thiomargarita* over the past 10 years have indicated their capacity for using nitrate as an alternative electron acceptor [24, 29]. Adaptations such as the intracellular storage of nitrate and elemental sulphur in vacuoles enable the bacteria to survive periods when electron donor and acceptor are limited in the ambient environment. The intracellular storage of nitrate may allow the bacteria to survive for up to 8 months [33]. Although the actual survival period of the bacteria in nature is uncertain, the principal conclusion is that sulphide oxidation can be decoupled from the contemporaneous presence of nitrate or

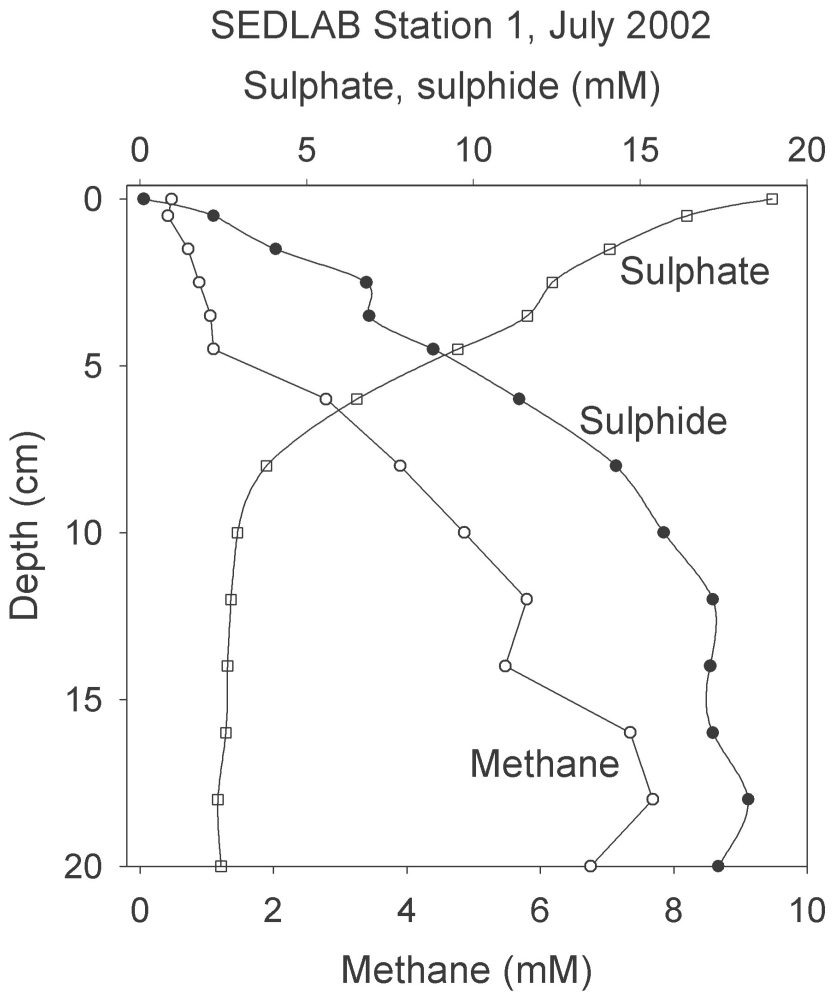

Figure 6. Representative depth profile of dissolved sulphate, sulphide, and methane concentration, here shown from SEDLAB Station 1, July 2002. Methane (○), sulphide (●), sulphate (□).

oxygen in the bottom waters. Therefore, sulphide oxidation can take place even when there is no dissolved nitrate or oxygen measurable in bottom waters because the large sulphur bacteria can retain a pool of intracellular nitrate to bridge periods with low or absent bottom water nitrate.

Experimental data indicate that a biofilm of *Beggiatoa* can quantitatively oxidize hydrogen sulphide [27], which is also in accordance with field microsensor measurements through *Beggiatoa* mats from Namibian shelf sedi-

ments that indicate complete removal of hydrogen sulphide in the mats (Stief and Brüchert, unpubl. data). Brüchert et al. [7] used data from 12 shelf stations to calculate the percentage of the hydrogen sulphide flux relative to bacterial sulphate reduction and found that between 4 and 51% of formed hydrogen sulphide diffuses across the sediment-water interface. In the presence of *Beggiatoa*, no hydrogen sulphide enters the water column, while *Thiomargarita* may reduce the diffusive upward sulphide flux by up to 45% [7]. The different physiological adaptations of these two bacterial species to hydrogen sulphide fluxes and concentrations make them good indicators for differences in the severity of bottom water anoxia and the potential occurrence of bottom water sulphide.

5.3 Regional Distribution

Fig. 7a shows the areal distribution of bacterial sulphate reduction rates on the Namibian shelf and slope. Areas with enhanced bacterial sulphate reduction correspond to areas of retention rather than to upwelling cells such as the Lüderitz upwelling cell. In the Lüderitz cell upwelling is almost perennial [9, 10]. Since upwelling mixes the water column in the cell continuously, phytoplankton biomass is not as high as further north, where the water column can become weakly stratified and water retention is higher [2]. As a consequence, rates of organic matter accumulation are also smaller in the Lüderitz cell. As less phytoplankton reaches the seafloor, and bottom water ventilation is better due to the upwelling of ESACW, rates of bacterial sulphate reduction in the sediment are correspondingly lower.

Diffusive hydrogen sulphide fluxes are always a fraction of the bacterial sulphate reduction rates (Fig. 7b). The highest fluxes are restricted to three areas: (1) Between 25°S and 24°S extending approximately from Sylvia Hill to Meob Bay, (2) from 23°30'S to 22°50'S, i.e, Conception Bay to Pelican Point including the area of Walvis Bay, and (3) the area from Cape Cross to Henties Bay. There is no significant agreement between the rates of bacterial sulphate reduction and hydrogen sulphide fluxes. South of Walvis Bay, the rates of sulphate reduction and the hydrogen sulphide fluxes roughly correlate, whereas to the north, none of the areas with enhanced bacterial sulphate reduction are evident in the hydrogen sulphide flux pattern. The highest hydrogen sulphide fluxes only coincide in the area inside Walvis Bay and are generally restricted to a very small area.

The distribution pattern of the large sulphur bacteria can provide answers to these discrepancies. *Beggiatoa* and *Thiomargarita* are concentrated in different areas, respectively (Fig. 8a and 8b). *Beggiatoa* is concentrated in the area north of Palgrave Point and is found north to Cape Frio, whereas *Thiomargarita* is most abundant in the area south of Palgrave Point and around Walvis Bay.

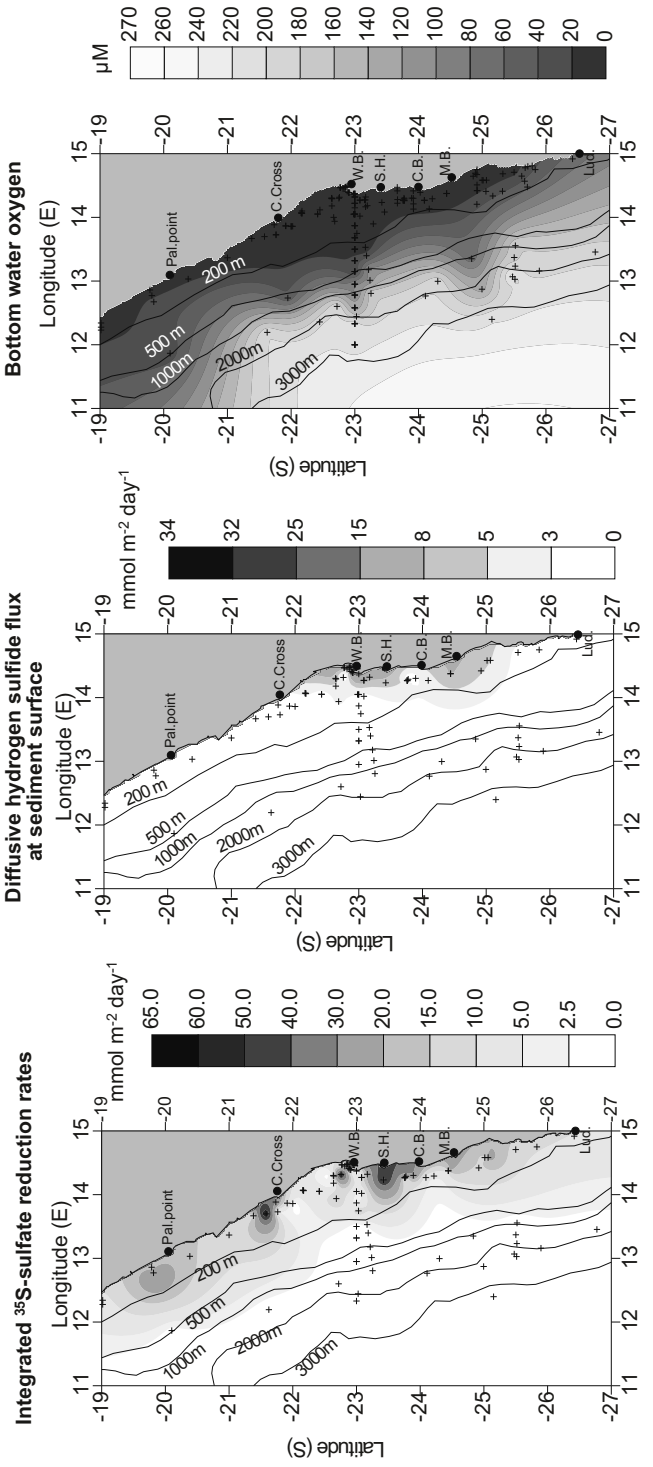

Figure 7. Areal distribution map of (a) depth-integrated bacterial sulphate reduction rates, (b) diffusive hydrogen sulphide fluxes across the sediment-water interface, (c) annually averaged bottom water dissolved oxygen concentrations.

Thiomargarita and *Beggiatoa* are also abundant south of Walvis Bay between 24°S and 25°30'S near Sylvia Hill and between Conception Bay and Walvis Bay. The distribution maps represent quasi-averages over 7 years of observation. It is important to note that significant intra- and interannual fluctuations in abundance exist. These are integrated into the maps for the areas where stations were revisited several times.

Field observations have consistently shown that *Beggiatoa* is absent from areas with bottom water hydrogen sulphide. *Thiomargarita*, in contrast, can tolerate hydrogen sulphide at least temporarily at millimolar concentrations and has been found to survive in environments repeatedly containing bottom water hydrogen sulphide [7]. This is confirmed by the distribution map of *Thiomargarita* and the areas where bottom water hydrogen sulphide has been found on the Namibian shelf (Fig. 8c). The difference in distribution between the two types of large sulphur bacteria may have to do with the slower metabolism of *Thiomargarita* relative to *Beggiatoa*, when growing with nitrate. The large size of *Thiomargarita* may allow them to store larger amounts of nitrate and survive for longer time periods under adverse conditions.

5.4 Temporal Variation

We assessed the intra- and interannual variability at a selected station in shallow depth (28 m), with shallow gas saturation (SEDLAB Station 1). Between May 2001 and May 2004, concentrations of porewater methane, hydrogen sulphide, and water column oxygen were determined nearly every two months (Fig. 9a-c). At this sampling frequency marked fluctuations in oxygen levels in the water column were detected, in concert with variations in methane concentration and with fluxes of hydrogen sulphide. There was no apparent periodicity in the observed fluctuations, and except for one period oxygen concentrations in the bottom water were below 22 μM. The most conspicuous feature was the extreme oxygen depletion over the whole water column, with drops in surface concentrations of oxygen to values as low as 67 μM. A relatively stable chemocline was only present during the austral summer 2001/2002 (October 2001 until May 2002). During this period, two low-oxygen periods occurred in December 2001 and in May 2002. Oxygen-rich water intruded after May 2002, but was interrupted by another low-oxygen period in October 2002, which was also terminated abruptly. Subsequently, oxygen levels dropped in the bottom water and the chemocline rose gradually throughout the year 2003 reaching the shallowest depth in March 2004. Data acquisition stopped in May 2004 with an apparent return to better ventilated conditions.

During time periods when a shallow chemocline was present, methane concentrations increased abruptly in the sediment so that the depth of methane

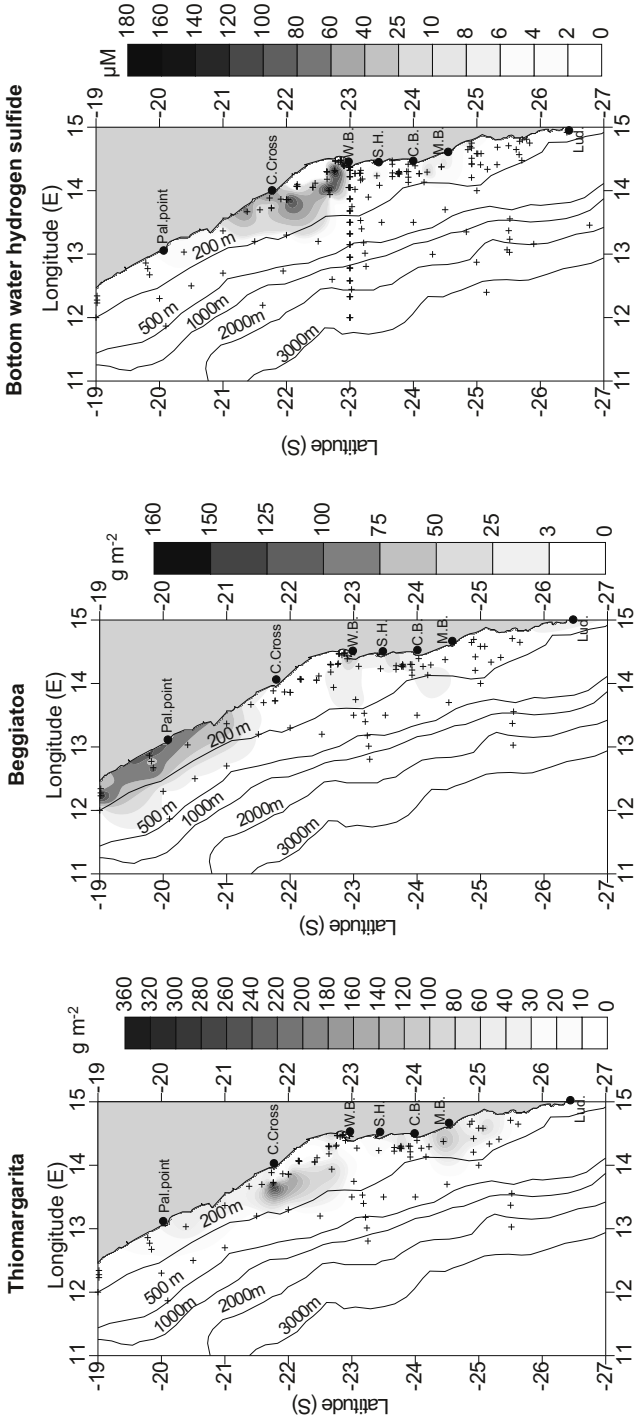

Figure 8. Areal distribution map of (a) Thiomargarita, (b) Beggiatoa, (c) annually averaged bottom water hydrogen sulphide.

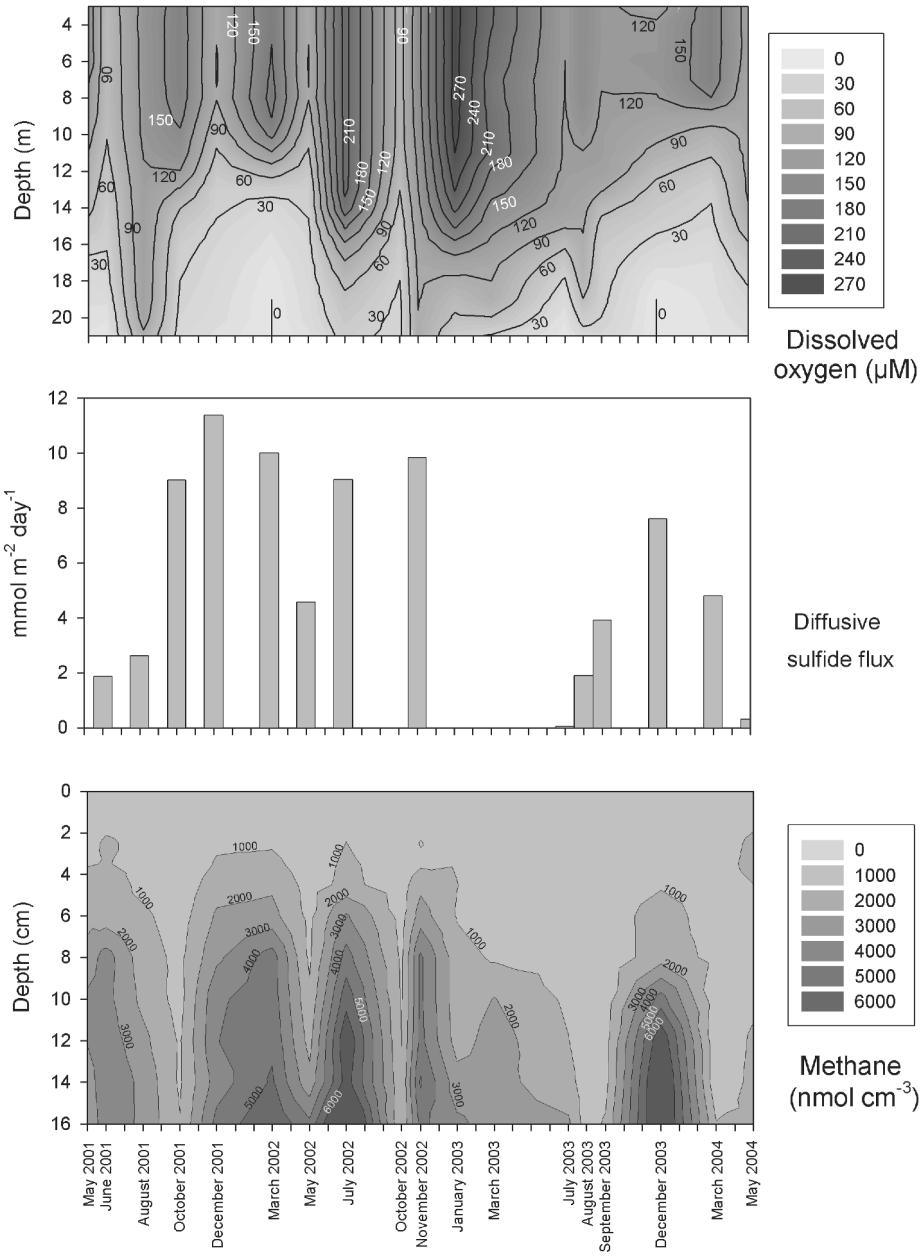

Figure 9. Time series plot from SEDLAB Station 1 of (a) water column dissolved oxygen, (b) diffusive sulphide flux, (c) sediment methane concentrations.

saturation rose to a sediment depth as shallow as 4 cm. Sulphide fluxes also increased during these periods. The sulphide fluxes ranged from 0.02 to 11.4 mmol m^{-2} day^{-1}, a variation of more than 2 orders of magnitude. The enhanced sulphide fluxes and methane concentrations did not coincide with the punctuated low-oxygen periods. In two cases, the low-oxygen period preceded the period of increased methane and sulphide fluxes. It appears that the period of good stratification was conducive for the accumulation of bottom water hydrogen sulphide (Fig. 4). Nitrate concentrations, which were below the detection limit in March 2002, support this interpretation. There was no bottom water hydrogen sulphide before March 2002, but it may have been missed because of the relatively long sampling gap. Coincidentally, during the summer 2001/2002, there were numerous observations of turquoise near-shore surface water discolorations and hydrogen sulphide smell suggesting that hydrogen sulphide was present in the water column [40]. It is clear that a higher sampling frequency than once every two months is required in order to capture the true dynamic nature of developing anoxia.

5.5 The Contribution of the Sedimentary Microbial Sulphur Cycle to System-Wide Oxygen Consumption

Overall oxygen consumption in the Namibian upwelling system takes place by aerobic respiration of organic material in the water column, hydrogen sulphide oxidation at the sediment-water interface, and oxidation of water column hydrogen sulphide. The proportions of these processes vary as a function of water depth, spatial occurrence of water column hydrogen sulphide and sulphide-oxidizing bacteria, and sediment sulphate reduction rates. We have divided the shelf into the total shelf and the inner shelf area, which we defined as the areas inside the isobaths of 300 m and 100 m, respectively. Table 2a shows that extreme anoxia (oxygen concentrations less than 1 μM) only occur in an area covering 8944 km^2, roughly 10 % of the total shelf area. Bottom waters characteristic of hypoxic conditions (< 22.3μM/0.5 ml/l) cover 46954 km^2, which is 55 % of the total shelf and an area larger than the inner shelf (21690 km^2). With few exceptions, hydrogen sulphide diffuses across the sediment-water interface only in areas of the inner shelf. For an estimate of the relative proportions of oxygen-producing and oxygen-consuming processes, area-integrated fluxes were calculated for oxygen production and consumption for the inner and total shelf, respectively (Table 2b). Oxygen production by photosynthesis and the import of oxygen by upwelling amount to 10.9 x 10^9 and 24.8 x 10^9 moles O_2 day^{-1} for the inner and total shelf, respectively (Table 2b). Aerobic water column respiration (1.8 and 21.7 x 10^9 moles O_2 day^{-1}) balances 16.5 % and 87.5 % of the photosynthetic oxygen production/import in the two areas, respectively. The combined water column and benthic sulphide

oxidation contributes 25 % and 9 % to the total oxygen consumption on the inner and total shelf, respectively. This comparison emphasizes the importance of sedimentary processes for the regulation of water column oxygen levels on the inner shelf. Although there are considerable uncertainties associated with the estimation of water column respiration, there is a reasonable match between the combined sediment and water column oxygen consumption versus primary production and import of oxygen, which gives further support to our estimates.

Table 2. Areal and volumetric estimates of Namibian shelf area between 29°S and 17°S, inventory of oxygen and water column hydrogen sulphide, and areal occurrence of sulphur bacteria.

Areal estimates	*Area (km^2)*
Shelf area (max. 300 m water depth) 29°S to 17°S	85472
Shelf (max. 100 m water depth) 29°S to 17°S	21690
Gas-charged area	1350
Area covered by craters, domes, and disrupted sea floor	380
Hydrogen sulphide, bottom water, > 1μM, 10 - 30 m thickness	27978
Bottom water dissolved oxygen, <44.6μM (1 ml/l)	78565
Bottom water dissolved oxygen, <22.3μM (0.5 ml/l)	46954
Bottom water dissolved oxygen, <11μM (0.25 ml/l)	31491
Bottom water dissolved oxygen, <1μM (0.022 ml/l)	8944
Thiomargarita >5 gm^{-2} biomass	50555
Beggiatoa, >5 g m^{-2} biomass	33143

6. SEDIMENTOLOGICAL CONTROL ON SULPHATE REDUCTION RATES AND METHANE ACCUMULATION

Three main regions with different sediment patterns were outlined from the acoustic records. The continental slope consists of soft silts forming a smooth surface with westward prograding sediment layers. At the shelf break the sea bottom consists of hardground and consolidated sediments suggesting a non-depositional environment. Well-stratified deposits with dipping reflectors are truncated and partly covered with silty/sandy sediments (Fig. 10). Strong bottom currents prevent the deposition of soft sediments. These sediments are apparently reworked deposits. They contain only small amounts of reactive organic material and support relatively low depth-integrated rates of sulphate reduction that are less than 1.5 mmol m^{-2} day^{-1} [7]. Porewater concentrations of dissolved sulphide are in the low μM range, and fluxes of hydrogen sulphide across the sediment-water interface are below detection. In addition, at depths greater than 150 m, no large sulphur bacteria have been observed [7].

Table 3. Area-integrated flux estimates of oxygen production and consumption due to respiration and sulphide oxidation for the Namibian shelf between 29°S and 17°S.

Source/sink	*Inner shelf (< 100 m water depth)*	*Total shelf (< 300 m water depth)*
	O_2 production (+) / consumption (-) 10^9 moles day^{-1}	
Estimated integrated primary production[1]	4.7	18.6
Import of oxygen with upwelling waters and poleward undercurrent[2]	6.2	6.2
Aerobic respiration in the water column[3]	-1.8	-21.7
Oxygen consumption of sulphide diffusing into the water column[4]	-0.1	-0.3
Sediment oxygen uptake for benthic sulphide oxidation[4,5]	-0.5	-1.9

[1] Primary production: 217 mmol C m^{-2} day^{-1} based on 0.37 Gt C yr^{-1} (Carr, 2002) for an area covering 389,000 km^2; Org. C : O_2 production (1:1)
[2] Upwelling: 1.6 Sv [34], O_2 concentration: 45μM
[3] Based on experimental oxygen consumption rates of 1.7 μM day^{-1} (see text)
[4] expressed in O_2 equivalents (mole O_2 : mole H_2S = 2:1)
[5] Calculated as the difference between depth-integrated sulphate reduction rate, diffusive hydrogen sulphide flux, and sulphide burial (see [7])

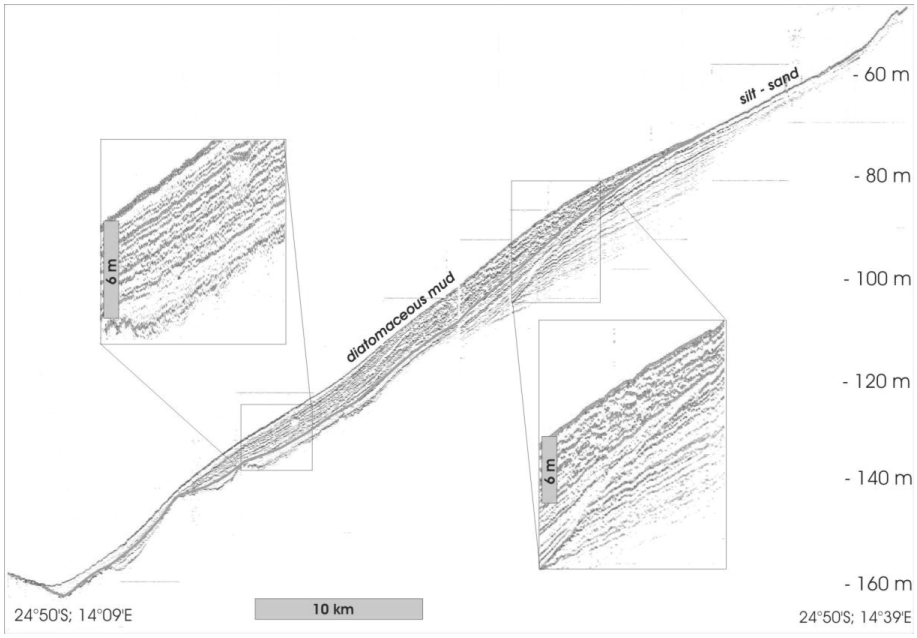

Figure 10. SES96 Sediment echosounder profile 1: cross section of the mud belt at 24°50S showing stratified, gas-free mud over westward prograding sandy layers. Towards the coast, at a depth of about 70 m, the muddy surface sediment changes to coarser (silt, sand) material.

The near-shore region (water depths of less then 150 m) is characterized by sedimentation of organic matter forming a NNW-SSE striking (coast parallel) diatom mud layer, which grows to more then 10 m thickness towards the coast (Fig. 11). At water depths between 80 m and 130 m, acoustic anomalies, so-called blankings, occur that indicate free gas accumulations at about 6 m depth in the mud layer (Fig. 11). The gas bubbles are concentrated under a less permeable layer inside the mud. Comprehensive acoustic investigations on gas-charged mud in Eckernförde Bay, Baltic Sea, used similar acoustic frequencies to our study [41] and found that between 2% (mean) and 8% of the pore space are occupied by bubbles.

In direction to the coast, the isolated acoustic gas blankings change into a permanent gas-charged layer at about 3 to <1 m sub-bottom depth. This gas-charged layer intersects the sea-bottom at water depths of about 40 m (Fig. 11). Near the coast, between 22° 50'S and 23°10'S, east of 14°15'E the flat sea bottom changes to morphological features like pockmarks (Fig. 11) and very rough sea bottom surface (Fig. 11). These features indicate recent eruptions of free gas and/or gas-charged mud blocks. Upward-travelling gas bubbles in the water column from one of the pockmarks were observed in the high-frequency channel of the SES96 echosounder during station work. The area affected by

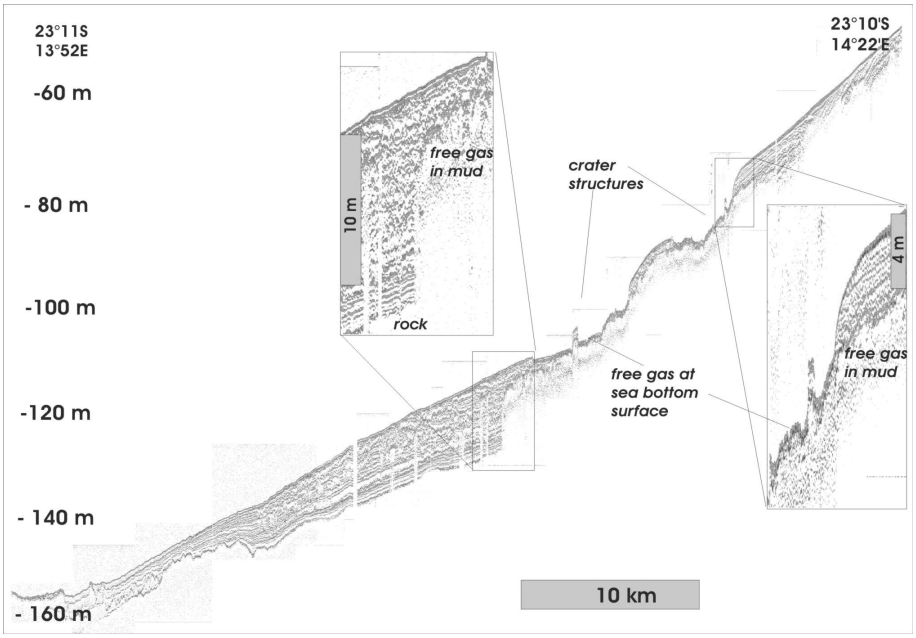

Figure 11. SES96 Sediment echosounder profile 2: cross section of the mud belt at 23° 10'S, showing pockmark/crater structures and abundant gas blankings.

pockmark structures covers about 380 km^2. Pockmarks occupy 5 to 10 percent of this area. The total gas-filled area has been estimated to cover as much as 1350 km^2 [14]. Free gas in the shelf sediments is restricted to an area between 22°S and 23°15'S between 40 m and 120 m water depth. Outside this area, a small patch was detected off Conception Bay at 24°S. Our data coverage is considered sufficiently tight to predict that no large gas-filled areas have remained undetected between 22° and 27°S.

7. TRANSPORT MECHANISMS OF HYDROGEN SULPHIDE TO THE WATER COLUMN

7.1 Catastrophic Methane Eruptions

Video observations of rising gas bubbles, sediment craters, and disrupted seafloor off Walvis Bay suggest locally enhanced transport of hydrogen sulphide and methane by eruptive degassing. A budget assessment of the available amount of hydrogen sulphide in the sediments is instructive to estimate the reservoir strength of the mud belt for the supply of hydrogen sulphide to the overlying water column. The gas-charged sediments, which cover 1350 km^2 (Table 2a) would contain about $2.0 \cdot 10^{11}$ moles hydrogen sulphide, if porewater

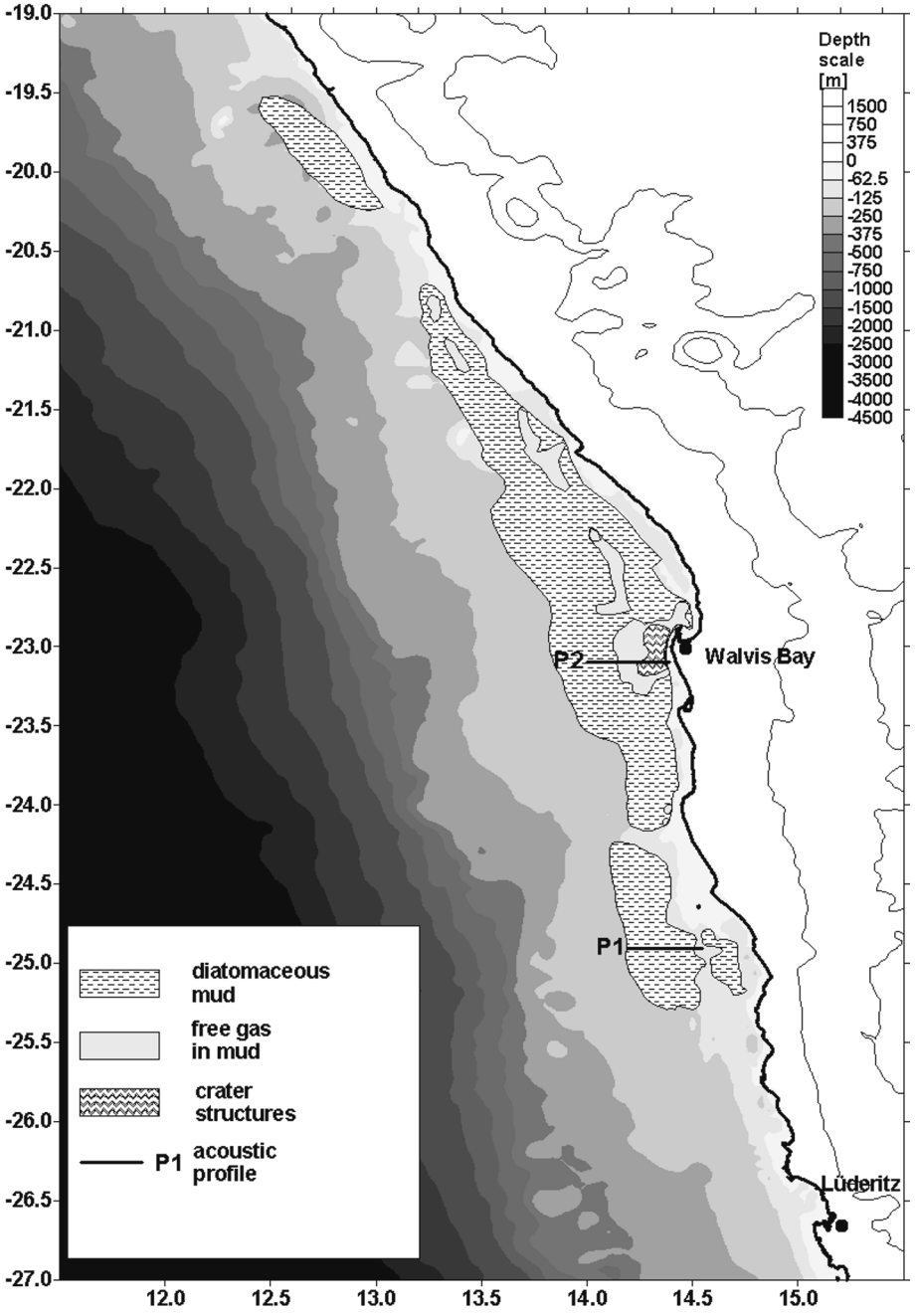

Figure 12. Distribution map of diatomaceous mud and gas-charged area. The area with abundant crater structures and disrupted seafloor is highlighted in dark-grey.

sulphide concentrations in the methane-containing zone are 15 mM [14]. Areal integration of the amount of hydrogen sulphide in the water column yielded an estimated 0.3 to 0.8 x 10^9 moles of hydrogen sulphide. Only between 0.2 and 0.4 % of this reservoir is required to replenish the bottom water with hydrogen sulphide to concentrations exceeding 1 μM.

We assessed the amount of hydrogen sulphide that would have been released during a violent sediment eruption, using as an example a crater with a diameter of 250 m and a depth of 10 m, which was mapped during METEOR expedition M57-3 [42]. The total volume of sediment missing from this crater is about 490,000 m^3. If this volume of sediment had an average porewater hydrogen sulphide concentration of 15 mM and a porosity of 0.8, then the total amount of hydrogen sulphide in the crater void would have been 5.9 x 10^6 moles. Assuming that the overlying seawater contained at least 6 μmoles of hydrogen sulphide per litre seawater, about 10^{12} litres of seawater could contain this concentration of hydrogen sulphide. For a water depth of 60 meters, this corresponds to an area covering 16 square kilometres. The calculation indicates that individual sediment eruptions may have an important local impact on hydrogen sulphide in the water column, but are of limited regional significance.

Sediments, which contain no free gas or free gas at more than 3 m sediment depth at the time of the acoustic echosounding surveys, have not likely emitted gas to the overlying water column in the past years. The size and outline of the gas-charged areas identified on echosounding lines conducted on cruises in August 2000, March 2003, and March 2004 coincide closely. Gas-free areas and areas with free gas at more than 3 m sediment depth all have good sediment stratification [5], a lack of surface structures, and from the core samples examined, a deep penetration of dissolved sulphate (Fig. 13a). The profile shape of pore water sulphate in Fig. 13a suggests that the dominant mode of sulphate transport has been by molecular diffusion. If these sediments once contained free gas near the sediment surface, sulphate would have been depleted a few centimetres below the sediment surface. After the gas release, sulphate would have diffused downward. It would take approximately 180 years for sulphate to diffuse over a distance of 3 m by molecular diffusion [18]. In addition, in sediments with diffusive interfaces between methane and sulphate more than 95 percent of the methane is oxidized anaerobically with sulphate, which counteracts the build-up of gas overpressure. For these reasons, it is unlikely that undisturbed areas surveyed have in the past contributed to methane gas emission.

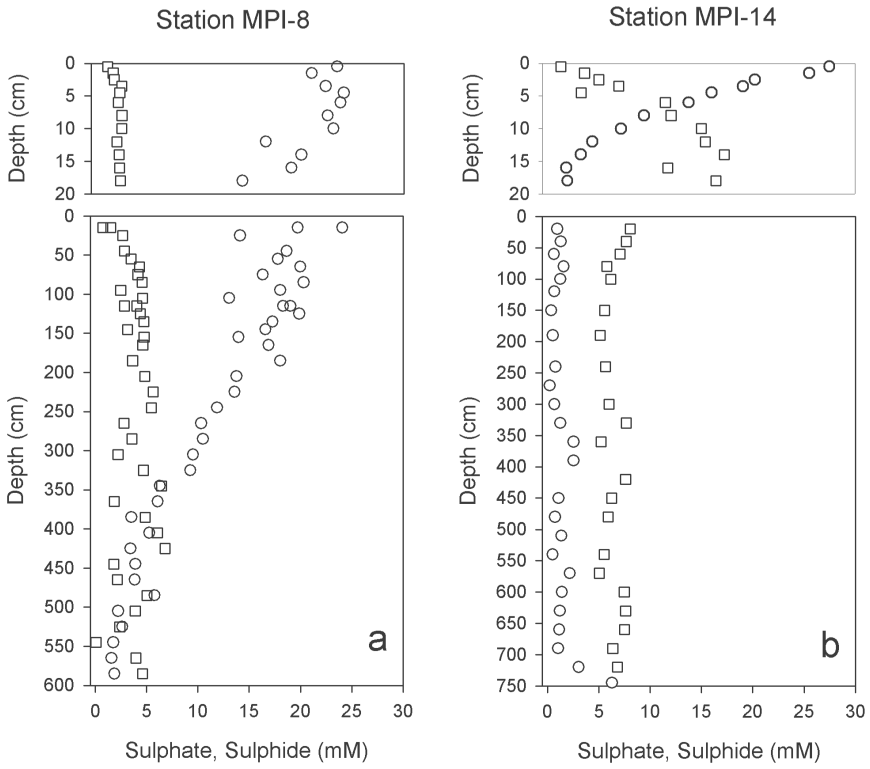

Figure 13. Comparative depth profile of sulphate and sulphide concentrations (a) from an area devoid of free gas (left profile) and (b) from an area where the gas-charged zone almost intercepts with the sea floor. ● (sulphate, multi-core), ○ (sulphate, gravity core), ■ (sulphide, multi-core), □ (sulphide (gravity core).

7.2 Methane Ebullition

Apart from catastrophic eruptions, advective transport due to methane ebullition in gas-charged areas would also enhance the exchange between sediment and seawater. Several studies have demonstrated that gas advection enhances pore water transport [22, 23, 28]. Co-transport of porewater methane and hydrogen sulphide is evident from the concentration profiles in one of the craters (Fig. 6 and 13b). The porewater profiles are linear just below the sediment surface and show highly significant correlations between hydrogen sulphide and methane. These profile shapes suggest mixing and advective transport of porewater and gas. The pH values of the porewaters range between 7.0 and 7.4. In this pH range, between 25 and 45 percent of dissolved sulphide is present as hydrogen sulphide gas, which can be transported together with methane. The

actual fluxes of hydrogen sulphide across the sediment-water interface in the gas-charged sediments are therefore likely higher than those calculated from molecular diffusion. However, gas bubbling on the Namibian shelf is apparently intermittent. An areal and temporal quantification of the fluxes during active gas emission has not yet been studied and remains difficult, because neither the rate of advection nor the frequency of such gas emissions is known.

7.3 Bottom Water Hydrogen Sulphide Replenishment by Production of Hydrogen Sulphide in the Topmost Sediment Layers

The area of gas-charged sediments is significantly smaller than the spatial occurrence of bottom water sulphide, and is much smaller than the area outlined by positive fluxes of hydrogen sulphide across the sediment-water interface (Table 2 and Fig. 7b). Gas-charged sediments occur over a much smaller area than hydrogen sulphide-containing waters. In particular, bottom water sulphide has often been observed as far south as 26°30'S [40], where gas saturation occurs in more than 6 m sediment depth (Fig. 13a). These observations suggest that processes other than ebullition and gas eruption are of significance for the production of water column hydrogen sulphide.

In shelf areas with less than 100 m water depth, sulphate reduction rates in the topmost 20 cm are high enough to generate a hydrogen sulphide flux that can produce μM concentrations of hydrogen sulphide in the bottom waters within a few days. In this process hydrogen sulphide is essentially inexhaustible because continuous replenishment of fresh deposited organic matter and short diffusion distance for seawater sulphate maintain the microbial production of hydrogen sulphide at the sediment surface. Using the areal estimates of 27978 km^2 for bottom hydrogen sulphide and the hydrogen sulphide fluxes calculated for this area (Table 2), it would take a maximum of 7.5 days to reach a sulphide concentration of 1 μM in a 10 m thick bottom water layer for the whole area. However, since the flux estimate is taking the whole area into account, in areas with significantly higher fluxes, locally bottom water hydrogen sulphide would accumulate much faster.

Key requirements for this process are a bottom boundary layer water that is stagnant and that contains very little dissolved nitrate and oxygen. Under these circumstances, bacterial sulphide oxidation with oxygen and nitrate is inhibited and the diffusive flux of sulphide from the sediment into the bottom waters is enhanced. Episodic in-shore movement and upward mixing of the bottom boundary layer would transport hydrogen sulphide into the oxic part of the water column where turbulent mixing with oxygen produces the colloidal elemental sulphur.

8. Summary

Temporally and spatially variable circulation patterns control the development and persistence of an isolated, stagnant bottom boundary layer that contains low concentrations of oxygen and nitrate. Preconditions are low wind stress and distance from the Angola-Benguela Front in order to deplete nutrient-rich SACW of nitrate.

Aerobic respiration in the water column consumes the major amount of oxygen supplied by upwelling and primary production. Sediments account for 9 to 25 % of the oxygen consumption. The major source of hydrogen sulphide is the diatomaceous mud belt, where excess organic matter deposition supports bacterial hydrogen sulphide and methane production. Water column bacterial sulphate reduction was found to contribute little to the development of water column hydrogen sulphide.

For the development of bottom water sulphidic conditions, bacterial sulphide oxidation at the sediment-water interface must be inhibited or ineffective. These conditions are only met after complete depletion of nitrate in the bottom waters. The large sulphur bacteria *Beggiatoa* spp. would represent an effective barrier against hydrogen sulphide. Nitrate-consuming processes in the water column such as anammox contribute to the development of complete nitrate depletion.

The development of bottom water sulphidic conditions is accelerated by advective transport mediated by gas ebullition and during catastrophic eruption events. The structure of the Namibian shelf and slope sediments indicate that this mechanism is active in an area between 23°S and 24°S in water depths less than 100 m.

The temporal and spatial variability of water column hydrogen sulphide occurrences suggest that several mechanisms are active on the shelf. The inshore area may be affected more strongly by gas ebullition, whereas the central shelf probably experiences mainly diffusive supply of hydrogen sulphide to the bottom waters. Possible linkages between the gas emanations and wind-driven circulation remain the subject of further research.

Acknowledgements

We would like to thank Lev Neretin for the invitation to contribute to this book and the two reviewers for their constructive comments. Tim Ferdelman provided unpublished data on sulphate reduction rates from 1997, and Daniela Riechmann provided bacterial counts from the METEOR cruise M48-2. We are grateful for scientific discussions with Anja van der Plas, Bo Barker Jørgensen, Tim Ferdelman, Kay-Christian Emeis, Helle Ploug, Marcel Kuypers, Gaute Lavik, and Heide Schulz. Gerd Bening, Chibola Chiklililwa, Kirsten Imhoff, Swantje Lilienthal, Martina Meyer, Gerald Nickel, Andrea Schipper, the late Bernd Schulz, Heidi Skrypzeck, Monika Trümper, and Tamara Zemskaya pro-

vided technical assistance for this study. Funding was provided by the Max-Planck Society, the DFG Research Center Ocean Margins at the University of Bremen, the BMBF and DFG programme GEOTECHNOLOGIEN, the DFG priority programme 516 (Meteor expeditions), the Benguela Environment Fisheries Interaction and Training Programme BENEFIT, and the Ministry of Fisheries, Namibia. This is publication no. GEOTECH-175 of the GEOTECHNOLOGIEN programme of BMBF and DFG, Grant 03G0580B NAMIBGAS.

References

[1] Aller R.C. and Rude P.D. Complete oxidation of solid phase sulfides by manganese and bacteria in anoxic marine sediments. Geochim Cosmochim Ac 1988; 52:751-65.

[2] Bailey G.W., Boyd A.J., Duncombe Rae C.R., Mitchell-Innes B. and van der Plas A. Synthesis of marine science research in the Benguela Current system during cruises linked to the BENEFIT training programme in 1999. S Afr J Sci 2001; 97:271-74.

[3] Berg P., Petersen-Risgaard N. and Rysgaard S. Interpretation and measured concentration profiles in sediment pore water. Limnol Oceanogr 1998; 43:1500-10.

[4] Bleil U. *Report and Preliminary Results of METEOR Cruise 34/1, Cape Town - Walvis Bay, 31.01.1996 -25.01.1996.* Bremen, Berichte Fachbereich Geowissenschaften, Universität Bremen, 1996.

[5] Borchers S.L., Schnetger B., Böning P. and Brumsack H.-J. Geochemical signatures of the Namibian diatom belt: Perennial upwelling and intermittent anoxia. Geochem Geophy Geosy 2005; 6:1-20.

[6] Boyd A.J. Intensive study of the currents, winds and hydrology at a coastal site off central South West Africa, June/July 1978. Investigational Report, Sea Fisheries Institute, Republic of South Africa, 1983; 1-47.

[7] Brüchert V., Jørgensen B.B., Neumann K., Riechmann D., Schlösser M. and Schulz H. Regulation of bacterial sulfate reduction and hydrogen sulfide fluxes in the central Namibian coastal upwelling zone. Geochim Cosmochim Ac 2003; 67:4505-18.

[8] Brüchert V., Pérez M.E. and Lange C.B. Coupled primary production, benthic foraminiferal assemblage, and sulfur diagenesis in organic-rich sediments of the Benguela upwelling system. Mar Geol 2000; 163:27-40.

[9] Campillo-Campbell C. and Gordoa A. Physical and biological variability in the Namibian upwelling system: October 1997-October 2001. Deep-Sea Res 2004; 51:147-58.

[10] Carr M.-E. Estimation of potential productivity in Eastern Boundary Currents using remote sensing. Deep-Sea Res 2002; 49:59-80.

[11] Chapman P. and Shannon L.V. The Benguela Ecosystem Part II. Chemistry and related processes. Oceanogr Mar Biol Ann Rev 1985; 23:183-251.

[12] Cline J.D. Spectrophotometric determination of hydrogen sulfide in natural waters. Limnol Oceanogr 1969; 14:454-59.

[13] Emeis K.-C., Bening G., Berger J., Brüchert V., Currie B., Endler R., Ferdelman T., Finke N., Graco M., Haferburg G., Heyn T., Kiessling A., Lage S., Leipe T., Mollenhauer G., Neumann K., Nickel G., Noli K., Riechmann D., Schippers A., Schneider R., Schulz H., Shidjuu A., Sonnabend H., Stregel S., Struck U., Treppke U., Vogt T. and Zemskaya T. *Cruise Report Meteor Expedition M48-2, Walvis Bay - Walvis Bay, August 8 - August 23, 2000.* Bremen, Berichte Fachbereich Geowissenschaften Universität , 2002.

[14] Emeis K.-C., Brüchert V., Currie B., Endler R., Ferdelman T.G., Kiessling A., Leipe T., Noli-Peard K., Struck U. and Vogt T. Shallow gas in shelf sediments of the Namibian coastal upwelling ecosystem. Cont Shelf Res 2004; 24:627-42.

[15] Hamukuaya H., O'Toole M. and Woodhead P.M.J. Observations of severe hypoxia and offshore displacements of Cape Hake over the Namibian Shelf in 1994. S Afr J Marine Sci 1998; 19:41-57.

[16] Hardman-Mountford N.J., Richardson A.J., Agenbag J.J., Hagen E., Nykjaer L., Shillington F.A. and Villacastin C. Ocean climate of the South East Atlantic observed from satellite data and wind models. Prog Oceanogr 2003; 59:181-221.

[17] Helly J.J. and Levin L.A. Global distribution of naturally occurring marine hypoxia on continental margins. Deep-Sea Res 2004; 51:1159-68.

[18] Jørgensen B.B. Bacteria and biogeochemistry, In *Marine Geochemistry*, H.D. Schulz and M. Zabel, eds. Berlin: Springer Verlag, 2000.

[19] Kiørboe T. and Jackson G.A. Marine snow, organic solute plumes, and optimal chemosensory behaviour of bacteria. Limnol Oceanogr 2001; 46:1309-18.

[20] Kiørboe T., Tiselius P., Mitchell-Innes B., Hansen J.L.S., Visser A.W. and Mari X. Intensive aggregate formation with low vertical flux during an upwelling-induced diatom bloom. Limnol Oceanogr 1998; 43:104-16.

[21] Kuypers M.M.M., Lavik G., Woebken D., Schmid M., Fuchs B.M., Amann R., Jørgensen B.B. and Jetten M.S.M. Massive nitrogen loss from the Benguela upwelling system through anaerobic ammonium oxidation. PNAS 2005; 102:6478-83.

[22] Martens C.S., Albert D.B. and Alperin M.J. Biogeochemical processes controlling methane in gassy coastal sediments-part 1. A model coupling organic matter flux to gas production, oxidation, and transport. Cont Shelf Res 1998; 18:1741-70.

[23] Martens C.S. and Klump J.V. Biogeochemical cycling in an organic-rich coastal marine basin-I. Methane sediment-water exchange processes. Geochim Cosmochim Ac 1980; 44:471-90.

[24] McHatton S.C., Barry J.P., Jannasch H.W. and Nelson D.C. High nitrate concentrations in vacuolate, autotrophic marine *Beggiatoa* spp. Appl Environ Microb 1996; 62:954-58.

[25] Mohrholz V., Schmidt M. and Lutjeharms J.R.E. The hydrography and dynamics of the Angola-Benguela frontal zone and environment in 1999. S Afr J Sci 2001; 97:199-208.

[26] Naqvi S.W.A., Jayakumar D.A., Narvekar P.V., Nalk H., Sarma V.V.S.S., D'Souza W., Joseph S. and George M.D. Increased marine production of N_2O due to intensifying anoxia on the Indian continental shelf. Nature 2000; 408:346-49.

[27] Nelson D.C., Jørgensen B.B. and Revsbech N.P. Growth pattern and yield of a chemoautotrophic *Beggiatoa* spp. in oxygen-sulfide microgradients. Appl Environ Microb 1986; 52:225-33.

[28] O'Hara S.C.M., Dando P.R., Schuster U., Bennis A., Boyle J.D., Chui F.T.W., Hatherell T.V.J., Niven S.J. and Taylor L.J. Gas seep induced interstitial water circulation: observations and environmental applications. Cont Shelf Res 1995; 15:931-48.

[29] Otte S., Kuenen J.G., Nielsen L.P., Paerl H.W., Zopfi J., Schulz H.N., Teske A., Strotmann B., Gallardo V.A. and Jørgensen B.B. Nitrogen, carbon, and sulfur metabolism in natural *Thioploca* samples. Appl Environ Microb 1999; 65:3148-57.

[30] Ploug H., Hietanen S. and Kuparinen J. Diffusion and advection within and around sinking, porous diatom aggregates. Limnol Oceanogr 2002; 47:1129-36.

[31] Poole R. and Tomczak M. Optimum multiparameter analysis of the water mass structure in the Atlantic Ocean thermocline. Deep-Sea Res I 1999; 46:1895-921.

[32] Schippers A. and Jørgensen B.B. Biogeochemistry of pyrite and iron sulfide oxidation in marine sediments. Gechim Cosmochim Ac 2002; 66:85-92.

[33] Schulz H.N., Brinkhoff T., Ferdelman T.G., Mariné H.M., Teske A. and Jørgensen B.B. Dense populations of a giant sulfur bacterium in Namibian sediments. Science 1999; 284:493-95.

[34] Shannon L.V. and Nelson G. The Benguela: Large scale features and processes and system variability, In *The South Atlantic, present and past circulation*, Wefer G., Berger W., Siedler G. and Webb D. J., eds. Berlin: Springer, 1996.

[35] Shillington F.A. The Benguela Upwelling System off south-western Africa, In *The Sea*, Robinson A.R. and Brink K.H., eds. New York: Wiley, 1998.

[36] Spiess V. *Digitale Sedimentechographie-Neue Wege zu einer hochauflösenden Akustostratigraphie*. Bremen: Fachbereich Geowissenschaften, Universität Bremen, 1993.

[37] Thamdrup B., Fossing H. and Jørgensen B.B. Manganese, iron, and sulfur cycling in a coastal marine sediment, Aarhus Bay, Denmark. Geochim Cosmochim Ac 1994; 58:5115-29.

[38] Tyrrell T. and Lucas M.I. Geochemical evidence of denitrification in the Benguela upwelling system. Cont Shelf Res 2002; 22:2497-511.

[39] Ulloa O., Escribano R., Hormazábal S., Quiñones R., Gonzales R. and Ramos M. Evolution and biological effects of the 1997-1998 El Nino in the upwelling ecosystem of northern Chile. Geophy Res Lett 2001; 28:1591-94.

[40] Weeks S.J., Currie B., Bakun A. and Peard K.R. Hydrogen sulphide eruptions in the Atlantic Ocean off southern Africa: implications of a new view based on SeaWIFS satellite imagery. Deep-Sea Res 2004; 51:153-72.

[41] Wilkens R.H. and Richardson M.D. The influence of gas bubbles on sediment acoustic properties: in situ, laboratory and theoretical results from Eckernförde Bay, Baltic Sea. Cont Shelf Res 1998; 18:1859-92.

[42] Zabel M., Brüchert V. and Schneider R.R. *The Benguela Upwelling System 2003, Cruise No. 57, 20 January - 13 April 2003, Meteor Berichte*. Hamburg: Universität Hamburg, 2004.

SEASONAL OXYGEN DEFICIENCY OVER THE WESTERN CONTINENTAL SHELF OF INDIA

S. Wajih A. Naqvi[1], H. Naik[1], D.A. Jayakumar[1,2], M.S. Shailaja[1], and P.V. Narvekar[1]

[1]*National Institute of Oceanography, Dona Paula, Goa 403 004, India*

[2]*Princeton University, Department of Geosciences, Princeton, NJ 08544-1003, USA*

Abstract The North Indian Ocean contains about two-third of the global continental-margin area affected by natural oxygen deficiency (O_2 < 0.2 mL L^{-1}) in the water column. Also, the littoral countries of this semi-enclosed basin account for a quarter of the world's population, making the sensitive O_2-depleted environment especially vulnerable to anthropogenic perturbations. We describe here factors responsible for the occurrence of O_2 deficient conditions, their evolution over the annual cycle, and their impact on biology and chemistry off the west coast of India. The O_2 deficiency in this region, associated with the seasonal (southwest monsoon) upwelling, seems to have intensified in recent years, presumably in response to enhanced nitrogen loading from land. The O_2 deficiency affects patterns of organic production and distribution of organisms including commercially important fishes, and modifies chemical fluxes through microbial reduction of polyvalent elements especially nitrogen (denitrification). While the extent of water-column denitrification over the shelf is modest (1.3-3.8 Tg N y^{-1}), a very substantial fraction of the nitrate undergoing reduction appears to end up as nitrous oxide, which accumulates to levels rarely seen elsewhere in the ocean. Relative changes in dissolved inorganic nitrogen (DIN) and dissolved inorganic phosphorus (DIP) closely conform to those predicted by the Redfield-Ketchum-Richards stoichiometry in the oxic and suboxic waters. However, a higher-than-expected buildup of DIP occurs in anoxic waters, probably due to dissolution of the iron-oxyhydroxo-phosphate complex from sediments. This DIP may support nitrogen fixation after the cessation of upwelling.

Keywords: Arabian Sea, Indian shelf, upwelling, primary production, suboxia, anoxia, nitrogen cycle, denitrification, nitrous oxide, remineralization ratios

1. INTRODUCTION

Photosynthetic production of oxygen (O_2), its exchange with the atmosphere, and turbulence caused by winds, waves and tides combine to keep seawater generally well oxygenated in all open-coastal areas except those affected by

L. N. Neretin (ed.), Past and Present Water Column Anoxia, 195–224.

an anthropogenically-enhanced nutrient supply from land or where upwelling brings up subsurface waters of low O_2 content that is further reduced through degradation of copious, locally-produced organic matter. In both cases, a high organic loading is the primary cause of O_2 depletion. This is often associated with strong near-surface stratification, which inhibits vertical mixing and associated aeration of subsurface waters. There are several examples of the first type of O_2 deficient environment, popularly known as 'dead zones' because of exclusion of many organisms including commercially important fishes. The largest and the best investigated 'dead zone' along an open-ocean coast develops every summer in the inner Gulf of Mexico as a consequence of fertilizer runoff by the Mississippi [43]. Coastal O_2 depleted environments of the second category are primarily of natural origin, found along the eastern boundaries of the Pacific and the Atlantic Oceans and along the northern boundary of the Indian Ocean [25, 28]. The total areas of the continental margin containing waters with $O_2 < 0.5$ mL L^{-1} (22 μM) and < 0.2 mL L^{-1} (9 μM) are estimated to be 1.15 x 10^6 and 0.76 x 10^6 km^2, respectively. The majority of these areas (59 and 63%, respectively) are found in the Indian Ocean north of the equator [25]. This is because the North Indian Ocean is semi-enclosed, bounded by land at low latitudes. As a consequence, an overall high biological production combines with a slow re-oxygenation at depth to produce some of the most intense O_2 depletion observed anywhere in the open ocean [35, 54, 57] within a depth range that includes a large portion of the continental margin.

Pelagic O_2 deficiency strongly influences biodiversity, ecosystem functioning and biogeochemical transformations. One of the most important biogeochemical consequences is the activation of alternate (anaerobic) pathways of respiration, mainly denitrification and sulphate (SO_4^{2-}) reduction. The former involves the reduction of oxidized nitrogen [mainly nitrate (NO_3^-)] to molecular nitrogen (N_2) when O_2 concentration falls close to zero, and the latter leads to the production of hydrogen sulphide (H_2S) when the water is completely stripped of both O_2 and NO_3^- [46]. Oxygen depletion in the North Indian Ocean is severe enough to allow these processes to occur in the water column.

The countries bordering the North Indian Ocean account for approximately a quarter of the world's human population, a great majority of which (about 1.4 billion people) lives in the three major South Asian countries – India, Pakistan and Bangladesh. The requirements of food and energy for such a large population are obviously enormous. For example, in order to sustain agricultural production, the South Asian countries consumed in 2002-2003 about 14 million tonnes of nitrogen (N) as synthetic fertilizer (out of the global consumption of about 85 million tonnes); this represents a roughly 46-fold increase over the amount used in 1960-61 [27]. Similarly, oil consumption, which accounts for roughly a third of all commercial energy sources in the

region, was about 2.7 billion barrels per day in 2002. Given the trend over the past decade (the energy consumption rose by 64% from 1992 to 2002 [20], reflecting rapid economic growth), it is expected that fuel consumption will continue to increase steeply in the foreseeable future. Moreover, the ongoing industrialization and urbanization are greatly influencing patterns of land use. Because of these demographic and economic factors, the disproportionately large continental-margin O_2 deficiency that exists in the North Indian Ocean acquires an even greater significance and underscores the vulnerability of the coastal O_2 deficient environment to human activities with potentially important global implications.

In this chapter we describe the factors responsible for the occurrence of suboxic/anoxic[1] conditions, their evolution over the annual cycle, and impact on the biology and chemistry along a segment of the continental margin – off the west coast of India – that not only experiences the most extreme conditions, but has also been the best studied.

2. HYDROGRAPHY AND CIRCULATION

Surface currents along the west coast of India, as in other parts of the North Indian Ocean, reverse every six months. During the summer or the southwest monsoon (SWM; June-September), the West India Coastal Current (WICC) flows toward the equator (Fig. 1b), carrying at its peak about 0.5 Sv (1 Sv = 10^6 m^3 s^{-1}) of water in the north and 4 Sv in the south [52]. As in other eastern boundary environments, the equatorward surface flow is accompanied by upwelling, which begins in the south (off the southwest coast of India and the west coast of Sri Lanka) sometime in May. The presence of a cyclonic eddy, the Lakshadweep Low (LL), located close to the islands it has been named after, also contributes to low sea surface temperatures and shallow thermocline extending beyond the continental shelf in this region [52]. Upwelling gradually propagates toward the north, persisting until November-early December along the northwest coast (e.g. off Mumbai), well after the collapse of the SWM winds [4]. Thus, the local winds alone do not seem to account for upwelling along the Indian west coast, and it is believed that the process is, to a large extent, remotely forced [32].

Hydrography of coastal waters is also profoundly influenced by the SWM rainfall. The heaviest precipitation (> 3000 mm y^{-1}) occurs along the central west coast (around 13-14^{o}N latitude) decreasing northward to < 1000 mm y^{-1} along the Gujarat coast (north of Mumbai), and more gently toward the south (e.g. ~2500 mm at Trivandrum). The large freshwater inputs to coastal region

[1] In order to classify the degree of O_2-deficiency operationally, we use the following criteria:
hypoxic – $0.1 < O_2$ (Winkler) ≤ 0.5 mL L^{-1}, $NO_2^- = 0$ μM, $NO_3^- > 0$ μM;
suboxic (denitrifying) – $O_2 \leq 0.1$ mL L^{-1}, NO_2^-, $NO_3^- > 0$ μM;
anoxic (sulphate reducing) – $O_2 = 0$ mL L^{-1}, NO_2^-, $NO_3^- = 0$ μM, $H_2S > 0$ μM.

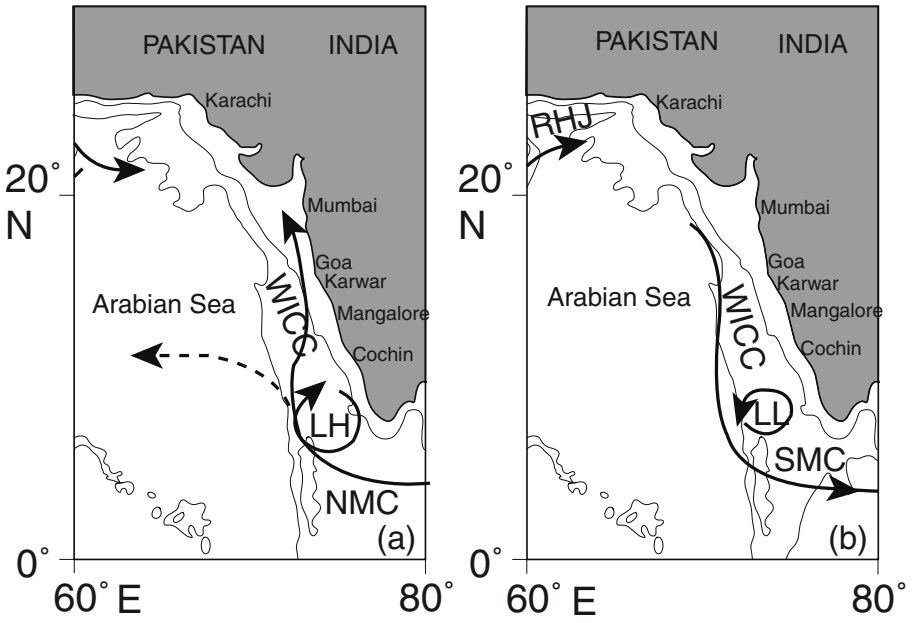

Figure 1. Major features of surface circulation in the eastern Arabian Sea during (a) Northeast Monsoon, and (b) Southwest Monsoon (RHJ - Ras-al-Hadd Jet; WICC – West India Coastal Current; LH – Lakshadweep High; LL – Lakshadweep Low; NMC – Northeast Monsoon Current; SMC – Southwest Monsoon Current) (modified from [48]).

create a lighter (warmer and fresher) water mass that floats over the cold, saline upwelled water, generally preventing the latter from surfacing [4, 38].

Despite lighter winds during the winter or northeast monsoon (NEM, December-March) it is, paradoxically, during this season that coastal circulation off India is the best organized (Fig. 1a). The LL is replaced by the Lakshadweep High (LH), an anticyclonic eddy. The now poleward-flowing WICC is not only better developed and stronger (transporting approximately 10 Sv of water off the southwest coast of India), it also flows against the wind [51], underscoring the importance of remote forcing [32]. This flow greatly influences biogeochemistry because it induces downwelling over the Indian shelf and brings waters from low latitudes, which are nutrient-impoverished. Moreover, its low density does not permit the development of the convective mixing regime (with elevated nutrient levels) that occurs elsewhere in the Arabian Sea at comparable latitudes (e.g. as far south as off Somalia [55]).

The effects of seasonal changes in circulation on the hydrographic structure and biogeochemical cycling extend beyond the continental margin [41]. During the SWM, when the surface flow is directed toward the equator, the subsurface current moves in the opposite direction [3,52]. The West India Undercurrent

(WIUC) may be identified from the distribution of temperature [upward sloping of isotherms at the top of this feature and downward tilt close to its bottom just off the continental shelf (Fig. 2a)], and even more clearly from those of salinity (Fig. 2b) and O_2 (Fig. 2c). Note that the water derived from the south has lower salinity and slightly higher O_2 content. As judged by the 35.400 salinity contour, the influence of the WIUC, at its peak, extends vertically down to approximately 400 m depth and horizontally up to 200 km from the continental slope at 15^oN latitude (Goa transect, Fig. 2b). The WIUC plays an important role in determining the redox status of subsurface waters off the western Indian continental margin where its relatively higher O_2 content inhibits denitrification, probably as far north as 17^oN latitude, as reflected by the distribution of nitrite (NO_2^-, Fig. 2d). This is why the seasonal suboxic zone over the Indian shelf is not contiguous with the perennial suboxic system found offshore [36].

3. EVOLUTION OF O_2 DEFICIENCY

Subsurface waters over the entire North Indian Ocean are characterized by very high nutrient contents (e.g. NO_3^- concentrations exceeding 20 μM are often found at depths shallower than 100 m [58]). Large quantities of nutrients from this layer can be brought up easily to the euphotic zone by upwelling and vertical mixing, resulting in high rates of phytoplankton production (PP). Over the Indian continental shelf, except off Gujarat in the north, such fertilization of the euphotic zone only occurs during periods of upwelling because, as already pointed out, the winter circulation is associated with downwelling and the absence of convective overturning. This imparts pronounced seasonality to PP (Table 1). The slow rate of upwelling in this region not only allows an efficient utilization of upwelled nutrients locally, but it also results in greater consumption of O_2 in the upwelled water that has low O_2 content to begin with (at the shelf break; Fig. 2). The presence of a low-salinity lens during the periods of upwelling further contributes to subsurface O_2 depletion.

Table 1. Primary Production (PP) over the Western Continental Shelf of India during the Southwest and Northeast Monsoons.

Period	*PP (g C m^{-2} d^{-1})*		*Number of*
	Range	*Mean ± Std Dev*	*Observations*
July 1998	0.18-3.96	1.29±1.51	5
August 1998	0.87-7.29	3.39±2.16	8
December 1999	0.29-0.56	0.35±0.14	3

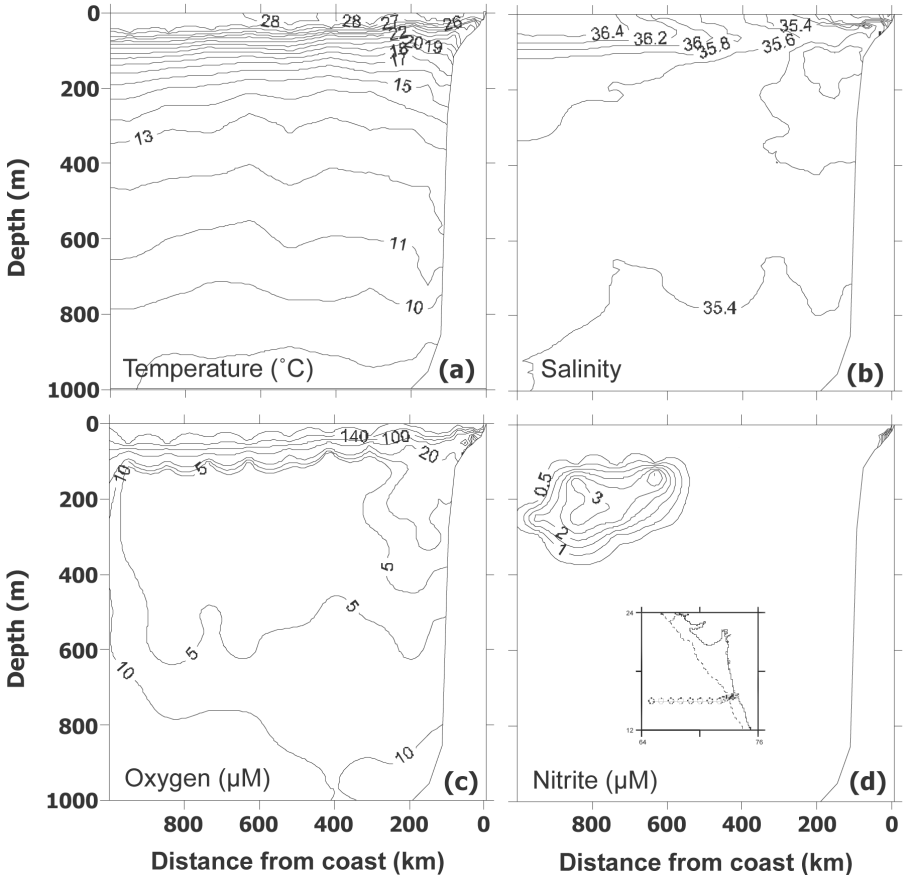

Figure 2. Variations in (a) temperature, (b) salinity, (c) O_2, and (d) NO_2^- in the upper 1 km of the water column along the Goa transect (location shown in the inset) during 1-6 December, 1998.

We present here data covering the annual cycle, collected at a quasi time-series station located over the inner shelf off Goa, and property distributions across the same segment of the shelf during the two monsoons. The time-series station, designated as the Candolim Time Series (CATS), has been sampled by us since 1997. With a water depth of around 28 m, the CATS site (15^{o}31'N, 73^{o}39'E) lies approximately 10 km off the coast (the village of Candolim). Due to logistic reasons (mainly the non-availability of a suitable vessel during the turbulent monsoon season), the sampling has not been as regular as needed for an optimal time series. However, during the crucial late SWM – early fall intermonsoon (FI) period (August-November) the station has been visited at least once a month between 1997 and 2004. The data have been pooled and averaged for various depth intervals on a fortnightly basis for August-December

and on a monthly basis for the remaining period. When plotted against time, these data reveal well-defined annual cycles of the measured variables, reflecting the seasonality of hydrographic and biogeochemical processes, including the evolution of O_2 deficiency (Fig. 3).

The temperature record (Fig. 3a) confirms the bimodal distribution pattern previously reported from the region [3, 53]. The highest values occur during the spring intermonsoon (SI; April-May) and late FI seasons; a minor minimum occurs during the NEM, but the main minimum is found during the SWM extending into the early FI. This is an apparent consequence of upwelling which, at its peak in September, lowers the near-bottom temperature below 21^oC.

The water column is vertically homogeneous during the NEM, but the salinity changes considerably (Fig. 3b). As stated earlier, the WICC brings fresher waters from the south, and this is reflected by lower salinities, particularly in February. The highest salinity values ($\geq$ 36.000) are recorded during the following SI season before the monsoon rainfall produces a low-salinity lens that persists from June/July to October/November (Fig. 3b).

The duration of O_2 deficient conditions is somewhat longer than would be expected from the temperature record (Fig. 3c) due to the occasional occurrence of near-bottom O_2 depletion during the SI. We speculate that this might be caused by the decay of *Trichodesmium* blooms. The lowest O_2 concentrations ($<$ 10 μM) are, however, confined only to the period of upwelling (July-November).

The decreases in O_2 in subsurface waters are mirrored by increases in NO_3^- (Fig. 3d). However, the NO_3^- concentration begins to fall as denitrification sets in by July/August, and in about one month all NO_3^- is used up by this process.

Traces of NO_2^- occur in subsurface waters even when the environment is not reducing (Fig. 3e), possibly produced through the assimilatory reduction of NO_3^- by phytoplankton, nitrification or denitrification in sediments. When the environment becomes denitrifying, NO_2^- accumulates in much higher concentrations with the peak values (averaging in excess of 6 μM) occurring slightly above the seafloor during August-September, and declining rapidly thereafter as subsurface waters become completely anoxic.

Low N_2O concentrations prevail throughout the water column during the NEM and SI seasons. However, a dramatic increase in N_2O concentration is noticed once the system becomes O_2 deficient (Fig. 3f). The highest concentrations (averaging in excess of 180 nM), observed after the subsurface waters turn reducing, are coincident with the highest NO_2^-. Toward the end of the suboxic period, and coinciding with the onset of SO_4^{2-} reduction, N_2O concentration declines sharply, but increases again to moderately high levels in November.

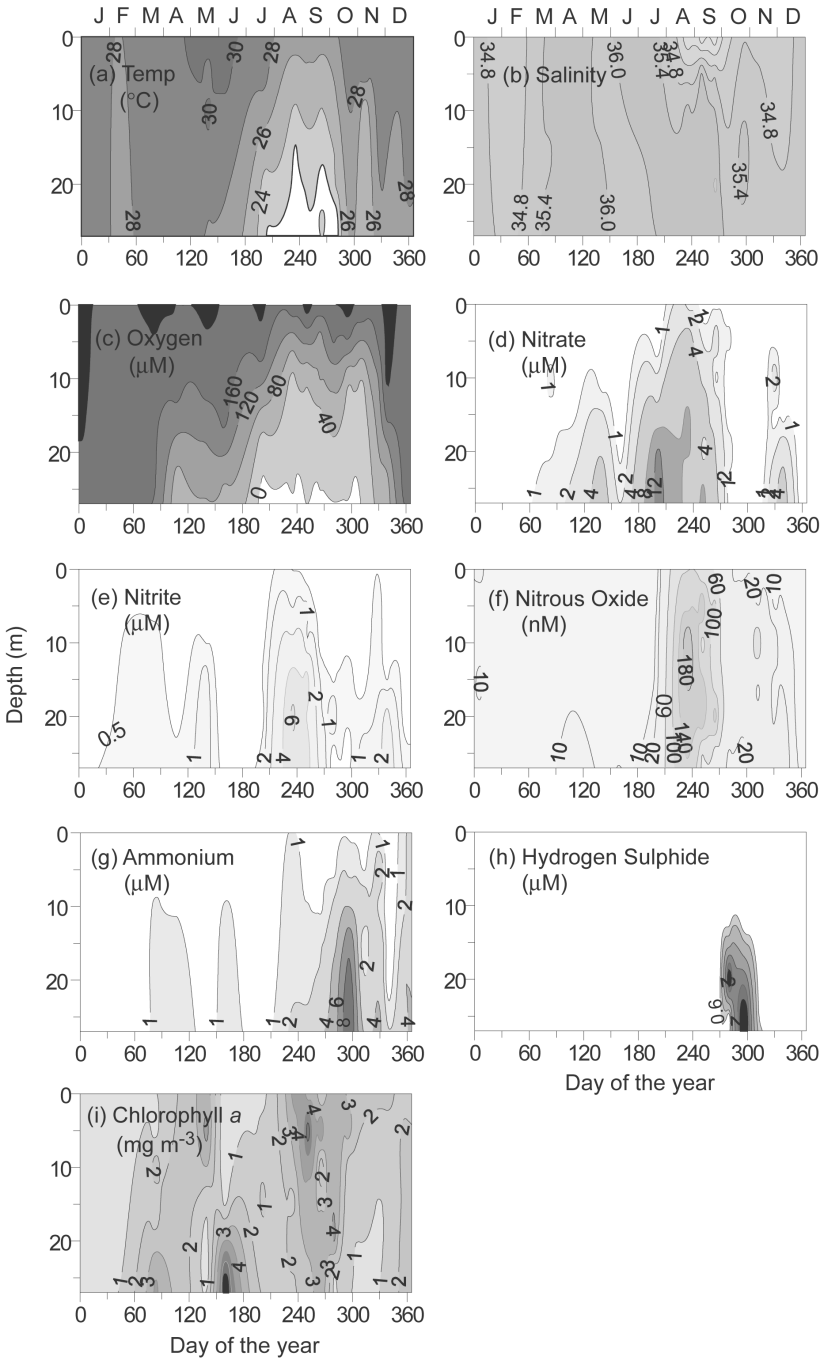

Figure 3. Monthly-/fortnightly-averaged records showing annual cycle of (a) temperature, (b) salinity, (c) O_2, (d-g) inorganic nitrogen species, (h) hydrogen sulphide, and (i) chlorophyll *a* at the Candolim Time Series (CATS) site (15^{o}31'N, 73^{o}39'E) based on observations from 1997 to 2004.

The disappearance of the oxidized nitrogen species (NO_3^-, NO_2^- and N_2O) coincides with the accumulation of both NH_4^+ and H_2S (Fig. 3g, h). Anoxic events are generally restricted to September and October, occasionally extending to November.

Distribution of chlorophyll *a* is relatively more patchy, in part because of fewer and less regular observations (Fig. 3i). The lowest values, particularly close to the surface, are recorded during the late NEM and late SI-early SWM periods. The low phytoplankton biomass during the early SWM is contrary to expectation and seems to reflect light limitation of PP due to high turbidity and cloud cover. Peak chlorophyll *a* concentrations are expectedly associated with the late SWM-early FI seasons.

The pattern of changes described above is also seen in cross-shelf sections of properties during the period of peak O_2 deficiency as exemplified by observations off Goa in September 1999 (Fig. 4a) and September 2002 (Fig. 4b). Upwelling is clearly indicated by the upsloping of isotherms on both occasions, with the strong near-surface temperature and salinity gradients caused by the above-mentioned low-salinity lens that caps the cold, saline upwelled water, especially near the coast. Around the shelf break, near-bottom water has low O_2, but it is still oxidizing (inferred from the high NO_3^- and undetectable NO_2^- concentrations; Fig. 4a). But as this water ascends over the shelf and loses the residual O_2, denitrification occurs first over the mid-shelf (as evidenced by the build-up of NO_2^- and depletion of NO_3^-) and SO_4^{2-} reduction follows over the inner-shelf (indicated by the accumulation of H_2S and NH_4^+). Along both sections, intense N_2O accumulation occurred at mid-depths, with the near-bottom waters characterized by its depletion, especially in September 2002 when the anoxic conditions were more severe.

Property distributions in the same region during January 1998 (Fig. 5a) and February 2002 (Fig. 5b), representing the NEM, show the absence of upwelling and the associated features described above. The water column was well oxygenated and generally nutrient-depleted.

The sections presented above are typical of the region north of at least 12^oN. Although upwelling-driven O_2 depletion in the water column also occurs south of this latitude, it does not always culminate in denitrification and SO_4^{2-} reduction. Nevertheless, as discussed in a following section, near-bottom O_2 concentrations have been known to fall below 0.25 mL L^{-1} as far south as off Cochin ($\sim 10^oN$), and on one occasion (in August 1998) denitrification did occur over the inner shelf in this region in conjunction with a bloom of the dinoflagellate *Noctiluca* [37]. Likewise, in September 2004 an incidence of fish mortality accompanied by stench emanating from the sea that caused sickness in children led to a public health alarm around Trivandum (Lat. 8.5^oN). This was probably due to a holococcolithophore bloom followed by O_2 depletion in coastal waters [44]. The inter-annual changes, implied by these observations,

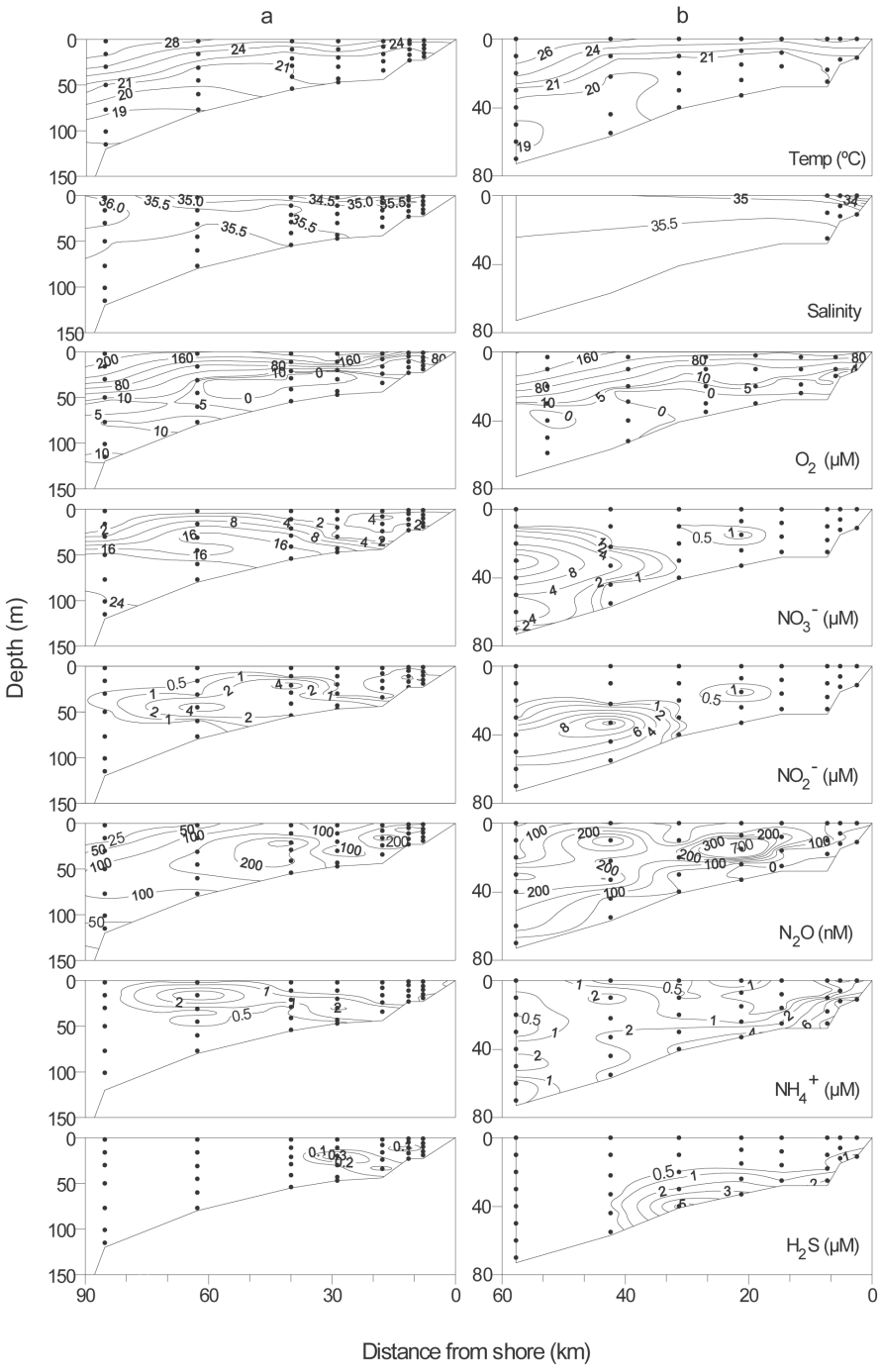

Figure 4. Vertical sections of temperature, salinity, O_2, inorganic nitrogen species and hydrogen sulphide off Goa (parts of the same transect as in Fig. 2) on (a) 22/9/1999, and (b) 18-20/9/2002.

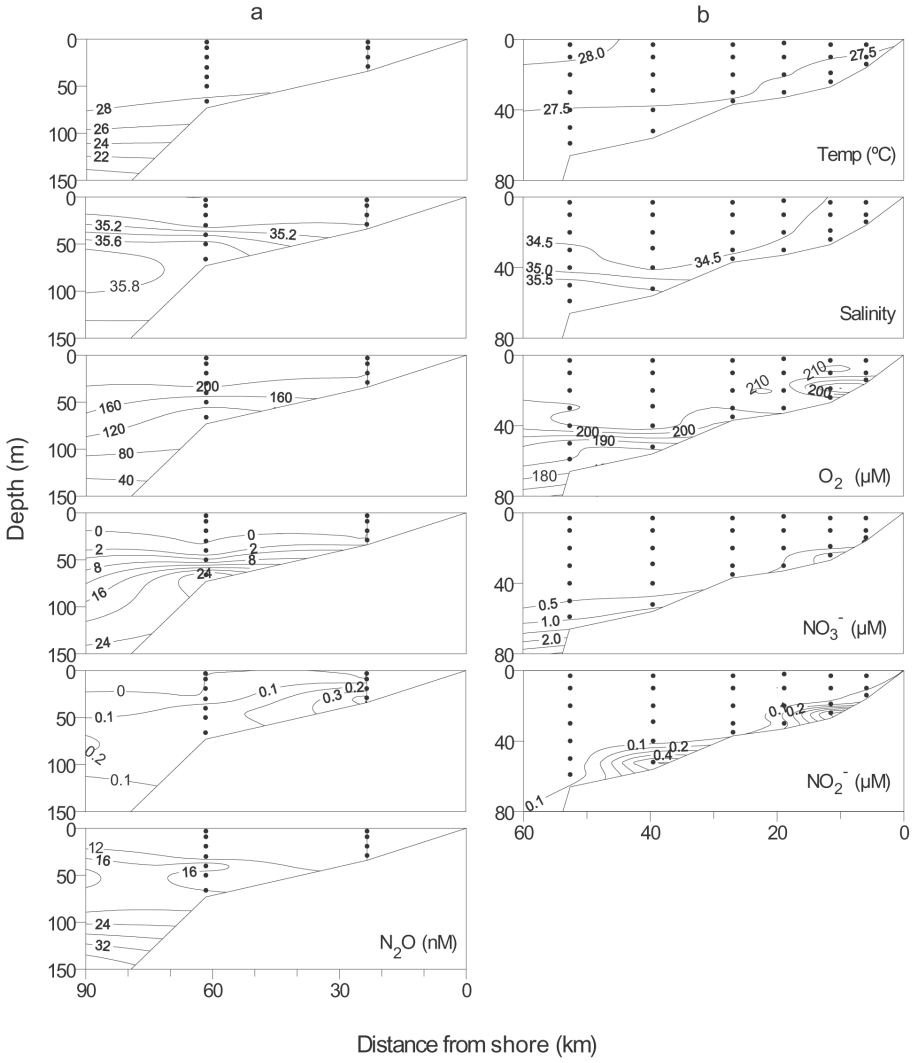

Figure 5. Vertical sections of temperature, salinity, O_2 and inorganic nitrogen species off Goa (parts of the same transect as in Fig. 2) on (a) 6-7/1/1998, and (b) 16/2/2002. H_2S was absent whereas NH_4^+ was generally below 0.5 μM on both occasions (data not presented). For technical reasons analysis for N_2O could not be performed on 16/2/2002.

are clearly demonstrated by numerous repeat sections [33], including those presented here. These changes must be related, albeit in a complex way, to the inter-annual changes in the strength of the SWM, which affects both the demand and supply of O_2 in subsurface waters. The severity of O_2-deficiency during and just after the SWM is probably determined by variations in productivity (through fertilization of the euphotic zone) and stratification (through freshening of the surface layer) in a given year.

4. RECENT INTENSIFICATION OF O_2 DEFICIENCY

Superimposed on the inter-annual variability one can detect a longer-term change when recent measurements are compared with previous observations that go back to the 1950s [3, 4, 8]. The time-series measurements made by Banse [3] off Cochin are worthy of special mention although extended observations were also made in shallow waters off Mumbai (Bombay) by Gogate [22] and off Calicut by Subrahmanyan [53]. Banse sampled two stations over the shelf having water depths of 25 and 55-60 m from August 1958 to January 1960, and another deeper station over the continental slope (depth ~2000 m) from November 1958 to May 1959. Combining these measurements with all other data then available, he provided a comprehensive description, on a seasonal basis, of hydrography along various segments of the west coast of the Indian subcontinent [3-5]. The time series records of temperature, salinity and O_2 at the mid-shelf station off Cochin [4] are very similar to the corresponding records off Goa presented here. For example, the lowest temperature (~21^{o}C) and the lowest bottom-water O_2 occur during September-October in both records. It is apparent from Banse's data that even in 1958-59 bottom-water O_2 sometimes fell below 10% of the saturation value off Cochin. Nitrite was occasionally present in concentrations up to 4 μM [3]. It is not clear if its production occurred through dissimilatory NO_3^- reduction in the water column, but if this process did take place it would have been on a limited scale. H_2S was never present in concentrations high enough to be noticed by its odor [Karl Banse, personal communication].

A more extensive set of hydrocast data for salinity, temperature and O_2 along numerous cross-shelf sections off the Indian west coast, was generated under the UNDP/FAO sponsored Integrated Fisheries Project (IFP) during 1971-1975. The sections were repeated in different seasons. This data set serves as an excellent reference for evaluating the extent of shift in O_2 distribution over the western Indian shelf. We utilize here data only along the section off Karwar (extending offshore from 14^{o}49'N, 74^{o}03'E) and at stations shallower than 60 m that were occupied between August and October. These data are compared with our own measurements made in the same region and during the same season (August-September) between 1997 and 2004 (Fig. 6, Table 2). As

expected, the O_2 data show considerable scatter. However, the range of values is much wider for the deeper layer (temperature < 24^{o}C) in case of the 1971-75 data set with the recent data clustering toward lower values (Fig. 6). In all cases the means and medians of subsurface O_2 concentrations are significantly lower for 1997-2004 than for 1971-1975 (Table 2). Moreover, on no occasion were the measured O_2 concentrations actually zero during the IFP cruises in contrast with numerous such values recorded in the recent data set (which are invariably associated with the presence of H_2S in concentrations reaching up to ~13 μM). This implies that even though H_2S was not measured on the IFP cruises, it was probably not present.

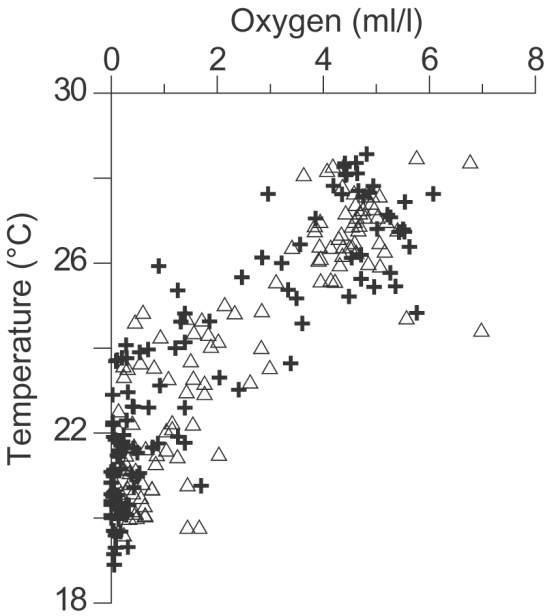

Figure 6. Comparison of O_2 concentrations with reference to temperatures over the inner- and mid-shelf regions (depths < 60 m) off Karwar, central west coast of India, during the upwelling period in 1971-75 (triangles) and 1997-2004 (crosses). Mean and median concentrations for various temperature ranges are given in Table 2.

Routine measurements of NO_3^- and NO_2^- were not made under the IFP, but the nutrient data subsequently collected on cruises conducted by the National Institute of Oceanography (NIO) [38, supplementary information], indicate that the subsurface environment was denitrifying, but not SO_4^{2-} reducing, at least until the 1980s. These observations lead us to conclude that the subsurface O_2 deficiency over the Indian shelf has intensified significantly since the 1970s, and that SO_4^{2-} reduction in the region, not recorded previously, is a manifestation of this change. The cause of this regime shift cannot be pinpointed with absolute

Table 2. Comparison of the mean and median O_2 concentrations (Winkler values in mL L^{-1} uncorrected for reagent blanks) for various temperature ranges off Karwar, central west coast of India, during 1971-75 and 1997-2004. Data from stations shallower than 60 m and for the upwelling period (August-October) only have been utilized (see also Fig. 6).

	1971-1975			1997-2004		
*Temp Range**	*Mean*	*Median*	*n*	*Mean*	*Median*	*n*
28-29	4.88	4.18	5	4.49	4.52	8
27-28	4.75	4.77	14	5.15	4.86	11
26-27	4.43	4.50	25	4.75	5.02	9
25-26	3.85	4.14	7	3.59	3.50	11
24-25	2.35	1.85	14	2.23	1.39	7
23-24	1.24	1.08	11	1.04	0.62	12
22-23	0.97	1.15	9	0.40	0.31	9
21.5-22	1.00	0.86	5	0.43	0.22	16
21-21.5	0.44	0.28	9	0.17	0.12	9
20.5-21	0.55	0.41	9	0.29	0.05	10
20-20.5	0.48	0.48	9	0.15	0.16	13
19-20	1.11	1.44	3	0.11	0.08	11

*inclusive of the upper limit

certainty. The two obvious possibilities involve modifications of ventilation and organic production, which in view of the precarious biogeochemical balance already existing in the region could be quite subtle.

Changes in physical forcing have been invoked to explain the recent development of hypoxia in the upwelling system off Oregon, on the west coast of the United States [24]. However, a preliminary analysis indicates that a temperature shift of comparable magnitude has not occurred over the Indian shelf. As a more reasonable and persuasive alternative, increased supply of nutrients from land has been suggested to have enhanced PP in the region, as in many other coastal areas [38]. Indeed, the fertilizer consumption in the region has undergone a 7-fold increase since the early 1970s, and this is expected to have affected river runoff. Based on the fertilizer consumption figure for 1990, Seitzinger et al. [49] estimated that the riverine flux of dissolved inorganic nitrogen (DIN) to the sea from South Asia could be as much as 4.2 Tg N y^{-1} (1 Tg = 10^{12} g). However, the measured concentrations of DIN in the Indian rivers near their mouths are not very high (<20 μM), and consequently terrestrial DIN inputs to the Arabian Sea via runoff probably do not exceed 0.1 Tg N y^{-1} [39]. The deposition of DIN (NO_3^-+NH_3/NH_4^+) from the atmosphere has been estimated to be an order of magnitude larger (1.6 Tg N y^{-1} [2]), although such deposition occurs over a larger area. If we assume that the Indian shelf receives 10% of the estimated atmospheric deposition over the Arabian Sea, the total anthropogenic nitrogen loading in the region would exceed 0.2 Tg N y^{-1}. This amount has

the potential to trigger a shift from natural suboxic to anthropogenic anoxic conditions. This is because the stoichiometries of primary production (C:N = 6.6) and denitrification (C:N = 1.1) are such that new inputs of DIN into suboxic waters get amplified by a factor of up to 6 [11]. That is, for each unit of DIN added to the surface waters up to 6 units of NO_3^- may be removed at depth if the additional organic matter produced is oxidized by NO_3^-. The potential increase in denitrification rate (>1 Tg N y^{-1}) is of the same order as the rate of denitrification over the shelf (see below).

5. IMPACT OF O_2 DEFICIENCY

5.1 Biological Impact

Phytoplankton Production . While elevated PP is a key factor responsible for the formation and sustenance of subsurface O_2 deficiency, the latter may, in turn, affect the quality and quantity of PP in several ways. One of them is by regulating the availability of both the macro and micro nutrients [especially DIN and iron (Fe)]. While NO_3^- is lost through denitrification, Fe is mobilized from the suspended matter and sediments. The loss of NO_3^- would lead to an initial decrease in PP. However, once the system turns anoxic nitrogen regenerated from organic matter would accumulate as NH_4^+ (the highest NH_4^+ concentration measured over the Indian shelf is about 21 μM), and its diffusion may sustain moderate PP in the thin oxygenated layer overlying the anoxic water. Within the O_2 deficient layer, which has sufficient nitrogenous nutrients and generally extends to the euphotic zone, the ambient O_2 concentrations may be too low for the "normal" phytoplankton to meet their metabolic requirements, thereby inhibiting PP (although some carbon fixation may still be carried out by anoxygenic photosynthetic organisms [45] about which nothing is known from this region so far). Results of our observations at two stations off Mangalore, presented in Figs. 7 and 8, provide rare evidence for such an effect.

One of the stations (M1A) was located over the inner shelf (Lat. 13^{o}08'N, Long. 74^{o}38'E; water depth 27 m; date of sampling 19/09/2001) and the other (M8) was positioned close to the shelf edge (Lat. 12^{o}54'N, Long. 74^{o}11'E; water depth 83 m; date of sampling 20/09/2001). At both locations, upwelled water reached depths $\leq$ 10 m, but redox conditions in subsurface waters were quite different. At M1A, denitrification had resulted in complete removal of NO_3^-, while H_2S and NH_4^+ accumulated at depths $\geq$ 10 m (Fig. 7). Station M8 was on the verge of being suboxic, with O_2 levels at depths $\geq$ 20 m being less than 30 μM and NO_3^- concentrations exceeding 20 μM (Fig. 8). In both cases, very low rates of PP, as measured by the ^{14}C technique, were recorded in the O_2 deficient waters (at depths > 10 m at the shallow station and > 20 m at the deeper one), in contrast with high values in the surface layer. Typically, PP peaked

a few meters below the surface (near the top of the shallow pycnocline); this phenomenon was more pronounced at M8 that had a thicker surface mixed layer. The other notable difference between the two stations was that the chlorophyll *a* concentration declined rapidly below the oxycline at M8 but not at M1A. This could be attributed to the preservation of chlorophyll in anoxic waters. In spite of the prevalence of anoxic conditions at very shallow depths, column-integrated primary production at M1A (1.47 g C m^{-2} d^{-1}) was comparable with that at M8 (2.15 g C m^{-2} d^{-1}).

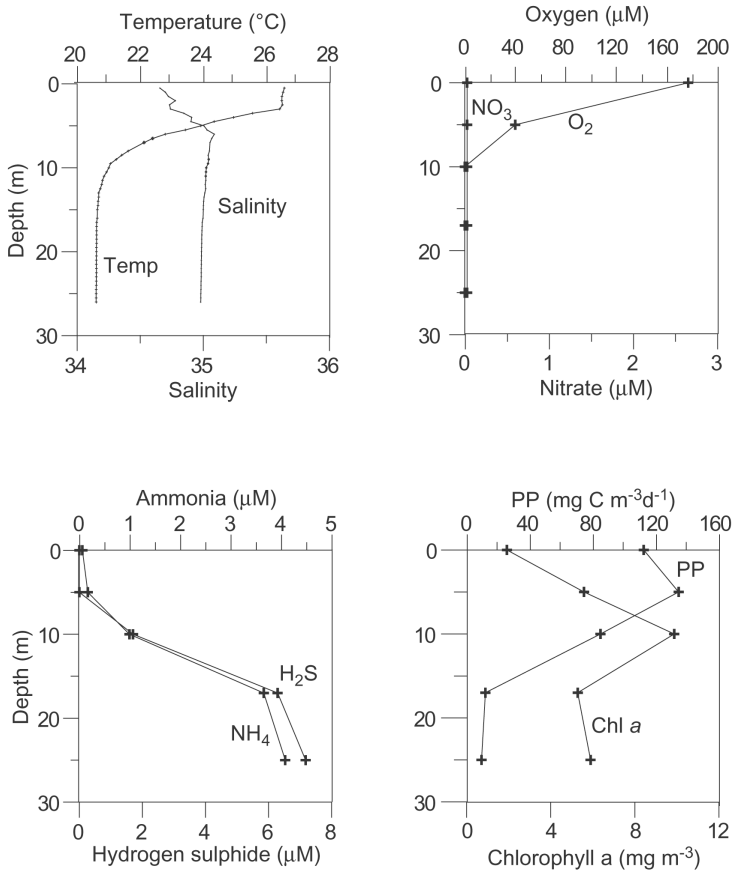

Figure 7. Vertical profiles of temperature, salinity, O_2, NO_3^-, NH_4^+, H_2S, primary productivity and chlorophyll *a* at Sta. M1A located over the inner shelf off Mangalore (13°08'N, 74°38'E; water depth 27 m; date of sampling 19/9/2001).

Since an observable suboxic layer did not exist above the anoxic bottom water, as a possible consequence of the thin oxygenated surface layer containing negligible amounts of NO_3^- and NO_2^- at Sta. M1A, PP at this station should have been fuelled entirely by NH_4^+. This represents an unusual situation since,

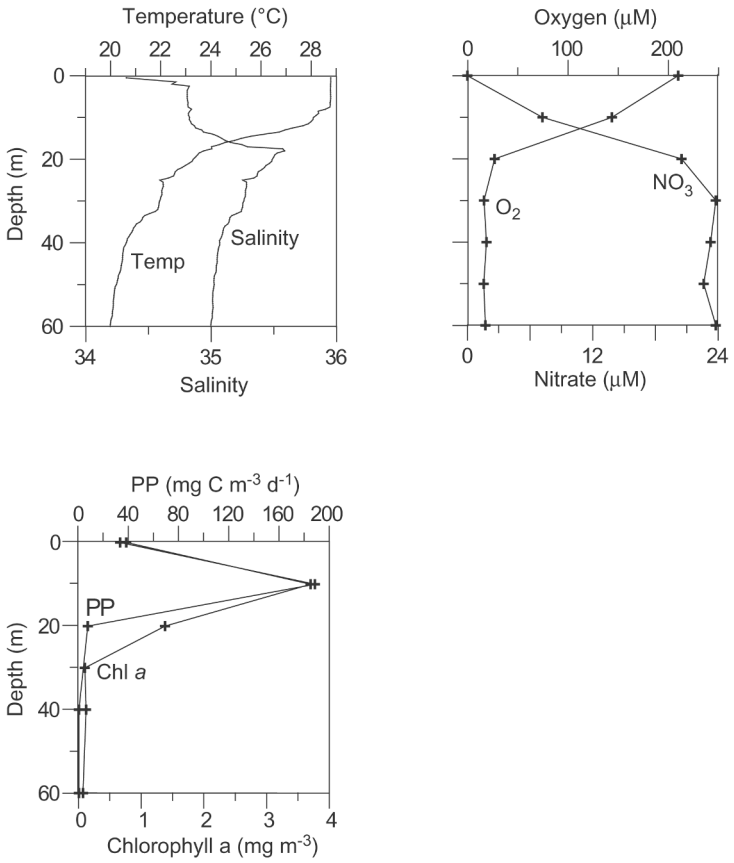

Figure 8. Vertical profiles of temperature, salinity, O_2, NO_3^-, primary productivity and chlorophyll *a* at Sta. M8 located close to the shelf edge off Mangalore (12°54'N, 74°11'E; water depth 83 m; date of sampling 20/9/2001).

with a few exceptions (e.g. off Peru [13, 14]), new production in the ocean is supported by NO_3^-. It is believed that diatoms require NO_3^- for their healthy growth and the presence of NH_4^+ in high concentrations has an inhibitory effect on NO_3^- uptake [19]. However, although the composition of phytoplankton was somewhat different, diatoms were by far the dominant micro phytoplankton group at both stations.

Zooplankton. Systematic long-term monitoring of zooplankton biomass and composition with reference to O_2 distribution has just been initiated. Previous data, such as those reproduced in Fig. 9, for a station located close to the CATS site, which was sampled over a period of 36 hours on 28-29 September

1986 [31], indicate much higher (by a factor of 5.5) zooplankton counts and biomass within the oxic mixed layer than in the O_2 depleted subsurface waters. Despite severe O_2 depletion, total zooplankton biomass (displacement volume) at this station was quite high (~12 mL m^{-3}). Copepods were the most abundant group (over 65%) and about 25% of all zooplankton were carnivores. Although almost all groups were present both above and below the pycnocline, the larger organisms tended to be concentrated in the surface layer. While the total biomass varied with the mixed layer thickness, the latter probably modulated by tidal mixing, there was little evidence for vertical diurnal migration. These observations indicate that the zooplankton avoid O_2 deficient waters.

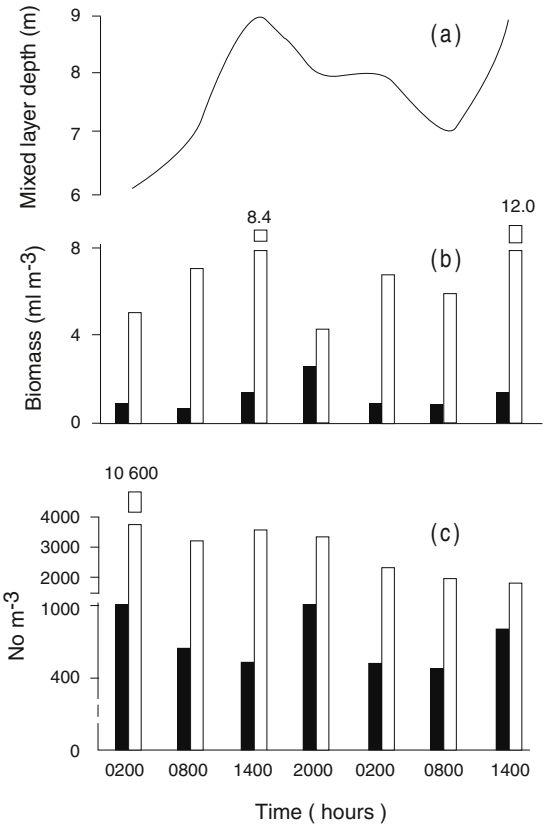

Figure 9. Variations in mesozooplankton biomass (b) and density (c) in relation to mixed layer depth (a) with time at an anchor-station off Goa (15°26'N, 73°35'E; water depth 32 m; dates of sampling 28-29/09/1986). Dark and light bars denote values below and within the mixed layer, respectively (redrawn from Madhupratap et al. [31]).

Benthos. At the time of the most intense upwelling, the entire continental shelf off India is enveloped by subsurface/bottom waters with $O_2 < 0.5$ mL L^{-1} [38], and this has long been known to have a profound impact on benthic fauna. Observations by Carruthers et al. [8] off Mumbai led them to conclude, "Scarcely any benthic animals were found in the depths where the oxygen content of the bottom water was less than 0.5 ml per litre. In shallow water, benthos consisted mainly of hermit crabs, *Jibia curba* shells and a few nereid and polychaete worms." The shift to anoxic conditions has since affected the benthic population even further as indicated by observations off Goa where surface sediments within the zone presently affected by bottom-water SO_4^{2-} reduction contain plenty of bivalve shells, but no live animals [B. Ingole, personal communication]. Sulphur bacteria such as *Thiomargarita*, *Thioploca* and *Beggiatoa* have not been reported from the coastal anoxic zone so far, perhaps due to the restriction of anoxic conditions to a season and also low free sulphide concentrations in interstitial waters. *Thioploca* mats have, however, been observed at greater depths along the continental slope off Pakistan [47].

Fisheries. The impact of near-bottom O_2 deficiency on fisheries has attracted much attention [3, 4, 8, 26]. The historical data, reviewed by Banse [4], could be taken to be representative of a pristine environment (i.e. before the increase in fertilizer consumption in South Asia). It is obvious that seasonal O_2 deficiency over the shelf had always affected fisheries along the west coast of India. According to Banse [4], "Off Cochin, the deoxygenation of near-bottom waters results in the regular disappearance of demersal fishes and in unprofitable trawling in a belt between the aerated water nearshore and the relatively new bottom water on the outer shelf. For the dominant fish, *Synagris japonicus*, oxygen concentrations of 0.25-0.5 ml/l seemed to be critical (Banse, 1959). . . The fact that off Bombay, as off Calicut, the oxygen content dropped to zero in near-bottom water suggests that there may possibly be a vast area on the outer shelf (and perhaps also on the middle shelf) approximately from Cochin to Karachi that is devoid of commercially important concentrations of demersal fishes during the southwest monsoon." Given the recent observations showing a decrease in the O_2 levels and an appearance of H_2S, the environment could only have become more hostile to demersal fishes (including prawns). On numerous cruises undertaken during the period August-October since 1997 we observed practically no bottom trawling activity between Cochin and Mumbai to a depth of at least 50 m and unusually intense trawling over the outer shelf. The zone of 'aerated water nearshore' referred to by Banse [4], when present, is generally no more than a few hundred meters wide as indicated by the results of our sustained observations off Goa. It usually disappears sometime in August when the O_2 deficient layer moves shoreward. This is associated with greatly enhanced fish catch, including that of the highly valued 'solar prawns'

(*Metapenaeus dobsoni*), if the fishing operations are permitted to be undertaken during the period. The demersal fishes are driven into inshore waters (estuaries and creeks), where they can be easily captured (once located, the stocks of solar prawns are usually depleted in 2-3 days time due to intense fishing).

Over the past few years there has been a substantial decrease in the demersal fish catch along the coast of India, as exemplified by the data from the state of Goa (Fig. 10). Significantly, a similar decline has not occurred in the case of the pelagic fishes, and therefore it is reasonable to conjecture that the onset of anoxic conditions (appearance of H_2S) might be the main cause of the declining demersal fish catch. Besides the adverse impact on fisheries, the O_2 deficiency has been known to result in fish-kills when the fishes are unable to escape from anoxic upwelled waters. Several instances of large scale fish-kills in the region, apparently caused by asphyxiation, have been recorded in the literature, with increasing recurrence in the last few years [37, 44].

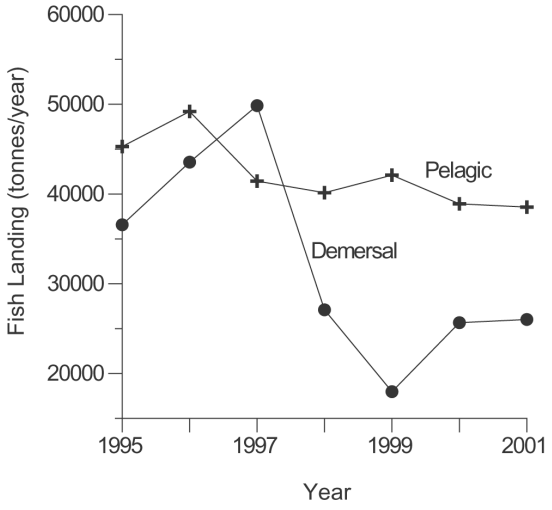

Figure 10. Annual pelagic and demersal fish landings in the state of Goa from 1995 to 2001 (courtesy Dr. Z.A. Ansari).

5.2 Geochemical Impact

Water-column Denitrification. Direct measurements of denitrification rate in the Arabian Sea through incubations of water samples spiked with $^{15}NO_3^-$ yielded higher values (21.6±46.8 pM d^{-1}) for the coastal suboxic zone than for the open-ocean one (8.8±3.8 pM d^{-1}), apparently reflecting greater organic carbon availability and higher temperatures over the shelf [17]. However, the measured rates for the coastal zone are lower than expected from the nutrient

data. Repeat observations at several sites over the inner shelf off the central west coast of India suggested an average NO_3^- consumption rate of 0.83 μM d^{-1} and applying this rate to an estimated volume of 1.2-3.6 x 10^{12} m^3 and a denitrification period of 3 months, the overall rate comes to 1.3-3.8 Tg N y^{-1} [33]. This is 4-12% of the denitrification rate estimated for the perennial suboxic zone of the open Arabian Sea. It may be pointed out that the rate of N_2 production may substantially exceed that of NO_3^- consumption because of the involvement of anaerobic ammonium oxidation (ANAMMOX) which under certain conditions (as observed over the continental shelf off Namibia) can be the dominant pathway of N_2 production [29]. Although such conditions (i.e. suboxia with high availability of NH_4^+ and NO_2^-) also exist in the coastal Arabian Sea, the quantitative significance of ANAMMOX in the region still remains to be evaluated.

Through the removal of fixed nitrogen from the water column, denitrification - both in water column and sediments (see below) - counters anthropogenic nitrogen loading. In fact, as pointed out above, due to the much lower ratio of carbon oxidation to NO_3^- reduction than the Redfield C:N value, denitrification has the potential to remove more nitrogen than the external inputs. This negative feedback probably constrains PP in the eutrophied environments (as long as they are not SO_4^{2-} reducing). However, while the loss of excessive nitrogen is undoubtedly good for the environment, the problem, as discussed below, is that a significant portion of the denitrified nitrogen might end up as N_2O, a potent greenhouse gas.

Sedimentary Respiration. As with the water column, seasonal cycles of PP and degree of oxygenation must also influence benthic respiration. As the period of maximal production is also one with the least oxygenation in bottom waters, one may expect a cycle wherein, on balance, organic matter accumulates in sediments during the upwelling period and is degraded during the rest of the year. Inorganic nutrients thus regenerated should then be expected to support PP during the non-upwelling periods, thereby dampening the seasonality in production to some extent. This aspect of benthic-pelagic coupling including variability of benthic respiration rates is yet to be studied in detail. Limited measurements of sedimentary denitrification, made mostly during the upwelling period following the acetylene block technique, have yielded values ranging from 0.27 to 1.45 pmol NO_3^- cm^{-2} s^{-1}, which are generally within the range of values from other areas [33, 34]. Scaling these rates to the area of the Indian shelf provides an estimate of the annual nitrogen loss ranging between 0.21 and 1.15 Tg, which implies that sedimentary denitrification is an important but not the dominant sink for fixed nitrogen in the region.

Nitrous Oxide Cycling and Fluxes. Perhaps the most important aspect of nitrogen cycling in the eastern Arabian Sea is the unprecedented accumulation of N_2O frequently observed during the late SWM - early FI period over the inner- and mid- shelf regions north of 12°N. The highest concentration (765 nM) recorded in the region is about four times the highest values reported from the eastern tropical South Pacific [9, 12]. As noted previously (in Section 3), the greatest accumulation of N_2O occurs in denitrifying waters associated with the buildup of NO_2^- the concentration of which can reach up to 16 μM. This is in sharp contrast to N_2O distribution in the perennial suboxic zone of the open ocean where N_2O profiles invariably exhibit a minimum associated with the NO_2^- maximum [16, 40]. However, the denitrifying waters sometimes contain N_2O in very low concentration as well, presumably due to its reduction to N_2 (Fig. 4). These observations strongly point to transient production of N_2O from NO_3^- through a reductive pathway.

For denitrification to be a net producer of N_2O, it is imperative that the activity of N_2O reductase be suppressed. There are two characteristics of this enzyme that might allow this to happen. First, N_2O reductase contains copper, and the non-availability of this element in a suitable form or quantity could lead to the denitrification sequence being terminated at N_2O. Such an effect has been demonstrated by culture experiments carried out under trace-metal clean conditions [23]. However, it is hard to conceive copper limitation in a shallow coastal environment even though the possibility of the metal being non-bioavailable due to speciation cannot be completely ruled out. Secondly, N_2O reductase is not readily available with denitrifiers and is synthesized as and when needed [21]. This enzyme also appears to be more sensitive to O_2 than the other denitrification enzymes [6]. Experimental evidence for the sensitivity of N_2O production to O_2 levels in a natural environment has been provided by Castro González and Farías [9]. It has been speculated that frequent incursions of O_2 into suboxic waters might deactivate N_2O reductase and its recovery would take some time after the reestablishment of suboxic conditions. This would allow N_2O build up in the water column. This hypothesis appears to be supported by results of incubation experiments [38].

Even when a net consumption of N_2O occurs in near-bottom waters, surface concentrations (5-436 nM, mean 37.3 nM, $n = 241$) during the upwelling period are almost always far in excess of the corresponding saturation values. Using the individual data and employing two different models of air-sea gas exchange [30, 56], N_2O flux to the atmosphere has been computed to range from –1.2 μmol m^{-2} d^{-1} (the only negative value indicating absorption of atmospheric N_2O by the ocean) to 3243.2 μmol m^{-2} d^{-1} at wind speeds ranging from 5 to 10 m s^{-1}. The average flux varied from 39.1 to 263.8 μmol m^{-2} d^{-1}. Since high surface N_2O levels prevail even during the early phase of upwelling [42], this flux has been extrapolated over a period of six months and an area of 180,000

km^2 to arrive at a total N_2O efflux of 0.05-0.38 Tg N_2O from the study region. This is roughly of the same magnitude as the most recent estimate of N_2O efflux (0.33-0.70 Tg N_2O y^{-1}) from the entire Arabian Sea [1].

The available data from the Indian coastal waters do not go back far enough in time to evaluate the extent to which N_2O concentrations might have been enhanced as a result of intensification of coastal O_2 deficiency. However, in view of the well known non-linear response of N_2O production to changes in ambient O_2 levels in the low range [12], we believe that the effect may be substantial. And, should this also apply to the other coastal hypoxic sites, then the human activities may be bringing about a significant increase in the emissions of N_2O from the ocean [38].

Stoichiometric Relationship. Degradation of marine organic matter with various oxidants is believed to follow approximately constant stoichiometries [46]. The data set from the Arabian Sea, representing all the three types of redox environments [oxic/hypoxic, suboxic (denitrifying) and anoxic (SO_4^{2-} reducing)], provides a rare opportunity to test the constancy of these ratios in the same region. For this purpose, data from 294 stations located over the shelf (depth $\leq$ 200 m) were pooled and the DIN ($NO_3^- + NO_2^- + NH_4^+$) was plotted against DIP (dissolved inorganic phosphate, $PO_4^{3-} + HPO_4^{2-} + H_2PO_4^-$). The diagram (Fig. 11) may be visualized in terms of the spatio-temporal evolution of anoxia in a parcel of initially-oxygenated water as it upwells over the continental shelf and undergoes sequential changes in redox conditions. First, the decay of organic matter in the presence of O_2 increases the concentrations of both DIN and DIP in general accordance with the Redfield stoichiometry (with a $\Delta N:\Delta P$ of 13.74, represented by Line I in Fig. 11)[2] until the O_2 concentration falls below the threshold for denitrification to set in. Once this threshold is crossed (at this point DIN concentration is on an average $\sim$24 μM), NO_3^- is used by the bacteria, and the concentration of DIN decreases rapidly, but that of DIP increases slowly. The computed $\Delta N:\Delta P$ for denitrifying water (-79.1, represented by Line II in Fig. 11) is slightly different from Richards' [46] value (-94.4) for the case when NH_3 is oxidized by NO_3^- but it is close to the value (-84.8) for the case when such an oxidation does not take place. When the system turns anoxic (after the complete loss of NO_3^- that seems to take place when DIP reaches an average concentration of 2.15 μM), the relative changes in DIN and DIP exhibit complete departure from the theoretical value. That is, as NH_3 released from organic matter cannot be oxidized by SO_4^{2-}, one would expect the DIN and DIP values to fall along Line III in Fig. 11. Such is not the case, though; instead, all data points are located to the left and above

[2]The slightly lower N:P remineralization ratio than the Redfield value (16) may reflect mixing between the oxic/hypoxic and suboxic/anoxic waters

this line. The nearly linear trend of these values, completely unexpected from the Redfield model, probably arises from mixing between two end members representing a situation such as that encountered at Sta. M1a (Fig. 7).

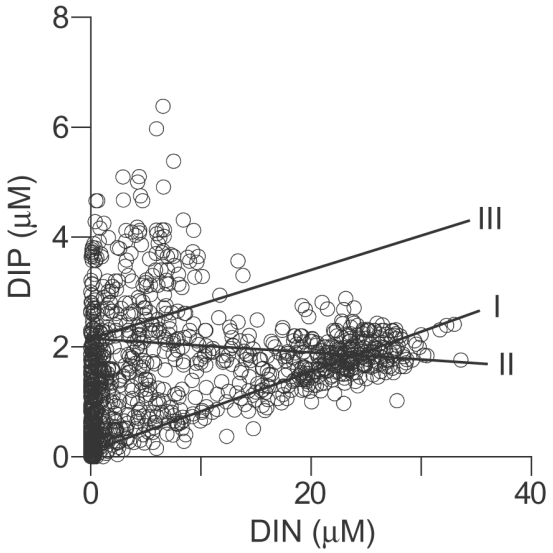

Figure 11. Plot of dissolved inorganic phosphorus (DIP) versus dissolved inorganic nitrogen (DIN = NO_3^- + NO_2^- + NH_4^+) for all samples taken from depths less than 200 m. Lines I and II have been derived from linear regressions between the observed DIN and DIP data within the oxic/hypoxic and suboxic waters with slopes ($\Delta N:\Delta P$) of 13.74 and -79.1, respectively, whereas Line III has been drawn arbitrarily from the intercept of Line II on the DIP axis with the Redfield ($\Delta N:\Delta P$) slope of 16 (modified from Naqvi et al. [38]).

The higher-than-expected DIP values in anoxic waters imply the involvement of processes other than simple degradation of organic matter by SO_4^{2-}. Under oxidizing conditions (Eh>~200 mV), DIP is known to get adsorbed onto iron hydroxide thereby forming complex iron-oxyhydroxo-phosphates (FeOP), which settle to the seafloor; DIP is released back from sediments to the overlying water when FeOP complex dissolves under reducing conditions [50]. It would appear that once the overlying waters turn anoxic over the Indian shelf DIP is mobilized in large quantities from the sediments, accounting for the observed departure of the DIN/DIP variations from the theoretical trend in anoxic waters.

The large excess of DIP in coastal waters produced during anoxic conditions in conjunction with adequate supply of Fe (both from land and through mobilization in suboxic/anoxic waters) should prime the system for N-fixation. This implies that N-fixation may be tightly coupled with denitrification in waters over the western Indian continental shelf. It is therefore not surprising that

extensive blooms of *Trichodesmium* occur on a regular basis in the eastern Arabian Sea following the cessation of upwelling (during the NEM and SI periods). Such blooms add new nitrogen to the system, partially compensating for the loss through denitrification and contributing significantly to biogeochemical cycles [15].

6. COMPARISON WITH OTHER AREAS

Of all the naturally-formed O_2 deficient zones, what distinguishes the one over the western Indian continental margin is its pronounced seasonality. Within the monsoon-affected North Indian Ocean itself, this shelf segment experiences the most severe O_2 depletion. Milder reducing conditions have recently been found to occur over the more productive, but better ventilated, Omani shelf (unpublished data collected during September 2004). However, such conditions were confined close to the seafloor, and did not produce the extreme effects, *viz.* N_2O and H_2S accumulation, observed off India. On the other side of the Indian subcontinent, in the Bay of Bengal, despite enormous river runoff, coastal waters do not turn suboxic for two reasons: (a) upwelling is much weaker in the Bay of Bengal as compared to the Arabian Sea, and (b) contrary to expectations, DIN loading by the South Asian rivers is not very large (<0.5 Tg N y^{-1} [39]).

In terms of the intensity of O_2 deficiency, the two other areas that are comparable with the eastern Arabian Sea are the eastern boundary current systems off Namibia (the Benguela Current [7, 10]) and Peru-Chile (the Humboldt Current [9, 12-14, 18]). The extent to which suboxic conditions extend offshore in these regions varies greatly owing to differences in the hydrography and respiration rate. Unlike the Pacific and the Indian Oceans, the suboxic zone does not extend much beyond the continental margin in the Atlantic Ocean, and O_2 content of waters upwelling over the Namibian shelf is initially >100 μM [7]. Respiration rates in this region therefore ought to be extremely high. In the eastern tropical Pacific Ocean, off the coasts of Peru and Chile, the suboxic zone extends hundreds of kilometers offshore from the shelf. Here too vigorous respiration [9] fuelled by high PP appears to be the principal cause for the development of an intense O_2 deficiency including episodes of naturally-caused SO_4^{2-} reduction. In the Arabian Sea, the suboxic zone over the shelf is not contiguous with the more extensive offshore suboxic zone with the WIUC flowing off the continental margin separating the two systems. However, the poleward undercurrent is ubiquitous to all upwelling systems, and the fact that it retains its slightly elevated O_2 content in the Arabian Sea implies low respiration rates. Given the less intense upwelling, O_2 deficiency over the Indian shelf should be caused more by restricted ventilation than by high productivity. Also, we postulate that

until the anthropogenic enhancement in recent times, respiration rates in this region were probably not high enough to trigger SO_4^{2-} reduction.

There are as yet no data on N_2O from the Namibian upwelling zone. Off Peru and Chile, enhanced N_2O production does occur in the O_2 deficient waters [9, 12], but with peak values generally occurring within the transition zone between the oxic and suboxic layers (associated with low NO_2^- [9]). This is at variance with the trend observed off India where N_2O often attains the highest concentrations in suboxic (NO_2^- bearing) waters, implying different mechanisms of N_2O production.

With regard to benthic processes, SO_4^{2-} reduction rates over the Indian shelf appear to be greatly subdued, with correspondingly lower concentrations of free sulphide in porewaters, than off Namibia. These differences, tentatively attributed to a combination of lesser availability of organic matter and greater abundance of reactive iron over the Indian shelf [S.W.A. Naqvi and V. Brüchert, unpublished data], should be investigated in detail.

Acknowledgements

This manuscript was prepared when SWAN was on leave from NIO as a Fellow at the Hanse Wissenschaftskolleg (HWK), Delmenhorst, Germany; the help and support of the HWK staff is gratefully acknowledged. We also wish to record our gratitude to Dr. M.D. George, Dr. S.G.P. Matondkar, Dr. D.M. Shenoy, Dr. V.V.S.S. Sarma, Ms. Witty D' Souza and Mr. Anil Pratihary for their contribution to collection of the data used here. The IFP data were kindly supplied to us by Prof. Karl Banse, who should also be thanked for generously sharing with us his vast knowledge of the oceanography of the Arabian Sea. Our guru of oceanic nitrogen cycling, Dr. Lou Codispoti, along with an anonymous reviewer made excellent suggestions that have greatly improved this article.

References

[1] Bange H.W., Andreae M.O., Lal S., Law C.S., Naqvi S.W.A., Patra P.K., Rixen T. and Upstill-Goddard R.C. Nitrous oxide emissions from the Arabian Sea: A synthesis. Atmos Chem Phys 2001; 1:61-71.

[2] Bange H.W., Rixen T., Johansen A., Siefert R.L., Ramesh R., Ittekkot V., Hoffmann M.R. and Andreae M.O. A revised nitrogen budget for the Arabian Sea. Global Biogeochem Cy 2000; 14:1283-97.

[3] Banse K. On upwelling and bottom-trawling off the southwest coast of India. J Mar Biol Assoc India 1959; 1:33-49.

[4] Banse K. Hydrography of the Arabian Sea shelf of India and Pakistan and effects on demersal fishes. Deep-Sea Res 1968; 15:45-79.

[5] Banse K. "Overview of the hydrography and associated biological phenomena in the Arabian Sea off Pakistan." In *Marine Geology and Oceanography of Arabian Sea and*

Coastal Pakistan, B.U. Huq and J.D. Milliman, eds. New York: Van Nostrand Rheinhold, 1984.

[6] Betlach M.R. and Tiedje J.M. A kinetic explanation for accumulation of nitrite, nitric oxide, and nitrous oxide during bacterial denitrification. Appl Environ Microbiol 1981; 42:1074-84.

[7] Brüchert V., Jørgensen B.B., Neumann K., Riechmann D., Schlosser M. and Schulz H. Regulation of bacterial sulfate reduction and hydrogen sulfide fluxes in the central Namibian coastal upwelling zone. Geochim Cosmochim Ac 2003; 67:4505-18.

[8] Carruthers J.N., Gogate S.S., Naidu J.R. and Laevastu T. Shoreward upslope of the layer of minimum oxygen off Bombay: Its influence on marine biology, especially fisheries. Nature 1959; 183:1084-87.

[9] Castro González M. and Farías L. N_2O cycling at the core of the oxygen minimum zone off northern Chile. Mar Ecol Prog Ser 2004; 280:1-11.

[10] Chapman P. and Shannon L.V. The Benguela ecosystem. 2. Chemistry and related processes. Oceanogr Mar Biol Ann Rev 1985; 23:183-251.

[11] Codispoti L.A., Brandes J.A., Christensen J.P., Devol A.H., Naqvi S.W.A., Paerl H.W. and Yoshinari T. The oceanic fixed nitrogen and nitrous oxide budgets: Moving targets as we enter the anthropocene? Sci Mar 2001; 65 (suppl 2):85-105.

[12] Codispoti L.A., Elkins J.W., Yoshinari T., Friederich G.E., Sakamoto C.M. and Packard T.T. "On the nitrous oxide flux from productive regions that contain low oxygen waters." In *Oceanography of the Indian Ocean*, B.N. Desai, ed. New Delhi: Oxford & IBH, 1992.

[13] Codispoti L.A., Friederich G.E., Packard T.T., Glover H.E., Kelly P.J., Spinrad R.W., Barber R.T., Elkins J.W., Ward B.B., Lipschultz F. and Lostaunau N. High nitrite levels off northern Peru – a signal of instability in the marine denitrification rate. Science 1986; 233:1200-02

[14] Codispoti L.A. and Packard T.T. Denitrification rates in the eastern tropical South Pacific. J Mar Res 1980; 38:453-77.

[15] Devassy V.P., Bhattathiri P.M.A. and Qasim S.Z. *Trichodesmium* phenomenon. Indian J Mar Sci 1978; 7:168-86.

[16] Devol A.H., Naqvi S.W.A. and Codispot L .A. "Nitrogen cycling in the suboxic waters of the Arabian Sea". In *Past and Present Water Column Anoxia*, L.N. Neretin, ed. Dordrecht: Springer, 2006.

[17] Devol A.H., Uhlenhopp A.G., Naqvi S.W.A., Brandes J.A., Jayakumar A., Naik H., Codispoti L.A. and Yoshinari T. Denitrification rates and excess nitrogen gas concentrations in the Arabian Sea oxygen deficient zone, submitted.

[18] Dugdale R.C., Goering J.J., Barber R.T., Smith R.L. and Packard T.T. Denitrification and hydrogen sulphide in Peru upwelling region during 1976. Deep-Sea Res 1977; 24:601-08.

[19] Dugdale R.C., Wilkerson F., Chai F., Barber R. and Peng T. (2002) Diatoms in control and at risk: climate feedbacks and anthropogenic forcing, Oceans Biogeochemistry and Ecosystems Analysis, International Open Science Conference, Abstract PS1: 3.2 Retrieved May 2005 from: `http://www.igbp.kva.se/obe/OBE_PS3.pdf`.

[20] Energy Information Administration (2004) South Asia regional overview Retrieved May 2005 from: `http://www.eia.doe.gov/emeu/cabs/sasia.html`.

[21] Firestone M.K. and Tiedje J.M. Temporal change in nitrous oxide and dinitrogen from denitrification following onset of anaerobiosis. Appl Environ Microbiol 1979; 38:673-79.

[22] Gogate S.S. *Some Aspects of Hydrobiology of Bombay Waters*, M.Sc. thesis, Bombay University, 1960 (unpublished).

[23] Granger J. and Ward B.B. Accumulation of nitrogen oxides in copper-limited cultures of denitrifying bacteria. Limnol Oceanogr 2003; 48:313-18.

[24] Granthan B.A., Chan F., Nielsen K.J., Fox D.S., Barth J.A., Huyer A., Lubchenco J. and Menge B.A. Upwelling-driven nearshore hypoxia signals ecosystem and oceanographic changes in the northeast Pacific. Nature 2004; 429:749-54.

[25] Helly J.J. and Levin L.A. Global distribution of naturally occurring marine hypoxia on continental margins. Deep-Sea Res 2004; 51:1159-68.

[26] Hida T.S. and Pereira W.T. Results of bottom trawling in Indian seas by R.V. *Anton Bruun*. Proc Indo-Pacific Fish Coun 1966; 11:156-71.

[27] International Fertilizer Industry Association (2004) Total fertilizer consumption statistics by region from 1970/71 to 2002/03, Table N Retrieved May 2005 from: `http://www.fertilizer.org/ifa/statistics/indicators/tablen.asp`.

[28] Kamykowski D. and Zentara S.J. Hypoxia in the world ocean as recorded in the historical data set. Deep-Sea Res 1990; 37:1861-74.

[29] Kuypers M.M.M., Lavik G., Wöbken D., Schmid M., Fuchs B.M., Amann R., Jørgensen B.B. and Jetten M.S.M. Massive nitrogen loss from the Benguela upwelling system through anaerobic ammonium oxidation. Proc Nat Acad Sci 2005; 102:6478-83.

[30] Liss P. S. and Merlivat L. "Air-sea exchange rates: Introduction and synthesis." In *The Role of Air-Sea Exchange in Geochemical Cycling*. P. Buat-Menard, ed. Dordrecht : D. Reidel Publishing Co, 1986.

[31] Madhupratap M., Nair S.R.S., Haridas P. and Padmavati G. Response of zooplankton to physical changes in the environment: Coastal upwelling along central west coast of India. J Coast Res 1990; 6:413-26.

[32] McCreary J.P., Kundu P.K. and Molinany R.L. A numerical investigation of the dynamics and mixed layer processes in the Indian Ocean. Progr Oceanogr 1993; 31:181-244.

[33] Naik, H. *Benthic Nitrogen Cycling with Special Reference to Nitrous Oxide in the Coastal and Continental Shelf Environments of the Eastern Arabian Sea*, Ph.D. thesis, Goa University, 2003 (unpublished).

[34] Naik H. and Naqvi S.W.A. Sedimentary nitrogen cycling over the western continental shelf of India. EOS – Trans Amer Geophys Union 2002; 83(4) OSM Suppl.: Abs. OS12I-05.

[35] Naqvi S.W.A. Some aspects of the oxygen-deficient conditions and denitrification in the Arabian Sea. J Mar Res 1987; 49:1049-72.

[36] Naqvi S.W.A. Geographical extent of denitrification in the Arabian Sea in relation to some physical processes. Oceanolog Acta 1991; 14:281-90.

[37] Naqvi S.W.A., George M.D., Narvekar P.V., Jayakumar D.A., Shailaja M.S., Sardesai S., Sarma V.V.S.S., Shenoy D.M., Naik H., Maheswaran P.A., Krishnakumari K., Rajesh G., Sudhir A.K. and Binu M.S. Severe fish mortality associated with 'red tide' observed in the sea off Cochin. Curr Sci 1998; 75:543-44.

[38] Naqvi S.W.A., Jayakumar D.A., Narvekar P.V., Naik H., Sarma V.V.S.S., D'Souza W., Joseph S. and George M.D. Increased marine production of N_2O due to intensifying anoxia on the Indian continental shelf. Nature 2000; 408:346-49.

[39] Naqvi S.W.A, Naik H., D' Souza W., Narvekar P.V., Paropkari A.L. and Bange H.W. "Carbon and nitrogen fluxes in the North Indian Ocean." In *Carbon and Nutrient Fluxes in Continental Margins: A Global Synthesis*, K.K. Liu, L. Atkinson, R. Quinones, and L. Talaue McManus, eds. Berlin: Springer-Verlag, in press.

[40] Naqvi S.W.A. and Noronha R.J. Nitrous oxide in the Arabian Sea. Deep-Sea Res 1991; 38:871-90.

[41] Naqvi S.W.A, Noronha R.J., Somasundar K. and Sen Gupta R. Seasonal changes in the denitrification regime of the Arabian Sea. Deep-Sea Res 1990; 37:693-711.

[42] Naqvi S.W.A., Yoshinari T., Jayakumar D.A., Altabet M.A., Narvekar P.V., Devol A.H., Brandes J.A. and Codispoti L.A. Budgetary and biogeochemical implications of N_2O isotope signatures in the Arabian Sea. Nature 1998; 394:462-64.

[43] Rabalais N.N., Turner R.E. and Wiseman Jr. W.J. Hypoxia in the Gulf of Mexico. J Environ Qual 2001; 30:320-29.

[44] Ramaiah N., Paul J.T., Fernandes V., Raveendran T., Raveendran O., Sunder D., Revichandran C., Shenoy D.M., Gauns M., Kurian S., Gerson V.J., Shoji D.T., Madhu N.V., Sree Kumar S., Lokabharathi P.A. and Shetye S.R. The September 2004 stench off the southern Malabar coast - A consequence of holococcolithophore bloom. Curr Sci 2005; 88:551-54.

[45] Repeta D.J., Simpson D.J., Jørgensen B.B. and Jannasch H.W. Evidence for anoxygenic photosynthesis from the distribution of bacteriochlorophylls in the Black Sea. Nature 1989; 342:69-72.

[46] Richards F.A. "Anoxic basins and fjords." In *Chemical Oceanography*, *Vol. 1*, J.P. Riley, G. Skirrow, eds. New York: Academic Press, 1965.

[47] Schmaljohann R., Drews M, Walter S., Linke P., von Rad U. and Imhoff J.F. Oxygen minimum zone sediments in the northeastern Arabian Sea off Pakistan: a habitat for the bacterium *Thioploca*. Mar Ecol Progr Ser 2001; 211:27-42.

[48] Schott F. and McCreary J.P. The monsoon circulation of the Indian Ocean. Prog Oceanogr 2001; 51:1-123.

[49] Seitzinger S.P., Kroeze C, Bouwman A.E., Caraco N., Dentener F. and Styles R.V. Global patterns of dissolved inorganic and particulate nitrogen inputs to coastal systems: Recent conditions and future projections. Estuaries 2002; 25:640-55.

[50] Shaffer G. Phosphate pumps and shuttles in the Black Sea. Nature 1986; 321:515-17.

[51] Shetye S.R., Gouveia A., Shenoi S.S.C., Michael G.S., Sundar D., Almeida A.M. and Santanam K. The coastal current off western India during northeast monsoon, Deep-Sea Res 1991; 38:1517-29.

[52] Shetye S.R., Gouveia A., Shenoi S.S.C., Sundar D., Michael G.S., Almeida A.M. and Santanam K. Hydrography and circulation off west coast of India during the Southwest Monsoon. J Mar Res 1990; 48:359-78.

[53] Subrahmanyan R. Studies on the phytoplankton of the west coast of India. II. Physical and chemical factors influencing the production of phytoplankton, with remarks on the cycles of nutrients and on the relationship of the phosphate-content to fish landings. Proc Indian Acad Sci (Biol Sci) 1959; B50:189-252.

[54] Swallow J. Some aspects of the physical oceanography of the Indian Ocean. Deep-Sea Res 1984; 31:639-50.

[55] van Weering T.C.E., Helder W. and Schalk P. Netherlands Indian Ocean Program 1992-1993: First Results and an introduction. Deep-Sea Res II 1997; 44:1177-93.

[56] Wanninkhof R. Relationship between wind speed and gas exchange over the ocean. J Geophys Res 1992; 97:7373-82.

[57] Warren B.A. Context of the suboxic layer in the Arabian Sea. Proc Indian Acad Sci (Earth Planet Sci) 1994; 103:301-14.

[58] Wyrtki K. *Oceanographic Atlas of the International Indian Ocean Expedition*. Washington, D.C.: National Science Foundation, 1971.

OXYGEN DEPLETION IN THE GULF OF MEXICO ADJACENT TO THE MISSISSIPPI RIVER

Nancy N. Rabalais[1] and R. Eugene Turner[2]

[1]*Louisiana Universities Marine Consortium, Chauvin, Louisiana 70344, USA*

[2]*Coastal Ecology Institute, Louisiana State University, Baton Rouge, Louisiana 70803, USA*

Abstract The seasonal formation of a bottom water layer severely depleted in dissolved oxygen has become a perennial occurrence on the Louisiana continental shelf adjacent to the Mississippi River system. Dramatic changes have occurred in this coastal ecosystem in the last half of the 20^{th} century as the loads of dissolved inorganic nitrogen tripled. There are increases in primary production, shifts in phytoplankton community composition, changes in trophic interactions, and worsening severity of hypoxia. The hypoxic conditions (dissolved oxygen less than 2 mg l^{-1}) cover up to 22,000 km^2 of the seabed in mid-summer. Dissolved oxygen concentrations seldom decrease to anoxia, but are often below 1 mg l^{-1} and down to 0.5 mg l^{-1}. The continental shelf of the northwestern Gulf of Mexico is representative of systems in which nutrient flux to the coastal ocean has resulted in eutrophication and subsequently hypoxia. The Mississippi River influenced continental shelf is similar to systems, such as deep basins and fjords, with regard to biogeochemical processes of oxic versus suboxic conditions in the water column and sediments. However, the suboxic conditions for the Gulf of Mexico are less persistent in time and space due to the dynamic nature of the open continental shelf system. Also, anoxia at the seabed is not as common or long lasting.

Keywords: continental shelf, Gulf of Mexico, Mississippi River, hypoxia, anoxia, eutrophication, nitrogen, phosphorus, silica

1. INTRODUCTION

Anoxic and suboxic conditions exist naturally in the world's oceans in fjords, deep basins, and oxygen minimum zones [19, 24]. Similar conditions frequently occur where upwelling systems associated with western boundary currents impinge on the continental shelf. Oxygen depletion in coastal waters not subject to upwelled nutrients results from eutrophication usually initiated and maintained by increased nutrient loads under stratified conditions. Not all coastal systems with elevated nutrient loads undergo eutrophication or develop hypoxia. The

L. N. Neretin (ed.), Past and Present Water Column Anoxia, 225–245.

processes of increased phytoplankton biomass, carbon accumulation, and oxygen depletion are more likely to occur in systems with long water residence times and where the water column is stratified by salinity, temperature, or both. The amount of suspended sediment delivered to a coastal system also may influence whether enhanced production will result from the changing nutrient inputs.

Nutrient load increases result from increasing human populations and their activities – application of nitrogen and phosphorus fertilizers, planting of leguminous crops, atmospheric deposition of nutrients, and municipal and industrial wastewater [1, 50]. The consequences can be desirable or undesirable, as perceived by humans. Increased nutrients stimulate increased primary production and increased secondary production, and often the yield of commercially important fisheries. The negative effects may include increased noxious or harmful algal blooms, diminished water clarity, shifts in trophic interactions that do not result in the diatom-zooplankton-fish food web, loss of essential habitat and oxygen depletion. Over the last half of the 20^{th} century, the impacts of eutrophication, including oxygen depletion, increased in frequency and severity and expanded geographically [3, 10, 27]. This trend will continue in the future with increasing nutrient loads [43].

The continental shelf of the northwestern Gulf of Mexico is representative of systems in which nutrient flux to the coastal ocean has resulted in eutrophication and subsequently hypoxia. One other shelf environment with a similar scenario of changing nutrient loads and worsening hypoxia is presented for the northwestern shelf of the Black Sea that receives discharges from the Danube, Dniepr, and Dniestr rivers (Zaitsev, present volume).

2. DISTRIBUTION AND DYNAMICS OF HYPOXIA

We define hypoxia as dissolved oxygen less than 2 mg l^{-1}, or ppm, because bottom-dragging trawls usually do not capture any shrimp or demersal fish below this level [40]. (Dissolved oxygen of 2 mg l^{-1} equates to 1.4 ml l^{-1} or 63 μM, and approximates 20% oxygen saturation in the 25 °C and 35 psu bottom water of the hypoxic zone.) Sharks will modify their behavior to escape oxygen concentrations that fall below 3 mg l^{-1}. When dissolved oxygen values are below 2 mg l^{-1}, they are often less than 1 mg l^{-1}, a level that is stressful or lethal to benthic macroinfauna.

The second largest zone of oxygen-depleted coastal waters in the world is found in the northern Gulf of Mexico on the Louisiana/Texas continental shelf, an area that is influenced by the freshwater discharge and nutrient load of the Mississippi River system [33] (Fig. 1). The mid-summer areal extent of hypoxic waters averaged 13,000 km^2 over the period 1985-2004, with the largest size mapped in 2002 at 22,000 km^2 (Fig. 2). The seasonal cycle of freshwater

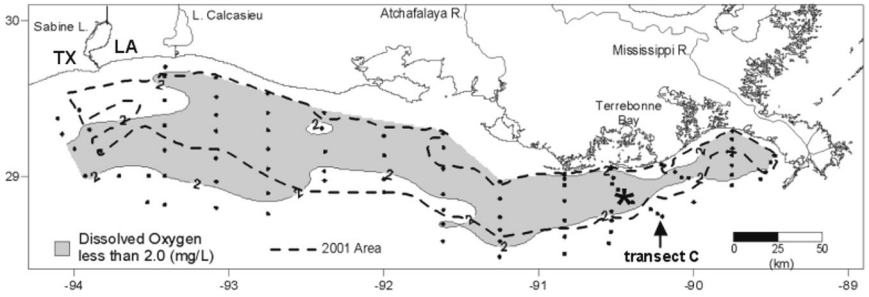

Figure 1. Distribution of bottom water hypoxia on the Louisiana/Texas coast in late July 2002 (stippled area) compared to July 2001 (area outlined by dashed line). Transect C and location of instrument mooring (*) identified. Data source: N.N. Rabalais, LUMCON.

discharge, nutrient flux, subtropical weather conditions, and circulation patterns that retain fresh water and associated constituents on the continental shelf controls the formation and maintenance of a spring-summer hypoxic zone. The seasonal formation of hypoxia is currently perennial, but hypoxia was not a dominant feature of the continental shelf prior to the major increase in nutrient loads beginning in 1960.

2.1 Physical Setting

The Mississippi River forms the largest watershed on the North American continent. It discharges an average 580 km^3 of fresh water per year to the northern Gulf of Mexico through two main distributaries—the main birdfoot delta southeast of the city of New Orleans, Louisiana and the Atchafalaya River delta 200 km to the west that carries about one-third of the flow [26]. The Mississippi and Atchafalaya rivers are the primary sources of fresh water, nitrogen and phosphorus to the northern Gulf of Mexico, delivering 80 percent of the freshwater inflow, 91 percent of the nitrogen load, and 88 percent of the phosphorus load [15]. Nutrient sources from atmospheric deposition, ground water and upwelled deeper Gulf water are estimated to be small or negligible [17, 36].

The fresh water, sediments, and dissolved and particulate materials are carried predominantly westward along the Louisiana/Texas inner to middle continental shelf, especially during peak spring discharge [36]. Although the area of the discharge's influence is an open continental shelf, the magnitude of flow, annual current regime and average 75-day residence time for fresh water result in an unbounded estuary stratified for much of the year. This stratification is

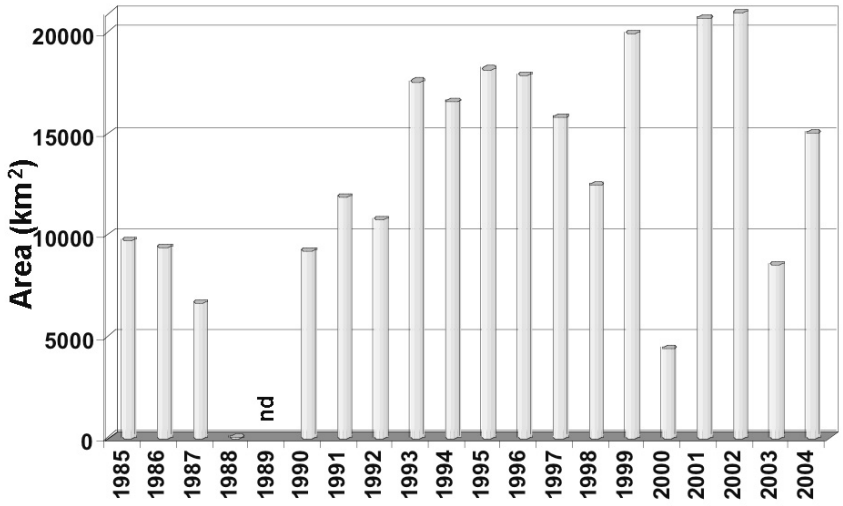

Figure 2. The areal extent of bottom water hypoxia in mid-summer on the Louisiana/Texas continental shelf from 1985-2004 (updated from [14]).

primarily due to salinity differences, and the stratification intensifies in summer with thermal warming of surface waters.

Mississippi River Watershed. The Mississippi River watershed drains 3.2 million km^2 encompassing 41 percent of the lower 48 United States. The Mississippi River has been modified for navigation and flood control with narrowing of the channel and levees extending along the river from Cairo, Illinois to the Gulf of Mexico. Fifty-six percent of the wetlands in the Mississippi River basin have been lost to agriculture, navigation, reservoirs and leveeing. Land use in the watershed that supports 27 percent of the U.S.'s population (about 70 million people) is predominantly agriculture [17], the conversion of which began in the early 1800s as settlers migrated west across the North American continent [46]. Artificial subsurface drainage in much of the croplands expedites the transport of nitrate from the soil to surface waters. This management practice coupled with the increase in fertilizer applications can only increase the flux of nitrate from agricultural fields to the streams. In addition to landscape changes, anthropogenic inputs of nitrogen and phosphorus have increased from agriculture, point sources, and atmospheric deposition.

The annual discharge of the Mississippi River system contributes sediment yields of 210 x 10^6 t, 1.6 x 10^6 t nitrogen, of which 0.95 x 10^6 t is nitrate and 0.58 x 10^6 t is organic nitrogen, 0.1 x 10^6 t phosphorus and 2.1 x 10^6 t silica [17]. The estimate of current river nitrogen export from the Mississippi River watershed over 'pristine' river (pre-agricultural and pre-industrial condition) nitrogen export is a 2.5- to 7.4-fold increase [20]. The average concentration and flux of nitrogen (per unit volume discharge) increased from the 1950s to 1980s, especially in the spring; this is consistent with increased use of fertilizer in the watershed [47].

Changes in River Constituents and Ecosystem Response. Changes in the coastal ecosystem are directly linked to the changes within the watershed and nutrient loading to the continental shelf, especially of nitrate, which tripled in the last half of the 20th century [36, 37, 46, 48]. Evidence from long-term data sets and the sedimentary record demonstrate that indices of increased marine productivity and subsequent worsening of oxygen stress are highly correlated with historic increases in riverine dissolved inorganic nitrogen concentrations and loads over the last 50 years [37] and implied nutrient load changes over the last 200 years [46]. Evidence comes in long-term changes in Secchi disk depth and diatom productivity, increased accumulation of diatom remains and marine-origin carbon in sediments, and indicators of worsening oxygen conditions in the sediments—glauconite abundance, benthic foraminiferan diversity and community composition, and ostracod diversity. The sediment data suggest that hypoxia was not a feature of the continental shelf before 1900 and that hypoxia *may* have existed at some level before the 1940–1950 time period, but that it has worsened since then. Recent models of how the size and intensity of hypoxia are related to nitrate flux from the Mississippi River [22, 42, 49] indicate that hypoxia as a widespread phenomenon was not likely on the Louisiana shelf before the early 1970s. Thus, the continental shelf hypoxia/anoxia adjacent to the Mississippi River results from anthropogenic activity within the watershed and subsequent eutrophication and oxygen deficiency in a physical setting conducive to the formation of hypoxia.

Because both the amount of fresh water delivered (an influence on stratification) and nitrogen loading (an influence on primary production) influence the distribution and dynamics of hypoxia, it is important to understand the interannual variability in discharge as it affects seasonal biological processes. Using two different approaches, Donner et al. [11] and Justić et al. [23] agreed that only 20 to 25 percent of the increased nitrate flux between the mid-1960s to the mid-1990s was attributable to greater runoff and river discharge, with the rest due to increased nitrogen loading from the landscape. With nitrate concentrations in the lower Mississippi River remaining near 100 μM since

the early 1990s [45], climate-driven changes in discharge now influence the seasonal formation of hypoxia more than they did before 1990.

Physical and Biological Processes. The relative influence of the physical features of the system and the progression of biological processes vary spatially and over an annual cycle and are directly linked with the dynamics of the Mississippi and Atchafalaya discharges.

The physical structure of the water column is defined by water masses that differ in temperature, salinity, or both. Fresh water from the rivers and seasonally-warmed surface waters reside above the saltier, cooler and more dense water masses near the bottom. The existence of a strong near-surface pycnocline, usually controlled by salinity differences, is a necessary condition for the occurrence of hypoxia, while a weaker, seasonal thermocline often guides the morphology of the bottom water hypoxia [51] (Fig. 3). Stratification goes through a well-defined seasonal cycle that is generally strongest during summer and weakest during winter [33]. These changes are responsive to the strength and phasing of river discharge, the changing frequency of cold front passages, regional circulation and air-sea heat exchange processes.

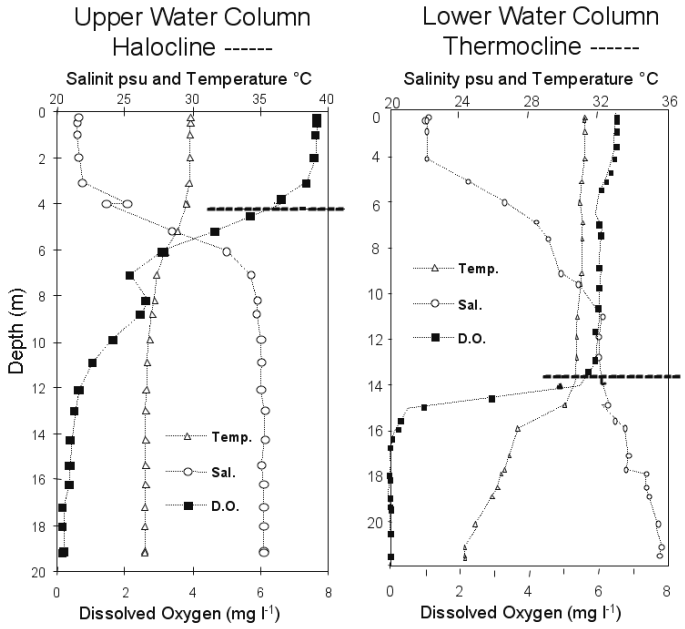

Figure 3. Left panel: example of upper water column halocline and oxycline. Right panel: example of upper water column halocline and lower water column thermocline and oxycline. Data source: N.N. Rabalais, LUMCON.

The concentrations and total loads of nitrogen, phosphorus and silica delivered to the coastal ocean influence the productivity of the phytoplankton community, the types of phytoplankton that are most likely to grow and the flux of phytoplankton-derived organic matter [12, 36, 45]. Phytoplankton not incorporated into the food web and fecal material generated via the food web sink into bottom waters where they are decomposed by aerobic bacteria. The source of the organic matter for this respiratory activity is mostly from marine phytoplankton growth stimulated by riverine-delivered nutrients, and not from the carbon in the Mississippi River [16]. The bacterial respiration in the lower water column and seabed results in a decline in oxygen concentration when oxygen is depleted faster than it can be replaced by vertical diffusion through the stratified water column.

2.2 Variability of Gulf of Mexico Hypoxia

The distribution of hypoxia on the Louisiana/Texas continental shelf reflects the interaction of physical and biological processes dominated by riverine inputs. Decreases in nutrient concentrations away from the Mississippi and Atchafalaya rivers are paralleled by decreases in surface water chlorophyll (Fig. 4) [34, 35]. Gradients away from the rivers result from mixing of the buoyant plumes and biological uptake and regeneration of nutrients. Dissolved inorganic nitrogen (DIN, nitrate+nitrite+ammonium) is high near the Mississippi River delta and composed primarily of nitrate. Down current from the delta, ammonium is the dominant DIN form and in sufficient supply to support primary production. Phosphate is uniformly present, and silicate concentrations are high near the delta and remain sufficient for diatom growth across a large area. There is an optimal distance and depth for the formation of hypoxia based on strength of the stratification, light conditions, nutrient availability and rates of primary production and flux of organic matter to the seabed. This is qualitatively illustrated in the compilation of 17 mid-summer surveys (1985-2002, Fig. 5) that shows the frequency of hypoxia is highest down current (west) from the freshwater and nutrient discharges from the Mississippi and Atchafalaya rivers. Empirical models strongly correlate the size of the mid-summer hypoxic area with the riverine nitrate load over several months prior to the mapping cruise [42, 49].

Spatial Extent. The hypoxic water mass is distributed across the Louisiana shelf west of the Mississippi River and onto the upper Texas coast (mapped in mid- to late July) [37]. Hypoxia extends from near shore to as much as 125 km offshore and in water depths up to 60 m. The size averaged 13,000 km^2 over the period 1985-2004, with a range from negligible in 1988 (a summer drought year for the Mississippi River basin) up to 22,000 km^2 (Fig. 2). Hypoxia may form in two distinct areas west of the Mississippi and Atchafalaya River

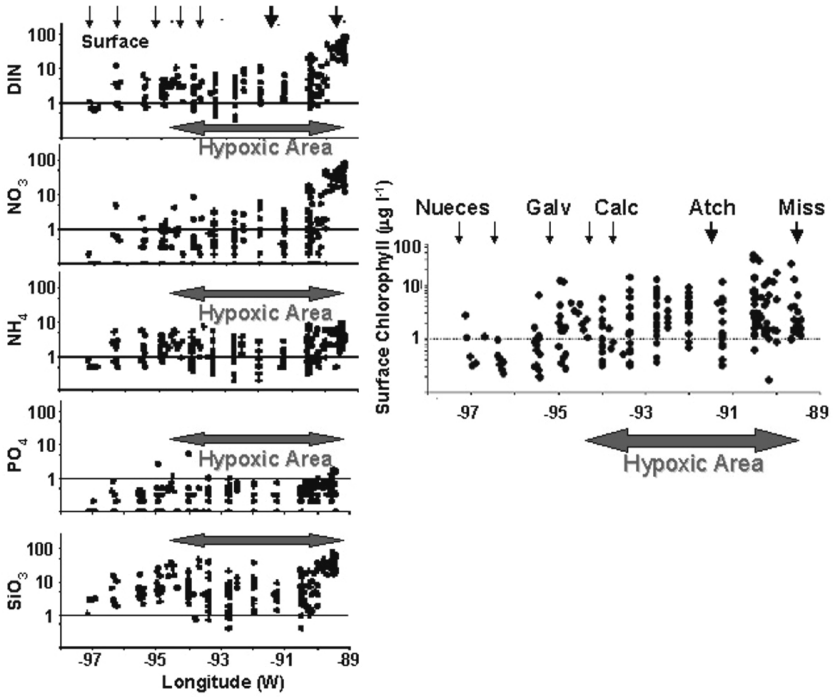

Figure 4. Concentration of surface water nutrients (μM) and chlorophyll biomass (μg l^{-1}) on the Louisiana/Texas shelf for multiple seasons in 1985-2002 (modified from [40]). The black arrows indicate the large inputs of fresh water and nutrients from the Mississippi and Atchafalaya Rivers, and minor contributions from the Calcasieu, Galveston, Nueces and other estuaries. The shaded horizontal arrows indicate the typical distance alongshore for the mid-summer hypoxic zone.

deltas (Fig. 6). The water between these two areas, however, is also depleted in oxygen (less than 3 mg l^{-1}). Hypoxia more often forms a single continuous zone (examples for 2001 and 2002 in Fig. 1). The 1998 hypoxic zone was atypically concentrated in deeper water than usual on the eastern Louisiana shelf. Although the bottom extent of hypoxia in 1998 was less than 1997 (Fig. 2), the volume of the hypoxic water mass in 1998 was greater than in 1997 [35]. The smaller area in 2003 resulted from a series of tropical storms that moved through the area two weeks prior to the mapping cruise and disrupted the stratification.

Most instances of hypoxia elsewhere in the northern Gulf of Mexico along the shelf farther to the west and also east of the Mississippi River delta are infrequent, short-lived, and limited in extent [30, 37]. Hypoxia on the upper Texas coast is usually an extension of the hypoxic zone off Louisiana [18, 28]. Hypoxia east of the Mississippi River is also isolated and ephemeral, but occurs

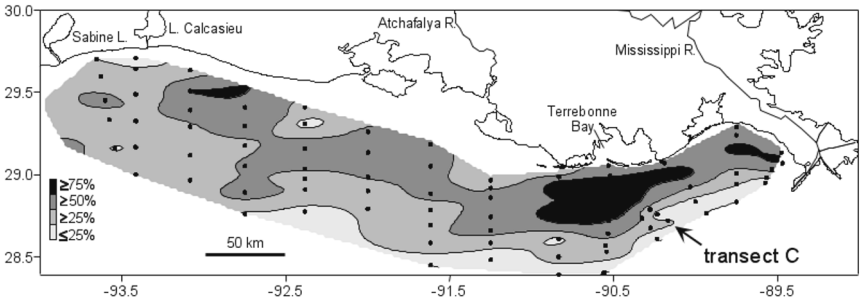

Figure 5. Distribution of frequency of bottom water hypoxia in mid-summer on the Louisiana/Texas shelf for 1985-2002 (modified from [14]).

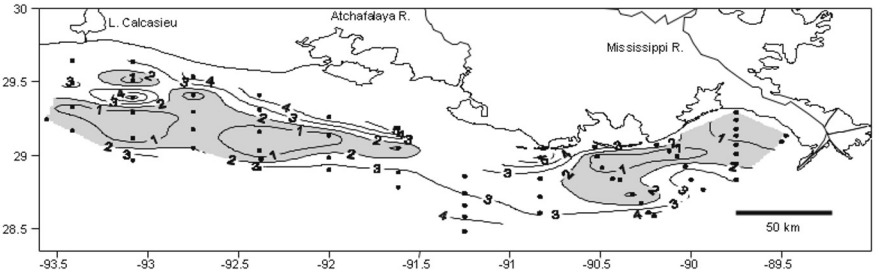

Figure 6. Isopleths of bottom water dissolved oxygen concentrations (mg l^{-1} for 7-17 July 1986 with values less than 2 mg l^{-1} stippled. Note the extent of values less than 3 mg l^{-1}, a level below which some nekton are excluded. Data source: N.N. Rabalais, LUMCON.

more frequently during flood stages of the Mississippi River when summer currents move more water to the east of the birdfoot delta. From limited data where both sides of the delta were surveyed ([44], National Marine Fisheries Service unpubl. data), there is no evidence that the area of low oxygen forms a continuous band around the delta.

Seasonal Variability. The broad spatial coverage of hypoxia has been routinely measured only once per year in mid-summer, and the spatial extent over the whole shelf during other parts of the year is less well known. More frequent sampling along a transect C on the southeastern Louisiana coast (labeled in Fig. 1 and 5) indicates that critically low dissolved oxygen concentrations occur from as early as late February through early October and nearly continuously from mid-May through mid-September [37]. Data from trawl surveys in the Mississippi River bight indicate that hypoxia occurs in that area in

6- to 10-m water depth as late as November (T. Romaire pers. comm.). Hypoxia is rare in late fall and winter. The monthly average value of bottom oxygen concentration along transect C illustrates the seasonal progression of worsening hypoxia across an increasingly greater area in May through August (Fig. 7). The persistence of extensive and severe hypoxia into September and October depends on the timing of the breakdown of vertical stratification from either tropical storms, passage of cold fronts or thermal turnover of the water column.

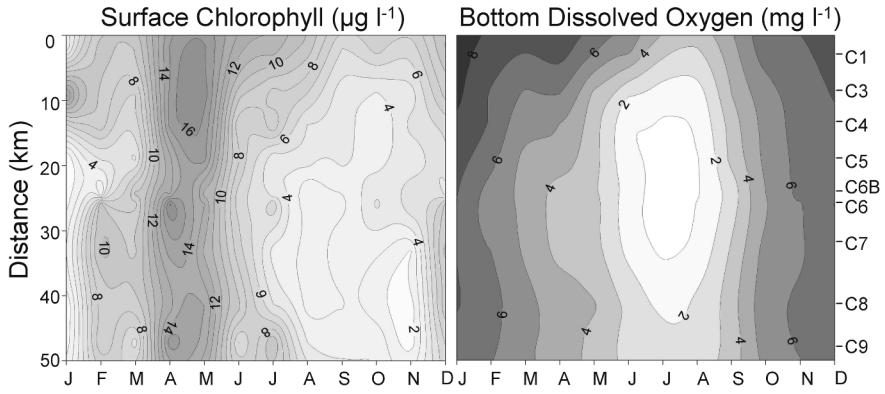

Figure 7. Long-term average (1985-1997) of surface water chlorophyll and bottom water dissolved oxygen by month for nine stations located 3 to 47 km from shore in water depths of 5 to 30 m. Data source: N.N. Rabalais, LUMCON.

Once hypoxia becomes established in mid-summer, much of the onshore-offshore variability in distribution can be attributed to wind-induced cross-shelf advection or tidal advection [38, 39]. The low oxygen water mass is displaced into deeper water following winds that produce downwelling-favorable conditions. Upwelling-favorable conditions push the hypoxic water mass closer to the barrier island shore.

Vertical Distribution. Hypoxia is sometimes found in a thin lens overlying the seabed, but more often occurs well up into the water column depending on the location of the pycnocline(s) (Fig. 3). Hypoxia may encompass from 10 to over 80 percent of the total water column, but is normally only 20 to 50 percent of the water column. At the high end of this range, hypoxic waters may reach to within 2 m of the surface in a 10-m water column, or to within 6 m of the surface in a 20-m water column.

Mid-water oxygen minima often occur below concentrations of phytoplankton at a density discontinuity in the upper or mid-water column. Where surface phytoplankton biomass is high, the sinking cells and fecal pellets

from zooplankton grazing settle through the water column and concentrate in fine layers at pycnoclines. Respiration in these interfaces often exceeds oxygen production via photosynthesis so that oxygen depleted layers form at or immediately below the concentration of organic matter. Examples are provided from within areas of hypoxia in July 2004 following a period of unseasonably high discharge of the Mississippi River (Fig. 8). Mid water oxygen minima, however, are not limited to areas of oxygen-depleted bottom water. These features are common near the Mississippi River plume in spring and diminish in frequency and strength with distance from the discharge.

High Frequency Oxygen Measurements. Continuously recording (15-min interval) oxygen meters have been deployed near the bottom at a 20-m station on transect C since 1990. There is variability within the year and between years, but the pattern (Fig. 9) that usually develops at this location includes: (i) gradual declines of bottom oxygen concentrations through respiration and more rapid reoxygenation from mixing events, (ii) persistent hypoxia and often anoxia for extended periods in May-September, (iii) isolated intrusions of higher oxygen content water from depth during upwelling-favorable wind conditions followed by a movement of the low oxygen water mass back offshore, and (iv) tropical storms, hurricanes or cold fronts in the late summer and fall that mix the water column sufficiently to prevent prolonged instances of low oxygen concentrations [33].

Another recording oxygen meter was deployed in a similar depth of 20-m but 77 km to the east and closer to the Mississippi River delta where the depth gradient of the shelf is much steeper [39]. At that station hypoxia occurred for only 44 percent of the record from mid-June through mid-October (compared to 75 percent at the station on transect C). There was a strong diurnal pattern in the oxygen time-series for the former and not for the latter. The dominant coherence of the diurnal peaks of oxygen concentration from the site in the Mississippi River bight with bottom pressure records suggests that the dissolved oxygen signal was due principally to advection of the interface between hypoxic and normoxic water by tidal currents.

3. BIOGEOCHEMICAL PROCESSES IN HYPOXIA

Most of the biogeochemical investigations of the highly productive plume of the Mississippi River have focused on surface waters with regard to bacterial production, respiration, carbon remineralization, and nutrient uptake and regeneration, and less often with similar processes in sediments overlain by hypoxic waters. Little is known about nutrient and carbon transformations within the mid-water hypoxic layers. The biogeochemical processes of oxic versus hypoxic conditions and oxic/anoxic interfaces in the water column and sediments

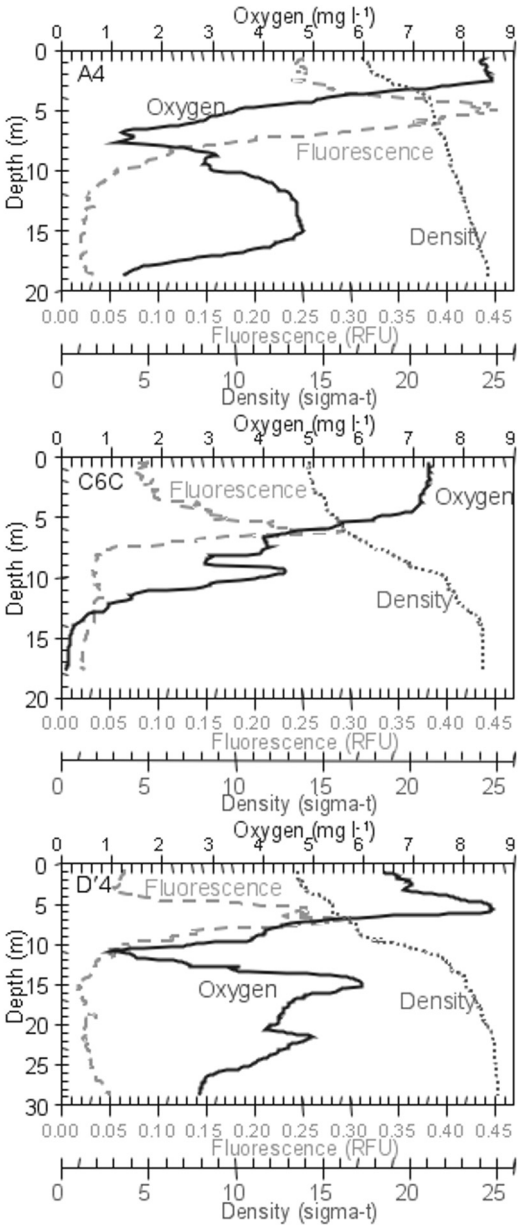

Figure 8. Examples of mid-water oxygen minima in areas of hypoxic bottom waters, July 2004. Oxygen, solid line; fluorescence, dashed line; density, dotted line. Station A4 is 37 km northwest of Southwest Pass of the Mississippi River, 20-m depth, 0035 GMT, sunrise; station C6C is 100 km west of Southwest Pass and 100 km east of the Atchafalaya River, 18-m depth, 1610 GMT, mid-morning; station D′4 is 120 km from Southwest Pass and 110 km from the Atchafalaya River, 30-m depth, 0555 GMT, midnight. Data are from a SeaBird system with SBE43 oxygen probe calibrated by Winkler titrations, derived density, and fluorescence from a Turner SCUFA. Data from: N.N. Rabalais, LUMCON.

Figure 9. Continuous bottom water dissolved oxygen in 20-m depth on the continental shelf west of the Mississippi River (April-November 1993) (mooring site in Fig. 1). The horizontal dashed line defines hypoxia. Data source: N.N. Rabalais, LUMCON.

of Louisiana shelf are similar to other areas of the world ocean. However, the suboxic conditions for the northern Gulf of Mexico are less persistent in time and space due to the dynamic nature of the open continental shelf system. Also, anoxia at the seabed is not as common or long lasting.

3.1 Hydrogen Sulfide

The occurrence of anoxia and production of H_2S in bottom waters on this shelf are limited even though the continental shelf is seasonally hypoxic over a large area and oxygen concentrations are often below 0.5 mg l^{-1}. While instrumentation may limit accuracy at levels below 0.1 mg l^{-1}, the presence of H_2S in bottom waters is a definitive indicator that the dissolved oxygen concentration is 0.0 mg l^{-1}. H_2S concentrations up to 50 μM have been measured in bottom water samples that emitted a strong odor of H_2S (N.N. Rabalais et al. unpubl.

data). H_2S concentrations of 2-5 μM were chemically detected, when there was still a faint H_2S odor. Thus, the 'odor indicator' has been used to determine the occurrence of anoxia. In a mid-summer survey of 80-90 stations, there are at most 10 stations in which the bottom water collections smelled of H_2S (N.N. Rabalais et al. unpubl. data). For the nine-station transect C, up to two stations per month in June through September can have the H_2S smell. The presence of sulfur-oxidizing bacteria at the sediment-water interface on many occasions, observed both by divers and video surveillance from remotely operated vehicles [31], indicates that extremely low oxygen concentrations, though not anoxic, commonly allow for the presence of these bacteria on the sediment surface.

3.2 Respiration and Oxygen Production

The Louisiana shelf hypoxic area, as represented by a 20-m station (mooring site, transect C, Fig. 1), is predominantly heterotrophic throughout the year [21]. The difference between bottom water oxygen deficit (measured oxygen content below the oxygen content at 100% saturation) and surface water oxygen surplus (measured oxygen content above the oxygen content at 100% saturation) is greatest in April-September.

Light conditions partially influence where hypoxic water masses are located and their severity. Extinction coefficients may be sufficiently improved at the edge of the hypoxia water mass to support benthic oxygen production. The Bierman et al. [2] model indicated that deeper light penetration might be more important with regard to hypoxia distribution in the western portion of the Louisiana shelf compared to the eastern area where the water clarity is lower (either due to suspended sediments or shading from high algal biomass). With sufficient light, photosynthesis at or near the sediment-water interface will occur and offset oxygen uptake processes to the point that anoxia does not frequently occur. The low oxygen concentration observed in respiration experiments (average 3.4 mg l^{-1}, n = 40), however, suggests that benthic oxygen production was relatively low [13].

The oxygen consumption rates in near-bottom waters were measured during several spring and summer cruises of multiple years [34, 44, 45]. Rates varied between 0.0008 to 0.29 mg O_2 l^{-1} hr^{-1}, and were sufficient to reduce the *in situ* oxygen concentration to zero in less than four weeks. The rates were inversely related to depth and decreased westward of the Mississippi River delta, consistent with the decrease in nutrients and chlorophyll *a* concentrations in surface waters. Respiration rates per unit chlorophyll *a* were highest in the spring, in shallower waters, and also closest to the Mississippi River delta. These results (1) indicate a strong vertical, rather than horizontal, coupling between oxygen consumption in bottom waters and organic loading from surface waters, and (2) are consistent with the hypothesis that the higher water column respiration

rates are driven by river-derived nutrients stimulating *in situ* organic production that sinks to the bottom layers.

Respiration in sediments is an additional oxygen sink for these waters. Dortch et al. [13] suggested that this oxygen sink may sometimes equal respiration in the overlying waters, but most results (field and modeling experiments) indicate that the sediment consumption is seldom more than one-third of the total oxygen uptake below the pycnocline. Current work by Z. Quiñones et al. (pers. comm.) with oxygen isotopes will better define these processes.

3.3 Low Redox Conditions

In general, the relationships between bottom water oxygen concentration and the concentration of dissolved inorganic nitrogen forms, phosphate and silicate are inverse (Fig. 10).

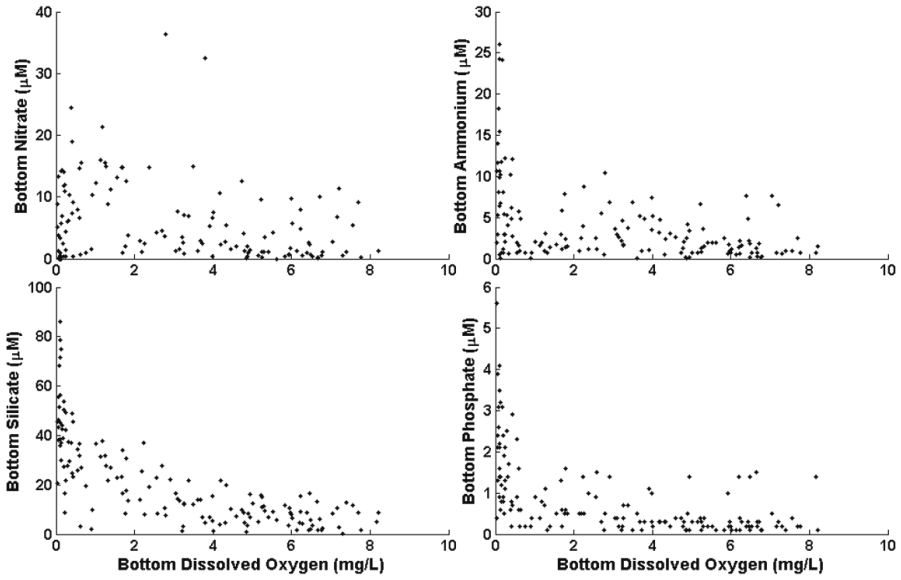

Figure 10. Comparisons of bottom water dissolved oxygen concentration and bottom water dissolved inorganic nutrient concentrations for a series of stations in 20 m depth on transect C within 1 km of each other between 1985-2002 for all months. Data source: N.N. Rabalais, LUMCON.

Most of the inorganic nitrogen is present as nitrate, but there are sometimes significant amounts of ammonium. Denitrification rates in sediments from stations within the hypoxic zone ranged between 150 and 410 μmol N m^{-2} hr^{-1} [8, 7]. The highest rates were observed when bottom water oxygen concentrations were between 1 and 3 mg l^{-1}. Denitrification activity was significantly lower at stations where dissolved oxygen was lower than 1 mg l^{-1} or greater

than 3 mg l^{-1}. Associated nutrient data indicated that the dominant form of nitrogen shifts from nitrate to ammonium as anoxia is approached (as in Fig. 10). The lower denitrification rates where oxygen was less than 1 mg l^{-1} may be due to nitrate limitation or an increase in the competitive advantage of microorganisms capable of dissimilatory nitrate reduction to ammonium. Suppression of denitrification at low oxygen concentrations will increase the residence time of bioavailable nitrogen and could act as a positive feedback mechanism in the formation of hypoxic bottom waters.

Limited data from benthic flux chambers deployed in hypoxic waters in Louisiana indicated a net flux of dissolved inorganic nitrogen into the sediments as a result of consumption of nitrate and nitrite (-1.2 mmol (NO_3^- + NO_2^-) m^{-2} d^{-1}) and an efflux of ammonium (2.5 mmol NH_4^+ m^{-2} d^{-1}) [41]. The overall net efflux of DIN was higher in waters with dissolved oxygen concentrations greater than 2 mg l^{-1} but still below saturation.

Preliminary measurements of nitrous oxide in a range of dissolved oxygen concentrations in the hypoxic area of the Louisiana shelf indicate that it is produced in low oxygen waters (M.B. Westley et al. unpubl. data). N_2O was sometimes present in waters at 5 μM O_2 or less, and its concentration was sometimes as high as two to three times higher than saturation levels. The concentration of N_2O increased with depth through a 20-m water column as dissolved oxygen declined with depth. On the other hand, Childs et al. [7] found no nitrous oxide production in any of their experimental overlying water.

Higher phosphate and silicate concentrations at the lower dissolved oxygen levels are consistent with strong fluxes from the sediments as they become anoxic or near anoxic. Higher dissolved silicate fluxes from the sediments under hypoxic bottom waters in Chesapeake Bay were related to the flux of organic matter from surface waters, but only one month after deposition events (shown as elevated sediment chlorophyll *a* concentrations) [4]. One expects then that the stations with higher silicate concentrations in bottom waters (Fig. 10) received a greater flux of silicate-based organic material in prior months.

Reduced forms of metals are often released from sediments during severe hypoxia. Mallini [25] found that dissolved Mn concentrations rapidly increased as oxygen concentrations fell below 63 μM. Extremely high dissolved Mn concentrations (1000 to 3200 μM) occurred in oxygen concentrations from 10 μM to anoxia.

The regeneration of nutrients in the lower water column or from the sediments could contribute to further nutrient-enhanced production in the upper mixed layer, if they diffuse or mix in significant amounts across the strong pycnocline present much of the year. The rates of these processes, if they occur, are not known, nor have they been estimated. Preliminary examination of vertical nutrient profiles does not indicate a transfer of high nutrients in hypoxic bottom waters into the overlying water column on the Louisiana shelf (N.N. Rabalais

et al. unpubl. data). Wind-induced mixing turned over the water column and introduced higher nutrients from the bottom into surface waters in shallow nearshore Louisiana shelf waters for a temporary enhancement of production [9]. The significance of bottom nutrient introduction to surface waters following mixing events in the hypoxic zone is not known.

4. CONSEQUENCES TO LIVING RESOURCES

Hypoxia is one manifestation of a suite of symptoms that may result from eutrophication. The effects of eutrophication, including hypoxia, are well known for some systems and include the loss of commercially important fisheries (e.g., Baltic and Black seas). The impacts of increased nutrient inputs and worsening hypoxia on overall system productivity are not well known for the Louisiana continental shelf food web. The hypoxic waters fall within an important commercial and recreational fishery zone that accounts for 25 to 30 percent of the annual coastal fisheries landings for the United States. The ability of organisms to reside, or even survive, either at the bottom or within the water column is affected as the depletion of oxygen progresses towards anoxia [31, 32]. When oxygen levels fall below critical values, those organisms capable of swimming (e.g., demersal fish, portunid crabs and shrimp) evacuate the area. Less motile fauna experience stress or die as oxygen concentrations fall to zero. Larger, longer-lived burrowing infauna are replaced by short-lived, smaller surface deposit-feeding polychaetes, and several taxa are absent from the fauna, for example, pericaridean crustaceans, bivalves, gastropods, and ophiuroids. These changes in benthic communities result in an impoverished diet for bottom-feeding fish and crustaceans and contribute, along with low dissolved oxygen, to altered sediment structure and sediment biogeochemical cycles.

Caddy [5] suggested that the fishery yield increases as nutrient loading increases, but, as the ecosystem becomes increasingly eutrophied, there is a drop in fishery yield. The benthos are the first resources to be reduced by increasing frequency of seasonal hypoxia and eventually anoxia; bottom-feeding fishes and crustaceans then decline. There is a negative relationship between the catch of brown shrimp (the largest economic fishery in the northern Gulf of Mexico) and the size of the mid-summer hypoxic zone [52]. The decadal average catch per unit effort of brown shrimp declined during the last forty years in which hypoxia was known to expand [14]. There are, however, changes in climate, river discharge, salinity of the estuary during critical development periods, acreage of nursery habitat and fishing effort that may also affect catch.

The point on the continuum of increasing nutrients versus fishery yields remains vague as to where benefits are subsumed by environmental problems that lead to decreased landings or reduced quality of production. There are indications of a shift from a demersal dominated fish community to a pelagic

dominated fish community over the last half of the 20^{th} century [6]. The pelagic food web on the Mississippi River influenced shelf has changed in the last several decades to the point where it is now poised to switch between one with, and one largely without, the diatom-zooplankton-fish food web [45]. There are also shifts in diatom community composition with implications for carbon flux [12] and increased jellyfish abundance from 1987 to 1997 [29]. While there have been no catastrophic losses in fishery resources in the northern Gulf of Mexico, the potential impacts of increasing trophic state and worsening oxygen conditions on ecologically and commercially important species and altered ecological processes warrant attention.

Acknowledgements

Funding for preparation of this manuscript was provided by the U.S. Dept. of Commerce, National Oceanic and Atmospheric Administration, Coastal Ocean Program grants to N.N. Rabalais and R.E. Turner. We thank B. Cole and A. Sapp for maintaining our data in a manner helpful to analysis of long-term trends and for assistance with the preparation of figures.

References

[1] Bennett E.M., Carpenter S.R. and Caraco N.F. Human impact on erodable phosphorus and eutrophication: a global perspective. BioScience 2001; 51:227-34.

[2] Bierman V.J. Jr., Hinz S.C., Zhu D., Wiseman W. J. Jr., Rabalais N.N. and Turner R.E. A preliminary mass balance model of primary productivity and dissolved oxygen in the Mississippi River Plume/Inner Gulf shelf region. Estuaries 1994; 17:886-99.

[3] Boesch D.F. Challenges and opportunities for science in reducing nutrient over-enrichment of coastal ecosystems. Estuaries 2002; 25:886-900.

[4] Boynton W.R. and Kemp W.M. "Influence of river flow and nutrient loads on selected ecosystem processes. A synthesis of Chesapeake Bay data." In: *Estuarine Science: A Synthesis Approach to Research and Practice*, Hobbie J.E. ed., Washington, DC: Island Press, 2000.

[5] Caddy J.F. Toward a comparative evaluation of human impacts on fishery ecosystems of enclosed and semi-enclosed seas. Reviews in Fisheries Science 1993; 1:57-95.

[6] Chesney E.J. and Baltz D.M. "The Effects of Hypoxia on the Northern Gulf of Mexico Coastal Ecosystem: A Fisheries Perspective" In: *Coastal Hypoxia: Consequences for Living Resources and Ecosystems*, Rabalais N.N., Turner R. E. eds., Coastal and Estuarine Studies 58, Washington, DC: American Geophysical Union, 2001.

[7] Childs C.R., Rabalais N.N., Turner R.E. and Proctor L.M. Sediment denitrification in the Gulf of Mexico zone of hypoxia. Mar Ecol-Prog Ser 2002; 240:285-90.

[8] Childs C.R., Rabalais N.N., Turner R.E. and Proctor L.M. Erratum. Mar Ecol-Prog Ser 2003; 247:310.

[9] Dagg M.J. Physical and biological responses to the passage of a winter storm in the coastal and inner shelf waters of the northern Gulf of Mexico. Cont Shelf Res 1988; 8:167-78.

[10] Diaz R.J. and Rosenberg R. Marine benthic hypoxia: A review of its ecological effects and the behavioural responses of benthic macrofauna. Oceanogr Mar Biol Annual Review 1995; 33:245-303.

[11] Donner S.D., Coe M.T., Lenters J.D., Twine T.E. and Foley J.A. Modeling the impact of hydrological changes on nitrate transport in the Mississippi River Basin from 1955 to 1994. Global Biochem Cy 2002; 16(3)10.1029/2001GB001396.

[12] Dortch Q., Rabalais N.N., Turner R.E. and Qureshi N.A. "Impacts of changing Si/N ratios and phytoplankton species composition." In: *Coastal Hypoxia: Consequences for Living Resources and Ecosystems*, Rabalais N.N., Turner R. E. eds., Coastal and Estuarine Studies 58, Washington, DC: American Geophysical Union, 2001.

[13] Dortch Q., Rabalais N.N., Turner R.E. and Rowe G.T. Respiration rates and hypoxia on the Louisiana shelf. *Estuaries* 1994; 17:862-72.

[14] Downing J.A. (chair), Baker J.L., Diaz R.J., Prato T., Rabalais N.N. and Zimmerman R.J. Gulf of Mexico Hypoxia: Land-Sea Interactions. Council for Agricultural Science and Technology, Task Force Report No. 134, 1999.

[15] Dunn D.D. Trends in Nutrient Inflows to the Gulf of Mexico from Streams Draining the Conterminous United States 1972 – 1993. U.S. Geological Survey, Water-Resources Investigations Report 96—4113, Prepared in cooperation with the U.S. Environmental Protection Agency, Gulf of Mexico Program, Nutrient Enrichment Issue Committee. Austin, TX: U.S. Geological Survey, 1996.

[16] Eadie B.J., McKee B.A., Lansing M.B., Robbins J.A., Metz S. and Trefry J.H. Records of nutrient-enhanced coastal productivity in sediments from the Louisiana continental shelf. Estuaries 1994; 17:754-65.

[17] Goolsby D.A., Battaglin W.A., Lawrence G.B., Artz R.S., Aulenbach B.T., Hooper R.P., Keeney D.R. and Stensland G. J. Flux and Sources of Nutrients in the Mississippi-Atchafalaya River Basin, Topic 3 Report for the Integrated Assessment of Hypoxia in the Gulf of Mexico. NOAA Coastal Ocean Program Decision Analysis Series No. 17. Silver Spring, MD: NOAA Coastal Ocean Program, 1999.

[18] Harper D.E. Jr., McKinney L.D., Nance J.M. and Salzer R.R. "Recovery responses of two benthic assemblages following an acute hypoxic event on the Texas continental shelf, northwestern Gulf of Mexico." In: *Modern and Ancient Continental Shelf Anoxia*, Tyson R.V., Pearson T.H. eds., London: Geol Soc Spec Publ No. 58, 1991.

[19] Helly J.J. and Levin L.A. Global distribution of naturally occurring marine hypoxia on continental margins. Deep-Sea Res Pt I 2004; 51:1159-68.

[20] Howarth R.W., Billen G., Swaney D., Townsend A., Jaworski N., Lajtha K. Downing J.A., Elmgren R., Caraco N., Jordan T., Berendse F., Freney J., Kudeyarov V., Murdoch P. and Zhao-Liang Z. Regional nitrogen budgets and riverine N & P fluxes for the drainages to the North Atlantic Ocean: Natural and human influences. Biogeochemistry 1996; 35:75-139.

[21] Justić D., Rabalais N.N. and Turner R.E. "Riverborne nutrients, hypoxia and coastal ecosystem evolution: Biological responses to long-term changes in nutrient loads carried by the Po and Mississippi Rivers." In: *Changes in Fluxes in Estuaries: Implications from Science to Management*, Dyer K.R., Orth R.J. eds., Fredensborg, Denmark: Olsen & Olsen, 1994.

[22] Justić D., Rabalais N.N. and Turner R.E. Modeling the impacts of decadal changes in riverine nutrient fluxes on coastal eutrophication near the Mississippi River Delta. Ecol Model 2002; 152:33-46.

[23] Justić D., Turner R.E. and Rabalais N.N. Climatic influences on riverine nitrate flux: Implications for coastal marine eutrophication and hypoxia. Estuaries 2003; 26:1-11.

[24] Kamykowski D. and Zentara S.J. Hypoxia in the world ocean as recorded in the historical data set. Deep-Sea Res 1990; 37:1861-74.

[25] Mallini L.J. Development of kinetic-colorimetric flow analysis techniques for determining dissolved manganese and iron and an assessment of the behavior of dissolved manganese in the far-field plume of the Mississippi River. Masters Thesis, University of Southern Mississippi, 1992.

[26] Meade R.H. ed. Contaminants in the Mississippi River, 1987-92. U.S. Geological Survey Circular 1133. Denver, CO: U.S. Geological Survey, 1995.

[27] Nixon S.W. Coastal marine eutrophication: A definition, social causes, and future concerns. Ophelia 1995; 41:199-219.

[28] Pokryfki L. and Randall R.E. Nearshore hypoxia in the bottom water of the northwestern Gulf of Mexico from 1981 to 1984. Mar Environ Res 1987; 22:75-90.

[29] Purcell J.E., Breitburg D.L., Decker M.B., Graham W.M. and Youngbluth M.J. "Pelagic cnidarians and ctenophores in low dissolved oxygen environments." In: *Coastal Hypoxia: Consequences for Living Resources and Ecosystems*, Rabalais N.N., Turner R.E. eds., Coastal and Estuarine Studies 58, Washington, DC: American Geophysical Union, 2001.

[30] Rabalais N.N. An Updated Summary of Status and Trends in Indicators of Nutrient Enrichment in the Gulf of Mexico. Environmental Protection Agency Publ. No. EPA/800-R-92-004. Stennis Space Center, MS: Gulf of Mexico Program, Nutrient Enrichment Subcommittee, 1992.

[31] Rabalais N.N., Harper D.E. Jr. and Turner R.E. "Responses of nekton and demersal and benthic fauna to decreasing oxygen concentrations." In: *Coastal Hypoxia: Consequences for Living Resources and Ecosystems*, Rabalais N.N. and Turner R.E. eds., Coastal and Estuarine Studies 58. Washington, DC: American Geophysical Union, 2001a.

[32] Rabalais N.N., Smith L.E., Harper D.E. Jr. and Justić D. "Effects of Seasonal Hypoxia on Continental Shelf Benthos." In: *Coastal Hypoxia: Consequences for Living Resources and Ecosystems*, Rabalais N.N. and Turner R.E. eds., Coastal and Estuarine Studies 58. Washington, DC: American Geophysical Union, 2001b.

[33] Rabalais N.N. and Turner R.E. "Hypoxia in the Northern Gulf of Mexico: Description, causes and change." In: *Coastal Hypoxia: Consequences for Living Resources and Ecosystems*, Rabalais N.N., Turner R.E. eds., Coastal and Estuarine Studies 58, Washington, DC: American Geophysical Union, 2001.

[34] Rabalais N.N., Turner R.E., Dortch Q., Justić D., Bierman V.J. Jr. and Wiseman W.J. Jr. Review. Nutrient-enhanced productivity in the northern Gulf of Mexico: past, present and future. Hydrobiologia 2002b; 475/476:39-63.

[35] Rabalais N.N., Turner R.E., Justić D., Dortch Q. and Wiseman W.J. Jr. Characterization of Hypoxia: Topic 1 Report for the Integrated Assessment of Hypoxia in the Gulf of Mexico. NOAA Coastal Ocean Program Decision Analysis Series No. 15. Silver Spring, MD: NOAA Coastal Ocean Program, 1999.

[36] Rabalais N.N., Turner R.E., Justić D., Dortch Q. and Wiseman W.J. Jr. Nutrient changes in the Mississippi River and system responses on the adjacent continental shelf. Estuaries 1996; 19:386-407.

[37] Rabalais N.N., Turner R.E. and Scavia D. Beyond science into policy: Gulf of Mexico hypoxia and the Mississippi River. BioScience 2002a; 52:129-42.

[38] Rabalais N.N., Turner R.E., Wiseman W.J. Jr. and Boesch D.F. "A brief summary of hypoxia on the northern Gulf of Mexico continental shelf: 1985—1988." In: *Modern and Ancient Continental Shelf Anoxia*, Tyson R.V., Pearson T.H. eds., London: Geol Soc Spec Publ No. 58, 1991.

[39] Rabalais N.N., Wiseman W.J. Jr. and Turner R.E. Comparison of continuous records of near-bottom dissolved oxygen from the hypoxia zone of Louisiana. Estuaries 1994; 17:850-61.

[40] Renaud M. Hypoxia in Louisiana coastal waters during 1983: implications for fisheries. Fish B-NOAA 1986; 84:19-26.

[41] Rowe G.T., Cruz Kaegi M.E., Morse J.W., Boland G.S. and Escobar Briones E.G. Sediment community metabolism associated with continental shelf hypoxia, northern Gulf of Mexico. Estuaries 2002; 25:1097-1106.

[42] Scavia D., Rabalais N.N., Turner R.E., Justić D. and Wiseman W.J. Jr. Predicting the response of Gulf of Mexico hypoxia to variations in Mississippi River nitrogen load. Limnol Oceanogr 2003; 48:951-56.

[43] Seitzinger, S.P., Kroeze C., Bouwman A.F., Caraco N., Dentener F. and Styles R.V. Global patterns of dissolved inorganic and particulate nitrogen inputs to coastal systems: recent conditions and future projections. Estuaries 2002; 25:640-55.

[44] Turner R.E. and Allen R.L. Bottom water oxygen concentration in the Mississippi River Delta Bight. Contrib Mar Sci 1982; 25:161-72.

[45] Turner R.E., Qureshi N., Rabalais N.N., Dortch Q., Justić D. and Cope J. Fluctuating silicate:nitrate ratios and coastal plankton food webs. Proceedings of the National Academy of Science, USA 1998; 95:13048-51.

[46] Turner R.E. and Rabalais N. N. Linking landscape and water quality in the Mississippi River basin for 200 years. BioScience 2003; 53:563-72.

[47] Turner R.E. and Rabalais N.N. Changes in Mississippi River water quality this century. Implications for coastal food webs. BioScience 1991; 41:140-48.

[48] Turner R.E. and Rabalais N.N. Coastal eutrophication near the Mississippi river delta. Nature 1994; 368:619-21.

[49] Turner R.E., Rabalais N.N., Swenson E.M., Kasprzak M. and Romaire T. Summer hypoxia in the northern Gulf of Mexico and its prediction from 1978 to 1995. Mar Environ Res 2005; 59:65-77.

[50] Vitousek P.M., Abler J.D., Howarth R.W., Likens G.E., Matson P.A., Schindler D.W., Schlesinger W.H. and Tilman D.G. Human alterations of the global nitrogen cycle: Sources and consequences. Ecol Appl 1997; 7:737-50.

[51] Wiseman W.J. Jr., Rabalais N.N., Turner R.E., Dinnel S.P. and MacNaughton A. Seasonal and interannual variability within the Louisiana Coastal Current: Stratification and hypoxia. J Marine Sys 1997; 12:237-48.

[52] Zimmerman R.J. and Nance J.M. "Effects of hypoxia on the shrimp fishery of Louisiana and Texas." In: *Coastal Hypoxia: Consequences for Living Resources and Ecosystems*, Rabalais N.N. and Turner R.E. eds., Coastal and Estuarine Studies 58, Washington, DC: American Geophysical Union, 2001.

ECOLOGICAL CONSEQUENCES OF ANOXIC EVENTS AT THE NORTH-WESTERN BLACK SEA SHELF

Yu. P. Zaitsev

Odessa Branch, Institute of Biology of the Southern Seas (OB IBSS) 37, Pushkinskaya Street, 65011 Odessa, Ukraine

Abstract The Black Sea, due to its geographical position and large drainage basin, morphometry and effective isolation, is one of the most characteristic examples of impacted marine areas. The main kind of man-made influence on the Black Sea ecosystem is the anthropogenic eutrophication. The main consequences of this impact during the period 1950-2000: excessive blooms of algae, decline in water transparency, depletion of oxygen in near-bottom layers of water on the North-western Black Sea shelf and cases of mass mortalities of benthic organisms are discussed.

Keywords: Black Sea, North-western shelf, eutrophication, hypoxia, anoxia, mass mortality.

1. INTRODUCTION

As a rule, development of hypoxic zones on the shelf is among the ecological consequences of man-made eutrophication. System-specific factors appear to modulate the response to the changes in nutrient load with some systems such as the Black Sea, Baltic Sea, northern Gulf of Mexico (Rabalais and Turner, present volume) to be very sensitive, while others such as San Francisco Bay, a number of estuarine systems around Europe are more 'robust' towards nutrient enrichment. Density stratification usually accelerates eutrophication effects. Among direct and indirect ecosystem responses are water transparency loss, vascular plants and macroalgae biomass changes, changes in nutrient regeneration, frequency of toxic/harmful algae blooms, habitat worsening for metazoans and pelagic and benthic invertebrates [4].

Up to the 1950s, phytoplankton blooms in the Black Sea were sporadic and unusual events, restricted to narrow coastal zones in the river mouth areas [19] and were described at first as exceptional natural phenomena. Titles of related articles of that time are enough indicative: "An interesting case of Black Sea surface water coloration" [12] or "A special case of Black Sea water blooming in spring 1959" [2]. Thanks to these and other relevant publications of specialists,

L. N. Neretin (ed.), Past and Present Water Column Anoxia, 247–256.

for example [6], we are able to consider the 1950s as a period of "ecological norm".

Until the middle 1960s, the most productive area of the Black Sea, its Northwestern shelf (NWS), in terms of biological diversity, biomass and biological productivity, was considered the principal "nursery" of the sea and the area of the most important stocks of commercial species of algae, invertebrates and fish and traditional fisheries [18]. In the manuscript I present an overview of the ecosystem changes on the NWS due to increased eutrophication such as water transparency, harmful algal blooms, the extent of hypoxic zone, and discuss structural changes in pelagic and benthic communities. The analysis showed deterioration of many ecosystem parameters and components during 1960s-1980s. In the late 1990s some signs of recovery of the NWS habitats were observed. Continuing monitoring of chemical parameters and biodiversity studies of the NWS are particularly important since the area is the key zone of the Black Sea in terms of its biological resources and their reproduction.

2. MAN-MADE EUTROPHICATION

First considerable changes in the Black Sea ecosystem, associated with man-made or cultural eutrophication, were noted in the NWS area in the late 1960s and early 1970s. Now it is obvious, that the main reason of these changes was the river runoff, because the largest Black Sea Rivers – Danube, Dnister and Dniper – are discharging just in this area.

It was established, that during the 1970s and 1980s, the influx of river-borne nutrients into the NWS area was considerably increased [3]. For example, the average influx of ammonium nitrogen in 1950-1960 was 52.2 thousand metric tones per year, and in 1986-1989, 206.4 thousand metric tones per year. Nitrite influx was 2.8 and 15.4 thousand tones per annum respectively, phosphates 14.6 and 69.8 (same units) and organic phosphorus 7.8 and 35.8 (same units).

As a result of these trends, the NWS area of the Black Sea became the largest heavily eutrophic (hypertrophic) marine zone in the whole Mediterranean basin [17].

It is generally accepted, that changes in phytoplankton communities, species diversity, number and biomass, are directly related to changes in the composition and concentration of the nutrient supply.

As a general rule, the most favored species in eutrophic conditions are the small-size planktonic algae such as *Dinoflagellates, Coccolithophores, Euglenoids* and some other. The average biomass in the NWS area of the Black Sea in the 1950s, 1960s, 1970s and 1980s was 670 $mg.m^{-3}$, 1,030 $mg.m^{-3}$, 18,690 $mg.m^{-3}$ and 30,000 $mg.m^{-3}$ respectively [7, 9, 11].

During major algal blooms, the phytoplankton community can become dominated by a single species to the near exclusion of others. These "red", "green"

or "brown" tides, so called because the algae are abundant enough to discolor the water, were described in different marine areas [5], but the Black Sea is especially rich in such examples. The first description of a large-scale red tide in the Black Sea, produced by mass development of Dinoflagellate *Prorocentrum cordatum* (syn. *Exuviaella cordata*) was given by Nesterova [10]. In August-September 1973, the density of this species attained 280 million cells.l^{-1}, representing 95 % of the total phytoplankton biomass. In 1983-1988, 24 cases of "monospecific" blooms in the Romanian NWS zone were recorded.

3. WATER TRANSPARENCY

Increasing in number of unicellular algae and detritus (composed mainly from dead phytoplankton) is an important reason of changes in marine and fresh water transparency. The reduction of Black Sea water transparency which began in the early 1970s [16] is a direct consequence of the increased density of suspended planktonic organisms, their external metabolites and detritus. The clouding of seawater, arising from the increased turbidity, especially in the NWS area, is well known to divers, underwater photographers and fishermen. Some areas of the Black Sea have now lost their former aesthetic attraction for tourists and photographers. However, the most serious consequences for the marine ecosystem were the biological effects, produced by the decreased water transparency.

Before these events, in the 1960s, Secchi disk readings of 15-18 m were recorded in offshore NWS waters. At a distance of 1 km from the shore the readings were 6-7 m. In the 1970s and 1980s, Secchi disk readings were 7-8 m and 2-2.5 m respectively for these two areas [18]. This implies that in the 1960s, the compensation point (the depth below which marine plants release more organic matter in respiration than they accumulate during photosynthesis because of the low light intensity) was situated at 45-55 m depth in the offshore NWS area and at 18-20 m depth in the near-coastal zone. In the 1970s, the depth of compensation point decreased to 20-25 m in the offshore shelf and to 6-8 m near the coasts.

In the 1970s, light illumination at depths of 25 m and more in the offshore areas and at depths of 8 m and more in coastal zone became a limiting factor for bottom macroalgal communities. This was the main reason for the sharp decline of the famous "Zernov's *Phyllophora* field" (an extensive meadow of red algae, harvested for the agaroids) in the central part of the NWS. In the 1950s, the area occupied by *Phyllophora* was 10,000 km^2, with a total biomass of algae of about 10,000,000 t. Toward 1980s, this area had diminished to 3,000 km^2 and biomass had declined to 1,400,000 t. In the early 1990s, these values had declined even further to 500 km^2 and 500,000 t respectively [18]. At that

same time another small *Phyllophora* field, situated at 10-15 m depth in eastern part of the NWS has continued its normal development.

Such a disastrous reduction of the Zernov's *Phyllophora* field means not only loss of commercially valuable "agar weed" stocks, but the disappearance of a large bottom biocoenosis with a specific red-colored fauna (*Phyllophora* fauna) and the loss of an important source of oxygen. According to some data, these seaweeds, in the period of their normal development, excreted in the bottom layers up to 2 Mio. m^3 of oxygen per day.

4. HYPOXIA AND ANOXIA IN NEAR-BOTTOM LAYERS OF WATER

At the beginning of the 1970s, the rate of sedimentation of dead planktonic organisms (mainly phytoplankton) to the seabed was found to be 15-20 times more than that observed in the 1950s. Decomposition of dead organic material requires oxygen dissolved in the water. As a result, the amount of oxygen consumed during the decomposition this organic fall-out increased and zones of hypoxia and anoxia began to appear on the shelf, first of all, in areas with pronounced stratification of water layers. This new environmental phenomenon in the Black Sea was first observed during a cruise of Odessa Branch IBSS RV "Miklukho-Maklay" in August-September 1973 [16]. Then, between the Danube river delta and the Dnister river estuary, over a surface area of 3,500 km^2 at depths from 10 to 20 m, a mass mortality of benthic invertebrates and fishes from hypoxia occurred. In more recent years, cases of mass mortality of benthic organisms from hypoxia have become ordinary phenomena, with scales depending on the meteorological, hydrological, chemical and biological peculiarities of summer season (Fig. 1).

Among the most common victims of hypoxia are practically all species of bottom invertebrates and fish. Among them there are mollusks (*Mytilus, Cerastoderma, Mya, Abra*), barnacles (*Balanus, Chtamalus*), shrimps (*Crangon, Palaemon*), ghost shrimps (*Upogebia, Calianassa*), crabs (*Carcinus, Macropipus, Pilumnus*), tunicates (*Botryllus*), and among fishes – species of gobies (*Gobiidae*), flatfishes (*Soleidae, Pleuronectidae, Scopthalmidae*), sturgeons (*Acipenseridae*). River damming was the additional factor for the decline in migratory fish stocks such as e.g., sturgeon stocks. Only few species of invertebrates: foraminiferans (*Ammonia tepida*), polychaets (*Nereis diversicolor, Melinna palmata*), mollusks (*Scapharca inaequivalvis*), nematods (species of *Desmoscolex, Tricoma* and *Cobbionema* genera) can survive for longer periods in the absence of dissolved oxygen.

The biological losses due to hypoxia and anoxia on the NWS are estimated at 100 to 200 t of animals per km^2 of seabed. In some years, areas depleted in oxygen reached 30,000-40,000 km^2 (Fig. 1). The total biological losses over 18 years, from 1973 to 1990, are estimated at 60 million tones, including 5 million

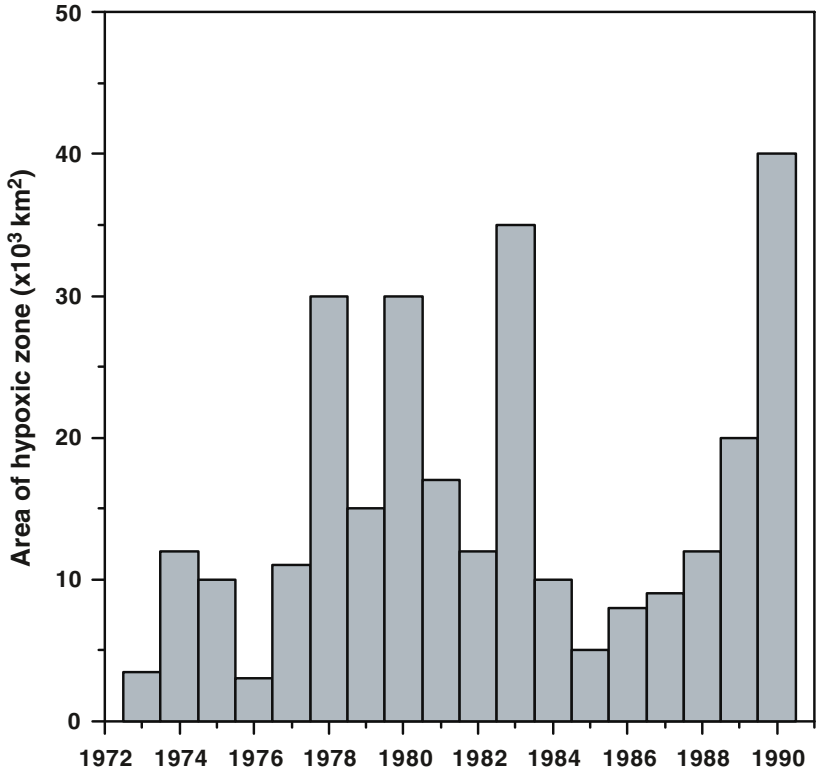

Figure 1. Surfaces of hypoxic zones (dissolved O_2 <= 2 mg.l^{-1}) on the North-western Black Sea shelf in 1973-1990.

tones of fish, both commercial and not commercial species, adult specimens and fry [20].

In autumn season, due to lowering in water temperature, disappearance of a strong pycnocline and turbulent mixing, bottom waters are re-oxygenated and life begins to return. Pelagic larvae of benthic organisms from the edge of the sea and shelf elevations settle down and give rise to new generations of animals, which develop until the next episode of hypoxia occurs next summer, or in two-three years. That is why the populations of benthic invertebrates and fish, except for the inhabitants of coastal marginal biotopes, are markedly young. Now it is very difficult to find old specimens. Overall, the stocks of benthos on the NWS have greatly decreased, including important commercial species – mussels, oysters, shrimps, and other invertebrates, as well as vertebrates turbot, flounder, gobies, sturgeons and other fish.

The following example illustrates the magnitude of the problem. At the beginning of the twentieth century, the Odessa Gulf and adjacent NWS areas were nicknamed "Kingdom of mussels" [19]. In the 1950s and 1960s, these mus-

sels, in canned form, were exported to Mediterranean markets. Today Odessa shops advertise foreign canned mussels, but not local mollusks. The reason of such a conversion of an exporter into an importer are not only the successful free-market relations in the Ukraine, but the drastic fall in commercial stocks of mussels on the NWS caused by deoxygenation of bottom water, which has been produced by man-made eutrophication.

The ecological situation in other shelf areas of the Black Sea, out of zones of strong impact of the river runoff, is better, but the largest NWS area, is a key zone in terms of biological resources of the Black Sea and their reproduction. This is the most productive area of the Black Sea regarding benthic and pelagic species. Until recently, this area produced more than 95% of all the standing stock of the red algae *Phyllphora nervosa* and *P. brodiaei*, the seagrasses *Zostera marina* and *Z. noltii* and the blue mussel *Mytilus galloprovincialis*; more than 90% of the turbot *Psetta maeotica*, the flounder *Platichthys flesus luscus*, and the mackerel *Scomber scombrus*; about 70% of the spiny dogfish *Squalus acanthias*, the thornback ray *Raja clavata*, the sprat *Sprattus sprattus phalericus*, the Black Sea shad *Alosa kessleri pontica*, the whiting *Merlangius merlangus euxinus*, and gobies (species of Gobiidae family); about 60% of the anchovy *Engraulis incrasicholus ponticus* and the horse mackerel *Trachurus mediterraneus ponticus*; and other fish, including sturgeons (Acipenseridae) were concentrated in this area. Therefore the NWS was an area for traditional harvesting of fish, marine mammals, mussels, *Phyllophora* and other biological resources.

In the late 1990s, some signs of recovery of the NWS and Black Sea ecosystems were observed. Some species of invertebrate and fish, considered to be rare or even extinct and inscribed into Black Sea Red Data Book [1], became quite common. According to author's observations, among them there are hermit crab (*Diogenes pugilator*), crabs *(Carcinus aestuarii* and *Pilumnus hirtellus*), bottom fishes, sole (*Solea nasuta*), dragonet (*Callionymus belenus*), sea horse (*Hippocampus ramulosus*), turbot (*Psetta maeotica*) and some other species.

In September-October 2003, during an international cruise of RV "Academic", in the frame of the UNDP-GEF Black Sea Ecosystem Recovery Project, comprehensive investigations of bottom organisms on the North-western and Western Black Sea shelves, under the guidance of the well-known specialist of the bottom fauna, Professor M.T. Gomoiu, were carried out. According to preliminary assessments, obvious evidences of a mass mortality of benthic organisms in this year were not registered (Prof. L.V. Vorobyova, personal communication).

5. BLACK SEA MARGINAL HABITATS IN EUTROPHICATION CONDITIONS

The distribution of normoxic, oligoxic and anoxic [8] habitats on the NWS is the main determining environmental factor in eutrophication conditions. Usually, oligoxic (having reduced levels of oxygen) and anoxic (devoid of oxygen) areas on the NWS occurs at depths from 7-10 to 35-40 m. Normoxic habitats (having normal level of oxygen) remain in the narrow coastal zone from the shore to 7-10m and in the deeper shelf zone from 40m to the upper level of the permanent anoxic zone at 130-130m depth.

The first zone (from the shore to the 7-10m depth) in spring, summer and autumn seasons is the most important in terms of numbers, biomass, productivity and diversity of plant and animal species. The appearance of hydrogen sulphide in this habitat is an exceptional and short-term event during wind-driven coastal upwelling. This is the reason that near-coastal biotopes are inhabited by a large variety of algae, mollusks crustaceans, worms and other invertebrates and coastal fish. There has even been a considerable increase in the populations of some invertebrates such as the amphipod, *Pontogammarus maeoticus* and the small pelagic coastal fish such as the silverside, *Atherina mochon pontica*, sand lance, *Gymnammodites cicerellus*, gobies such as the round goby, *Neogobius melanostomus*, Blenniidae species. Schools of young and adult silversides, migrating just near the shoreline, are very dense numbering up to one-two thousand of fish per one cubic meter of water. Such rich food attracts pelagic predators to the shore and during recent years there has been a successful hook fishery of the garfish, *Belone belone euxini*, bluefish, *Pomatomus saltator*, and even the rare Black Sea salmon, *Salmo trutta labrax*. This is a new kind of recreational fishery in the Odessa Gulf and other coastal areas, and one of very few positive consequences of its man-made eutrophication.

6. THE CRITICAL 1970s

The major recurrent phytoplankton blooms, events of hypoxia and anoxia in the 1970s were not limited to the Black Sea. Similar events from the late 1960s to early 1980s were noted in the Baltic Sea, Southern North Sea, Northern Adriatic Sea, the Persian Gulf, the Inland Sea of Japan, the Gulf of Mexico, New York Bight [5], Elands Bay in South Africa [14], the Bay of Fundy in Canada [15] and other coastal areas.

Such a coincidence in time of similar ecological events in different coastal marine areas suggests that there may be a common causative factor influencing eutrophication on a global scale. There are reasons to believe that this factor was the sudden global increase in economic activity in the 1960s. One of ecologically important manifestations of this activity was the Indicative World Plan (IWP) for agricultural development, which has been named the “Green

Revolution". Its aim was to increase the production and availability of food. The IWP proved to be highly effective, but one of its environmental consequences was the sharp increase in the nutrient influx to different water bodies, including inland seas and coastal marine waters. The global consumption of nitrogen and phosphorus fertilizers has greatly increased during last several decades (Fig. 2).

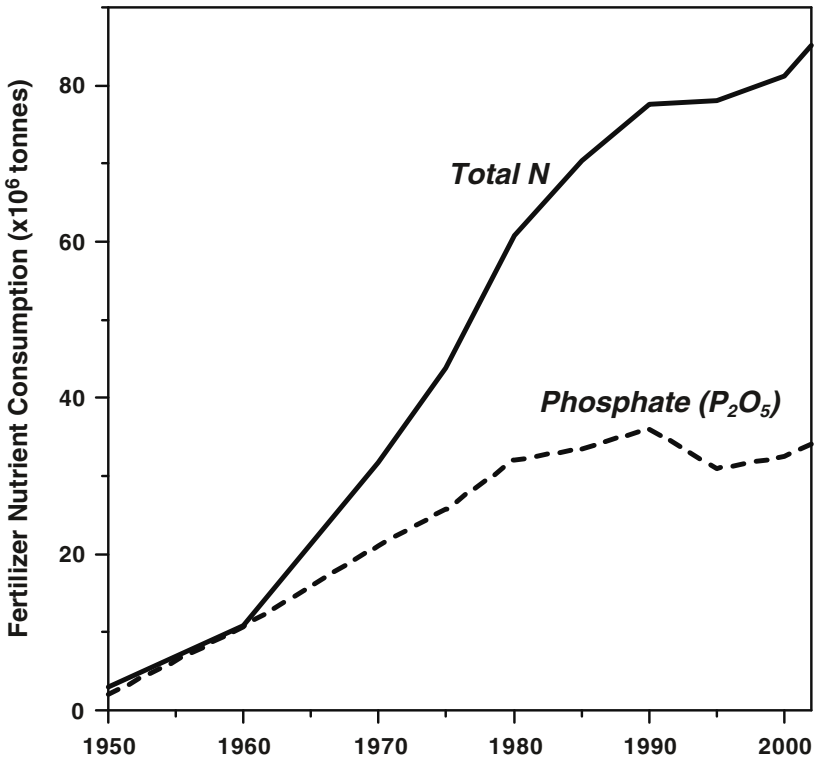

Figure 2. World's nitrogen (N) and phosphate (P_2O_5) fertilizer consumption in 1960-2003 [13].

It is evident that there was a sharp increase in fertilizer use in the 1960s, 1970s and 1980s and stabilization at the high level after 1990s [13]. The fertilizers use trend in the world resembles the trend in phytoplankton blooms in some marine coastal waters. This is a major reason why the 1970s was a crucial period for marine ecosystems. In marine ecology it is therefore quite realistic to call this period "the critical 1970s" [19]. The Black Sea, due to its geographical position and large drainage basin, its morphometry and high isolation from the World Ocean, is the most strongly pronounced example in this respect, but the event was not an entirely exceptional one.

References

[1] *Black Sea Red Data Book*. Dumont H.J. ed., New York: UN Office for Project Services, 1999.

[2] Bodeanu N. and Chirila V. Un caz aparte de "inflorire" a apei in Marea Neagra in primavera anului 1959. Comunicarile Academiei RPR 1960; 10(8):681-686 (in French).

[3] Bronfman A.M., Vorobyova L.V. and Garkavaya G.P. "Main features and tendencies of anthropogenic changes in the ecosystems of the North-western Black Sea shelf." In: *Proceedings of the Black Sea Symposium Ecological Problems and Economical Prospects* Istanbul: Turkey, 1991 September 16-18.

[4] Cloern J.E. Our evolving conceptual model of the coastal eutrophication problem. Marine Ecol Progr Series 2001; 210:223-53.

[5] *Global marine biological diversity. A strategy for building conservation into decision making*, Norse E.A. ed., Washington D.C., Island Press, 1993.

[6] Ivanov O.I. On the mass development of phytoplankton organisms in the North-western part of the Black Sea in 1954-1956. Naukovi zapisky Odesk. Boil. St. 1959; 1:6-25 (in Russian).

[7] Ivanov A.I. "Phytoplankton." In: *Biology of the North-western part of the Black Sea*, Vinogradov K.A. ed., Kiev: Naukova Dumka, 1967 (in Russian).

[8] Lincoln R.J., Boxhall G.A. and Clark P.F. *A Dictionary of Ecology, Evolution and Systematics*. Cambridge: Cambridge University Press, 1985.

[9] Mashtakova G.P. "Influence of the river runoff on the productivity of phytoplankton in the North-western part of the Black Sea." In: *Proceedings of the Conference Perspectives of Black Sea fisheries Development*, Odessa: USSR, 1971 September 13-17.

[10] Nesterova D.A. Development of the Peridinean Exuviaella cordata and "red tide" phenomenon in the North-western part of the Black Sea. Biologya morya 1979; 5:24-29 (in Russian).

[11] Nesterova D.A. Features of phytoplankton successions in the North-western part of the Black Sea. Hydrobiologicesky zhurnal 1987; 23:16-21 (in Russian).

[12] Skolka H. and Petranu A. Un caz interesant de colorare a apei siperficiale a Marii Negre. Biol Anim 1960; 12:175-80 (in French).

[13] Total fertilizer consumption statistics by region from 1960 to 2003 compiled by International Fertilizer Association. `http://www.fertilizer.org/ifa/statistics.asp`.

[14] Villier G. Recovery of a population of white mussel, *Donax swrra* at Eland Bay, South Africa, following a mass mortality. Fisheries Bulletin (South Africa Sea Fisheries Branch) 1979; 12:69-74.

[15] White A.W. Recurrence of kills of Atlantic herring (*Clure harengus*) caused by Dinoflagellate toxins transferred through herbivorous zooplankton. Canada of Fisheries and Aquatic Science. 1980; 37:2262-65.

[16] Zaitsev Yu.P. The North-western part of the Black Sea as a subject matter of recent hydrobiological studies. Biologya morya 1977; 43:3-7 (in Russian).

[17] Zaitsev Yu.P. Cultural eutrophication of the Black Sea and other South European Seas. La mer 1991; 1:1-7.

[18] Zaitsev Yu.P. Recent changes in the trophic structure of the Black Sea. Fisheries Oceanography 1992; 1:180-89.

[19] Zaitsev Yu.P. "Eutrophication of the Black Sea and Its Major Consequences." In: *Black Sea Pollution Assessment*, Mee L.D. and Topping G. eds., New York: United Nations Publications, 1998.

[20] Zaitsev Yu.P. Impact of Eutrophication on the Black Sea fauna. GFCM (FAO) Studies and Reviews 1993; 64:59-86.

III

BIOGEOCHEMISTRY AND MICROBIOLOGY OF THE NITROGEN CYCLE

NITROGEN CYCLING IN SUBOXIC WATERS: ISOTOPIC SIGNATURES OF NITROGEN TRANSFORMATION IN THE ARABIAN SEA OXYGEN MINIMUM ZONE

Joseph P. Montoya[1] and Maren Voss[2]

[1] *School of Biology, Georgia Institute of Technology, 311 Ferst Dr., Atlanta, GA 30332, USA*

[2] *Baltic Sea Research Institute Warnemünde, Seestrasse 15, 18119 Rostock, Germany*

Abstract The natural abundance of the stable isotopes of nitrogen provides a powerful in situ tracer for N cycle processes in and around suboxic zones. Denitrification in the suboxic zone of the Arabian Sea raises the $\delta^{15}N$ of the residual nitrate, which is mixed into the surface layer during periods of deep convection and upwelling. Complete assimilation of available nitrate during primary production transfers this isotopic signature into surface particulate matter, which then contributes to the flux of sinking organic matter. A small fraction of the nitrogen is ultimately deposited on the seafloor with an isotopic signature well above the $\delta^{15}N$ of average oceanic NO_3^-. We illustrate the patterns in isotopic variation of organic matter in and near one of the major oceanic suboxic zones with data from the German JGOFS cruise in the Arabian Sea in May-June 1995. On this cruise, we collected samples of particulate organic matter and nutrients along a transect on 65°E between 21°N and the equator. Interestingly, we also encountered a massive bloom of N_2-fixing cyanobacteria during this cruise. This bloom introduced isotopically depleted N into upper water column particles as well as sinking organic matter. Nonetheless, we found enriched nitrogen isotope values in suspended particles throughout the upper 1500m of the water column as far south as the equator. This lateral spread of the isotopic signature of denitrification is of obvious importance in paleoceanographic studies of the nitrogen cycle, as is the interaction between N_2-fixation and denitrification in setting the isotopic composition of organic matter in the water column.

Keywords: Denitrification, marine nitrogen cycle, stable isotope biogeochemistry, N_2-fixation

1. INTRODUCTION AND BACKGROUND

The major Oxygen Minimum Zones (OMZs) of the world ocean are characterized by partial to complete consumption of midwater NO_3^-, leading to significant removal of combined nitrogen from the ocean. On long time scales, the interplay between denitrification in OMZs and N_2-fixation elsewhere in the

L. N. Neretin (ed.), Past and Present Water Column Anoxia, 259–281.

global ocean appears to play a dominant role in regulating the oceanic content of combined nitrogen, and therefore oceanic productivity.

The earliest estimates of the rate of pelagic denitrification were derived by coupling measurements of the spatial distribution of NO_3^- in an OMZ to circulation models to provide an estimate of the absolute rate of NO_3^- disappearance along the mean flow path [15, 18, 42]. More recently, a variety of geochemical [25] and isotopic [10] budgeting approaches have been used to constrain the rate of denitrification in different OMZs. Direct tracer-based measurements have not been widely used to quantify denitrification in the field to date. This likely reflects the practical difficulties of maintaining suboxic conditions while preparing and incubating experimental samples, and the scaling problems associated with relating experimental results to the OMZ as a whole. Nonetheless, tracer experiments have played a critical role in elucidating the role of "alternative" denitrification pathways in marine systems, particularly in sedimentary contexts [19, 33].

The stable isotopes of nitrogen provide a natural analog to tracer experiments and can often be used to elucidate the role of different processes in the nitrogen cycle. For example, the biomass and detritus formed through biological production in the upper ocean acquire an isotopic signature that reflects the source(s) of N supporting productivity and/or the subsequent processing of that organic matter. Within the water column, the remineralization of sinking particles leads to characteristic patterns of variation in the natural abundance of ^{15}N with depth [e.g., 5, 38, 41, 56]. Although deep water NO_3 acts as an important, and often dominant, isotopic end-member for primary production in the surface ocean, the isotopic composition of sinking organic matter may also be affected by N_2-fixation in the surface layer. The ^{15}N composition of particulate matter at depth therefore provides an integrative measure of the sources of N fueling primary production at the surface. This signal can propagate to the bottom, where it can enter the sedimentary record, providing information on long-term variation in critical oceanic N cycle processes [3, 4, 17, 23, 27, 31].

1.1 Isotopic Fractionation

Most biological transformations of nitrogen in the ocean are accompanied by significant kinetic isotopic fractionation, which leads to predictable alterations in the natural abundance of the stable isotopes of N. The degree of isotopic fractionation reflects the different reaction rates for molecules containing the two isotopes of nitrogen and is commonly expressed as a fractionation factor, α:

$$\alpha = {}^{14}k/{}^{15}k \tag{1}$$

where ^{14}k and ^{15}k are the rate constants for reaction of molecules containing the light and heavy isotopes, respectively. Using this convention, "normal" isotopic fractionation that discriminates against the heavy isotope has a fractionation factor greater than unity. The inverse convention is also used by some authors [e.g., 35], requiring careful attention when comparing fractionation factors reported in different publications.

While the fractionation factor describes the relative reaction rates of the different isotopic species, the isotopic discrimination factor, ϵ, provides a simpler expression of the magnitude of fractionation:

$$\epsilon = (\alpha - 1) * 1000 \tag{2}$$

To a good approximation, the discrimination factor is equal to the instantaneous difference in δ^{15}N between the substrate and product of a reaction

$$\epsilon = \delta^{15}N_{substrate} - \delta^{15}N_{product} \tag{3}$$

as long as residual substrate remains and is undergoing reaction. As a reaction progresses in a closed system, both the residual substrate and the product formed will become progressively enriched in ^{15}N, following a typical Rayleigh fractionation trajectory (Fig. 1). Conservation of mass and isotopes requires that the δ^{15}N of the combined substrate and product pool remain constant throughout the course of reaction. Note that complete conversion of substrate to product will leave no measurable isotopic imprint since the accumulated product will have exactly the same δ^{15}N as the initial pool of substrate even if the reaction itself discriminates strongly between isotopes (Fig. 1). The effect of isotopic fractionation is thus observable only under conditions of partial consumption of the available substrate pool.

1.2 Isotopic Fractionation in the Water Column

Deep water NO_3^- is the dominant pool of combined nitrogen in the ocean, and its isotopic composition integrates a variety of processes and inputs. In OMZs, suboxic conditions promote denitrification as a respiratory pathway supporting heterotrophic microbial growth. Both field and laboratory experiments have shown that denitrification discriminates strongly (20 - 30 ‰) between the stable isotopes of nitrogen [6, 16, 57]. As a result, the partial denitrification characteristic of many pelagic systems (e.g., the Eastern Tropical Pacific and the Arabian Sea) generates a strong isotopic enrichment in the residual NO_3^-, as shown schematically in Fig. 1. In contrast, sedimentary denitrification typically goes to completion within the sediment, resulting in no expression of the isotope effect associated with the denitrification process itself [8, 9]. In other words, sedimentary denitrification is effectively invisible from an isotopic standpoint (Fig. 2), removing combined nitrogen from the ocean

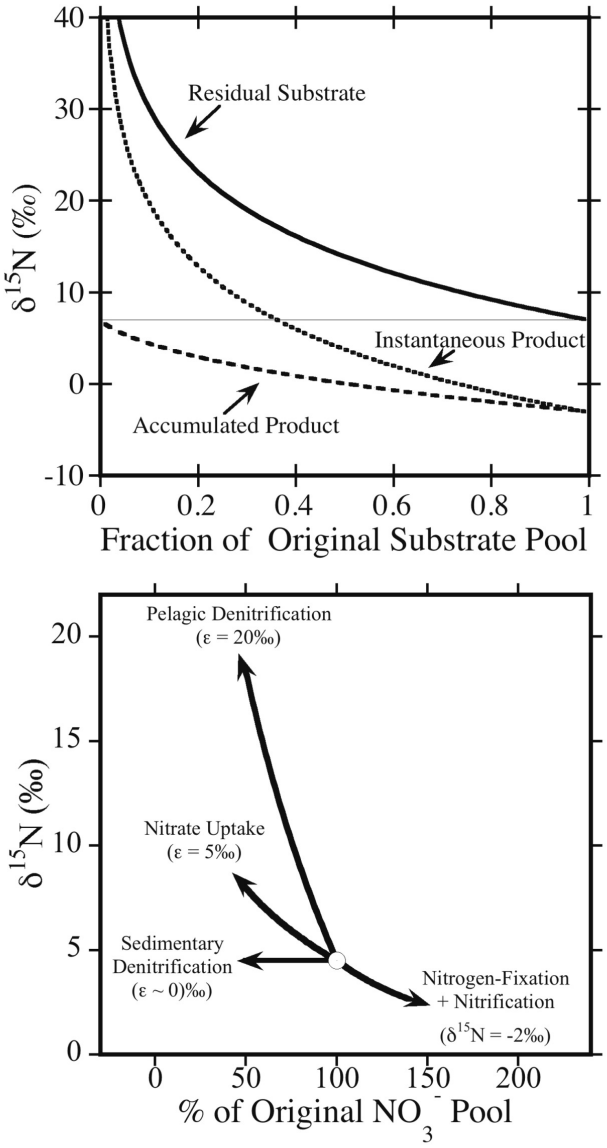

Figure 1. Effects of isotopic fractionation. Upper panel: Trajectory of $\delta^{15}N$ of the substrate and product of a reaction with an isotope discrimination factor (ϵ) of 10‰. As reaction proceeds from right to left, the $\delta^{15}N$ of the residual substrate and accumulated produce pool increase, as does the $\delta^{15}N$ of the product formed at any instant. Lower panel: Schematic showing the effect of various N cycle processes on the $\delta^{15}N$ of NO_3^-. Trajectories for denitrification, nitrate uptake, and sedimentary denitrification were calculated using a closed-system Rayleigh model with isotope discrimination factors (ϵ) as shown. The trajectory associated with N_2-fixation was calculated using a mass balance model for remineralization and nitrification of newly fixed N with a $\delta^{15}N$ of -2‰.

without any impact on the isotopic composition of the dissolved inorganic nitrogen left behind.

In the upper water column, assimilatory uptake of NO_3^- by phytoplankton can have a measurable impact on the $\delta^{15}N$ of the residual NO_3^- (Fig. 1). Phytoplankton discriminate against $^{15}NO_3^-$ during uptake [40, 45, 46, 59, 60], which can lead to significant alteration of residual NO_3^- at the base of the surface mixed layer. A typical value for the discrimination factor for NO_3^- uptake is about 5‰, though the actual expressed fractionation varies significantly with growth rate and environmental conditions.

Although most marine organisms require access to combined nitrogen (e.g., NO_3^-, NH_4^+) as a substrate for growth, a variety of prokaryotes are able to reduce and assimilate N_2 into biomass. These "diazotrophs" are taxonomically diverse [61] and recent work in the Pacific has demonstrated that unicellular cyanobacteria occur throughout the mixed layer and make a significant contribution to the pelagic nitrogen budget [39, 62]. N_2-fixation shows modest discrimination against ^{15}N, producing organic matter that is slightly depleted in ^{15}N relative to tropospheric N_2. The best known oceanic diazotroph, the colonial nonheterocystous cyanobacterium *Trichodesmium*, typically has a $\delta^{15}N$ of about -1 to -2‰ [14, 38], while the heterocystous *Richelia* that lives endosymbiotically within diatoms has a $\delta^{15}N$ of about -1‰ [38].

Of the processes shown in Figure 1, N_2-fixation is the one most likely to lower the $\delta^{15}N$ of NO_3^- while adding to the oceanic pool of combined nitrogen. It's important to note that the process of N_2-fixation doesn't directly alter the oceanic NO_3^- pool; instead, the organic matter formed by N_2-fixing organisms is ultimately rematerialized and contributes to the subsurface pool of NO_3^- through nitrification of the NH_4^+ produced during remineralization. Nitrification is thus a critical step in the conversion of organic matter to NO_3^-, and a potential source of ^{15}N-depleted NO_3^- in the water column [49, 54] due to the isotopic fractionation associated with oxidation of NH_4^+ [35]. In the upper and mid water column of oligotrophic waters, however, the isotopic fractionation associated with nitrification itself is unlikely to have a major impact on the $\delta^{15}N$ of NO_3^- since little or no residual substrate (NH_4^+) typically accumulates in the water column. Unless an appreciable fraction of the NH_4^+ produced in the water column remains in solution unconsumed by nitrifiers, nitrification simply transfers the isotopic signature of remineralized NH_4^+ into the NO_3^- pool.

The isotopic enrichment of NO_3^- therefore provides an integrative measure of the biological sinks and sources of nitrogen within a water column. The impact of local processes such as denitrification in an OMZ may also propagate laterally for substantial distances from the site of activity through advection [e.g., 34]. In addition, both denitrification and N_2-fixation create isotopic patterns that can propagate into other components of the ecosystem, including

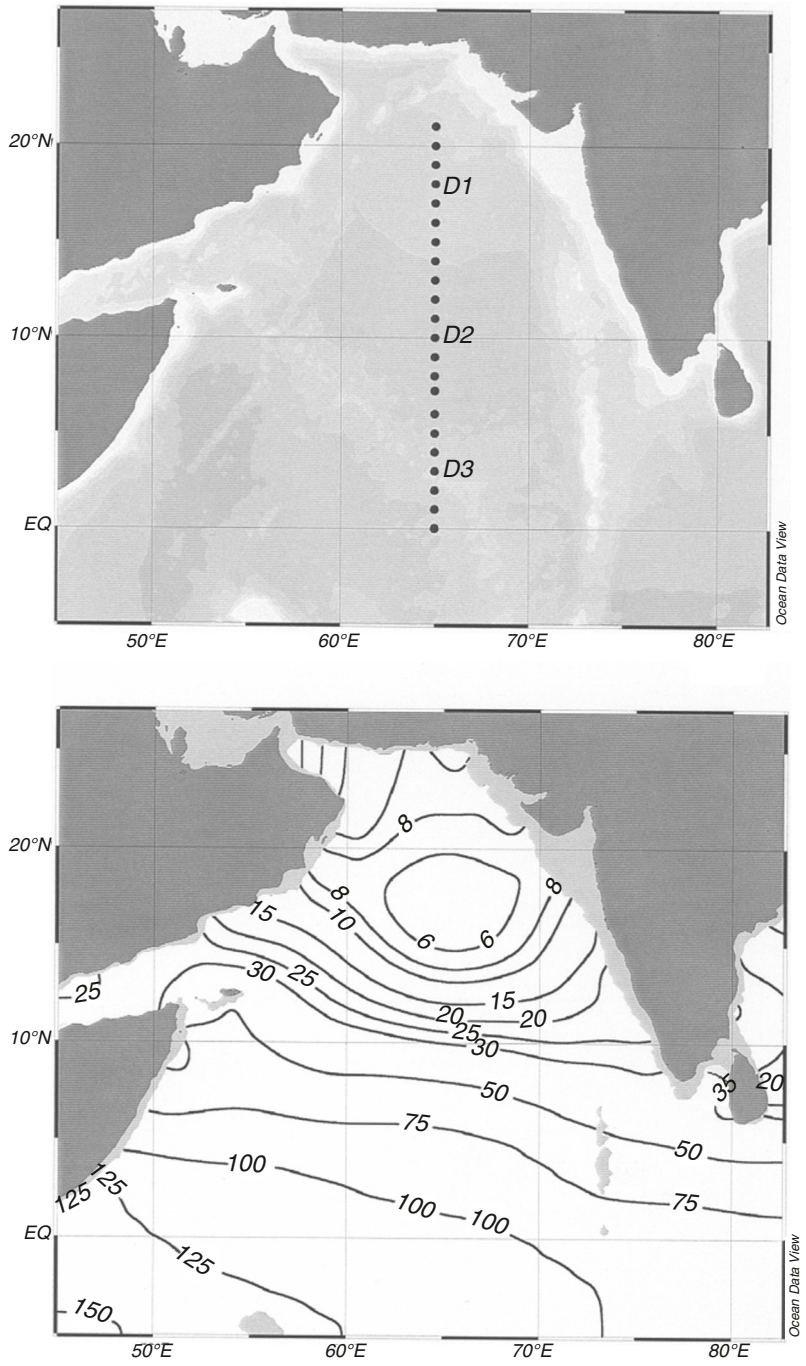

Figure 2. Charts showing stations occupied during cruise ME32/3 (upper panel) and climatologic distribution of O_2 (μmol L^{-1}) at 300 m depth (lower panel). Charts prepared using Ocean Data View [52] and objectively analyzed data from the World Ocean Atlas 2001.

near surface biota [37, 38, 57] and benthic sediments [4, 23]. In effect, isotopic discrimination creates a natural isotopic perturbation that can potentially be exploited in studies of the impact of denitrification on an ecosystem and global level. Here, we will use data from the German Arabian Sea JGOFS program as an example of the impact of denitrification and N_2-fixation on the stable isotopic composition of organic nitrogen in the water column in and around a major oceanic OMZ.

2. ARABIAN SEA FIELD PROGRAM

As part of the German JGOFS program, we collected samples of suspended and sinking particles in 1995 during a meridional transect through the central Arabian Sea. This cruise occurred in the intermonsoon period just before the Southwest Monsoon and our data allow us to evaluate the horizontal and vertical propagation of isotopic signatures associated with processes occurring within the OMZ as well as in the surface mixed layer above. Our data provide interesting isotopic insights into the regional nitrogen cycle, particularly with respect to the interaction between denitrification and N_2-fixation and the propagation of the isotopic signature associated with the OMZ southward into areas well removed from the site of active denitrification.

2.1 Sample Collection and Analysis

We collected samples during a German JGOFS cruise to the Arabian Sea in May 1995 (cruise ME 32-3, 5 May - 5 June 1995). Sampling stations were located at 1 degree intervals along a transect at 65°E longitude from 21° N to the equator (Fig. 2). Samples were collected from the upper 1500 m of the water column with a CTD-rosette system equipped with Neil Brown sensors and twelve 10L Niskin bottles. In addition to the standard upper water column sampling at thirteen transect stations, we carried out time-series studies and vertical flux measurements at 18°N (D1, 8 days), 10°N (D2, 7 days) and 3°N (D3, 3 days).

Multiple casts were required to obtain enough water for all the chemical and biological analyses carried out at each station. At the time-series stations, a large rosette equipped with six 30L water bottles (Hydrobios) was used to supplement the standard rosette, allowing rapid collection of large volumes of water from selected depths. However, a post-cruise comparison of nutrient and DIC data from the two rosettes showed a systematic mismatch in regions of the water column with strong gradients in chemical properties. We attribute this to a design flaw in the 30L bottles, which have a mouth aperture significantly smaller than the diameter of the bottle itself, leading to poor flushing of the bottle volume. To correct for this sampling bias, we used the nutrient concentrations

measured in the 30L bottles to estimate a nominal sampling depth for the particulate samples obtained from those bottles.

We deployed drifting Kiel-type sediment traps [63] at 100 m depth during all three time-series studies. At 18°N and 10°N, a second drifting trap was deployed at 500 m depth. The shallow (100 m) trap was recovered daily for replacement of its single sample bottle. The deeper trap (500 m) was equipped with a carousel of sample bottles programmed for daily sampling and was deployed for the entire time-series study at each site. All sample bottles were filled with a brine solution to preserve organic matter and to prevent washout of the material collected. Immediately after trap recovery, the samples were split with a rotating splitter [7] and filtered for later analysis of the particulate matter.

Concentrations of nutrients and oxygen were measured using standard methods [24]. Samples of particulate organic carbon and nitrogen (POC, PON) were collected by gentle vacuum filtration onto precombusted (12 hrs 450°C) Whatman GF/F filters and kept frozen at -20°C during the cruise and transport to the laboratory.

All stable isotope and particulate organic matter concentration measurements were carried out by continuous-flow isotope ratio mass spectrometry using an elemental analyzer (CE/Fisons NA 1108) interfaced to a mass spectrometer (Finnigan MAT Delta S). Prior to analysis, sample filters were decalcified by fuming with HCl for 24 hours, then dried and formed into pellets in Sn cups. All isotope data are reported as δ^{15}N or δ^{13}C values using atmospheric N_2 and PDB, respectively, as isotopic reference materials. A sample of peptone (Merck) was run after every fifth sample to provide a working standard for the isotopic and elemental analyses. The standard deviation for replicate samples is less than 0.2 ‰.

2.2 General Distribution of Water Column Properties

The upper water column was well-stratified throughout our transect, with the surface mixed layer extending through the upper 50 to 100m of the water column (Fig. 3). All stations sampled showed a clear subsurface minimum in O_2 concentration beginning at about 150 - 200 m depth and extending to more than 1000 m depth. Oxygen concentrations in the upper 200 m of the water column ranged from 0 to >267 μmol l^{-1} along our transect. The core of the Arabian Sea OMZ occurred between 18˚N and 14˚N, but hypoxic conditions extended well south of this region, forming a tongue of oxygen depleted water extending southward and centered around 800m depth (data not shown).

Nitrate concentrations were at or near the limit of detection in the surface mixed layer (Fig. 3). A sharp gradient in concentration extended through the pycnocline with maximal concentrations occurring below 150 m (Fig. 3). In

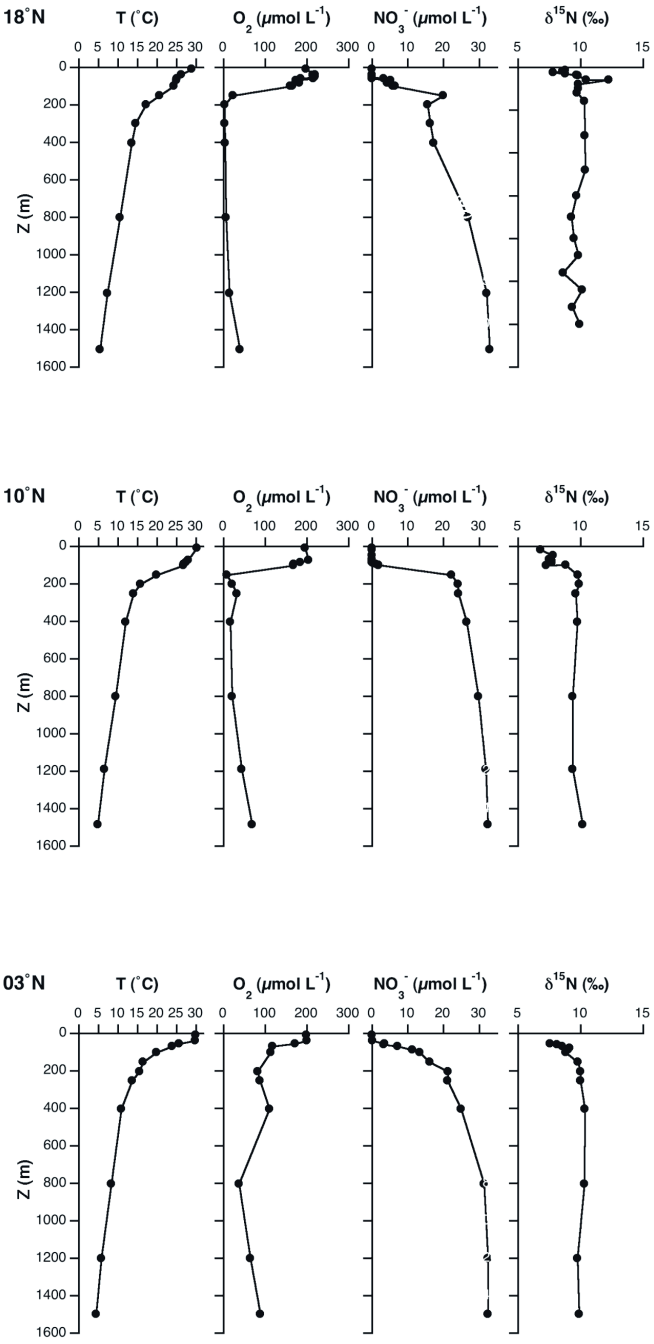

Figure 3. Profiles of temperature, O_2 concentration, NO_3^- concentration, and $\delta^{15}N$ of suspended particles at the three time-series stations carried out at 18°N, 10°N, and 3°N.

the northern portion of our transect, in the core region of the OMZ, we found a clear minimum in NO_3^- concentration between 200 and 400 m. This local minimum reflects the impact of denitrification (Fig. 1) in removing NO_3^- from the water column.

The isotopic composition of suspended particles ($\delta^{15}N$) showed relatively little vertical structure below the surface on this transect, with all subsurface values falling between 9 and 11‰ (Fig. 3). In contrast, we found a well-defined surface minimum in $\delta^{15}N$ with values as low as 4‰ near 10°N (Fig. 4). Below the surface mixed layer, $\delta^{15}N$ values increased and reached 9‰ between 80 and 100m depth at most stations.

The low $\delta^{15}N$ values we observed in suspended particles at the surface were associated with an extensive surface bloom of *Trichodesmium*. This bloom extended over about 20% of the surface area of the Arabian Sea [12]. The rates of primary production and N_2-fixation by *Trichodesmium* were both high within the bloom, and *Trichodesmium* accounted for roughly 80% of total surface primary production, and about a quarter of total water column primary production [12]. As a result of the spatial extent of the bloom and the intense production by *Trichodesmium* within the bloom, N_2-fixation appeared to support most of the new production in the Arabian Sea at the time of sampling [12].

2.3 Sinking Particles

Our sediment trap collections show both vertical and lateral variations in the $\delta^{15}N$ of sinking organic matter (Table 1, Fig. 4). In general, the materials collected in the shallow (100 m) trap had an isotopic composition similar to (10°N) or enriched (3°N, 18°N) in ^{15}N relative to the average particle field in the upper 100 m of the water column. The low $\delta^{15}N$ of sinking particles collected by the shallow trap at our 10°N station coincided with the peak abundances of *Trichodesmium* in the upper water column (Fig. 4).

At the two time series stations at 18°N and 10°N, we deployed a second trap at 500 m depth. Interestingly, sinking particles collected by the deeper trap had a significantly lower $\delta^{15}N$ than materials collected by the shallow trap (Fig. 4). Although materials collected in the 500 m trap at 10°N showed substantial variation from day to day (SD = 2.7‰), the mean value over the 6 days of deployment was lower than the surface PN at that station, which was dominated by *Trichodesmium* (Fig. 4).

3. DISCUSSION

The Arabian Sea, with its well-developed oxygen minimum zone (OMZ) is one of the major regions of pelagic denitrification in the world ocean and provides a large midwater habitat for denitrifying bacteria. The consumption of NO_3^- by bacteria leads to a deficit in NO_3^- relative to other nutrients

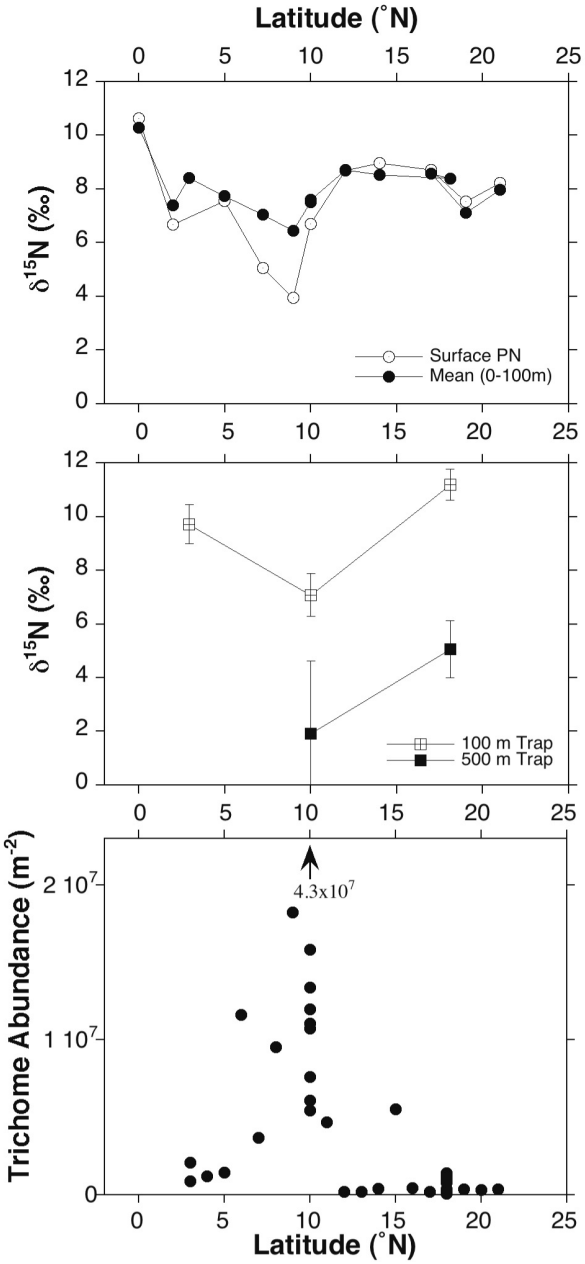

Figure 4. Meridional distribution of δ^{15}N of suspended and sinking PN and *Trichodesmium* abundance at the surface. Upper panel: δ^{15}N of PN collected in the upper 10 m of the water column and the mean, concentration-weighted δ^{15}N of PN in the upper 100 m of the water column. Middle panel: δ^{15}N of material collected in the sediment traps deployed at 100 and 500 m depth (mean $\pm$ SD). Lower panel: Abundance of *Trichodesmium* in the upper 20 - 50 m of the water column (trichomes m^{-2}).

Table 1. Summary of the stable isotope composition of suspended and sinking particles in the Arabian Sea. The $\delta^{15}N$ of suspended particles is the concentration-weighted mean for the upper 100 or 1500 m of the water column. Where we analyzed suspended particles from multiple casts (i.e., at 18° and 10°N), the range of means is given. For the sediment traps, mean isotope compositions (± SD) were calculated from multiple intervals, each interval lasting 1 day.

Latitude (°N)	*Suspended PN (0 - 100 m)*	*Suspended PN (0 - 1500 m)*	*Sinking PN (100 m)*	*Sinking PN (500 m)*
21	8.8	9.8	n.d.	n.d.
19	7.8	9.4	n.d.	n.d.
18	8.8-10.0	9.3-10.3	11.2 ± 0.58 (N= 7)	5.1 ± 1.1 (N= 7)
17	8.9	9.3	n.d.	n.d.
14	8.8	9.5	n.d.	n.d.
12	8.8	9.4	n.d.	n.d.
10	7.8-8.2	9.4-9.6	7.1 ± 0.8 (N= 6)	1.9 ± 2.7 (N= 6)
9	6.8	8.7	n.d.	n.d.
7	7.5	9.8	n.d.	n.d.
5	8.0	9.7	n.d.	n.d.
3	8.3	9.9	9.7 ± 0.7 (N= 2)	n.d.
2	7.9	9.9	n.d.	n.d.
0	10.3	8.2	n.d.	n.d.

and an enrichment in the ^{15}N content of the residual nitrate. The impact of this isotopic fractionation has been documented in both laboratory and field studies of suboxic systems [6, 10, 16, 34, 36, 57]. The residual NO_3^- exiting pelagic OMZs can be advected laterally for substantial distances [e.g., 34, 51], potentially transporting the isotopic signature of partial denitrification to regions well removed from the OMZ proper.

The isotopic signature of denitrification can also propagate upward to the surface through vertical mixing, especially in a monsoonal system like the Arabian Sea. The subsequent uptake of isotopically enriched nitrate by phytoplankton in the mixed layer will result in formation of suspended particles with $\delta^{15}N$ values that are much higher than is typical of waters well removed from OMZs [1, 5, 38, 41, 56]. Some fraction of the organic matter produced will sink out of the surface layer, further transporting the isotopic signature of denitrification activity vertically through the water column and into the deep sea.

Surface blooms of N_2-fixing cyanobacteria, primarily *Trichodesmium*, have been reported in the coastal and open waters of the Arabian Sea in the oligotrophic intermonsoon periods [11, 20, 21, 22, 32], making it one of the few places in the world where both N_2-fixation and pelagic denitrification are known to occur simultaneously and at significant rates in the same water column.

During our German JGOFS cruise, we encountered a massive bloom of *Trichodesmium* [12], which had a clear impact on the water column nitrogen budget and the δ^{15}N of suspended particles at the surface.

3.1 Subsurface Processes in the Arabian Sea

The Arabian Sea is contained within a single, roughly triangular basin extending from about 25°N to the Carlsberg ridge in the south with a maximal depth of about 4000m. The hydrology of intermediate waters in the Arabian Sea reflects significant inputs of Indian Deep Water from the South with as well as warm, salty water from both the Persian Gulf in the northwest and the Red Sea to the southwest [55, 58]. The slow and tortuous path followed by the northward-flowing Indian Deep water along with the low initial O_2 concentration of waters entering the Arabian Sea from the north lead to extensive development of suboxic conditions in the water column of the Arabian Sea [55]. The core of the OMZ is about 800 m thick in the central Arabian Sea as far south as about 14°N, and low O_2 concentrations (< 10 μmole L^{-1}) extend to about the same latitude (Fig. 2).

The elevated δ^{15}N signature characteristic of particles (Fig. 3) in the Arabian Sea is consistent with the effects of denitrification within the OMZ. The relative uniformity of the δ^{15}N we measured in suspended particles below the surface mixed layer suggests that the isotopic composition of the particle field is determined primarily by processes occurring either at the surface (e.g., primary production) or within the upper reaches of the OMZ (e.g., heterotrophic production), rather than by processes occurring in situ within the core of the OMZ proper.

A number of lines of evidence indicate that the highest rates of denitrification occur just below the nitracline in the upper margin of the OMZ, a scenario consistent with our isotope data. For example, the portion of the water column between 300 and 400 m depth is characterized by high electron transport system activity [43], high N_2O concentrations [44], and elevated δ^{15}N values for NO_3^- [10]. Although this characteristic isotopic signature originates at depth within the OMZ, vertical mixing, particularly during the strong Southwest Monsoon, can transport isotopically enriched NO_3^- into the surface mixed layer. This vertical mixing and recharge of the surface layer with nutrients through mixing associated with the monsoon presumably occurs twice a year, a time scale that matches well with the 1 year ventilation time estimated by Naqvi and Shailaja based on the rate of metabolic activity within the OMZ [43]. Finally, a high temporal resolution study in the eastern central Arabian Sea revealed internal wave oscillations of several tens of meters beneath the thermocline which were strongest during the period immediately after onset of the Southwest Monsoon [50]. Such internal wave activity could also help to move isotopically

enriched NO_3^- upward into the euphotic zone. In any case, the two, monsoon-associated mixing events each year would be enough to lead to considerable ^{15}N enrichment of the particle pool at the surface through assimilation of residual NO_3^- mixed upward from the zone of active denitrification in the upper part of the OMZ.

3.2 Surface Processes

As noted above, the $\delta^{15}N$ values we measured in suspended particles (Fig. 3) are quite high relative to values typical of particles in regions of the open ocean well removed from suboxic water masses [1, 5, 38, 41, 56]. In addition to creating a characteristic isotopic signature, denitrification in the OMZ significantly alters the relative abundance of nutrients in the water column by removing NO_3^- independently of PO_4^{3-}. This contrasts strongly with assimilatory processes, which remove both NO_3^- and PO_4^{3-} from solution in roughly Redfield proportions and therefore have minimal impact on the relative concentrations of the two ions. The net result of denitrification activity in the OMZ is that subsurface waters in the Arabian Sea show a clear deficit in NO_3^- availability relative to PO_4^{3-} (Fig. 5). This departure from Redfield stoichiometry can be described using the N* parameter [25], which quantifies the degree to which NO_3^-:PO_4^{3-} concentration ratios depart from the oceanic mean. The nutrient distributions within the Arabian Sea yield uniformly negative N* values, with a minimum below -12.5 μmol kg^{-1} in the core of the OMZ (Fig. 5). As a result, vertical mixing processes can promote primary production but will induce nitrogen limitation of production because of the NO_3^- deficit arising through denitrification.

The intermonsoon period we sampled is characterized by little wind stress and dissolved nutrient concentrations were at or below the limit of detection in the surface mixed layer throughout our transect (Fig. 4). These conditions are ideal for bloom formation by *Trichodesmium*, and our cruise track passed through one of the largest such blooms ever documented [12].

N_2-fixation produces organic matter with an isotopic composition depleted in ^{15}N relative to atmospheric N_2, and therefore a significantly lower $\delta^{15}N$ than average marine sources of nitrogen [38]. This isotopic contrast is accentuated in the Arabian Sea, where the isotopic fractionation associated with denitrification leads to an overall increase in the $\delta^{15}N$ of organic matter. Not surprisingly, samples of suspended particles collected within the upper 10 m of the water column in the bloom show significantly lower $\delta^{15}N$ values than surface particle samples collected north and south of the densest portion of the bloom (Fig. 4, upper panel). Although *Trichodesmium* biomass was most concentrated near the surface, our vertical profiles of the $\delta^{15}N$ of suspended particles indicate that nitrogen fixation made a measurable contribution to the nitrogen budget

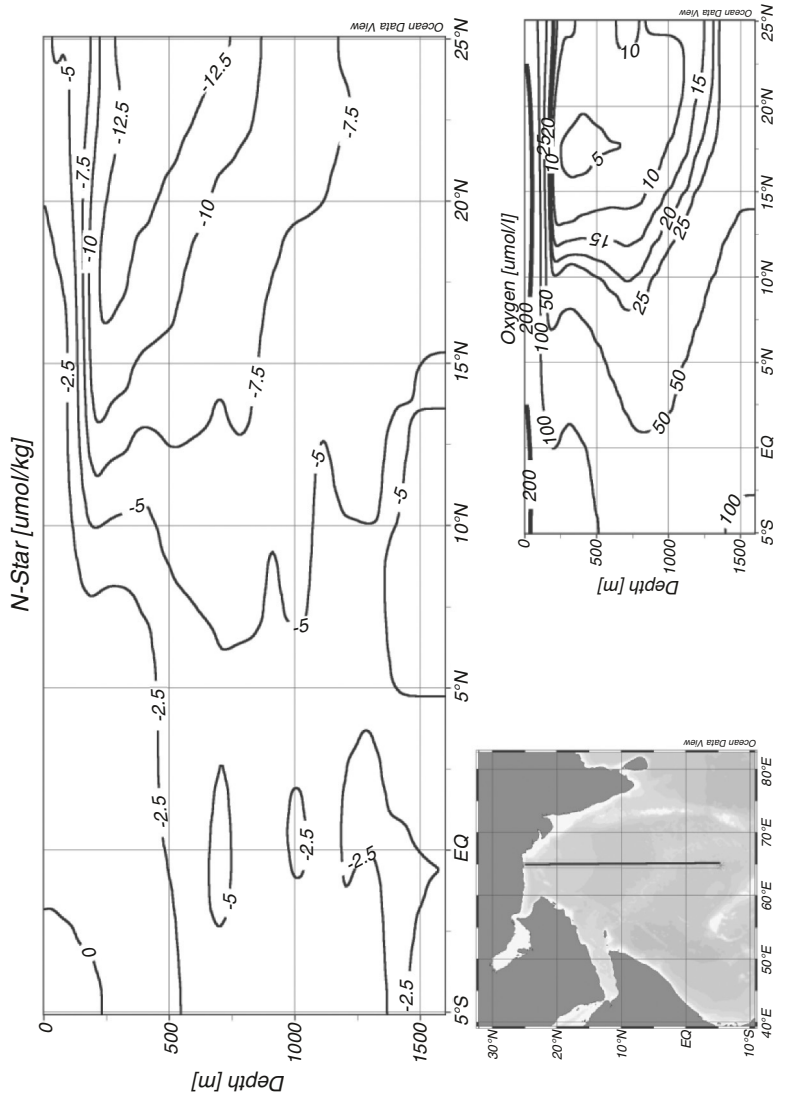

Figure 5. Meridional section along 65°E showing the climatologic distribution of O_2 (lower right) and N* (top) along our cruise track. Charts prepared using Ocean Data View [52] and objectively analyzed data from the World Ocean Atlas 2001.

of the entire upper 200 m of the water column (Fig. 3). An isotope mixing model revealed that diazotroph nitrogen constituted about a quarter of the total pool of suspended particulate nitrogen in the upper 100 m of the water column [12]. On a larger scale, the low $\delta^{15}N$ values of surface particles and the integrated biomass of the upper water column (0 - 100 m, Table 1) in the region of the *Trichodesmium* bloom demonstrates that N_2-fixation made a significant contribution to the overall nitrogen budget between roughly 12°N and 3°N (Fig. 4).

3.3 Interactions Between Suspended and Sinking Particles

Studies in other oceanic areas have demonstrated that the isotopic signature of N_2-fixation can propagate into other components of the pelagic ecosystem [37, 38], though the actual mechanism of transfer of diazotroph nitrogen into the food web is not yet well understood. In the Arabian Sea, the surface N_2-fixation signature had a clear impact on the field of sinking organic matter sampled by our sediment traps (Fig. 4, middle panel), and a more modest effect on the mean $\delta^{15}N$ of suspended particles in the upper 100 m of the water column (Fig. 4, upper panel). Under calm sea and wind conditions, *Trichodesmium* tends to aggregate at the surface as a result of the positive buoyancy imparted to healthy trichomes by their internal gas vesicles [13]. This behavior may have contributed to the absence of a clear N_2-fixation signal in the isotopic composition of suspended particles below 200 m in the core of the bloom at 10°N (Fig. 3).

Our time series at 10°N is particularly interesting because we deployed traps at both 100 and 500 m at this station, which was located within the densest part of the *Trichodesmium* bloom (Figs. 3 and 5). The sinking particles collected by the 100 m trap are strongly depleted in ^{15}N relative to the sinking particles collected at this depth at 18°N and 3°N outside the core of the bloom. Interestingly, the material sinking into the 100 m trap had a mean $\delta^{15}N$ only slightly lower than the mean $\delta^{15}N$ of particles in the upper 100 m of the water column (Fig. 4, Table 1) and higher than the $\delta^{15}N$ of material collected right at the surface (Fig. 4), suggesting that this trap effectively sampled the entire mixed layer.

In contrast, the trap at 500 m collected material with a substantially lower mean $\delta^{15}N$ (Fig. 4, Table 1). A decrease in the $\delta^{15}N$ of sinking particles with depth has been observed in other oceanic areas [e.g., 2, 56], albeit over a much greater depth range than the 500 m in our study. Although we cannot rule out the possibility that the difference in $\delta^{15}N$ between traps reflects temporal changes in the $\delta^{15}N$ of sedimenting organic matter, the low $\delta^{15}N$ of material collected in our trap at 500 m could also arise from preferential remineral-

ization of organic matter with a high $\delta^{15}N$ during passage through the water column. If so, then much of the flux at 100 m must be rapidly remineralized, making a minimal contribution to the deeper flux. Few organisms feed actively on *Trichodesmium* [47, 48], which is known to have toxic (allelopathic) effects on both phytoplankton and zooplankton [26, 28, 29, 30]. Allelopathic compounds produced by *Trichodesmium* may also reduce the rate of degradation and remineralization of sinking organic material derived from *Trichodesmium* blooms at the surface, which in turn would result in an increasing relative contribution of *Trichodesmium* to the sinking flux with greater depth. The contrast between the 100 m and 500 m traps would then imply that the deeper trap is much more effectively sampling particles originating at the very surface, where *Trichodesmium* dominated both the biomass and the isotopic signature of the suspended particles.

Our time series at 18°N shows a similar decrease in the $\delta^{15}N$ of sinking particles between the traps at 100 and 500 m. In this case, the material collected by the trap at 100 m was enriched in ^{15}N by about 1 to 2‰ relative to the particle field in the upper 100 m of the water column. *Trichodesmium* was present in the upper water column at this station, though not at concentrations approaching those we saw at 10°N (Fig. 3). We deployed only one trap at 100 m depth at our short (2 day) time series at 3°N. The sinking particles at this depth have a $\delta^{15}N$ very similar to the mean value for particles in the upper 100 m of the water column.

We did not collect sinking particles at greater depth during this study, but the data from our time series at 10°N clearly show the potential for N_2-fixation in the surface layer to have a strong local impact on the $\delta^{15}N$ of sinking particles at depth. Interestingly, the diazotroph signature is expressed more clearly at 500 m than at 100 m depth, likely reflecting differences in sinking rate and extent of degradation of organic matter from different sources (i.e., *Trichodesmium* vs. other primary producers). Taken together, the sediment trap samples from our three time series stations suggest that the particles leaving the surface mixed layer are imprinted with the mean isotopic composition of the upper water column, and that a substantial fraction of the particle flux at 100 m is remineralized during transit through the upper part of the OMZ. Since NH_4^+ doesn't accumulate in the water column, most or all of the remineralized nitrogen must be nitrified, adding NO_3^- with a relatively low $\delta^{15}N$ to the dissolved pool. In effect, the sinking flux of organic matter will tend to reduce both the isotopic and the mass effects of denitrification on the NO_3^- pool in the upper part of the OMZ.

3.4 Advection

Biological processes are critical in driving the vertical movement of material and isotopic signatures, but physical processes dominate the lateral movement of organic matter and its associated stable isotope signature on a regional scale. Most research to date on the hydrography of the Arabian Sea has focused on the monsoonal wind patterns and the induced alternating surface flows. Comparatively little has been published about mid and deep water circulation [53], despite its obvious importance in determining the distribution of physical and chemical properties below the surface mixed layer.

As a result of the monsoons, the surface circulation changes seasonally in the Arabian Sea. In summer the Southwest Monsoon drives coastal upwelling in the western Arabian Sea and surface currents are anticyclonic (clockwise) with flows from the northwest to the southeast in the eastern Arabian Sea and to the north along the western boundary of the basin. During the winter, the flow is driven by the Northeast Monsoon and water moves in the opposite direction [55]. Interestingly, the depth to which these monsoon-driven currents extend has not been well studied though it is clearly an important determinant of the effectiveness of advection in altering the horizontal distribution of organic matter and dissolved constituents in the Arabian Sea.

Our isotopic measurements suggest that advection plays a critical role in distributing the elevated $\delta^{15}N$ values generated by denitrification in the OMZ to regions well removed from the OMZ itself. For example, the $\delta^{15}N$ of suspended particles is much higher than values typical of non-OMZ regions all the way to the southern end of our transect at the equator, a pattern that reflects advective transport of both NO_3^- and POM. In the Arabian Sea, low O_2 concentrations extend to only to about 10°N (Fig. 2), so the high $\delta^{15}N$ of particles further south must reflect advective transport of isotopically enriched NO_3^- and/or organic matter.

4. CONCLUDING REMARKS

Although the isotope budget of the Arabian Sea is clearly dominated by the effect of denitrification within the large OMZ in the north-central basin, N_2-fixation in the surface layer also makes an important contribution to the isotopic systematics of the system. The interaction between denitrification and N_2-fixation clearly plays a critical role in controlling the relative abundance of NO_3^- and PO_4^{3-} in the ocean on long time scales, but to our knowledge, massive blooms of N_2-fixers have not been observed above any of the other major OMZs in the world ocean. The seasonal oligotrophy of surface waters in the Arabian Sea, in combination with the strong nitrogen limitation arising through denitrification below the surface, produce conditions that strongly favor N_2-fixation as a strategy for growth. With respect to both the mass and the isotopic

composition of oceanic combined nitrogen, N_2-fixation and denitrification have diametrically opposed effects and the occurrence of both processes within the same water column creates unique challenges in interpreting the isotopic systematics of the basin. Clearly, this may also complicate the interpretation of the sedimentary $\delta^{15}N$ record, which has typically been viewed in terms of denitrification intensity alone.

The isotopic contrast between sinking particles at 100 and 500 m depth provides another example of the complex interplay between denitrification and N_2-fixation in this basin. While denitrification sets the overall baseline isotopic composition of the basin, N_2-fixation can act locally to lower the $\delta^{15}N$ of both suspended and sinking particles. Because our cruise coincided with a major bloom of *Trichodesmium*, our data likely represent one extreme in the spectrum of interaction between denitrification and N_2-fixation in the Arabian Sea and field studies at other seasons will likely reveal a simpler propagation of the high $\delta^{15}N$ associated with denitrification through the water column.

Finally, our data also provide strong support for the view that the $\delta^{15}N$ of sedimentary organic nitrogen acts as an integrative proxy for nitrogen cycle processes on a regional scale [e.g., 4]. In particular, we found elevated $\delta^{15}N$ values in suspended particles well south of the OMZ and in a region where denitrification doesn't occur. Further studies of the role of the surface circulation in redistributing the isotopic signature of denitrification throughout the basin are clearly warranted.

Acknowledgements

We thank our colleagues on cruise ME32/3 as well as the officers and crew of the F/S Meteor for their assistance at sea. Financial support for this project was provided by the German Ministry for Education, Science and Technology "Der Stickstoffkreislauf im Arabischen Meer als Antrieb für neue Produktion und Exportfluß von organischem Kohlenstoff" Förderkennzeichen 03F0241D and NSF grants OCE9530187, OCE9977528, and OCE0425583 to JPM.

References

[1] Altabet M.A. A time-series study of the vertical structure of nitrogen and particle dynamics in the Sargasso Sea. Limnol Oceanogr 1989; 34(7):1185-1201.

[2] Altabet M.A., Deuser W.G., Honjo S. and Stienen C. Seasonal and depth-related changes in the source of sinking particles in the North Atlantic. Nature 1991; 354:136-39.

[3] Altabet M.A. and FranÃ§ois R. Sedimentary nitrogen isotopic ratio records surface ocean nitrate utilization. Global Biogeochem Cy 1994; 8:103-16.

[4] Altabet M.A., FranÃ§ois R., Murray D.W. and Preil W.L. Climate-related variations in denitrification in the Arabian Sea from sediment $^{15}N/^{14}N$ ratios. Nature 1995; 373:506-09.

[5] Altabet M.A. and McCarthy J.J. Vertical patterns in ^{15}N natural abundance in PON from the surface waters of warmâ^core rings. J Mar Res 1986; 44:185-201.

[6] Barford C.C., Montoya J.P., Altabet M.A. and Mitchell R. Steady state nitrogen isotope effects of N_2 and N_2O production in Paracoccus denitrificans. Appl Environ Microb 1999; 65(3):989-94.

[7] Bodungen B.v., Wunsch M. and FÃ…rderer H. Sampling and analysis of suspended particles in the North Atlantic. In *Marine Particles: Analysis and Characterization*, Hurd D.C. and Spencer D.W., eds., Geophysical Monograph Series, 1991.

[8] Brandes J.A. and Devol A.H. A global marine fixed nitrogen isotopic budget: Implications for Holocene nitrogen cycling. Global Biogeochem Cy 2002; 16(4):1120, doi: 10.1029/2001GB001856.

[9] Brandes J.A. and Devol A.H. Isotopic fractionation of oxygen and nitrogen in coastal marine sediments. Geochim Cosmochim Ac 1997; 61:1793-1801.

[10] Brandes J.A., Devol A.H., Yoshinari T., Jayakumar D.A. and Naqvi S.W.A. Isotopic composition of nitrate in the central Arabian Sea and eastern tropical North Pacific: A tracer for mixing and nitrogen cycles. Limnol Oceanogr 1998; 42(7):1680-89.

[11] Bryceson I. Seasonality of oceanic conditions and phytoplankton in Dar es Salaam waters. Univ Sci J (Dar Univ.) 1982; 8:66-76.

[12] Capone D.G., Subramanian A., Montoya J.P., Voss M., Humborg C., Johansen A.M., Siefert R.L. and Carpenter E.J. An extensive bloom of the $N_2$2-fixing cyanobacterium, Trichodesmium erythraeum, in the central Arabian Sea during the spring intermonsoon. Mar Ecol-Prog Ser 1998; 172:281-92.

[13] Capone D.G., Zehr J.P., Paerl H.W., Bergman B. and Carpenter E.J. Trichodesmium, a globally significant marine cyanobacterium. Science 1997; 276(23 May):1221-29.

[14] Carpenter E.J., Harvey H.R., Fry B. and Capone D.G. Biogeochemical tracers of the marine cyanobacterium Trichodesmium. Deep-Sea Res 1997; 44:27-38.

[15] Cline J. and Richards F.A. Oxygen deficient conditions and nitrate reduction in the eastern tropical North Pacific Ocean. Limnol Oceanogr 1972; 17:885-900.

[16] Cline J.D. and Kaplan I.R. Isotopic fractionation of dissolved nitrate during denitrification in the eastern tropical North Pacific Ocean. Mar Chem 1975; 3:271-99.

[17] Codispoti L.A., Brandes J.A., Christensen J.P., Devol A.H., Naqvi S.W.A., Paerl H.W. and Yoshinari T. The oceanic fixed nitrogen and nitrous budgets: Moving targets as we enter the Anthropocene? Sci Mar 2001; 65:85-105.

[18] Codispoti L.A. and Richards F.A. An analysis of the horizontal regime of denitrification in the eastern tropical North Pacific. Limnol Oceanogr 1976; 21:379-88.

[19] Dalsgaard T., Canfield D.E., Petersen J., Thamdrup B. and Acuna-Gonzalez J. N_2 production by the anammox reaction in the anoxic water column of Golfo Dulce, Costa Rica. Nature 2003; 422:606-08.

[20] Devassy V.P. Trichodesmium red tides in the Arabian Sea. In Dr. S.Z. Qusim Sixtieth Birthday Felicitation Volume, 1987.

[21] Devassy V.P., Bhattathiri P.M.A. and Qasim S.Z. Trichodesmium phenomenon. Indian J Mar Sci 1978; 7: 168-86.

[22] Dugdale R.C., Goering J.J. and Ryther J.H. High nitrogen fixation rates in the Sargasso Sea and the Arabian Sea. Limnol Oceanogr 1964; 9:507-10.

[23] Ganeshram R.S., Pedersen T.F., Calvert S.E. and Murray J.W. Large changes in oceanic nutrient inventories from glacial to interglacial periods. Nature 1995; 376:755-58.

[24] Grasshoff K., Erhardt M. and Kremling K. Methods of seawater analysis: Verlag Chemie, 1983.

[25] Gruber N. and Sarmiento J.L. Global patterns of marine nitrogen fixation and denitrification. Global Biogeochem Cy 1997; 11(2):235-66.

[26] Guo C. and Tester P.A. Toxic effect of the bloom-forming Trichodesmium sp. (Cyanophyta) to the copepod Acartia tonsa. Nat Toxins 1994; 2(4):222-27.

[27] Handley L.L. and Raven J.A. The use of natural abundance of nitrogen isotopes in plant physiology and ecology. Plant Cell Environ 1992; 15:965-85.

[28] Hawser S.P. and Codd G.A. The toxicity of Trichodesmium blooms from Caribbean waters. In *Marine pelagic cyanobacteria: Trichodesmium and other diazotrophs*, Carpenter E.J., Capone D.G. and Rueter J.G., eds., Dordrecht, Kluwer Academic Publishers, 1992.

[29] Hawser S.P., Codd G.A., Capone D.G. and Carpenter E.J. A neurotoxin from the marine cyanobacterium Trichodesmium thiebautii. Toxicon 1991; 29:277-78.

[30] Hawser S.P., O'Neil J.M., Roman M.R. and Codd G.A. Toxicity of blooms of the cyanobacterium Trichodesmium to phytoplankton. J Appl Phycol 1992; 4:79-86.

[31] Howell E.A., Doney S.C., Fine R.A. and Olson D.B. Geochemical estimates of denitrrification in the Arabian Sea and the Bay of Bengal during WOCE. Geophys Res Lett 1997; 24:2549-52.

[32] Kromkamp J., De Bie M., Goosen N., Peene J., Van Rijswijk P., Sinke J. and Duinevel G.C.A. Primary production by phytoplankton along the Kenyan coast during the SE monsoon and November intermonsoon 1992, and the occurrence of Trichodesmium. Deep-Sea Res Pt II 1997; 44(6-7):1195.

[33] Kuypers M.M.M., Sliekers A.O., Lavik G., Schmid M., Jorgensen B.B., Kuenen J.G., Sinnighe Damsté J.S., Strous M. and Jetten M.S.M. Anaerobic ammonium oxidation by anammox bacteria in the Black Sea. Nature 2003; 422:608-11.

[34] Liu K.-K. and Kaplan I.R. The eastern tropical Pacific as a source of ^{15}N-enriched nitrate in seawater off southern California. Limnol Oceanogr 1989; 34:820-30.

[35] Mariotti A., Germon J.C., Hubert P., Kaiser P., Letolle R., Tardieux A. and Tardieux P. Experimental determination of nitrogen kinetic isotope fractionation: some principles; illustration for the denitrification and nitrification processes. Plant Soil 1981; 62:413-30.

[36] Mariotti A., Germon J.C., LeClerc A., Catroux G. and Letolle R. Experimental determination of kinetic isotopic fractionation of nitrogen isotopes during denitrification. In *Stable Isotopes*, Schmidt H.-L., Forstel H. and Heinzinger K. eds., Amsterdam, Elsevier, 1982.

[37] McClelland J.W., Holl C.M. and Montoya J.P. Nitrogen sources to zooplankton in the Tropical North Atlantic: Stable isotope ratios of amino acids identify strong coupling to N_2-fixation. Deep-Sea Res I 2003; 50:849-61.

[38] Montoya J.P., Carpenter E.J. and Capone D.G. Nitrogen-fixation and nitrogen isotope abundances in zooplankton of the oligotrophic North Atlantic. Limnol Oceanogr 2002; 47:1617-28.

[39] Montoya J.P., Holl C.M., Zehr J.P., Hansen A., Villareal T.A. and Capone D.G. High rates of N_2-fixation by unicellular diazotrophs in the oligotrophic Pacific. Nature 2004; 430:1027-31.

[40] Montoya J.P. and McCarthy J.J. Nitrogen isotope fractionation during nitrate uptake by marine phytoplankton in continuous culture. J Plankton Res 1995; 17(3):439-64.

[41] Montoya J.P., Wiebe P.H. and McCarthy J.J. Natural abundance of ^{15}N in particulate nitrogen and zooplankton in the Gulf Stream region and Warm-Core Ring 86A. Deep-Sea Res 1992; 39, Suppl. 1:363-92.

[42] Naqvi S.W.A. Some aspects of the oxygen-deficient conditions and denitrification in the Arabian Sea. J Mar Res 1987; 45:1049-72.

[43] Naqvi S.W.A. and Shailaja M.S. Activity of the respiratory electron transport system and respiration rates within the oxygen minimum layer of the Arabian Sea. Deep-Sea Res II 1993; 40(3):687-96.

[44] Naqvi S.W.A., Yoshinari T., Jayakumar D.A., Altabet M.A., Narvekar P.V., Devol A.H., Brandes J.A. and Codispoti L.A. Budgetary and biogeochemical implications of N_2O isotope signatures in the Arabian Sea. Nature 1998; 394(30 July):462-64.

[45] Needoba J.A. and Harrison P.J. Influence of low light and a light: dark cycle on NO_3-uptake, intracellular NO_3-, and nitrogen isotope fractionation by marine phytoplankton. J Phycol 2004; 40(3):505-16.

[46] Needoba J.A., Waser N.A.D., Harrison P.J. and Calvert S.E. Nitrogen isotope fractionation by 12 species of marine phytoplankton during growth on nitrate. Mar Ecol-Prog Ser 2003; 255:81-91.

[47] O'Neil J.M. and Roman M.R. Grazers and associated organisms of Trichodesmium. In *Marine Pelagic Cyanobacteria: Trichodesmium and other Diazotrophs*, Carpenter E.J., Capone D.G. and Reuter J.G. eds., Dordrecht, Kluwer Academic Publishers, 1992.

[48] O'Neil J.M. and Roman M.R. Ingestion of the cyanobacterium Trichodesmium spp. by the harpacticoid copepods Macrosetella, Miracia and Oculocetell. Hydrobiologia 1994; 292/293:235-40.

[49] Ostrom N.E., Macko S.A., Deibel D. and Thompson R.J. Seasonal variation in the stable carbon and nitrogen isotope biogeochemistry of a coastal cold ocean environment. Geochim Cosmochim Ac 1997; 61(14):2929-42.

[50] Rao R.R., Mathew B. and Kumar P.W.H. A summary of results on thermohaline variability in the upper layers of the east central Arabian Sea and Bay of Bengal during summer monsoon experiments. Deep-Sea Res 1993; 8:1647-72.

[51] Saino T. and Hattori A. Geographical variation of the water column distribution of suspended particulate organic nitrogen and its ^{15}N natural abundance in the Pacific and its marginal seas. Deep-Sea Res 1987; 34:807-27.

[52] Schlitzer R. Ocean Data View. Alfred Wegener Institute for Polar and Marine Research: Bermerhaven, Germany, 2004.

[53] Shetye S.R., Gouveia A.D. and Shenoi S.S.C. Circulation and water masses of the Arabian Sea. In *Biogeochemistry of the Arabian Sea*, Lal D. ed., Bangalore, Indian Academy of Science, 1994.

[54] Sutka R.L., Ostrom N.E., Ostrom P.H. and Phanikumar M.S. Stable nitrogen isotope dynamics of dissolved nitrate in a transect from the North Pacific Subtropical Gyre to the Eastern Tropical North Pacific. Geochim Cosmochim Ac 2004; 68(3):517-27.

[55] Tomczak M. and Godfrey S.J. Regional Oceanography: An introduction. London: Pergamon 1994.

[56] Voss M., Altabet M.A. and v. Bodungen B. $\delta^{15}N$ in sedimenting particles as indicator of euphotic-zone processes. Deep-Sea Res 1996; 43:33-47.

[57] Voss M., Dippner J. and Montoya J.P. Nitrogen isotope patterns in the oxygen deficient waters of the Eastern Tropical North Pacific (ETNP). Deep-Sea Res 2001; 48:1905-21.

[58] Warren B.A. Context of the suboxic layer in the Arabian Sea. In *Biogeochemistry of the Arabian Sea*, Lal D. ed., Indian Academy of Science, 1994.

[59] Waser N.A., Yin K., Yu Z., Tada K., Harrison P.J., Turpin D.H. and Calvert S.E. Nitrogen isotope fractionation during nitrate, ammonium and urea uptake by marine diatoms and coccolithophores under various conditions of N availability. Mar Ecol-Prog Ser 1998; 169:29-41.

[60] Waser N.A.D., Harrison P.J., Nielsen B., Calvert S.E. and Turpin D.H. Nitrogen isotope fractionation during the uptake and assimilation of nitrate, nitrite, ammonium, and urea by a marine diatom. Limnol Oceanogr 1998; 43(2):215-24.

[61] Zehr J.P., Mellon M.T. and Zani S. New nitrogen-fixing microorganisms detected in oligotrophic oceans by amplification of nitrogenase (nifH) genes. Appl Environ Microb 1998; 64(9):3444-50.

[62] Zehr J.P., Waterbury J.B., Turner P.J., Montoya J.P., Omoregie E., Steward G.F., Hansen A. and Karl D.M. New nitrogen-fixing unicellular cyanobacteria discovered in the North Pacific Central Gyre. Nature 2001; 412:635-38.

[63] Zeitzschel B., Diekmann P. and Uhlmann L. A new multisample sediment trap. Mar Biol 1978; 45:285-88.

NITROGEN CYCLING IN THE SUBOXIC WATERS OF THE ARABIAN SEA

Allan H. Devol[1], S. Wajih A. Naqvi[2], Louis A. Codispoti[3]

[1] *University of Washington, School of Oceanography, Box 357940, Seattle, WA 98195-7940, USA*

[2] *National Institute of Oceanography, 403004 Dona Paula, Goa, India*

[3] *University of Maryland Center for Environmental Science, Horn Point Laboratory, 2020 Horns Point Rd, P.O. Box 775, Cambridge, MD 21613, USA*

Abstract Arabian Sea contains one of the world's three large oxygen deficient zones (ODZ). Within the ODZ oxygen concentration is vanishingly small between about 200 and 800 m depth and in this depth interval denitrification is the major mode or organic matter oxidation. This makes the Arabian Sea a globally important sink in the marine combined nitrogen cycle. Within the ODZ nitrate concentration profiles typically show a local minimum near 250 m and nitrate is depleted relative to phosphate. Stoichiometrically based estimates of the amount of nitrate removed from the water column, or the nitrate deficit, suggest maximum values of ~12 μM. However, the amount of excess nitrogen gas, which is presumably a result of denitrification, has been estimated to be almost twice this value. Although the reason for this discrepancy between the nitrate deficit and the quantity of excess nitrogen gas remains unresolved, possible causes include non-Redfield stoichiometry for denitrification, contributions due to nitrogen fixation either in the Arabian Sea or in the ODZ source waters, anammox, or sedimentary denitrification. Nitrate deficit based estimates of overall denitrification rate are about 40 Tg N a^{-1}, but if the larger excess nitrogen gas measurements are correct they suggest the rate could be correspondingly higher. Nitrate is enriched in the heavy N isotope within the denitrification zone due to denitrification. During upwelling this enriched N is brought into the euphotic zone where it is take up by phytoplankton. When remains of the phytoplankton sink and become incorporated into the sediment the resulting sediments are also enriched in the heavy isotope relative to other areas of the ocean. However, during glacial periods the N in the sediment was not enriched suggesting better ventilation of the ODZ waters and a lack of denitrification. Nitrous oxide, an important green-house gas and an intermediate in both denitrification and nitrification typically displays local maxima at the upper and lower boundaries of the ODZ, while it is found in very low concentrations within the ODZ. Low values in the ODZ are the result denitrification and this is evidenced by enrichment in the heavy isotopes of both N and O. Maxima at the boundaries of the ODZ may result from either

L. N. Neretin (ed.), Past and Present Water Column Anoxia, 283–310.

nitrification or denitrification and the N is depleted in the heavy isotope, while the O is enriched.

Keywords: Arabian Sea, oxygen-deficient zone, nitrogen cycling, nitrogen isotopes, nitrous oxide

1. INTRODUCTION

Nitrogen has long been long recognized as a major nutrient limiting primary carbon fixation in vast areas of the world's oceans [14, 32, 35]. Furthermore, through its control of marine primary production, it has been suggested that changes in the atmospheric concentration of carbon dioxide (CO_2) during the last glacial-interglacial transition were linked to, or driven by, changes in the marine nitrogen cycle [1, 10, 60]. Thus, it is important to understand nitrogen cycling in the contemporary ocean not only because it influences present day nitrogen availability and the amount and rate of primary production, but also to gain insights into past climate and possible future global change.

Despite nitrogen's importance, its biogeochemical cycling in the oceans is not well understood. This is perhaps best exemplified by the current controversy over the state of the combined nitrogen budget. The dominant input of combined nitrogen to the ocean is believed to be through fixation of atmospheric di-nitrogen (N_2) by cyanobacteria, while the principal canonical removal term is reconversion of combined nitrogen to N_2 by denitrification. Some investigators believe the contemporary budget is more or less in balance [25, 43], while others have proposed marine nitrogen budgets that are severely out of balance with losses due to denitrification far exceeding inputs from nitrogen fixation [19, 26, 62]. The recent discovery that anaerobic ammonium (NH_4^+) oxidation to N_2 (anammox) may be common in suboxic zones of the oceans further complicates understanding of the marine nitrogen cycle [23, 27, 54]. Denitrification and anammox take place in suboxic environments after virtually all the oxygen has been depleted, as do several other respiratory processes that can potentially produce N_2 (Codispoti et al. [21] define suboxic as waters in which dissolved oxygen is vanishingly small but sulfate reduction has not been initiated). These suboxic environments are found in certain water-column areas and in the sediments of most shelf and upper slope environments. In today's oceans there are three major suboxic water masses: the intermediate waters of the eastern tropical North and South Pacific and the Arabian Sea [19].

2. THE ARABIAN SEA OXYGEN DEFICIENT ZONE (ODZ)

Oxygen deficient conditions (defined as $O_2 \leq$ 2-4 μM; [21]) in the intermediate waters (~200-1000 m) of the Arabian Sea were first noticed during the 1933-34 John Murray Expedition [41]; but their spatial extent was not

established untill the 1962-1965 International Indian Ocean Expedition [95]. Although the complete depletion of dissolved oxygen with the concomitant appearance of hydrogen sulfide (H_2S) has been reported [50] these conditions do not appear to be common in the open-ocean oxygen deficient zone in the Arabian Sea. However, H_2S has been observed during the occurrence of seasonal anoxia over the Indian shelf [74] and also off Peru [20, 33].

Circulation in the northern Indian Ocean is governed by two distinctly opposite monsoon cycles that are known to produce some of the greatest seasonal variability observed in any ocean basin [88]. During the Southwest Monsoon (June-September) strong southwesterly winds produce offshore Ekman transport resulting in coastal upwelling off the Arabian Coast and open-ocean upwelling due the wind stress curl [64]. The combination of upwelled nutrients, high aeolian dust flux and near constant, intense irradiance results in high primary production in a section extending about 1000 km off shore from the Arabian coast (1.5 g C m^{-2} d^{-1}; [6]). The Northeast Monsoon (December-February) is characterized by moderate winds from the Himalayas that send cool, dry air over the region, that combined with reduced winter solar radiation promote convective mixing. This raises surface nutrient concentration but not to levels as high as during the SW Monsoon, which again stimulates high productivity [6]. Comprehensive studies of primary production, long-term sediment trap deployments and detailed studies of the water-column distributions document the seasonality and interannual variability of the production cycle [75]. The high primary productivity creates high oxygen demand in intermediate waters and is one of the two primary factors responsible for the development of oxygen deficient conditions in the Arabian Sea, the other being the limited supply of oxygen to the intermediate layers (150-1000m). The oxygen deficient zone is supplied with water advecting in from three major areas: the southern Indian Ocean, the Persian Gulf, and the Red Sea. The majority of water entering the ODZ is ultimately derived from the southern Indian Ocean. This water outcrops around 45°S, where the surface oxygen concentration is high, but by time it reaches the southern border of the ODZ (~14°N) it loses almost all of its dissolved oxygen (Fig 1; [77]). Thus the combination of high oxygen demand and low oxygen source waters results in the strong and persistent ODZ in the Arabian Sea.

Upon oxygen depletion a suite of oxidized compounds serves as terminal electron acceptors for organic matter oxidation [38]. By far the most abundant suboxic electron acceptor in the open ocean is nitrate (NO_3^-). Thus, denitrification is believed to be the major mode of respiration in the oxygen deficient zone of the Arabian Sea [19, 67]. Canonically, denitrification proceeds via the series of reductions described by:

$$NO_3^- \rightarrow NO_2^- \rightarrow NO \rightarrow N_2O \rightarrow N_2 \qquad (1)$$

Nitrite (NO_2^-), nitric oxide (NO) and nitrous oxide (N_2O) are obligatory intermediates that sometimes escape to the environment where they can either accumulate and be exported or be re-assimilated and reduced. These features are clearly reflected in vertical profiles through the ODZ (Fig. 2). Although the NO_3^- concentrations begin to increase below the mixed layer, they have a local minimum near 250 m that reflects NO_3^- removal by denitrification. More or less coinciding with this minimum is a maximum in NO_2^-, an intermediate of denitrification; this feature is often referred to as the secondary nitrite maximum (SNM). Nitrous oxide typically shows local maxima on either side of the SNM also reflecting its nature as an intermediate. The oxygen deficient zone in the Arabian Sea generally thickens from south to north; NO_2^- concentrations first increase and then decrease in the same direction with the highest values occurring in the central Arabian Sea (Fig. 3). This high NO_2^- concentration is frequently interpreted as indicating increased denitrification rates [20, 63]. In the northwestern corner of the Arabian Sea, the input of Persian Gulf water is clearly evident as a southward penetrating tongue of slightly more oxygenated water (>5 μM).

The rate of water column denitrification in the Arabian Sea is generally believed to be globally significant. However, published estimates differ widely (from 0.1 to 44 Tg N yr^{-1}) with a majority falling between 21 and 44 Tg N yr^{-11} [19, 31, 46, 59, 66, 71]. These rates are strictly for canonical denitrification (N_2 produced from NO_3^-) but new information suggests that such estimates may be too low due to inappropriate stoichiometries and underappreciated pathways (see below). In addition to nitrogen oxides, oxides of Fe, Mn and I can also serve as oxidants under suboxic conditions, but the importance of these electron acceptors in suboxic oxidation of organic matter in the Arabian Sea water column is not known.

3. DENITRIFICATION RATE IN THE ARABIAN SEA

Various methods have been used to estimate denitrification rate in the Arabian Sea including stoichiometric relationships, measurements of the enzymatic activity of the electron transport system (ETS), and direct measurements of the amount of excess nitrogen gas. In combination with residence times or mass transport calculations these measurements yield areal denitrification rates.

Stoichiometric calculations involve calculation of an "expected NO_3^-" concentration (*sensu* Codispoti and Richards [15]), i.e., the NO_3^- concentration in a parcel of ODZ water expected before denitrification took place. Given an expected NO_3^- concentration and an analytical determination of the actual inorganic nitrogen concentration ($NO_3^- + NO_2^- + NH_4^+$), the measured can be subtracted from the expected to give a "NO_3^- deficit" or the amount of NO_3^-

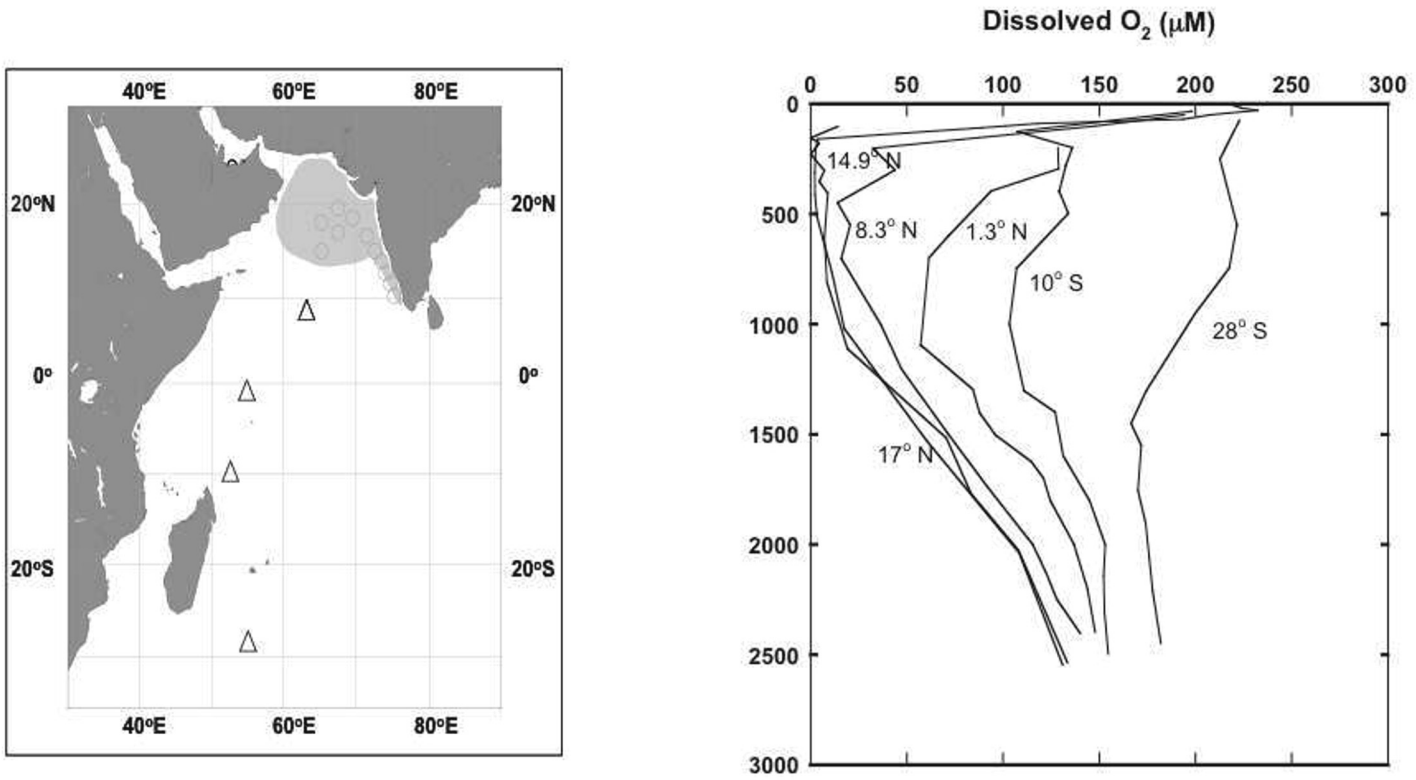

Figure 1. Station locations for the 4 WOCE stations used in this study, and the general extent of the ODZ in the Arabian Sea (right). Profile of dissolved oxygen in the Indian Ocean south of the Arabian Sea oxygen deficient zone, ODZ, and within the ODZ (left). The two stations in the ODZ are JGOFS stations (TT 43; M1 and N7 respectively).

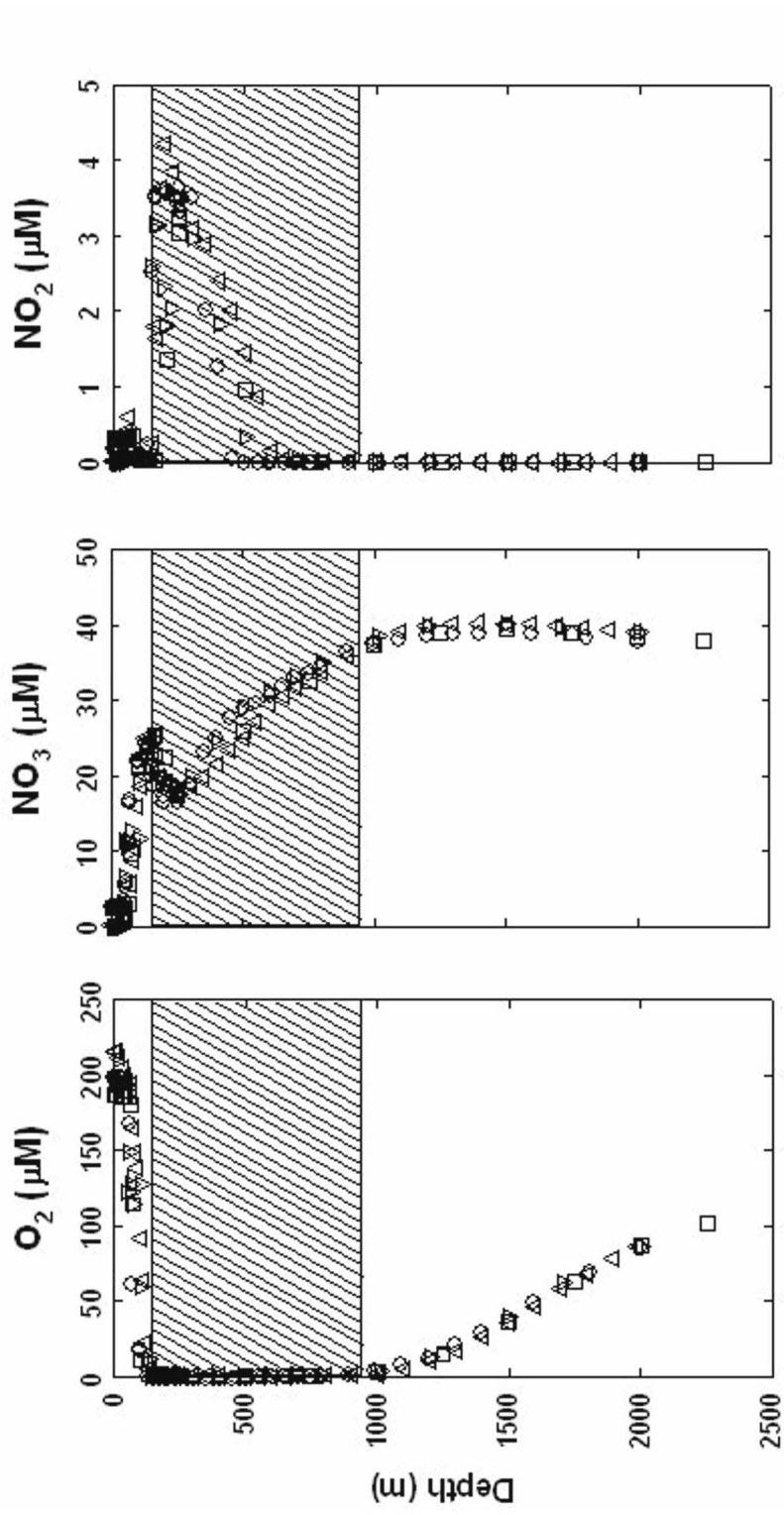

Figure 2. Dissolved oxygen (left), nitrate (center) and nitrite (right) in the heart of the oxygen deficient zone at four times during the year. The cross hatched area shows the approximate boundaries of the ODZ. Data used are from US JGOFS cruises, TGT 43, TGT 45, TGT 50 (Redrawn from [28]).

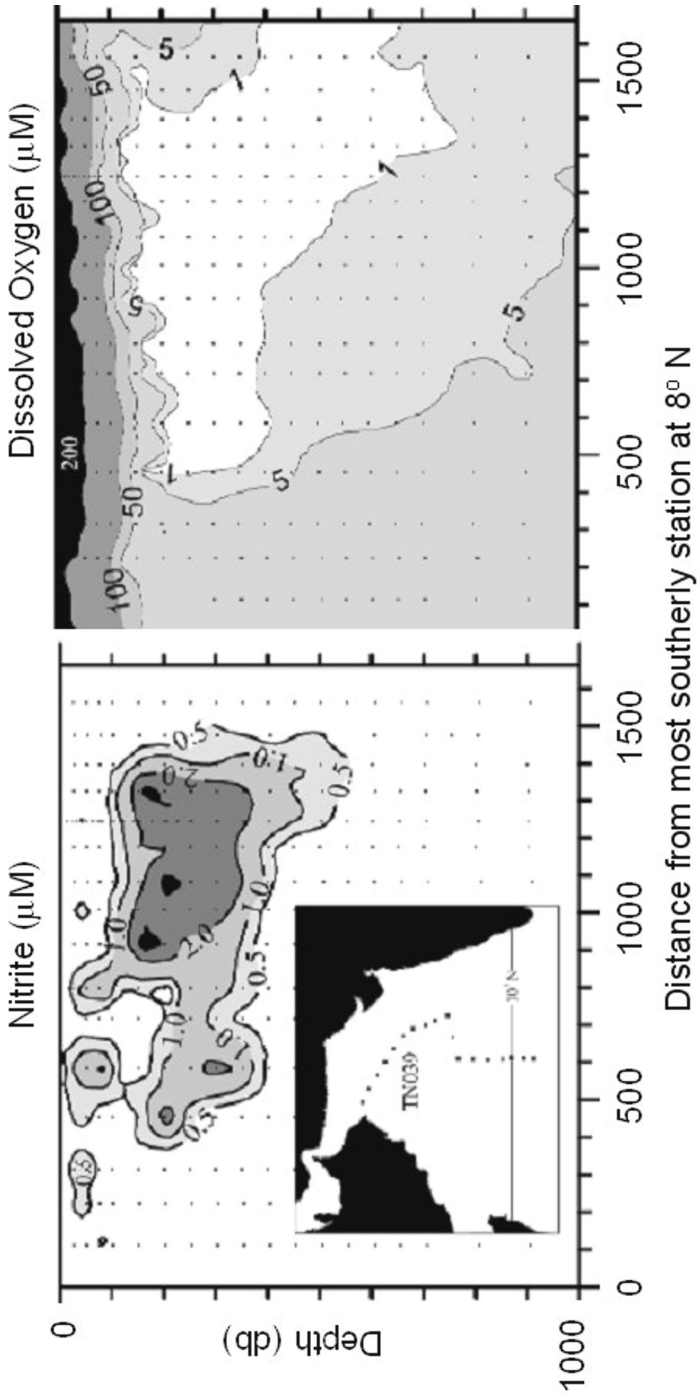

Figure 3. Nitrite and oxygen sections through the central part of the ODZ (from [19]).

removed by denitrification. Two primary methods have been used to calculate expected NO_3^-, both based on Redfieldian stoichiometry. The first is based on the "semi-conservative" water-mass tracer "*NO*" [9]. Stoichiometrically, every mole of O_2 respired will remineralize approximately 1/9 of a mole of NO_3^- so that "*NO*", defined as

$$NO = [O_2] + 9.1[NO_3^-], \tag{2}$$

should be a conservative property in most water masses. Then, given *NO* in any particular water mass, the amount of NO_3^- expected can be calculated by rearranging the above equation to the following:

$$NO_3^-\,(\text{expected}) = (NO - O_2)/9.1 \tag{3}$$

Naqvi and Sen Gupta [68, 70] and Mantoura et al. [59] have derived predictive *NO*-θ relationships for the non-denitrifying waters (outside the ODZ) in the Arabian Sea (θ = potential temperature). Given this relationship, *NO* can be used to calculate the amount of NO_3^- expected in the water column if there were no significant denitrification, and the nitrogen deficit, N_{deficit}, can then be calculated as:

$$N_{deficit} = NO_3^-\,_{(expected)} - [NO_3^-\,_{(measured)} + NO_2^-\,_{(measured)}] \tag{4}$$

However, extrapolation of these relationships into the ODZ is not entirely straightforward because the waters above and below the ODZ have different θ-S relationships. This has resulted in different authors utilizing different *NO*-θ relationships.

Nitrate deficits calculated from equation 4 using the *NO*-θ relationships developed by Naqvi [66] are shown in Fig. 4. Nitrate deficits are typically negative in the surface layers, increase dramatically in the oxycline and then decline toward zero deficit at the bottom of the ODZ, around 800 m. The negative values in the surface layers may be attributable to atmospheric exchange (alteration of the oxygen saturation state but not the nutrient concentration) and/or photosynthesis [72].

A different approach was taken by Codispoti et al. [19] to estimate NO_3^- deficit from the extensive, high-quality JGOFS nutrient data. Their calculation was based on the N* concept of Gruber and Sarmeinto [43], which relies on the stoichiometric assumption that for every phosphorus regenerated during organic matter degradation a fixed number of nitrogens are also regenerated. Therefore, if one knows the phosphate concentration of a water mass, the nitrate concentration can be predicted by stoichiometry. Deviations from this stoichiometry can be used to calculate the $N_{deficit}$. Briefly, Codispoti et al. used

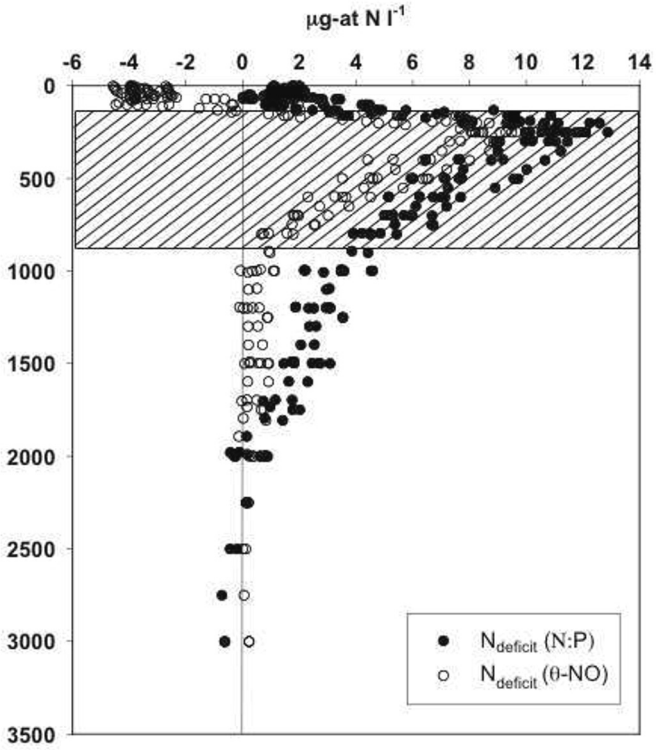

Figure 4. Comparison of nitrate deficit calculated from θ-NO relationships, and from N:P regressions. The cross hatched area shows the approximate boundaries of the ODZ. Data used are US JGOFS data (see caption to Fig 2).

Type II linear regressions of reactive phosphate (PO_4^{3-}) *vs* inorganic nitrogen ($IN=NO_3^- + NO_2^- + NH_4^+$) on samples from depths between 100 and1500 db, with oxygen concentrations >65 μM/l to determine the N-P relationship for the intermediate water before the onset of denitrification. The resulting equation was:

$$N_{deficit} = [(14.89\, PO_4^{3-} - 0.28) - IN]\,\mu M * 0.86\,(r^2 = 0.998), \qquad (5)$$

where $N_{deficit}$ is the estimate of the inorganic nitrogen removed from a water parcel by denitrification, $14.89 = \Delta IN/\Delta PO_4^{3-}$ (by atoms), 0.28 is the PO_4^{3-} intercept at IN, and 0.86 accounts for the PO_4^{3-} released by the organic material re-mineralized by denitrification assuming that N/P in local organic matter is 14.89, and that consumption of 94.4 NO_3^- by denitrification releases one PO_4^{3-} [38, 81]. Partially because this equation is independent of dissolved oxygen, it does not result in negative nitrate deficits in the surface layer (Fig 4). The

maximum predicted deficit is about 30% larger (12 vs 9 μM) and remains larger and extends about 1000 m deeper than the deficits calculated from *NO-θ* relationships. The observation that the denitrification signal penetrates well below the ODZ, to almost 2000 m is supported by isotopic data (See section 5).

Estimation of denitrification rate from NO_3^- deficit requires knowledge of the time over which the deficit has accumulated. Typically, this is taken as the residence time of intermediate waters within the ODZ. Mantoura et al. [59] vertically integrated NO_3^- deficits calculated from *NO-θ* relationships, extrapolated them to the area of the denitrification zone, and then combined them with a CFC derived residence time of 10 years to arrive at a denitrification rate of 11.9 Tg N yr^{-1} for the entire ODZ volume. Besides the uncertainty involved in the nitrate deficit calculation, this estimate also compounds the uncertainties in the area of the denitrification zone and the residence time. In an effort to circumvent these uncertainties, Naqvi [66] took a different approach and determined NO_3^- deficit on an east-west section across the Arabian Sea. He calculated the diffusive and advective losses of NO_3^- deficits from the ODZ, the latter from geostrophic transport of intermediate water across this section. The rate so obtained was 29.5 Tg N yr^{-1}, approximately three times as great as Mantoura et al.'s estimate. Howell et al. [46] combined data on NO_3^- deficit and CFC ages to compute a rate of 21 Tg N yr^{-1}.

Another technique that has been used to quantify denitrification in the Arabian Sea is the measurement of ETS activity [71]. This method utilizes crude enzyme extracts of material filtered from ODZ waters to which electron donors (NADH and NADPH) are added and the rate of electron passage to an artificial electron acceptor is measured. This technique measures only to canonical denitrification. Using this technique, Naqvi and Shailaja [71] determined the denitrification rate in the Arabian Sea to be 24-33 Tg N yr^{-1}; Although this estimate is independent of any residence time calculation, it is still dependent on the estimate of the area of the denitrification zone (when adjusted to an area of 1.5 x 10^{12} m^2, this range expands to 31.9-43.9 Tg N yr^{-1}; [28]). Moreover, it also involves assumptions concerning the conversion of ETS activity to denitrification rate.

A final way investigators have attempted to quantify denitrification in the Arabian Sea is to measure the end product of the process, N_2. Devol et al. [28] report measurements of nitrogen gas in waters from the Indian Ocean, especially the Arabian Sea, made by isotope ratio mass spectrometry. Results are presented as normalized nitrogen:argon ratios, $(N_2{:}Ar)_n=(N_2{:}Ar)_s\ /(N_2{:}Ar)_e$ where $(N_2{:}Ar)_s$ is the sample ratio and $(N_2{:}Ar)_e$ is the atmospheric equilibrium ratio, such that at equilibrium with the atmosphere $(N_2{:}Ar)_n=1.00$. Once subducted below the euphotic zone the noble gas Ar should maintain its equilibrium saturation but biological processes, such as denitrification (and possibly

others) can change N_2 saturation state. Devol et al. [28] present four profiles from the Indian Ocean south of the Arabian Sea oxygen deficient zone (Fig. 5), which are nearly identical to profile from other oxygenated waters of the Atlantic, Pacific and Southern Ocean ([44]; Uhlenhopp et al., unpublished). Although the N_2:Ar ratio increases slightly with depth, this increases is due to the effects of bubble injection during water mass formation rather than any biological alteration [44]. In contrast, the profile of $(N_2{:}Ar)_n$ in the waters of the ODZ contains a distinct maximum indicative of the excess of nitrogen gas resulting from denitrification (Fig. 5). To quantify the excess, "background" values obtained by averaging the four profiles outside the suboxic zone were subtracted from the ODZ values. The resulting fractional N_2 excesses were multiplied by the in situ equilibrium N_2 saturations to give the actual concentrations of excess N_2 (Fig 5; [28]). Excess N_2 values were zero at the top of the ODZ, reached a maximum of about 22 μg-at/l at 250 m and then decrease more or less exponentially to background values around 2000 m (Fig. 5). Interestingly, the shape of the excess N_2 profile is similar to the shape of the NO_3^- deficit profile determined by Codispoti et al. [19], but the absolute amount of excess N_2 is about twice as much as the NO_3^- deficit. The position of both the excess N_2 and NO_3^- deficit maxima near the top of the suboxic zone is likely due to the fact that the rain rate of organic matter is greater there.

Reasons for the large discrepancy between the N_2 excess values and the NO_3^- deficits are unclear but the discrepancy suggests sources of combined nitrogen for N_2 production in addition to just NO_3^-. It also suggests NO_3^- deficits underestimate the true denitrification rate, i.e. the conversion of combined N to N_2 gas. Because NH_4^+ concentrations in the ODZ are uniformly low, part of the difference is likely due to oxidation of the NH_4^+ liberated from organic matter decomposition during denitrification to N_2, possibly by anammox bacteria [48]. However, given Redfield organic matter and the denitrification stoichiometry of Froelich et al. [38], NH_4^+ oxidation could only account for a 15% increase over the nitrate deficit. Even the protein rich stoichiometry for denitrification proposed by Van Mooy et al. [91] would increase the N_2 production by only about 27%. Although, nitrogen gas production coupled to manganese (and iodine) cycling has been suggested for sedimentary environments [36, 57], these oxidations are likely to be only minor contributors in the open Arabian Sea (Codispoti et al. [19]). A potential source of excess N_2 is from denitrification or anammox in the sediments in contact with the ODZ. The Arabian Sea is a semi-enclosed basin with continental margin on three sides and radium distributions show that sedimentary signals penetrate into the interior waters [89]. Given a sedimentary denitrification rate of the same order as that off the West Coast of the US (~1.5 mM m^{-2} d^{-1}; [45]) and a sediment area in contact with the ODZ of 4.5×10^{11} m^2 [28], potential sedimentary denitrification could be 3.9 Tg N yr^{-1}.

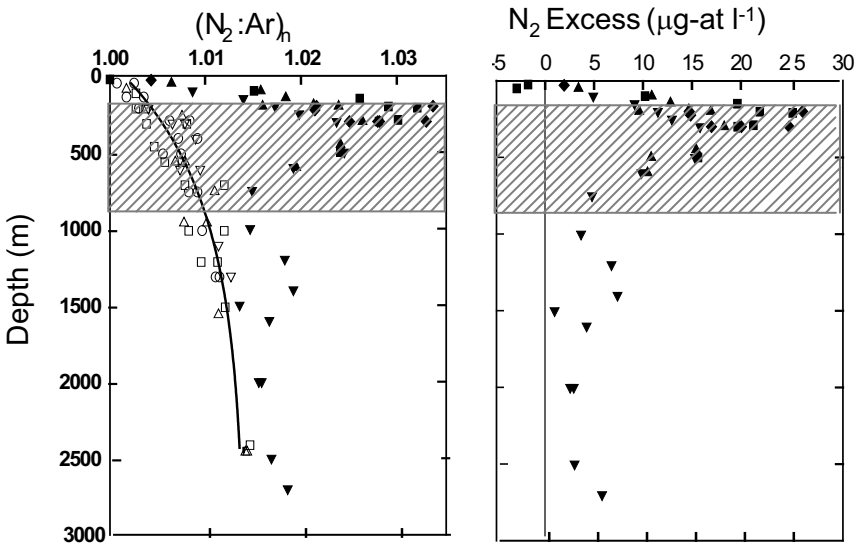

Figure 5. N:Ar ratio profiles (left) from the four WOCE stations (open symbols) as well as those in the ODZ (Solid symbols) and Composite N_2 excess profile (right). Symbols are as follows 28 °S, open triangles; 10 °S open circles; 1 °S open inverted triangles; 8 °N open squares; Jan. 98, solid squares; Dec. 98, solid triangles; Apr. 96, solid inverted triangles; and Sept. 99, solid diamonds. The cross hatched area shows the approximate boundaries of the ODZ (Redrawn from [28]).

This is close to the upper end of the range (0.4-3.5 N yr^{-1}) for sedimentary denitrification for the Arabian Sea reported by Naik [65]. Sulfate reduction is probably the dominant carbon oxidation pathway in the sediment bordering the ODZ. Moreover, there are several strains of sulfide oxidizing bacteria, e.g. *Thioploca, Beggiatoa and Thiomargarita*, that derive energy from the reduction of NO_3^- to NH_4^+ [49] and mats *Thioploca*, are known to occur in sediments of the Arabian Sea ODZ [84]. The NH_4^+ produced by these processes will diffuse into the overlying water where anammox could convert it to N_2 [20]. It may be noted that the chemoautotrophic reduction of NO_3^- to NH_4^+ does not involve regeneration of PO_4^{3-}. It should be noted however, that because sedimentary processes also regenerate PO_4^3, they could only contribute to the excess N_2 to the extent that nitrogen is preferentially recycled relative to phosphorus. ODZ sediments have been found to support phosphogenesis with the apatite precipitation rate varying between 0.08 and 1.04 μmole P cm^{-2} yr^{-1} [83]. Thus, one might expect higher N/P export ratio from the ODZ sediments than ex-

pected from the Redfieldian stoichiometry [19], and this could contribute to the observed excess of N_2 over the NO_3^- deficit.

Nitrogen fixation in the Arabian Sea could also elevate N_2 yields during denitrification because N-fixers have N:P ratios much greater than Redfield (up to 100; [43, 51]). Capone et al. [11] have shown that blooms of the nitrogen fixing organism *Trichodesmium* can at times cover 20% of the Arabian Sea and that N-fixation at times can supply all the nitrogen for new production. Further, Brandes et al. [8] have recently estimated that 20% of the primary production in the Arabian Sea is fueled by nitrogen fixation (see following section). Given an N:P ratio of 60 for nitrogen fixers and a 20% contribution to new production in the Arabian Sea, N-fixation would increase the N:P ratio of the sinking flux to ~ 24.8 , similar to that Karl et al. [51] observe at station ALOHA, 22.4. This would be a 50% increase and thereby increase the N_2 excess (up to 50% if all N_2 production were driven by this vertical flux

It appears that there is no single mechanism that could explain the discrepancy between NO_3^- anomaly and excess N_2 in the Arabian Sea ODZ; instead, there are a number of identifiably processes that could supply the extra N_2 over that derived from the reduction of NO_3^-. Consequently, it is likely that the discrepancy results from some combination of these processes. In any case, the N_2/Ar data clearly indicate that the current estimates for water column denitrification in the Arabian Sea may be too low with respect to those derived from the nitrate deficit or the ETS activity (which also involved lower ratios of N_2 production to NO_3^- consumption). Codispoti et al. [19] scaled up the current "best estimate" (30 Tg N yr^{-1}) of canonical denitrification by a factor of 2, taking into account both the underestimation of nitrate deficits by earlier workers and the likelihood of other sources of N_2 production in addition to NO_3^- reduction, to suggest that that the rate of water column denitrification in the Arabian Sea may be as high as 60 Tg N yr^{-1}. It may be noted that this estimate pertains to the perennial, open ocean suboxic zone, and it does not include denitrification in the seasonal suboxic system over the Indian shelf. However, the latter is an order of magnitude smaller in magnitude even though the specific rates are much higher (Naqvi et al., this volume; [28]).

4. N_2O AND THE ODZ

Nitrous oxide is a by-product or an intermediate of both nitrification and denitrification and each processes likely plays a role in determining the N_2O distributions in the Arabian Sea suboxic zone. Although N_2O is quantitatively of only minor significance as a combined nitrogen species in seawater, it is nevertheless an important gaseous constituent because of its high greenhouse efficiency – on a per molecule basis it is 200-300 times as effective as CO_2 in trapping infrared radiation [58]. A typical profile of N_2O in the suboxic zone of

the Arabian Sea is shown in Fig. 6. Surface waters are generally supersaturated [4, 29, 56, 69, 80, 93]. Below the mixed layer, concentrations increase to about 10 times the saturation values forming a local maximum. This feature usually coincides with the lower boundary of the oxycline [69]. Within the core of the ODZ, N_2O concentrations decrease to very low values, but at the lower transition from suboxic back to oxic conditions the concentrations again increase to highly supersaturated values. Below this deeper maximum, N_2O concentrations fall steadily with depth but remain well above saturation at least down to 2500 m [69, 72, 73].

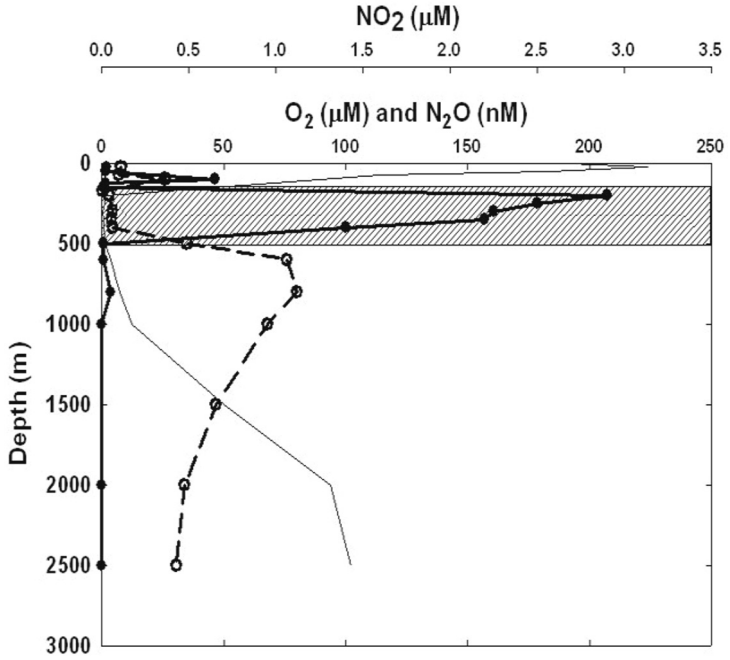

Figure 6. Vertical profiles of N_2O (open circles, dotted line), NO_2 (solid circles, solid line) and O_2 (line only). The ODZ depth interval is shown by crosshatching. Composite redrawn from figures in [72] .

In the oxygenated waters N_2O concentrations are positively correlated with the apparent oxygen utilization (AOU), albeit with separate relationships in the upper and deep waters [69]. The linear relationships between N_2O and AOU observed in various oceanic areas have been interpreted to reflect N_2O production through nitrification [34, 78, 97]. However, as the oxygen concentrations approach suboxia at the boundaries of the ODZ, N_2O accumulates to levels much above those predicted by the N_2O-AOU regression line. Enhanced

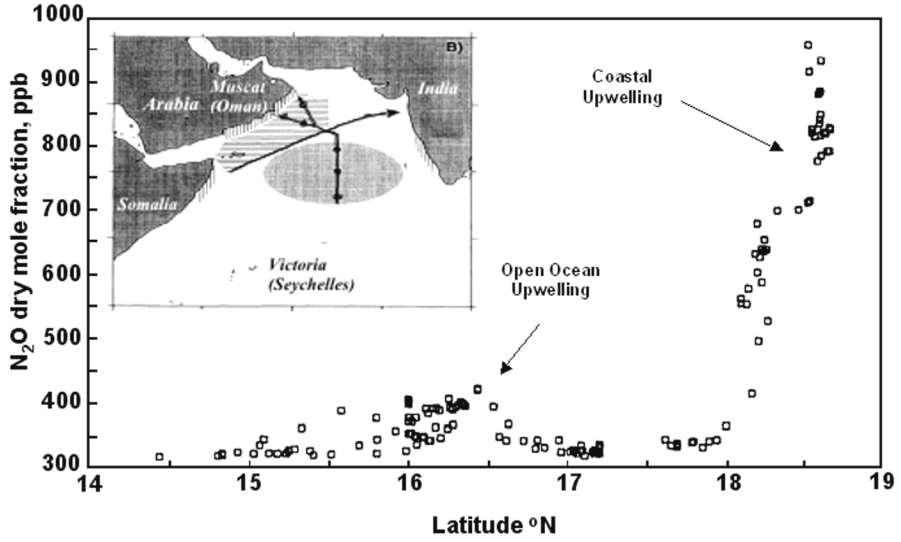

Figure 7. Surface N_2O concentrations in July-August in the Arabian Sea along the cruise track shown in the inset. The vertically hatched area is the area of coastal upwelling, while the horizontally hatched area is the area of open-ocean upwelling during the southwest monsoon. The area of downwelling with a deep mixed layer is shaded gray and the arrow represents the Finlader atmospheric jet that drives the South-West Monsoon. (redrawn from [4]).

production of N_2O in oxygen-poor (but not suboxic/anoxic) waters may result from enhanced yield of N_2O during nitrification at low oxygen levels [41], denitrification [96] or a possible coupling between the two processes [69]. As discussed below, isotopic measurements reveal different compositions of N_2O within the shallower and deeper maxima, suggesting the involvement of various formative mechanisms.

The low N_2O concentrations within the core of the ODZ are typical of other open-ocean ODZs [16, 18, 22]. The N_2O minimum coincides with the SNM, which suggests a net consumption of N_2O by denitrifiers. This is in contrast with the trend seen in the more variable, shallower denitrifying systems [17, 18], including that occurring seasonally over the Indian shelf (Naqvi et al., this volume), where denitrification can sometimes lead to enormous buildups of N_2O in the water column. Naqvi et al. [74] attributed this to the low N_2O reductase activity in "young", rapidly denitrifying systems since denitrifiers usually have to synthesize this enzyme after the development of suboxic conditions [18].

The proximity of the shallower N_2O maximum to the sea surface sustains high concentrations (in excess of the saturation values) in surface waters as mentioned earlier. The energy needed for the entrainment of N_2O-rich subsur-

face water into the surface layer is provided by monsoon forcing (e.g. through upwelling during the southwest monsoon and convective overturning during the northeast monsoon). However, as a consequence of the non-uniformity of monsoon forcing in space and time, N_2O distributions in the Arabian Sea surface waters shows considerable seasonal and spatial variations. The highest surface saturations have been found to occur during the southwest monsoon within zones of coastal upwelling off Somalia (up to 330%; [30]), Oman (up to 230%, Fig 7; [4]) and India (8250%; Naqvi et al., this volume). Widespread winter cooling in the open northern and central Arabian Sea occasionally raises the saturation level above 400% [47]. The lowest surface saturations (99-105%) have been reported from the central Arabian Sea during the spring intermonsoon, a period of strong vertical stability [4, 55].

Recently, Bange et al. [5] utilized over 2400 surface N_2O measurements made between 1977 and 1997 to compute mean seasonal and annual N_2O concentrations within 1^ox1^o grids. The annual emission rate calculated from these data is 0.33-0.70 Tg N_2O. As expected, coastal regions during the SW monsoon appear to account for the bulk of the fluxes. However, this data set did not include the very high N_2O concentrations off the Indian west coast, which suggest a seasonal (May-October) flux of N_2O from the shelf ranging from 0.06 to 0.39 Tg N_2O [74]. Inclusion of these data would push up Bange et al.'s [4] estimate to ~0.4-1 Tg N_2O yr^{-1}, amounting to up to one-fifth of total oceanic emissions of N_2O (4.7 – 6.3 Tg N_2O yr^{-1}; [76]).

5. ISOTOPIC CONSEQUENCES OF NITROGEN CYCLING IN THE ODZ

There are two naturally occurring stable isotopes of nitrogen, ^{14}N and ^{15}N, with ^{14}N far more abundant, 99.63%. Because of this mass difference, the activation energy for biological reactions involving the heavier isotope, ^{15}N, is slightly greater than that for the lighter isotope, resulting in a slower reaction. Consequently, there occurs a kinetic discrimination against the heavier isotope leading to an increase in the $^{15}N/^{14}N$ ratio in the reactants and a decrease in the ratio in the products. The isotope composition is typically expressed as the part per thousand change in the isotope ratio, δ = ‰, relative to a standard; in the case of nitrogen the standard is air. These isotopic fractionations are very useful in the study of nitrogen cycling in the oceans.

Isotope measurements have been made for three of the major nitrogen species involved in nitrogen cycling in the Arabian Sea ODZ [8, 72, 73, 98]. At a station in the heart of the ODZ with a well developed SNM, the isotopic composition of NO_3^- shows a dramatic increase in $\delta^{15}N$ (Fig. 8). Outside the ODZ's the isotopic composition of NO_3^- is relatively constant (4-6‰; [86, 92]). Deep-water $\delta^{15}N$–NO_3 values in the Arabian Sea are within this range. However, as one moves up in the water column the $\delta^{15}N$ of NO_3^- increases dramatically to

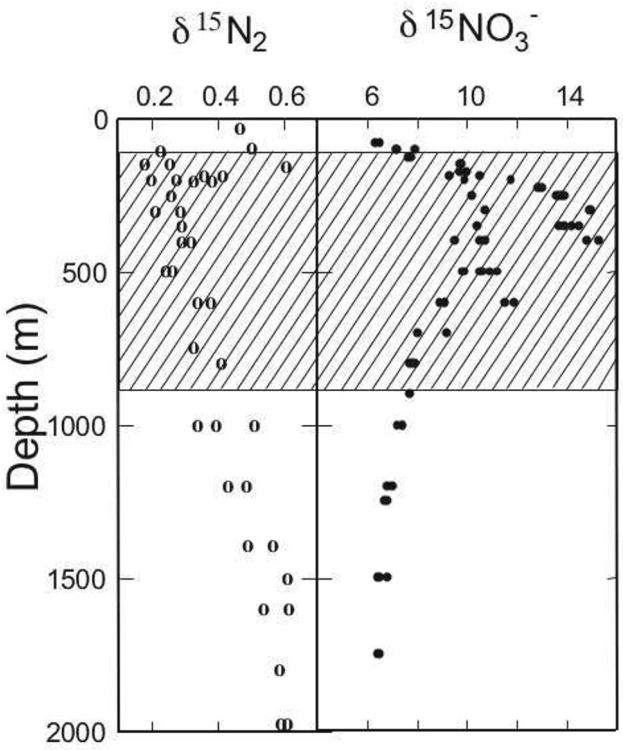

Figure 8. Composite profiles of $\delta^{15}N_2$ and $\delta^{15}NO_3^-$ from profiles taken in the heart of the ODZ (Data from Brandes 1996). The cross hatched area shows the approximate boundaries of the ODZ.

a maximum of about 15‰, more or less coincident with the SNM. Above the SNM the $\delta^{15}N$ of NO_3^- decreases to about 6‰ at the base of the mixed layer. The large enrichment of ^{15}N in NO_3^- within the heart of ODZ is undoubtedly due to fractionation during denitrification, especially as it is corroborated by the mirror-image decrease in $\delta^{15}N$ of N_2 (Fig 8). Laboratory culture studies suggest a fractionation factor, ε, for denitrification of 17-20‰ [25, 61]. Given the data shown in Fig. 8 and nitrate deficits calculated from hydrographic data, Brandes et al. [8] fitted the Rayleigh fractionation equation, to arrive at a fractionation factor of 22‰ (Rayleigh fraction: $\Delta\delta^{15}N\text{-}NO_3^- = 10^3(\alpha - 1)\ln f_{NO_3}$, where α is the ratio of reaction rates of ^{15}N and ^{14}N and f_{NO_3} is the fraction of the initial NO_3^- removed by denitrification). The Rayleigh fraction equation represents a closed system; however, Brandes et al. [8] also used an open-system advection-reaction model to calculate a fractionation factor of 25‰. Altabet et al. [3] reported a similar, but slightly higher, value for ε. As theses values are very similar to fractionation factors calculated similarly for

the ODZ's of the eastern tropical North Pacific [3, 8], it appears that open-ocean-water-column denitrification may display a relatively constant isotope fractionation.

Interestingly, the NO_3^- isotope composition at the base of the mixed layer is characterized by a relative depletion of ^{15}N ($\delta^{15}N \sim 6‰$). In non-ODZ areas the trend toward the surface is exactly the opposite, i.e., the $\delta^{15}N$ of NO_3^- increases toward the surface due to the preferential uptake of $^{14}NO_3^-$ by phytoplankton [2, 86]. Thus, there appears to be a requirement for a source of isotopically light fixed nitrogen in the Arabian Sea mixed layer. This light fixed nitrogen must either be laterally advected to the central Arabian Sea or generated locally through nitrogen fixation, which produces fixed nitrogen with an isotopic signature near 0‰ [94]. The principal water mass that forms the upper portion of the thermocline, characterized by light $\delta^{15}N$ - NO_3^- values, is the Arabian Sea high salinity surface water. This water is formed in the northern Arabian Sea during winter [53]. The nitrate content of this water is expected to be determined by local processes (regeneration from organic matter and vertical supply from the deeper layers) rather than the long range transport from the south. Hence nitrogen fixation appears to be the most likely process responsible for the observed decrease in $\delta^{15}N$ of NO_3 in near surface waters.

Brandes et al. [8] estimated the amount of nitrogen fixation required to match the observed NO_3^- isotope distribution. They assumed the water upwelled to the mixed layer originated at 200 m, which had an isotopic composition of 11‰. If all the upwelled NO_3^- were utilized by primary producers in the mixed layer above 80 m, then a simple mixing calculation suggested that 40% of the fixed nitrogen must have come from nitrogen fixation. This gave them a rate of 6 TgN y^1. Because newer primary production data [6] is about twice as great as estimates [79] used by Brandes et al., this might be a low estimate for N-fixation. Conversely, the upwelling depth chosen by Brandes et al., is deeper than that suggested by the analysis of USJGOFS data [63], which would lower Brandes et al.'s estimate. Nevertheless, the nitrogen fixation rate in the Arabian Sea appears to be lower by several times than the denitrification rate indicating that on balance the Arabian Sea is a substantial sink of fixed nitrogen.

Dual isotopic analysis of N_2O also shows a pattern of enrichment of both ^{15}N and ^{18}O (relative to the more abundant ^{16}O) – sometimes exceeding 30‰ (versus air) and 60‰ (versus Standard Mean Ocean Water), respectively - in strongly denitrifying waters (Fig. 9; [72, 73, 98]). In general, the maxima in $\delta^{15}N$ and $\delta^{18}O$ are associated with the minimum of N_2O concentration. At sites located at the periphery of the perennial denitrification zone where the intermediate N_2O concentration minimum was weakly developed, enrichments in the two heavier isotopes were not as great as at those at strongly denitrifying locations [72]. It is obvious, therefore, that the isotopic anomalies in the denitrifying waters result from the preferential loss of light N_2O to N_2.

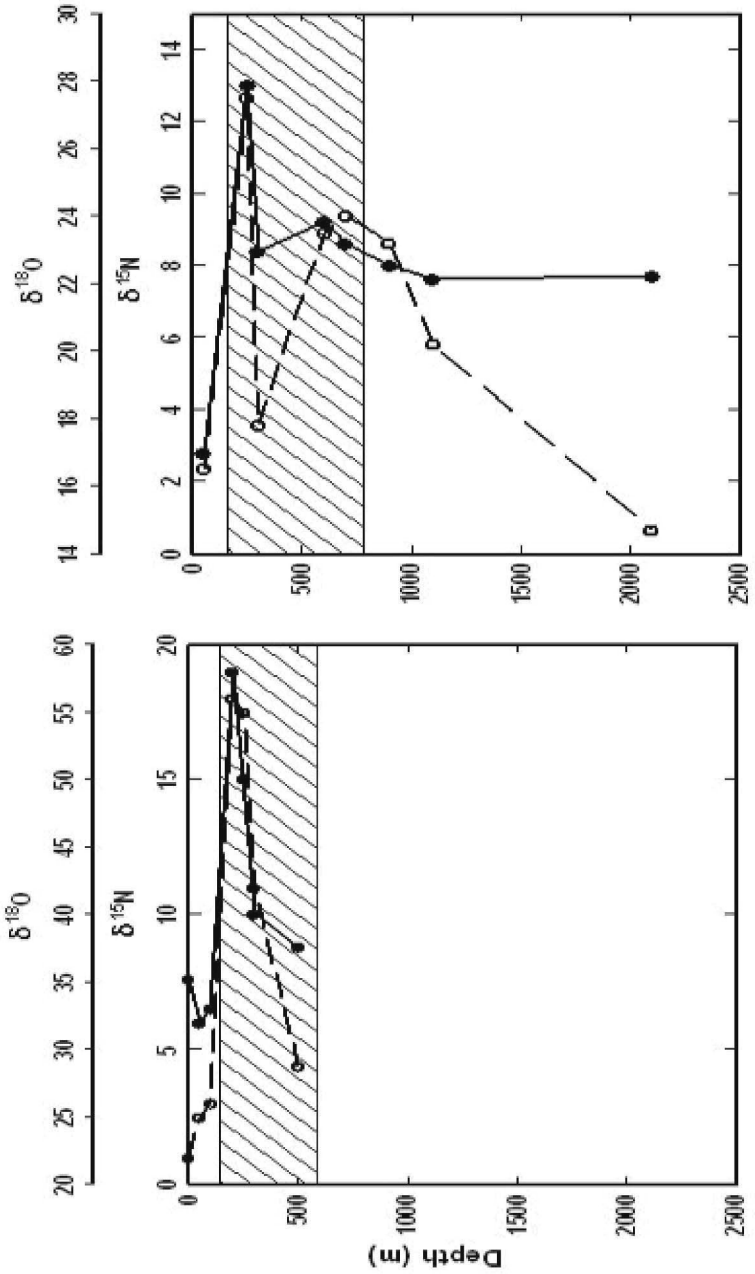

Figure 9. N (solid line) and O (dashed line) isotopic composition of N_2O at two stations in the Arabian Sea: (left) Cruise *SK87* station 11, well within the ODZ at ~19°N and (right) Cruise *SS106* station 14 at the southern boundary of the ODZ at ~15°N. The cross hatched area shows the approximate boundaries of the ODZ. (Redrawn from [72]).

Moving upwards out of the ODZ, the $\delta^{15}N$ and $\delta^{18}O$ values for N_2O fall rapidly across the oxycline with mixed-layer $\delta^{15}N$ values typically lower than the atmospheric equilibrium value of roughly 7‰ [52]. The lightest values, more pronounced for N than for O, are found close to the base of the mixed layer where nitrification activity should be maximal [16]. As stated earlier, an N_2O concentration maximum is also observed at about the same level. Experimental studies have revealed that N_2O produced through nitrification is depleted in the heavier isotopes especially ^{15}N [96]. The upper-pycnocline isotopic minima have also been reported to occur in the Pacific Ocean and they were explained by invoking production through nitrification [31]; it is reasonable to assume that the same process may be predominantly responsible for the enhanced N_2O production below the mixed layer in the Arabian Sea as well. The relatively high $\delta^{18}O$ values of N_2O within the surface waters [73] also support nitrification as the likely mechanism. This is because of the fact that as a result of intense oxygen consumption the residual dissolved oxygen, used for oxidation of NH_4^+, is enriched with ^{18}O, and this signal is expected to be reflected in the isotopic composition of N_2O formed as a by product of nitrification. As an alternative, Naqvi et al. [73] suggested that N_2O having light N but relatively heavy O might be formed from some intermediate of the nitrification process, e.g. NO that may subsequently be reduced to N_2O. The capping of the suboxic layer by the layer with light N_2O prevents the escape of the heavy N_2O from the ODZ to the atmosphere [73], except in rare cases when the water from the suboxic zone itself is brought up through upwelling or vertical mixing (Naqvi et al., in preparation).

A decrease in the extent of ^{15}N and ^{18}O isotope enrichment also occurs across the lower suboxic-oxic interface as the depth increases, but N_2O remains relatively enriched in both heavy isotopes relative to the tropospheric average values even in the deep waters. Heavy isotope enrichments of somewhat smaller magnitude have also been reported for the deep waters of the Pacific Ocean [52]. The reasons for the isotopic enrichment are not very clear, but causative factors may include consumption/production through denitrification within micro-reducing sites and/or long-range transport of heavy N_2O (e.g. from continental margins).

5.1 Glacial-Interglacial Denitrification Signals in the Arabian Sea

The transition from the last glacial maximum (LGM, about 20,000 yr B.P.) to the current interglacial was accompanied by ~85 ppm change in atmospheric CO_2 content. Whether this CO_2 change caused the transition or merely was a response to it is not yet resolved. To transfer carbon from the atmosphere and sequester it in the deep ocean many models invoke higher productivity

during the LGM. This could have been driven by greater nitrogen fixation [10], diminished denitrification [12, 13, 40, 60], greater NO_3 utilization in the present high nutrients – low chlorophyll regions [37, 87]) or a combination of some or all of the above possibilities. Although increased productivity driven by greater relative nitrogen fixation (which causes an increase in the combined nitrogen inventory) would enhance oceanic capacity to sequester atmospheric CO_2, it would also lead to greater oxygen demand at depth and, presumably, more denitrification (which causes a decrease in the combined nitrogen inventory). Clearly, the interactions between nitrogen fixation, primary production, deep-water oxygen depletion and denitrification are far from resolved.

The high productivity and suboxic conditions in the Arabian Sea result in preservation of excellent sedimentary records of past conditions in the oceans, especially in margin areas where the ODZ impinges on the sediments. The lack of oxygen in waters overlying the ODZ sediments also precludes large benthic organisms and bioturbation such that sediments from these zones are frequently laminated [85]. Furthermore, denitrification in suboxic waters produces ^{15}N-enriched nitrate, which, upon being upwelled into the photic zone, becomes incorporated into the plankton. Remains of these plankton imprint the denitrification signal in the organic rain to the sediments where the isotopic signal of denitrification becomes part of the sedimentary record [3, 82]. Consequently, down-core records of $\delta^{15}N$ have been treated as records of denitrification in the past [2, 3, 39, 40].

In the Arabian Sea, contemporary sediments have an isotopic $\delta^{15}N$ of ~8‰, and this highly positive signal is prevalent throughout the Holocene; in contrast, lighter isotopic values (~5-6‰) occur in sediments that accumulated during the LGM and indeed during all glacial stages [1, 2, 3, 39, 40, 90]. These values are typical of non reducing environments in today's ocean. This implies that water-column denitrification was either absent or it was much weaker during glacial times. Spectral analysis of the sedimentary $\delta^{15}N$ records showed a high degree of cyclicity associated with the three Milankowitch bands of 100,000, 41,000 and 23,000 year frequencies [2]. The association with the 23,000 year precessional band which dominantly regulates the monsoon strength is particularly strong. Higher resolution records indicate variations on an even shorter (millennial) time scale, closely linked with the climatic changes recorded by the Greenland ice cores [1, 90]. For example, the $\delta^{15}N$ records in sediment cores from the Oman Margin (Fig. 10; [1]) show oscillations that are remarkably similar in structure and timing to the Dansgaard/Oeschger (D/O) events recorded in the Greenland (GISP2) ice cores (D/O events are warm periods punctuating the last glacial with a frequency of about 1600 y; [24]). Moreover, when smoothened with a 3000 yr running average – to account for the dampening effect of the residence time of nitrogen in the sea – the Arabian Sea denitrification records are incredibly similar to the Antarctic temperature

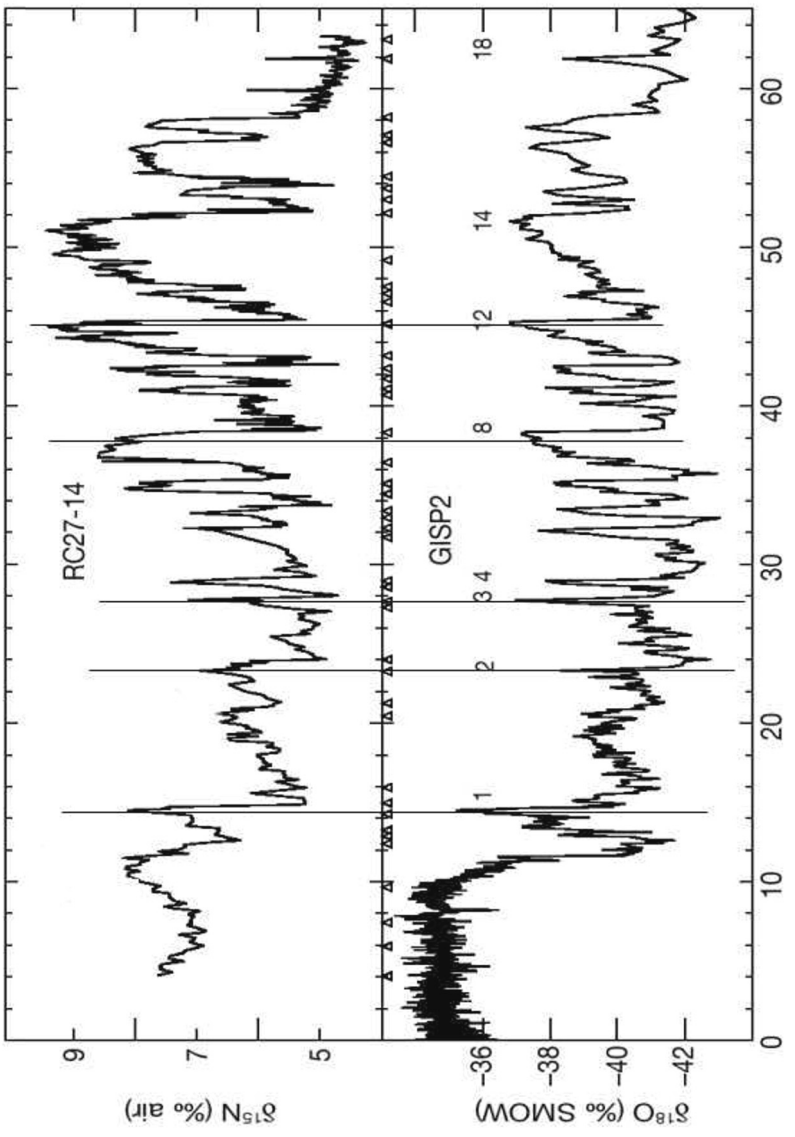

Figure 10. Correlation between δ^{15}N in sediment cores in the Arabian Sea (core RC27-14) with the GISP2 ice-core record of temperature (δ^{18}O of ice is a proxy for temperature with more positive values being higher temperature). Lines added to show the strong correlation. Numbers in lower panel refer to Dansgaard-Oeschger events. Triangles indicate stadial-interstadial mid-points used to synchronize the two records. Redrawn from [1].

and CO_2 records, leading Altabet et al. [1] to conclude that changes in denitrification in the ODZ of the Arabian Sea, and probably in other similar areas of the eastern tropical Pacific, had a major impact on global climate.

Acknowledgements

We express our gratitude to the Department of Ocean Development (DOD), Government of India, for generously allotting time on Sagar Kanya and Sagar Sampada for this project. AHD and LAC were supported by the NSF through grants OCE 9416626 and OCE 0118036. SWAN supported by the DOD (under the project "Land Ocean Interactions in the Coastal Zone") and by the Council of Scientific and Industrial Research (CSIR).

References

[1] Altabet M., Higginson M. J. and Murray D. W. The effect of millennial-scale changes in Arabian Sea denitrification on atmospheric CO_2. Nature 2002; 415:159-62.

[2] Altabet M. A., Francois R., Murray D. W. and Prell W. L. Climate-related variations in denitrification in the Arabian Sea from sediment $^{15}N/^{14}N$ ratios. Nature 1995; 373:506-09.

[3] Altabet M. A., Murray D. W. and Prell W. L. Climatically linked oscillations in Arabian Sea denitrification over the past 1 m.y.: Implications for the marine N cycle. Paleoceanography 1999; 14(6):732-43.

[4] Bange H. W., Rapsomanikis S. and Andreae M. O. Nitrous oxide in coastal waters. Global Biogeochem Cycl 1996; 10:197-207.

[5] Bange H.W., Andreae M.O.,Lal S., Law C.S., Naqvi S.W.A., Patra P.K., Rixen T. and Upstill-Goddard R.C. Nitrous oxide emissions from the Arabian Sea: A synthesis. Atmos Chem Phys 2001; 1:61-71.

[6] Barber R.T., Marra J., Bidigare R.R., Codispoti L.A., Halpern D., Johnson Z., Latasa M., Goericke R. and Smith S.L. Primary productivity and its regulation in the Arabian Sea during 1995. Deep-Sea Res II 2001; 48:1127-72.

[7] Brandes J.A. *Isotopic effects of denitrification in the marine environment.* Ph.D. Thesis, University of Washington, Seattle, 1996.

[8] Brandes J. A., Devol A. H., Yoshinari T., Jayakumar D. A. and Naqvi S. W. A. Isotopic composition of nitrate in the central Arabian Sea and eastern tropical North Pacific: A tracer for mixing and nitrogen cycles. Limnol Oceanogr 1998; 43:1680-89.

[9] Broecker W. S. "NO", a conservative water-mass tracer. Earth and Planet Sci Lett 1974; 23:100-07.

[10] Broecker W. S. and Henderson G. M. The sequence of events surrounding Termination II and their implications for the cause of glacial-interglacial CO_2 Changes. Paleooceanography 1998; 4:352-64.

[11] Capone D. G., Subramaniam A., Montoya J. P., Voss M., Humborg C., Johansen A. M., Siefert R. L. and Carpenter E. J. An extensive bloom of the N_2-fixing cyanobacterium *Trichodesmium erythraeum* in the central Arabian Sea. Mar Ecol Progr Series 1998; 172:281-92.

[12] Christensen J. P., Smethie W. M. and Devol A. H. Benthic nutrient regeneration and denitrification off the Washington continental shelf. Deep-Sea Res 1987; 34:1027-47.

[13] Christensen J.P. Carbon export from continental shelves, denitrification and atmospheric carbon dioxide. Cont Shelf Res 1994; 14:547-76.

[14] Codispoti L.A. "Phosphorus vs nitrogen limitation of new and export production" In: *Productivity of the oceans: Present and past*, Berger W.H., Smetacek V.S. and Wefer G. eds., New York: Wiley and Sons, 1989.

[15] Codispoti L.A. and Richards F.A. An analysis of the horizontal regime of denitrification in the eastern tropical North Pacific Ocean. Limnol Oceanogr 1976; 21:379-88.

[16] Codispoti L.A. and Christensen J.P. Nitrification, denitrification and nitrous oxide cycling in the eastern tropical South Pacific Ocean. Mar Chem 1985; 16:277-300.

[17] Codispoti L.A., Friederich G.E., Packard T.T., Glover H.T., Kelly P.J., Spinrad R.W., Barber R.T., Elkins J.W., Ward B.B., Lipschulz F. and Lostanau N. High nitrite levels off the coasts of Peru: A signal of instability in the marine denitrification rate. Science 1986; 233:1200-02.

[18] Codispoti L.A., Elkins J.W., Yoshinari T., Friederich G.E., Sakamoto C.M. and Packard T.T. "On the nitrous oxide flux from productive regions that contain low oxygen waters." In: *Oceanography of the Indian Ocean*, Desai B.N. ed., New Delhi: Oxford & IBH, 1992.

[19] Codispoti L. A., Brandes J. A., Christensen J. P., Devol A. H., Naqvi S. W. A., Pearl H. W. and Yoshinari T. The oceanic fixed nitrogen and nitrous oxide budgets: Moving targets as we enter the anthropocene? Sci Mar 2001; 65:85-105.

[20] Codispoti L. A. and Packard T. T. Denitrification rates in the eastern tropical South Pacific. J Mar Res 1980; 38:453-77.

[21] Codispoti L. A., Yoshinari T. and Devol A. H. "Suboxic respiration in the oceanic water-column." In: *Respiration in Aquatic Ecosystems*, del Giorgio P. A. and Williams P. J. l. B. eds., Blackwell Scientific, 2005.

[22] Cohen Y. and Gordon L. I. Nitrous oxide in the oxygen minimum of the eastern tropical North Pacific: evidence for its consumption during denitrification and possible mechanisms for its production. Deep-Sea Res 1978; 25:509-24.

[23] Dalsgaard T., Canfield D. E., Petersen J., Thamdrup B. and Acuña-Gonzáles J. N_2 production by the anammox reaction in the anoxic water column of Gulfo Dulce, Costa Rica. Nature 2003; 442:606-08.

[24] Delwiche C. C. and Steyn P. L. Nitrogen isotope fractionation in soils and microbial reactions. Environ Sci Technol 1970; 4:929-35.

[25] Deutsch C., Gruber N., Key R. M. and Sarmiento J. L. Denitrification and N_2 fixation in the Pacific Ocean. Global Biogeochem Cycl 2001; 15:483-506.

[26] Devol A. H. Direct measurement of nitrogen gas fluxes from continental shelf sediments. Nature 1991; 349:319-21.

[27] Devol A. H. Solution to a marine mystery. Nature 2003; 422:575-76.

[28] Devol A. H., Uhlenhopp A. G., Naqvi S. W. A., Brandes J. A., Jayakumar D. A., Naik H., Gaurin S., Codispoti L. A. and Yoshinari T. Denitrification rates and excess nitrogen gas concentrations in the Arabian Sea oxygen deficient zone. Deep-Sea Res. (in press)

[29] de Wilde H. P. J. and Helder W. Nitrous oxide in the Somali Basin: the role of upwelling. Deep-Sea Res II 1997; 44:1319-40.

[30] Dore J.E., Popp B.N., Karl D.M. and Sasone F.J. A large source of atmospheric nitrous oxide from subtropical North Pacific surface waters. Nature 1998; 396:63-66.

[31] Dueser W. G., Ross E. H. and Mlodzinska M. J. Evidence for and rate of denitrification in the Arabian Sea. Deep-Sea Res 1978; 24:431-45.

[32] Dugdale R. C. and Goering J. J. Uptake of new and regenerated forms of nitrogen in primary productivity. Limnol Oceanogr 1967; 12:196-206.

[33] Dugdale R.C., Goering J.J., Barber R.T., Smith R.L. and Packard T.T. Denitrification and hydrogen sulfide production in Peru upwelling during summer. Deep-Sea Res 1977 24:601-08.

[34] Elkins J.W., Wofsy S.C., McElroy M.B., Colb C.E. and Kaplan W.A. Aquatic sources and sinks for nitrous oxide. Nature 1978; 175:602-06.

[35] Falkowski P. G., Barber R. T. and Smetacek V. Biogeochemical controls and feedbacks on ocean primary production. Science 1998; 281:200-06.

[36] Farrenkoph A. M., Luther G. W. I., Truesdale V. W. and Van der Weijden C. H. Sub-surface iodine maxima: evidence for biologically catalyzed redox cycling in Arabian Sea OMZ during the southwest intermonsoon. Deep-Sea Res II 1997; 44:1391-1409.

[37] François R., Altabet M. A., Yu E. F., Sigman D. M., Bacon M. P., Frank M., Bohrmann G., Bareille G. and Labeyrie L. D. Contribution of Southern Ocean surface-water stratification to low atmospheric CO_2 concentrations during the last glacial period. Nature 1997; 389:929-35.

[38] Froelich P. N., Klinkhammer G. P., Bender M. L., Luedtke N. A., Heath G. R., Cullen D., Dauphin P., Hammond D., Hartman B. and Maynard V. Early oxidation of organic matter in pelagic sediments of the equatorial Atlantic: Suboxic diagenesis. Geochim Cosmochim Acta 1979; 43:1075-90.

[39] Ganeshram R. S., Pedersen T. F., Calvert S. E. and Murray J. W. Large changes in oceanic nutrient inventories from glacial to interglacial periods. Nature 1995; 376:755-58.

[40] Ganeshram R.S., Pedersen T.F., Calvert S.E., McNeill G.W. and Fontugne M.R. Glacial-interglacial variability in denitrification in the world's oceans: Causes and consequences. Paleoceanography 2000; 15:361-76.

[41] Gilson H.C. The nitrogen cycle. Scientific Reports. John Murray Expedition 1933-34, 1937; 2:21-81.

[42] Goreau T.J., Kaplan W.A., Wofsy S.C., McElroy M.B., Valois F.W. and Watson S.W. Production of NO_2 and N_2O by nitrifying bacteria at reduced concentrations of oxygen. Appl Environ Microbiol 1980; 40:526-32.

[43] Gruber N. and Sarmiento J. Global patterns of marine nitrogen fixation and denitrification. Global Biogeochem Cycl 1997; 11:235-66.

[44] Hamme R. C. and Emerson S. R. Mechanisms controlling the global oceanic distribution of the inert gases argon, nitrogen and neon. Geophys Res Lett 2003; 23:35(1)-35(4).

[45] Hartnett H. E. and Devol A. H. The role of a strong oxygen deficient zone in the preservation and degradation of organic matter: a carbon budget for the continental margins of NW Mexico and Washington. Geochim Cosmochim Acta 2003; 67:247-64.

[46] Howell E. A., Doney S. C., Fine R. A. and Olson D. B. Geochemical estimates of denitrification in the Arabian Sea and Bay of Bengal during WOCE. Geophys Res Lett 1997; 24:2549.

[47] Jayakumar D.A. *Biogeochemical Cycling of Methane and Nitrous Oxide in the Northern Indian Ocean*. Ph.D. Thesis, Goa University, 1999.

[48] Jetten M. S. M., Sliekers O., Kuypers M., Dalsgaard T., van Niftrik L., Cirpus I., van de Pas-Schoonen K., Lavik G., Thamdrup B., Le Paslier D., Op den Camp H. J. M., Hulth S., Nielsen L. P., Abma W., Third K., Engstrom P., Kuenen J. G., Jørgensen B. B., Canfield D. E., Damste J. S. S., Revsbech N. P., Fuerst J., Weissenbach J., Wagner M., Schmidt I., Schmid M. and Strous M. Anaerobic ammonium oxidation by marine and freshwater planctomycete-like bacteria. Appl Microbiol Biotech 2003; 63(2):107-14.

[49] Jørgensen B.B. and Gallardo V.A. *Thioploca spp*: filamentous sulfur bacteria with nitrate vacuoles. FEMS Microbiol Ecol 1999; 28:301-13.

[50] Ivanenkov V. N. and Rozanov A.G. Hydrogen sulphide contamination of the intermediate water layers of the Arabian Sea and the Bay of Bengal. Okeanologiia 1961; 1:443-49 (in Russian).

[51] Karl D. M., Letelier R., Hebel D. V., Bird D. F. and Winn C. D. "*Trichodesmium* blooms and new production in the North Pacific gyre." In: *Marine and Pelagic Cyanobacteria: Trichodesmium and the Diazotrophs*, Carpenter E. J. ed., Kluwer, 1992.

[52] Kim K. R. and Craig H. ^{15}N and ^{18}O Characteristics of nitrous-oxide: A global perspective. Science 1990; 262:1855-57.

[53] Kumar S. P. and Prasad T. G. Winter cooling in the northern Arabian Sea. Current Science 1996; 71:834-41.

[54] Kuypers M. M. M., Sliekers A. O., Lavik G., Schmid M., Jørgensen B. B., Kuenen J. G., Sinninghe Damste J. S., Strous M. and Jetten M. S. M. Anaerobic ammonium oxidation by anammox bacteria in the Black Sea. Nature 2003; 422:608-11.

[55] Lal S. and Patra P.K. Variabilities in the fluxes and annual emissions of nitrous oxide from the Arabian Sea. Global Biogeochem Cycles 1998; 12:321-27.

[56] Law C. S. and Owens N. J. P. Significant flux of atmospheric nitrous oxide from the northwestern Indian Ocean. Nature 1990; 346:826-28.

[57] Luther G. W., Sundby B., Lewis B. L., Brendel P. J. and Silverberg N. Interactions of manganese with the nitrogen cycle: Alternative pathways to dinitrogen. Geochimica et Cosmochimica Acta 1997; 61(19):4043-52.

[58] Manne A.S. and Richels R.G. An alternative approach to establishing trade-offs among greenhouse gases. Nature 2001; 410:675-77.

[59] Mantoura R. F. C., Law C. S., Owens N. P. J., Burkill P. H., Woodward M. S., Howland R. J. M. and Llewellyn C. A. Nitrogen biogeochemical cycling in the northwestern Indian Ocean. Deep-Sea Res 1993; 40:651-71.

[60] McElroy M. A. Marine biologic controls on atmospheric CO_2 and climate. Nature 1983; 302:328-29.

[61] Mariotti A., Germon J. C., Hubert P., Kaiser P., Letolle R., Tardieux A. and Tardieux P. Experimental determination of nitrogen kinetic isotope fraction: Some principles; Illustrations for the denitrification and nitrification processes. Plant and Soil 1981; 62:413-30.

[62] Middelburg J. J., Soetaert K. and Herman P. M. J. Evaluation of the nitrogen isotope-pairing method for measuring benthic denitrification: a simulation analysis. Limnol Oceanogr 1996; 41:1839-44.

[63] Morrison J. M., Codispoti L. A., Smith S., Wishner K., Flagg C., Gardner W. E., Gaurin S., Naqvi S. W. A., Manghnani V., Prosperie L. and Gundersen J. S. The oxygen minimum zone in the Arabian Sea during 1995. Deep-Sea Res II 1999; 46:1903-32.

[64] Morrison J.M., Codispoti L.A., Gaurin S, Jones B., Manghanani V. and Zheng Z. Seasonal variation of the hydrographic and nutrient fields during the US JGOFS Arabian Sea process study. Deep-Sea Res II 1998; 45:2053-2101.

[65] Naik H. *Benthic Nitrogen Cycling with Special Reference to Nitrous Oxide in the Coastal and Continental Shelf Environments of the Eastern Arabian Sea.* Ph.D. Thesis, Goa University, 2003.

[66] Naqvi S. W. A. Some aspects of the oxygen-deficient conditions and denitrification in the Arabian Sea. J Mar Res 1987; 45:1049-72.

[67] Naqvi S. W. A. "Denitrification processes in the Arabian Sea." In: *Biogeochemistry of the Arabian Sea* Lal D. ed., Indian Academy of Sciences, 1994.

[68] Naqvi S. W. A. and Sen Gupta R. Seasonal changes in the denitrification regime of the Arabian Sea. Deep-Sea Res 1990; 37:593-611.

[69] Naqvi S. W. A. and Noronha. R. J. Nitrous oxide in the Arabian Sea. Deep-Sea Res 1991; 38:971-80.

[70] Naqvi S. W. A. and Sen Gupta R. "NO", a useful tool for the estimation of nitrate deficits in the Arabian Sea. Deep-Sea Res 1985; 32:665-74.

[71] Naqvi S. W. A. and Shailaja M. S. Activity of the respiratory electron transport system and respiration rates within the oxygen minimum layer of the Arabian Sea. Deep-Sea Res 1993; 40:687-96.

[72] Naqvi S. W. A., Yoshinari T., Brandes J. A., Devol A. H., Jayamumar D. A., Nervekar P. V., Altabet M. A. and Codispoti L. A. Nitrogen isotope studies in the suboxic Arabian Sea. Proc Indian Acad Sci (Earth Planet Sci) 1998; 107:367-78.

[73] Naqvi S. W. A., Yoshinari T., Jayakumar D. A., Altabet M. A., Narvekar P. V., Devol A. H., Brandes J. A. and Codispoti L. A. Budgetary and biogeochemical implications of N_2O isotopic signatures in the Arabian Sea. Nature 1998; 394:462-64.

[74] Naqvi S.W.A., Jayakumar D.A., Narvekar P.V., Naik H., Sarma V.V.S.S., D'Souza W., Joseph S. and George M.D. Increased marine production of N_2O due to intensifying anoxia on the Indian continental shelf. Nature 2000; 408:346-49.

[75] Naqvi S.W.A., Naik H. and Narvekar P.V. "The Arabian Sea." In: *Biogeochemistry of Marine Systems*, Black K. and Shimmield G. eds., Oxford: Blackwell Publishing, 2003.

[76] Nevison C. D., Weiss R. F. and Erickson D. J. Global oceanic emissions of nitrous oxide. J Geophys Res 1995; 100:15809-15820.

[77] Olson D. B., Hitchcock G. L., Fine R. A. and Warren B. A. Maintenance of the low oxygen layer in the central Arabian Sea. Deep-Sea Res 1993; 40:673-86.

[78] Oudot C., Andre C. and Montel Y. Nitrous oxide production in the tropical Atlantic Ocean. Deep-Sea Res 1990; 37:183-202.

[79] Owens N.P.J. and others. Size-fractionated primary production and nitrogen assimilation in the northwestern Indian Ocean. Deep-Sea Res II 1993; 40:697-709.

[80] Patra P. K., Lal S., Venkotaramani S., de Sousa S. N., Sarma V. V. S. S. and Sardesai S. Seasonal and spatial variability of N_2O distribution in the Arabian Sea. Deep-Sea Res I 1990; 46:529-43.

[81] Richards F. A. "Anoxic basins and fjords." In: *Chemical Oceanography*, Vol. 1, Riley J. P. and Skirrow G. eds., Academic Press, 1965.

[82] Schafer P. and Ittekkot V. Isotope biogeochemistry of nitrogen in the Northern Indian Ocean. Mitt Geol-Palaont Inst Univ Hamburg 1995; 78:67-93.

[83] Schenau S., Slomp C.P., and de Lange G.J. Phosphogenesis and active phosphorite formation in sediments from the Arabian Sea oxygen minimum zone. Mar Geol 2000; 169:1-20.

[84] Schmaljohann R., Drews M., Walter S., Linke P., von Rad U. and Imhoff J.F. Oxygen minimum zone sediments in the northeastern Arabian Sea off Pakistan: a habitat for the bacterium *Thioploca*. Mar Ecol Progr Ser 2001; 211:27-42.

[85] Schulz H., von Rad U. and von Stackelberg U. "Laminated sediments from the oxygen-minimum zone of the northeastern Arabian Sea." In: *Palaeoclimatology and Palaeoceanography from Laminated Sediments*. Kemp A.E.S. ed., Geol Soc Spec Publ, 116, London: Geological Society, 1996.

[86] Sigman D. M. *The role of biological production in Pleistocene atmospheric carbon dioxide variations and the nitrogen isotope dynamics of the Southern Ocean.* Ph.D. Thesis, Mass Inst Technol, 1997.

[87] Sigman D. M. and Boyle E. A. Glacial/interglacial variations in atmospheric carbon dioxide. Nature 2000; 407:859-69.

[88] Smith S., Roman M., Prusova I., Wishner K., Gowing M., Codispoti L. A., Barber R., Marra J. and Flagg C. Seasonal response of zooplankton to monsoonal reversals in the Arabian Sea. Deep-Sea Res II 1998 45:2369-2403.

[89] Somayajulu B. L. K., Sarin M. M. and Remesh R. Denitrification in the eastern Arabian Sea: Evaluation of the role of continental margins using Ra isotopes. Deep-Sea Res II 1996; 43:111-17.

[90] Suthhof A., Ittekkot V. and Gaye-Haake B. Millennial-oscillation of denitrification intensity in the Arabian Sea during the late Quaternary and its potential influence on atmospheric N_2O and global climate. Global Biogeochem Cycl 2001; 15:637-49.

[91] Van Mooy B. A. S., Keil R. G. and Devol A. H. Impact of suboxia on sinking particulate organic carbon: Enhanced carbon flux and preferential degradation of amino acids via denitrification. Geochim Cosmochim Acta 2002; 66:457-65.

[92] Wu J. P., Calvert S. E. and Wong C. S. Nitrogen isotope variations in the subarctic northeast Pacific: Relationships to nitrate utilization and trophic structure. Deep-Sea Res I 1997; 44:287-314.

[93] Upstill-Goddard R.C., Barnes J. and Owens N.J.P. Nitrous oxide and methane during the 1994 SW monsoon in the Arabian Sea/ northwestern Indian Ocean. J Geophys Res 1999; 104:30067-84.

[94] Wadda E. and Hattori A. *Nitrogen in the Sea: Forms, Abundances and Rate Processes*. CRC Press, 1990.

[95] Wyrtki K. Oceanographic Atlas of the International Indian Ocean Expedition. National Science Foundation, 1971.

[96] Yoshida N., Morimoto H., Hirano M., Koike I., Matsuo S., Wada E., Saino T. and Hattori A. Nitrification rates and ^{15}N abundances of N_2O and NO_3 in the western North Pacific. Nature 1989; 342:895-97.

[97] Yoshinari T. Nitrous oxide in the sea. Mar Chem 1976; 4:189-202.

[98] Yoshinari T., Altabet M.A., Naqvi S.W.A., Codispoti L.A., Jayakumar A., Kuhland M. and Devol A.H. Nitrogen and oxygen isotopic composition of N_2O from suboxic waters of the eastern tropical North Pacific and the Arabian Sea - measurement by continuous-flow isotope ratio monitoring. Mar Chem 1997; 56:253-64.

ANAEROBIC AMMONIUM OXIDATION IN THE MARINE ENVIRONMENT

Marcel M.M. Kuypers[1], Gaute Lavik[1] and Bo Thamdrup[2]

[1]*Max-Planck-Institute for Marine Microbiology, Department of Biogeochemistry, Celsiusstr. 1, 28359 Bremen, Germany*

[2]*Danish Center for Earth System Science, Institute of Biology, University of Southern Denmark, Campusvej 55, DK-5230 Odense, Denmark*

Abstract Oceanographers noticed already many years ago that far less ammonium accumulated in anoxic fjords and basins, than would be expected from the stoichiometry of heterotrophic denitrification. It was suggested that this 'missing' ammonium was oxidized with nitrate to free N_2. Since then several other workers have argued based on chemical profiles that ammonium is oxidized anaerobically in oxygen deficient marine sediments and waters with either nitrate or manganese oxides as electron acceptor. While there is as yet no direct evidence for the anaerobic ammonium oxidation with manganese oxides in either sediments or anoxic water columns, more and more evidence is being provided for anaerobic ammonium oxidation with nitrite/nitrate. The first direct evidence for the anaerobic oxidation of ammonium was provided in a waste water bioreactor, where so-called 'anammox' bacteria belonging to the Order *Planctomycetales* directly oxidize ammonium to N_2 with nitrite as the electron acceptor. Although the anammox process was generally seen as a promising process for waste water treatment, it was believed to be insignificant in the natural environment due to the extremely slow generation times (more than 2 weeks) of the anammox organisms. However, recent studies provide direct evidence for anaerobic oxidation of ammonium by nitrate and/or nitrite in marine sediments, oxygen minimum zones, anoxic fjords and basins as well as Arctic sea ice. Phylogenetic analysis of 16S ribosomal RNA sequences show that the bacteria involved are closely related to anammox bacteria from waste water bioreactors. The combined biogeochemical and microbiological data available indicates that anammox may contribute significantly to the loss of reactive nitrogen in the ocean.

Keywords: anaerobic ammonium oxidation, anammox, denitrification, nitrogen cycle, marine, suboxic, review

L. N. Neretin (ed.), Past and Present Water Column Anoxia, 311–335.

1. INTRODUCTION

Large amounts of dissolved inorganic carbon (DIC), fixed inorganic nitrogen (NH_4^+, NO_2^-, NO_3^-) and phosphate in the ocean surface waters are consumed by algae and cyanobacteria during photosynthesis. The atomic ratio of C, N and P of the produced organic matter is similar throughout the marine realm [10, 72] and on average phytoplanktonic biomass is characterized by a C:N:P ratio of 106:16:1 [47]. In principle, carbon dioxide, ammonium and phosphate are released in the same ratio, the so-called Redfield ratio, upon mineralization of this phytoplankton-derived organic matter [47]. When this mineralization occurs under oxic conditions, ammonium will be oxidized with oxygen via nitrite to nitrate by nitrifying organisms (mainly chemoautotrophic bacteria). The nitrate can subsequently be used again to produce new phytoplankton biomass. Alternatively, nitrate can be used in oxygen-deficient marine environments by predominately facultative anaerobic prokaryotes to oxidize organic matter in the absence of oxygen. During this process (i.e. heterotrophic denitrification) nitrate is reduced to N_2. Oceanographers noticed many years ago that oxygen-deficient waters and sediments are characterized by nitrate to phosphate ratios that are significantly lower than Redfield (N:P < 16). This nitrate deficit has been attributed to heterotrophic denitrification, which releases phosphate upon organic matter decomposition while nitrate is lost as N_2. The organic matter mineralization through denitrification should also release ammonium, which, in the absence of oxygen, it was thought should remain as ammonium [14]. Although the idea that ammonium may be oxidized anaerobically in the ocean was floating around for a fairly long period [27], evidence was not specifically provided until early/mid 1960s. It was Richards who first noticed that far less ammonia accumulated in Lake Nitinat, an anoxic fjord on Vancouver Island (Canada), than would be expected from the stoichiometry of heterotrophic denitrification according to equation (1) [48, 50]:

$$(CH_2O)_{106}\,(NH_3)_{16}\,H_3PO_4 + 84.8HNO_3 \rightarrow 106CO_2 + 16NH_3 + 42.4N_2 + 148.4H_2O + H_3PO_4 \quad (1)$$

He suggested that this 'missing' ammonia was oxidized with nitrate to free N_2 according to equation (2) [48]:

$$5NH_3 + 3HNO_3 \rightarrow 4N_2 + 9H_2O \quad (2)$$

Since then several other workers have argued based on chemical profiles that ammonium is oxidized anaerobically in oxygen deficient marine sediments and waters with either nitrate or manganese oxides as electron acceptor (e.g. [1, 4, 17, 31, 39, 60]).

Mulder and co-workers [38] were the first to provide direct evidence for the anaerobic oxidation of ammonium in a waste water bioreactor. They argued that ammonium was oxidized with nitrate to N_2 according to equation (2) and named this biological process 'Anammox.' Van de Graaf et al. [76] showed that in these bioreactors ammonium is oxidized to N_2 with nitrite instead of nitrate as the electron acceptor. Recently, Strous et al. (1999) [65] discovered organisms capable of anaerobic ammonium oxidation ('anammox') in waste waters treatment plants. These so-called 'anammox' bacteria belonging to the Order *Planctomycetales* directly oxidize ammonium to N_2 with nitrite as the electron acceptor:

$$NH_4^+ + NO_2^- \rightarrow N_2 + 2H_2O \quad (3)$$

Anammox bacteria are chemoautotrophs [55, 59, 65] and 0.07 mol CO_2 is fixed per mol ammonium oxidized [66].

Although the anammox process is generally seen as a promising process for waste water treatment, it was believed to be insignificant in the natural environment due to the extremely slow generation times (more than 2 weeks) of the anammox organisms [82]. However, recent studies of a variety of marine settings using biogeochemical and microbiological techniques [11, 12, 19, 35, 51, 53, 70, 73] indicate that the anaerobic oxidation of ammonium by nitrate and/or nitrite may contribute significantly to the loss of reactive nitrogen in the ocean.

2. TRACING ANAMMOX IN THE ENVIRONMENT

2.1 Labeling Experiments

Incubation experiments with addition of ^{15}N-labeled nitrogen species have been a useful tool for elucidating anaerobic ammonium transformations and quantifying the rates in both sediments and anoxic water columns. Consumption of $^{15}NH_4^+$ and concomitant production of ^{15}N-labeled N_2 provided the first experimental evidence for anaerobic ammonium oxidation in marine sediments [70]. This transformation was only observed in the presence of nitrate, which was reduced via nitrite. Through the separate analysis of $^{14}N^{15}N$ and $^{15}N^{15}N$ production, experiments with labeling of nitrate, ammonium, or both, demonstrated that N_2 formed through a 1-to-1 pairing of N from both sources, as characteristic of anammox. The sediment process was further tied to anammox through the demonstration of a typical microbial temperature response, and by showing that nitrite could be used en lieu of nitrate [12, 73].

Labeling experiments also provided evidence of anammox in anoxic waters. Anaerobic oxidation of $^{15}NH_4^+$ to N_2 was observed in both the anoxic basin of Golfo Dulce, Costa Rica, and in the suboxic zone of the Black Sea [11, 35]. The results from Golfo Dulce exhibited three features characteristic of

anammox [11]: 1) ^{15}N-labeled N_2 accumulated linearly without a lag phase in incubations with $^{15}NH_4^+$, indicating that the label was not transformed via intermediates such as NO_2^- or NO_3^-; 2) ^{15}N from NH_4^+ was recovered as $^{14}N^{15}N$ rather than $^{15}N^{15}N$, consistent with isotope pairing during anammox [75] and inconsistent with a direct oxidation coupled to Mn reduction; and 3) the production of ^{15}N-labeled N_2 from $^{15}NO_3^-$ was stimulated by the addition of NH_4^+. Furthermore, it occurred with a lag phase consistent with a gradual labeling of the NO_2^--pool, with NO_2^- being the direct oxidant for NH_4^+. These three characteristics, possibly supplemented with results from incubations with $^{15}NO_2^-$ [12], form a checklist of criteria for the demonstration of anammox with ^{15}N-techniques.

N-15-labelling provides a very sensitive technique for the determination of anammox rates. For example, rates of the order of 1 nM h^{-1} were determined in incubations over ~2 days with water from Golfo Dulce [11]. As an additional advantage, incubations with $^{15}NO_3^-$ or $^{15}NO_2^-$ allow for the simultaneous determination of anammox and denitrification, giving insights to the relative importance of the two sinks for fixed N [70]. This partitioning rests on the characteristic patterns of isotope pairing in N_2 formed through the two pathways. In contrast to the 1-to-1 pairing of nitrogen atoms from nitrite and ammonium during anammox, the reduction of two equivalent molecules of nitrate or nitrite via nitric oxide to nitrous oxide results in random pairing of the isotopes in N_2 formed through denitrification, with $^{14}N^{14}N$, $^{14}N^{15}N$, and $^{15}N^{15}N$ forming at a ratio of $(1-F)^2$:$2F(1-F)$:$(1-F)^2$, where F is the fraction of ^{15}N in the nitrogen source [29, 41, 84]. Thus, in experiments with $^{15}NO_3^-$ or $^{15}NO_2^-$ and $^{14}NH_4^+$, $^{15}N^{15}N$ only forms through denitrification, and total denitrification as well as the production of $^{14}N^{15}N$ through this pathway can be calculated from the ratio above. Subsequently the production of $^{14}N^{15}N$ through anammox is quantified as the difference between measured $^{14}N^{15}N$ production and the production of this mass through denitrification, and $^{14}N^{14}N$ production though anammox is calculated from this excess and an expected RATIO of $^{14}N^{14}N$:$^{14}N^{15}N$ from anammox of $(1-F)$:F [70].

The accuracy of the $^{15}NO_3^-/^{15}NO_2^-$ incubation approach depends critically on an accurate determination of the fraction of ^{15}N (F) in the electron acceptor, nitrate or nitrite, utilized by the two processes. Kinetic isotope effects have been neglected in the calculations as they should bias the results by a few percent at most. The available data suggests that the increase in NO_3^- or NO_2^- concentrations through the amendments does not influence the measured rates. Thus, apparent half-saturation concentrations (K_m) with respect to NO_2^- for both anammox and denitrification are low (< 3 μM) [12, 73] compared to the natural concentrations of these species, and anammox appears to be NH_4^+-limited in anoxic waters [11]. Although rates determined in incubations with $^{15}NH_4^+$ may thus overestimate the rates *in situ*, they are valuable as

direct evidence of anaerobic ammonium oxidation, as discussed above. As yet no comparisons of incubation-based and -independent anammox rates are available, but such should be an important component of future investigations.

2.2 Membrane Lipids

Specific lipid biomarkers, so-called 'ladderane' lipids, were used to trace anammox bacteria in particulate organic matter collected from various depths across the suboxic zone of the Black Sea [35]. Ladderane lipids [62] are the main building blocks of a unique bacterial membrane that surrounds the 'anammoxosome', a special compartment of the anammox cell, where the anaerobic oxidation of ammonium to N_2 takes place (Fig. 1). During the anammox process the intermediates hydrazine and hydroxylamine are formed, which readily diffuse through conventional biomembranes [78]. The energy loss associated with the loss of 10% hydrazine from the anammox cells would lead to a 50% decrease in biomass yield [62]. Therefore, the limitation of diffusion is extremely important for these bacteria. The biomembrane surrounding the anammoxosome is more resistant to diffusion than conventional biomembranes due to dense and rigid ladderane lipids. Therefore, the ladderane based biomembrane is probably a unique adaptation to the anammox metabolism. This is supported by the fact that ladderane lipids were not found in phylogenetically related planctomycetes that do not have the capacity to anaerobically oxidize ammonium [62]. In addition to their unique structure, ladderane lipids are characterized by a specific isotopic signature that can be used to trace these biomarkers in the environment. Compound specific stable isotope analysis show that lipids derived from anammox bacteria are depleted in ^{13}C by up to 50‰ compared to dissolved CO_2 [59]. This large isotopic offset may indicate that anammox bacteria use the acetyl-CoA pathway for carbon fixation [59].

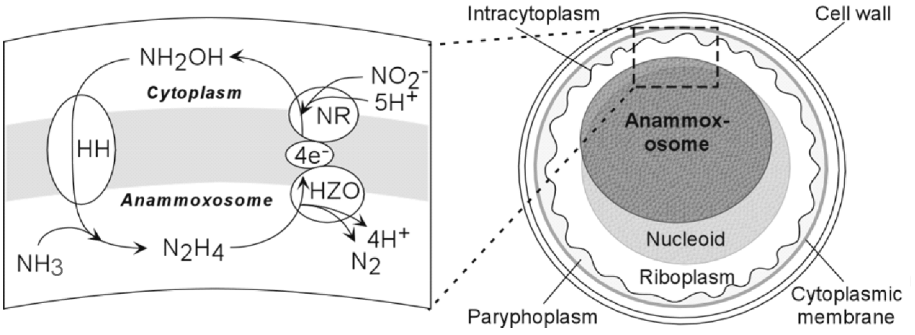

Figure 1. Morphology of the anammox cell and proposed model for the anammox process; HH: hydrazine (N_2H_4) hydrolase; HZO: hydrazine oxidizing enzyme; NR: nitrite reducing enzyme.

2.3 Molecular Techniques

DNA/RNA based techniques are widely used to identify organisms involved in anaerobic ammonium oxidation in waste water bioreactors (e.g. [15, 16, 56-58, 65]). Phylogenetic analyses of the 16S ribosomal RNA sequences indicate that all known anammox bacteria belong to the order Planctomycetales [58]. There are presently at least three known anammox genera; *Candidatus* 'Brocadia', *Candidatus* 'Kuenenia' and *Candidatus* 'Scalindua'[58]. The average sequence similarity between members of these genera is generally low, with less than 85% sequence similarity between members of *Candidatus* 'Brocadia' and *Candidatus* 'Scalindua'.

Only a few studies have used molecular ecological techniques to trace anammox bacteria in the marine environment [23, 35, 51]. Anammox derived 16Sr-RNA sequences have been reported from Black Sea water and from Danish estuarine sediments [35, 51]. The sequences from these different settings are nearly identical indicating a low diversity of marine anammox bacteria. The anammox bacterium from the Black Sea, tentatively named *Candidatus* Scalindua sorokinii is nearly identical (98.1%) to a sequence recently obtained from a bioreactor shown to have anammox activity [35, 58]. Based on the sequence obtained from the Black Sea, an oligonucleotide probe has been designed, labeled with Cy3 fluorochrome, for fluorescence *in situ* hybridization (FISH). This probe gave a bright and specific signal with cells from the Black Sea that have the unusual doughnut shape characteristic for anammox bacteria in bioreactors. Cells hybridizing with this specific FISH probe were also found in Randers Fjord sediment [51].

3. DISTRIBUTION OF ANAMMOX IN THE MARINE ENVIRONMENT

3.1 Sediments

To date, anammox has been detected in practically all the sediments for which results of anammox assays have been published. These include marine sites in the Kattegat/Skagerrak area where anammox was first reported [19, 70], in Long Island Sound [19], and around Greenland [54], as well as locations in the Thames estuary [73]. Recently, anammox bacteria were also reported from an African fresh water wetland [32]. Within the small array of marine sites, anammox rates varied by nearly two orders of magnitude between ~5 and 240 μM N_2 d^{-1}, with both extremes represented in the Thames estuary. The rates decreased towards the mouth of the Thames estuary and towards deeper water in Kattegat/Skagerrak thus correlating with the metabolic activity of the sediment. The site with the lowest salinity in the Thames (2‰) was an outlier in this trend with a relatively low anammox rate.

Although denitrification rates varied in an overall similar manner, they were less variable than anammox rates in the Thames and more variable in Kattegat/Skagerrak sediments. As a result, the relative contribution of anammox to N_2 production decreased from 8 to 1% towards the mouth of the Thames, while it increased from 2 to 79% from the shallowest to the deepest site in Kattegat/Skagerrak [19, 70, 73]. Overall, the small dataset suggests that anammox is generally of little importance for N_2 production (< 10%) in nearshore sediments, while it is more important and may even dominate in open water sediments (Fig. 2). Some factors controlling the process and its importance relative to denitrification will be discussed below.

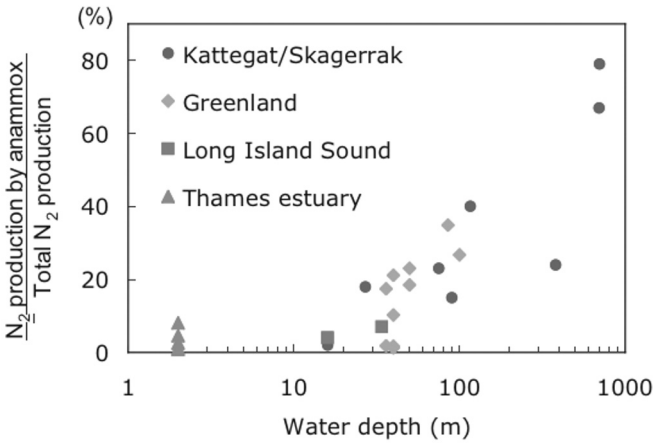

Figure 2. The relative contribution of anammox to N_2 production from anammox plus denitrification in marine sediments as a function of water depth (note log scale). Contributions were determined in jar-type incubations of surface sediment horizons. Measurements from the Thames estuary were arbitrarily set at 2 m depth. Data from [19, 54, 70, 73].

The existing reports on anammox in sediments are based on experiments with homogenized sediment from discrete sediment horizons, and rates are reported on a per-volume basis, typically for a sediment horizon that corresponds only roughly to the anoxic, NO_3^-/NO_2^--containing layer where anammox and denitrification are expected. If the total N_2 flux from the sediment is known, either from direct measurement (e.g. [13, 61]) or from whole-core incubations with $^{15}NO_3^-$ (the isotope pairing technique; [41, 52]), depth-integrated rates of anammox and denitrification can be estimated by combination of the N_2 flux and the relative importance of the two processes determined in the homogenized sediment. A whole-core approach for the direct determination of both anammox and denitrification rates was recently suggested by Risgaard-Petersen et al. [52]. This approach is a modification of the isotope pairing technique previously developed for measurement of denitrification in sediments

[41], and it involves incubation of sediment cores with different proportions of $^{14}NO_3^-$ and $^{15}NO_3^-$ in the overlying water, at a constant total nitrate concentration. Such an approach would circumvent potential effects of sediment homogenization on the rates, as often observed for other microbial processes (e.g., [28]), but the technique with its underlying assumptions awaits practical testing.

3.2 Anoxic Fjords and Basins

Golfo Dulce. Golfo Dulce is a 50 km long and 10 km wide embayment on the Pacific coast of Costa Rica with a 200 m-deep inner basin and a sill at ~60 m [79]. The water chemistry, first described by Richards and coworkers [49], is characterized by a broad anoxic, NO_3^--containing zone reaching from ~100 m depth to near the bottom with hydrogen sulfide detected only in the deepest ~20 m [11, 49, 68]. Low-oxygen NO_3^--rich waters of the Eastern Tropical North Pacific oxygen minimum zone appear regularly to spill over the sill and disturb the stratification in the outer bay, whereas deep oxygenation has not been observed at the head of the bay (refs. above; B. Thamdrup, T. Dalsgaard, M.M. Jensen, J. Acuña-Gonzales, unpublished results).

Richards and coworkers [49] noted both ammonium and DIN deficiencies in the waters of Golfo Dulce and attributed this to denitrification and anaerobic ammonium oxidation with nitrate. These observations were repeated in 2001 and the activity of denitrification and of anammox as a sink for ammonium was directly demonstrated through incubations [11]. Anammox was detected at all four depths investigated between 100 and 180 m at each of two stations (Fig. 3). Rates varied between 2 and 20 nM h^{-1} with no clear trends with depth or between stations. In contrast, denitrification rates tended to increase with water depth with particularly high rates at 180 m, and rates were higher at the inner than at the outer station. As a result, the relative contribution of anammox to N_2 production varied between 13 and 68% for individual depths. The depth-integrated contributions from anammox were 35 and 19% at the outer and inner station, respectively. The high rates of denitrification in the deepest waters, which lowered the depth-integrated contributions from anammox, were suggested to be coupled to sulfide oxidation. Except for the deepest part of the water column, ammonium concentrations were near the detection limit, and ammonium-limitation of anammox was indicated by 2 – 4-fold increases in rates after ammonium addition. Thus, anammox efficiently scavenged the ammonium released from mineralization in the water column.

Except for the sulfidic near-bottom water, the water-column chemistry of Golfo Dulce resembles that of the oceanic oxygen deficiency zones, with elevated concentrations of NO_2^- (up to 2 μM in Golfo Dulce) and very low ammonium concentrations. The finding and significance of anammox in Golfo

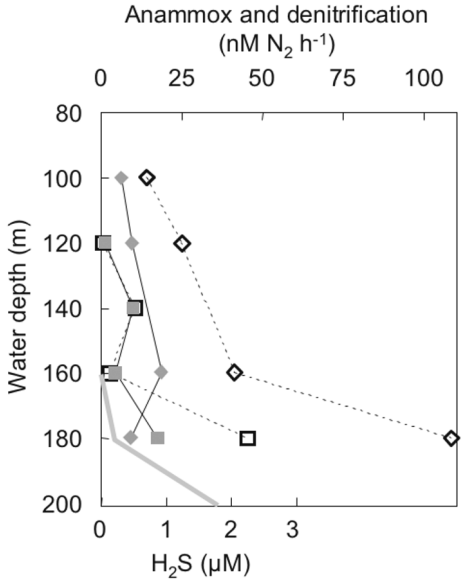

Figure 3. Rates of anammox (filled grey symbols) and denitrification (open symbols) and the concentration of hydrogen sulfide (dark grey line; bottom axis) in the anoxic water column of Golfo Dulce. Diamonds and squares indicate two different stations A and B. Hydrogen sulfide data is from station B. Anoxia was found from ~110 m at Station A and ~90 m at Station B. Data from Dalsgaard et al. [11].

Dulce suggest that this process may also contribute substantially to the ammonium and DIN deficiencies in oxygen deficient oceanic waters. The bay provides an easily accessible model system for further studies of the process.

Mariager Fjord. Mariager Fjord is a long and narrow fjord on the east coast of Jutland, Denmark, which in its inner part harbors a small euxinic basin known as Dybet (maximum depth 28 m). Stratification is occasionally disrupted during winter, but then reestablishes during spring. Oxygen and hydrogen sulfide usually meet at a sharp interface, but a "suboxic" zone low in both these species is occasionally observed [22, 46, 83]. The suboxic zone may be a non-steady-state phenomenon related to intrusions around the depth of the chemocline, as indicated by day-to-day variations in chemocline structure [83]. Near the chemocline a small peak in NO_2^- of ~1 μM may coexist with 10 – 20 μM NH_4^+ [83].

Investigations of anammox in the water column of Mariager Fjord in 2001 and 2002 did not find any clear evidence for the process in samples collected across the chemocline [44]. Sampling was done with a pump system at a depth resolution of 0.2 – 0.3 m. Denitrification rates exceeded 100 nM N_2 h^{-1} and

increased with water depth, suggesting that the process was fueled by hydrogen sulfide. Hydrogen sulfide is the major primary electron donor for the redox processes in the Mariager Fjord chemocline [46, 83]. Thus, in an extension of the conclusions from the deepest waters in Golfo Dulce, the results from Mariager Fjord suggest that anammox is of little importance in systems that are to a large extent fueled by sulfide oxidation.

Black Sea. The Black Sea is the world's largest anoxic basin and is a model for both modern and ancient anoxic environments. It is characterized by a high ammonium concentration in the deep waters (up to 100 μM), while only trace amounts of fixed inorganic nitrogen are present in the suboxic zone. This apparent ammonium sink in the suboxic zone strongly suggests that ammonium is oxidized anaerobically to N_2 [39, 48, 70]. During an R/V Meteor cruise in December 2001 the role of anammox in the Black Sea water column was investigated using microbiological and biogeochemical techniques [35]. Water samples from various depths were incubated anaerobically after addition of ^{14}N-nitrite and ^{15}N-ammonium to check for anammox activity in the suboxic zone. The potential anammox activity determined this way showed a clear peak in the zone of nitrite and ammonium disappearance, whereas no significant anammox activity was observed outside the suboxic zone. Ladderane' lipids [62] were used to trace anammox bacteria in particulate organic matter collected from various depths across the suboxic zone. Three different ladderane lipids were detected in the saponified total lipid extracts with a depth distribution similar to that of the potential anammox activity, indicating that anammox bacteria could indeed be responsible for the anaerobic oxidation of ammonium. Phylogenetic analysis of the 16S rRNA sequences from Black Sea water at the depth of maximum ladderane abundance (90 m) confirmed that the Planctomycetes, tentatively named *Candidatus* Scalindua sorokinii, from the suboxic zone of the Black Sea are related to bacteria known to be capable of anammox (87.9 % sequence similarity to *Kuenenia*, 87.6% to *Brocadia*) [35]. The sequence obtained from the Black Sea was nearly identical (98.1%) to a sequence recently obtained from a bioreactor shown to have anammox activity [58]. Ladderane biomarkers (Fig. 1) and cells hybridizing with the FISH probe specific for anammox bacteria were also found in the suboxic zone at the shelf break (Fig. 4; Station 7617, 43 38,04'N 30 02,54'E), indicating that anammox bacteria are not restricted to the strongly stratified central basin but are also present in the more dynamic peripheral current [64].

Assuming that the concentration profile of ammonium represents a steady state, an anaerobic ammonium oxidation rate of ~0.007 μM day^{-1} was calculated for the suboxic zone of the central basin using a reaction diffusion model. This rate is comparable to aerobic ammonium oxidation rates (0.005-0.05 μM day^{-1}) determined for the nitrate maximum of the western central basin of

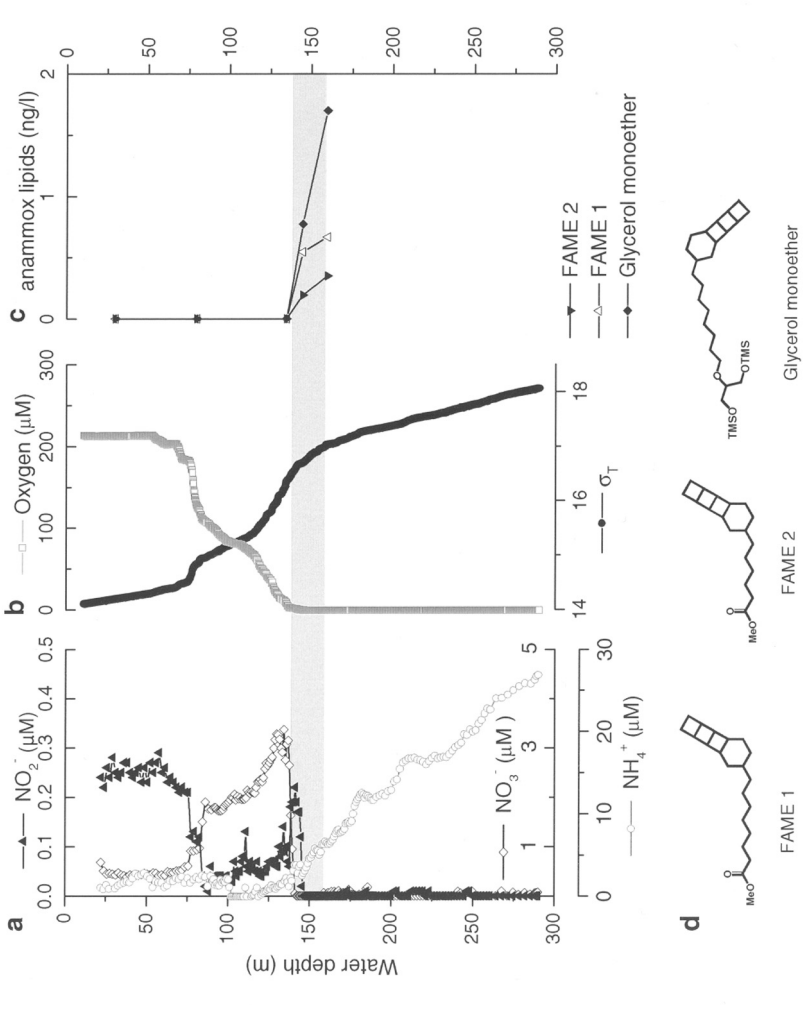

Figure 4. Chemical zonation and distribution of anammox indicators across the Black Sea chemocline at Station 7617 (43 38.04'N 30 02.54'E). **(a)** Fixed inorganic nitrogen species, **(b)** water density and oxygen concentrations, **(c)** peak of three ladderane membrane lipids specific for anammox bacteria, and **(d)** molecular structures of the three ladderane membrane lipids specific for anammox bacteria presented in **(c)**. The suboxic zone is indicated by gray shading.

the Black Sea [81]. An anammox rate of 2-20 fmol ammonium cell^{-1} day^{-1} (1 fmol = 10^{-15} mol) was found in laboratory bioreactors [65]. Assuming a similar range of cell specific activity for the Black Sea, 300-3000 anammox cells ml^{-1} would be needed to account for the observed ammonium oxidation rates in the suboxic zone. Counts of cells stained with the newly designed FISH probe (Amxbs820) gave an anammox cell density of ~1900 (±800) cells ml^{-1} (0.75% of all cells counted by DAPI) at the nitrite peak.

The rates of net ammonium and nitrate consumption calculated as a function of depth indicate that nitrate reduction by denitrifiers coupled to anammox accounts for a substantial loss of fixed inorganic nitrogen. Assuming that the area (3 * 10^5 km^2) below the shelf break (< 200 m) [64] represents the total surface area of the suboxic zone, 0.3 Tg fixed inorganic nitrogen per year may be lost through nitrate reduction coupled to anammox.

3.3 Oxygen Minimum Zones

Nutrient measurements indicate that 30-50% of the total nitrogen loss in the ocean occurs in the oxygen deficient waters of oxygen minimum zones [9, 25]. The extremely low concentration of ammonium could indicate that anammox bacteria also play an important role in the nitrogen removal from oxygen minimum zone (OMZ) waters (e.g. [11, 14, 80]).

Recently, evidence was provided for extensive anammox activity in the OMZ waters of the Benguela upwelling system [34]. Upwelling of nutrient-rich South Atlantic mid-waters in the Benguela current system along the southwest African continental margin sustains some of the highest primary production rates in the ocean [7, 8]. Although the upwelling water is generally well oxygenated (> 200 μM O_2), bottom waters become severely oxygen depleted (< 10 μM O_2) over large areas of the southwest African shelf. This is the result of oxygen consumption associated with the decomposition of settling algal biomass [8]. A strong N-deficit (a decrease in the ratio of fixed inorganic N to P; [74]) in the bottom waters has been attributed to denitrification [8, 74]. Water in the Benguela OMZ is exchanged rapidly and concentrations of oxygen vary significantly [8]. These conditions at first glance seem to be unfavorable for anammox bacteria, with their slow growth rate and anaerobic physiology, are able to thrive under such highly dynamic conditions.

During an R/V *Meteor* cruise in March/April 2003 the role of denitrification and anammox in Namibian shelf waters was investigated by combining microbiological and biogeochemical techniques. As observed previously [8], nitrate concentrations drop at the base of the oxic zone (<10 μM O_2). This decrease in nitrate has previously been attributed to the conversion of nitrate to N_2 by denitrifying bacteria [8, 74]. The N:P ratios for dissolved inorganic nutrients << Redfield indicate extensive loss of nitrogen from the oxygen de-

ficient Namibian shelf waters. Ammonium should have accumulated in these waters if heterotrophic denitrification was solely responsible for the nitrogen loss [48, 50]. The low ammonium concentrations (below detection limit) in the suboxic zone could indicate that anammox bacteria play an important role in the nitrogen removal from the Benguela OMZ waters [11, 14, 80].

The N-deficit in the OMZ clearly shows that large amounts of fixed inorganic nitrogen are being removed from the Namibian suboxic waters. *In situ* ^{15}N-labeling experiments indicate that nitrate is not directly converted to N_2 by heterotrophic denitrification in the suboxic zone. Instead, nutrient profiles, anammox rates, abundances of anammox cells, and specific biomarker lipids indicate that fixed nitrogen is lost through anammox coupled to a) reduction of nitrate to nitrite by heterotrophic denitrifiyers or anammox bacteria and b) aerobic ammonium oxidation. Data from the Chilean OMZ show a similar dominance of anammox over heterotrophic denitrification (B. Thamdrup, T. Dalsgaard, M.M. Jensen, O. Ulloa, unpublished results). Depth integrated rates indicated that 1-5 mmol fixed inorganic nitrogen per square meter per day was lost from the suboxic waters of the Benguela upwelling system due to anammox. Assuming that the main area (~100,000 km^2) of suboxic shelf water extends from 28° to 18° south [8], 1.4 ± 1 Tg fixed nitrogen per year might be lost through anammox from the Benguela system.

3.4 Arctic Sea Ice

Anammox activity was recently also reported for Arctic sea ice [53]. Anaerobic processes occur in the lower 0.5 m of sea ice, in brine systems, which become anoxic as a result of oxygen dilution by melting of deoxygenated ice crystals and oxygen consumption associated with decomposition of ice algae and/or detritus incorporated during ice formation. The organic matter degradation also leads to high concentrations of dissolved organic carbon and ammonium in sea ice. Incubation experiments with addition of ^{15}N-labeled nitrogen species to melted sea ice indicate that substantial amounts of fixed inorganic nitrogen (100-300 nmol N L^{-1} sea ice d^{-1}) are lost from sea ice as N_2 as a result of heterotrophic denitrification and anammox. Anammox accounts for up to 19% of the total N_2 production in the investigated sea ice.

4. ANAEROBIC OXIDATION OF AMMONIUM WITH MANGANESE OXIDES

With standard reduction potentials for Mn oxide/Mn^{2+} couples only slightly lower than that of the NO_3^-/N_2 couple (e.g. [69]), Mn oxides are potential electron acceptors in anaerobic ammonium oxidation. In their seminal study of early diagenesis, Froehlich and coworkers [24] assumed that N_2 was the end product

of the mineralization of organic N with Mn oxides as terminal electron acceptor. Further indications of anaerobic ammonium oxidation by Mn oxides include the observation of an ammonium deficiency in anoxic Mn-oxide rich sediment from the Panama Basin [2] and of transient accumulation of nitrate in anoxic sediment incubations, with the maximum nitrate concentrations correlating with the Mn content of the sediment [31]. Both these findings were suggested to result from an anaerobic Mn oxide-dependent nitrification-like process in conjunction with denitrification. Alternatively, Luther and co-workers [36], based on differences in porewater chemistry and nutrient fluxes between Mn-rich and Mn-poor sediments, as well as abiotic experiments with Mn oxides, suggested that Mn oxides oxidize ammonium directly to N_2. Since this reaction requires fresh oxide surfaces, it was suggested to be most important in the presence of O_2, where surfaces would be continuously regenerated through Mn^{2+} oxidation. Manganese oxide-based ammonium oxidation has also been suggested to be active in the Black Sea water column [40].

In order to directly demonstrate and quantify ammonium oxidation coupled to Mn reduction in sediments, Thamdrup and Dalsgaard [69] amended a metabolically active anoxic manganese-rich sediment with ^{15}N-labeled ammonium, and monitored the production of ^{15}N labeled N_2. No such production was detectable, however, and it was concluded that the process was insignificant for nitrogen cycling in this sediment. Subsequent studies at several other locations with manganese concentrations more typical of coastal sediments also failed to detect any anaerobic ammonium oxidation in the absence of nitrate or nitrite [19, 70].

As discussed previously (See chapter 3.2), anaerobic ammonium oxidation in the water column of Golfo Dulce was attributed to the anammox process with no indications of a coupling to Mn oxides [11], despite relatively high concentrations of particulate Mn and soluble Mn^{2+} [68]. Thus, there is as yet no direct evidence for the process in either sediments or anoxic water columns. It remains to be determined to which extent the anammox process may explain the phenomena that have been attributed to ammonium oxidation by Mn oxides.

5. FACTORS CONTROLLING ANAMMOX IN THE MARINE ENVIRONMENT

5.1 Temperature

With recent reports of anammox activity in melted sea ice and high-Arctic sediments [53, 54], the process has been found at temperatures of -1.8 – 16 °C in natural environments, the upper limit being reached in Golfo Dulce [68]. In sediment from Skagerrak and Greenland with a stable *in situ* temperature of ~6 °C and ~-1 °C, respectively, anammox exhibited a psychrotolerant temperature response in short-term experiments with highest rates at ~15 °C and no activity

above 35 °C [12, 54]. The increase in rate with increasing *in situ* temperature corresponded to Q_{10} -values of 2.2 - 2.5. Denitrification was more favored by higher temperatures and the relative importance of anammox in N_2 production decreased continuously with increasing temperature above 6 °C.

Short-term temperature responses reflect the physiology of the active microbial community and cannot be used to predict or interpret changes in activity in response to, e.g., seasonal temperature variations, or between sites with different temperatures. However, the results indicate differences between the natural anammox community and the well-studied anammox population of wastewater systems, which has an optimum temperature of 37 °C [65]. Viewed together, the results suggest that the distribution of anammox activity in the environment will not be excluded by temperatures between freezing and 40 ° C.

5.2 Organic Matter

The activity of anammox bacteria in the environment may not be directly dependent on the availability of organic compounds if they are capable of autotrophy, as are those known from wastewater systems [59]. The recent demonstration of acetate and propionate oxidation coupled to nitrate and/or nitrite reduction by anammox bacteria from wastewater bioreactors shows, however, that organic matter cannot be excluded as either carbon or energy source for anammox bacteria in the marine environment [26].

While direct use of organic matter by anammox bacteria needs further exploration, it is clear that organic matter is the main source of NH_4^+ through ammonification. This likely explains the general correlation of anammox rates and sediment metabolism, as an indicator or organic carbon availability, observed in sediments (see above). It has also been suggested that a correlation of anammox with organic content of the sediment was caused by NO_2^- availability, with greater reductive NO_2^- production in more C_{org}-rich sediments [73]. Nitrite is, however, only an intermediate in the reduction of NO_3^- to N_2 or NH_4^+, and NO_2^- consumption through these pathways could also be expected to be stimulated with increased availability of organic substrates. Further aspects of interactions between anammox bacteria and NO_3^-/NO_2^- reducers are discussed below.

The Black Sea and Golfo Dulce exemplify wide differences in the tightness of coupling between anammox and ammonification. In the Black Sea, anammox is an interface process fueled by NH_4^+ transported from the deeper basin, and largely independent of local sources [35]. In much of the water column in Golfo Dulce, anammox is NH_4^+-limited and tightly coupled to the local mineralization of organic N [11]. In sediments, both these situations are possible, and in a given environment the NH_4^+ source may fluctuate over time between local sources

and transport from deeper horizons. Specific relationships between anammox bacteria, denitrifiyers and nitrifiers will be discussed in the following sections.

With organic matter as the ultimate source of NH_4^+ for anammox, stoichiometric considerations may put certain constraints on the role of anammox in the N cycle. In environments such as the intermediate depths in Golfo Dulce where anammox scavenges all the ammonium released during mineralization, which is ultimately coupled to denitrification, the contribution of the process to N_2 production should be tied to the mineralization ratio of N to C. For example, during the complete mineralization of Redfieldian organic matter through denitrification and anammox 16 of 55.2 mol N_2, or 29%, is produced through anammox [11]:

$$(CH_2O)_{106}(NH_3)_{16}H_3PO_4 + 94.4NO_3^- + 94.4H^+ \rightarrow 106CO_2 + 16NH_4^+ + 16NO_2^- + 39.2N_2 + 145.2H_2O + H_3PO_4 \quad (4)$$

$$16NH_4^+ + 16NO_2^- \rightarrow 16N_2 + 32H_2O \quad (5)$$

The anammox contributions in Golfo Dulce, excluding the bottom depths, were 58 and 32% at the two stations, which would indicate a higher N:C ratio during mineralization than in the equations above [11]. Sediment trap studies indicate a preferential mineralization of organic N during water-column denitrification [43, 77], which may help explain these deviations.

5.3 Interaction with Denitrifiers

The biogeochemical relationship between anammox bacteria and denitrifiers appears quite complex. As discussed above, anammox depends on ammonification, which in environments such as Golfo Dulce may to a large extent be carried out by denitrifiers that oxidize N-containing organics. Further interactions with denitrifiers include the potential dependence on denitrification as a source of NO_2^-, as well as competition for NO_2^-.

Nitrite has been shown as the electron acceptor utilized by anammox bacteria for ammonium oxidation from wastewater systems [76], and patterns of isotope pairing during marine anammox suggest that this is also true for anammox bacteria in natural environments [12]; (see also above). Nitrate reduction is the main source of NO_2^- in Golfo Dulce and the Black Sea [12, 35], where NO_2^- accumulates in the anoxic waters, similar to observations in oceanic oxygen minimum zones (e.g. [9]). Nitrite may also accumulate transiently to high levels during anoxic incubations of NO_3^--amended sediment [70], while in other cases NO_2^- concentrations remain low [73].

It is not clear which factors regulate the accumulation of NO_2^- during NO_3^- reduction in waters and sediments. Denitrifiers are often thought to

dominate NO_3^- reduction and thereby NO_2^- production. They only form a subset, however, of a large variety of organisms capable of nitrate reduction to nitrite [84], including at least some anammox bacteria [26]. An identification of the dominating NO_2^--producing organisms in natural environments would contribute to an understanding of NO_2^- dynamics and their significance for anammox.

Under the assumption that nitrite consumption by anammox can be described by Michaelis-Menten kinetics, the apparent half-saturation concentration, K_m, for NO_2^- during anammox in natural environments has been constrained to $< 3\ \mu$M [12, 73]. For the one sedimentary setting where kinetic studies were performed in some detail, by examining the time course of NO_2^- depletion, the apparent K_m for NO_2^- during denitrification was similarly low and there was no change in the relative importance of anammox and denitrification during NO_2^- depletion [12]. With maximum NO_2^- concentrations in natural environments of only a few μmol per liter, tighter constraints on the K_m values are however needed for a determination of how competition for NO_2^- may affect the balance between anammox and denitrification.

5.4 Oxygen Sensitivity and the Interaction with Aerobic Ammonium Oxidizers

Little is known about the oxygen tolerance of anammox bacteria in the marine environment. Experimental work with enrichment cultures showed that the anammox metabolism is inhibited by oxygen concentrations as low as 1 μM [67]. The inhibition is fully reversible and anammox enrichment cultures that have been exposed to oxygen, resume activity immediately after the reestablishment of anaerobic conditions [67]. As such anammox bacteria might be able to thrive in oxygen deficient environments that regularly experience incursions of oxygenated water, such as the oxygen minimum zones of coastal upwelling areas. At higher oxygen concentrations anammox bacteria could be dormant, and become active again under anaerobic conditions. Alternatively, marine snow aggregates are abundant in many oxygen deficient environments, and could provide the anammox bacteria with anaerobic micro-environments at low ambient oxygen concentrations ($< 25\ \mu$M) [45].

Intriguingly, in the so called Completely Autotrophic Nitrogen removal Over Nitrite (CANON) process in oxygen limited bioreactors, aerobic and anaerobic ammonia oxidizing bacteria cooperate to remove ammonium at ambient oxygen concentrations as high as 10 μM [42, 63, 71]. In these bioreactors, anaerobic and aerobic ammonia oxidizing bacteria form small (micrometer to millimeter size) aggregates, with the aerobic ammonia oxidizers restricted to the outer shell ($< 100\ \mu$M) while the anammox bacteria occur in the central anoxic part

[42]. The ammonium is partly oxidized under oxygen limitation to nitrite by aerobic ammonium oxidizers, such as *Nitrosomonas* and *Nitrosospira* (eq. 6).

$$NH_4{}^+ + 1.5O_2 \rightarrow NO_2{}^- + H_2O + 2H^+ \quad (6)$$

The produced nitrite is subsequently used as an electron acceptor by the anammox bacteria to oxidize ammonium to dinitrogen gas (eq. 3). The stoichiometry of the CANON process can be represented by eq. 7.

$$2NH_4{}^+ + 1.5O_2 \rightarrow N_2 + 3H_2O + 2H^+ \quad (7)$$

There is so-far no direct evidence for the CANON process in the marine environment. However, the CANON process combined with enzyme catalyzed hydrolysis of organic nitrogen would provide an alternative explanation for the fact that the relative contribution of anammox to the total N_2 production is far larger [11, 70] in certain environments than the 29% expected from the stoichiometry (eqs. 4 and 5) of the complete mineralization of Redfieldian organic matter through denitrification and anammox (see also chapter 5.2).

6. ANAMMOX AND THE CHEMICAL EVOLUTION OF EARTH'S SURFACE

The present chemical composition of the oceans and atmosphere is the result of evolving biological processes and geological activity interacting throughout Earth's history. During some stages, nitrogen limitation of biological production is thought to have played an important role in the configuration of the biogeochemical cycles and as a driving force in biological evolution [3, 20]. Anammox introduces the possibility of $NH_4{}^+$ removal under anoxic conditions to the N cycle. This shunt seems of particular relevance on early Earth, where the atmosphere and oceans are thought to have been anoxic (e.g. [3]). Anammox depends on $NO_2{}^-$, and before the rise of O_2, $NO_2{}^-$ and $NO_3{}^-$ may mainly have been supplied at a low flux from atmospheric processes [33]. Biological N fixation as a source of $NH_4{}^+$ is believed to have evolved early in Earth's history and in the diversification of life [6, 20, 21]. Thus, a niche for anammox bacteria may have existed since the Archean, but due to the low flux of $NO_2{}^-/NO_3{}^-$ the process may not have had a large impact on the N cycle [30]. As O_2 accumulated, nitrification became possible and likely supplied substantial amounts of $NO_2{}^-/ NO_3{}^-$ for denitrification and anammox, leading to a configuration of the N cycle similar to that of modern euxinic basins. In conjunction with possible trace-metal limitation of N_2 fixation in the sulfidic oceans, this stimulation of the oxidative N cycle may have led to substantial limitation of primary production [3, 20]. The unique ladderane lipids of the anammoxosome membrane potentially provide a specific biomarker of anammox activity in the geological

record [62]. For this, however, an assessment of the long-term stability of these compounds in sediments is needed.

7. ANAMMOX AND THE MARINE NITROGEN CYCLE

Phytoplankton growth is nitrogen limited in many oceanic regions [9, 20] due to basin scale imbalances between N_2-fixation and fixed inorganic nitrogen (NH_4^+, NO_2^-, NO_3^-) removal by anaerobic microbial activity (Fig. 5). Nutrient measurements and stable nitrogen isotope modeling indicate that 400-480 Tg of fixed nitrogen per year is lost from the Ocean, with oxygen minimum zones and continental margin sediments as the main areas of nitrogen loss [5, 9]. The discovery of anammox as a distinct novel pathway of N_2 production in marine environments calls for a quantification of its global significance, and an identification of the main factors that regulate this process.

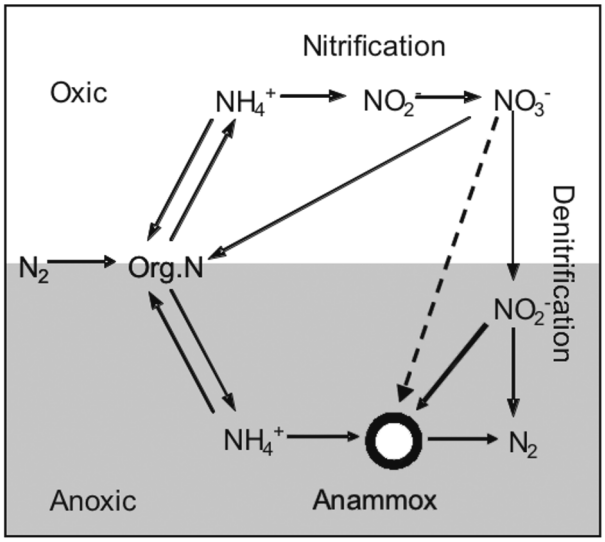

Figure 5. Simplified marine nitrogen cycle including the anammox 'sink'; Org. N: organic nitrogen.

The relative contribution of anammox to the total fixed nitrogen loss as N_2 is still unclear. But the widespread occurrence of anaerobic ammonium oxidation with nitrite to N_2 in marine sediments, anoxic basins and fjords [11, 12, 35, 51, 54, 70, 73] indicates that anammox bacteria could be responsible for substantial loss of fixed nitrogen from the ocean. Devol [14] argued that it is possible that anammox accounts for 30-50% of the N_2 production in the ocean. Theoretically, 29% of the N_2 production during the complete mineral-

ization of Redfieldian organic matter through denitrification and anammox, is produced through anammox (eqs. 4, 5) [11, 14]. The preferential mineralization of nitrogen rich proteins through denitrification, releases more ammonium than predicted by standard Redfield stoichiometry (eqs. 4) [11, 14]. If proteins are the only substrate for denitrification, the relative contribution of anammox to the total N_2 production increases to 48% [14]. In sediments and anoxic basins like the Black Sea, ammonium diffuses upwards into the suboxic zone from the underlying sulfidic zone [14, 35] where large amounts of ammonium are released upon mineralization of organic nitrogen through fermentation/sulfate reduction. In such environments where ammonium is supplied from outside the suboxic zone, the relative importance of anammox can exceed 48% [11, 14, 19, 30, 70, 80].

Prognostic diagenetic modeling indicates that, globally, most benthic denitrification takes place in slope and hemipelagic sediments [37]. The role of anammox in such locations awaits quantification. However, the general trend towards increased relative importance of anammox with increasing water depth and decreasing organic loading (Fig. 2) further substantiates that this process may indeed be a major nitrogen sink in the ocean.

The extremely low concentration of ammonium and typical abundance of nitrite could indicate that anammox bacteria also play an important role in the nitrogen removal from oxygen minimum zone waters (e.g. [11, 14, 80]). Nutrient measurements indicate that 30-50% of the total nitrogen loss in the ocean occurs in these oxygen minimum zones [9, 25]. The pelagic nitrogen removal takes place within only ~0.1% of the ocean volume, and hence moderate variations in the extent of oxygen minimum zones may have a large impact on the global nitrogen cycle [9, 25]. This nitrogen loss has been fully attributed to nitrate reduction to N_2 by heterotrophic bacteria (denitrification) [9, 18, 25] because until recently there was no other process known that could transform fixed inorganic nitrogen into N_2. In fact, to the best of our knowledge there is so far no published evidence from ^{15}N-labeling experiments that nitrate is directly converted to N_2 by heterotrophic denitrifiers in the OMZ waters of the ocean. Recent results show that anammox bacteria are responsible for massive loss of fixed nitrogen as gaseous N_2 from the Benguela OMZ water [34]. The possibility that anammox is also a dominant process for nitrogen removal in other OMZ waters of the ocean should now be explored.

References

[1] Aller R.C. Bioturbation and manganese cycling in hemipelagic sediments, Philos Trans R Soc of Lond A Math Phys Sci 1990; 331:51-58.

[2] Aller R.C., Hall P.O.J., Rude P.D. and Aller J.Y. Biogeochemical heterogeneity and suboxic diagenesis in hemipelagic sediments of the Panama Basin, Deep-Sea Res Pt I 1998; 45:133-65.

[3] Anbar A.D. and Knoll A.H. Proterozoic ocean chemistry and evolution: A bioinorganic bridge? Science 2002; 297:1137-42.

[4] Bender M., Jahnke R., Weiss R., Martin W., Heggie D.T., Orchardo J. and Sowers T. Organic carbon oxidation and benthic nitrogen and silica dynamics in San Clemente Basin, a continental borderland site, Geochim Cosmochim Acta 1989; 53:685-97.

[5] Brandes J.A. and Devol A.H. A global marine-fixed nitrogen isotopic budget: Implications for Holocene nitrogen cycling, Global Biogeochem Cy 2002; 16.

[6] Braun S.T., Proctor L.M., Zani S., Mellon M.T. and Zehr J.P. Molecular evidence for zooplankton-associated nitrogen-fixing anaerobes based on amplification of the nifH gene, Fems Microbiol Ecol 1999; 28:273-79.

[7] Carr M.-E. Estimation of potential productivity in eastern boundary currents using remote sensing, Deep Sea Res II 2002; 49:58-80.

[8] Chapman P. and Shannon L.V. The Benguela ecosystem. Part II. Chemistry and related processes, Oceanogr Mar Biol Ann Rev 1985; 23:183-251.

[9] Codispoti L.A., Brandes J.A., Christensen J.P., Devol A.H., Naqvi S.W.A., Paerl H.W. and Yoshinari T. The oceanic fixed nitrogen and nitrous oxide budgets: Moving targets as we enter the anthropocene? Sci Mar 2001; 65:85-105.

[10] Copin-Montegut C. and Copin-Montegut G. Stoichiometry of carbon, nitrogen and phosphorus in marine particulate matter, Deep Sea Res 1983; 30:31-46.

[11] Dalsgaard T., Canfield D.E., Petersen J., Thamdrup B. and Acuña-González J. Anammox is a significant pathway of N_2 production in the anoxic water column of Golfo Dulce, Costa Rica, Nature 2003; 422:606-08.

[12] Dalsgaard T. and Thamdrup B. Factors controlling anaerobic ammonium oxidation with nitrite in marine sediments, Appl Environ Microb 2002; 68:3802-08.

[13] Devol A.H. Direct measurement of nitrogen gas Fluxes from continental-shelf sediments, Nature 1991; 349:319-21.

[14] Devol A.H. Solution to a marine mystery, Nature 2003; 422:575-76.

[15] Egli K., Bosshard F., Werlen C., Lais P., Siegrist H., Zehnder A.J.B. and van der Meer J.R. Microbial composition and structure of a rotating biological contactor biofilm treating ammonium-rich wastewater without organic carbon, Microbial Ecol 2003; 45:419-32.

[16] Egli K., Fanger U., Alvarez P.J.J., Siegrist H., van der Meer J.R. and Zehnder A.J.B. Enrichment and characterization of an anammox bacterium from a rotating biological contactor treating ammonium-rich leachate, Arch Microbiol 2001; 175:198-207.

[17] Emerson S., Jahnke R., Bender M., Froelich P., Klinkhammer G., Bowser C. and Setlock G. Early diagenesis in sediments from the Eastern Equatorial Pacific. I. Pore water nutrient and carbonate results, Earth Planet Sc Lett 1980; 49:57-80.

[18] Emery K.O., Orr W.L. and Rittenberg S.C. Nutrient budgets in the ocean, In: *Essays in the Natural Sciences in Honor of Captain Allan Hancock*. Univ. of Southern California Press: Los Angeles. p. 229-310, 1955.

[19] Engström P., Dalsgaard T., Hulth S. and Aller R.C. Anaerobic ammonium oxidation by nitrite (anammox): implications for N_2 production in coastal marine sediments, Geochim Cosmochim Ac 2005; 69:2057-65.

[20] Falkowski P.G. Evolution of the nitrogen cycle and its influence on the biological sequestration of CO_2 in the ocean, Nature 1997; 387:272-75.

[21] Fani R., Gallo R. and Lio P. Molecular evolution of nitrogen fixation: The evolutionary history of the nifD, nifK, nifE, and nifN genes, J Mol Evol 2000; 51:1-11.

[22] Fenchel T., Bernard C., Esteban G., Finlay B.J., Hansen P.J. and Iversen N. Microbial diversity and activity in a danish fjord with anoxic deep-water, Ophelia 1995; 43:45-100.

[23] Freitag T.E. and Prosser J.I. Community structure of ammonia-oxidizing bacteria within anoxic marine sediments, Appl Environ Microb 2003; 69:1359-71.

[24] Froelich P.N., Klinkhammer G.P., Bender M.L., Luedtke N.A., Heath G.R., Cullen D., Dauphin P., Hammond D. and Hartman B. Early oxidation of organic matter in pelagic sediments of the eastern equatorial Atlantic: Suboxic diagenesis, Geochim Cosmochim Ac 1979; 43:1075-90.

[25] Gruber N. and Sarmiento J.L. Global patterns of marine nitrogen fixation and denitrification, Global Biogeochem Cy 1997; 11:235-66.

[26] Güven D., Dapena A., Kartal B., Schmid M., Maas B., van de Pas-Schoonen K., Sozen S., Mendez R., op den Camp H., Jetten M.S.M., Strous M. and Schmidt I. Propionate oxidation and methanol inhibition of the anaerobic ammonium oxidizing bacteria, Appl Environ Microb 2005; 71:1066-71.

[27] Hamm R.E. and Thompson T.G. Dissolved nitrogen in the sea water of the Northeast Pacific with notes on the total carbon dioxide and dissolved oxygen, J Mar Res 1941; 4:11-27.

[28] Hansen J.W., Thamdrup B. and Jorgensen, B.B. Anoxic incubation of sediment in gas-tight plastic bags: a method for biogeochemical process studies, Mar Ecol-Prog Ser 2000; 208:273-82.

[29] Hauck R.D., Melsted S.W. and Yankwich P.E. Use of N-isotope distribution in nitrogen gas in the study of denitrification, Soil Science 1958; 86:287-91.

[30] Hulth S., Aller R.C., Canfield D.E., Dalsgaard T., Engström P., Gilbert F., Sundbäck K. and Thamdrup B. N removal in marine environments: recent developments and future research challenges, Mar Chem 2005; 94:125-45.

[31] Hulth S., Aller R.C. and Gilbert F. Coupled anoxic nitrification/manganese reduction in marine sediments, Geochim Cosmochim Ac 1999; 63:49-66.

[32] Jetten M.S.M. et al. Anaerobic ammonium oxidation by marine and freshwater planctomycete-like bacteria, Appl Microbiol Biot 2003; 63:107-14.

[33] Kasting J.F. and Walker J.C.G. Limits on oxygen concentration in the prebiological atmosphere and the rate of abiotic fixation of nitrogen, J Geophys Res-Oc Atm 1981; 86:1147-58.

[34] Kuypers M.M.M., Lavik G., Woebken D., Schmid M., Fuchs B.M., Amann R., Jørgensen B.B. and Jetten M.S.M. Massive nitrogen loss from the Benguela upwelling system through anaerobic ammonium oxidation, PNAS 2005; 102:6478-83.

[35] Kuypers M.M.M., Sliekers A.O., Lavik G., Schmid M., Jørgensen B.B., Kuenen J.G., Sinninghe Damsté J.S., Strous M. and Jetten M.S.M. Anaerobic ammonium oxidation by anammox bacteria in the Black Sea, Nature 2003; 422:608-11.

[36] Luther G.W., Sundby B., Lewis B.L., Brendel P.J. and Silverberg N. Interactions of manganese with the nitrogen cycle: Alternative pathways to dinitrogen, Geochimi Cosmochim Ac 1997; 61:4043-52.

[37] Middelburg J.J., Soetaert K., Herman P.M.J. and Heip C.H.R. Denitrification in marine sediments: A model study, Global Biogeochem Cy 1996; 10:661-73.

[38] Mulder A., van de Graaf A.A., Robertson L.A. and Kuenen J.G. Anaerobic ammonium oxidation discovered in a denitrifying fluidized bed reactor, FEMS Microbiol Ecol 1995; 16:177-84.

[39] Murray J.W., Codispoti L.A. and Frederich G.E. Oxidation-reduction environments - The suboxic zone in the Black Sea, In: *Aquatic Chemistry*, Huang C.P., O'Melia C.R. and Morgan J.J., Eds. American Chemical Society: Washington DC., 1995.

[40] Murray J.W., Lee B.S., Bullister J. and Luther G.W. III, The suboxic zone of the Black Sea, In: *Environmental degradation of the Black Sea: Challenges and remedies*, S. Besiktepe, U. Ünülata, and A. Bologa, Eds., Kluwer Academic Publisher: Dordrecht, 1999.

[41] Nielsen L.P. Dentrification in sediment determined from nitrogen isotope pairing, FEMS Microbiol Ecol 1992; 86:357-62.

[42] Nielsen M., Bollmann A., Sliekers A.O., Jetten M., Schmid M., Strous M., Schmidt I., Larsen L.H., Nielsen L.P. and Revsbech N.P. Kinetics, diffusional limitation and microscale distribution of chemistry and organisms in a CANON reactor, FEMS Microbiol Ecol 2005; 51:247-56.

[43] Pantoja S., Sepulveda J.S. and Gonzalez H.E. Decomposition of sinking proteinaceous material during fall in the oxygen minimum zone off northern Chile, Deep-Sea Res Pt I 2004; 51:55-70.

[44] Petersen J. The role of anammox in the marine nitrogen cycle, M.Sc. thesis, Institute of Biology, University of Southern Denmark, Odense 2002. (In Danish)

[45] Ploug H. Small-scale oxygen fluxes and remineralization in sinking aggregates, Limnol Oceanogr 2001; 46:1624-31.

[46] Ramsing N.B., Fossing H., Ferdelman T.G., Andersen F. and Thamdrup B. Distribution of bacterial populations in a stratified fjord (Mariager fjord, Denmark) quantified by in situ hybridization and related to chemical gradients in the water column, Appl Env Microbiol 1996; 62:1391-1404.

[47] Redfield A.C., Ketchum B.H. and Richards F.A. The influence of organisms on the composition of sea water, In: *The Sea*, M.N. Hill, Ed., Interscience Press: New York, 1963.

[48] Richards F.A. Anoxic Basins and Fjords, In: *Chemical Oceanography*, J.P. Ripley and G. Skirrow, Eds., Academic Press: London and New York, 1965.

[49] Richards F.A., Anderson J.J. and Cline J.D. Chemical and physical observations in Golfo Dulce, an anoxic basin on Pacific coast of Costa-Rica, Limnol Oceanogr 1971; 16:43-&.

[50] Richards F.A., Cline J.D., Broenkow W.W. and Atkinson L.P. Some consequences of the decomposition of organic matter in lake Nitinat an anoxic fjord, Limnol Oceanogr (suppl.) 1965; 10:R185-R201.

[51] Risgaard-Petersen N., Meyer R.L., Schmid M., Jetten M.S.M., Enrich-Prast A., Rysgaard S. and Revsbech N.P. Anaerobic ammonium oxidation in a estuarine sediment, Aquatic Microbial Ecol 2004; 36:293-304.

[52] Risgaard-Petersen N., Nielsen L.P., Rysgaard S., Dalsgaard T. and Meyer R.L. Application of the isotope pairing technique in sediments where anammox and denitrification coexist, Limnol Oceanogr Methods 2003; 1:63-73.

[53] Rysgaard S. and Glud R.N. Anaerobic N_2 production in Arctic sea ice, Limnol Oceanogr 2004; 49:86-94.

[54] Rysgaard S., Glud R.N., Risgaard-Petersen N. and Dalsgaard T. Denitrification and anammox activity in Arctic sediments, Limnol Oceanogr 2004; 49: 1493-1502.

[55] Schmid M., Maas B., Dapena A., van de Pas-Schoonen K., van de Vossenberg J., Kartal B., van Niftrik L., Schmidt I., Cirpus I., Kuenen J.G., Wagner M., Damsté J.S.S., Kuypers M., Revsbech N.P., Mendez R., Jetten M.S.M. and Strous M. Biomarkers for in situ detection of anaerobic ammonium-oxidizing (anammox) bacteria, Appl Environ Microb 2005; 71:1677-84.

[56] Schmid M., Schmitz-Esser S., Jetten M. and Wagner M. 16S-23S rDNA intergenic spacer and 23S rDNA of anaerobic ammonium-oxidizing bacteria: implications for phylogeny and *in situ* detection, Environ Microbiol 2001; 3:450-59.

[57] Schmid M., Twachtmann U., Klein M., Strous M., Juretschko S., Jetten M., Metzger J., Schleifer K.H. and Wagner M. Molecular evidence for genus level diversity of bacteria capable of catalyzing anaerobic ammonium oxidation, Syst Appl Microbiol 2000; 23:93-106.

[58] Schmid M., Walsh K., Webb R., Rijpstra W.I.C., van de Pas-Schoonen K., Verbruggen M.J., Hill T., Moffett B., Fuerst J., Schouten S., Sinninghe Damsté J.S., Harris J., Shaw P., Jetten M. and Strous M. *Candidatus* 'Scalindua brodae', sp.nov., *Candidatus* 'Scalindua wagneri', sp. nov., two new species of anaerobic ammonium oxidizing bacteria, System Appl Microbiol 2003; 26.

[59] Schouten S., Strous M., Kuypers M.M.M., Rijpstra W.I.C., Baas M., Schubert C.J., Jetten M.S.M. and Damste J.S.S. Stable carbon isotopic fractionations associated with inorganic carbon fixation by anaerobic ammonium-oxidizing bacteria, Applied and Environ Microbiol 2004; 70:3785-88.

[60] Schultz H.D., Dahmke A., Schinzel U., Wallman K. and Zabel M. Early diagenetic processes, fluxes, and reaction rates in sediments of the South Atlantic, Geochim Cosmochim Ac 1994; 58: 2041-60.

[61] Seitzinger S., Nixon S., Pilson M.E.Q. and Burke S. Denitrification and N_2O Production in near-Shore Marine-Sediments, Geochim Cosmochim Ac 1980; 44:1853-60.

[62] Sinninghe Damsté J.S., Strous M., Rijpstra W.I.C., Hopmans E.C., Geenevasen J.A.J., van Duin A.C.T., van Niftrik L.A. and Jetten M.S.M. Linearly concatenated cyclobutane (ladderane) lipids from a dense bacterial membrane, Nature 2002; 419:708-12.

[63] Sliekers A.O., Derwort N., Campos Gomez J.L., Strous M., Kuenen J.G. and Jetten M. Completely autotrophic nitrogen removal over nitrite in one single reactor, Water Res 2002; 36:2475-82.

[64] Sorokin Y.I. In *The Black Sea - Ecology and oceanography. Biology of Inland Waters*, Martens K., ed., Leiden: Backhuys Publishers, 2002.

[65] Strous M., Fuerst J.A., Kramer E.H.M., Logemann S., Muyzer G., van de Pas-Schoonen K.T., Webb R., Kuenen J.G. and Jetten M.S.M. Missing litotroph identified as new planctomycete, Nature 1999; 400:446-49.

[66] Strous M., Kuenen J.G. and Jetten M.S.M. Key physiology of anaerobic ammonium oxidation, Appl Environ Microb 1999; 65:3248-50.

[67] Strous M., vanGerven E., Kuenen J.G. and Jetten M. Effects of aerobic and microaerobic conditions on anaerobic ammonium-oxidizing (Anammox) sludge, Appl Environ Microb 1997; 63:2446-48.

[68] Thamdrup B., Canfield D.E., Ferdelman T.G., Glud R.N. and Gundersen J.K. A biogeochemical survey of the anoxic basin Golfo Dulce, Costa Rica, Revista De Biologia Tropical 1996; 44:19-33.

[69] Thamdrup B. and Dalsgaard T. The fate of ammonium in anoxic manganese oxide-rich marine sediment, Geochim Cosmochim Ac 2000; 64:4157-64.

[70] Thamdrup B. and Dalsgaard T. Production of N_2 through anaerobic ammonium oxidation coupled to nitrate reduction in marine sediments, Appl Environ Microb 2002; 68:1312-18.

[71] Third K.A., Sliekers A.O., Kuenen J.G. and Jetten M.S.M. The CANON system (completely autotrophic nitrogen-removal over nitrite) under ammonium limitation: Interaction and competition between three groups of bacteria, Syst Appl Microbiol 2001; 24:588-96.

[72] Toggweiler J.R. An ultimate limiting nutrient, Nature 1999; 400:511-12.

[73] Trimmer M., Nicholls J.C. and Deflandre B. Anaerobic ammonium oxidation measured in sediments along the Thames estuary, United Kingdom, Appl Environ Microb 2003; 69:6447-54.

[74] Tyrrell T. and Lucas M.I. Geochemical evidence of denitrification in the Benguela upwelling system, Cont Shelf Res 2002; 22:2497-2511.

[75] van de Graaf A.A., de Bruijn P., Robertson L.A., Jetten M.S.M. and Kuenen J.G. Metabolic pathway of anaerobic ammonium oxidation on the basis of N-15 studies in a fluidized bed reactor, Microbiol 1997; 143:2415-21.

[76] Van de Graaf A.A., Mulder A., De Bruijn P., Jetten M.S.M., Robertson L.A. and Kuenen J.G. Anaerobic oxidation of ammonium is a biologically mediated process, Appl Environ Microb 1995; 61:1246-51.

[77] Van Mooy B.A.S., Keil R.G., and Devol A.H. Impact of suboxia on sinking particulate organic carbon: Enhanced carbon flux and preferential degradation of amino acids via denitrification, Geochim Cosmochim Ac 2002; 66:457-65.

[78] van Niftrik L.A., Fuerst J.A., Damste J.S.S., Kuenen J.G., Jetten M.S.M. and Strous M. The anammoxosome: an intracytoplasmic compartment in anammox bacteria, FEMS Microbiol Lett 2004; 233:7-13.

[79] Vargas J.A. Pacific coastal ecosystems of Costa Rica with emphasis on the Golfo Dulce and adjacent areas: A synoptic view based on the R.V. Victor Hensen expedition 1993/94 and previous studies. Preface, Rev Biol Trop 1996; 44:U1-U4.

[80] Ward B.B. Significance of anaerobic ammonium oxidation in the ocean, Trends Microbiol 2003; 11:408-10.

[81] Ward B.B. and Kilpatrick K.A. Nitrogen transformations in the oxic layer of permanent anoxic basins: the Black Sea and the Cariaco Trench, In *Black Sea Oceanography*, Izdar E. and Murray J.W., Eds., Kluwer Academic Publishers: Dordrecht, 1991.

[82] Zehr J.P. and Ward B.B. Nitrogen cycling in the ocean: New perspectives on processes and paradigms, Appl Environ Microb 2002; 68:1015-24.

[83] Zopfi J., Ferdelman T.G., Jorgensen B.B., Teske A. and Thamdrup B. Influence of water column dynamics on sulfide oxidation and other major biogeochemical processes in the chemocline of Mariager Fjord (Denmark), Mar Chem 2001; 74:29-51.

[84] Zumft W.G. Cell biology and molecular basis of denitrification, Microbiol Mol Biol Rev 1997; 61:533-616.

DIVERSITY, DISTRIBUTION AND BIOGEOCHEMICAL SIGNIFICANCE OF NITROGEN-FIXING MICROORGANISMS IN ANOXIC AND SUBOXIC OCEAN ENVIRONMENTS

Jonathan P. Zehr[1], Matthew J. Church[2], and Pia H. Moisander[3]

[1] *University of California Santa Cruz, Ocean Sciences Department, 1156 High Street, Santa Cruz, CA 95064, USA*

[2] *University of Hawaii, School of Ocean and Earth Science and Technology, Honolulu, HI 96822, USA*

[3] *NASA Ames Research Center, Exobiology Branch, Moffett Field, CA 94035, USA*

Abstract Nitrogen fixation, the reduction of atmospheric dinitrogen (N_2) to biologically available ammonium, has been important in the balance of biologically available nitrogen since early in the evolution of life on Earth. The nitrogen fixation reaction requires ATP and reductant and also reduces H^+ to H_2. Nitrogenase is composed of two multi-subunit metalloproteins. There are at least three evolutionarily related nitrogenase gene families that require different metals (Mo, V or Fe) in the cofactor for the protein component (Component I) that contains the active site for N_2 reduction. The requirements for metals probably played an important role in the evolution of nitrogenases, as the oceans progressed from anoxic waters containing relatively high concentrations of reduced Fe, to low-Fe oxic waters. The nitrogenase genes are distributed widely throughout prokaryotic taxa, and thus, nitrogen fixation is found in diverse anaerobic, aerobic, and facultative microorganisms, with equally diverse physiological strategies. Many of these organisms can be found at oxic-anoxic interfaces and in anoxic waters.

Nitrogenase expression and activity is regulated in the presence of both NH_4^+ and O_2, which are biogeochemically important variables in anoxic ecosystems. It has generally been assumed that N_2 fixation is unimportant in anoxic waters since ammonium concentrations tend to be high in these environments. N_2 fixation is known to be quantitatively important in oxygenated surface waters of the oceans and in oxic waters overlying anoxic basins, with much of this N_2 fixation catalyzed by cyanobacteria. N_2 fixation occurs in marine anoxic habitats such as salt marshes and in sediments, but has not been reported in anoxic water columns. N_2 fixation studies in hypersaline Mono Lake indicate that N_2 fixing microorganisms do express nitrogenase in anoxic waters, but in general, the

L. N. Neretin (ed.), Past and Present Water Column Anoxia, 337–369.

significance of nitrogenase gene expression and activity has yet to be determined in anoxic water columns.

Keywords: Nitrogen fixation, *nif*, anaerobes, biogeochemical cycles, marine nitrogen cycle, evolution, anoxic environments.

1. INTRODUCTION

Nitrogen fixation is the primary pathway for introduction of fixed nitrogen into the biosphere and comprises a central process in the global nitrogen cycle. Microbially mediated N_2 fixation accounts for an annual input of ~ 1.5 x 10^{13} mol N yr^{-1} globally, with approximately half of this annual N_2 fixation in the oceans. Oceanic N_2 fixation has received increasing attention in the past two decades as basin-scale nitrogen budgets provide conflicting estimates of the magnitude of N_2 fixation. In addition, previously unrecognized N_2-fixing microorganisms have recently been discovered and the contributions of these poorly characterized microorganisms to ocean nitrogen budgets are not yet known.

Nitrogen fixation in the water columns of oxic ocean basins has received considerable attention, but to date, little research has focused on N_2 fixation in anoxic ocean basins. Anoxic waters have played a pivotal role in the evolution of N_2 fixation on Earth as the oceans were anoxic over large periods of the Earth's history. N_2 fixation is an energetically expensive reaction that is highly regulated. The characteristics of the enzyme and the chemical reaction are important for understanding how and why N_2 fixation evolved in anoxic oceans, and why it could occur in anoxic water columns. In this chapter, we review the properties of N_2 fixation, what is known about N_2 fixation in the oceans, and examine N_2 fixation in anoxic marine environments, including anoxic basins.

2. THE BIOCHEMISTRY AND MOLECULAR BIOLOGY OF NITROGEN FIXATION

2.1 Chemical Reaction

Biological N_2 fixation is the enzymatic reduction of N_2 to ammonia (NH_3). Enzymes that catalyze this reaction are called nitrogenases. The reduction of one molecule of N_2 requires 8 low potential electrons to form 2 molecules of NH_3 and one molecule of hydrogen (H_2). N_2 fixation is an energetically expensive reaction requiring approximately 16 ATP molecules per molecule of N_2 reduced corresponding to 2 ATP per electron [29]. The low potential electrons are provided by oxidation of ferredoxin or flavodoxin :

$$N_2 + 8H^+ + 8e^- + 16MgATP \rightarrow 2NH_3 + H_2 + 16MgADP + 16P_i$$

H_2 is an unavoidable byproduct of N_2 fixation. The evolution of H_2 reduces the efficiency of N_2 fixation by consuming ATP. Many diazotrophs have an uptake hydrogenase that catalyzes the recapture of the energy lost in H_2 production. It is impossible to eliminate the hydrogenase reaction coincident with N_2 fixation apparently because hydride ions must be bound to the active site prior to binding N_2 [29].

2.2 Nitrogenase Structure and N_2-fixation Genes

Nitrogenase is composed of two multi-subunit metalloproteins, termed Component I (dinitrogenase, or the MoFe protein) and Component II (dinitrogenase reductase, or the Fe protein). Both proteins have Fe-S reaction centers. The Fe protein of Component II passes electrons to the MoFe protein, thereby reducing the MoFe protein and allowing the reduction of N_2 to occur at the active site of Component I [53]. Each cycle of N_2 fixation requires association of Component I and II, hydrolysis of 2 MgATP, transfer of an electron from Component II to Component I, and dissociation of the two proteins [17]. The rate-limiting step for the reaction appears to be the dissociation of Component I and II [102]. The cycle is repeated, with the Component I protein progressing to increasingly reduced states until 8 electrons are transferred and N_2 is formed [17]. Nitrogenase has a relatively slow turnover time of 5 electrons per second, thereby catalyzing the reduction of 1 molecule of N_2 in 1.25 seconds [98, 102].

N_2 is not present the only substrate for nitrogenase. If N_2 is not present, hydrogen is formed from water. Other substrates that are reduced by nitrogenase are acetylene (to ethylene and ethane), hydrogen cyanide, hydrogen azide, nitrou oxide, and carbon monoxide [98]. These other compounds are sometimes competitive substrates or inhibitors, depending on the concentrations of substrates and proteins [17]. Carbon monoxide is an inhibitor for all of these other substrates [29].

Nitrogenases consist of three gene families that contain molybdenum (Mo), vanadium (V), or iron (Fe) in the cofactor (FeMo cofactor in the case of the Mo enzyme). They are three different, but evolutionarily related gene families. These enzymes are termed conventional (Mo nitrogenase), alternative (V nitrogenase, *vnfHDGK* encoded), or second alternative (Fe, *anfHDGK* encoded) nitrogenases (Fig. 1).

The nitrogenases are metalloproteins, and both components contain Fe. Component I of the conventional Mo containing enzyme is composed of a tetramer of $\alpha_2\beta_2$ subunits each containing two pairs of FeS clusters, P clusters and one FeMo cofactor. The FeMo cofactor is composed of $MoFe_3S_3$ linked to Fe_4S_3 with 3 sulfurs [53] that lie within the α subunits of the protein. These sites form the presumed active site for N_2 fixation [17, 53]. The P clusters lie at the interfaces between the α and β subunits and are involved in shuttling electrons between the Fe protein and the active site. The P clusters are composed of

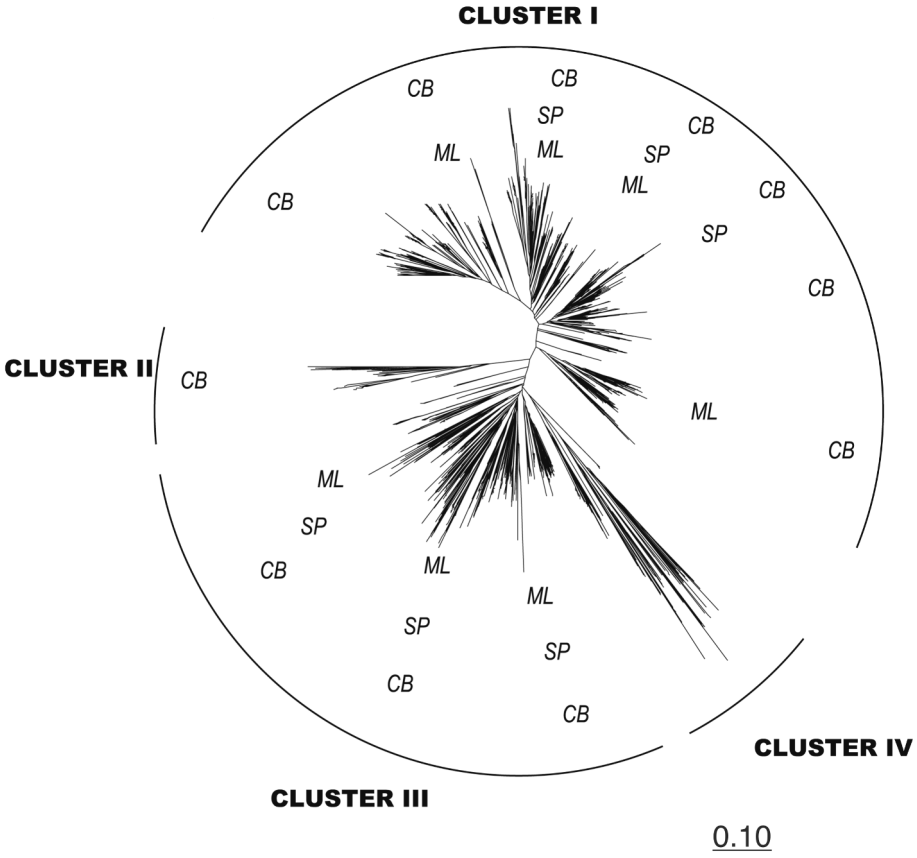

Figure 1. Phylogenetic tree of N_2 fixing microorganisms based on approximately 2000 *nifH* sequences in GenBank [142]. Sequences that cluster in Cluster III, which contains nitrogenases from many anaerobes, have been detected in some aquatic environments, but are particularly abundant in Mono Lake which had an anoxic water column [123]. The sequences in the tree indicate Cluster III nitrogenases that have been detected. CB= Chesapeake Bay, GN= Guerrero Negro microbial mat, ML= Mono Lake, SP= *Spartina* marsh sediments.

Fe_8S_8 clusters (actually formed from two Fe_4S_4 clusters) [53]. Component II is a homodimer (α_2) containing an Fe_4S_4 cluster. Component II serves to reduce Component I through 8 successive reductions per molecule of N_2 converted to NH_3. The *nifH* gene encodes component II.

Although all three nitrogenases reduce N_2, the characteristics of the reaction and interaction with substrates as well as sensitivity to environmental conditions such as oxygen and temperature differ. The alternative nitrogenases are more sensitive to oxygen, have a lower ratio of H_2 production per N_2 reduced,

and do not reduce acetylene to ethylene [29]. Instead of ethylene, the alternative nitrogenases release small amounts of ethane (C_2H_6) from acetylene. The production of ethane can be used as an indicator for the presence of alternative nitrogenases. In addition, the V nitrogenase may be less affected by lower temperatures [29].

Nitrogenase genes are found in a wide diversity of prokaryotes that possess equally diverse physiological capabilities [98]. The phylogeny of N_2-fixing microorganisms based on 16S rRNA was reviewed by Young [136]. However, rRNA phylogenies do not provide useful tools for identifying N_2-fixing microorganisms, since the nitrogenase genes are not distributed evenly throughout closely related taxa. For example, some species of *Klebsiella* fix N_2 while others do not. The most extensive phylogenetic analyses of diazotrophic prokaryotes are based on *nifH* genes (encoding Component II). There are now thousands of partial and full length *nifH* sequences in GenBank, largely derived by PCR amplification of DNA from environmental samples [142]. *nifH* gene phylogeny appears concordant with ribosomal RNA phylogeny [136, 142]. Several microorganisms have multiple copies of nitrogenase genes; *Azotobacter vinelandii* and *A. chroococcum* each contain conventional, alternative and second alternative nitrogenases [10, 29]. The evolution of the different nitrogenases, which require different metals, may reflect the chemical evolution of the biosphere.

There are three major clusters of *nifH* genes that encode active nitrogenases (termed Clusters I-III). The Cluster I *nifH* genes contain the cyanobacteria, most of the proteobacteria, and the *Bacillus* group of the *Firmicutes* (gram positive organisms) (Fig. 1). Cluster II contains second alternative nitrogenases, which contain Fe instead of Mo or V as a component of the cofactor of Component I (dinitrogenase) (Fig. 1).

Cluster III contains the nitrogenases found in methanogens, sulfate reducers (including delta proteobacteria and *Firmicutes*), the clostridia group of the Firmicutes, and genes from other anaerobic microorganisms such as green sulfur bacteria (*Chlorobium* spp.). The Cluster III nitrogenases are presumed to contain Mo, and protein structure studies have shown that the nitrogenase in *Clostridium* is structurally similar to Cluster I nitrogenases [53, 114]. The Cluster III nitrogenases are particularly interesting and relevant to discussions of anoxic water columns, since this cluster contains *nif* genes from anaerobic microorganisms, including sulfate reducers and Archaea. These prokaryotes may have played an important role in the evolution of N_2 fixation, and are present in modern day anoxic water columns.

The final groups of *nifH* sequences are in a deeply divergent group of sequences (termed Cluster IV, or designated Clusters IV and V in [105]). These deeply divergent groups of sequences contain genes that are not involved in N_2

fixation, including the *nif*-like genes of Archaea and the protochlorophyllide reductases.

Within the Archaeal methanogens, the nitrogenase genes are homologues of those found in Bacteria, and there are at least 6 *nif* genes (H, D, K, E, N, X) found in both the Archaea and the Eubacteria. Some Archaeal nitrogenase genes are *nif* homologs of unknown function [76]. Most of the methanogen nitrogenases are Cluster III nitrogenases, and are presumed to be Mo-containing enzymes, although vanadium-containing nitrogenases may be present in selected methanogens [76]. N_2 fixation by methanogens is regulated at the transcriptional and post-transcriptional level by ammonium; however, the mechanism of this repression appears different than regulation in Proteobacteria [76].

2.3 Regulation of Nitrogen Fixation

Nitrogenase is highly regulated at both transcriptional and post translational levels. Regulation occurs through cascades of regulatory proteins that activate transcription, and by post-translational mechanisms that inactivate nitrogenase through modification of the Fe protein. The mechanisms of regulation differ among microorganisms, and for many organisms the mechanisms are not well understood. Nitrogenase regulatory systems are generally assumed to operate analogously to model organisms such as *Klebsiella*.

Fixation of N_2 is energetically more expensive than utilization of ammonium (NH_4^+). N_2 fixation is also sensitive to oxygen (O_2). As a result, nitrogenase gene expression appears to be regulated by the presence of NH_4^+ and O_2 at transcriptional and post-translational levels in many organisms. In *Klebsiella*, oxygen presence results in binding of a protein (*nifL*) to the *nif* activator *nifA*, preventing activation of transcription [52]. The mechanism in other bacteria, such as the purple nonsulfur bacteria [89] is not as well known.

Oxygen and ammonium are two major variables in aquatic environments [55], and are particularly relevant to the study of N_2 fixation in anoxic environments since anoxic basins often accumulate relatively high concentrations of ammonium. Two important questions are: 1) what are the mechanisms that regulate N_2 fixation in aerobic waters? and 2) how and why do anaerobic microorganisms utilize nitrogenase in anoxic waters that are typically characterized by high concentrations of ammonium? The regulation of nitrogenase is a complex topic [52] and only major factors of relevance to water column N_2 fixation will be highlighted here.

Nitrogenase is rapidly inactivated by oxygen *in vitro* [126], suggesting N_2 fixation is a strictly anaerobic process [37]. The sensitivity of nitrogenase to O_2 is particularly relevant in the oceans because O_2 levels are at or above saturating concentrations throughout much of the sunlit portion of the upper oceans. As a

result, O_2 may be an important factor limiting N_2 fixation in the modern, oxic ocean.

Despite the apparent sensitivity of nitrogenase to O_2, there is substantial variability in oxygen sensitivity *in vivo* [37, 50]. A number of aerobic microorganisms, including heterotrophic bacteria and O_2 evolving cyanobacteria are capable of *in vivo* aerobic N_2 fixation. It appears that it is not oxygen itself that is toxic to nitrogenase, and that oxygen inactivation does not occur at the FeS centers [37, 126]. Thorneley and Ashby [126] demonstrated that Component II of nitrogenase actually reduces oxygen without inactivation, and is only inactivated by the products of oxygen reduction, such as superoxide or hydrogen peroxide. Thus, Component II of nitrogenase may serve as an "autoprotection" mechanism against inactivation by oxygen for nitrogenase, reducing oxygen to water, as long as the concentration of Component II exceeds the concentration of oxygen by about fourfold [126].

N_2-fixing microorganisms have evolved several ways of avoiding oxygen inactivation of nitrogenase. Aerobic heterotrophic bacteria, such as *Azotobacter,* utilize several mechanisms to help balance oxygen requirements with oxygen sensitivity. Such mechanisms include the production of polysaccharides, maintaining relatively high respiration rates and thus low oxygen concentrations, and production of the Shethna or FeSII protein that appears to provide conformational protection to nitrogenase [50]. Some facultative microorganisms only express nitrogenase under anaerobic or microaerophilic conditions, controlled by a regulatory network involving *nifL* and *nifA* [52]. Most cyanobacteria protect N_2 fixation by the oxygen-sensitive nitrogenase from oxygen evolved through photosynthesis by temporal and spatial mechanisms [6, 7].

In at least some species of nonsulfur purple bacteria, including *Rhodospirillum*, N_2 fixation is regulated in response to light, oxygen and fixed nitrogen availability. These microorganisms grow photoheterotrophically under anaerobic conditions. A reversible post-translational mechanism for regulating nitrogenase activity has been well characterized in some microorganisms involving enzymatic ADP-ribosylation of the Fe protein [107]. The modification and demodification of nitrogenase are catalyzed by specific enzymes (DRAT and DRAG) that respond to ammonium, oxygen, and light [77]. This mechanism is present in other microorganisms as well. A shift in apparent molecular weight of the Fe protein of nitrogenase (which is indicative of the ADP ribosylation) has been observed in cyanobacteria, [90, 137], but the ADP-ribosylation mechanism itself has never been demonstrated in cyanobacteria [37].

The N_2 fixation proteins and genes of strict anaerobes, such as clostridia and sulfate reducers, have been characterized to some extent, but little is known about their regulation due to the lack of model genetic systems. N_2 fixation in sulfate reducing bacteria also appears regulated similar to other microbes in response to oxygen or ammonium [99]. In present anoxic environments (sedi-

ments, microbial mats, and water columns), there are generally relatively high concentrations of ammonium, potentially obviating the need for N_2 fixation. However, N_2 fixation (or acetylene reduction) has been detected despite micromolar concentrations of porewater ammonium in salt marsh sediments [5, 97]. Despite the potential repression of nitrogenase by NH_4^+, studies of extant microbial mats indicate that many microorganisms express nitrogenase genes in anoxic regions of the mats where NH_4^+ is present. Similarly, N_2 fixation has been reported in sediments, where ammonium is usually found at high concentrations. The presence of N_2 fixation genes in microorganisms that thrive in anaerobic environments, including sulfate reducers and methanogens suggests that either anaerobic microorganisms benefit (or have benefited in the past) from N_2 fixation, or that the N_2 fixation apparatus serves (or has served in the past) another purpose.

Nitrogenase expression has been demonstrated in non sulfur purple bacteria grown photoheterotrophically in the presence of ammonium when alternate electron sinks are unavailable (the Calvin-Benson-Basham pathway or DMSO) [127]. In this case, nitrogenase acts as an electron sink under specific physiological conditions. It's unknown how widespread the use of nitrogenase as an electron sink may be in other anaerobes, but it could provide clues as to the original function of the protein. However, the conditions under which this has been demonstrated are specific to photoheterotrophic growth under anaerobic conditions.

In contrast to ammonium, the availability of nitrate does not appear to completely repress nitrogenase synthesis or activity [143]. Nitrate assimilation is energetically costly and some cyanobacteria do not appear to regulate N_2 fixation in the presence of nitrate [35]. For example, *Nodularia* appears to continue to fix N_2 even when nitrate is present, although these cyanobacteria may lack the ability to reduce nitrate [112]. Thus, under some circumstances, N_2 fixation can proceed in the presence of nitrate [61].

Nitrogen fixation is dependent upon the availability of metals (Mo or V, and Fe) for active enzyme synthesis. The availability of these metals partly depends on oxygen and pH. The expression of the conventional and alternative nitrogenases appears regulated in response to the availability of Mo and V [10]. In the modern day oxygenated ocean, Fe availability is low (typically in the picomolar to nanomolar range) due to the low solubility of the Fe (Fe^{3+}) hydroxides. Mo concentrations (in the form of MoO_4) are relatively high (typically nanomolar to micromolar range) but Mo availability has been hypothesized to limit N_2 fixation due to competitive uptake of sulfate (an analogue of molybdate) [54]. Possible limitation of N_2 fixation due to competition between Mo and sulfate uptake remains unresolved and evidence to the contrary has been provided [96].

How the availability of fixed inorganic nitrogen, other nutrients, trace metals and concentration of oxygen interact to regulate N_2 fixation in an ecosystem context is beyond the scope of this review, and elaborately covered by others [38, 49, 55, 61, 94, 131]. One critical factor to consider is the interaction between Fe and phosphorus [111]; the nitrogenase requirement for Fe has been suggested to control phosphorus availability [73, 134]. Often the N:P ratio, rather than the concentration of N or P individually, is believed to control N_2 fixation [48]. Temperature can determine the distribution of individual diazotrophic species and has been hypothesized to explain the lack of heterocystous species in the tropical and subtropical ocean [119].

The ecosystem regulation of N_2 fixation has been studied in aerobic water columns overlying anoxic basins, but not within anoxic water columns themselves. Anoxic basins can promote the solubilization of metals, but can also promote precipitation, depending upon chemical composition and salinity. Anoxic conditions can also promote P dissolution and solubilization, which can stimulate N_2 fixation by decreasing the N:P ratio. Thus, there are complex ways that anoxia interact with the availability of nutrients and metals needed for N_2 fixation.

3. EVOLUTION OF NITROGENASE

The Earth's atmosphere has always been dominated by N_2 [39]. However, ammonium may have been present in the early Earth's atmosphere, and this has been argued to preclude the need for N_2 fixation [128]. Nonetheless, nitrogenase, or some form of pre-nitrogenase genes, could have initially served a function other than for N_2 fixation (Fig. 2). In addition to cleaving the triple N_2 bond, nitrogenase also reduces cyanide. This capability could have been particularly advantageous during periods in the Earth's history when methane was prevalent in the Earth's atmosphere and cyanide was formed through photooxidation of methane [62]. However, cyanide can be assimilated by other pathways and can be used directly as a source of nitrogen. Nonetheless, it is conceivable that nitrogenase may have initially served as detoxyases and later used for making atmospheric N_2 biologically available [34, 62, 105].

Ammonium in the early Archean could have been rapidly depleted by the evolution of living organisms [104]. The composition of the atmosphere was changing throughout the Archean. The high atmospheric concentrations of CO_2 and CH_4 declined, and coincident with these changes rates of abiotic (photochemical and catalyzed by lightning) production of reduced nitrogen compounds probably decreased [62, 83] (Fig. 2). In addition, autotrophic life forms evolved that would have depleted the fixed nitrogen reserves [104].

The oceans are believed to have been anoxic, even subsequent to the development of oxygenic photosynthesis [1, 19, 100]. Thus, N_2 fixation likely

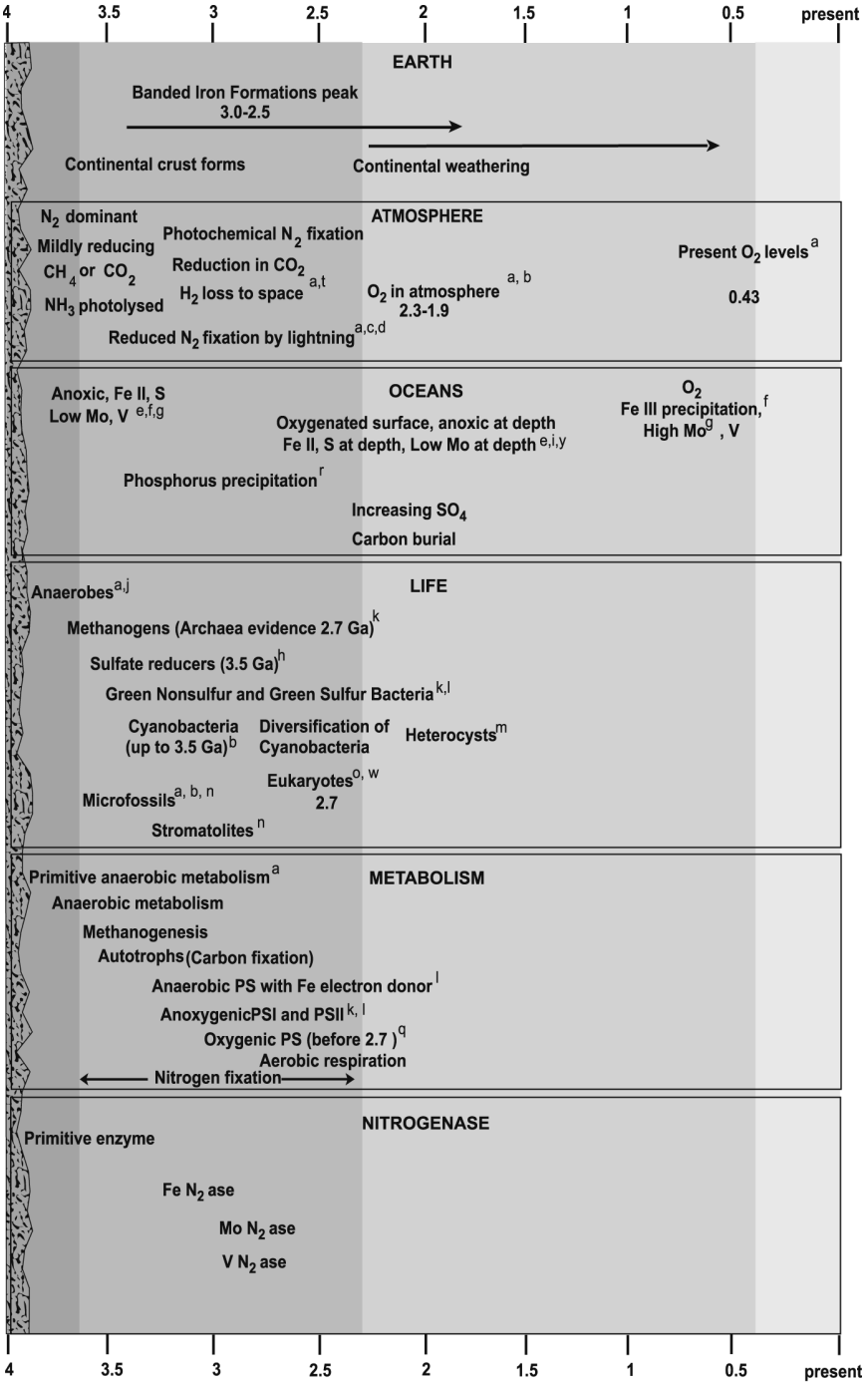

Figure 2. Major events in the evolution of the Earth, the atmosphere, oceans and life. Meteor bombardment ends by 3.8 Ga, allowing planet to become habitable. [a][113], [b][115], [c][83], [d][62], [e][1], [f][7]. [g][110]. [h][116], [i][19], [j][30]. [k][87,88]. [l][46], [m][41], [n][4],[o][125], [p][68], [q][14], [r][11], [s][63], [t][51], [u][104], [v][120], [w][16] [x][105], [y][100], [z][2].

evolved during periods when the oceans were anoxic, reducing, and rich in ferrous Fe (Fe^{2+}) [104]. The early ocean probably had high concentrations of Fe^{2+}, but low concentrations of sulfate and sulfide [110]. Although the high concentrations of Fe^{2+} may have removed some of this sulfide by precipitation, chemical models suggest that relatively high concentrations of sulfide remained [110]. Fe and S, required for nitrogenase, were probably present in the Archean ocean. Extant anoxic basins have high sulfate which differs from these early Earth scenarios [110]. However, the availability of Mo and V in the Archean oceans may have been low, due to the precipitation of MoO_4 and VO_4 with sulfides or FeS [7]. Once the surface oceans became oxic these metals might have become more biologically available [7, 105], and could have selected for the Mo and V nitrogenases.

It is difficult to accurately model the chemistry of the early oceans since we know so little about the ionic composition at that time in Earth's history. The early ocean may have even been much more saline [67], which would make the modern anoxic basins good analogues for the early Earth (except for the presence of sulfate). During the Proterozoic, the surface oceans appear to have become oxic, while the deep ocean remained anoxic, mildly reducing, and relatively Fe^{2+}-rich. Sediment records indicate that sulfate reduction became an increasingly important process during the Proterozoic [116]. The subsequent oxidation of sulfide to sulfate would have titered any atmospheric oxygen that was formed by oxygenic photosynthesis. This may be part of the explanation for the lag between the evolution of oxygenic photosynthesis and the oxygenation of the atmosphere (Fig. 2). Contemporary anoxic basins where sulfate reduction plays a central role in anaerobic metabolism are likely analogous to the microbiology of the deep oceans during this period. Intriguingly, numerous sulfate reducers have N_2 fixation genes, suggesting that sulfate reducers could have been involved in early N_2 fixation.

There is a large degree of uncertainty regarding when life evolved. Earth became habitable around 3.8 Ga after the frequent meteor bombardments ended, and evidence of life in the form of microfossils has been reported from 3.5 Ga rocks [69, 115]. Considerable controversy surrounds the interpretation of these fossils, ranging from chemical artifacts [12], to evidence for early microbes, including cyanobacteria. The first microbes probably predated these 3.5 Ga microfossils, with prokaryotic life likely arising approximately 3.8 Ga [88].

The first microbes are thought to have been anaerobic chemoheterotrophs [30, 88] with methanogenesis, a process catalyzed by the Archaeal methanogens, likely the earliest metabolic process [63, 84]. Various taxa of methanogens contain nitrogenase genes [76]. Similarly, sulfate reducers likely evolved prior to 3.5 Gya [20, 116], and the nitrogenase of sulfate reducing Proteobacteria as well as some Archaea, fall within the deeply branching Cluster III *nif* sequences.

This cluster contains nitrogenases from strict anaerobes, and may represent the earliest form of nitrogenase. Nitrogenase genes in Cluster III are found in modern anoxic environments [142].

The nitrogenases of cyanobacteria form a cluster of deeply branching lineages not unlike ribosomal RNA cyanobacterial phylogeny [40, 133, 139]. Heterocyst-forming cyanobacteria (heterocysts are specialized cells that do not evolve oxygen and are the site of N_2 fixation in some filamentous species) form tight phylogenetic clusters in both *nifH* and rRNA trees, and appear to have evolved late in the evolution of cyanobacteria [40, 139]. Akinetes of heterocystous cyanobacteria have been reported in microfossils dating to as recently as 1.5 Ga [41]. However, the concentration of oxygen in Earth's atmosphere between 2-0.5 Ga was only a fraction of the present atmospheric level. Thus, the heterocyst evolved prior to severe oxygen stress in the oceans, except perhaps in shallow embayments, where the local concentration of oxygen could have been high due to blooms of cyanobacteria. Blooms of heterocyst-forming cyanobacteria still occur in embayments and estuaries such as the Baltic Sea and Lake Alexandrina in Australia. In the modern world, microenvironments play pivotal roles in shaping ecosystem diversity and function; similar microhabitats undoubtedly were important in the evolution and diversification of early life on the Earth.

There would have been strong selection for carbon fixation early in the evolution of life, since organic molecules would have quickly been consumed by heterotrophic microorganisms. Autotrophic carbon-fixing microbes were likely present by 3.8 Ga [108] and the evolution of CO_2 fixation may have partially been responsible for depleting ammonia on the early Earth [104, 118]. The first phototrophic autotrophs were probably phototrophic bacteria that used Fe for electron donors [46, 88]. Chlorophyllide reductases, used in the synthesis of bacteriochlorophyll, have a high degree of similarity in protein structure and gene sequence to nitrogenase, and probably evolved from the nitrogenase genes [18, 105]. Thus, N_2 fixation may have predated anoxygenic photosynthesis. Oxygenic photosynthesis evolved more recently, followed by aerobic respiration. Cyanobacteria appeared between 3.8 Ga [115] and 2.7 Ga [14, 115, 125], but evolved and diversified relatively quickly [40, 74]. Oxygenic photosynthesis and the diversification of cyanobacteria must have evolved between 3.5 Ga (if the microfossils are indeed of cyanobacterial origin, and if cyanobacteria had evolved oxygenic photosynthesis by that time) and 2 Ga, when the atmosphere became oxygenated (based on the presence of red beds formed by precipitation of iron). Oxygenic photosynthesis would have predated the accumulation of oxygen in the atmosphere since oxygen produced would have had to titer the reduced Fe and sulfide in the oceans before accumulating in the atmosphere. Atmospheric oxygen concentrations that would have selected

for heterocysts could only have occurred in localized environments under these conditions.

Nitrogenase genes are widely distributed throughout the prokaryotic kingdom, but are not uniformly distributed across closely related taxa. Since the genes are so highly conserved (very similar in DNA and amino acid sequence in very different microorganisms), it has been argued that nitrogenase genes either evolved early, or were laterally (horizontally) transferred later after most of the major lineages had diverged [99, 136]. Most phylogenetic analyses, including those based on recent analyses of large datasets conclude that the nitrogenase genes evolved early, prior to the separation of the Archaea from the Bacteria [34, 76, 105, 136, 138]. Gene duplications and lateral gene transfer must also have been involved in order to explain the distribution of the different nitrogenase gene families [105]. Regardless of how early nitrogenase evolved, the genes must have evolved when at least the deep oceans were anoxic (Fig. 2).

Although it is difficult to speculate about the early evolution of metabolic pathways [84], the sequence of events that shaped the Earth's chemistry and led to nitrogen limitation of productivity in the oceans paralleled the evolution of N_2 fixation, autotrophy and photosynthesis. Nitrogenase had to have evolved early [105] prior to the diversification of the cyanobacteria, and prior to the oxygenation of the atmosphere. The first nitrogenase protein may have been the Fe nitrogenase, which could have evolved in a Fe rich ocean, that had low concentrations of Mo and V [105]. The Mo and V enzymes would then have evolved from duplication of the Fe nitrogenase more recently, perhaps after oxidation of the surface ocean, or when localized oxidized environments allowed MoO_4 and VO_4 to remain in solution. Since the formation of these oxidized environments presumably followed the diversification of life and evolution of oxygenic photosynthesis, the Mo and V nitrogenases would have had to have been horizontally transferred in order to give rise to the current distribution of the Mo and V enzymes throughout the prokaryotic tree [105]. Alternatively, the Mo and V nitrogenases could have evolved near hydrothermal vents, where metal concentrations might have been high enough to select for these metalloenzymes.

The fixation of N_2 in anoxic water columns is likely to be important in the evolution of life on earth, as well as in the modern day ocean basins. The nitrogenase enzymes and N_2 fixation have undoubtedly been shaped by the conditions of the early oceans, including anoxia. Coincident with changes in oxygen concentrations were changes in metal and ion chemistry of importance to N_2 fixation.

4. DIVERSITY OF AEROBIC AND ANAEROBIC N_2-FIXING MICROORGANISMS

Although N_2 fixation is a property found only in prokaryotes, the phylogenetic and physiological diversity of N_2-fixing microorganisms spans most of the prokaryotic kingdom [136]. N_2 fixation is found in a wide diversity of anaerobic, aerobic, and facultative microorganisms, with equally diverse physiological strategies including anoxygenic and oxygenic phototrophy, photoheterotrophy, chemoheterotrophy, and chemolithotrophy. Archaea and Eubacteria contain diazotrophic representatives, and within the Eubacteria various members of the proteobacteria (alpha, beta, gamma and delta), cyanobacteria, clostridia, green and purple sulfur bacteria all appear to have the genetic potential for N_2 fixation. There are selected phylogenetic groups within the Eubacteria and Archaea that do not contain N_2-fixing representatives, including *Planctomyces* and *Flavobacter*, but this may reflect a lack of information on the genomic diversity of these groups rather than evolutionary patterns. Relatively few N_2-fixing microorganisms have yet been targeted by genome sequencing projects, and our knowledge of most of the prokaryote N_2 fixers remains quite poor.

Characterizing the diversity of N_2 fixing microorganisms in marine environments continues to be hampered by the difficulties of cultivating microorganisms from oligotrophic environments. Many isolates have been obtained from organic matter-rich environments, such as salt marshes and sediments [5]. Diazotrophic microorganisms were plated from the oligotrophic oceans in early studies that predate characterizations of microbes by rRNA sequence analysis [64]. Efforts to cultivate diazotrophs from oceanic environments is an area ripe for progress in future studies, as new high throughput cultivation techniques have recently been developed [58, 103]. Here we review some of the diversity of cultivated microorganisms that fix N_2, in order to provide context for the observed physiological diversity in marine diazotrophic communities.

The American Type Culture Collection contains over 650 bacterial isolates from the marine environment. Genera that are included in this collection that could be diazotrophic are *Vibrio*, *Bacillus*, *Alcaligenes*, *Rhodopseudomonas*, *Clostridium*, *Spirochaeta*, *Methanococcus*, *Desulfobacter* and *Desulfonema*. Paerl and Zehr [95] provide a list of marine cultivated microorganisms that are available from culture collections. Various microorganisms have been cultivated from salt marshes such as vibrios, rhizobia, spirilli and pseudomonads [5]. Many of these organisms are facultative or obligate anaerobes and are typically found at oxic/anoxic interfaces and could also be present in anoxic water columns. These collections would serve as important sources of microorganisms in investigations of diversity and activity of N_2 fixing microorganisms in anoxic marine environments.

4.1 Heterotrophs

In the oxygenated oceans, diazotrophic bacteria are likely to be largely aerobic, utilizing either photoautotrophic or aerobic heterotrophic metabolism. Representatives of diverse aerobic proteobacteria lineages fix N_2; however, even within N_2-fixing genera, not all species appear capable of diazotrophy [136]. For example, the genera *Vibrio* and *Klebsiella* contain many species that do not appear to be able to fix N_2.

Azotobacter species are obligate aerobic diazotrophic chemoheterotrophs that fix N_2. They have been isolated from salt marshes or sediments [27]. Other known aerobic chemoheterotrophs include *Rhizobia, Bradyrhizobia* and *Beijerinckia*, but they have not been isolated from the marine environment. Aerobic bacteria of a wide variety of morphologies (rods, cocci) have been isolated from seawater samples, but acetylene reduction by yeasts cultivated by these methods were also reported [135]. Part of the problem of isolating N_2-fixing microorganisms is the contamination of media reagents with trace nitrogen compounds that can serve as nitrogen sources for oligotrophs. Kawai and Sugahara [64] isolated aerobic N_2 fixing microorganisms from seawater and sediments. These authors reported abundances much lower than total heterotrophs, but again, due to the problems of removing trace nitrogen compounds, it is not clear whether they enumerated oligotrophs or N_2-fixers. Martinez et al. [78] described N_2-fixing bacteria in association with free-floating mats of diatoms. These bacteria are probably aerobes, since the mats are in aerobic waters, but could be facultatively anaerobic. Anaerobic microzones can occur in aggregates in aerobic water columns [93].

Methane oxidizers and methylotrophs are obligate aerobes that include a variety of diazotrophs. A number of methanotrophs including *Methylocystis* sp., *Methylosinus* sp., and *Methylobacter* sp. contain *nif* genes and are capable of N_2 fixation [3]. The methane oxidizers may be important in aquatic systems, particularly at oxic/anoxic interfaces.

Representatives of diazotrophs are found among all groups of proteobacteria, the green and purple sulfur bacteria, purple nonsulfur bacteria, methanogens, sulfate reducers and clostridia. The anaerobic and microaerophilic diazotrophs include members of both the Archaea and Eubacteria. Diverse physiological capabilities characterize anaerobic N_2 fixers, with organisms deriving energy from both phototrophy and chemotrophy. A suite of electron acceptors can be utilized for anaerobic respiration including nitrate (denitrifiers such as *Bradyrhizobium*), sulfate (sulfate reducers such as *Desulfovibrio*), CO_2 (methanogens such as *Methanosarcina*), Mn (manganese reducers such as *Arthrobacter*), Fe (iron reducers such as *Geobacter*), and organics (fermentation such as *Klebsiella*). Facultative diazotrophs include the photoheterotrophic purple bacteria. *Rhodospirillum* and *Rhodobacter* are aerobic heterotrophs which can grow

photoheterotropically in the light under anoxic conditions. Spirochaetes are commonly found in marine environments and are obligately anaerobic or facultatively anaerobic.

The recently characterized oceanic aerobic anoxygenic photosynthetic bacteria (*Roseobacter* and *Erythrobacter*) have not yet been shown to be N_2 fixers, although it seems likely that some representatives of this group may be diazotrophic.

Most of the sulfate reducers (mostly delta proteobacteria) appear to fix N_2, as do many of the purple sulfur (mostly gamma proteobacteria) bacteria [136]. Numerous genera of green and purple sulfur bacteria fix N_2, and both of these groups are often found at the interface between oxic and anoxic layers in the water column, as well as in microbial mats [120].

The observation that members of Archaea contain *nif* genes and can fix N_2 provides additional evidence that nitrogenases likely evolved early in prokaryote evolution. Among the anaerobic Archaea, N_2 fixation has been observed in three orders of methanogenic *Euryarchaeota*: *Methanococcales*, *Methanomicrobiales* and *Methanobacteriales* [76]. To date, none of the *Crenarchaeota* that have been genetically characterized appear to have the capacity for N_2 fixation [76].

4.2 Phototrophs

The cyanobacteria include five major different morphologies that have formed the basis of cyanobacterial taxonomy [106]. Diverse cyanobacteria are N_2 fixers including representatives of all five morphological groups [129]. Many of these have been isolated from marine environments, although most have been isolated from benthic environments rather than pelagic habitats.

Cyanobacterial blooms in lakes and estuaries are often composed of filamentous heterocystous diazotrophs. The blooms of *Nodularia* are well known in the Baltic Sea and around the world. Heterocystous free-living cyanobacteria, although not abundant, have been observed in the open ocean as well [22]. One of the most abundant heterocystous species in the open ocean is the cyanobacterial symbiont *Richelia*, which forms a symbiotic association with the diatom *Rhizosolenia*. There are other similar symbioses observed between marine diatoms and heterocystous cyanobacteria, although the taxonomic and phylogenetic relationship of this filamentous group is not yet known.

Filamentous nonheterocystous cyanobacterial species are found in many marine microbial mats and in the open ocean. *Trichodesmium* is one of the most abundant diazotrophs in oligotrophic subtropical and tropical waters. Other nonheterocystous species have been observed, usually in association with *Trichodesmium* aggregates [117]. Diverse unicellular cyanobacteria also fix N_2, including representatives of the genera *Synechocystis*, and *Cyanothece*.

N_2 fixing unicellular cyanobacteria play important roles in the ecology and biogeochemistry of diverse environments ranging from microbial mats to the open ocean.

4.3 Chemolithotrophs

A variety of chemolithotrophic bacteria have the ability to fix N_2. These include the Fe oxidizers, such as *Thiobacillus*. Some species of the sulfur oxidizing *Beggiatoa* are also diazotrophic. These microorganisms oxidize sulfide to elemental sulfur aerobically for energy, and are found at interfaces between sulfidic and oxic zones. The availability of reduced compounds in anoxic water columns supports a variety of chemolithotrophic metabolisms. Anoxic environments support diverse chemolithotrophic bacteria, and it seems likely that members of these anaerobic prokaryote assemblages might fix N_2.

5. MARINE N_2-FIXATION

Nitrogen fixation in the oceans occurs in the water column and the benthos. Highest rates of N_2 fixation are typically found in intertidal and shallow water cyanobacterial mats, and in salt marshes [49]. N_2 fixation in sediments occurs at low rates, presumably because of the high ammonium concentrations, analogous to anoxic water columns. Cyanobacteria are important in N_2 fixation in both the water column and in microbial mats. Heterocystous species (such as the symbiont of diatoms, *Richelia*) and unicellular species (e.g. the recently reported *Crocosphaera*, [141]) play a role in N_2 fixation in the open ocean. Blooms of free-living planktonic heterocystous species are found in certain coastal and estuarine waters.

5.1 N_2 Fixation in Surface Oceans

The surface waters of large regions of the world's oceans have vanishingly low concentrations of bioavailable-fixed inorganic nitrogen (NO_3^-, NO_2^-, NH_4^+). Nitrate + nitrite (NO_3 + NO_2) concentrations in the surface waters of oligotrophic ocean ecosystems are typically 10-100 nmol L^{-1}, and NH_4^+ concentrations range 10-50 nmol L^{-1}. Rapid recycling of nitrogen in the upper ocean appears to support > 90% of measured primary production in large areas of the world's oceans. Inputs of allochthonous nitrogen to the upper ocean are restricted to 1) diffusive fluxes across the thermocline, 2) convective overturn and mixing of nitrogen from depth, 3) advection from frontal regions, mesoscale eddies, and other hydrodynamic processes, 4) atmospheric deposition, and 5) biologically-mediated N_2 fixation. Losses of fixed nitrogen from the upper ocean include assimilation and export by plankton (including sedimentation), and denitrification. The contributions of these various sources and sinks of fixed nitrogen are variable in both time and space; however, the balance among

these processes ultimately constrains plankton productivity and fixed nitrogen availability in the upper ocean.

Recent increases in anthropogenic CO_2 emissions have stimulated interest in the role of the oceans in modulating global climate. As a result, there has been considerable interest in quantifying the processes that limit N_2 fixation and the role of N_2 fixing microorganisms on biogeochemical fluxes and inventories in the oceans. Initial studies suggested that N_2 fixation supplied little fixed nitrogen to plankton assemblages in the oceans, and that the oceans were inhabited by relatively few species of diazotrophs. However, numerous lines of evidence now suggest that in large regions of the open ocean, N_2 fixation plays a central role in modifying elemental cycling in the sea, and might even play a prominent role in regulating global climate [33, 43, 60, 79].

The most prominent oceanic diazotrophs are species of the non heterocystous, filamentous cyanobacteria genus *Trichodesmium*. Filaments of *Trichodesmium* often grow to be several millimeters in length, making them easily identifiable, even from space, as the filaments accumulate to surface blooms. As a result, estimates of oceanic N_2 fixation have relied heavily on rates of N_2 fixation by colonies of *Trichodesmium*. Extrapolation of measured N_2 fixation rates to ocean basin scales suggests *Trichodesmium* may be responsible for ~20-100 μmol N m^{-2} d^{-1} [21, 60, 82]. These rates are comparable to diffusive NO_3 fluxes to the upper ocean in subtropical and tropical ocean ecosystems. However, analysis of *nifH* genes in oceanic plankton has indicated there may be a much greater diversity of diazotrophic plankton than previously suspected. A number of studies have identified uncultivated cyanobacterial, proteobacterial, and Cluster III *nifH* genes from plankton samples in the North Pacific and North Atlantic oceans [13, 32]. Nitrogenase genes of unicellular cyanobacteria were found [140], that have also been found elsewhere in the oceans [32]. *NifH* mRNA of unicellular cyanobacteria have also been detected [141]. These unicellular cyanobacteria appear to actively fix N_2 at rates comparable to filamentous cyanobacteria based on ^{15}N tracer studies (ranging ~2-500 μmol N m^{-2} d^{-1}) [82].

Recent direct measurements of N_2 fixation support geochemical determinations of oceanic N_2 fixation. Depth profiles of the elemental stoichiometry of NO_3^- and PO_4^{3-} have been utilized to quantify excess NO_3^- relative to PO_4^{3-}, referred to as the N* anomaly [26, 43, 79]. Depletions of upper ocean CO_2 inventories in the absence of NO_3^- in both the Atlantic and Pacific may be supported by N_2 fixation, and can be used to quantify the amount of nitrogen required to support CO_2 uptake in the upper ocean. In addition, measurements of the isotopic signatures (^{15}N) of particles exported from the upper ocean combined with long-term analyses of nutrient stoichiometry all suggest N_2 fixation plays an important role in supporting plankton production and carbon export in the oceans [28, 60]. The use of these approaches to quantify N_2 fixation suggest

diazotrophs supply 48-530 μmol N m^{-2} d^{-1} to the upper ocean of the Atlantic [43, 45, 79] and 93-137 μmol N m^{-2} d^{-1} to the Pacific [26, 59, 75].

5.2 N_2 Fixation in the Baltic Sea

The Baltic Sea is an estuarine environment that has anoxic basins in restricted areas. The natural water column stratification in the Baltic Sea includes thermal stratification in the summer at ca. 10-20 m depth, and permanent salinity stratification, a halocline, that both separate the upper water masses from the deeper (> ~60-80 m) more saline waters. During periods of several years up to decades when the input of ocean water is limited, the water beneath the halocline can become hypoxic or anoxic. This occurs as a result of oxygen consumed by organic matter decomposition in the deep waters [36]. The topography of the Baltic Sea basin defines the areas that become anoxic. The most permanent anoxic areas include a few deep basins, including Gotland and Landsort Deeps.

Widespread N_2-fixing cyanobacterial blooms, dominated by the genera *Nodularia*, *Aphanizomenon*, and *Anabaena,* are an annual occurrence. N_2-fixing cyanobacterial blooms dominated by *Nodularia* spp. and *Aphanizomenon* sp. typically follow the approximate boundaries of the halocline. N_2 fixers in the Baltic Sea may also include unicellular species [132]. Sediment pigment records indicate that cyanobacterial blooms have been present in the Baltic Sea throughout the past 8000 years [9]. The size of the blooms vary from year to year, and although some evidence suggests blooms have intensified during the past decades fueled by anthropogenic eutrophication [31], their periodic occurrence appears to form a natural component of this ecosystem.

Cyanobacterial blooms in the Baltic Sea can benefit from or be dependent upon sources of nutrients and trace elements in anoxic layers. The main connection between presence of anoxic bottom layers and cyanobacterial surface bloom intensities in the Baltic Sea lies in the supply of bioavailable P and low N:P ratio water from anoxic layers to the euphotic zone. In the late summer, primary productivity in the open Baltic Sea is primarily N-limited, although P is often the secondary limiting nutrient for productivity [42, 66]. This situation leads to a competitive advantage for the N_2-fixing cyanobacteria. In contrast to the overall phytoplankton productivity which is N- or N+P limited, the growth of cyanobacteria and their rate of N_2 fixation most often appear P-limited [81].

In oxygenated Baltic Sea water, P has a tendency to precipitate with ferric hydroxides, while in the absence of oxygen, P is solubilized and released from sediments as phosphate [23, 85]. Certain upwelling and frontal zones that act by introducing PO_4^{3-} from the deep water to the euphotic zone, such as the entrance to the Gulf of Finland, serve as seed areas for cyanobacterial

blooms [70, 86]. In addition, euphotic zone wintertime P concentrations may be important proxies for predicting the intensity of the forthcoming cyanobacterial blooms that occur in the subsequent summer [65].

In Baltic Sea deep waters, another microbially mediated process, denitrification, counteracts the inputs of new nitrogen from N_2 fixation by removing dissolved inorganic nitrogen from the system [72], thus enhancing N limitation and potentially favoring N_2 fixation. Due to the processes of PO_4^{3-} release and denitrification, Baltic Sea bottom waters typically have a low N:P ratio, suggested to favor N_2-fixing cyanobacterial blooms [86].

6. N_2-FIXATION IN ANOXIC ENVIRONMENTS

Nitrogen fixation has received little attention in most anoxic basins. Many, if not most, anoxic environments have high concentrations of NH_4^+ due to decomposition of organic matter and lack of photosynthetic uptake. Furthermore, N_2 fixation enzymes require metals, Fe and Mo, whose availability are affected by redox chemistry.

There are few reports of attempts to measure N_2 fixation in anoxic water columns, presumably either because it is assumed not to be an important process or because of lack of positive results with N_2 fixation assays. Although N_2 fixation has not been measured in many anoxic water columns, there are analogous habitats that have been studied. These include sediments, microbial mats and salt marsh rhizospheres. The same gradients in oxygen, nutrients and metals that are present in anoxic water columns are found in these habitats, but over smaller vertical length scales.

6.1 Microbial Mats and Salt Marshes

Microbial mats are believed to have been important in the evolution of life on Earth. Remnants of mats, in the form of stromatolites, are some of our earliest records of life [25]. Early microbial communities were probably important in the exchange and cycling of materials between microbes, including genetic information. Modern day mats mimic these early communities, and often contain layers of cyanobacteria that are important in carbon fixation as well as N_2 fixation. The hydrogen produced by N_2-fixing cyanobacteria in ancient mats has been speculated to have resulted in hydrogen loss to space, facilitating oxygenation of the Earth's atmosphere [51]. Oxygen availability within the mats closely follows the diurnal cycle in photosynthesis and light, and anoxic environments are frequently found in mats [121]. Once photosynthesis ceases, microaerophilic or anaerobic N_2 fixation can occur. The deeper layers of mats are typically anoxic and dominated by sulfate reducing microorganisms as well as other anaerobes, many of which contain nitrogenase genes. Expression of nitrogenase by these anaerobic organisms (Cluster III nitrogenases) has been

detected by molecular techniques in extant microbial mats [91, 122]. It is not clear why these organisms fix N_2 in environments where concentrations of ammonium can be high, but the chemical conditions and microbial survival strategies are likely to be similar to those found in anoxic basins.

Nitrogen fixation has been studied extensively in salt marshes [49]. Sulfate reducing bacteria have been implicated in N_2 fixation in a number of studies [49]. Sulfate reducing bacteria and potentially other anaerobes have been shown to express nitrogenase genes in salt marsh sediments [15]. The high sulfate concentrations and anoxia are likely to be similar to anoxic water columns, suggesting that similar activities may be present in anoxic water columns as well.

6.2 Anoxic Water Columns

Anoxic basins can be extremely productive regions due to the interface between anoxic and oxic regions, and associated juxtaposition of nutrients, trace metals and microbial processes (Fig. 3). Examples of anoxic basins in extant oceans include the Black Sea and the Cariaco Trench. High ammonia concentrations in anoxic water columns in places such as the Black Sea [71], certain Northern European fjords [101, 130], and the Baltic Sea [44] suggest N_2 fixation to be unlikely; however, the presence of N_2-fixers and rates of N_2 fixation have not been intensively studied in these systems. Delta proteobacteria related to sulfate reducers, many of which are known to be N_2 fixers, were reported at high abundances in anoxic and microaerophilic water columns in a Danish fjord [101].

Nitrogen fixation varies extensively in time and space in these basins with rates varying from the undetected to high rates associated with cyanobacterial blooms. There is also considerable seasonal, annual and decadal variability in N_2 fixation in these waters. N_2 fixation is controlled by the availability of nutrients, and is selected for by the availability of nutrients relative to the stoichiometric requirements for life. In waters overlying anoxic layers, the availability of trace metals (Fe, V, Mo) can be affected by the chemistry of the oxic and anoxic waters, and the availability of other nutrients (P). Anoxic layers may control surface water cyanobacterial N_2 fixation by its effect on the N:P ratio in the nutrient supply [47].

The Mediterranean Sea has low concentrations of nutrients, but N_2 fixation has not been extensively studied. Cyanobacterial N_2 fixation is occasionally present in the Mediterranean surface waters but is believed to be of minor importance [8]. However, sediment stable isotopic record from the eastern Mediterranean Sea suggests widespread N_2 fixation has been present in the water column of the basin during anoxic deep water events that have reoccurred over geological time scales [109, 124]. Records in these organic carbon rich

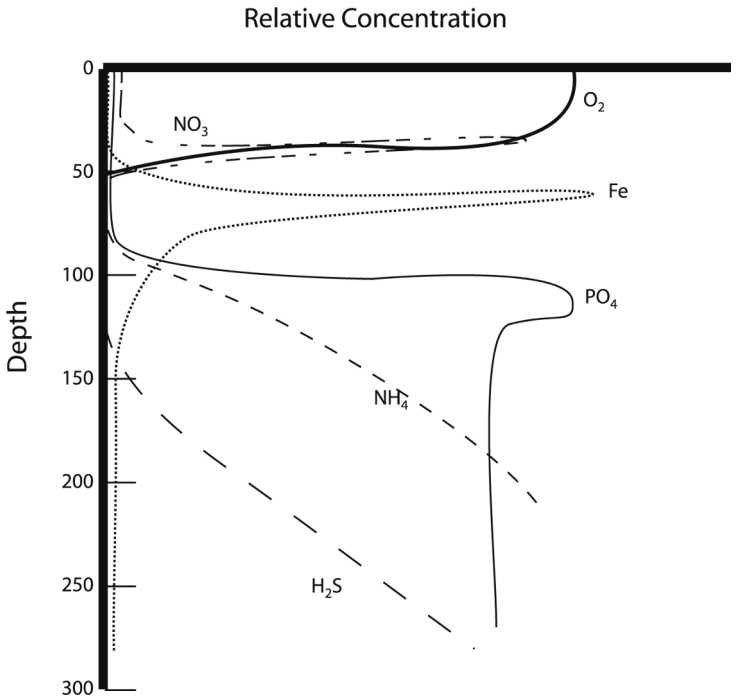

Figure 3. Typical depth profile of water chemistry of the Black Sea, from data collected at different times and stations, based on Millero [80]. Profiles indicated vary with depth depending upon the sampling location. The profile shows typical distributions of water chemistry parameters important for N_2 fixation.

sediment deposits, sapropels, also indicate that blooms of rhizosolenid diatoms that can harbor endosymbiotic N_2-fixing cyanobacteria have co-occurred with the anoxic periods [109]. Endosymbiotic diazotrophs could be an important source of new nitrogen into the Mediterranean Sea [24].

6.3 Mono Lake

Mono Lake is a hypersaline alkaline lake that may mimic life on early Earth. For many years, Mono Lake was meromictic (Fig. 4), with an oxycline that was within the photic zone and a chemocline that was below the photic zone. Productivity in the lake is believed to be nitrogen limited, but below the oxycline there are high concentrations of ammonia/ammonium [56].

Diverse N_2-fixing microorganisms are found throughout the oxic and anoxic portions of the Mono Lake's water column [123]. *NifH* genes found in Mono Lake include a relatively high abundance of genes grouping with Cluster III *nifH* genes, including many anaerobes (Fig. 1). Many *nif* genes that clustered with genes from sulfate reducers, clostridia, and green sulfur bacteria were

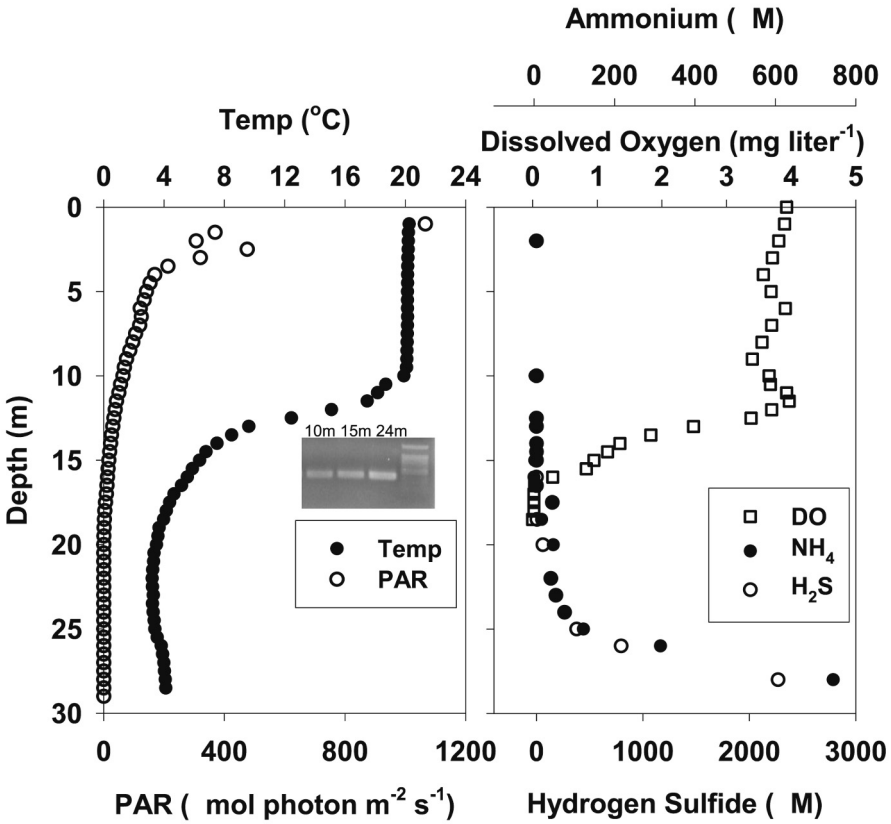

Figure 4. Depth profile of water chemistry of hypersaline Mono Lake during meromixis in August, 2001. Agarose gel shows amplification products of reverse-transcriptase polymerase chain reaction (RT-PCR) of *nifH* from 10, 15, and 24 m depths. Amplification by RT-PCR indicates that nitrogenase is being expressed in the anoxic water column.

detected in the anaerobic portion of the Mono Lake water column. *NifH* gene expression has been detected in the anoxic water column (Fig. 4). However, despite presence of diverse *nifH* genes and evidence supporting *nifH* expression in the system, attempts to measure N_2 fixation with ^{15}N in the Mono Lake water column have been unsuccessful [123]. N_2 fixation in this ecosystem is not likely to be constrained by the availability of trace elements, since it occurs in algal aggregates in the littoral region of the lake [92]. It is somewhat surprising that N_2 fixation has not been detected in the water column, even though primary production in this system is believed to be nitrogen limited [57]. However, there

is a substantial supply of ammonium to the photic zone from the anoxic deeper waters.

It appears that N_2 fixation may occur in anoxic zones even if fixed nitrogen is present, although at low rates. It is possible that that this low level of N_2 fixation is performed by a small group of microorganisms or is somehow involved in minor redox reactions as an electron sink. N_2 fixation could occur in anoxic water columns for similar reasons.

7. CONCLUDING REMARKS

The importance of N_2 fixation in providing fixed nitrogen for the world's oceans is now clear, but the process is not well-understood: previously unrecognized diazotrophs are still being discovered, and how the availability of nutrients and trace metals control N_2 fixation and primary productivity is still largely unknown.

N_2 fixation evolved under anoxic conditions, although the evolution of N_2 fixation and the underlying genes is speculative and poorly understood. Anoxic marine environments represent conditions where evolutionarily ancient biogeochemical processes and microbial communities are found. Since nitrogenase evolved under anoxic conditions, it may also be expressed in anoxic water columns. There simply is too little data on the presence and expression of nitrogenase genes in anoxic water columns to know how important of a process it is. It may, for example, play a role in localized regions at the interface between oxic and anoxic regions.

Given the concentrations of fixed inorganic nitrogen in the form of ammonium and organic nitrogen in extant anoxic water columns, it seems unlikely that N_2 fixation plays an important role in the N budget except in aerobic waters overlying anoxic water columns. However, in the anoxic or microaerobic environments examined so far, including microbial mats, sediments, estuaries and Mono Lake, there is a high diversity of N_2-fixing microorganisms [142]. In Mono Lake, at least a few of these microorganisms are expressing the nitrogenase genes. This raises intriguing questions: What is the role of N_2 fixation in anoxic environments? Does nitrogenase serve another function for microorganisms in these environments? Why is the diversity of nitrogenase-containing microorganisms so high in these environments? What are the selection forces and why do these microorganisms still retain the nitrogenase genes in their genomes?

It is clear that N_2 fixation is important in the aerobic open ocean, and in oxygenated waters of many anoxic basins such as the Baltic Sea. However, more research is needed to determine if N_2 fixation occurs within the anoxic water column. It is an intriguing question because of the parallel with the anoxic

oceans of the early Earth, but also to understand the factors that determine the distribution of microorganisms, genes and genomes in the modern world.

Acknowledgements

We thank Janet Siefert and James Kasting for helpful suggestions, and Sandra Roll and Bob Jellison for Mono Lake data. Bethany Jenkins, Cynthia Short and Grieg Steward contributed to the Mono Lake study. This work was supported by grants from NASA Exobiology and the NSF (MCB-9977892, OCE-9977460, OCE-9981437).

References

[1] Anbar A. D. and Knoll A. H. Proterozoic ocean chemistry and evolution: A bioinorganic bridge? Science 2002; 297:1137-42.

[2] Arnold G. L., Anbar A. D., Barling J. and Lyons T. W. Molybdenum isotope evidence for widespread anoxia in mid-proterozoic oceans. Science 2004; 304:87-90.

[3] Auman A. J., Speake C. C. and Lidstrom M. E. *nifH* sequences and nitrogen fixation in type I and type II methanotrophs. Appl Environ Microbiol 2001; 67:4009-16.

[4] Awramik S. M., Schopf J. W. and Walter M. R. Carbonaceous filaments from North Pole, Western Australia: Are they fossil bacteria in archean stromatolites? A discussion. Precambrian Res 1988; 39:303-09.

[5] Bagwell C. E. and Lovell C. R. Persistence of selected *Spartina alterniflora* rhizoplane diazotrophs exposed to natural and manipulated environmental variability. Appl Environ Microbiol 2000; 66:4625-33.

[6] Bergman B. B., Gallon J. R., Rai A. N. and Stal L. J. N_2 fixation by non-heterocystous cyanobacteria. FEMS Microbiol Rev 1997; 19:139-85.

[7] Berman-Frank I., Lundgren P. and Falkowski P. Nitrogen fixation and photosynthetic oxygen evolution in cyanobacteria. Res Microbiol 2003; 154:157-64.

[8] Béthoux J. P., Morin P., Chaumery C., Connan O., Gentili B. and Ruiz-Pino D. Nutrients in the Mediterranean Sea, mass balance and statistical analysis of concentrations with respect to environmental change. Mar Chem 1998; 63:155-69.

[9] Bianchi T. S., Engelhaupt E., Westman P., Andren T., Rolff C. and Elmgren R. Cyanobacterial blooms in the Baltic Sea: Natural or human-induced? Limnol Oceanogr 2000; 45:716-26.

[10] Bishop P. E. and Premakur R. "Alternative nitrogen fixation systems." In: *Biological Nitrogen Fixation*, Stacey G., Burris R. H. and Evans H. J. eds., New York: Routledge, Chapman and Hall, Inc., 1992.

[11] Bjerrum C. J. and Canfield D. E. Ocean productivity before about 1.9 Gyr ago limited by phosphorus adsorption onto iron oxides. Nature 2002; 417:159-162.

[12] Brasier M., Green O., Lindsay J. and Steele A. Earth's oldest (similar to 3.5 Ga) fossils and the 'Early Eden hypothesis': Questioning the evidence. Orig Life Evol Biosph 2004; 34:257-69.

[13] Braun S., Proctor L., Zani S., Mellon M. T. and Zehr J. P. Molecular evidence for zooplankton-associated nitrogen-fixing anaerobes based on amplification of the *nifH* gene. FEMS Microbiol Ecol 1999; 28:273-279.

[14] Brocks J. J., Logan G. A., Buick R. and Summons R. E. Archean molecular fossils and the early rise of eukaryotes. Science 1999; 285:1033-36.

[15] Brown M. M., Friez M. J. and Lovell C. R. Expression of *nifH* genes by diazotrophic bacteria in the rhizosphere of short form *Spartina alterniflora*. FEMS Microbiol Ecol 2003; 43:411-17.

[16] Buick R. The antiquity of oxygenic photosynthesis: evidence from stromatolites in sulphate-deficient Archaean lakes. Science 1992; 255:74-77.

[17] Burgess B. K. and Lowe D. J. Mechanism of molybdenum nitrogenase. Chem Rev 1996; 96:2983-3011.

[18] Burke D. H., Hearst J. E. and Sidow A. Early evolution of photosynthesis-clues from nitrogenase and chlorophyll iron proteins. P Natl Acad Sci USA 1993; 90:7134-38.

[19] Canfield D. E. and Teske A. Late Proterozoic rise in atmospheric oxygen concentration inferred from phylogenetic and sulphur-isotope studies. Nature 1996; 382:127-132.

[20] Canfield D. E. A new model for Proterozoic ocean chemistry. Nature 1998; 396:450-53.

[21] Capone D. G., Zehr J. P., Paerl H. W., Bergman B. and Carpenter E. J. *Trichodesmium*: a globally significant marine cyanobacterium. Science 1997; 276:1221-29.

[22] Carpenter E. J. Nitrogen fixation by marine Oscillatoria (*Trichodesmium*) in the world's oceans. In: *Nitrogen in the Marine Environment*, Carpenter E. J. and Capone D. G. eds., New York: Academic Press, 1983.

[23] Conley D. J., Humborg C., Rahm L., Savchuk O. P. and Wulff F. Hypoxia in the Baltic Sea and basin-scale changes in phosphorus biogeochemistry. Environ Sci Technol 2002; 36:5315-20.

[24] D'Alcala M. R., Civitarese G., Conversano F. and Lavezza R. Nutrient ratios and fluxes hint at overlooked processes. J Geophys Res Oceans 2003; 108:Art. No 8106.

[25] Des Marais D. J. and Walter M. R. Astrobiology: Exploring the origins, evolution, and distribution of life in the Universe. Annu Rev Ecol Syst 1999; 30:397-420.

[26] Deutsch C., Gruber N., Key R. M., Sarmiento J. L. and Ganachaud A. Denitrification and N-2 fixation in the Pacific Ocean. Global Biogeochem Cycles 2001; 15:483-506.

[27] Dicker H. and Smith D. Effects of salinity on acetylene reduction (nitrogen fixation) and respiration in a marine *Azotobacter*. Appl Environ Microbiol 1981; 42:740-44.

[28] Dore J. E., Brum J. R., Tupas L. M. and Karl D. M. Seasonal and interannual variability in sources of nitrogen supporting export in the oligotrophic subtropical North Pacific Ocean. Limnol Oceanogr 2002; 47:1595-1607.

[29] Eady R. R. Structure-function relationships of alternative nitrogenases. Chem Rev 1996; 96:3013-30.

[30] Ehrlich H. L. *Geomicrobiology*, 2nd edn. New York City: Marcel Dekker, Inc., 1990.

[31] Elmgren R. Understanding human impact on the Baltic ecosystem: Changing views in recent decades. Ambio 2001; 30:222-31.

[32] Falcon L. I., Carpenter E. J., Cipriano F., Bergman B. and Capone D. G. N_2 fixation by unicellular bacterioplankton from the Atlantic and Pacific oceans: Phylogeny and in situ rates. Appl Environ Microbiol 2004; 70:765-70.

[33] Falkowski P. G. Evolution of the nitrogen cycle and its influence on the biological sequestration of CO_2 in the ocean. Nature 1997; 387:272-75.

[34] Fani R., Gallo R. and Lio P. Molecular evolution of nitrogen fixation: The evolutionary history of the *nifD*, *nifK*, *nifE*, and *nifN* genes. J Mol Evol 2000; 51:1-11.

[35] Flores E. and Herrero A. "Assimilatory nitrogen metabolism and its regulation." In: *The Molecular Biology of Cyanobacteria*, Bryant D. A. ed., The Netherlands: Kluwer Academic Publishers, 1994.

[36] Fonselius S. Oxygen and hydrogen sulphide conditions in the Baltic Sea. Mar Pollut Bull 1981; 12:187-94.

[37] Gallon J. R. Tansley Review No. 44/Reconciling the incompatible: N_2 fixation and O_2. New Phytol 1992; 122:571-609.

[38] Galloway J., Dentener F. J., Capone D. G., Boyer E. W., Howarth R. W., Seitzinger S. P., Asner G. P., Cleveland C. C., Green P. A., Holland E. A., Karl D. M., Michaels A. F., Porter J. H., Townsend A. R. and Vorosmarty C. J. Nitrogen cycles: past, present and future. Biogeochemistry, 2004; 70:153-226 .

[39] Galloway J. N. "The global nitrogen cycle." In: *Treatise on Geochemistry*, Schesinger W. ed., San Francisco: Elsevier Health Sciences, 2003.

[40] Giovannoni S. J., Turner S., Olsen G. J., Barns S., Lane D. J. and Pace N. R. Evolutionary relationships among cyanobacteria and green chloroplasts. J Bacteriol 1988; 170:3584-92.

[41] Golubic S. and Lee S. J. Early cyanobacterial fossil record: preservation, palaeoenvironments and identification. Eur J Phycol 1999; 34:339-48.

[42] Granéli E., Wallström K., Larsson U., Graneli W. and Elmgren R. Nutrient limitation of primary production in the Baltic Sea area. Ambio 1990; 19:142-51.

[43] Gruber N. and Sarmiento J. L. Global patterns of marine nitrogen fixation and denitrification. Global Biogeochem Cycles 1997; 11:235-66.

[44] Gundersen K. The distribution and biological transformations of nitrogen in the Baltic Sea. Mar Pollut Bull 1981; 12:199-205.

[45] Hansell D. A., Bates N. R. and Olson D. B. Excess nitrate and nitrogen fixation in the North Atlantic Ocean. Mar Chem 2004; 84:243-65.

[46] Hartman H. Photosynthesis and the origin of life. Orig Life Evol Biosph 1998; 28:515.

[47] Haug G. H., Pedersen T. F., Sigman D. M., Calvert S. E., Nielsen B. and Peterson L. C. Glacial/interglacial variations in production and nitrogen fixation in the Cariaco Basin during the last 580 kyr. Paleoceanography 1998; 13:427-32.

[48] Hecky R. E. and Kilham P. Nutrient limitation of phytoplankton in freshwater and marine environments: A review of recent evidence on the effects of enrichment. Limnol Oceanogr 1988; 33:796-822.

[49] Herbert R. A. Nitrogen cycling in coastal marine ecosystems. FEMS Microbiol Rev 1999; 23:563-90.

[50] Hill S. "Physiology of nitrogen fixation in free-living heterotrophs." In: *Biological Nitrogen Fixation*, B. R. H. Stacey G. and Evans H.J. eds., New York, London: Chapman and Hall, Inc, 1992.

[51] Hoehler T., Bebout B. M. and Des Marais D. J. The role of microbial mats in the production of reduced gases on the early Earth. Nature 2001; 412:324-27.

[52] Hoover T. "Control of nitrogen fixation genes in *Klebsiella pneumoniae*." In: *Prokaryotic Nitrogen Fixation*, Triplett E. W. ed., Norfolk, England: Horizon Scientific Press, 2000.

[53] Howard J. B. and Rees D. C. Structural basis of biological nitrogen fixation. Chem Rev 1996; 96:2965-82.

[54] Howarth R. W. and Cole J. J. Molybdenum availability, nitrogen limitation, and phytoplankton growth in natural waters. Science 1985; 229:653-55.

[55] Howarth R. W. and Marino R. Nitrogen fixation in freshwater, estuarine, and marine ecosystems. 2. Biogeochemical controls. Limnol Oceanogr 1988; 33:688-701.

[56] Jellison R. and Melack J. M. Meromixis in hypersaline Mono Lake, California.1. Stratification and vertical mixing during the onset, persistence, and breakdown of meromixis. Limnol Oceanogr 1993; 38:1008-19.

[57] Jellison R. and Melack J. M. Algal photosynthetic activity and its response to meromixis in hypersaline Mono Lake, California. Limnol Oceanogr 1993; 38:818-37.

[58] Kaeberlein T., Lewis K. and Epstein S. S. Isolating "uncultivable" microorganisms in pure culture in a simulated natural environment. Science 2002; 296:1127-29.

[59] Karl D., Letelier R., Hebel D., Tupas L., Dore J., Christian J. and Winn C. Ecosystem changes in the North Pacific subtropical gyre attributed to the 1991-92 El Nino. Nature 1995; 373:230-34.

[60] Karl D., Letelier R., Tupas L., Dore J., Christian J. and Hebel D. The role of nitrogen fixation in biogeochemical cycling in the subtropical North Pacific Ocean. Nature 1997; 388:533-38.

[61] Karl D., Michaels A., Bergman B., Capone D., Carpenter E., Letelier R., Lipschultz F., Paerl H., Sigman D. and Stal L. Dinitrogen fixation in the world's oceans. Biogeochemistry 2002; 57/58:47-98.

[62] Kasting J. F. and Siefert J. L. Biogeochemistry - The nitrogen fix. Nature 2001; 412:26-27.

[63] Kasting J. F. and Siefert J. L. Life and the evolution of Earth's atmosphere. Science 2002; 296:1066-68.

[64] Kawai A. and Sugahara I. Microbiological studies on nitrogen fixation in aquatic environments - III. On the nitrogen fixing bacteria in offshore regions. Bull Jap Soc Sci Fish 1971; 37:981-85.

[65] Kiirikki M., Inkala A., Kuosa H., Pitkänen H., Kuusisto M. and Sarkkula J. Evaluating the effects of nutrient load reductions on the biomass of toxic nitrogen-fixing cyanobacteria in the Gulf of Finland, Baltic Sea. Boreal Environ Res 2001; 6:131-46.

[66] Kivi K., Kaitala S., Kuosa H., Kuparinen J., Leskinen E., Lignell R., Marcussen B. and Tamminen T. Nutrient limitation and grazing control of the Baltic plankton community during annual succession. Limnol Oceanogr 1993; 38:893-905.

[67] Knauth L. P. Salinity history of the Earth's early ocean. Nature 1998; 395:554-55.

[68] Knoll A. H. and Holland H. D. Oxygen and Proterozoic evolution: An update. In: *Effects of Past Global Change on Life*, Stanley S. ed., Washington, D.C.: National Academy Press, 1995.

[69] Knoll A. H. *Life on a Young Planet: The first three billion years of evolution on Earth*. Princeton: Princeton University Press, 2003.

[70] Kononen K., Kuparinen J., Mäkelä K., Laanemets J., Pavelson J. and Nõmmann S. Initiation of cyanobacterial blooms in a frontal region at the entrance to the Gulf of Finland, Baltic Sea Limnol Oceanogr 1996; 41:98-112.

[71] Konovalov S. K. and Murray J. W. Variations in the chemistry of the Black Sea on a time scale of decades (1960-1995). J Mar Syst 2001; 31:217-43.

[72] Kuparinen J. and Tuominen L. Eutrophication and self-purification: Counteractions forced by large-scale cycles and hydrodynamic processes. Ambio 2001; 30:190-94.

[73] Kustka A., Carpenter E. J. and Sañudo-Wilhelmy S. A. Iron and marine nitrogen fixation: progress and future directions. Res Microbiol 2002; 153:255-62.

[74] Lazcano A. and Miller S. L. How long did it take for life to begin and evolve to cyanobacteria? J Mol Evol 1994; 39:546-54.

[75] Lee K., Karl D. M., Wanninkhof R. and Zhang J. Z. Global estimates of net carbon production in the nitrate-depleted tropical and subtropical oceans. Geophys Res Lett 2002; 29:1907, doi.10.1029/2001GLO14198.

[76] Leigh J. "Nitrogen fixation in methanogens-the Archaeal perspective." In: *Prokaryotic Nitrogen Fixation; a Model System for the Analysis of a Biological Process*, Triplett E. W. ed., Wymondham, Norfolk: Horizon Scientific Press, 2000.

[77] Ludden P. W., Roberts G. P., Lowery R. G., Fitzmaurice W. P., Saari L., Lehman L., Lies D., Woehle D., Wirt H., Murrell S. A., Pope M. R. and Kanemoto R. H. "Regulation of nitrogenase activity by reversible ADP-ribosylation of dinitrogenase reductase." In: *Nitrogen Fixation: Hundred Years After*, Bothe H., De Bruijn F. J. and Newton W. E. eds., Stuttgart, Germany: Gustav Fischer, 1988.

[78] Martinez L., Silver M. W., King J. M. and Alldredge A. L. Nitrogen fixation by floating diatom mats: a source of new nitrogen to oligotrophic ocean waters. Science 1983; 221:152-4.

[79] Michaels A. F., Olson D., Sarmiento J. L., Ammerman J. W., Fanning K., Jahnke R., Knap A. H., Lipschultz F., Prospero J. M. Inputs, losses and transformations of nitrogen and phosphorus in the pelagic North Atlantic Ocean. Biogeochemistry 1996; 35:181-226.

[80] Millero F. J. *Chemical oceanography*. Boca Raton, Florida: CRC Press, Inc., 1996.

[81] Moisander P. H., Steppe T. F., Hall N. S., Kuparinen J. and Paerl H. W. Variability in nitrogen and phosphorus limitation for Baltic Sea phytoplankton during nitrogen-fixing cyanobacterial blooms. Mar Ecol Prog Ser 2003; 262:81-95

[82] Montoya J. P., Holl C. M., Zehr J. P., Hansen A., Villareal T. A. and Capone D. G. High rates of N_2 fixation by unicellular diazotrophs in the oligotrophic Pacific Ocean. Nature 2004; 430:1027-32.

[83] Navarro-Gonzalez R., McKay C. P. and Mvondo D. N. A possible nitrogen crisis for Archean life due to reduced nitrogen fixation by lightning. Nature 2001; 412:61-64.

[84] Nealson K. H. and Rye R. "Evolution of metabolic pathways." In: *Treatise on Geochemistry*, Schesinger W. ed., San Francisco: Elsevier Health Sciences, 2003.

[85] Nehring D. Phosphorus in the Baltic Sea. Mar Pollut Bull 1981; 12:194-98.

[86] Niemi A. Blue-green algal blooms and N:P ratio in the Baltic Sea. Acta Bot Fenn 1979; 110:57-61.

[87] Nisbet E. G. and Sleep N. H. The habitat and nature of early life. Nature 2001; 409:1083-91.

[88] Nisbet E. G. and Fowler C. M. R. "The early history of life." In: *Treatise on Geochemistry*, Schlesinger W. ed., San Francisco: Elsevier Health Sciences, 2003.

[89] Oelze J. and Klein G. Control of nitrogen fixation by oxygen in purple nonsulfur bacteria. Arch Microbiol 1996; 165:219-25.

[90] Ohki K., Zehr J. P. and Fujita Y. Regulation of nitrogenase activity in relation to the light-dark regime in the filamentous non-heterocystous cyanobacterium *Trichodesmium* sp. NIBB 1067. J Gen Microbiol 1992; 138:2679-85.

[91] Omoregie E. O., Crumbliss L. L., Bebout B. M. and Zehr J. P. Determination of nitrogen-fixing phylotypes in *Lyngbya* sp and *Microcoleus chthonoplastes* cyanobacterial mats from Guerrero Negro, Baja California, Mexico. Appl Environ Microbiol 2004; 70:2119-28.

[92] Oremland R. S. Nitrogen fixation dynamics of two diazotrophic communities in Mono Lake, California. Appl Environ Microbiol 1990; 56:614-22.

[93] Paerl H. W. and Prufert L. E. Oxygen-poor microzones as potential sites of microbial N_2 fixation in nitrogen-depleted aerobic marine waters. Appl Environ Microbiol 1987; 53:1078-87.

[94] Paerl H. W., Bebout B. M. and Prufert L. E. "Physiological ecology and environmental control of N_2 fixation in marine and freshwater microbial associations." In: *Nitrogen Fixation: Hundred Years After*, Bothe H., de Bruijn F. J. and Newton W. E. eds, Stuttgart, Germany: Gustav Fischer, 1988.

[95] Paerl H. W. and Zehr J. P. "Marine nitrogen fixation." In: *Microbial Ecology of the Oceans*, Kirchman D. L. ed., New York: Wiley-liss, 2000.

[96] Paulsen D. M., Paerl H. W. and Bishop P. E. Evidence that molybdenum-dependent nitrogen-fixation is not limited by high sulfate concentrations in marine environments. Limnol Oceanogr 1991; 36:1325-34.

[97] Piceno Y. M. and Lovell C. R. Stability in natural bacterial communities: I. Nutrient addition effects on rhizosphere diazotroph assemblage composition. Microb Ecol 2000; 39:32-40.

[98] Postgate J. *Nitrogen Fixation*, 3rd edn. Cambridge, UK: The Press Syndicate of the University of Cambridge, 1998.

[99] Postgate J. R. and Eady R. R. "The evolution of biological nitrogen fixation." In: *Nitrogen Fixation: Hundred Years After*, Bothe H., de Bruijn F. J. and Newton W. E. eds., Stuttgart, Germany: Gustav Fischer, 1988.

[100] Poulton S. W., Fralick P. W. and Canfield D. E. The transition to a sulphidic ocean similar to 1.84 billion years ago. Nature 2004; 431:173-77.

[101] Ramsing N. B., Fossing H., Ferdelman T. G., Andersen F. and Thamdrup B. Distribution of bacterial populations in a stratified fjord (Mariager Fjord, Denmark) quantified by in situ hybridization and related to chemical gradients in the water column. Appl Environ Microbiol 1996; 62:1391-1404.

[102] Rangaraj P., Ruttimann-Johnson C., Shah V. K. and Ludden P. W. "Biosynthesis of the iron-molybdenum and iron-vanadium cofactors of the *nif*-and *vnf*-encoded nitrogenases." In: *Prokaryotic Nitrogen Fixation: a Model System for the Analysis of a Biological Process*, Triplett E. W. ed., Norfolk: Horizon Scientific Press, 2000.

[103] Rappe M. S., Connon S. A., Vergin K. L. and Giovannoni S. J. Cultivation of the ubiquitous SAR11 marine bacterioplankton clade. Nature 2002; 418:630-33.

[104] Raven J. A. and Yin Z. H. The past, present and future of nitrogenous compounds in the atmosphere, and their interactions with plants. New Phytol 1998; 139:205-19.

[105] Raymond J., Siefert J. L., Staples C. R. and Blankenship R. E. The natural history of nitrogen fixation. Mol Biol Evol 2004; 21:541-54.

[106] Rippka R., Deruelles J., Waterbury J. B., Herdman M. and Stanier R. Y. Generic assignments, strain histories and properties of pure cultures of cyanobacteria. J Gen Microbiol 1979; 111:1-61.

[107] Roberts G. P., Ludden P. W., Burris R. H., Fitzmaurice W. P., Fu H.-A., Nielsen G., Liang J.-H., Lehman L., Woehle D., Lies D., Wirt H., Montgomery S., Davis R. and Bao Y. "The genetics and biochemistry of the reversible ADP-ribosylation systems of *Rhodospirillum rubrum* and *Azospirillum lipoferum*." In: *Nitrogen Fixation: Achievements and Objectives*,

Gresshoff P. M., Roth L. E., Stacey G. and Newton W. E. eds., New York: Routledge, Chapman and Hall, Inc., 1990.

[108] Rosing M. T. ^{13}C-depleted carbon microparticles in > 3700-Ma sea-floor sedimentary rocks from west Greenland. Science 1999; 283:674-76.

[109] Sachs J. P. and Repeta D. J. Oligotrophy and nitrogen fixation during eastern Mediterranean sapropel events. Science 1999; 286:2485-88.

[110] Saito M. A., Sigman D. M. and Morel F. M. M. The bioinorganic chemistry of the ancient ocean: the co-evolution of cyanobacterial metal requirements and biogeochemical cycles at the Archean-Proterozoic boundary? Inorg Chim Acta 2003; 356:308-18.

[111] Sañudo-Wilhelmy S. A., Kustka A. B., Gobler C. J., Hutchins D. A., Yang M., Lwiza K., Burns J., Capone D. G., Raven J. A. and Carpenter E. J. Phosphorus limitation of nitrogen fixation by *Trichodesmium* in the central Atlantic Ocean. Nature 2001; 411:66-69.

[112] Sanz-Alférez S. and Campo F. F. d. Relationship between nitrogen fixation and nitrate metabolism in the *Nodularia* strains M1 and M2. Planta 1994; 194:339-45.

[113] Schlesinger W. H. *Biogeochemistry; an analysis of global change*, 2nd edn. San Diego, London: Academic Press, 1997.

[114] Schlessman J. L., Woo D., JoshuaTor L., Howard J. B. and Rees D. C. Conformational variability in structures of the nitrogenase iron proteins from *Azotobacter vinelandii* and *Clostridium pasteurianum*. J Mol Biol 1998; 280:669-85.

[115] Schopf J. W. *Life's origins: The beginnings of biological evolution*. Berkeley, Los Angeles, London: University of California Press, Ltd., 2002.

[116] Shen Y. A., Buick R. and Canfield D. E. Isotopic evidence for microbial sulphate reduction in the early Archaean era. Nature 2001; 410:77-81.

[117] Siddiqui P. J. A., Carpenter E. J. and Bergman B. B. "*Trichodesmium*: Ultrastructure and protein localization." In: *Marine Pelagic Cyanobacteria: Trichodesmium and Other Diazotrophs*, Carpenter E. J., Capone D. G. and Rueter J. G. eds., The Netherlands: Kluwer Academic Publishers, 1992.

[118] Sprent J. I. and Raven J. A. "Evolution of nitrogen-fixing symbioses." In: *Biological Nitrogen Fixation*, Stacey G., Burris R. H. and Evans H. J. eds., New York: Chapman and Hall, 1992.

[119] Staal M., Meysman F. J. R. and Stal L. J. Temperature excludes N_2-fixing heterocystous cyanobacteria in the tropical oceans. Nature 2003; 425:504-07.

[120] Stal L. J. "Cyanobacterial mats and stromatolites." In: *The Ecology of Cyanobacteria*, Whitton B. A. and Potts M. eds., Dodrecht/London/Boston: Kluwer Academic Publishers, 2000.

[121] Stal L. J. Coastal microbial mats: the physiology of a small-scale ecosystem. S Afr J Bot 2001; 67:399-410.

[122] Steppe T. F. and Paerl H. W. Potential N_2 fixation by sulfate-reducing bacteria in a marine intertidal microbial mat. Aquat Microb Ecol 2002; 28:1-12.

[123] Steward G. F., Zehr J. P., Jellison R. P., Montoya J. P. and Hollibaugh J. T. Vertical distribution of nitrogen-fixing phylotypes in a meromictic, hypersaline lake. Microb Ecol 2003; 47:30-40.

[124] Struck U., Emeis K. C., Voss M., Krom. M. D. and Rau G. H. Biological productivity during sapropel S5 formation in the Eastern Mediterranean Sea: Evidence from stable isotopes of nitrogen and carbon. Geochimica Cosmochimica Acta 2001; 65:3249-66.

[125] Summons R. E., Jahnke L. L., Hope J. M. and Logan G. A. 2-Methylhopanoids as biomarkers for cyanobacterial oxygenic photosynthesis. Nature 1999; 400:554-57.

[126] Thorneley R. N. F. and Ashby G. A. Oxidation of nitrogenase iron protein by dioxygen without inactivation could contribute to high respiration rates of Azotobacter species and facilitate nitrogen fixation in other aerobic environments. Biochem J 1989; 261:181-87.

[127] Tichi M. A. and Tabita F. R. Maintenance and control of redox poise in *Rhodobacter capsulatus* strains deficient in the Calvin-Benson-Bassham pathway. Arch Microbiol 2000; 174:322-33.

[128] Towe K. M. Evolution of nitrogen fixation. Science 2002; 295:798-99.

[129] Turner S., Huang T. C. and Chaw S. M. Molecular phylogeny of nitrogen-fixing unicellular cyanobacteria. Bot Bull Acad Sinica 2001; 42:181-86.

[130] Velinsky D. J. and Fogel M. L. Cycling of dissolved and particulate nitrogen and carbon in the Framvaren Fjord, Norway: stable isotopic variations. Mar Chem 1999; 67:161-80.

[131] Vitousek P. M., Cassman K., Cleveland C., Crews T., Field C. B., Grimm N. B., Howarth R. W., Marino R., Martinelli L., Rastetter E. B. and Sprent J. I. Towards an ecological understanding of biological nitrogen fixation. Biogeochemistry 2002; 57:1-45.

[132] Wasmund N., Voss M. and Lochte K. Evidence of nitrogen fixation by non-heterocystous cyanobacteria in the Baltic Sea and re-calculation of a budget of nitrogen fixation. Mar Ecol Prog Ser 2001; 214:1-14.

[133] Wilmotte A. "Molecular evolution and taxonomy of the cyanobacteria." In *The Molecular Biology of the Cyanobacteria*, Bryant D. A. ed., The Netherlands: Kluwer Academic Publishers, 1994.

[134] Wu J., Sunda W., Boyle E. A. and Karl D. M. Phosphate depletion in the western North Atlantic Ocean. Science 2000; 289:759-62.

[135] Wynn-Williams D. D. and Rhodes M. E. Nitrogen fixation in seawater. J Appl Bacteriol 1974; 37:203-16.

[136] Young J. P. W. "Phylogenetic classification of nitrogen-fixing organisms." In *Biological Nitrogen Fixation*, Stacey G., Evans H. J. and Burris R. H. eds., New York: Chapman and Hall, 1992.

[137] Zehr J. P., Wyman M., Miller V., Duguay L. and Capone D. G. Modification of the Fe protein of nitrogenase in natural populations of *Trichodesmium thiebautii*. Appl Environ Microbiol 1993; 59:669-676.

[138] Zehr J. P., Mellon M., Braun S., Litaker W., Steppe T. and Paerl H. W. Diversity of heterotrophic nitrogen fixation genes in a marine cyanobacterial mat. Appl Environ Microbiol 1995; 61:2527-32.

[139] Zehr J. P., Mellon M. T. and Hiorns W. D. Phylogeny of cyanobacterial *nifH* genes: evolutionary implications and potential applications to natural assemblages. Microbiology 1997; 143:1443-50.

[140] Zehr J. P., Mello M. T. and Zani S. New nitrogen fixing microorganisms detected in oligotrophic oceans by the amplification of nitrogenase (*nifH*) genes. Appl Environ Microbiol 1998; 64:3444-50.

[141] Zehr J. P., Waterbury J. B., Turner P. J., Montoya J. P., Omoregie E., Steward G. F., Hansen A. and Karl D. M. Unicellular cyanobacteria fix N_2 in the subtropical North Pacific Ocean. Nature 2001; 412:635-638.

[142] Zehr J. P., Jenkins B. D., Short S. M. and Steward G. F. Nitrogenase gene diversity and microbial community structure: a cross-system comparison. Environ Microbiol 2003; 5:539-54.

[143] Zevenboom W., Vanderdoes J., Bruning K. and Mur L. R. A non-heterocystous mutant of *Aphanizomenon flos-aquae*, selected by competition in light-limited continuous culture. FEMS Microbiol Lett 1981; 10:11-16.

IV

BIOGEOCHEMISTRY OF CARBON AND SULFUR CYCLES. MICROBIAL METAL REDUCTION

FRACTIONATION OF STABLE ISOTOPES OF CARBON AND SULFUR DURING BIOLOGICAL PROCESSES IN THE BLACK SEA

Mikhail V. Ivanov[1] and Alla Yu. Lein[2]

[1] *Winogradsky Institute of Microbiology RAS, Pr. 60-letija Oktaybrya 7/2, 117312 Moscow, Russia*

[2] *Shirshov Institute of Oceanology RAS, 37 Nakhimovsky prosp., 117997 Moscow, Russia*

Abstract The paper presents literature and authors' own data on the isotopic composition of sulfur and carbon compounds in the water column and bottom sediments of the Black Sea. The fractionation factors of stable isotopes have been compared with the rates of sulfate reduction, photo- and chemosynthesis, methanogenesis, and anaerobic oxidation of methane. In the water column and bottom sediments, the inverse relationship between ^{32}S and ^{34}S fractionation and sulfate reduction rate (measured in situ with the use of $Na^{35}SO_4$) was observed. The isotopic composition of hydrogen sulfide in the water column ($\delta^{34}S$ = -40.0‰) differs greatly from $\delta^{34}S$ of the reduced sulfur compounds of bottom sediments; this confirms the hypothesis that H_2S forms in the water column itself. Seasonal dynamics of $\delta^{13}C$ of phytoplankton-produced organic carbon was revealed; it was demonstrated that some changes in the isotopic composition of POC occur in the chemocline as a result of the photo- and chemosynthetic activity of microorganisms. The data on the isotopic composition of the three main sources of the Black Sea methane are presented. $\delta^{13}C$ of the biogenic methane produced in bottom sediments reaches -67.6‰; $\delta^{13}C$ of methane from cold methane seeps reaches -65.8‰; $\delta^{13}C$ of methane from mud volcanoes ranges from -30.0‰ to -75.0‰. The large-scale process of microbial oxidation of methane results in the production of methane-derived carbonates ($\delta^{13}C$ values range from -27.2‰ to -45.6‰). Using the data on the rates of methanogenesis and anaerobic oxidation of methane as well as the data on the isotopic composition of methane, the balance between the methane flux into the water column and its oxidation has been calculated. It was found that the annual methane production and oxidation in the anoxic zone of the Black Sea are 62.9 and $77.7 \cdot 10^{10}$ mol m^{-2}, respectively. About 80% of methane production is concentrated in the water column and 20% of methane is produced in mud volcanoes and cold seep areas (10% each).

Keywords: Black Sea, water column, bottom sediments, isotopic composition ($\delta^{34}S$ and $\delta^{13}C$), hydrogen sulfide, sedimentary sulfides, particulate organic carbon (POC),

L. N. Neretin (ed.), Past and Present Water Column Anoxia, 373–417.

methane, sulfate reduction, methanogenesis, anaerobic oxidation of methane (AOM), cold methane seeps, mud volcanoes

1. INTRODUCTION

The presence of hydrogen sulfide dissolved in the water column of the deep Black Sea was discovered more than hundred years ago during the expedition of the Russian Geographic Society [4]. At that time a microbial origin of hydrogen sulfide produced in the Black Sea was assumed [100]. In the following years, two alternate hypotheses were made in order to explain the origin of H_2S. Biologists and chemists had an opinion that most of the Black Sea hydrogen sulfide was produced by sulfate-reducing bacteria in the water column and sediments. Some geologists offered the migratory hypothesis by which H_2S discharges into the sea from ancient rocks through tectonic fractures or from mud volcanoes at the sea bottom [92].

Various arguments were made in order to prove the microbiological hypothesis. Danilchenko and Chigirin [18] have observed decrease in the SO_4^{2-}/Cl^- ratio with depth and argued that hydrogen sulfide is produced in the water column. These investigations were continued by Skopintsev [90] and Bezborodov and Eremeev [6]. Issachenko [53] and Kriss [62] investigated the distribution of sulfate-reducing and putrefactive bacteria in details. They suggested that the bulk of the Black Sea hydrogen sulfide is produced in bottom sediments. Sorokin [91] came to the same conclusion when he carried out first experiments estimating the rates of sulfate reduction under in situ conditions with $Na^{35}SO_4$.

The investigations of the isotopic composition of hydrogen sulfide and sulfate in the water column and pore waters were started by Vinogradov, Grinenko and Ustinov [94] and continued by a number of Russian and foreign scientists. The detailed analysis of the data obtained and their role in understanding of the sulfur cycle of the Black Sea are main objectives of this review.

Microbial processes of the sulfur and carbon cycles are closely related. Most of well known species of sulfate reducing bacteria are heterotrophs consuming two moles of organic carbon to reduce one mole of sulfate. Many microorganisms participating in the oxidative part of the sulfur cycle are chemo- and photoautotrophs producing organic compounds at the expense of aerobic or light-dependent anaerobic oxidation of H_2S and other reduced compounds of sulfur.

The second objective of our work is to discuss the processes of production and consumption of organic carbon in the Black Sea with particular emphasis on the $^{12}C/^{13}C$ fractionation. Investigations of the stable isotopic composition of particulate organic matter in the Black Sea began in 1969 during the "Atlantis II" cruise [24, 25]. Most of recent studies have analyzed $\delta^{13}C$ of suspended organic matter in the water column and bottom sediments of the central Black Sea. We have studied biogeochemical processes on the north-western shelf

of the Black Sea during project EROS 21 [63]. Four large rivers (Danube, Dniper, Dniestr, and Bug) affected the region of our investigations. Therefore samples were collected during flood period in spring (April - May) and in mid-summer (July - August). We analyzed samples having the isotopic composition of particulate organic carbon (POC) of the terrigenous and planktonic origin [50, 70]Furthermore, we studied the influence of autotrophic microorganisms located at the upper sulfide boundary on the carbon isotopic composition of POC in the central Black Sea [50].

The third task of the review is to discuss the effects of the stable carbon isotope fractionation during microbial processes of organic matter consumption. During the "Atlantis II" cruise (March-April, 1969), depletion in ^{13}C of dissolved inorganic carbon (DIC) with depth in the water column of the Black Sea was discovered [25].

During last 25 years three important discoveries were made which stimulated interest in the origin of methane and its cycle in the Black Sea. In 1988, a group of Ukrainian scientists discovered numerous methane jets from bottom sediments in the western Black Sea – cold methane seeps [83]. Two years later it was proved that the intense microbial oxidation of methane with the formation of large (up to 3-4 m high) carbonate constructions occurs at the outlets of methane seeps under strictly anaerobic conditions [48]. Around this time the process of anaerobic oxidation of methane was discovered in the water column of the Western gyre in the Black Sea [84]. Finally, methane gas hydrates were found in deep-sea sediments of the Black Sea [33, 60, 61].

The isotopic composition of methane carbon and hydrogen is one of the characteristics of the low-temperature (microbial) vs. high-temperature genesis of methane [99]. One of the tasks of the review is to summarize the data on the isotopic composition of methane carbon in the Black Sea.

2. FRACTIONATION OF STABLE SULFUR ISOTOPES DURING SULFATE REDUCTION IN THE BLACK SEA WATER COLUMN

Prior to large-scale investigations of the isotopic composition of Black Sea sulfur compounds [36, 75, 93, 94, 98] and our investigations of sulfate reduction rates using ^{35}S [46, 65-68], most researchers believed that most part of dissolved sulfide is not produced in the water column, but diffuses from bottom sediments [62, 90].

Sorokin, who was the first to use $Na^{35}SO_4$ to determine sulfate reduction rate (SRR) in the water column and bottom sediments of the Black Sea expressed the same point of view [91]. Sorokin's erroneous assumption resulted from the use of $Na^{35}SO_4$ with insufficiently high specific activity. He was able to measure SRR only in the samples with active sulfate reduction: in the surface sediments, in the upper layer of the H_2S zone, and in the near-bottom water.

Sorokin has not detected SRR in the most part of the water column. In more recent studies based on this method we [66-68] and Gulin [34] found that main part of the Black Sea hydrogen sulfide is produced in the water column. Sorokin subscribed to this view in his latest monograph [92]. According to our data, the annual hydrogen sulfide production in the deep-sea sediments is $5.53 \cdot 10^6$ tons of sulfur, while in the water column the annual production is $20.2 \cdot 10^6$ tons of sulfur [67, 68]. Table 1 summarizes literature data on the annual sulfide production in water column and sediments of the Black Sea.

Table 1. Annual H_2S production in the water column and bottom sediments of the Black Sea anoxic zone (depth below 200 m, total area – 306×10^3 km^2).

References	*[66 – 68]*	*[34]*	*[1]*	*[92]*
Water column g m^{-2} y^{-1}	66	140	10	114
Bottom sediments g m^{-2} y^{-1}	18	16	17	12
Annual production 10^6 t	26	48	8	27

All the data on the isotopic composition of hydrogen sulfide dissolved in the water column measured at 17 stations (Fig. 1) are presented in Table 2. Figure 2 shows the typical water column distribution of $\delta^{34}S$ H_2S with depth. It is evident from these data that the isotopic composition of sulfur in the upper layers of the hydrogen sulfide zone is less depleted in ^{34}S than in the deeper water column, where $\delta^{34}S$ values are the lowest (up to -42‰) and relatively uniform independent of the location. The difference between the isotopic composition of sulfide and sulfate ($\delta^{34}S = 19.3$‰) in the Black Sea water is more than 60‰.

So far no experiments with pure cultures of sulfate-reducing bacteria and "natural populations" [14, 17, 37, 55] have resulted in such considerable difference between the $\delta^{34}S$ values of sulfate and hydrogen sulfide. The maximum fractionation factor in these experiments was 46‰. It is notable that in most of the studies the lower fractionation factors have been observed at higher cell-specific sulfate reduction rates and vice versa [14, 17, 55].

German scientists who have studied fractionation processes in 36 pure cultures of sulfate reducers used a wide range of substrates. Their results casted doubt that the inverse relationship between the sulfur isotopic fractionation and the specific rate of sulfate reduction exists [23]. Despite the fact that the authors have experimented with cells of different sizes, they expressed obtained specific SRRs in moles/cell/day, which was an error. For example, one cell of a rod-shaped sulfate-reducer (cell size 0.5×1.2 μm) contains 0.2 μm^3 of biomass, the volume of a large spherical cell of *Desulfosarcina variabilis* (2 μm

Table 2. The isotopic composition of hydrogen sulfide in the Black Sea water column.

Number of stations	$^{34}S‰$		*Reference*
	The upper part of the H_2S zone	*Deeper part of water column*	
2	Depth 180-300 m −39.8* −38.7 ÷ −40.9 [4]	Depth 300-200 m −40.0 −39.1 ÷ −41. 3[15]	[93]
2	Depth 250 m −38.8	Depth 500-2100 m −40.1 −39.8 ÷ −40.5 [4]	[66, 68]
3	Depth 100-170 m −38.6 −35.2 ÷ −40.5 [11]	Depth 170-2000 m −40.5 −39.3 ÷ −41.3 [15]	[36]
2	Depth 105-170 m −37.9 −36.2 ÷ −39.0 [4]	Depth 180-1890 m −40.6 −40.3 ÷ −42.4 [17]	Unpublished data
5	Depth 121-250 m −36.5 −32.4 ÷ −39.5 [8]	Depth 250-2180 m −39.7 −34.7 ÷ −42.0 [62]	[79]
4	Depth 110-200 m −28.3 −23.3 ÷ −33.1 [2]	Depth 300-1500 m −33.4 −28.4 ÷ −36.1 [15]	[94]
14	−38.1 −32.47 ÷ −40.9 [28]	−40.0 −34.7 ÷ −42.4 [108]	Total**

* numerator – the average $\delta^{34}S$
denominator – range of $\delta^{34}S$ values, number in brackets – number of samples
** Without data of Vinogradov et al. [94].

in diameter) is 4.2 μm^3, but one cell of a giant filamentous sulfate-reducing bacteria *Desulfonema magnum* (7 μm in diameter × 15 μm in length) contains 580 μm^3 of biomass. Hence the author's data given in [23] should be recalculated on a cell volume base to make the conclusion about the relationship between the sulfur fractionation factor and cell-specific SRR credible.

Started from 1973 in our laboratory we have carried out a range of experiments demonstrating the relationship between the sulfur isotope fractionation and sulfate reduction rates in reduced sediments of the Pacific Ocean [44, 45, 64] and the Black Sea [65-70]. Unlike the aforementioned experiments with natural bacterial populations where the samples of bottom sediments were sup-

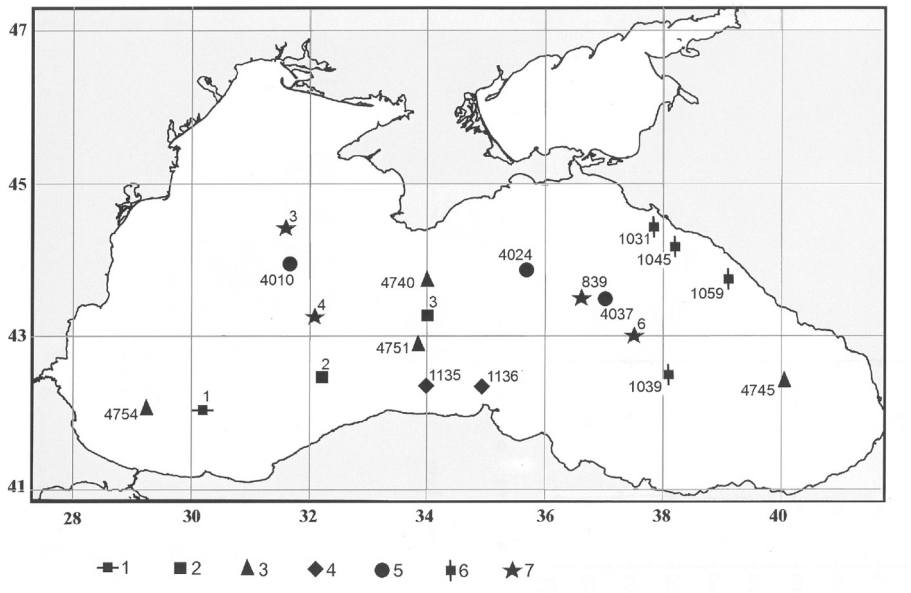

Figure 1. Stations sampled for sulfur isotopic composition of hydrogen sulfide and sulfate. 1-2 [36]; 3 – [94]; 4 – [93]; 5-6 [79]; 7 – our data.

plemented with substrates utilized by sulfate reducers (these substrates would increase the rates of sulfate reduction), our experiments were carried out without the addition of any organic substrate under conditions close to in situ conditions. To determine rates, a method with the use of $Na^{35}SO_4$ of high sensitivity was developed. It was first proposed in the 1950s [43] and later specifically modified to study marine sediments recovered during Pacific expedition in 1973 [44].

The lowest SRR in sediments on the continental slope off California and in the South China Sea measured with this method, varied between 7 and 125 nM/day per 1 kg. These sediments contained isotopically light pyrite ($\delta^{34}S$ = -44.5 ÷ -45.8‰). In the sediments sampled at smaller depths on the upper part of the slope, SRR increased to 1.16 – 1.74 μM/day, and $\delta^{34}S$ of pyrite varied from -24.2 to -26.9‰ [64]. The analysis of these data suggests that at lower SRRs, which are characteristic for oceanic deep-sea sediments, higher isotope fractionation between sulfate and sulfide is observed [45, 64]. Similar, in the deep-sea water column of the Black Sea very low SRRs (Table 3) play a crucial role producing isotopically light hydrogen sulfide (Tables 2 and 3).

An alternative way of explaining the extremely light isotopic composition of sulfides is the effect of isotopic fractionation during microbial disproportionation of S^0, $S_2O_3^{2-}$ and SO_3^{2-} [14, 16, 37, 57, 82]. The fact that the disproportionation is performed by many microorganisms in nutrient-rich media

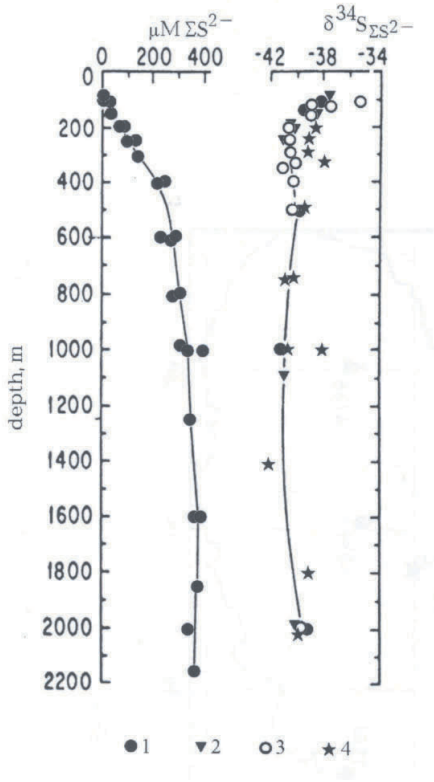

Figure 2. Concentration and $\delta^{34}S$ values of dissolved sulphide in water of the anoxic zone of the Black Sea: 1 – Station 1; 2 – Station 2; 3 – Station 3 [36] and 4 – data from [93].

with elemental sulfur, thiosulfate, and sulfite is beyond the question [13]. Hydrogen sulfide produced during this reaction is substantially enriched in the lighter sulfur [14 - 16]. However, it is totally unfounded to use the disproportionation mechanism to explain the extremely light isotopic composition of H_2S in Black Sea waters. It suffices to remind the data obtained by Luther [74], who had studied the distribution of sulfur species in sulfidic waters of the Black Sea and did not reveal the presence of sulfite and thiosulfate. The concentration of elemental sulfur in the sulfidic water was very low – less than 30 nM [74]. The higher S^0 concentrations (up to 65 nM) were found only in the upper part of the Black Sea sulfidic zone, where, in contrast to deep waters, active hydrogen sulfide oxidation occurs [74]. The combination of two factors – less depleted in ^{34}S hydrogen sulfide and the higher rate of sulfate reduction in the upper part of the sulfide zone (Table 2 and 4) – likely favors our viewpoint on the inverse relationship between the SRR and $\delta^{34}S$ - H_2S rather than a pronounced effect of the disproportionation. Our data indicating that hydrogen

Table 3. Sulfate reduction rate (SRR) and the isotopic composition of hydrogen sulfide (δ^{34}S, ‰) in the deep part of the Black Sea water column (unpublished data).

Station, water depth	*Sampling depth, m*	*SRR, nmol l^{-1} d^{-1}*	*$\delta^{34}S$, ‰*
Station 4988, 1989 m	180	8.4	–40.3
	190	-	–40.3
	200	43.1	–
	210	-	–41.4
	250	74.0	–41.3
	275	-	–41.6
	300	9.0	–
	350	10.3	–41.7
Station 839, 2160 m	500	4.0	–40.0
	700	4.0	–
	1500	-	–40.2
	2100	35	–40.4

sulfide is less depleted in δ^{34}S at the boundary between reduced and oxidized zones of the Black Sea compared to deeper layers (Tables 2-4) are supported by Muramoto's data [78]. The material collected from sedimentary traps at water depths of 500 and 1000 m contained pyrite produced at the upper boundary of H_2S zone with δ^{34}S values from -32.7 to -38.5‰ [78].

3. FRACTIONATION OF SULFUR ISOTOPES DURING SULFATE REDUCTION IN THE UPPER HOLOCENE SEDIMENTS OF THE BLACK SEA

In the Upper Holocene sediments of the Black Sea, anaerobic decomposition of organic matter by sulfate-reducing bacteria is the main mineralization process. In sediments of the anaerobic zone (at water depths below 200 m), the most active process of sulfate reduction was detected in the upper sediments (in the so-called 'fluff layer') rich in organic matter [1, 46, 62, 66, 91, 97]. Even in shallow-water sediments, sulfate reduction occurs in the uppermost sediments covered with a thin (less than 1 mm) layer of brown silt [65, 69, 70, 73, 97]. Only in wintertime when water temperature drops and the influx of allochthonous and autochtonous organic matter decreases, the uppermost shelf sediments become aerobic. Active sulfate reduction leads to the accumulation of reduced sulfur compounds in sediments – up to 1.5% d.w.[69, 95]. It is followed by the fractionation of the stable sulfur and carbon isotopes. Table 5 shows fluctuations of δ^{34}S of terminal products of the reduction processes in more than a hundred samples of sedimentary pyrite and pore water sulfates.

Table 4. Sulfate reduction rate (SRR) and $\delta^{34}S$ of H_2S in the water column at the oxic/anoxic interface of the Black Sea (unpublished data).

Station 6, depth 2123 m, May 1998 43°00′N, 34°30′E					*Station 4, depth 1980 m, May 1998 44°20′N, 32°10′E*					*Station 5096, depth 1989 m, Aug. 1992 45°25′N, 32°10′E*				
Water depth, m	*O_2, mM·l^{-1}*	*H_2S, mM·l^{-1}*	*SRR nmol $l^{-1}\cdot d^{-1}$*	*$\delta^{34}S$, ‰*	*Water depth, m*	*O_2, mM·l^{-1}*	*H_2S, mM·l^{-1}*	*SRR, nmol $l^{-1}\cdot d^{-1}$*	*$\delta^{34}S$, ‰*	*Water depth, m*	*O_2, mM·l^{-1}*	*H_2S, mg.l^{-1}*	*SRR, nmol $l^{-1}\cdot d^{-1}$*	*$\delta^{34}S$, ‰*
115	0	2.2	49	–	115	0	6.6	125	–	100	11.0	7.0	12	–
120	0	6.6	33	–36.1	120	0	8.9	60	–37.8	105	15.0	7.0	150	–37.9
135	0	–	231	–	125	0	11.1	78	–	110	11.0	6.0	8	–38.6
125	0	–	186	–										
140	0	–	120	–38.1	160	0	–	625	–	130	11.0	20.0	446	–
145	0	15.6	22	–	170	0	–	–	–35.2	150	2.0	30.0	400	–36.2
										160	0	38.0	10	–39.0
180	0	–	64	–38.6	180	0	–	498	–37.8	180	0	45.0	6	
					200	0	44.6	443	–	200	0	60.0	11	–41.3
200	0	31.2	–	–40.0	250	0	–	17	–41.8					

The $\delta^{34}S$ of sulfate in pore waters is in the range between 0.8‰ in the upper sediments due to the influence of river water and 53.8‰ in the pore water of shallow-water sediments with active sulfate reduction. The range of $\delta^{34}S$ of pyrite is very wide: 1.5‰ in littoral sediments of the north-western shelf and up to -43‰ in surface layers of continental slope and shelf sediments (Table 5).

When both, the average and the range of $\delta^{34}S$ of pyrite, are compared with the daily production of sulfate reduction in the upper 30 cm layer, the relationship between the isotopic composition of pyrite and sulfate reduction rate is evident. The most isotopically heavy pyrite was found in sediments close to river mouth and in coastal marine sediments with the maximum intensities of H_2S production (with the average $\delta^{34}S$ values of pyrite ranged from -10.1 to -11.0‰ – Table 5, No. 1-3). In sediments on the north-western and Bulgarian shelf (Table 5, No. 4-6), pyrite was less enriched with ^{34}S as the intensity of sulfate reduction decreased from 2.6 to 0.89 mmol m^{-2} day^{-1}. The difference between $\delta^{34}S$ of sulfate from the pore water and pyrite was maximal (61.4‰ – Table 5, No. 5) in shelf sediments with the minimum sulfate reduction rate. Pyrite in sediments of the continental slope and deep water zone of the Black Sea was less depleted in ^{34}S: the average $\delta^{34}S$ varied from -29.7 to -32.8‰; the maximum values were higher than -40.0‰ (Table 5, No. 8-10).

Hence, in lithologically homogeneous sediments (aleuropelitic shelf sediments with shell fragments of benthic clams – Table 5, No. 3-7, and carbonate/clay sediments of the hydrogen sulfide zone – Table 5, No. 8-10), the isotopic composition of the pyrite sulfur depends entirely on the intensity of sulfate reduction.

Unlike the Black Sea water column, where the isotopic composition of the sulfate sulfur is not affected by sulfate reduction, considerable and regular changes in the $\delta^{34}S$ of sulfate of pore waters are observed in bottom sediments with depth. Table 6 shows changes in $\delta^{34}S$ values of pore water sulfate, acid-volatile sulfides, and the sum of elemental, pyrite, and organic sulfur in bottom sediments of various zones of the Black Sea. The data presented (Table 6, No. 1-5) indicate that at all stations on the north-western shelf (depths less than 80 m), consumption of sulfate along with changes in its isotopic compositions have been observed in the upper 0-1 cm. Shallow-water sediments were anaerobic except of a brownish thin layer at the interface with the oxygen-containing water. Active SRR was measured in surface sediments (Table 6, No. 2-5). A group of German scientists also detected active sulfate reduction in the surface layer (fluff layer) of sediments on the north-western shelf during the R/V "Petr Kottsov" cruise in September 1997 [54, 97]. Significant changes in the isotopic composition of sulfate of pore waters were detected only in 5-10 and 10-15 cm layers of deep-sea sediments (Table 6, stations 616 and 601). Residual sulfate was significantly depleted in ^{32}S at all shallow-water stations

Table 5. Sulfur isotope composition of pore water sulfates and pyrite and productivity of sulfate reduction (PSR) in the upper layer of sediments from various regions of the Black Sea.

	Short description of sampling site	$\delta^{34}S$, ‰		$\Delta^{34}S = (\delta^{34}S_{SO_4} - \delta^{34}S_{pyrite})$, ‰	*PSR*[1]	*Reference*
		SO_4^{2-} *in pore waters*	*Pyrite*			
1	Sandy-clay reduced sediments in estuaries of Kuban, Dnister, and Danube, water depth 1.5-17 m. Upper sediments 0-5 cm.	9,6 0.8 – 14.6 [8]	-10.1 −1.5 ÷ −27.0 [9]	19.7	-	[73]
2	Pelitic shallow water sediments in the estuary of Danube river, water depth 0-20 m layer 0-15 cm; 1988.	36.6 21.5 – 53.8 [11]	-10.3 −4.4 ÷ −15.8 [10]	46.9	-	[70]
3	Same as (2), layer 0-30 cm; 1975.	26.0 19.6 – 49.8 [16]	-11,0 −1.5 ÷ −19.6 [36]	37.0	12710 [2]	[70]
4	Clay sandy sediments with fragmented and intact shells of Mactra and Oyster, water depth 15-40 m, layer 0-30 cm	27.6 20.6 – 34.1 [4]	-18.7 −15.2 ÷ −23.5 [7]	46.3	2600[2]	[70]
5	The same as (4), water depth > 40 m, north-western shelf, layer 0-30 cm	21.6 18.1 – 27.5 [10]	-39.8 −32.5 ÷ −43.0 [7]	64.4	770[3] 8902	[70]

6	The same as (5) on Bulgarian shelf, water depth 22-86 m.	19.9 18.0 – 21.8 [12]	-29.3 −19.9 ÷ −44.5 [9]	49.2	1200[2]	[46]
7	Clay-sandy sediments with fragments of shells off Tuapse, water depth 51-81 m.	–	-28.6 −21.6 ÷ −32.6 [6]	–	–	[73]
8	Laminated coccolith ooze, upper part of the continental slope, water depth 200-1000 m.	21.4 20.0 – 24.4 [8]	-29.7 −24.2 ÷ −40.0 [9]	51.1	750[3] 1250[2]	[70]
9	Laminated coccolith ooze, continental slope, water depth 1000-2000 m.	23.5 20.0 – 24.7 [11]	-32.8 −24.0 ÷ −37.7 [10]	56.3	2217[2]	[70]
10	Laminated coccolith ooze in the central Black Sea, water depth > 2000 m	24.9 20.0 – 31.4 [7]	-31.9 −24.9 ÷ −36.4 [13]	56.0	1100[2] 450[3]	[46, 93, 94]

[1] PSR – productivity of sulfate reduction, mmol m^{-2} d^{-1}
[2] [70]
[3] [97]
[4] numerator – the average $\delta^{34}S$, ‰,
denomerator – range of $\delta^{34}S$ values, number in brackets – number of samples

with active sulfate reduction. $\delta^{34}S$ of sulfate was 49.8‰ at 30-40 cm below the surface (Table 6, station 17) and even 53.8‰ at a depth of 16-18 cm (Table 6, station 65B). The data in Table 6 suggest that the isotopic composition of both, monosulfide and pyrite sulfur, become isotopically heavier with depth in the sediment at most stations. SRR decreases with depth in the sediment (Table 6; [97]). The isotope fractionation of sulfur is inversely correlated with SRR. Sulfate-reducing bacteria in the subsurface use isotopically heavier sulfate and as a result produce hydrogen sulfide with higher ^{34}S content.

Transformation of sulfide ions produced from sulfate by sulfate reducing bacteria depends on specific geochemical conditions in which sulfate reduction occurs. In the absence or at low content of iron oxide, the bulk of microbially produced sulfide transforms into hydrogen sulfide: $S^{2-} + 2H_2O = H_2S + 2OH^-$. This reaction is the principal one during sulfate reduction in the water column. In bottom sediments, where iron oxide is abundant, the bulk of sulfide precipitates in the form of acid-soluble hydrotroilite ($FeS \cdot nH_2O$), the first product of diagenetic reactions in reduced bottom sediments. Production of elemental and organic sulfur and pyrite as the final product of the diagenetic transformation of reduced sulfur compounds, occur in bottom sediments during further physiochemical reactions. The mechanisms of these reactions are poorly understood [95].

Reduced sulfur compounds were found in Black Sea sediments. However, their isotopic composition is poorly known. The literature data are listed in Table 7 show that the average $\delta^{34}S$ values of different reduced sulfur compounds in surface sediments of the hydrogen sulfide zone of the Black Sea are rather similar. However, they differ greatly from the $\delta^{34}S$ of hydrogen sulfide dissolved in the water column ($\delta^{34}S$ = -40.0‰; Table 2). A comparison between the average $\delta^{34}S$ of H_2S of pore waters, monosulfide (acid-volatile) sulfur, and $\delta^{34}S$ of the sum of pyrite, elemental, and organic (chromium-reducible) sulfur in anoxic sediments of the Black Sea (Table 7) shows that the isotopic composition of monosulfide sulfur and H_2S is heavier in most cases. These sulfur forms are the latest diagenetic products of hydrogen sulfide, which is produced from isotopically heavy sulfate of pore waters.

The following conclusions can be made from the data obtained:

1. The isotopic composition of sulfate in the upper oxic water column varies from 18.4 – 18.6‰ to 19.0‰ [80, 94]). In the deep water zone, the isotopic composition of sulfate is close to the oceanic isotopic composition (19.5 - 20.2‰) [80, 93, 94].

2. The isotopic composition of the Black Sea H_2S and other reduced compounds of sulfur is dependent on the rate of sulfate reduction. The highest value of fractionation (up to 60‰) is observed in the deeper part of the water column with the lowest SRR (^{34}S of $H_2S = -40.0$‰, Table 2). In

Table 6. Sulfate reduction rates (SRR μmol dm^{-3} d^{-1}) and the sulfur isotopic composition of sulfate in pore waters, acid–volatile sulfides (AVS) and chromium reducible sulfur (CRS) [70].

	Station	*Sediment layer, cm*	SO_4^{2-} *mmol l*$^{-1}$	*SRR*	$\delta^{34}S$ *of* SO_4^{2-}, ‰	$\delta^{34}S$ *of AVS*, ‰	$\delta^{34}S$ *of CRS*, ‰
1	Station 65B, depth 11m,	0 – 0,5	–	8.0	31.56	–9.46	–
	black clay sediment with	1.0 – 3.0	–	3.2	52.05	–18.73	–
	H_2S smell, Dniestr mouth	3.0 – 5.0	–	3.4	48.97	–19.90	–6.24
		10.0 –12.0	–	3.2	49.55	–23.04	–6.83
		16.0 – 18.0	–	3.5	53.81	–22.81	–7.22
2	Station 11,	0 – 1.0	73.1	14.6	24.6	–2.0	–16.4
	depth 11m,	2.0 – 4.0	6.3	14.6	–	–10.0	–15.9
	black grey	5.0 – 8.0	1.0	13.5	23.0	–2.7	–12.8
	sediment with	9.0 – 14.0	9.9	13.0	22.9	3.2	–10.6
	strong smell of	21.0 – 30.0	1.3	9.4	32.8	4.2	–14.4
	H_2S, Danube delta						
3	Station 17,	0 – 1.0	5.9	16.7	20.0	–11.7	–17.5
	depth 26 m, carbonate	3.0 – 5.0	67.5	15.6	20.0	–	–
	terrigenous sediment of	8.0 – 12.0	15.3	14.6	23.9	–20.7	–19.6
	the costal zone,	14.0 – 18.0	13.8	12.5	30.8	–8.2	–9.0
	Danube front area	22.0 – 30.0	4.7	8.8	43.8	–16.4	–16.4
		30.0 – 40.0	2.5	5.7	49.8	–	–
4	Station 19,	0 – 20	151.0	16.7	22.3	–10.2	–13.7
	depth 20 m, same	3.0 – 5.0	31.6	12.5	25.4	2.0	–9.9
	sediment as Station 17,	6.0 – 10.0	75.0	9.9	28.6	0.6	–9.7
	Danube front area	11.0 – 15.0	155.0	7.3	32.0	–	–
		20.0 – 30.0	25.3	2.1	–	–2.0	–10.0

5	Station 568, depth 80 m, sandy–clay sediment with shells, Bulgarian shelf area	0 – 2.0 5.0 – 10.0 21.0 – 40.0	11.9 2.7 1.5	20.0 12.1 –	19.4 20.7 20.8	–6.0 –2.5 –6.3	– –42.0 –37.7
6	Station 601, depth 1000 m, finely laminated coccolith ooze, Bulgarian sector	0 – 2.0 2.0 – 5.0 10.0 – 150 30.0 – 50.0	1.64 0.34 0.07 0.006	15.45 9.7 – 0.4	19.4 20.0 20.2 21.4	–2.0 – – –	–40.0 –24.2 –37.0 –1.0
7	Station 616, depth 1562 m same type of sediment as at station 601	0–2.0 5.0–10.0 25.0–45.0	– – – –	– 14.4 –	19.6 20.0 20.8	– – –	–34.1 –34.3 –33.0
8	Station 545, depth 2002 m finely laminated coccolith ooze	2.0–5.0 10.5–15.0 50.0–70.0	1.76 0.125 0.95	– – –	20.0 21.9 23.4	– – –6.0	–33.0 –30.4 –23.4
9	Station 4752–2, depth 2003 m, same type of sediment as at station 545	0–5.0 10.0–25.0 33.0–48.0	– – –	– – –	21.0 25.0 31.4	–29.4 –22.1 –0.8	–27.4 –24.9 –25.3

Table 7. The sulfur isotope composition ($\delta^{34}S$) of various reduced sulfur compounds in the upper layer of bottom sediments.

Station and depth, m	*Layer, cm*	*H_2S + FeHS*	*S^0*	*FeS_2*	*S_{org}*	*Reference*
			Shelf sediments, oxic zone			
St. 2, 110 m	1–3	–20.5	–206	–19.9	–12.0	[94]
St. 3, 108 m	1–3	–21.1	–24.6	–20.0	+3.4	
St. 708, 51 m	0–30	–	–22.2(3)	–28.6(5)	–13.9(3)	[73]
St. 752, 87 m	0–30	–	–23.3(3)	–28.5(5)	–17.0(3)	
Average	–	–20.5	–22.7	–27.1	–12.7	
			Sediments of the anoxic zone			
St. 4740, 2008 m	0–10	–24.0	–30.8	–33.2	–30.8	
St. 4751, 2216 m	0–10	–21.1	–	–	–19.3	
St. 4752, 2003 m	0–5	–29.4	–24.9	–27.4	–28.1	
St. 4750, 2163 m	0–5	–32.1	–31.3	–30.6	–28.9	[94]
St. 4753, 1773 m	0–10	–27.4	–25.9	–33.7	–30.1	
St. 4745, 1704 m	0–10	–31.2	–35.3	–33.7	–33.5	
St. 4754, 1179 m	0–10	–30.5	–28.3	–26.3	–23.9	
Average		–28.0	–29.7	–30.8	–27.8	

the upper layers of the hydrogen sulfide zone with a source of suspended organic matter from the zones of active photo- and chemosynthesis SRR is much higher. The isotopic composition of sulfur of hydrogen sulfide in these layers is heavier ($\delta^{34}S$ = -35.2 ÷ -39.0‰; Table 4).

3. In bottom sediments, minimum fractionation and the isotopically heavy sulfides were found in coastal sediments with high SRR. In deep-sea sediments of the hydrogen sulfide-containing zone with lower SRR, the average isotope difference between sulfate and reduced sulfur is -56‰; the average isotopic composition of the sum of the reduced sulfur compounds is -31.8‰ (Table 5).

4. In subsurface sediments with active sulfate reduction, sulfate is enriched with ^{34}S up to $\delta^{34}S$ = 49.8 – 53.8‰ (Table 6), due to depletion of the residual sulfate. The enrichment of all forms of reduced sulfur in ^{34}S in the subsurface happens due to their formation from isotopically heavy residual sulfate (Table 6 and 7).

5. Because of a considerable difference in the isotopic compositions of hydrogen sulfide in the water column ($\delta^{34}S_{average}$ = -40.0‰; Table 2)

and of reduced sulfur compounds in surface sediments of the hydrogen sulfide zone ($\delta^{34}S$ = -31.8; Table 5), it is evident that the flux of dissolved sulfide from bottom sediments into the water column does not influence the balance of sulfur compounds in the Black Sea. The bulk of hydrogen sulfide of the water column is produced during sulfate reduction in the water column itself. Hence, the results of the isotopic/geochemical analysis of the Black Sea sulfur compounds confirm previous sulfur balance estimations [67, 68].

At the end of the section on the isotopic composition of reduced and oxidized sulfur compounds let us consider other than sulfate reduction mechanisms of sulfur isotopes fractionation.

Many investigators of the sulfur isotopic composition of pyrite in marine sediments with oxic near-bottom waters suggested that in the production of isotopically light pyrite ($\delta^{34}SO_4^{2-}$ - $\delta^{34}S_{pyrite}$ > 45‰), disproportionation of elemental sulfur, thiosulfate, and sulfite (derived from the H_2S oxidation with bottom water oxygen) is of considerable importance [14]. In the Black Sea, such conditions exist only in shelf sediments. Sediments at water depths below 180-200 m are permanently anoxic. We assume that the disproportionation reactions in shelf sediments may occur, but their role in the formation of the isotopic composition of sedimentary pyrite in the Black Sea anoxic zone are of minor importance due to the absence of the H_2S oxidation.

The arrival of terrigenous pyrite in littoral sediments is theoretically possible, however, detailed microscopical observations have shown that the major portion of sulfide minerals in sediments are represented by pyrite framboids as well as pyrite precursors: hydrotroilite, mackinawite, and greigite [98]. Muramoto et al. [78] performed a quantitative analysis of the flux of pyrite produced in the upper part of the sulfide water column and in bottom sediments of the deep-sea basin. The estimated flux (10 mg or 0.32 mmol/m^2/year) comprised less than 2% of the annual bacterially produced hydrogen sulfide under m^2 of bottom sediments (16-18 g per year – Table 1).

4. THE ISOTOPIC COMPOSITION OF ORGANIC CARBON IN THE BLACK SEA WATER COLUMN

The first data on the isotopic composition of carbon of Black Sea plankton were published by Deuser [24]. He analyzed 10 samples of plankton from the surface down to 100 m water depth at 7 stations taken during the cruise of R/V "Atlantis II" in March-April 1969 (Fig. 3). Fry et. al. [36] published the results on the isotopic composition of POC of 30 samples collected at station 2 during the cruise of R/V "Knorr" in May 1988 (Fig. 3). Samples were collected from the surface down to a depth of 240 m. Kodina et al. [58] published the data

on $\delta^{13}C$ of POC collected at 5 stations in various zones of the Black Sea in September 1992 (Fig. 3).

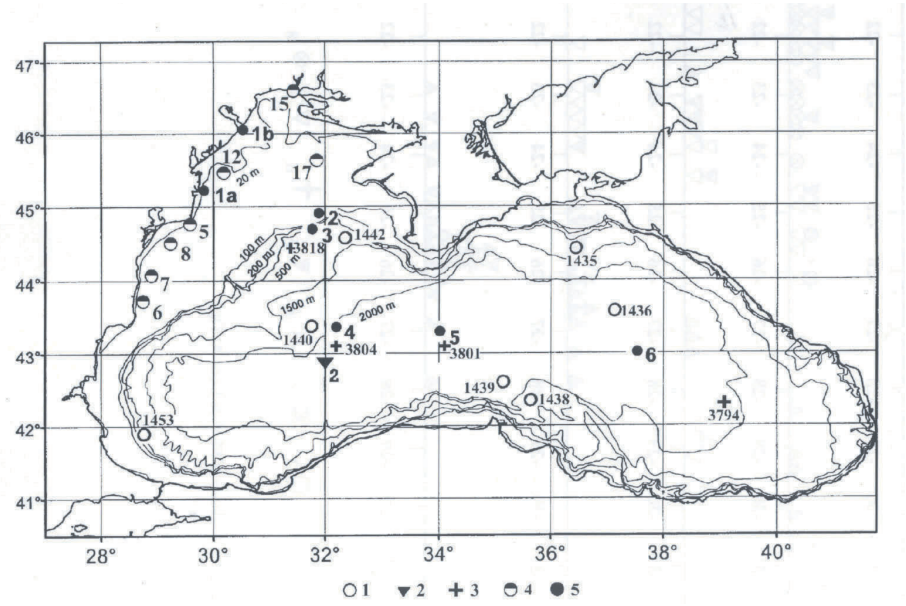

Figure 3. Stations sampled for POC isotopic composition: 1 – March-April 1969 [24]; 2 – May 1989 [36]; 3 - September-October 1992 [58]; 4 – May 1997 [70]; 5 - May 1998 [50].

We analyzed the isotopic composition of POC obtained at ten stations on the north-western shelf and at 4 stations in the deep water zone of the Black Sea (Fig. 3) [50, 70]. Figure 5 shows all data on $\delta^{13}C$ of POC in the water column of the Black Sea. The isotopic studies of POC during cruises of 1995-1997 of the International Project EROS 21 [63] have been conducted in the north-western zone of the Black Sea [10, 70, 87]. One of the goals was to find out the isotopic composition of terrigenous organic matter flowing into the Black Sea from Danube, Dniper, and Dniestr. These rivers account for a half of the total river discharge in the Black Sea.

Important data on the isotopic composition of POC of terrigenous origin were obtained from the Danube delta in April 1997 as well as from the zone near the mouth of Dniper and Dniestr in May 1997. The average $\delta^{13}C$ of POC in seven samples collected in three zones was -28.1‰ (ranging from -24.4‰ to -31.5‰) (Table 8, No. 1-3). The samples of POC collected in spring 1977 over the shelf area at various distances from the river mouth were less depleted in ^{13}C because of the presence of the isotopically heavy plankton (Table 8, No. 4-7).

Table 8. The isotopic composition of POC (δ ^{13}C, ‰) in water samples from north-western shelf collected in different seasons.

N	*Place of sampling*	*Time of sampling*	$\delta^{13}C$, ‰	*Reference*
1	Danube river	April 1997	-28.1 −24.4 ÷ −31.5 [7]	[10]
2	Dniper mouth	May 1997	-29.0 −28.5 ÷ −29.5 [2]	[70]
3	Dnister mouth	May 1997	-28.5 −28.2 ÷ −28.8 [2]	[70]
4	North-western shelf	May 1997	-26.07 −24.4 ÷ −28.8 [15]	[70]
5	North-western shelf	April-May 1997	-25.0 −22.3 ÷ −27.7 [7]	[10]
6	Danube-Black Sea mixing zone	April-May 1997	-26.66 −24.3 ÷ −28.3 [21]	[87]
7	North-western shelf	May 1998	-25.3 −24.2 ÷ −27.1 [7]	[50]
8	North-western shelf	August 1995	-20.0 −19.3 ÷ −20.7 [2]	[70]
9	North-western shelf	September-October 1992	-21.46 −20.6 ÷ −22.2 [10]	[58]

Numerator – the average δ^{13}C ‰;
denominator – range of δ^{13}C; number in brackets – number of samples.

δ^{13}C of POC in summer of 1995 and early autumn of 1992 was very different. In the fall the input of terrigenous material and the phytoplankton production were low (Table 8, No. 8 and 9).

Table 9 shows published data on the isotopic composition of POC in the upper water column of the deep Black Sea. These data demonstrate that seasonal dynamics of δ^{13}C of POC is characteristic not only for the north-western shelf, but for the whole sea as well. Samples of POC collected in spring [24] and during summer phytoplankton bloom [58] are less depleted in ^{13}C than the samples that we [50] and Fry et al. [36] collected in May during low phytoplankton production [9] (Fig. 4). The chart (Fig. 5) shows data for δ^{13}C of POC for two contrasting (by primary production) periods. The average data between two seasons differ by 2.5 – 4.2‰.

Table 9. The isotope composition of POC in the upper water column of the central Black Sea.

	Water layer, m	*Station number*	*Date*	$\delta^{13}C$, ‰	*Reference*
1	0 – 100	7	25.03 – 06.04 1969	–23.0* $-21.8 \div -24.1$ [10]	[20]
2	0 – 40	1	05.1988	–25.2 $-24,4 \div -26,0$ [5]	[36]
3	0 – 35	4	09. – 10. 1992	–22.64 $-21.4 \div -24.8$ [11]	[58]
4	0 – 40	6	05. 1998	–27.2 $-24,2 \div -30,2$ [7]	[50]

* Numerator – the average δ^{13}C, ‰;
denominator – range of δ^{13}C values; number in brackets – number of samples.

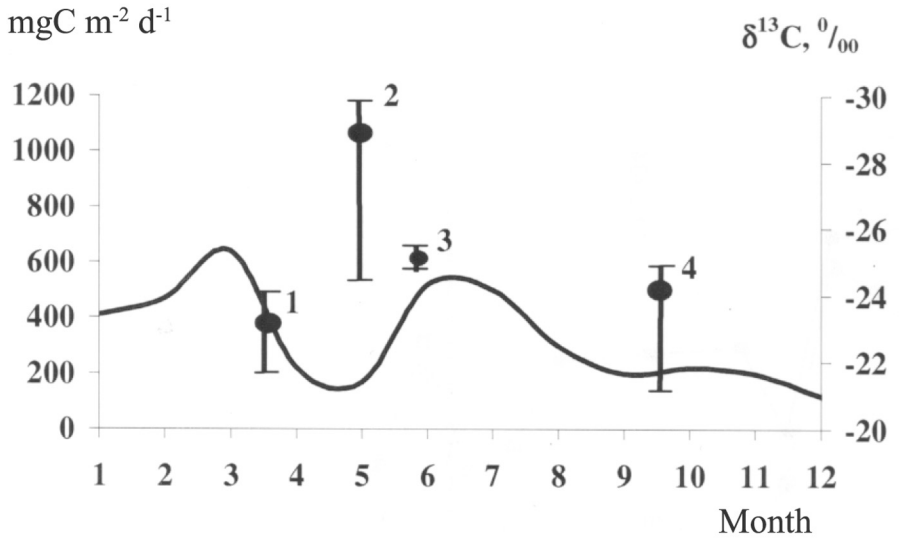

Figure 4. Seasonal variability of the primary production (solid line) and δ^{34}C of POC in the western cyclonic gyre [9]. Vertical lines and numbers show the time of sampling: 1 – beginning of April 1969 [20]; 2 – beginning of May 1998 [50]; 3 – end of May 1988 [36]; 4 – end of September 1992 [58].

This may be a result of seasonal differences in specific rates of photosynthesis. The literature data point to an inverse relationship between the carbon

isotope fractionation and the specific rate of photosynthesis studied under natural conditions and in pure cultures of marine phytoplankton [35].

Detailed investigations of $\delta^{13}C$ of POC were carried out at 9 stations in the deep water zone (Fig. 5). As illustrated in Fig. 5, seasonal changes of $\delta^{13}C$ of POC in the oxic zone are opposite to changes in the anoxic zone. In May, there is a substantial decrease in the carbon isotopic composition of POC in comparison with the end of March [24, 36, 50]. The opposite situation is observed at the end of September when the quantity of POC in surface waters increases due to active photosynthesis (Table 10). In general, POC concentrations decrease significantly with depth. The isotopic composition of POC in the layer of its maximum content differs from the isotopic composition of POC in the photosynthetic zone. Specifically, in accordance with the data [58], at water depths of 110 – 135 m at every of 4 stations a distinct increase in POC content (up to 125 mg/l) was accompanied by ^{13}C depletion of POC compared to the upper layers (Table 10, Footnote). Since considerable fractionation of carbon isotopes during aerobic mineralization of organic matter does not occur [35], main reasons for changes in $\delta^{13}C$ of POC along the water column profile are seasonal changes in photosynthetic rates (Fig. 5) and in the carbon isotopic composition of phytoplankton biomass.

Table 10. Particulate organic matter from Black Sea surface layers and its isotopic composition.

Date of sampling	Surface layer (0-1 m)		Layer 1-20 m		Reference
	C_{org}, mg l^{-1}	$\delta^{13}C$, ‰	C_{org}, mg l^{-1}	$\delta^{13}C$, ‰	
May 1988	48	–25.5	93	–25.1	[36]
September-October 1992 *	148	–21.8	158	–21.9	[58]

*$\delta^{13}C$ (average) POC in the layer 110 – 135 m (zone of the deep-sea POC maximum) = –24.1 ‰ (range from –23.0 to –25.8‰) [58]

Since fractionation of carbon isotopes occurs not only during photosynthesis by phytoplankton, but also during chemosynthesis and bacterial photosynthesis [38], attempts to reveal this effect at the boundary between the oxic and anoxic waters of the Black Sea were made. The carbon isotopic composition of POC in the chemocline was studied in 1988 during the cruise of R/V "Knorr" [36]. Despite the fact that samples from the chemocline were collected in 3 m intervals, changes in $\delta^{13}C$ of POC at the upper boundary of the sulfide zone and below were not revealed (Fig 6a). Other scientists who participated in this cruise analyzed both, the distribution of microorganisms and their activity, at the same depths where samples for carbon isotopic composition were collected. Neither an increase in the quantity nor an increase in the CO_2 dark fixation rates

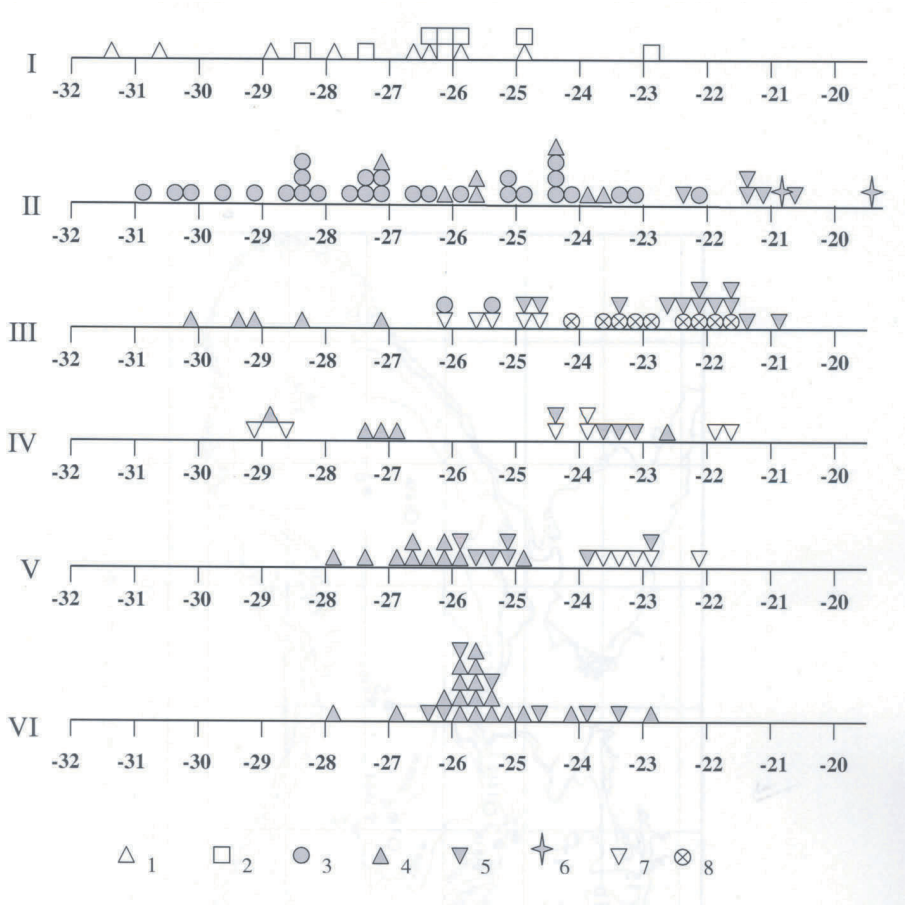

Figure 5. Seasonal changes of the carbon isotopic composition in different areas of the Black Sea. I – Danube river and Danube estuary; II – north-western shelf; III-VI – central part of the Black Sea: III – euphotic zone (0-40 m); IV – decomposition zone (40-90 m); V – upper part of the H_2S zone (above 200 m); VI – deep-water H_2S zone (below 200 m) 1 – Danube river, April-May [10], 2 – Danube estuary, April-May [87]; 3 – North-Western shelf, May [87, 70]; 4 – May [49]); 5 – August-September [58, 32]; 6 – July [70]; 7 – end of May [36]; 8 – March-April [20].

were revealed in the chemocline [8, 56]. Kodina and her colleagues [58] have detected carbon isotopic signal in the chemocline. Samples with isotopically light carbon were collected at 5 m (station 3804), 15 m (station 3794), and 20 m (station 3794) above the upper boundary of the sulfide zone (Fig. 6c). The isotopic trend was explained by the fractionation of carbon isotopes by the chemolithoautotrophic bacteria [31, 32, 58, 59].

We have investigated the possible effect of autotrophic microorganisms on the isotopic composition of POC in the chemocline during the joint Russian-Swiss expedition in May 1998 [50]. The distribution of microorganisms, rates of CO_2 dark fixation, sulfate reduction, and methanogenesis as well as the isotopic composition of POC, oxygen and hydrogen sulfide content along the transect to the deep-sea zone have been studied (Fig. 3). Water samples were collected in the chemocline as well as every 5 m above and below. Figure 6c shows the data on δ^{13}C-POC; the results of hydrochemical and microbiological analyses at stations 3 and 5 (Fig. 3) are listed in Table 11. Significant changes in the isotopic composition of POC are evident in the upper layer (15-20 m) of the sulfide zone. This can be explained by the presence of autotrophic microorganisms, because the total number of microorganisms and dark CO_2 fixation rates increase in this zone. The analysis of δ^{13}C distribution in deeper layers showed that the isotopically light organic matter consisting of the autotrophic microbial biomass was rapidly consumed by anaerobic bacteria. The main consumers of this fresh organic matter were heterotrophic sulfate reducers as demonstrated by the peak of sulfate reduction rates under the layer with maximum rate of dark CO_2 fixation. This phenomenon was first discovered by Sorokin [91] and confirmed later in our studies (Table 11) [50].

The noticeable lightening of the isotopic composition of POC in the chemosynthesis zone was recently reported by a group of Turkish scientists at two stations in the south-western Black Sea [102]. In addition to δ^{13}C determinations of POC, the rate of dark CO_2 fixation has been measured, which revealed active chemosynthesis in the upper sulfide zone [101]. The maximum depletion of POC in δ^{13}C isotope in the chemosynthesis zone at one of the stations was 5‰ compared to POC samples from the oxycline. Similar to our observations, isotopically light organic matter was rapidly consumed in the zone below the chemosynthesis layer [102]. In meromictic Lake Mogil'noye on Kil'din Island (Barents Sea) we have discovered similar isotope effect due to activity of autotrophic microorganisms in the upper sulfide zone [49].

In sum, δ^{13}C values of POC in the sulfide zone of the Black Sea (below 200 m) range between -24.0 and -26.0‰; the average δ^{13}C of POC of 22 samples is -25.3‰ (Fig. 5). These data are of great interest for understanding the organic carbon genesis in Black Sea sediments.

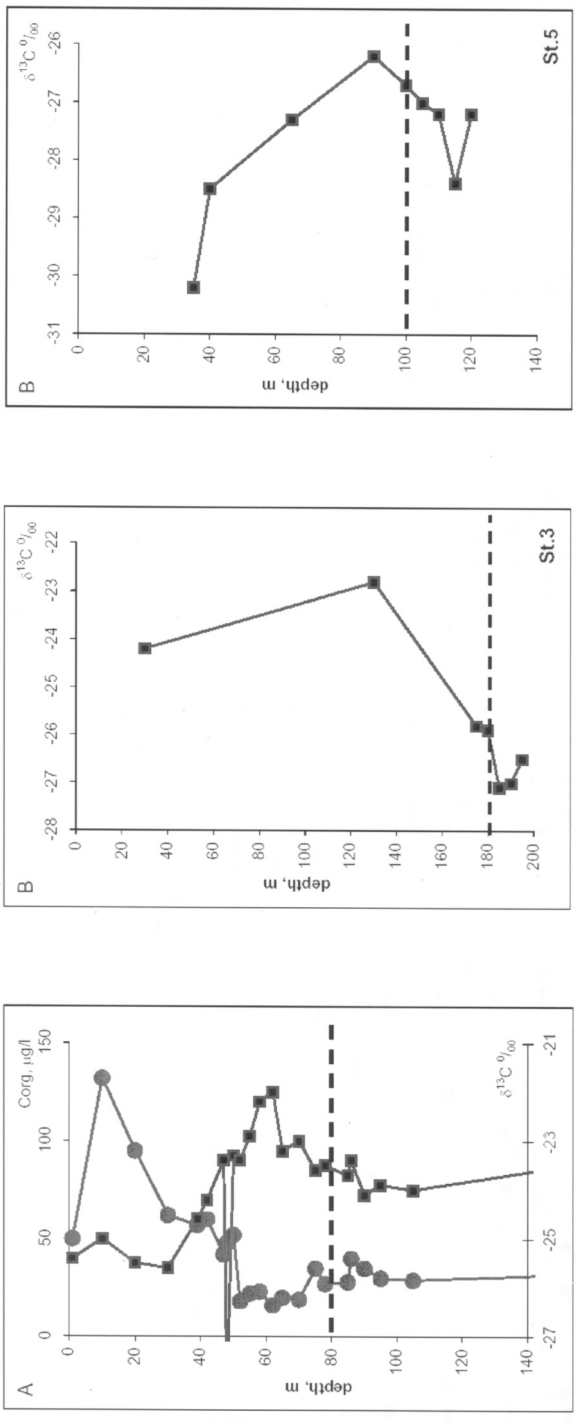

Figure 6. POC content [1] and carbon isotopic composition of POC [2] in water column of the Black Sea. A – Station 2 [36]; B - Stations 3 and 5 [49]; C – Stations 3794, 3801 and 3804 [58].

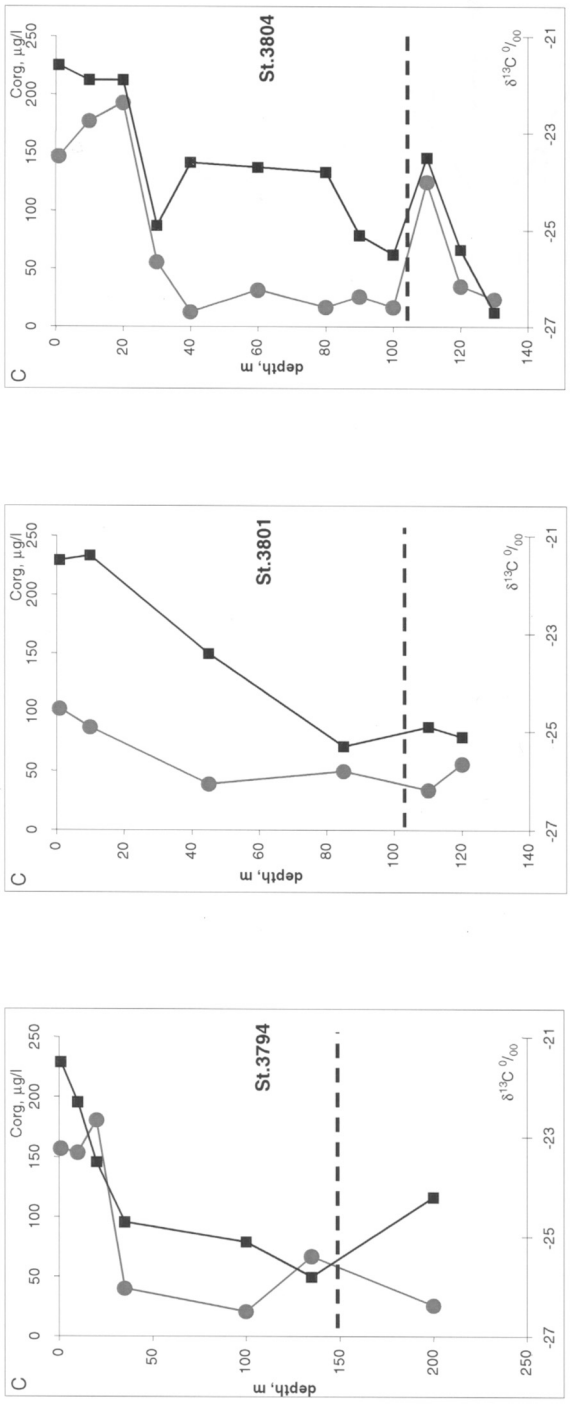

Figure 6 continued.

Table 11. Hydrogen sulfide and oxygen contents, sulfate reduction (SRR) and CO_2 fixation rates, and the isotopic composition of POC at depths, relative to the H_2S upper boundary at two stations in the Black Sea [49].

St. 3, depth 592 m, H_2S zone – below 180 m						*St. 5, total depth 2172 m, H_2S zone – from 105 m*					
Depth, m	*O_2, µmol l^{-1}*	*H_2S, µmol l^{-1}*	*CO_2 fixation, nmol l^{-1} d^{-1}*	*SRR nmol l^{-1} d^{-1}*	*$\delta^{13}C$ of POC, ‰*	*Depth, m*	*O_2, µmol l^{-1}*	*H_2S, µmol l^{-1} d^{-1}*	*CO_2 fixation, nmol l^{-1} d^{-1}*	*SRR, nmol l^{-1} d^{-1}*	*$\delta^{13}C$ of POC, ‰*
+5	11.0	0	< 0.05	-	-25.8	+20	1	0	< 0.05	-	-24.9
0	< 1.0	< 1.0	< 0.05	3.9	-25.9	0	0	< 1	0.07	1.76	-29.2
-5	< 1.0	2.2	< 0.05	2.10	-27.1	-5	0	0.4	0.05	1.22	-25.6
-10	< 1.0	4.5	0.55	5.20	-27.0	-10	0	2.2	0.22	0.76	-26.5
-15	0	8.0	0.35	3.90	-26.5	-15	0	4.5	0.73	3.35	-27.3
-20	0	13.4	0.62	6.51	-24.9	-20	0	6.7	1.70	1.52	-27.8
-30	0	22.3	0.66	7.56	-25.5	-25	0	8.9	1.70	0.76	-27.2
-40	0	29.0	1.45	5.73	-	-30	0	11.2	1.25	0.50	-26.9
-90	0	31.2	0.24	6.51	-26.7	-45	0	15.6	1.25	4.57	-27.5
						-95	0	31.2	1.31	6.09	-25.9

5. THE ISOTOPIC COMPOSITION OF CARBON IN BOTTOM SEDIMENTS

Published data on the isotopic composition of organic carbon are listed in Table 12, which shows that seasonal differences in the isotopic composition are found only in the uppermost sediments on the north-western shelf: abundance of terrigenous organic matter in April-May shifts the average isotopic composition of organic carbon by -1.7‰ compared to the data obtained in August (Table 12, No. 1 and 3).

Table 12. The carbon isotopic composition of organic matter in surface sediments of the Black Sea.

	Place of sampling	*Time of sampling*	$\delta^{13}C$, ‰	*Reference*
1	North-western shelf, 0–1 cm	August	–25.15* −24.3 ÷ −26.0 [2]	[70]
2	North-western shelf, 0–1 cm	May	–26.8 −24.8 ÷ −27.5 [5]	[50]
3	North-western shelf, 0–1 cm	August	–23.8 −22.5 ÷ −26.5 [15]	[32]
4	North-western shelf, 0–40 cm	August	–25.3 −24.2 ÷ −26.9 [21]	[70]
5	Deep-sea, > as 2000 m, 4 Stations, 0–10 cm	October	–25.7 −25.5 ÷ −26.0 [11]	[67]
6	Deep-sea 2 stations, 0–40 cm	-	–24.4 −24.0 ÷ −25.6 [14]	[12]
7	Continental slope, 0–60 cm	-	–23.4÷ –25.7 [15]	[59]

*Numerator – the average δ^{13}C, ‰;
denominator - range of δ^{13}C; number in brackets - number of samples.

The range of δ^{13}C of organic carbon in sediments on the north-western shelf (Table 12, No. 3) is close to published data ([59]; Table 12, No 7). They are however in contradiction with the Galimov's opinion [31, 32] on certain zonality of δ^{13}C distribution in sediments from various geochemical zones of the Black Sea. His results were based on a small number of samples in the uppermost (0 – 1 cm) sediments collected in summer. In summer isotopically heavy organic matter of the planktonic origin accumulates in shallow regions. However, this organic matter is quickly degraded, therefore the isotopic composition of organic matter from the shelf sediments is slightly different from

the average isotopic composition of organic carbon in deep-sea sediments (-25.3‰ and -24.4 – -25.7‰, respectively) (Table 12, No. 4–6).

Microbiological, hydrochemical and isotopic data (Table 13) point to the intense organic matter mineralization in shallow sediments of the Black Sea. The fact that the total alkalinity increases with depth is a direct evidence of ongoing mineralization processes. The alkalinity increase was maximal in shallow-water sediments at stations 11 and 16 where the rate sulfate reduction was high and minimal in deep-sea sediments at station 28 (129 m water depth) (Table 13). Mineralization of organic matter by sulfate-reducing bacteria in shelf sediments occurs under anaerobic conditions. It is well known that an excess of calcium ions as well as alkalinization are caused by the uptake of SO_4^{2-} ion during sulfate reduction. Both processes shift the carbonate equilibrium toward the precipitation of the early diagenetic calcium carbonate. A decrease in calcium concentration along the depth profile in littoral sediments is illustrated by the example of station 16 (Table 13). Precipitation of early diagenetic carbonates can be proved by considerable lightening of the isotopic composition of total carbonates. Precipitation was evident in sediments with high rates of sulfate reduction (stations 11 and 16). Less isotopically light carbonate minerals were discovered at the open shelf stations (station 1, Table 13) and in sediments from the shelf edge (station 28, Table 13).

Active anaerobic decomposition of organic matter accompanied by the change in the isotopic composition of DIC was discovered in the water column as well. According to [25], the isotopic composition of DIC is lighter with depth in the sulfide zone: -4.0‰ at 500 m, - 5.5‰ at 1000 m, - 6.5‰ at 1500 m, and -6.9‰ in the near-bottom water at 2200 m. Since $\delta^{13}C$ values change simultaneously with an increase in the H_2S content, it is obvious that both processes result from activity of sulfate reducing bacteria.

While microorganisms play the main role in the distribution and redistribution of stable sulfur isotopes in the Black Sea, the isotopic composition of organic carbon depends on the balance of allochthonous organic matter discharged by rivers and autochthonous organic matter synthesized by plankton. In spring, an increase in the inflow of terrigenic material leads to lighter carbon isotopic composition of POC in the water column and in upper layers of shallow sediments. It becomes heavier during the periods of intensive blooms of phytoplankton in early spring and summertime.

The average $\delta^{13}C$ of organic carbon in the central part of the Black Sea is -25.0‰ (Table 12, No. 5 and 6). This value is about the same as the isotopic composition of POC of the deep-water zone (-25.3‰) (Fig. 5). The relative content of hydrocarbons of different origin determine the carbon isotope composition of total POC [96]. It has been found that organic matter in upper deep-sea sediments consists of 56% of hydrocarbons of the terrigenous origin

Table 13. Alkalinity and dissolved calcium content in pore waters, sulfate reduction rate (SRR) and the carbon isotopic composition of organic carbon, HCO_3^- and calcium carbonate in shallow-water sediments of the north-western shelf of the Black Sea [70].

Station/ water depth	*Sediment layer, cm*	*SRR µmol dm^{-3} day^{-1}*	*Alka-linity, mM*	*Ca^{2+}, mg l^{-1}*	*C_{org}*	*$\delta^{13}C$, ‰ HCO_3^-*	*$CaCO_3$*
11/	0–1.0	73.1	4.5	–	–25.2	–18.6	–10.9
11m	0.5–8.0	6.3	8.5	–	–25.4	–18.0	–11.4
	9.0–14.0	9.9	12.5	–	–26.9	–19.0	–10.5
	21.0–25.0	–	18.0	–	–25.9	–22.0	–8.6
16/	0–1.0	12.8	4.0	14.0	–24.1	–	–11.8
16m	1.0–6.0	5.6	5.0	12.0	–24.9	–	–13.8
	8.0–12.0	21.3	14.0	12.0	–25.5	–	–10.8
	20.0–30.0	5.9	25.0	9.0	–25.6	–	–11.3
	30.0–40.0	–	–	5.0	–26.0	–	–11.3
1/	0–3.0	–	3.5	–	–	–	–
55m	4.0–5.0	2.6	3.8	–	–23.5	–	–4.3
	7.0–20.0	1.7	3.9	–	–24.2	–	–2.7
	20.0–25.0	6.4	4.1	–	–24.3	–	–7.0
28/	0–13.0	5.5	2.2	–	–26.3	–11.4*	–2.1
129m	20.0–26.0	2.2	4.0	–	–25.5		–2.2

* For sediment layer 0-26.0 cm

with $\delta^{13}C$ = -27‰ (Table 8) and 44% of planktonic and bacterial origin with the average isotopic composition of organic carbon of -23‰.

Local variations of the isotopic composition of POC in the chemocline zone due to carbon fractionation by autotrophs and insignificant enrichment of DOC with the light isotope ^{12}C in the deep water column as a result of heterotrophic microbial activity have little effect on the carbon isotope cycle of the Black Sea.

6. FRACTIONATION OF CARBON ISOTOPES DURING THE METHANE CYCLE IN THE BLACK SEA

The biogeochemical methane cycle in the Black Sea is less understood in comparison with the sulfur cycle, particularly the isotopic composition of carbon and hydrogen of the Black Sea methane and products of methane oxidation. Before cold methane seeps [83] and associated with them carbonate construc-

tions [48] as well as active mud volcanoes [41] were discovered, the distribution of methane have only been studied at few stations in the deep-sea. It was reported that methane concentration increases mostly linear down to 500-600 m to 10-13 μmol l^{-1}; below methane concentration is constant [40, 84]. The shape of the methane profile with depth suggested that methane produced by microorganisms in bottom sediments diffuses into the water column.

Microbiological investigations of the distribution and geochemical activity of microorganisms involved in the methane production and oxidation have started in 1980s [46, 64]; extensive studies have been performed in recent years [29, 30, 49, 52]. Figure 7 shows main results of these investigations. The data indicate that methane concentration increases monotonically from the upper boundary of the sulfidic zone to the bottom at stations in the upper part of the continental slope (up to 600 m) (Fig 7, A). At deep-sea stations in the western part of the sea (Fig. 7B), pronounced peak of methane concentration at 400-600 m was explained by lateral migration of methane from abundant cold seeps located in the upper part of the continental slope. Methane content increases in the near-bottom water (Fig. 7A, 7B). At many of deep-sea stations, methane content in bottom sediments is lower than in the near-bottom water (Fig 7D, E). This phenomenon was first discovered by Berlin et al. [5] and was later confirmed in our investigations in different Black Sea regions [29, 30, 52].

Figure 7 shows the vertical distribution of the rates of methanogenesis and anaerobic oxidation of methane. These rates were estimated using $^{14}CO_2$ and $^{14}CO_3COONa$ for methanogenesis and $^{14}CH_4$ for methane oxidation [30, 51]. Integrated over 1 m^2 data demonstrate that methane oxidation exceeds methane production in the water column. The integrated microbial production of methane in the water column is 62.9 10^{10} moles per year in the entire anaerobic zone (306 10^3 km^2, depths more than 200 m). The annual methane oxidation is 77.8 10^{10} mol per year. Rates of methanogenesis and anaerobic methane oxidation in Late Holocene sediments (upper 0-40 cm) are much lower – 27.6 10^7 mol and 24.6 10^7 mol, respectively [52, 72]. The data show that microbial methanogenesis in the anaerobic water column accounts for more than 80% of the methane content. However, the water column receives annually no less than 14.8 10^{10} moles of methane from various external sources – underwater mud volcanoes and cold methane seeps [52, 72]. The bulk of methane coming from these two sources, as well as its origin (biogenic or thermogenic) have not been adequately investigated. The investigation of the isotopic composition of methane as well as of its heavier gaseous homologues are the most important isotopic-geochemical problems of the Black Sea.

The values of $\delta^{13}C$ of methane from surface [2, 39, 40, 51] and subsurface sediments (4.8 – 6.3 m; [40]) are shown in Fig. 8. These values indicate a biogenic origin of methane produced during CO_2 reduction with hydrogen. According to results of our experiments with radioactively labeled substrates,

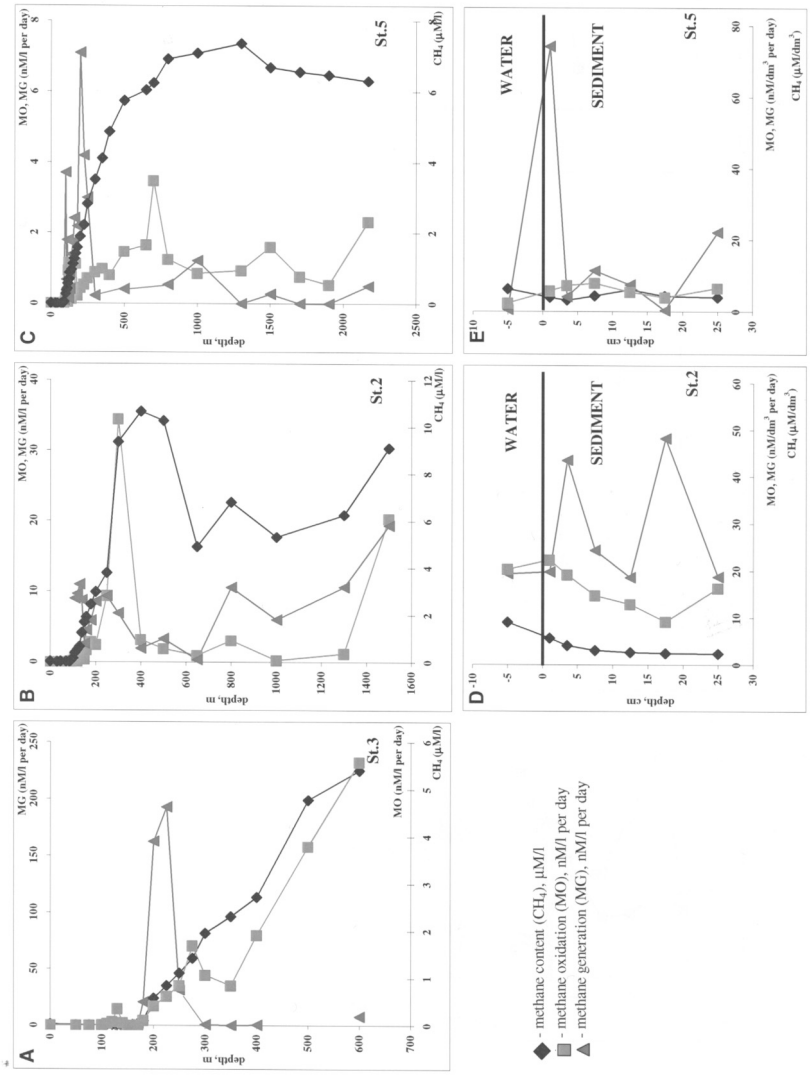

Figure 7. Depth distributions of methane, methane production and methane oxidation rates in the water column (A, B, C) and sediments (D, E) of the Black Sea [52]. A - Station 3, upper part of the western continental slope; B – Station 2, deeper part of the western continental slope, and C – central part of the western gyre.

autotrophic methanogenesis is responsible for more than 90% of methane production in the water column and sediments of the Black Sea [52, 72].

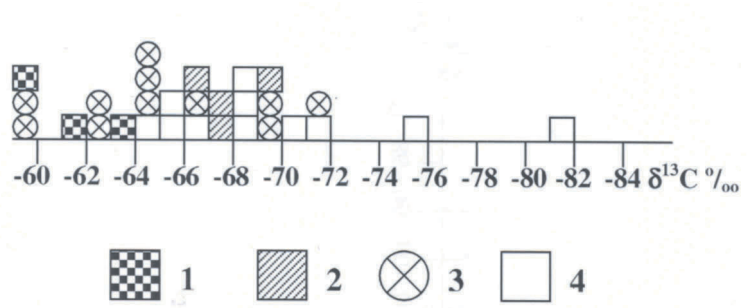

Figure 8. Carbon isotopic composition of methane in sediments of the Black Sea. 1 – [40]; 2 – [2, 71]; 3 – [39]; 4 – [51].

Four methane samples studied by Hunt [40] were collected at depths of 4.8-6.3 m below the sediment surface in deep part of the Black Sea in the zone where (as many suggest) a biogenic methane appears [5, 92]. However methane samples analyzed by Hunt [40] had $\delta^{13}C$ values typical for biogenic methane. More isotopically lighter methane ($\delta^{13}C$ up to -91‰) has been recently found in sediments of the central Black Sea [88].

Cold methane seeps discovered in 1988 during the expedition of the Institute of Biology of the Southern Seas (Sevastopol) are active sources of methane [83]. By now, methane seeps have been discovered around the whole periphery of the Black Sea at different depths up to 2100 m [28]. The annual flux of methane into the water column of the western part of the Black Sea from these sources have been estimated to be 9.8 10^{10} mol. According to Dimitrov's data [26], CH_4 emission to the atmosphere in the area of cold seeps varies from 2 to 10 10^{10} mol of methane per year.

The first analysis of the isotopic composition of methane coming in the form of bubble streams from a carbonate construction (at 226 m water depth) gave $\delta^{13}C$ of -58.2‰ [48], the value indicative of its microbiological origin. We carried out extensive investigations of the isotopic composition of methane from the Black Sea seeps in samples collected directly from vents by submarine "Jago" during the international expedition within the framework of GOSTDABS project (under the leadership of Prof. W. Michaelis, Hamburg University) in June – July 2001. Table 14 shows the chemical composition of gases as well as the isotopic composition of carbon and hydrogen of methane from gas seeps [71]. A group of German participants of GOSTDABS has obtained similar to our results. The carbon isotopic composition of methane in cold seeps varied from -62.4 to -68.3‰ [81]. $\delta^{13}C$ and δD data given in Table 14 unambigu-

ously demonstrate the biogenic origin of methane formed by microbiological reduction of CO_2 with hydrogen [99]. Extremely low content of heavy gaseous homologues of methane in gaseous fluids of seeps also suggested biogenic origin of methane. The analysis of our samples (Table 14) shows that the content of these homologues does not usually exceed 0.001% [71]; content of heavy hydrocarbons in gas samples collected on the Bulgarian shelf was 0.1-0.4% [26]. Therefore, the biogenic origin of methane from cold seeps is confirmed by (i) the carbon and (ii) hydrogen isotopic composition of emitted methane, and by (iii) the composition of methane homologues.

Table 14. Chemical composition of gases and the isotopic composition of methane (δ^{13}C and δ D) from cold methane seeps of the Dnieper Canyon [71].

Station	*Depth, m*	*Composition of gases, vol %*				$\delta^{13}C$ *(PDB),* ‰	δD *SMOW,* ‰
		CH_4	H_4	N_2	CO_2		
14	182	95.0	–	–	–	–68.2	–
21	225	99.0	0.17	0.90	0.00	–68.1	–
33	324	95.1	0.25	4.60	0.26	–70.5	–144
38	230	99.0	0.02	0.90	0.80	–64.0	–132
46	111	99.1	0.01	0.00	0.90	–65.0	–
51	371	94.9	0.02	5.10	0.05	–63.0	–
55	226	99.6	0.00	0.17	0.26	–66.5	–201
61	64	96.2	0.01	3.60	0.10	–65.0	–
68	321	98.8	0.02	1.10	1.10	–68.5	–169
85	230	96.8	0.01	3.20	0.00	–62.4	–

There is no reason to believe that all methane is produced in modern sediments of the Black Sea. Methane distribution with depth in sediments down to 3.0-3.5 m revealed a constant increase in methane concentrations up to 50-75 mM in pore water [54]. Rates of methanogenesis measured with $NaH^{14}CO_3$ have showed that microbial methanogenesis occurs in the whole sequence of Holocene sediments down to a depth of at least 2.6 m [46]. Methanogenesis in sediments of the western Caspian Sea have been detected to sediment depths as high as 100 m [47]. Many researchers associated the distribution of methane seeps with fractures in the sea bed. Biogenic methane emitted along these fractures comes from the sapropel layer rich in organic carbon.

Mud volcanoes and sub-sea gas hydrates in the lower part of the continental slope (700-750 m water depth) and in the deep basin are the third source of the Black Sea methane [33, 41, 61]. Mud volcanoes are located on tectonic dislocations, which suggests that methane emitted from volcanoes can be of thermocatalytic origin. The data on the isotopic composition of methane from

mud volcanoes and gas hydrates of the Black Sea (Table 15) obtained so far suggest that the interpretation of methane origin in these areas is not straightforward. The carbon isotopic composition typical for thermocatalytic methane (δ^{13}C of -30.0‰ to -50.0‰) was detected only over large mud volcanoes in the central part of the Western gyre and in Sorokin Trench [11, 42] (Table 15). The isotopic data obtained in other mud volcanoes and gas hydrates showed much lighter carbon isotopic composition of methane (δ^{13}C from -55.0‰ to -75‰) (Table 15). These values are typical for methane produced during CO_2 reduction with hydrogen by autotrophic methanogens [99]. The data on the composition of gaseous methane homologues are less unique; their content in the samples collected in the central Black Sea does not reach several per cents [42]. Such composition is more indicative of the thermocatalytic methane. In contrast, samples from Sorokin Trench contained less than one per cent of these homologues. The authors reported that some samples with light isotopic composition of methane carbon sometimes contained abundant gaseous homologues of methane [42].

The data on the isotopic and gas composition of mud volcanic fluids are scarce. Most of them have been published as briefs submitted to various conferences. The fact that mud volcanoes are located along tectonic fracture zones does not necessarily indicate that gas emitting from these fractures is generated at greater depths and at high temperatures. Methane of a biogenic origin (formed in Black Sea sediments of 12-15 km thick during past geological epochs) may come to the surface along geological fractures. This is true for methane generated in non-consolidated Pleistocene sediments with high organic carbon content.

The isotopic composition of methane dissolved in the aerobic and anaerobic water columns of the Black Sea is poorly studied. Table 16 shows a few data points published in the literature and data kindly offered to us by Prof. R. Seifert, which were obtained during GOSTDABS expedition. During this expedition, dissolved methane and methane collected directly from bubble streams were sampled by a group of German scientists on board submersible “Jago”. Most investigations were carried out in the Dniper Canyon with active methane seeps. The analysis of the isotopic composition of methane sampled at the site of its outcome and from bubble streams at various depths has been performed. The results showed that along a gas bubble path, the isotopic composition of methane is getting heavier because of the selective dilution of the isotopically lighter methane (Table 16, No. 2 and 3). Dissolved methane was considerably heavier than methane sampled from bubble streams at the same depths in the water column (Table 16, No. 3 and 4). This phenomenon can be explained by active anaerobic oxidation of methane [3], which occurs within the sulfide zone (see above, Fig. 7).

Table 15. The carbon isotope composition of methane from mud volcanoes and gas hydrates.

	Description of sites	$\delta^{13}C$, ‰	*Reference*
1	Large mud volcanic structures of the central part of the sea	−30.0 ÷ −50.0	[42]
	and Sorokin Trench	−40.0 ÷ −42.0	[11]
2	Small mud volcanoes of Sorokin Trench	−55.0 ÷ −75.0	[42]
3	Gas hydrates and host sediments	−61.0 ÷ −65.0	
4	Gas hydrates from Dvurechensky mud volcano*	−62.0 ÷ −66.0	[7]
5	Sediments of volcanic structures and gas hydrates	−61.8 ÷ −63.5	[11]
6	Gas from sediments at volcanic structures	−63.9	Data from CRIMEA Expedition

* δ D of methane in the sample varied from –185 to –209 ‰ SMOW.

An active process of microbial methane oxidation causes the increase of the isotopic composition of residual methane (up to $\delta^{13}C$ = -19.0‰) in the chemocline (Table 16, No. 3 and 5). In the oxic zone, isotopically light methane ($\delta^{13}C$ varied from -40.0‰ to -60.6‰; Table 16) has been detected. This methane is generated in anaerobic microniches (zooplankton intestines, pellets, and other particles) due to the activity of anaerobic methanogens. Our experiments with $^{14}CO_2$ and $^{14}CH_3COONa$ have demonstrated that the rate of methanogenesis in one liter of water from the oxic zone may be as high as 170-180 nl of CH_4 per day; the excess of microbial methane production over its consumption varies between 0.6 to 5.4 ml m^{-2} per day for the whole oxic zone [86]. These new experimental data explain a sharp increase in the methane content within the oxic zone, which many investigators have described [27, 29, 52]. A bulk of methane in the sulphidic zone is oxidized upon contact with waters containing dissolved oxygen. Methane produced during methanogenesis on particles in the oxic zone is the main source of methane emitting to the atmosphere [86]. Unfortunately, the isotopic composition of methane in the sulphidic zone of the central part of the Black Sea was not adequately studied. Schubert et al. [88] reported $\delta^{13}C$ of methane of -50‰ in the central Black Sea. The heavier

Table 16. The carbon isotope composition of the Black Sea methane.

	Description of samples	$\delta^{13}C$, ‰	*Reference*
1	Methane from the upper Holocene sediments	−67.6* / −60.4 ÷ −91.0	Figure 8
2	Methane from cold seeps	−65.8 / −62.0 ÷ −72.0	Figure 9
3	Methane from bubble streams	−64.5 / −58.5 ÷ −68.4	[89]
4	Dissolved methane in the sulfidic zone	−55.4 / −50.8 ÷ −58.0	[89]
5	Dissolved methane in the chemocline zone	−35.2 / −19.0 ÷ −48.5	[89] [88]
6	Dissolved methane in the oxic zone	−54.3 / −40.0 ÷ −66.6	[89] [88]
7	Thermogenic methane dissolved in the sulfidic zone above mud volcanoes	−45.7 / −43.0 ÷ −47.5	[89]
8	Methane from mud volcanoes	−30.0 ÷ −50.0	Table 15

*Numerator – the average δ^{13}C;
denominator – range of δ^{13}C.

isotopic composition of methane ($\delta^{13}C_{average}$ = -45.7‰) was found at depths of 900-2070 m at station 28 around mud volcano in the central part of the western gyre.

Using the total amount of microbial methane produced in the water column (M_{bio} = 62 10^{10} M year^{-1}) as well as the total amount of methane oxidized (M_{tot} = 77.7 10^{10} M year^{-1}), we can calculate the total production of methane from seeps and mud volcanoes ($M_{sip} + M_{volc.}$ = 14.8 10^{10} M year^{-1}) [52].

We also know δ^{13}C of methane from external sources: from cold seeps of δ^{13}C = -65.8‰ (Table 16); from mud volcanoes of $\delta^{13}C_{volc}$ = -40‰ (Table 16). The δ^{13}C of biogenic methane is -67.6‰ (Table 16 No. 1), the rating value of δ^{13}C of total dissolved methane ($\delta^{13}C_{tot}$) is -64.5‰. The δ^{13}C of dissolved methane (-55.4‰; Table 16, No. 3) increased by -9.1‰ (a difference in the carbon isotope composition between methane in bubbles and anaerobically oxidized methane) served as a basis for our calculations. We calculated the δ^{13}C of external methane coming from mud volcanoes and seeps using the isotope-mass balance:

$$\delta^{13}C_{sip+volc} = \frac{\delta^{13}C_{bio} \times M_{bio} - \delta^{13}C_{tot} \times M_{tot}}{M_{sip}+_{volc}} = -51.3‰$$

We calculated the total amount of methane coming from volcanoes (M_{volc}) and seeps (M_{sip}):

$$M_{volc} = \frac{M_{sip+volc} \times \delta^{13}C_{sip} - M_{sip+volc} \times \delta^{13}C_{sip+volc}}{(\delta^{13}C_{volc} - \delta^{13}C_{sip})} = 7,8 \times 10^{10}\text{moles/year}$$

The annual flux of methane from external sources (mud volcanoes and cold methane seeps) should be similar (7.8 and 7.0 10^{10} moles/year, respectively). It is noticebale that our calculation of the annual flux of methane from seeps is close to the estimation of Egorov and his colleagues (9.8 10^{10} moles/year) who used a different method of calculation [28].

In cold seeps and mud volcanoes, a large-scale anaerobic methane oxidation is associated with the methane release. This process is followed by accumulation of the isotopically light organic matter of bacterial mats and methane-derived carbonate minerals. First analyses which we carried out in 1989 [48] revealed that the $\delta^{13}C$ values of aragonite from carbonate constructions ranged between -35 to -42‰; $\delta^{13}C$ of organic matter of microbial mats was -82.5‰.

Figure 9 shows the results of more detailed investigations of the isotopic composition of organic matter and lipid fraction of mats as well as of aragonite from carbonate constructions and calcite from their base [69, 71, 77]. Insignificant depletion in ^{13}C of organic carbon compared to that of methane is the result of fractionation of carbon isotopes during the synthesis of microbial biomass. The lipid fraction is far more depleted in ^{13}C. Inorganic carbon dissolved in seawater takes part in the formation of carbonate minerals as well, along with the isotopically light carbon dioxide produced during methane oxidation. The carbon of carbonate minerals is therefore less depleted in ^{13}C compared to carbon of the microbial biomass. The difference in the isotopic composition of aragonite from carbonate constructions and of calcite from its base can be explained by the fact that carbonate minerals at the base contain isotopically heavy carbonate precipitated from the water column.

7. CONCLUSIONS

1. The results of detailed investigations of the isotopic composition of hydrogen sulfide and sulfates in the water column and bottom sediments of the Black Sea have confirmed that hydrogen sulfide is produced mostly in the anaerobic water column due to activity of sulfate-reducing bacteria.

2. A comparison between the data on the rates of sulfate reduction and $\delta^{34}S$ of hydrogen sulfide has confirmed the results of laboratory experiments

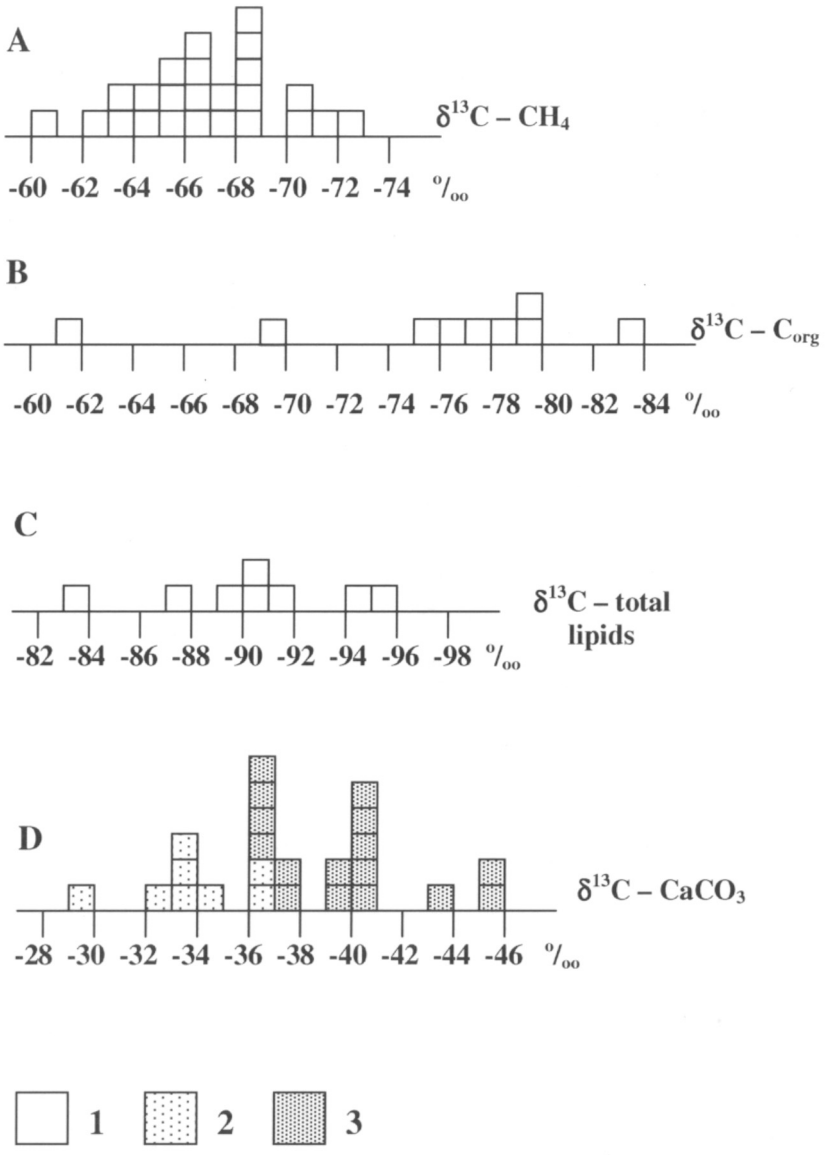

Figure 9. Carbon isotopic composition of methane from cold seeps (A), organic carbon of microbial mats covered carbonate constructions (B); organic carbon of total lipids (C) and carbonate minerals, formed as result of anaerobic oxidation of methane (C) [69, 70, 71]. 1 – $\delta^{13}C$ of CH_4, organic carbon and lipids of bacterial mats; 2 – $\delta^{13}C$ of calcite; 3 – $\delta^{13}C$ of aragonite.

on the inverse relationship between the rate of sulfate reduction and $^{32}S/^{34}S$ fractionation.

3. Distinct seasonal changes of the isotopic composition of POC have been observed. In early spring and summertime during phytoplankton blooms, POC is less depleted in ^{13}C.

4. An additional depletion in ^{13}C of POC was observed in the zone of active development of phototrophic and chemoautotrophic microorganisms at the oxic/anoxic interface. The isotopically light biomass of autotrophic microorganisms is rapidly consumed by anaerobic heterotrophic microorganisms, mainly by sulfate-reducing bacteria.

5. Analysis of the geochemical activity of microorganisms participating in the methane cycle as well as from the data on the isotopic composition of the Black Sea methane show that about 80% of methane dissolved in the water column is generated due to in situ activity of methanogens. Methane fluxes from cold seeps and mud volcanoes are responsible for an additional 10% of the methane production each. Methane coming from bottom sediments does not play any significant role in the methane balance of the water column.

6. A large-scale anaerobic methane oxidation was detected in the water column, bottom sediments, and close to cold seep vents and mud volcanoes. This process is followed by the accumulation of isotopically light carbonate minerals and extremely light organic carbon of bacterial mats.

7. In anaerobic microniches of organic matter particles suspended in the aerobic water column, autotrophic methanogenesis takes place. This process results in the formation of isotopically light methane, in aerobic waters. A portion of this methane migrates from the water column to the atmosphere.

Acknowledgments

This work was supported by the Russian Academy of Sciences (grant MCB RAS).

References

[1] Albert D-B., Taylor C. and Martens C.S. Sulphate reduction rate and low molecular weight fatty acid concentrations in the water column and surfical sediments of the Black Sea. Deep Sea Res 1995; 42:1239-60.

[2] Alekseev E.A. and Lebedev V.S. "Carbon isotope composition of CO_2 and CH_4 of the Black Sea bottom sediments." In *Dissipated gases.* Moscow, VNIIYAGG, 1975. (In Russian)

[3] Alperin M.J., Reeburgh W.S. and Whiticar M.I. Carbon and hydrogen isotope fractionation resulting from anaerobic methane oxidation. Global biogeochemical cycles 1988; 2:279-88.

[4] Andrusov N.I. Preliminary report about participation in deep-water cruise. Izvestiya Russkogo geographicheskogo obchestva, 1890; 26(5):25-38. (In Russian)

[5] Berlin Yu.M., Bolshakov A.N., Verchovskaya Z.I., Egorov A.V., Marina M.M. and Trotsuk V.Ya. "Methane in the Danube and Kisil-Ermak prodelta sediments." In *Lithologiya i Geochimiya osadkoobrazovaniya.* Akad. Nauk SSSR, I. Okeanologii 1987; 116-126. (In Russian)

[6] Bezborodov A.A. and Eremeev L.G. Variability in structure of O_2-H_2S zone: dramatical or synoptical. Morskoy Hydrophizicheskiy Zhurnal (Sevastopol) 1991; (1):59-68. (In Russian)

[7] Blinova V.N., Ivanov M.K. and Bohrman G. Study of hydrocarbon gases in deposits from mud volcanoes in Sorokin Trench. Methane seepage, mud volcanoes and hydrates in the Black Sea (2004). Leibniz-Institut für Meereswissenschaften, Deutchland.

[8] Bird D.F. and Karl D.M. Microbial biomass and population diversity in the upper water column of the Black Sea. Deep Sea Res 1991; 38:1069-82.

[9] Bologa A.S., Frangopol P.T., Vedernicov V.I., Stelmach L.V., Yunev O.A., Yilmaz A. and Oguz T. "Distribution of planktonic primary production in the Black Sea." In *Environmental degradation at the Black Sea: challenges and remedies.* Besiktepe S.T., Unliiata U., Bologa A. eds., Kluwer Academic Publishers Dorchester, 1999.

[10] Breas O., Guillou C., Lancelot C., Martin Y.-M., Mousty F. and Reniero F. Measurments of the $^{13}C/^{12}C$ particulate and dissolved organic matter in the Black Sea and Danube river. Joint Res. Centre-Ispra, Environ. Institute Ispra, Italy, 2000.

[11] Byakov Y.A., Kruglyakova R.P. and Kruglyakov M.V. Gas hydrates of the Black Sea sediment section: genesis, geophysical methods for their discovery and mapping. Gas in marine sediments. Abstract book of the 7th International conference. Baku, 2002; 24-26.

[12] Calvert S.E, Thode H.D., Yeung D.A. and Karlin R.E. A stable isotope study of pyrite formation in the Late Pleistocene and Holocene sediments of the Black Sea. Geochim Cosmochim Ac 1996; 60:1261-70.

[13] Canfield D.E. Isotope fractionation by natural populations of sulfate-reducing bacteria. Geochim Cosmochim Ac 2001a; 65:1117-24.

[14] Canfield D.E. "Biogeochemistry of sulphur isotopes." In *Stable isotope geochemistry.* Valley J.W. and Cole D.R. eds., Review in Mineralogy and Geochemistry 2001; 43:607-36.

[15] Canfield D.E., Thamdrup B. and Fleischer S. Isotope fractionation and sulfur metabolism by pure and enrichment cultures of elemental sulfur-disproportionating bacteria. Limnol Oceanogr 1998; 43:253-54.

[16] Canfield D.E. and Thamdrup B. The production of ^{34}S-depleted sulfide during bacterial disproportionation of elemental sulfur. Science 1994; 266:1973-75.

[17] Canfield D.E., Raiswell R. and Bottrell S. The reactivity of sedimentary iron minerals toward sulfide. Am J Sci 1992; 292:659-83.

[18] Castro H.F., Williams N.H. and Ogram A. Phylogeny of sulfate-reducing bacteria. FEMS Microbiol Ecol 2000; 31:1-9.

[19] Chambers L.A., Trudinger P.A., Smith J.W. and Burns M.S. Fractionation of sulfur isotopes by continuous cultures of *Desulfovibrio desulfuricans*. Can J Microbiol 1975; 21:1602-07.

[20] Chambers L.A., Trudinger P.A., Smith J.W. and Burns M.S. A possible boundary condition in bacterial sulfur isotope fractionation. Geochim Cosmochim Ac 1976; 46:721-28.

[21] Cypionka H., Smock M.E. and Böttcher M.E. A combined pathway of sulfur compound disproportionation in *Desulfovibrio desulfuricans*. FEMS Microbiol Lett 1998; 166:181-86.

[22] Danilchenko P.T. and Chigirin N.I. About origin of hydrogen sulfide in the Black Sea. Tr. Sevastopol'skoi biol. St. Akad. Nauk SSSR 1926; (10):141-52. (In Russian)

[23] Detmers J., Brüchert V., Habicht K.S. and Kuever J. Diversity of sulfur isotope fractionations by sulfate reducing prokaryotes. Appl Environ Microbiol 2001; 67:888-94.

[24] Deuser W.G. Isotopic evidence for diminishing supply of available carbon during diatom bloom in the Black Sea. Nature 1970a; 225:1069-71.

[25] Deuser W.G. Carbon-13 in Black Sea waters and implications for the origin of hydrogen sulphide. Science 1970b; 168(3937):1575-77.

[26] Dimitrov L. Contribution to atmospheric methane by natural seepages on the Bulgarian continental shelf. Continental Shelf Res 2002; 22:2429-42.

[27] Egorov V.N. Methane distribution in the water column and bottom sediments of the NE part of the Black Sea. NATO ARW Past and present water column anoxia, 4 - 8. Oct. 2003, Crimea, 34-36.

[28] Egorov V.N., Polikarpov G.G., Gulin S.B., Artemov Yu.G., Stakosov M.A. and Kostova S.K. Modern concept about forming-casting and ecological role of methane gas seeps from bottom of the Black Sea. Morskoy ecologicheskii zhurnal 2004; 3:5-26. (In Russian).

[29] Gal'chenko V.F., Lein A.Yu. and Ivanov M.V. (a). Methane content in the bottom sediments and water column of the Black Sea. Microbiol 2004; 73(2):258-70.

[30] Gal'chenko V.F., Lein A.Yu. and Ivanov M.V. (b). Rates of microbial production and oxidation of methane in the bottom sediments and water column of the Black Sea. Microbiol 2004, 73(2):271-83.

[31] Galimov E.M., Kodina L.A., Zhiltsova L.I. and Vlasova L.N. Organic carbon geochemistry in the northwestern Black Sea – Danube river system. Geochemistry International 1999; 7:675-85.

[32] Galimov E.M., Kodina L.A., Zhiltsova L.I., Tokarev V.G., Vlasova L.N., Bogacheva M.P., Korobeinik G.S. and Vaisman T.I. Organic carbon geochemistry in the northwestern Black Sea – Danube river system. Estuar Coast and Shelf Sci 2002; 64(3):631-41.

[33] Ginsburg G.D. and Soloviev V.A. *Submarine Gas Hydrates.* Statoil, Norway, 1998.

[34] Gulin M.B. Study of bacterial processes of sulphate reduction and chemosyntesis in waters of the Black Sea. Ph.D. thesis, Institute of the Biology of the Southern Seas, Sevastopol, 1991; 20. (In Russian)

[35] Freeman K.H. "Isotope biogeochemistry of marine organic carbon." In *Stable isotope geochemistry.* Valley J.W. and Cole D.R. eds., Rev mineral geochem 2001; 43:579-606.

[36] Fry D., Jannash H.-W., Molinaux S.I., Wirsen S.O., Muramoto J.A. and King S. Stable isotope studies of the carbon, sulphur and nitrogen cycles in the Black Sea and Cariaco Trench. Deep Sea Res 1991; 38:1003-19.

[37] Habicht K.S. and Canfield D.E. Isotope fractionation by sulfate-reducing natural populations and the isotopic composition of sulfide in marine sediments. Geology 2001; 29:555-58.

[38] Hayes J.M. "Fractionation of carbon and hydrogen isotopes in biosynthetic processes." In *Stable isotope geochemistry.* Valley J.W. and Cole D.R. eds., Rew. in mineralogy and geochemistry 2001; 43:225-78.

[39] Hunt Y.M. and Whelan Y.K. Dissolved gases in the Black Sea sediments. Init. Rep. Deep Sea Drilling Project 1978; 42:661-65.

[40] Hunt Y.M."Hydrocarbon geochemistry of the Black Sea". In *The Black Sea – Geology, Chemistry and Biology* E.T. Degens and D.A.Ross, eds. Amer Ass Petrol Geology Tulsa, Oklahoma, USA, 1974; 26:499-504.

[41] Ivanov M.K., Limonov A.F. and van Weering Tjce. Comparative characteristics of the Black Sea and Mediterranian mud volcanoes. Mar Geol 1996; 132:253-71.

[42] Ivanov M.K. and Stadnitskaya A. Methane-seeps related processes in the Black Sea NATO ARW Past and present water column anoxia, 4 – 8 Oct. 2003 Crimea Ukraine, 39-41.

[43] Ivanov M.V. Using isotopes for studying the rates of sulfate reduction in Belovod Lake. Microbiologiya 1956; 25:3.

[44] Ivanov M.V., Lein A.Yu. and Kashparova E.V. "The intensity of formation and diagenetic transformation of reduced sulfur compounds in the Pacific Ocean sediments." In *Biogeochemistry of diagenesis of ocean sediments.* Volkov I.I. ed., Nauka, 1976.

[45] Ivanov M.V. and Lein A.Yu. Distribution of microorganisms and their role in processes of diagenetic mineral formation. In *Geochemistry of diagenesis of the Pacific Ocean sediments.* Nauka, Moscow, 1980.

[46] Ivanov M.V., Vainshtein M.B., Gal′chenko V.F., Gorlatov S.N. and Lein A.Yu. "Distribution and geochemical activity of the bacteria in the sediments." In *Oil and gas genetic studies of the Bulgarian sector of the Black Sea* Publ. House. Bulgar. Acad. Sci. Sofia, 1984. (In Russian).

[47] Ivanov M.V., Belyaev S.S., Laurinavichus K.S. and Obraztsova A.Ya. Microbial H_2S and CH_4 formation in modern and quaternary sediments of the Caspian Sea. Geochimistry International 1980; 3:416-22.

[48] Ivanov M.V., Polykarpov G.G., Lein A.Yu., Gal′chenko V.F., Egorov V.N., Gulin S.B., Gulin M.B., Rusanov I.I., Miller Yu.M. and Kuptsov V.I. Biogeochemistry of carbon cycle at the Black Sea methane seeps. Doklady Academii Nauk SSSR, 1991; 320(5):1235-40. (In Russian).

[49] Ivanov M.V., Rusanov I.I., Pimenov N.V., Bairamov I.I., Yusupov S.K., Savvichev A.S., Lein A.Yu. and Sapozhnikov V.V. Microbial processes of the carbon and sulfur cycles in the Lake Mogil′noe. Mikrobiology 2001; 70(5):675-86.

[50] Ivanov M.V., Lein A.Yu., Miller Yu.M., Yusupov S.K., Pimenov N.V., Wherly B., Rusanov I.I. and Zehnder A. The effect of microorganisms and seasonal factors on the isotopic composition of particulate organic carbon from the Black Sea. Microbiology 2000; 69(4):541-52.

[51] Ivanov M.V., Pimenov N.V., Rusanov I.I. and a. Lein A.Yu. Microbial processes of the methane cycle at the northwestern shelf of the Black Sea. Estuarine Coastal and Shelf Science 2002; 54:589-99.

[52] Ivanov M.V., Rusanov I.I., Lein A.Yu., Pimenov N.V., Yousupov S.K. and Gal′chenko V.F. Biogeochemistry of methane cycle in the anaerobic zone of the Black Sea. NATO ARW Past and present water column anoxia, 4-8 0ct. 2003, Crimea, Ukraine, 42-43.

[53] Issatshenko B.L. (1929) "Characteristics of bacteriological processes in the Black Sea and Sea of Azov." In Issatehenko B.L., *Selected Papers,* USSR, Acad. of Sciences, 1951; I:364-374. (In Russian)

[54] Jorgensen B.B., Weber A. and Zopfi J. Sulfate reduction and anaerobic methane oxidation in Black Sea sediments. Deep Sea Res I 2001; 48:2097-120.

[55] Kaplan I.R. and a. Rittenberg S.C. Microbiological fractionation of sulphur isotopes. J Gen Microbiol 1964; 34:195-212.

[56] Karl D.M. and Knauer G.A. Microbial production and particle flux in the upper 350 m of the Black Sea. Deep Sea Res 1991; 38(2):921-42.

[57] Krämer M., Cypionka H. Sulfate formation via ATP sulfurylase in thiosulfate- and sulfite-disproportionating bacteria. Arch. Microbiol 1989; 151:232-37.

[58] Kodina L.A., Bogacheva M.P. and Lyutsarev S.V. Particulate organic carbon in the Black Sea: Isotopic composition and genesis, Geochemistry International 1996; 9:884-90.

[59] Kodina L.A. and Vlasova L.N. Distribution of organic carbon stable isotopes in the upper layer of the Black Sea. Geochemistry International 2000; 11:1209-18.

[60] Korsakov O.D., Byakov Yu.A. and Stupak S.N. Gas hydrates of the Black Sea Trench. Sovetskaya geologiya 1989; 12:3-10. (In Russian)

[61] Kremlev A.N. and Ginsburg G.D. The first results of the search for submarine gas hydrates in the Black Sea. Geologiya i Geophisika 1989; 4:110-11. (In Russian)

[62] Kriss A.E. *Marine Microbiology (Deep Sea).* Oliver and Boyd, Edinburg, 1963.

[63] Lancelot C., Martin J.-M., Panin M. and Zaitsev Yu.P. The North - western, Black Sea: A pilot site to understand the complex interaction between human activities and the coastal environment. Estuar Coast Shelf Sci 2002; 54(3):641.

[64] Lein A.Yu. The isotopic mass balance of sulfur in oceanic sediments (the Pacific Ocean as an example). Marine Chemistry 1985; 16:249-57.

[65] Lein A.Yu. "Formation of carbonate and sulfide minerals during diagenesis of reduced sediments." In *Environmental biogeochemistry and geomicrobiology.* Krumbein W. ed., Ann Arbor Sci Publ, 1978.

[66] Lein A.Yu., Ivanov M.V. and Vainshtein M.B. Hydrogen sulphide balance in the deep-sea zone of the Black Sea. Microbiology 1990; 59(4):656-65.

[67] Lein A.Yu. and Ivanov M.V. Hydrogen sulfide production in shelf sediments and its balance in the Black Sea. Microbiology 1990; 59(5):921-8.

[68] Lein A.Yu. and Ivanov M.V. "On the sulfur and carbon balances in the Black Sea (1991)." In *Black Sea Oceanography,* Izdar E. and Murray J.W. eds., Kluwer Acad. Publ., Dordrecht/Boston/London, 1992.

[69] Lein A.Yu., Ivanov M.V., Pimenov N.V. and Gulin M.B. Geochemical characteristics of the carbonate constructions formed during microbial oxidation of methane under anaerobic conditions. Microbiologiya 2002; 70:78-90. (In Russian)

[70] Lein A., Pimenov N., Guillou C., Martin J.-M., Lancelot C., Rusanov I., Yusupov S., Miller Yu. and Ivanov M. Seasonal dynamics of the sulfate reduction rate on the north-western Black Sea shelf. Estuar Coast Shelf Sci. 2002; 54(3):385-403.

[71] Lein A.Yu., Ivanov M.V. and Pimenov N.V. Genesis of methane from cold methane seeps of the Dniepr canyon of the Black Sea. Dokl. Acad. Nauk 2002: 387:242-4. (In Russian)

[72] Lein A.Yu. and Ivanov M.V. The biggest methane basin on Earth. Priroda 2005; 2:19-26.

[73] Liu Lei. Sulfur compounds and their isotopic composition in the Caucasus shelf and slope sediments. Ph.D. thesis, Shirshov Inst. Oceanol. Moscow, 1993. (In Russian)

[74] Luther G.W. III "Sulfur and iodine speciation in the water column of the Black Sea." In *Black Sea Oceanography.* Izdar E. and Murray J.W. eds., NATO ASI Series, Series C; Mathematical and Physical Sciences. Kluwer, 1991.

[75] Lyons T.W. "Upper Holocene sediments of the Black Sea; Summary of Leg 4 box cores (1988 Black Sea Oceanographic Expedition)." In *Black Sea Oceanography.* Izdar E. and Murray J.W. eds., NATO Asi Series, Series C; Mathematical and Physical Sciences. Kluwer, 1991.

[76] Lyons T.W. Sulfur isotopic trends and pathways of iron sulfide formation in Upper Holocene sediments of the anoxic Black Sea. Geochim Cosmochim Ac 1997; 61:3367-82.

[77] Michaelis W., Seifert R. and Nauhaus K. et al. Microbial reefs in the Black Sea fueled by anaerobic oxidation of methane. Science 2002; 297:1013-1015.

[78] Muramoto J., Honjo S., Fry B., Hay B.J., Howarth R.W. and Cisne J.L. Sulfur, iron and organic carbon flaxes in the Black Sea: sulfur isotope evidence for origin of sulfur fluxes. Deep Sea Res II 1991; 38(2A):1151-84.

[79] Neretin L.N., Bottcher M. and Volkov I.I. The stable isotope composition of sulfur species in the Black Sea water column. Mineral Mag 1998; 62A:1075-6.

[80] Neretin L.N., Volkov I.I., Bottcher M.E. and Grinenko V.A. A sulfur budget for the Black Sea anoxic zone. Deep Sea Res I 2001; 48:2569-93.

[81] Pape T., Seifert R., Blumenberg M., Naubaus K., Widdel K., Raitner J., Konderding P., Wong H.-K. and Michaelis W. Results of GHOSTDABS Projelt, Topic Biogeochemistry. Methane seepages, mud volcanoes and hydrates in the Black Sea. Leibniz Institut fur Meereswissenschaften, 2004.

[82] Pfening P., 1987 (cited by Canfield D.E., 2001 b).

[83] Polikarpov G.G., Egorov V.N., Nezdanov A.I. et al. Active gas seeping from the Black Sea continental slope. Doklady Academii Nauk Ukrainian SSR. Ser. B. 1989, 12:13-16. (In Russian)

[84] Reeburgh W.S., Ward B.B., Whalen S.C., Sandbeck K.A., Kilpatrick K.A. and Kerthof L.J. Black Sea methane geochemistry. Deep Sea Res 1992; 38:1189-210.

[85] Rusanov I.I., Savvichev A.S., Yusupov S.K., Pimenov N.V. and Ivanov M.V. Production of exometabolites in the microbial oxidation of methane in marine ecosystems. Microbiology 1998; 67(5):590-6.

[86] Rusanov I.I., Yusupov S.K., Savvichev A.S., Lein A.Yu., Pimenov N.V. and Ivanov M.V. Microbial methane generation in aerobic Black Sea water column. Dokl. Acad. Nauk. 2004; 398(5):1-3. (In Russian)

[87] Saliot A., Derieux S., Sadouni N., Bouloubassi I., Fillaux J., Dagaut J., Momzikoff A., Gondry G., Guillow C., Breas O., Cauwet G. and Deliat G. Winter and spring characterization of particulate and dissolved organic matter in the Danube – Black Sea mixing zone. Estuar Coast Shelf Sci 2002; 54:355-67.

[88] Schubert K.J., Kaizer E.J., Knypers M. and Wehrly B. Methane formation and oxidation in the Black Sea. NATO ARW Past and present water column anoxia, 4-8 October 2003, Crimea Ukraine, 82-83.

[89] Seifert R. Preliminary results of GOSTDABS project (personal communication), 2002.

[90] Skopintsev B.A. *Formation of modern chemical composition of the Black Sea waters.* Hydrometeoizdat, Leningrad, 1975. (In Russian)

[91] Sorokin Yu.I. Experimental study of bacterial sulfate reduction in the Black Sea with the use of ^{35}S. Microbiology 1962; 31:402-10.

[92] Sorokin Yu.I. *The Black Sea: Ecology and Oceanography.* Backhuys Publishers, Leiden, 2002.

[93] Sweeney R.E. and Kaplan I.R. Stable isotope composition of dissolved sulfate and hydrogen sulfide in the Black Sea. Mar Chem 1980; 9:145-52.

[94] Vinogradov A.P., Grinenko V.A. and Ustinov V.I. Isotopic composition of sulfur compounds in the Black Sea. Geochimiya 1962; 10:857-61. (In Russian)

[95] Volkov I.I. The geochemistry of sulphur in the oceanic sediments. Nauka, Moscow, 1984.

[96] Wakeham S.G., Beier J.A., Glifford C.H. "Organic matter sources in the Black Sea as inferred from hydrocarbon distributions." In *Black Sea Oceanography,* Izdar E. and Murray I.W. eds., Kluwer Acad. Publ., Dordrecht/Boston/London, 1991.

[97] Weber A., Riess W., Wenzhoefer F., Jorgensen B.B. Sulphate reduction in Black Sea sediments: in situ and laboratory radiotracer measurements from the shelf to 2000 m depth. Deep Sea Res I 2001; 48:2073-96.

[98] Wilkin R.T. and Arthur M.A. Variation in pyrite texture, sulfur isotope composition, and iron systematics in the Black Sea: evidence for late Pleistocene to Holocene excursions of the $O_2 - H_2S$ redox transition. Geochim Cosmochim Ac 2001; 65:1399-416.

[99] Whiticar M.J., Faber E. and Schoell M. Biogenic methane formation in marine and freshwater environments: CO_2 reduction vs. acetate fermentation – Isotope evidence. Geochem Cosmochim Ac 1986; 50:693-709.

[100] Zelinsky N.D. About hydrogen sulfide fermentation in the Black Sea and Odessa estuaries. Zhurnal Rossiyskogo Physico-khimicheskogo Obshestva 1893; 5:25. (In Russian)

[101] Yilmaz A., Coban Yildiz, Morcos E. and Bologa A. "Sources of surface and midwater of organic carbon by photo- and chemo-autotrophic production in the Black Sea." In *Oceanography of Eastern Mediterranian and the Black Sea.* Yilmaz A. ed., Tubitak Publishers, Icel, Turkey, Ankara, 2003.

[102] Coban Yildiz, Altaber M.A., Yilmaz A., Tugrul S. and Salihoglu I. "Carbon and nitrogen isotopic ratios of suspended particulate organic matter in the Black Sea water column." In *Oceanography of Eastern Mediterranian and the Black Sea.* Yilmaz A. ed., Tubitak Publishers, Icel, Turkey, Ankara, 2003.

RECENT STUDIES ON SOURCES AND SINKS OF METHANE IN THE BLACK SEA

Carsten J. Schubert[1], Edith Durisch-Kaiser[1], Lucia Klauser[1], Francisco Vazquez[1], Bernhard Wehrli[1], Christian P. Holzner[2], Rolf Kipfer[2], Oliver Schmale[3], Jens Greinert[3] and Marcel M.M. Kuypers[4]

[1] *EAWAG, Surface Waters, Seestrasse 79, 6047 Kastanienbaum, Switzerland*

[2] *EAWAG, Water Resources and Drinking Water, Überlandstrasse 133, 8600 Dübendorf, Switzerland*

[3] *Leibniz-Institute of Marine Sciences (IFM-GEOMAR), Wischhofstrasse 1-3, 24148 Kiel, Germany*

[4] *Max Planck Institute for Marine Microbiology, Celsiusstrasse 1, 28359 Bremen, Germany*

Abstract This study focuses on the influence of gas seepage on methane sources and sinks, aerobic and anaerobic oxidation of methane and the mediating microbial organisms in the Black Sea. We present data from two cruises that took place in 2001 and 2003. Seven stations (two from the shelf, four from the upper and lower slope, and one from the central basin) were compared with respect to methane concentration and isotope signature. The stations differed in methane concentration depending on the location on the slope. A strong change in the concentration and isotopic composition of methane was observed below the oxic/anoxic interface, coinciding with increased levels of archaeal biomarkers (archaeol and sn-2-hydroxy-archaeol). Concentration and isotopic composition of methane in the water column and sediments indicate that sediments from the shelf, slope, and deep basin are only minor sources of methane. The main methane sources are seeps located on the shelf and upper slope, but also in the deep basin. The comparison of two shelf stations with and without methane seepage showed a difference in methane concentrations, isotopic composition and oxidation rates, but the presence of similar methanotrophic microbial assemblages. Also two deep stations at a seep and outside of a seep area were compared, but here methane concentrations and oxidation rates were not different from each other. Anaerobic methane oxidizers (ANME-1 and ANME-2 group) were observed at both stations with slightly higher cell counts at the seep station.

Keywords: Black Sea, methane concentration, methane isotopic composition, methane oxidation, methane seeps, methanotrophs

L. N. Neretin (ed.), Past and Present Water Column Anoxia, 419–441.

1. INTRODUCTION

Methane is an important greenhouse gas which has increased from a level of 850 ppb before industrialization to 1.7 ppm today, further increasing with approximately 1 % per year [6, 34]. Although methane concentration in the atmosphere is small compared to CO_2 (360 ppm), its impact as a greenhouse gas in the atmosphere is about 24 times higher [15]. Main methane sources of the earth today are of human origin. The largest natural sources are wetlands and termite guts. A large proportion of the methane flux to the atmosphere comes from anthropogenic sources that are either energy related (i.e. mining and gas drilling) or agricultural (i.e. ruminants, rice agriculture and biomass burning beside landfills) [6]. Despite considerable sources of methane in the seafloor, the ocean generally contributes only a small amount of ~5-20 Tg methane per year (<2%) to the atmosphere [6] due to microbial aerobic and anaerobic oxidation processes in sediments and water column [35, 36]. Recent research has focused a lot on the role of gas hydrates as the largest reservoir of methane on earth that has been overlooked before 20-30 years ago [25]. Methane clathrates are now found at almost all continental margins with a suitable temperature-pressure field. [26] including the north-western part of the Black Sea [5, 16].

The Black Sea has a surface area of 423,000 km^2 and a maximal depth of 2212 m, and represents the world largest anoxic basin [39]. After a freshwater period during the last glacial, the Black Sea turned into a brackish basin when the Bosporus established a full connection to the Mediterranean about 7150 yrs ago [13, 40]. Due to large freshwater inflow by rivers the surface water now has a salinity of 17.5–18.5 ‰, whereas the deep water salinity is 22.3 ‰ [31]. Anoxia developed 7500 yrs ago due to the stable stratification of the Black Sea waters [20]. The aerobic surface waters are separated from anoxic deep waters by a chemocline at 100-200 m water depth depending on the geographical location [45]. On the shelf and upper continental slope where large rivers like the Danube enter the Black Sea the chemocline may even reach down to 300 m [45]. The water column contains substantial but varying amounts of methane, which has been attributed to methanogenesis in the water column [17] and sediments [37], as well as to the release of methane from gas reservoirs such as methane hydrates [16]. Whereas methane concentrations in the oxic surface waters are in the nanomolar range, methane concentrations in the anoxic deep water are much higher, sometimes exceeding 10 μM. The inventory of methane in the Black Sea adds up to 96 Tg methane [37, 44]. It is still not clear which role the deposited sediments play in the methane turnover in the Black Sea, i.e. whether they function as a methane source or sink. Reeburgh et al. [37] have suggested that sediments on the slope emit methane into the water column whereas basin sediments serve as a methane sink.

Another important question is the identity, distribution and activity of microbial organisms responsible for anaerobic and aerobic methane oxidation in the Black Sea water column. Biomarker and compound specific stable isotope investigations on particulate material collected from the anoxic water column showed that archaea may be involved in methane oxidation [43, 49]. Methane oxidation rates are around 10^{-3} nM d^{-1} in the upper water layer and increase to a few nanomoles per day below 100 m [37]. However, beside these organic geochemical investigations there are no published molecular biological reports so far that really identified those organisms.

Relatively recent findings especially in the north-western part of the Black Sea are methane seeps [2, 18]. At these locations methane enters the water column in the aerobic as well as in the anaerobic water zone and tremendously influences the methane inventory of the Black Sea.

In order to better understand methane turnover in the Black Sea we measured methane concentrations in the sediments at two shallow sites on the NW and SW slope and at a deep site in the central basin. Additionally, we investigated several biogeochemical parameters related to methane in the water column at shallow and deep methane seeps and non-seep sites. Measurements were performed in sediments as well as in the water column to investigate further the sink/source behavior of the seafloor. Methane stable carbon isotopic composition was determined for further insight into the oxidation/formation patterns of methane. Additional biomarker and molecular investigations of particulate water column material were performed to reveal which organisms are involved in the methane oxidation. The data presented are partly preliminary results from ongoing research that will be further evaluated in the future.

2. METHODS AND MATERIALS

2.1 Sampling

During cruise M51-4 in December 2001 with the German research vessel *R/V Meteor* water column profiles and sediment cores were sampled at the following stations: 7605 (42 30,71'N, 30 14,69'E) at 2130 m water depth in the central basin, 7617 (43 38,04'N, 30 02,54'E) at 1560 m water depth from the NW slope, and 7623 (41 44,77'N, 31 10,28'E) at 876 m water depth from the SW slope (Fig. 1). Additionally, samples were recovered during the CRIMEA cruise with *R/V Professor Vodyanitskiy* in 2003. Presence of gas seepage was identified hydroacoustically by an echosounder system sensitive to gas bubbles onboard. Water samples were taken at two shallow sites, namely a gas plume site above a cold seep (CTD-038: 44° 50'N, 31° 59'E, 92 m water depth) and a near by reference site without seepage (CTD-055: 44° 51'N, 32° 01'E, 76 m). Also two deep stations were sampled, a gas plume site (CTD-072: 44° 17'N, 35° 02'E, 1985 m) and a reference site without seepage to the west

(CTD-064: 44° 14'N, 32° 30'E, 1658 m, Fig. 1). Water samples were taken with a rosette system equipped with 10 l Niskin bottles. To sample the gas plume at the seep stations, the vessel was either anchored (shallow water) or the rosette was fired while drifting over the plume site, after careful mapping of the plume dimensions using side scan sonar (deep stations). Oxygen profiles were recorded using a CTD system calibrated by Winkler titration.

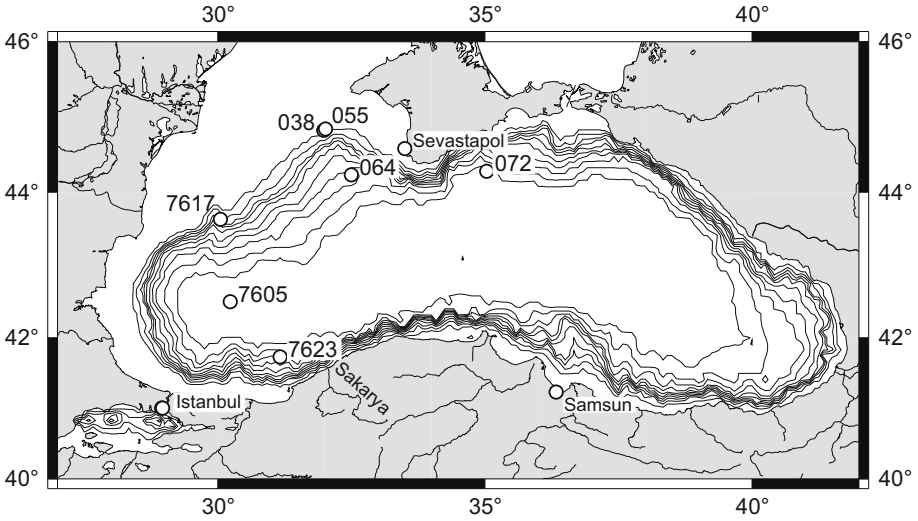

Figure 1. Map of the Black Sea showing sampling stations. Stations 7605 (central basin), 7617 (north-western slope), and 7623 (south-western slope) were sampled during the Meteor cruise in 2001 and Stations 038 (seep site on the north-western shelf), 055 (reference site on the north-western shelf), 064 (reference site on the lower slope southwest of Crimea), and 072 (seep site on the lower slope south of Crimea) were sampled during the CRIMEA cruise in 2003.

2.2 Methane Concentration and Isotopic Composition

For water sampling, 120 ml serum bottles were filled from the Niskin bottle directly after retrieval of the rosette. The water samples were poisoned with NaOH pellets, crimped immediately with a butyl-rubber stopper, and kept in the dark at 4 to 8 degrees. In the laboratory, a 20 ml helium headspace was introduced and equilibration between both phases was achieved. For sediment sampling a 5-mL cut-off plastic syringe was inserted through small holes in the core liner and the samples were placed in 50-mL serum vials containing 6 mL of 2.5 % NaOH solution. These vials were crimp sealed with butyl-rubber stoppers, shaken, and allowed to sit at room temperature for some hours before the measurement. Quantification of methane was accomplished by injecting 1 to 5 mL of headspace from the serum vials into a Hewlett-Packard 5890 Series II gas chromatograph equipped with a flame ionization detector. Injector

temperature was 200°C and the detector was at 225°C. The column, 6' x 1/8" stainless steel packed with Poropak Q (80/ 100 mesh), was maintained at 40°C. The carrier gas was N_2 flowing at 25 mL min^{-1}, and the retention time for CH_4 was about 0.7 min. Peak areas were quantified with an HP 3396 Series II electronic integrator. A known amount of standard gas (Scotty, Supelco) was injected in quadruplicate and served for quantification. Analytical precision was ± 5%.

For CH_4 analysis aboard *R/V Professor Vodyanitskiy*, a modification of the vacuum degassing method described by Lammers and Suess [27] was used [38]. 1600 ml of water were injected into pre-evacuated 2200 ml glass bottles leading to quantitative degassing. The gas phase was subsequently recompressed to atmospheric pressure and the CH_4 concentration of the extracted gas was determined by gas chromatography. A Shimadzu GC14A gas chromatograph equipped with a flame ionization detector was used in connection with a Shimadzu CR6A Integrator. Nitrogen was used as carrier gas, and separation was performed using a 4 m 1/8' SS column packed with Porapack Q (50/80 mesh) run isothermally at 50°C.

The carbon isotopic composition of dissolved methane ($\delta^{13}C_{CH4}$) was determined by a method described earlier [41]. Precision of the method was ± 1 ‰.

2.3 CH_4 Oxidation Rates

Water for measuring microbial methane oxidation was filled in triplicates in 20 ml crimp-seal bottles and capped gas-tight. From each triplicate, one sample was killed with 50 μl concentrated formaldehyde solution which functioned as a blank. Aliquots of 50 μl tritiated methane (^{3}H-CH_4) were added to the bottles and incubated in the dark at ambient temperatures imitating natural conditions. Immediately after the incubation an aliquot of the water was mixed with scintillation cocktail (Ultima Gold, Packard) and measured to determine the actual amount of tracer added to the sample. After the samples stood uncovered overnight they were bubbled for 20 min with nitrogen to eliminate all unreacted tritiated methane. An aliquot of the bubbled water was mixed with the scintillation cocktail and measured again. Measurements were performed by means of a scintillation counter (1600CA Tri-Carb, Packard). Turnover rates (k value, d^{-1}) were calculated from the ratio of tracer remaining in the water to total tracer added.

2.4 Lipid Analysis

Particulate organic matter for lipid analyses was collected from specific water depths by filtration of large volumes (up to 1,000 l) of water through 142 mm diameter glass fiber filters (GFF; nominal pore size 0.7μm, precombusted at

370° C) with in situ pumps. The GFF were extracted for 24 h in a Soxhlet apparatus to obtain the total lipid extracts. Aliquots of the total extracts were saponified after addition of an internal standard and separated into fatty acid and neutral lipid fractions. The fatty acid fractions were methylated (BF_3-MeOH, Sigma) and the neutral fractions were derivatized (BSTFA, Sigma) and analyzed by gas chromatography and gas chromatography–mass spectrometry for the quantification and identification of lipids, respectively.

2.5 Fluorescence in Situ Hybridization (FISH) and Cell Counts

Bacterial abundance was determined by epifluorescence microscopy (Zeiss Axioscope 2, 1,000 magnification) of DAPI (4',6-diamidino-2-phenylindole)-stained cells. Bacterial cells were fixed by the addition of concentrated formaldehyde solution (5 % final concentration) for 15 min at room temperature and thereafter recovered by gentle vacuum filtration (20 and 50 ml for each sample) on to polycarbonate filters with a pore size of 0.2 μm (GTPB, Millipore). After washing with PBS and water, the filters were transferred into sterile PP petri dishes, sealed and stored frozen at –20 °C for FISH. The protocol of Pernthaler et al. [33] was used for the hybridization procedure. The following oligonucleotide probes (MWG, Germany) were used to describe the microbial communities: Arch915 for members of the domain *Archaea*; Eel MS 932 (ANME-2 group); ANME-1, distantly related to *Methanosarcinales* [4]; and MG84/705 and MA450, describing methanotroph groups I and II [9], respectively. Probes were labeled with the indocarbocyanine fluorescent dye CY3 and fluorescein (MWG, Germany).

3. RESULTS

3.1 Oxygen Profiles

The water column of the sampled stations clearly showed a chemocline separating the water column in an oxic and anoxic zone. Figure 4 shows the oxygen profiles of the investigated stations. At the NW station 7617 and at the central station 7605 oxygen concentrations reached up to 220 μM, the SW station 7623 had surface water oxygen concentrations below 67 μM. These low concentrations may be caused by the Sakarya river inflow and its particulate organic matter load at the sampling site. The central station 7605 showed relatively stable values of 220 μM at the surface down to 55 m and then a very fast decrease to values around zero below 100 m. Oxygen depletion was also found below approximately 100 m at the SW station and below 140 m at the NW station. Here, the transition between the oxic and the anoxic layer was not as abrupt as observed at the other two stations. Stations 064 and 072 on the

lower Crimean slope had their oxic-anoxic interfaces at approximately 120 m and 180 m, respectively, whereas the shelf stations 038 and 055 were situated fully in the oxic part of the water column. It has been previously observed that the chemocline is deeper at the slope compared to the central basin (e.g. [45] and references therein).

3.2 Sediment Methane Concentrations

Short sediment cores of up to 40 cm length were retrieved at stations 7617 and 7623 on the upper slope and at station 7605 in the central basin. Methane concentration profiles of all three cores looked relatively similar with concentrations around 10 and 12 μM at the surface and decreasing values towards the core bottom with concentrations between 4 and 8 μM (Fig. 2). The profile shape with higher concentrations at the surface and lower concentrations at the bottom indicates a methane flux from the top to the bottom of the core.

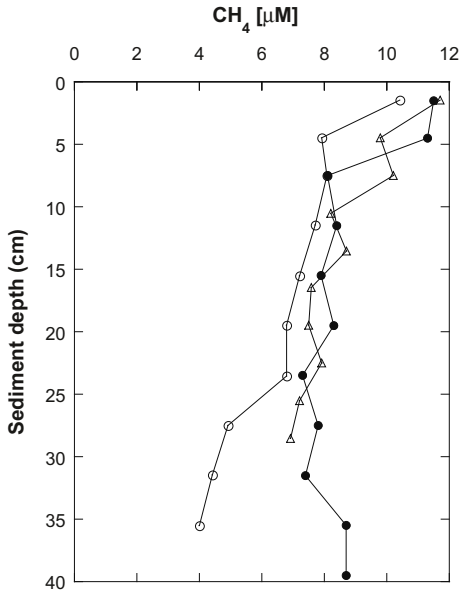

Figure 2. Methane concentrations in three sediment cores recovered from the NW slope (7617, open triangles), SW slope (7623, open circles), and the central basin (7605, full circles). The linear decrease of methane from top to bottom of the cores indicates a diffusive flux of methane from the water column into the sediments.

3.3 Water Column Methane Concentrations

All stations except the seep station 038 showed methane concentrations of 8 to 50 nM with increasing depth in the oxic water column. At the seep station 038,

methane reached 10 times higher values of up to 550 nM above the seep (Fig. 3). Below the chemocline at most stations methane values increased rapidly to approximately 10 μM at about 500 m, and remained stable around 10.5 to 11.3 μM from 500 to 2100 m water depth. Exceptions were the upper slope stations in the North-West (7617) where methane concentrations increased from 0.4 to 2.7 μM from 150 to 295 m, and in the South-West (7623), where methane concentrations increased from 0.5 at 150 m to 4.5 μM at 340 m (Fig. 4). The water columns sampled at the lower slope position (064 and 072) showed very similar concentration profiles with maximum values of 12.5 μM (Fig. 5).

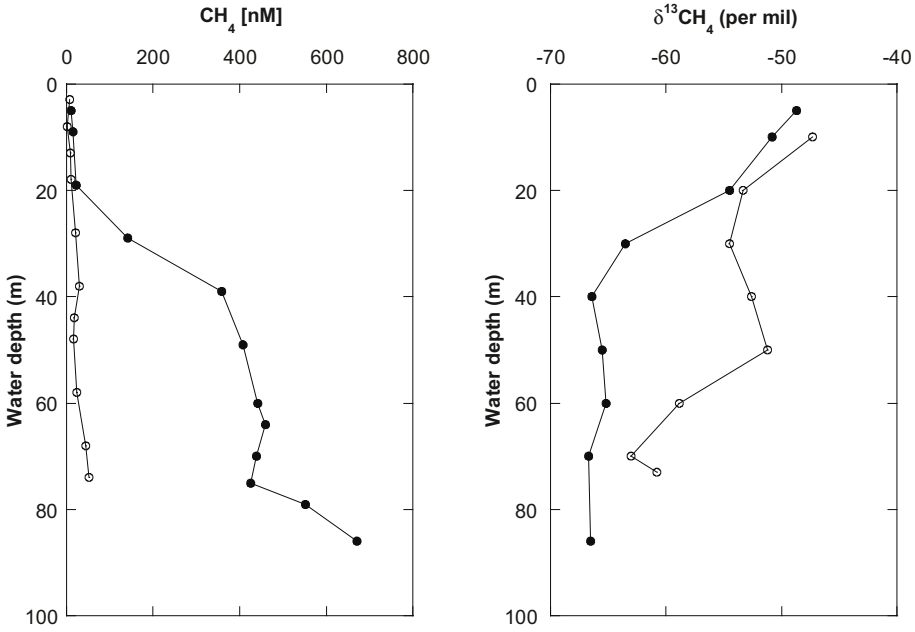

Figure 3. Water column methane concentrations (nM) at the seep 038 (full circles) and reference site 055 (open circles) located on the north-western shelf of the Black Sea. Carbon isotopic composition ($\delta^{13}C_{CH4}$ vs. VPDB) of the dissolved methane from the water column above the seep site (038, full squares) and reference site (055, open squares).

3.4 Isotopic Composition of Water Column Methane

The stable carbon isotopic composition of methane was measured at the north-western station (7617), the central station (7605), at the lower slope station (064), and at the two shelf stations (038, seep and 055, reference, Fig. 4,5,3). At the central station (7605, Fig. 4) $\delta^{13}C_{CH4}$ values in the anoxic deep water varied around - 54 ‰ and the shallowest sample taken at 30 m water depth had a $\delta^{13}C_{CH4}$ value of -42 ‰. A striking change in isotope fractionation

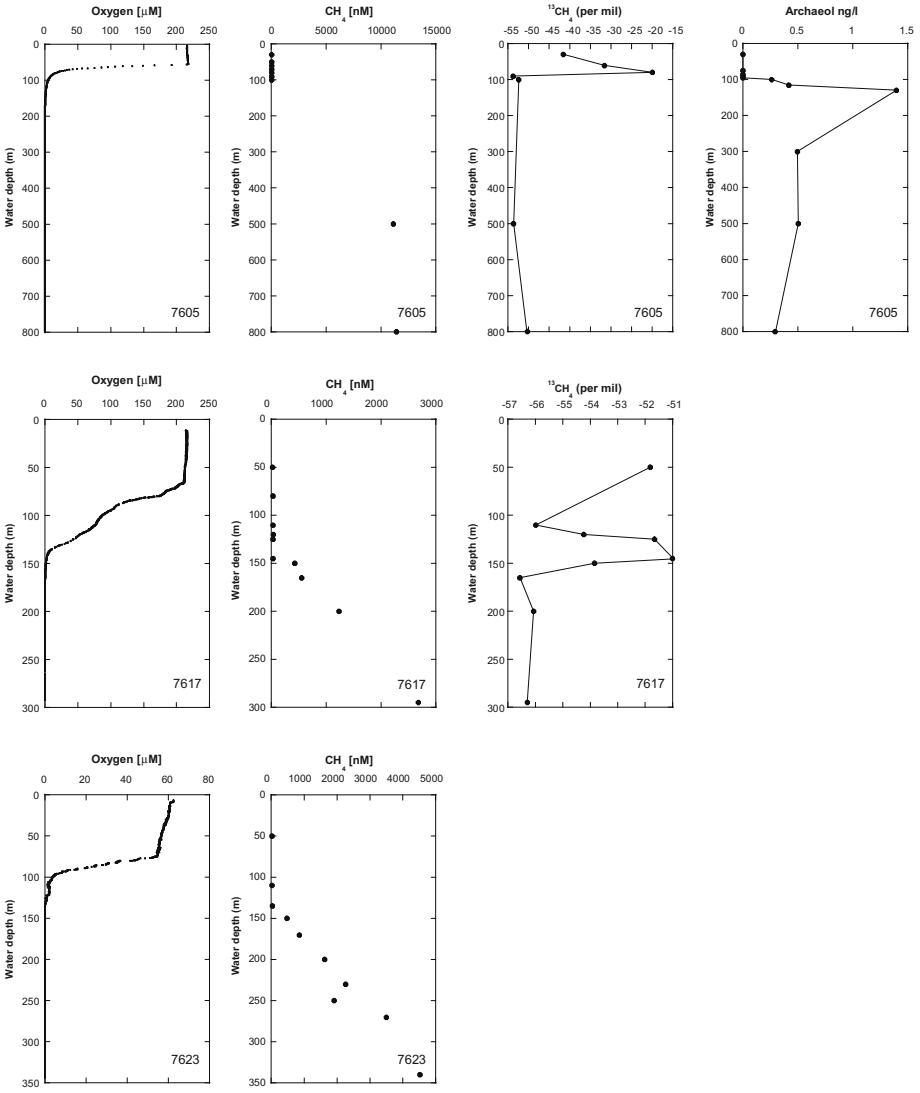

Figure 4. Oxygen (μM) and methane concentrations (nM) of stations 7605, 7617, and 7623, the carbon isotopic composition of methane ($\delta^{13}C_{CH4}$ vs. VPDB) of stations 7605, 7617 and the depth distribution of Archaeol (ng/l) extracted from particulate material collected from the water column at station 7605. Note the difference in the depth of the chemocline between stations and the change in isotopic composition of the methane due to oxidation.

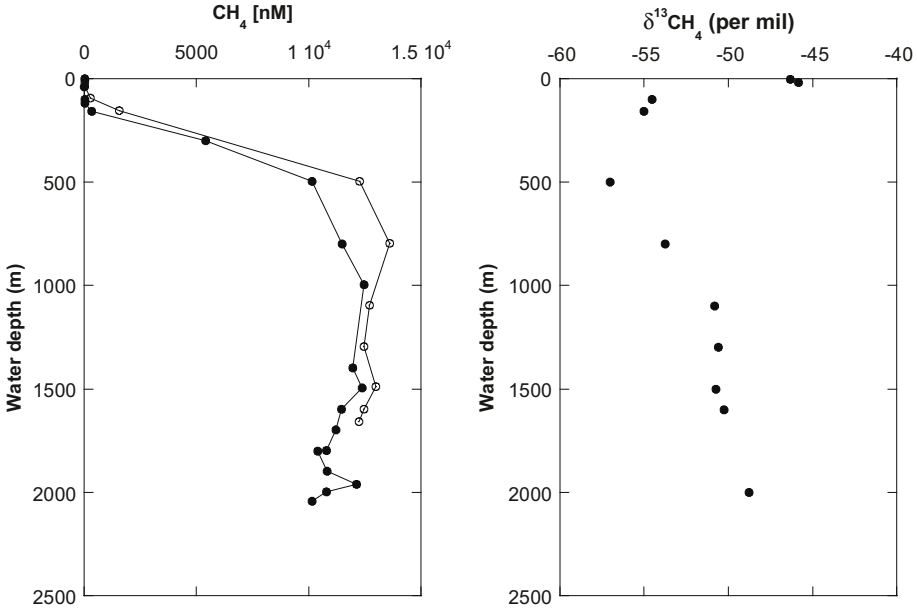

Figure 5. Depth profile of methane concentrations of reference site 064 (light circles) and a composite profile of seep sites 068 and 075 that were sampled very close to station 072 (dark circles). Carbon isotopic composition of the dissolved methane from the water column above the reference site 064. The depletion in the isotopic values from approximately 800 to 500 m water depth indicates an additional source of methane from the upper to middle slope.

occurred just below the chemocline at 100 m water depth, Here, $\delta^{13}C_{CH4}$ increased to -20 ‰. At the north-western station (7617, Fig. 4) the samples from 300 to 165 m had $\delta^{13}C_{CH4}$ values around – 56 ‰ followed by a significant increase to -51‰. The top sample at 50 m water depth had $\delta^{13}C_{CH4}$ values of -52 ‰. The stable carbon isotopic composition of methane at site 064 (Fig. 5) varied between -49 and -51 ‰ VPDB. Above 800 m $\delta^{13}C_{CH4}$ values decreased to a minimum of -58 ‰ VPDB at 500 m and subsequently increased again above 160 m to $\delta^{13}C_{CH4}$ values of -46 ‰ VPDB near the surface. The isotopic composition of the dissolved methane in the oxic water column near the seafloor at the two shelf stations (Fig. 3) differed with a $\delta^{13}C_{CH4}$ value of -67 ‰ VPDB at the bottom of the seep site (038) from the $\delta^{13}C_{CH4}$ value of -58 ‰ VPDB at the bottom of the reference site (055). A constant increase in $\delta^{13}C_{CH4}$ values from -67 ‰ VPDB to -49 ‰ VPDB from the bottom to the surface could be noted at the seep station (038).

3.5 Lipid Biomarkers for Methane Oxidizers in the Water Column

Lipids indicative for methane oxidizing bacteria and/or archaea were investigated at the two upper slope sites (7617, 7623), and at the central site (7605). Two glycerol-ethers namely archaeol and sn-2-hydroxyarchaeol, indicative of methanogenic or methanotrophic archaea, depending on the isotope signature [14, 23], were detected in the water column. Both compounds were only present in the anaerobic zone of the Black Sea and totally absent in the aerobic water layer. Concentrations in the anaerobic layer could be determined only for archaeol. They were found directly below the chemocline at 100 m in low abundances of 0.3 to 1.5 ng/l (Fig. 4). sn-2-Hydroxyarchaeol could be detected only as a trace compound in the samples at 130 m from the central station (7605) and from 170 m at the SW station (7623) where it occurred with ~0.1 ng/l. These concentrations are very low compared to those that are found in sediments off Oregon where up to 8 μg/g sediment of both compounds have been measured [4]. Due to the low abundance it was not possible to measure isotope signatures, hence it cannot be concluded whether the biomarkers are of methanogenic or methanotrophic origin.

3.6 Methane Oxidation Rates

Methane oxidation rates using tritium labeled methane were measured at the two shallow stations 038 (seep) and 055 (reference) and at the deep slope stations 064 (reference) and 072 (seep). There was on average a 30 times higher oxidation rate at the seep site (0.02 to 1.6 nM d^{-1}) compared to the shallow reference site (0.001 to 0.05 nM d^{-1}). In contrast, at the deep sites no significant difference was observed between reference and seep sites with the anoxic water column values of 0.03 to 3.1 nM d^{-1}.

3.7 Fluorescence in Situ Hybridization of Methanotrophic Microorganisms

To identify the methanotrophic community that is responsible for anaerobic methane oxidation in the anoxic Black Sea water column, filtered samples from the lower slope stations 064 (reference) and 072 (seep) were investigated by FISH (a method using specific fluorescently labeled gene probes which allows the detection of microorganisms under the microscope). Using 16S rRNA-targeted oligonucleotide probes specific to both groups, it was possible to detect ANME-1 and ANME 2 group cells, usually found in sediments, in the water column of the Black Sea. Cell counts of filters from the water column above the methane seep site revealed ANME-1 and ANME-2 cells in concentrations of up to 4 % of all DAPI stained cells (Table 1, [8]). Interestingly, cells counts

declined to below 1.2 % above 800 m, the depths where the bubble flare could not any longer be detected in the water column. At the reference station the ANME-1 and ANME-2 cells were lower than at the seep site and represented only around 1 to 2 % of total cells.

Table 1. Occurrence of ANME-1 and ANME-2 cells at the reference (064) and seep site (72) on the lower slope. Higher abundances of ANME-1 cells were measured at 1500 and 2000 m where a bubble plume could be observed with hydroacoustical means (echosounder) up to 1200 m in the water column (+ >2%, - <1.2%).

Station 064			*Station 072*		
Depth (m)	% ANME-1	% ANME-2	Depth (m)	% ANME-1	% ANME-2
160	+/-	+/-	500	-	-
500	+	-	1200	+	-
800	+/-	-	1500	+	+
1600	+/-	-	2000	+	+/-

The identification of aerobic methanotrophic bacterial cells using FISH showed at both shallow stations (038 and 055) a share of 0.1 to 4.5 % of methanotrophs type I cells of total DAPI stained cells. Methanotrophs type II were only detected with 2 % of total DAPI stained cell counts at one depth (038, 83 m) very close to the sediment. We have tested our FISH probes with pure cultures of methanotrophic bacteria of type I and II to ensure our cell detection/counting. Differences in cell numbers between our work and the data provided by Gal'chenko et al. [12] (see discussion) might have their origin in the different methods (immunofluorescence versus FISH), or in natural changes of the microbial population.

4. DISCUSSION

The following discussion compares the results of the two recent expeditions to what is known about the Black Sea methane budgets and fluxes. A closer look is taken at the interaction between the Black Sea water column and the atmosphere, the methane sink and source relationships in the sediments and water column, and at the identity of microorganisms that are responsible for methane oxidation in the oxic and anoxic part of the Black Sea water column. We especially focus on the significance of recently discovered methane seeps that have not or only marginally been considered in former publications [5, 16, 28, 42].

4.1 The Oxic Water Column as a Source of Methane to the Atmosphere

Methane concentrations in the non-seep oxic water column (055) decrease from 50 nM at around 76 m to concentrations of <10 nM at the sea surface. At the seep site (038) methane concentrations are 10 times higher above the seafloor in 80 m with values of up to 550 nM (Fig. 3). However, due to aerobic consumption of methane, surface water methane concentrations (uppermost 10 m) at the seep site are only 1.6 times higher than at the non-seep site with values of up to 16 nM. Oxidation rates at the seep site (up to 1.6 nM d^{-1}) were on average approximately 30 times higher relative to the reference station (0.001 to 0.05 nM d^{-1}). The relative turnover was 97 % at the seep and 87 % at the reference site. The oxidation of methane could also be traced using the stable carbon isotopic composition of the methane at the seep station. Here, a constant increase in the $\delta^{13}C_{CH4}$ values at the seep station from -67 ‰ VPDB (bottom) to -49 ‰ VPDB (5 m below water surface) over the entire water column clearly shows the preferably usage of light ^{12}C methane by the aerobic methanotrophs (Fig. 3).

The percentage of aerobic methanotrophs from the total cell number determined by DAPI varied between 0.1 to 4.5 % at both sites. Intriguingly, only methanotrophic bacteria of type I were detected with the exception of one sample from 100 m water depth at the seep site, where type II methanotrophs represented 2 % of total cell counts. This is at odds with earlier studies reporting that methanotrophs of type I and II are equally abundant in the water column [12]. Furthermore, Gal'chenko and coworkers found methanotrophs of type I and II representing up to 10 % of the total cell counts in the water column, whereas our findings indicate that they represent less than 5 % of the total cell counts (see results for possible explanation).

Comparing surface water methane concentrations with the methane concentration expected assuming atmospheric equilibrium [51], we find that the surface water at the seep and reference sites is 3 to 5 times supersaturated with respect to methane and therefore both stations act as a source for atmospheric methane. This is in agreement with other investigations that have measured methane fluxes from the Black Sea water column to the atmosphere [1, 42]. The latter authors found an air-sea methane flux above a shallow seep area of 0.96–2.32 nmol m^{-2} s^{-1} that is 3 times higher than calculated for the surrounding shelf (0.32–0.77 nmol m^{-2} s^{-1}) and 5 times higher than assessed for open Black Sea waters (water depth >200 m, 0.19–0.47 nmol m^{-2} s^{-1}). Hence, we can conclude that the gas seeps of the upper slope and shelf, where methane emanates in to the oxic water column, contribute substantially to the methane emission. The total number of active seeps at the upper slope and shelf is

still unknown, hence the emission of methane from the water column to the atmosphere related to gas seepage cannot be constrained at this point.

4.2 Variations in Methane Concentration in the Water Column Over Time

The key publication that deals with methane in the Black Sea arose from the 1988 *R/V Knorr* expedition [37]. Reeburgh et al. [37] showed one methane profile from the central basin with low concentrations (< 10 nM) in the oxic zone above 100 m, increasing concentrations from 100 to 550 m, and very stable concentrations around 11 μM down to 2200 m. Additionally, Reeburgh et al. [37] showed methane concentration data from the deep anoxic waters measured by Scranton [44] that were above 12 μM and speculated that this might hint to a methane decrease in the time between the two studies, i.e., 1975 and 1988. However, our measurements from 2001 and new measurements during the CRIMEA cruises in 2003 and 2004 are all between 10.5 and 13.1 μM and therefore close to Reeburgh's et al. [37] data. Hence, we conclude that any increase or decrease in this range could be reflecting regional variability, and that methane concentrations appear to be relatively stable over the past 30 years.

4.3 Sources of Methane to the Water Column

There are three potential sources for methane in the Black Sea: (1) methane is released from the sediments to the water column, (2) methane is produced in the water column or (3) methane seeps emit methane from deeper reservoirs to the water column.

(1) Methane contribution from the sediments to the water column: Depending on the location in the Black Sea the organic matter burial rates are very different. In front of rivers, high amounts of marine and terrestrial organic material are delivered to the sediments and degraded under anoxic conditions by iron, manganese, and sulfate reduction, eventually leading to methanogenesis. On the other hand, towards the central part of the Black Sea terrestrial contribution is limited and organic matter input depends on export of phytoplankton biomass to the seafloor [46]. Lander investigations by Friedl et al. [10] and Friedrich et al. [11] showed that no or only negligible amounts of methane were formed during degradation of organic material in sediments underlying oxic and anoxic bottom waters of the north-western Black Sea shelf. Additionally, Jørgensen et al. [21] could show on a sediment transect located on the north-western shelf and including sediments from water depths from 100 to 1200 m that, although methane is produced deeper in the sediments, no methane reaches the sediment surface and escapes to the water column due to the anaerobic oxidation of methane at the sulfate/methane transition zone. This is also

obvious from sediment methane concentration profiles presented by Sorokin [45]. Sediment methane concentration profiles from our investigation (Fig. 2) show high concentrations at the surface and lower concentrations at the bottom of the cores indicating that sediments from the slope and the basin are a sink for water column methane rather than a source. Dissolved water column methane diffuses into the sediments and is consumed by methanotrophic organisms. In contrast to the methane concentration profiles measured in this study (low μM range), Reeburgh et al. [37] measured concentrations in the mM range and suggested a high flux of methane from the shelf sediments to the water column. However, this is at odd with our findings and the results by Jørgensen et al. [21], Friedl et al. [10], and Friedrich et al. [11]. One explanation for the very high methane concentrations of the sediment core from Reeburgh et al. [37] may be that sediments were recovered from a seep system, an assumption made earlier also by Jørgensen et al. [21].

Most likely, sediments are only a source of methane where the gas is transported by advective processes such as fluid flow and ebullition of free gas. A high number of gas seeps that have been found close to the Crimea peninsula [16, 29] and meanwhile all around the shelf of the Black Sea (results by EU projects CRIMEA; METROL, ASSEMBLAGE) support this hypothesis.

(2) Whether methane is formed in the deep anoxic water column by methanogenesis is highly debated. Ivanov et al. [19] suggested that methane is formed in the order of 63 x 10^{10} mole per year during the process of organic matter degradation in the water column. Reeburgh et al. [37] argued that methane formation in the water column should be negligible, because sulfate reducers outcompete methanogenic bacteria for fermentation products at the presence of sufficient sulfate. Results from Konovalov et al. ([24], and manuscript in preparation) show that the profiles of ammonium and sulfide are in agreement with what would be expected when both constituents were solely derived from organic matter degradation by sulfate reduction, and that sulfate reduction would balance the export flux from surface water. This means that there is only very little place for methanogenesis in the water column and presumably not in the amount proposed by Ivanov et al. [19]. If methanogenesis is a significant process in the water column, this should show up in the isotope signature, as well as in the presence of specific biomarker lipids. We have found only minute amounts of archaeal biomarkers indicative of methanogenic archaea at site 7605. Here, they coincide with a substantial increase in the δ^{13}C of methane, pointing to a zone of anaerobic methanotrophy rather than methanogenesis. We, therefore, conclude that methanogenesis is not a significant process in the water column compared to methane oxidation.

(3) Several hundred seeps emitting methane to the water column were discovered during the last years especially on the NW shelf and south of Crimea ([2] [18] and CRIMEA Cruise Reports 2003, 2004). These seeps are so com-

mon that for instance only during the two cruises linked to the CRIMEA project more than 1000 new seeps where discovered (CRIMEA Cruise Report 2004). Gas seepage is not only found on the shelf, but occurs also on the upper and lower slope [5]. Indications for methane fluxes from seeps at the upper to middle slope could be seen in the $\delta^{13}C_{CH4}$ profile of station 064 (Fig. 5). A decrease in $\delta^{13}C_{CH4}$ values in the water column at 800 to 500 m water depth shows that methane escaping from seeps located at the deeper shelf and slope leaves an imprint on the $\delta^{13}C_{CH4}$ depth profile. This is supported by higher methane concentrations in water depths around 600 m, where the methane profile clearly deviates from other biogeochemical parameters such as NH_4 and H_2S, hence indicating an additional methane source (Konovalov, unpubl. model results). Sorokin [45] showed that the stable carbon isotope composition of methane seeping out of the Black Sea bottom is ~-58 ‰ VPDB and that the age of the methane as determined by ^{14}C dating lies between 3.500 to 5000 years BP. The $\delta^{13}C_{CH4}$ values at station 064 at around 500 m of ~ – 58 ‰ VPDB are actually very close to the values measured for methane escaping the seeps on the shelf and slope indicating a methane source from seepage. The age of the methane further confirms the argument that the methane is not formed by recent methanogenesis in the uppermost sediments, but is delivered from older Black Sea sediment deposits.

Comparing reference site (064) and seep site (072) on the lower slope, methane concentrations below 500 m water depth at both sites were more or less similar with 10-12.5 μM. First it seemed surprising that the methane plume at the seep site which was traced by acoustical means (echosounding) from 2000 m water depth up to 800 m water depth was not reflected in the methane concentration. Most likely, the huge background concentration of 12 μM methane in the deep water masks the signature of the plume. Accordingly, a plume concentration of around 500 nM as detected at the shallow seep (038) would not be resolved at a background of 12 μM.

One method to determine the methane input from seeps into the water is the distribution of noble gases in the water column. The concentrations of dissolved atmospheric noble gases in lake and ocean water correspond closely to the equilibrium concentrations determined by the surface water temperature and salinity that prevailed during gas exchange with the atmosphere [7, 22]. Noble gases are chemically inert, and therefore any observed deviations from the initial equilibrium concentrations can be used for modeling the purely physical processes. The release of gas bubbles into the water column stimulates a secondary gas exchange between the ascending gas phase and the surrounding water by gas stripping and dissolution and therefore affects the local noble gas concentrations [50].

Neon concentrations in the deep water were approximately constant with depth for each of the two profiles, but the mean Neon concentration determined

in the plume was 3.2 % lower than that determined for the reference profile (Fig. 6). This clearly proofs that a gas exchange takes place between the rising bubbles and the surrounding water; i.e., that the gas plume strips dissolved Neon from the water into the rising gas bubbles. It is, however, important to note that the observed Neon depletion in the water column is an integrated signal over the time the seep was and is active including horizontal and vertical mixing of the deep water of the Black Sea.

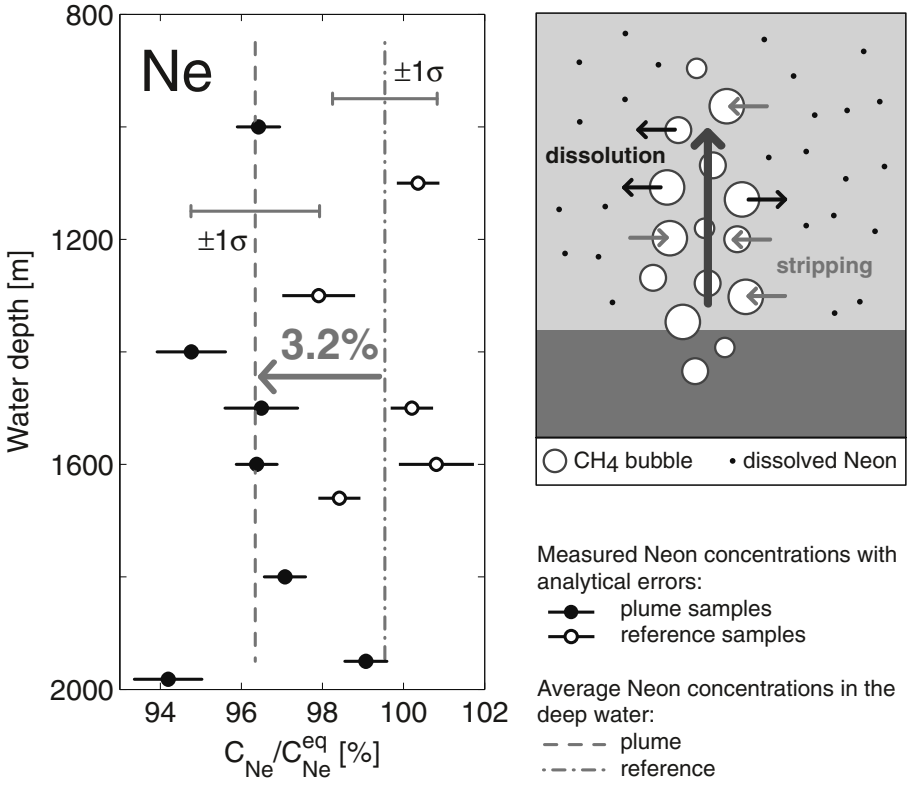

Figure 6. Atmospheric Ne concentrations (normalized to atmospheric equilibrium concentrations) in the deep water of the Black Sea (left hand panel).Water samples from the reference site (open circles) showed on average 3.2 % higher Ne concentrations than water samples of the flare from the seep site (closed circles). On the right hand panel a conceptual model shows how the gas bubbles strip the dissolved Ne from the surrounding water into the bubbles.

In conclusion we propose that a significant fraction of the methane that is found today in the water column of the Black Sea is derived from gas seeps that are mainly distributed on the shallow shelf and slope but can also be found in the deep parts of the Black Sea.

4.4 Methane Sinks

The main sinks in the methane budget of the Black Sea are, as pointed out earlier by Reeburgh et al. [37], central basin sediments, the oxidation of methane in the oxic and anoxic water column (AOM), and evasion to the atmosphere. One of the big questions as to sinks of methane in the Black Sea is the identity of methane oxidizers in the anaerobic part of the water column. It has been shown earlier that members of the order *Methanosarcinales* together with sulfate reducing bacteria are involved in the anaerobic oxidation of methane in the Black Sea [3, 30, 47]. At active gas seeps of the Black Sea, methanotrophic mats were found containing high amounts of strongly depleted archaeol and sn-2-hydroxyarchaeol. Interestingly we found archaeol and sn-2-hydroxyarchaeol in the water column of the Black Sea, coinciding with a strong fractionation against ^{13}C methane and high methane oxidation rates, indicating that methane is oxidized by organisms related to methanogenic archaea just below the chemocline. Unfortunately, due to the low concentration of these compounds in the water column it was not possible to measure their carbon isotopic composition, which would be needed for an ultimate proof that these organisms are involved in AOM. Schouten et al. [43] and Wakeham et al. [49] showed that ^{13}C depleted archaeal derived biphytanes occur in the anoxic water column of the Black Sea providing evidence that methane consuming archaea are present. Isotopically depleted phytane ($\delta^{13}C$ = -51 ‰) released after chemical (HI) treatment from an archaeal lipid precursor (e.g. archaeol, hydroxy-archaeol) has been described in the anoxic water column of the Black Sea (Wakeham et al. 2004). This $\delta^{13}C$ value is, however, rather heavy compared to values measured in sedimentary lipids extracted from venting sites (around –100 ‰, [4]) and the possibility remains that these compounds originate from methanogenic archaea.

Recently, Vetriani and co-workers [48] provided evidence based on 16S rRNA sequences and T-RFLP in one Black Sea water sample at 305 m that archaea phylogenetically related to the ANME-2 cluster are present. Using 16S rRNA-targeted oligonucleotide probes specific to both groups, we were able to detect ANME-1 and ANME 2-related cells in the water column of the Black Sea. Cell counts of samples from the water column above the methane seep (072) revealed ANME-1 and ANME-2 cells in concentrations of up to 4 % of all DAPI stained cells. Above the reference site (064) only up to 2 % ANME-1 and ANME-2 were detected. We believe that these organisms are at least partly responsible for anaerobic methane oxidation in the water column of the Black Sea but it is likely that there are other groups yet to be discovered. Incubation experiments revealed no difference in methane oxidation rates between the reference and seep site. This may be due to the fact that actual

methane concentrations at the two sites as shown above are not significantly different and cell counts were in the same range.

Interestingly, in the sediments of most methane seeps ANME-1 and ANME-2 archaea occurred in a consortium with sulfate reducers of the δ-proteobacteria groups *Desulfosarcina/Desulfococcus* [4, 30, 32]. However, no cell consortia in the water column could be observed and the methane oxidizers occurred rather as single cells. Investigations by 16S rDNA based methods are ongoing to further resolve the question which organisms are involved in the anaerobic oxidation of methane in the Black Sea water column.

From the carbon isotopic composition of the methane it is obvious that the chemocline is especially interesting when looking for methane sinks. At the central station (7605) and at the north-western station (7617) a strong isotopic enrichment of the methane was measured just below the chemocline (Fig. 4) providing strong evidence for enhanced microbial activity, i.e., methane oxidation. From tracer experiments by Reeburgh et al. [37] and own results we know that in the Black Sea water column rates of anaerobic oxidation of methane are 100 times higher than aerobic oxidation rates. However, since the strongest isotopic fractionation occurs where oxygen is already present, although in small amounts, we cannot exclude that aerobic methanotrophs contribute to the methane consumption. Higher sampling resolution at the chemocline is necessary to support this conclusion.

5. CONCLUSIONS

We have evaluated the different methane sources to the Black Sea water column and conclude that a significantly fraction of the methane derives from methane seeps located mainly on the shelf but also on the upper and lower slope. Significant microbial methane oxidation was indicated by increasing $\delta^{13}C_{CH4}$ values especially at the chemocline, but also in the oxic water column. Methanotrophic bacteria of type I are mainly responsible for aerobic methane oxidation in the oxic water column. Methane oxidation rates above the methane seep in the shallow water are approximately 30 times higher compared to a reference station. Methane concentrations and methane oxidation rates from a deep seep and a deep reference station were similar, but an additional input of methane via seepage was indicated by neon depletion in the water column due to gas ebullition. The carbon isotopic composition of methane in the anoxic water column indicates a methane source deriving from the deeper shelf/slope. Anaerobic methane oxidizers (ANME-1 and ANME-2 group) were detected over the deep seep and above the reference station. Detailed investigations are ongoing to better resolve the communities involved in anaerobic methane oxidation. To further understand the methane budget in the Black Sea it is important to determine more specifically methane oxidation rates especially

in the chemocline a boundary playing a crucial role. Additionally, rates of methanogenesis in the water column should be constrained to evaluate more precisely the sources of methane.

Acknowledgements

We like to thank Bo Barker Jørgensen from the MPI in Bremen who made it possible that Edith Durisch-Kaiser could join the research cruise with *R/V Meteor* to the Black Sea in 2001. We are especially indebted to Antje Boetius who has helped and supported us during the last years. Gabi Klockgether is thanked for her excellent analytical assistance. We especially acknowledge Marc De Batist and his enthusiasm with which he is leading the CRIMEA project. We thank all the people from the CRIMEA EU project and the captain and crew from *R/V Meteor* and R/V *Professor Vodyanitskiy* who helped us with sampling during the cruises. Funding came from the EU Project CRIMEA (EVK-2-CT-2002-00162), BBW grant (No.02.0247), the Max Planck Society and EAWAG.

References

[1] Amouroux D., Roberts G., Rapsomanikis S. and Andreae M. O. Biogenic gas (CH_4, N_2O, DMS) emission to the atmosphere from near-shore and shelf waters of the north-western Black Sea. Estuar Coast Shelf S 2002; 54:575-87.

[2] Blinova V.N., Ivanov M.K. and Bohrmann G. Hydrocarbon gases in deposits from mud volcanoes in the Sorokin Trough, north-eastern Black Sea. Geo-Mar Lett 2003; 23:250-57.

[3] Blumenberg M., Seifert R., Reitner J., Pape T. and Michaelis W. Membrane lipid patterns typify distinct anaerobic methanotrophic consortia. P Natl Acad Sci USA 2004; 101:11111-6.

[4] Boetius A., Ravenschlag K., Schubert C.J., Rickert D., Widdel F., Gieseke A., Amann R., Jorgensen B. B., Witte U. and Pfannkuche O. A marine microbial consortium apparently mediating anaerobic oxidation of methane. Nature 2000; 407:623-26.

[5] Bohrmann G., Ivanov M., Foucher J.P., Spiess V., Bialas J., Greinert J., Weinrebe W., Abegg F., Aloisi G., Artemov Y., Blinova V., Drews M., Heidersdorf F., Krabbenhoft A., Klaucke I., Krastel S., Leder T., Polikarpov I., Saburova M., Schmale O., Seifert R., Volkonskaya A. and Zillmer M. Mud volcanoes and gas hydrates in the Black Sea: new data from Dvurechenskii and Odessa mud volcanoes. Geo-Mar Lett 2003; 23:239-49.

[6] Cicerone R.J. and Oremland R.S. Biogeochemical aspects of atmospheric methane. Global Biogeochem Cy 1988; 2:299-327.

[7] Craig H. and Weiss R. F. Dissolved gas saturation anomalies and excess helium in the ocean. Earth Planet Sc Lett 1971; 10:289.

[8] Durisch-Kaiser E., Wehrli B. and Schubert C.J. Evidence for intense archaeal and eubacterial methanotrophic activity in the Black Sea water column. Appl Environ Microbiol 2005; submitted.

[9] Eller G., Stubner S. and Frenzel P. Group-specific 16S rRNA targeted probes for the detection of type I and type II methanotrophs by fluorescence in situ hybridization. FEMS Microbiol Lett 2001; 198:91-7.

[10] Friedl G., Dinkel C. and Wehrli B. Benthic fluxes of nutrients in the northwestern Black Sea. Mar Chem 1998; 62:77-88.

[11] Friedrich J., Dinkel C., Friedl G., Pimenov N., Wijsman J., Gomoiu M. T., Cociasu A., Popa L. and Wehrli B. Benthic nutrient cycling and diagenetic pathways in the northwestern Black Sea. Estuar Coast Shelf S 2002; 54:369-83.

[12] Gal'chenko V.F., Abranochkina F.N., Bezrukova L.V., Sokolova E.N. and Ivanov M.V. Species composition of aerobic methanotrophic microflora in the Black Sea. Mikrobiologiya 1988; 57:305-11.

[13] Gorur N., Cagatay M.N., Emre O., Alpar B., Sakinc M., Islamoglu Y., Algan O., Erkal T., Kecer M., Akkok R. and Karlik G. Is the abrupt drowning of the Black Sea shelf at 7150 yr BP a myth? Mar Geol 2001; 176:65-73.

[14] Hinrichs K.-U., Hayes J.M., Sylva S.P., Brewer P.G. and DeLong E.F. Methane-consuming archaebacteria in marine sediments. Nature 1999; 398:802-05.

[15] IPPC. Climate Change 2001: The Scientific Basis. Contribution of the Intergovernmental Panel on Climate Change, Greenhouse Gases (pp. 241-287).

[16] Ivanov M.K., Limonov A.F. and Woodside J.M. "Extensive deep fluid flux through the sea floor on the Crimean continental margin (Black Sea)." In *Gas Hydrates: Relevance to World Margin Stability and Climate Change*, Henriet J.-P. and Mienert J. eds., Geological Society London, 1998.

[17] Ivanov M.V., Pimenov N.V., Rusanov, II and Lein A.Y. Microbial processes of the methane cycle at the north-western shelf of the Black Sea. Estuar Coast Shelf S 2002; 54:589-99.

[18] Ivanov M.V., Polikarpov G.G., Lein A.Y., Galchenko V.F., Egorov V.N., Gulin M.B., Rusanov I.I., Miller Y.M. and Kupzov V.I. Biogeochemistry of carbon cycle on the Black Sea region of CH_4 gas seeps. Dokladi Academy Nauk USSR, 1989; 320:1235-40.

[19] Ivanov M.V., Rusanov I.I., Lein A.Y., Pimenov N.V., Yusupov S.K. and Galchenko V.F. Biogeochemistry of methane cycle in the anaerobic zone of the Black Sea, *Past and present water column anoxia. NATO Advanced Research Workshop* Crimea, Ukraine: NATO, 2003.

[20] Jones G.A. Constraining the initiation and evolution of anoxia in the Black Sea by AMS radiocarbon dating. Radiocarbon 1991; 33:211-12.

[21] Jørgensen B.B., Weber A. and Zopfi J. Sulfate reduction and anaerobic methane oxidation in Black Sea. Deep-Sea Res Pt I 2001; 48:2097-120.

[22] Kipfer R., Aeschbach-Hertig W., Peeters F. and Stute M. "Noble gases in lakes and ground waters." In *Noble gases in geochemistry and cosmochemistry.* Porcelli D., Ballentine C. and Wieler R. eds., Mineralogical Society of America, Geochemical Society, 2002.

[23] Koga Y., Morii H., Akagawa-Matsushita M. and Ohga M. Correlation of polar lipid composition with 16S rRNA phylogeny in methanogens. Further analysis of lipid component parts. Biosci Biotech Biochem 1998; 62(2):230-36.

[24] Konovalov S.K., Ivanov L.I. and Samodurov A.S. Fluxes and budget of sulphide and ammonia in the Black Sea anoxic layer. J Marine Syst 2001; 31:203-16.

[25] Kvenvolden K.A. Methane hydrates and global climate. Global Biogeochem Cy 1988; 2:221-29.

[26] Kvenvolden K.A., Ginsburg G. and Soloviev V. Worldwide distribution of subaquatic gas hydrates. Geo-Mar Lett 1993; 13:32-40.

[27] Lammers S. and Suess E. An improved head-space analysis method for methane in seawater. Mar Chem 1994; 47:115-25.

[28] Lein A.Y. Methane flows from cold methane seeps in the Black and Norwegian Seas: Quantitative estimates. Geochem Int 2005; 43:395-409.

[29] Luth C., Luth U., Gebruk A.V. and Thiel H. Methane gas seeps along the oxic/anoxic gradient in the Black Sea: manifestations, biogenic sediment compounds, and preliminary results on benthic ecology. Marine Ecology 1999; 20:221-49.

[30] Michaelis W., Seifert R., Nauhaus K., Treude T., Thiel V., Blumenberg M., Knittel K., Gieseke A., Peterknecht K., Pape T., Boetius A., Amann R., Jorgensen B.B., Widdel F., Peckmann J.R., Pimenov N.V. and Gulin M.B. Microbial reefs in the Black Sea fueled by anaerobic oxidation of methane. Science 2002; 297:1013-15.

[31] Murray J.W., Top Z. and Özsoy E. Hydrographic properties and ventilation of the Black Sea. Deep-Sea Res 1991; 38:663-89.

[32] Orphan V.J., House C.H., Hinrichs K.U., McKeegan K.D. and DeLong E.F. Direct phylogenetic and isotopic evidence for multiple groups of archaea involved in the anaerobic oxidation of methane. Geochim Cosmochim Ac 2002; 66:A571-A571.

[33] Pernthaler A., Preston C.M., Pernthaler J., DeLong E.F. and Amann R. Comparison of fluorescently labeled oligonucleotide and polynucleotide probes for the detection of pelagic marine bacteria and archaea. Appl Environ Microb 2002; 68:661-7.

[34] Rasmussen R.A. and Khalil M.A.K. Atmospheric methane in the recent and ancient atmospheres - Concentrations, trends, and interhemispheric gradient. J Geophys Res-Atmos 1984; 89:1599-1605.

[35] Reeburgh W.S. "Global methane biogeochemistry." In *The Atmosphere*, Keeling R.F. ed., Oxford, Elsevier-Pergamon, 2003.

[36] Reeburgh W.S. " "Soft spots" in the global methane budget." In *Microbial growth on C1 compounds*,Lidstrom M.E. and Tabita F.R. eds., Amsterdam, Kluwer Academic Publishers, 1996.

[37] Reeburgh W.S., Ward B.B., Whalen S.C., Sandbeck K.A., Kilpatrick K.A. and Kerkhof L.J. Black Sea methane geochemistry. Deep-Sea Res 1991; 38, Supplement 2:1189-1210.

[38] Rehder G., Keir R.S., Suess E. and Rhein M. Methane in the northern Atlantic controlled by microbial oxidation and atmospheric history. Geophys Res Lett 1999; 26:587-90.

[39] Ross D.A. and Degens E.T. "Recent Sediments of the Black Sea." In *The Black Sea - Geology, Chemistry and Biology*, Degens E.T. and Ross D.A. eds., Tulsa, OK, American Association of Petroleum Geologists Memoir 20, 1974.

[40] Ryan W.B.F., Pitman W.C. III, Major C.O., Shimkus K., Moskalenko V., Jones J.A., Dimitrov P., Gorur N., Sakinc M. and Yuce H. An abrupt drowning of the Black Sea shelf. Mar Geol 1997; 138.

[41] Sansone F.J., Popp B.N. and Rust T.M. Stable carbon isotopic composition of low-level methane in water and gas. Anal Chem 1997; 69:40-4.

[42] Schmale O., Greinert J. and Rehder G. Methane emission from high-intensity marine gas seeps in the Black Sea into the atmosphere. Geophys Res Lett 2005; 32.

[43] Schouten S., Wakeham S.G. and Damste J.S.S. Evidence for anaerobic methane oxidation by archaea in euxinic waters of the Black Sea. Org Geochem 2001; 32:1277-81.

[44] Scranton M.I. *The marine geochemistry of methane.* Ph.D. Thesis. W.H.O.I./M.I.T. Joint Program, Woods Hole, 1977.

[45] Sorokin Y.I. *The Black Sea, Eoclogy and Oceanography*, Leiden, Backhuys Publishers, 2002.

[46] Teodoru C., Friedl G., Friedrich J., Roehl U., Sturm M. and Wehrli B. Spatial distribution and recent changes in the carbon, nitrogen, and phosphorus accumulation in the sediments of the Black Sea. Global Biogeochem Cy, 2005; submitted.

[47] Thiel V., Blumenberg M., Pape T., Seifert R. and Michaelis W. Unexpected occurrence of hopanoids at gas seeps in the Black Sea. Org Geochem 2003; 34:81-7.

[48] Vetriani C., Tran H.V. and Kerkhof L.J. Fingerprinting microbial assemblages from the oxic/anoxic chemocline of the Black Sea. Appl Environ Microbiol 2003; 69:6481-8.

[49] Wakeham S.G., Lewis C.M., Hopmans E.C., Schouten S. and Damste J.S.S. Archaea mediate anaerobic oxidation of methane in deep euxinic waters of the Black Sea. Geochim Cosmochim Ac 2003; 67:1359-74.

[50] Wüest A., Brooks N.H. and Imboden D.M. Bubble plume modeling for lake restoration. Water Resour Res 1992; 28:3235-50.

[51] Yamamoto S., Alcauskas J.B. and Crozier T.E. Solubility of methane in distilled water and seawater. J Chem Eng Data 1976; 21:78-80.

SHEWANELLA: NOVEL STRATEGIES FOR ANAEROBIC RESPIRATION

Thomas J. DiChristina, David J. Bates, Justin L. Burns, Jason R. Dale, Amanda N. Payne

Georgia Institute of Technology, 311 Ferst Drive, Atlanta, Georgia 30332, USA

Abstract Metal-reducing members of the genus *Shewanella* are important components of the microbial community residing in redox-stratified freshwater and marine environments. Metal-reducing gram-negative bacteria such as *Shewanella*, however, are presented with a unique physiological challenge: they are required to respire anaerobically on terminal electron acceptors which are either highly insoluble (Fe(III)- and Mn(IV)-oxides) and reduced to soluble end-products or highly soluble (U(VI) and Tc(VII)) and reduced to insoluble end-products. To overcome physiological problems associated with metal solubility, metal-respiring *Shewanella* are postulated to employ a variety of novel respiratory strategies not found in other gram-negative bacteria which respire on soluble electron acceptors such as O_2, NO_3 and SO_4. The following chapter highlights the latest findings on the molecular mechanism of Fe(III), U(VI) and Tc(VII) reduction by *Shewanella*, with particular emphasis on electron transport chain physiology.

Keywords: *Shewanella*, metal reduction, anaerobic respiration, iron, uranium, technetium, dissolution, precipitation.

Although members of the genus *Shewanella* were first isolated nearly 75 years ago from spoiling dairy products and fish [78, 91], only recently have they received attention as important members of natural microbial communities. *Shewanella* have been isolated from a variety of marine, freshwater and terrestrial subsurface environments, including marine basins and sediments (Black Sea, Baltic Sea, Mississippi and Amazon River deltas, North Sea, Antarctic and Arctic Oceans, Mariana Trench at a depth of 11,000 m), freshwater rivers, lakes and sediments (Oneida Lake, NY, Lake Michigan), corroding oil pipelines (Alberta, Canada) and uranium-contaminated subsurface aquifers (New Mexico) [87]. *Shewanella* have also recently been detected in the surface waters of the Sargasso Sea [88], a finding that dramatically expands the normal range of *Shewanella* habitats.

Shewanella are members of the gamma subdivision of the Proteobacteria [15, 87]. *Shewanella* display remarkable respiratory versatility as they are

L. N. Neretin (ed.), Past and Present Water Column Anoxia, 443–469.

able to respire a wide variety of compounds as alternate electron acceptor, including oxygen (O_2), nitrate (NO_3^-), nitrite (NO_2^-), Mn(III,IV), Fe(III), trimethylamine-*N*-oxide (TMAO), sulfite (SO_3^{2-}), thiosulfate ($S_2O_3^{2-}$), S(0), fumarate, Cr(VI), U(VI), Tc(VII) and potentially several others [15, 53]. The remarkable respiratory versatility displayed by *Shewanella* is thought to provide a competitive advantage in redox-stratified environments where terminal electron acceptor type and abundance fluctuates on relatively small spatial and temporal scales. Over 75% of the cultivatable microorganisms from the Mn-reducing zone of the Black Sea water column are most similar to *Shewanella* [64], and nearly identical abundances are detected in the microaerobic and anoxic zones of the water column of the Gotland Deep, the main anoxic basin of the Central Baltic Sea [6].

The biogeochemical reactions catalyzed by *Shewanella* may influence the aqueous geochemical and mineralogical reaction network within redox-stratified environments. *Shewanella* may play an important role in carbon cycling by catalyzing the anaerobic mineralization of low molecular weight organic compounds in sulfate-deplete environments [1, 65, 85]. The most remarkable activity displayed by *Shewanella*, however, is their ability to couple the oxidation of organic carbon and hydrogen to either the reductive dissolution of solid phase Fe(III)- and Mn(IV)-oxides or the reductive precipitation of toxic metals and radionuclides such as Cr(VI), U(VI) and Tc(VII). The reductive precipitation reactions form the basis of alternate in situ bioremediation strategies since the relative solubility (and hence mobility) of Cr, U and Tc is greatly diminished at lower oxidation states [41, 44].

Compared to the wealth of knowledge on the molecular basis of other bacterial respiratory processes (e.g., aerobic respiration, denitrification, sulfate reduction, methanogenesis) [51], little is known about the molecular details of bacterial metal reduction. Recent sequencing of the *S. oneidensis* MR-1 genome has facilitated studies on the mechanistic details of metal reduction by *Shewanella* [29]. Genome-enabled research on *Shewanella* will be greatly expanded in the near future with the genome sequencing of seven additional *Shewanella* strains, including *S. putrefaciens* 200, *S. amazonensis*, *S. baltica* OS15, *S. frigidimarina* NCIMB 400, *S. denitrificans* OS217T, *S.* sp. PV-4 and *S. putrefaciens* CN-32 (DOE-JGI 2004 Microbial Sequencing Program). The following chapter highlights the latest findings on the molecular mechanism of Fe(III), U(VI) and Tc(VII) reduction by *Shewanella*, with particular emphasis on electron transport chain physiology.

1. MECHANISM OF IRON REDUCTION

Microbial Fe(III) reduction is involved in several globally significant environmental processes, including the biogeochemical cycling of Fe, Mn, trace elements and phosphate, degradation of natural and contaminant organic matter, weathering of Fe(III)-containing clays and minerals and biomineralization of Fe(II)-bearing minerals such as magnetite [19, 43, 48, 66]. The molecular mechanism of microbial Fe(III) reduction, however, is poorly understood. Fe(III)-respiring gram-negative bacteria are presented with a unique physiological problem: they are required to respire anaerobically on terminal electron acceptors that are largely found in crystalline form or as amorphous (oxy)hydroxide particles presumably unable to contact inner membrane (IM)-localized electron transport systems. To overcome this problem, Fe(III)-respiring bacteria are postulated to employ a variety of novel respiratory strategies not found in other gram-negative bacteria which respire on soluble electron acceptors such as O_2, NO_3 and SO_4. These strategies include 1) direct enzymatic reduction of insoluble Fe(III) oxides via outer membrane (OM)-localized metal reductases [56], 2) a two-step, electron shuttling pathway in which exogenous electron shuttling compounds (e.g., humic acids, melanin, phenazines, antibiotics, anthraquinone-2,6-disulfonate; AQDS) are first microbially reduced and subsequently chemically oxidized by the Fe(III) oxides in a second (abiotic) electron transfer reaction [10, 11, 18, 30, 68, 86], 3) an analogous two-step reduction pathway utilizing endogenous (quinone-like) electron shuttling compounds [76, 68] and 4) a two-step, Fe(III) solubilization-reduction pathway in which solid Fe(III) oxides are first non-reductively dissolved by bacterially-produced organic ligands, followed by uptake and reduction of the soluble organic Fe(III) forms by periplasmic Fe(III) reductases [47]. Several metal-reducing members of the genus *Shewanella* are able to respire solid Fe(III) oxides via all four mechanisms. Mechanistic details of the four pathways for reduction of solid Fe(III) by *Shewanella* are summarized in the following section.

1.1 Direct Enzymatic Reduction at the Outer Membrane

Shewanella catalyzes the reduction of solid Fe(III) oxides via an electron transport chain arranged in modular fashion. Primary dehydrogenase complexes are linked to terminal reductase complexes via a menaquinone pool [58]. Hydrogenases and flavin-containing dehydrogenases [41, 56] oxidize a variety of electron donors (e.g., H_2, formate, lactate) and transfer electrons via the menaquinone pool. Lipid soluble menaquinones are required for Fe(III) reduction by *Shewanella* membrane fractions supplied with either formate or NADH as electron donor [76]. Menaquinol is postulated to diffuse to the quinol oxidation site of CymA, a 21 kDa tetraheme *c*-type cytochrome which oxidizes

menaquinol and subsequently transfers electrons to downstream components of the electron transport chains terminating with reduction of Fe(III), Mn(IV), NO_3^- and fumarate [54, 60, 77]. Menaquinol oxidation and concurrent reduction of CymA releases protons to the periplasmic space, thereby generating a proton motive force. Electrons are transferred to one of four *c*-type hemes within CymA, followed by inter-heme electron transfer (according to decreasing heme redox potential) until a final transfer is made to subsequent electron carriers in the periplasmic space [28]. *cymA*-deficient mutants of *S. putrefaciens* are unable to reduce NO3-, Fe(III), Mn(IV) or fumarate as terminal electron acceptor [59]. CymA is therefore an integral part of the *Shewanella* electron transport system.

After CymA, the *Shewanella* electron transport system deviates from that generally observed in gram-negative bacteria respiring on soluble electron acceptors. Fe(III) reduction activity is detected in wild-type OM fractions [57], and is severely impaired in mutants lacking a variety of OM proteins, including several multi-heme *c*-type cytochromes (see below). Electron transport from CymA to solid Fe(III) oxides is postulated to proceed via an electron transport chain spanning the periplasmic space and terminating on the outside face of the OM [57]. Some of the most convincing evidence supporting this hypothesis has been derived from genetic studies with *S. putrefaciens* [16, 17]. Initial gene cloning studies have demonstrated that a 23.3 kb *S. putrefaciens* wild-type DNA fragment confers Fe(III) and Mn(IV) reduction activity to a set of Fe(III) and Mn(IV) reduction-deficient mutants. The smallest complementing fragment contains one open reading frame (ORF) whose translated product displays 87% sequence similarity to *Aeromonas hydrophila* ExeE, a member of the GspE family of proteins found in Type II protein secretion systems. GspE insertional mutants (constructed by targeted replacement of wild-type *gspE* with an insertionally inactivated *gspE* construct) are unable to respire anaerobically on solid Fe(III) or solid Mn(IV), yet retain the ability to respire all other electron acceptors. Nucleotide sequence analysis of regions flanking *gspE* reveal one partial and two complete ORFs whose translated products display 55%-70% sequence similarity to the GspD-G homologs of Type II protein secretion systems. A heme-containing Fe(III) reductase is present in the peripheral proteins loosely attached to the outside face of the wild-type OM, yet is missing from this location in the *gspE* mutants. Membrane fractionation studies with the wild-type strain support this finding: the heme-containing Fe(III) reductase is detected in the OM but not the IM or cytoplasmic fractions. These findings provide the first genetic evidence linking anaerobic Fe(III) and Mn(IV) respiration to Type II protein secretion and provide additional biochemical evidence supporting OM localization of *Shewanella* Fe(III) reductases [16, 17].

A contiguous cluster of 12 Type II protein secretion genes (*gspC-N* homologs) has also been identified in the *S. oneidensis* MR-1 genome. A Type II

protein secretion mutant of *S. oneidensis* (constructed by targeted replacement of wild-type *gspD*, encoding the putative OM secretion of type II secretion, with an insertionally-inactivated *gspD* construct), is unable to respire anaerobically on solid Fe(III) or solid Mn(IV), yet retains the ability to respire all other electron acceptors, including soluble Fe(III) and AQDS [18]. As observed with the Fe(III) respiration-deficient *gspE* insertional mutant of *S. putrefaciens*, a heme-containing Fe(III) reductase is present in the peripheral proteins loosely attached to the outside face of the wild-type OM, yet is missing from this location in the *gspD* insertional mutant. Type II protein secretion may therefore be required for direct enzymatic reduction of solid Fe(III) and solid Mn(IV) by all metal-reducing members of the genus *Shewanella*. The ability to respire solid Fe(III) and solid Mn(IV) is rescued in the *S. oneidensis gspD* insertional mutant by addition of AQDS, an indication that the AQDS electron shuttling pathway (Mechanism No. 2; see below) may functionally replace the Type II protein secretion-linked pathway for anaerobic respiration on solid Fe(III) and Mn(IV) oxides [18].

The OM proteins involved in the terminal steps of electron transport to solid Fe(III) remain unknown, yet most likely include several *c*-type cytochromes. The *S. oneidensis* MR-1 genome encodes 42 predicted *c*-type cytochromes [29, 55], including those in the *mtrDEF-omcA-mtrCAB* gene cluster which may encode several Fe(III) terminal reductase components. MtrA and MtrD [73] are decaheme *c*-type cytochromes that display 99% similarity to each other, suggesting they may provide complementary function. MtrA and MtrD are OM-associated, but are oriented toward the periplasm [73] and therefore not in position to contact solid Fe(III) directly. MtrB is a putative beta-barrel protein required for Fe(III) and Mn(IV) reduction activity [5, 62]. *mtrB* mutants are completely abolished in Mn(IV) reduction activity and are severely impaired (but not completely abolished) in Fe(III) reduction activity, yet retain the ability to reduce all other electron acceptors [5]. MtrB is postulated to be involved in OM localization of *c*-type cytochromes (e.g., OmcA, MtrC) involved in electron transfer to Fe(III) and Mn(IV) [62]. MtrC (OmcB) is an OM decaheme, *c*-type cytochrome required for both Fe(III) and Mn(IV) reduction. OmcA, on the other hand, is an OM decaheme *c*-type cytochrome involved only in Mn(IV) reduction [61]. *omcA*-deficient mutant strains reduce Mn(IV) at 45% wild-type rates. Interestingly, *mtrC* overexpression in an *omcA*-deficient mutant restores Mn(IV) reduction activity to greater than wild-type rates. MtrC overexpression may therefore compensate for the absence of OmcA in the *Shewanella* Mn(IV) reduction pathway, which suggests at least partial overlap in the roles of these OM cytochromes in the Mn(IV) reduction pathway [63]. The functions of MtrC and OmcA in solid Fe(III) oxide reduction remain unknown.

Lipopolysaccharides (LPS) and OM proteins may play a critical role in establishing and maintaining contact with solid Fe(III) oxides. The ability of

Shewanella cells to adhere to solid Fe(III) oxides may be controlled by the composition and length of the LPS molecules [35]. *Shewanella* cells respond to anaerobic conditions by synthesizing cell surface components with affinity for Fe(III) minerals: biological forces measured at the interface between cantilever-attached *Shewanella* cells and goethite indicate that attractive forces between the cell surface and Fe(III) mineral increase approximately five-fold under anaerobic conditions [49]. A working model of the Type II protein secretion-linked pathway for direct (enzymatic) reduction of solid Fe(III) oxides at the *Shewanella* OM is displayed in Fig. 1.

1.2 Exogenous Electron Shuttling Pathway

A variety of Fe(III)-reducing bacteria, including *Shewanella*, employ redox-active compounds (e.g., humic acids, melanin, phenazines, antibiotics, AQDS) as electron shuttles to reduce extracellular Fe(III) oxides [46]. The Fe(III) and Mn(IV) reduction-deficiencies of *Shewanella* Type II protein secretion mutants are rescued by addition of AQDS [18]. *S. oneidensis gspD* insertional mutants are unable to respire anaerobically on solid Fe(III) or Mn(IV), yet retain the ability to respire all other electron acceptors, including AQDS. The ability to respire 50 mM solid Fe(III) or Mn(IV) is rescued in the *S. oneidensis gspD* insertional mutants by addition of 50 μM AQDS, an indication that the AQDS electron shuttling pathway functionally replaces the Type II protein secretion-linked pathway for respiration on solid Fe(III) and Mn(IV). AQDS is toxic to *Shewanella* cells above a critical concentration threshold and the efflux pump protein TolC protects *Shewanella* cells from AQDS toxicity by mediating AQDS efflux [79]. Electron transfer to AQDS also requires the OM protein MtrB, although its role in AQDS reduction remains unknown [79].

Solid Fe(III) reduction by *Shewanella* is also stimulated by redox-active antibiotics and phenazines [30]. Phenazines display remarkable similarity in structure to AQDS, and most likely act in a similar manner to shuttle electrons between *Shewanella* cells and solid Fe(III) oxides. Redox-active antibiotics (e.g. bleomycin) also function as shuttles for extracellular electron transfer to solid electron acceptors. Bacterially-produced phenazines (e.g., synthesized by *Pseudomonas chlororaphis* PCL1391) stimulate Fe(III) reduction by bacteria unable to produce them (e.g. *S. oneidensis* MR-1) [30]. In addition, melanin (a humic acid analog synthesized by *S. algae* BrY in the presence of high concentrations of tyrosine) will enhance rates of Fe(III) oxide reduction. Melanin may have a dual function by acting as both an electron shuttle and an Fe(II)-complexing agent that prevents Fe(II) from blocking Fe(III) oxide surface sites [86]. A working model of the exogenous electron shuttling pathway for reduction of solid Fe(III) oxides is displayed in Fig. 2.

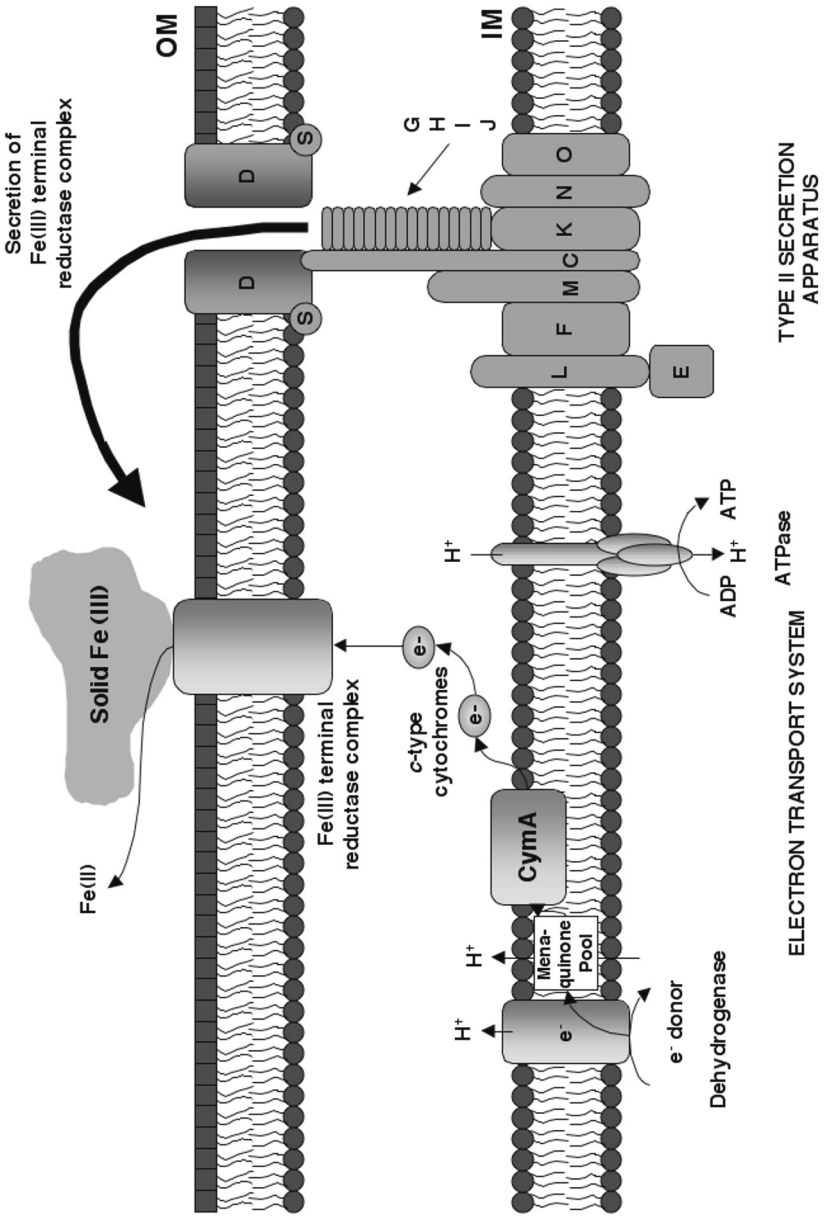

Figure 1. Working model for type II protein secretion-linked direct enzymatic reduction of solid Fe(III)-oxides at the outer membrane.

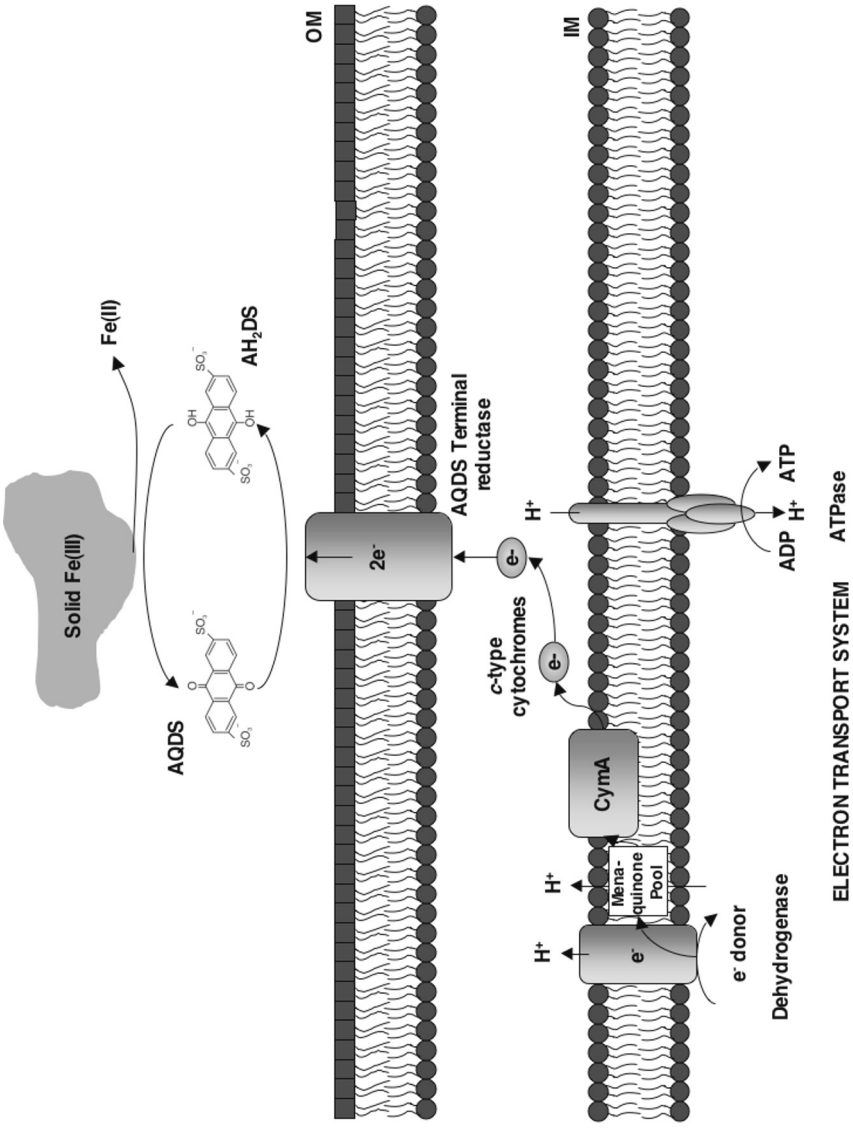

Figure 2. Working model for exogenous shuttling pathway with AQDS as electron shuttle.

1.3 Endogenous Electron Shuttling Pathway

Although the exact identity of an endogenous electron shuttle has yet to be determined, preliminary studies indicate that *Shewanella* may synthesize and release quinone-like compounds that act as shuttles for electron transfer to solid Fe(III) oxides [68]. *S. algae* BrY produces melanin as a soluble electron shuttle for reduction of insoluble Fe(III) oxides [86]. *S. algae*-produced melanin oxidizes cytochromes at the cell surface and reduces solid Fe(III) oxides extracellularly [86]. *S. oneidensis* MR-1 mutants defective in *menC* (encoding *o*-succinylbenzoic acid synthase) are deficient in menaquinone production and are unable to reduce AQDS, fumarate, thiosulfate, sulfite, DMSO or solid Fe(III) and Mn(IV) [68]. Menaquinone is detected in the spent media of the wild-type strain, but not the *menC* mutants. Spent media from the wild-type complemented the *menC* mutant, while spent media from *menC* mutant did not. *S. oneidensis* MR-1 mutants defective in either *menD* or *menB* (encoding components of the menaquinone biosynthetic pathway) are also unable to reduce solid Fe(III) oxides [76]. Vitamin K_2 (a menaquinone analog) restores the ability of the *menD* or *menB* mutants (and corresponding membrane fractions) to reduce either Fe(III) or Mn(IV) [76]. It should be noted that the endogenous electron shuttle pathway may be the consequence of cell lysis and inadvertent spillage of menaquinol into the culture medium. Lipid-soluble menaquinol or vitamin K2 then diffuse into bacterial membranes and functionally complement the *menB-D* mutants. Definitive evidence on the identity of the endogenous electron shuttle will therefore require further research. A working model of the endogenous electron shuttling pathway for reduction of solid Fe(III) oxides is displayed in Fig. 3.

1.4 Fe(III) Solubilization by Bacterially Produced Organic Ligands

An electrochemical signal attributed to soluble organic-Fe(III) is detected in a variety of marine and freshwater environments with Au/Hg voltammetric microelectrodes [83]. Soluble organic-Fe(III) may therefore represent a dominant, yet underappreciated electron acceptor in anaerobic aquatic systems. Microbial Fe(III) reduction rates are higher with soluble organic-Fe(III) in pure cultures of *S. putrefaciens* [2] and in freshwater sediments amended with nitrilotriacetic acid (NTA). *S. putrefaciens* reduces soluble organic-Fe(III) at rates three orders of magnitude faster than amorphous or crystalline Fe(III) forms. The mechanism of formation of soluble organic-Fe(III) generally involves non-reductive dissolution of amorphous Fe(III) oxides by multidentate organic ligands (forming mononuclear complexes with the Fe(III) oxides) at circumneutral pH. The strength of binding between Fe(III) and the complexing organic ligands influences soluble organic-Fe(III) reduction activity: organic ligands with strong

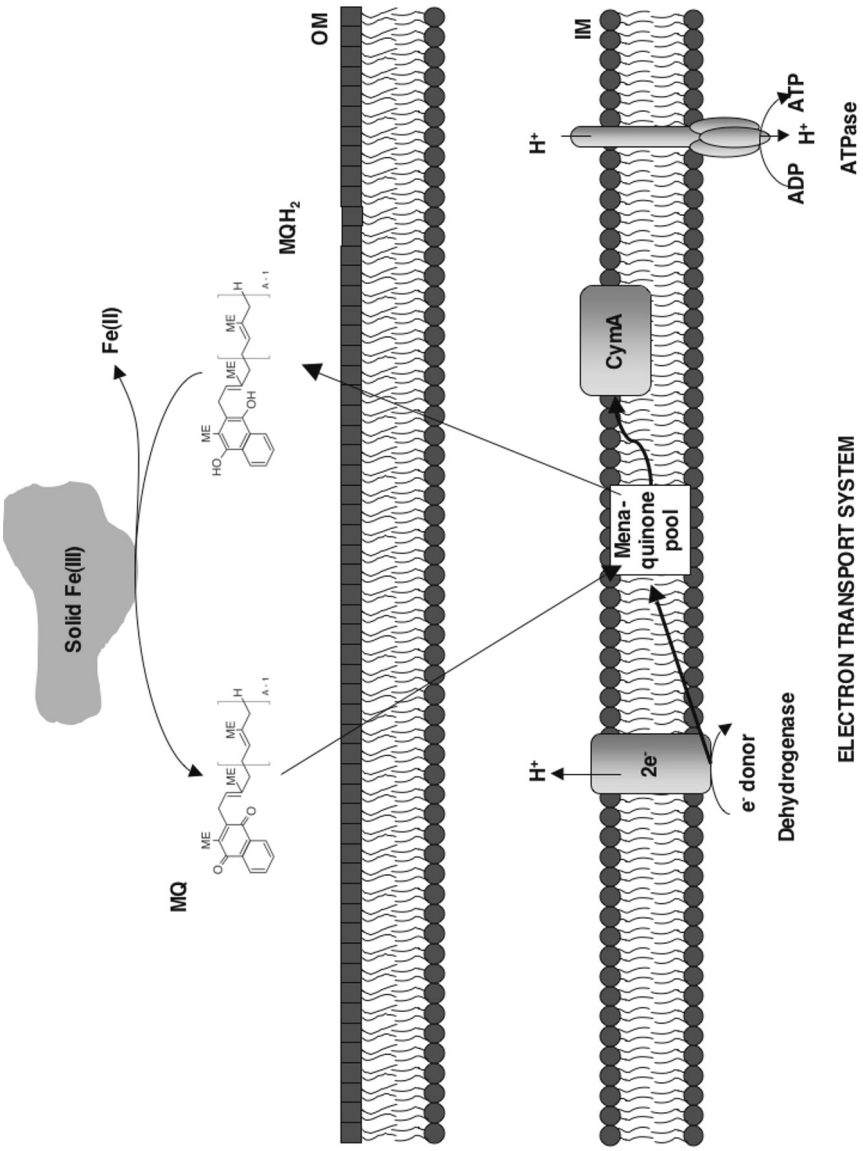

Figure 3. Working model for endogenous electron shutting pathway with menaquinones as electron shuttle.

Fe(III)-binding capability decrease (and in some cases totally inhibit) Fe(III) reduction activity by *S. putrefaciens* [26].

Some Fe(III)-reducing bacteria generate relatively high concentrations of soluble organic-Fe(III) in the absence of exogenous chelating compounds, an indication that such bacteria synthesize and release organic ligands to solubilize Fe(III) prior to reduction [67]. Soluble organic-Fe(III) is detected electrochemically in *Shewanella* cultures incubated anaerobically with either ferrihydrite or goethite [83]. Detection of soluble organic-Fe(III) prior to detection of Fe(II), suggests that soluble organic-Fe(III) is an intermediate in the reduction of solid Fe(III) oxides. Since lactate is the only organic ligand added to the *Shewanella* batch cultures and lactate-Fe(III) complexes do not react with Au/Hg electrodes, electrochemical detection of soluble organic-Fe(III) suggests that *Shewanella* synthesizes and releases organic ligands to non-reductively dissolve Fe(III) prior to reduction.

A soluble organic-Fe(III) reductase has not been definitively identified. *Shewanella* Type II protein secretion mutants (see above) are unable to reduce solid Fe(III) oxides, yet retain the ability to reduce all other electron acceptors, including soluble organic-Fe(III). The inability of the Type II protein secretion mutants to target Fe(III) reductases to the OM suggests that the Type II protein secretion mutants reduce soluble organic-Fe(III) in the periplasmic space. When expressed in *E. coli*, the *S. oneidensis* decaheme *c*-type cytochrome MtrA displays soluble organic-Fe(III) reductase activity [73], although confirmation in *S. oneidensis* has yet to be reported. In *S. frigidimarina*, the transcriptional activator IfcR is translated in the presence of soluble Fe(III) and is essential for expression of *ifcO* and *ifcA*. IfcO is a putative OM beta-barrel protein postulated to function as a soluble Fe(III) transporter. IfcA is a flavin-containing *c*-type cytochrome with a small (10 kDa) tetraheme cytochrome domain capable of reducing soluble Fe(III) [73]. A working model of the two-step, Fe(III) solubilization-reduction pathway in *Shewanella* is displayed in Fig. 4.

2. MECHANISM OF URANIUM REDUCTION

Members of the genera *Shewanella* [44], *Desulfovibrio* [45], *Clostridium* [22], *Geobacter* [9], *Thermus* [34], *Pyrobaculum* [32], and *Desulfosporosinus* [82] display U(VI) reduction activity. *Shewanella* and *Geobacter* enzymatically reduce U(VI) to U(IV) via a dissimilatory process that supports anaerobic growth, however the molecular mechanism of U(VI) reduction is poorly understood. Cytochrome c_3 of U(VI)-reducing (but non-respiring) *Desulfovibrio vulgaris* displays U(VI) reductase activity *in vitro* [45, 71]. Cytochrome c_3 couples H_2 oxidation to U(VI) reduction. Cytochrome c_7 of *Geobacter sulfurreducens* also displays U(VI) reductase activity *in vitro*, however, mutants deficient in either cytochrome c_3 or c_7 retain U(VI) reduction activity *in vivo*

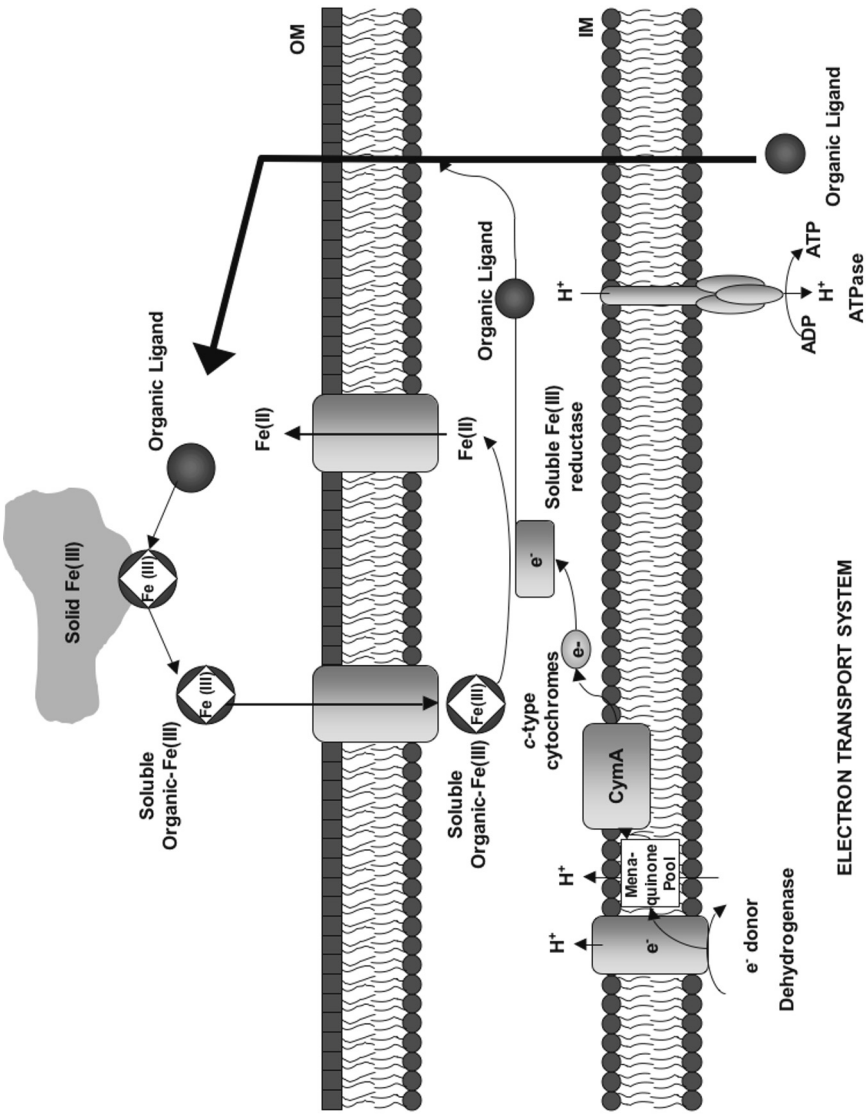

Figure 4. Working model for Fe(III) solubilization-reduction pathway with endogenous organic ligand as Fe(III)-chelating compound.

[42]. The effects of U(VI) chemical speciation, electron donors and competing electron acceptors on U(VI) reduction activity by *Shewanella* have recently been reported. In addition, the identity and subcellular location of reduction products have been described, and genetic analysis of U(VI) reduction-deficient mutant strains is underway.

2.1 U(VI) Chemical Speciation

U(VI) chemical speciation is an important variable controlling microbial U(VI) reduction activity. In oxidizing aqueous environments at circumneutral pH (and in the absence of phosphate), U(VI) is found as soluble uranyl ion (UO_2^{2+}) complexes or as the crystalline solid metaschoepite ($UO_3 \cdot 2H_2O$). U(IV) precipitates in reducing environments as uraninite (UO_2). The relative solubility of U(VI) compared with uraninite (only 10^{-8} M at pH >5; [74]) forms the basis of alternate bioremediation strategies.

Uranyl ion is highly soluble and readily complexes with either inorganic (e.g., hydroxyl, carbonate, phosphate, sulfate and calcium) or organic (e.g., acetate, malonate, citrate and oxalate) ligands in aqueous solution. The complexing ligand changes the reduction potential of U(VI), thus affecting microbial reduction activity. In terms of reduction potential, hydroxo complexes are the most favorable form of complexed U(VI). Complexation by carbonate decreases the reduction potential of U(VI). Complexation of U(VI)-carbonate by calcium (forming $Ca\text{-}UO_2\text{-}CO_3$ complexes) decreases the reduction potential to such an extent that U(VI) reduction by *S. putrefaciens* CN32 nearly ceases [7]. The formation of $Ca\text{-}UO_2\text{-}CO_3$ complexes also inhibits U(VI) reduction by *D. sulfuricans* and *G. sulfurreducens*. Neither fumarate nor Tc(VII) reduction activities are inhibited by Ca^{2+}, indicating that the effects of Ca^{2+} are U(VI) reduction-specific.

In the absence of carbonate or at pH less than 6 in the presence of carbonate, organic ligands bound to U(VI) also affect uranium solubility and bioavailability. Citrate, for example, binds U(VI) with varying strength as a function of pH [70]. At pH greater than 6 and at low citrate concentrations, the highly soluble $(UO_2)_3Cit_2$ species predominates over the $(UO_2)_2Cit_2$ species. *S. alga* reduces U(VI) bound to citrate and other multidentate aliphatic complexes such as malonate and oxalate more rapidly than U(VI) bound to monodentate aliphatic complexes such as acetate, while the opposite trend is found with *D. desulfuricans* [25]. U(VI) adsorbs to carboxyl, phosphoryl, and amine functional groups on the *S. putrefaciens* 200 cell surface, and a ligand exchange reaction may take place between the cell surface or U(VI) terminal reductase(s) and the U(VI) complexes prior to reduction [26].

2.2 Electron Donors and Competing Electron Acceptors

U(VI) reduction by *Shewanella* is coupled to oxidation of hydrogen, lactate, formate or pyruvate [44]. U(VI) reduction rates are highest with H_2 as electron donor [38] . Two explanations may account for the increased rate of U(VI) reduction coupled to H_2 oxidation [3, 38]. First, electron flow through the electron transport chain may be more rapid when coupled to H_2 rather than lactate oxidation. Periplasmic H_2 hydrogenases may pass electrons through the electron transport chain more rapidly than those generated from cytoplasmic membrane-localized lactate dehydrogenase. Secondly, mass flux of neutrally charged H_2 to the enzymatic site of oxidation may be faster than negatively charged lactate. The negative charge of the lactate ion inhibits diffusion across the cell surface to the cytoplasmic membrane, thereby requiring an active transport system.

The presence of competing terminal electron acceptors also interferes with microbial U(VI) reduction. Thermodynamic predictions indicate that electron acceptors are utilized in order of highest free energy yield, a likely explanation for the inhibition of U(VI) reduction in the presence of nitrate [21]. Thermodynamic considerations alone, however, do not explain the observed preference for some Fe(III) species over U(VI). Although the reduction of U(VI) coupled to the oxidation of organic compounds should yield greater free energy than Fe(III) [12], and despite the high solubility of U(VI), ferrihydrite inhibits U(VI) reduction by *S. alga* BrY [90]. Inhibition by hematite or goethite, however, is not observed. Amorphous Fe(III) hydroxides such as ferrihydrite are able to compete with U(VI) as electron acceptor, while U(VI) is favored over more crystalline forms of Fe(III). Kinetic factors, such as organism-Fe(III) oxide attachment rate or enzyme-mediated electron transfer rates may enhance the Fe(III) reduction rates relative to U(VI).

Electron transport to Mn(IV) provides a greater free energy yield than electron transport to U(VI), and is therefore predicted to be a preferred electron acceptor [12, 36]. Bioavailable Mn(IV)-oxides such as birnessite and bixbyite follow this prediction, however, U(VI) is reduced concurrently with less soluble forms of Mn(IV) [24]. To determine if this finding is due to electron acceptor competition or abiotic oxidation of U(IV) by Mn(IV), *S. putrefaciens* CN32 was incubated with U(VI) and pyrolusite (β-$MnO_{2(s)}$) [39]. Extracellular, cell surface-associated, and periplasmic $UO_{2(s)}$ aggregates were detected by Transmission Electron Microscopy (TEM) when cells were incubated only with U(VI). Upon addition of pyrolusite, extracellular $UO_{2(s)}$ was depleted but periplasmic and cell surface-associated $UO_{2(s)}$ remained. These results suggest that U(IV) functions as an electron shuttle and is oxidized by the extracellular pyrolusite. U(VI) is completely reduced provided the OM of intact cells physi-

cally separates (sequesters in the periplasmic space) $UO_{2(s)}$ from extracellular pyrolusite.

Humic acids have recently gained attention for their potential role as shuttles for electron transfer between anaerobically respiring *Shewanella* and solid Fe(III)-oxides (see above). Addition of AQDS to *S. putrefaciens* CN32, however, does not enhance the reduction rate of either soluble or insoluble forms of U(VI) [23]. AQDS actually inhibits U(VI) reduction activity, most likely by re-directing electrons away from the U(VI) reduction pathway.

2.3 U(IV) Localization

The subcellular location of U(VI) reduction in *Shewanella* is unknown, however, U(IV) is detected extracellularly, associated with the cell surface and within the periplasmic space of *S. putrefaciens* reducing soluble forms of U(VI) [39]. U(IV) is not detected in the cytoplasm. U(VI) reductases may therefore be localized within the gram-negative cell envelope, or soluble U(VI) diffusion (or transport) across the OM facilitates contact with U(VI) reductases located in the periplasm or cytoplasmic membrane. U(VI) reduction products are nanometer-size $UO_{2(s)}$ particles during U(VI) reduction by *Desulfosporosinus* [82]. Nanoparticles produced in the periplasm are either exported via OM porins or other export mechanisms where they aggregate extracellularly to form larger particles. Aggregation of U(IV) particles prior to export from the cell may result in the periplasmic deposits detected on TEM images of U(VI)-respiring cells [39]. U(IV) particles detected in the culture supernatant also leads to the intriguing possibility that anaerobically-respiring *Shewanella* are able to actively excrete U(IV) particles as a means of avoiding build-up of toxic insoluble end-products during U(VI) reduction. *S. putrefaciens* CN32 is also capable of reducing solid forms of U(VI) [23]. The mechanism by which *Shewanella* species reduce metaschoepite is unknown, but U(VI) terminal reductase localization to the outer membrane to contact solid U(VI) is possible.

2.4 Genetic Analysis

A genetic system has recently been developed to determine the molecular mechanism of U(VI) reduction by *S. putrefaciens* [89]. *S. putrefaciens* respiratory (Urr) mutants unable to reduce U(VI) were isolated and tested for the ability to respire on a suite of alternate compounds as electron acceptor, including oxygen (O_2), nitrate (NO_3^-), fumarate, trimethylamine-*N*-oxide (TMAO), dimethyl sulfoxide (DMSO), manganese oxide (MnO_2), ferric iron (Fe(III)), chromate (Cr(VI)), arsenate (As(V)), selenite (Se(IV)), pertechnetate (Tc(VII)), thiosulfate (S(II)), and sulfite (S(IV)) [89]. Ethyl methane sulfonate (EMS) was used as a chemical mutagen to generate the set of Urr mutants of *S. putrefaciens* 200. Approximately 13,000 colonies arising from EMS-treated cells were trans-

ferred to agar growth medium supplemented with U(VI)-carbonate as electron acceptor and incubated under microaerobic conditions. The resulting colonies were examined for production of a brown precipitate (presumably U(IV)) on their surface. Strains unable to produce the U(IV) precipitate were subsequently tested for anaerobic growth in liquid medium supplemented with U(VI) as sole electron acceptor. Strains displaying a U(VI) reduction-deficient phenotype on the rapid plate assay were also unable to respire U(VI) in anaerobic liquid growth medium. All Urr mutant strains also lacked the ability to respire NO_2^-. In particular, Urr mutant strain U14 retained the ability to respire all electron acceptors except U(VI) and NO_2^-. These results suggest that the electron transport chains terminating with the reduction of NO_2^- and U(VI) share common respiratory components, possibly including the NO_2^- reductase itself.

Three types of respiratory NO_2^- reductases are found in bacteria: Cu-containing NirK, cytochrome *cd*$_1$-containing NirS and *c*-type cytochrome NrfA [52]. In the NO_3^- reduction pathways of denitrifying bacteria such as *Alcaligenes faecalis* and *Pseudomonas stutzeri*, NirK and NirS reduce NO_2^- to nitric oxide (NO), which is subsequently reduced to N_2 via a nitrous oxide (N_2O) intermediate. In the NO_3^- reduction pathways of *E. coli* and *Wolinella succinogenes*, on the other hand, periplasmic NrfA catalyzes the 6-electron reduction of NO_2^- to NH_3 [81]. The *S. oneidensis* MR-1 genome was scanned for putative NO_2^- reductases via Basic Local Alignment Search Tool (BLAST) analysis. Only the *nrfA* homolog was found in the *S. oneidensis* genome: Locus SO3980 is 79% similar (65% identical) to *nrfA* of *Escherichia coli*.

In *E. coli*, NrfA requires three intermediary components (NrfB-D) to receive electrons from the menaquinone pool. NrfD is a putative inner-membrane quinol oxidase that transfers electrons from the menaquinone pool to NrfC. NrfC is a FeS protein that delivers electrons to the soluble *c*-type cytochrome NrfB, which subsequently delivers electrons to NrfA [31]. *W. succinogenes*, in contrast, requires only one intermediary component: inner-membrane associated NrfH (a NapC/NirT homolog; [80]), which displays quinol:NrfA oxidoreductase activity. Interestingly, the *S. oneidensis* genome contains ORFs encoding proteins similar to both NrfB and NrfH. NrfB displays similarity to MtrA and MtrD, the paralogous proteins involved in Fe(III) reduction [73]. In addition, CymA, a recently discovered NapC/NirT homolog also required for NO_2^- reduction [77] transfers electrons from the menaquinone pool to the Fe(III) terminal reductase complexes in *S. oneidensis* [59, 60, 77] (Figs. 1-4). The periplasmic location of the Nrf system in *E. coli* and *W. succinogenes* is consistent with the observed subcellular location of U(IV) in U(VI)-respiring *Shewanella*. A working model for the U(VI) reduction pathway in *S. oneidensis* is displayed in Fig. 5.

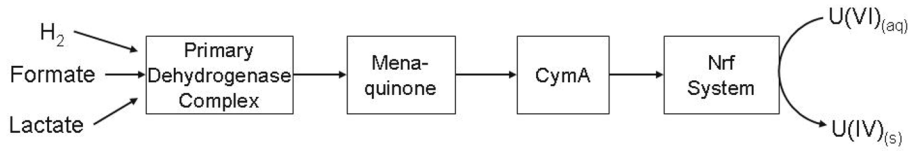

Figure 5. Working model for U(VI) reduction pathway in S. oneidensis.

3. MECHANISM OF TECHNETIUM REDUCTION

Molecular studies on the ability of microorganisms to reduce Tc(VII) have been focused in *E.coli*, however the ability to reduce Tc(VII) has been recently established in *Shewanella putrefaciens* CN32, *Shewanella oneidensis* MR-1 and *Shewanella putrefaciens* 200R [40, 50, 72, 91]. Tc(VII) is also reduced under acidic conditions by *Thiobacillus thiooxidans* [50], under alkaline conditions by *Halomonas* strain Mono [33] and at high temperature by *Pyrobaculum islandicum* [32]. Reduction of soluble Tc(VII) results in formation of Tc(IV) which precipitates as insoluble TcO_2 and is immobilized in the environment. Immobilization also occurs via formation of strong surface complexes with hydroxylated surface sites on Al and Fe oxides and clays in the absence of aqueous complexing agents [20, 27, 55, 75, 91].

3.1 The Role of Hydrogenases in Tc(VII) Reduction

E. coli possesses four hydrogenases, designated as hydrogenases 1-4. Hydrogenases 1 and 2 share little homology to hydrogenases 3 and 4. Hydrogenases 3 and 4 share high homology to each other and are both expressed as part of the formate-hydrogen lyase complex [4]. The Tc(VII) reductase in *E.coli* has been identified as the Ni-Fe hydrogenase 3 component of the formate-hydrogen lyase complex [40]. Hydrogenase expression is determined by pH: hydrogenase-4 (encoded by the *hyf* operon) is expressed under alkaline conditions while hydrogenase-3 (encoded by the *hyc* operon) is expressed under acidic conditions [4]. The formate hydrogen-lyase complex in *E.coli* is composed of formate dehydrogenase plus multiple components of the respective hydrogenase encoding operons (i.e., *hyf* and *hyp* operons). The bi-directional nature of hydrogenase-3 (HycE) enables both the production of H_2 during formate oxidation and the direct oxidation of H_2.

S. oneidensis MR-1 does not possess a formate-hydrogen lyase complex and possesses only two hydrogenases, neither of which share significant homology to hydrogenase 3 or 4 of *E.coli* . The first *S. oneidensis* MR-1 hydrogenase (Locus SO2098; HyaB) displays high homology to the IM-bound Ni-Fe hydrogenase HydB of *Wolinella succinogenes*, while the second *S. oneidensis* MR-1 hydrogenase (Locus SO3920; HydA) displays high homology to the (putative)

D subunit of the NADP-reducing hydrogenase of *Thermotoga maritima* (Table 1) [72]. In terms of hydrogenase function, *S. oneidensis* MR-1 appears most similar to *Alcaligenes eutrophus* where the cytoplasmic, soluble hydrogenase (HydA) regenerates NADH, while the membrane bound Ni-Fe hydrogenase (HyaB) generates reducing power [37]. In organisms containing only the membrane bound hydrogenase, reducing power is generated by reverse electron transport, generally carried out by membrane bound bi-directional hydrogenases (e.g., hydrogenases 3 and 4 in *E.coli*). Thus *S. oneidensis* MR-1 appears to share close similarity to the hydrogen uptake and utilization systems of *Acaligenes eutrophus* and little physiological similarity to the hydrogen uptake and utilization systems of *E.coli.* It will be interesting to determine if the *S. oneidensis* MR-1 hydrogenases display Tc(VII) reduction activity.

Table 1. BLAST analysis of non-redundant protein database with *S. oneidensis* MR-1 loci SO2098 (HyaB) and SO3920 (HydA).

Locus	Best Hit	% Identity	% Similarity	Expect
SO2098 (HyaB)	*Wollinella succinogenes* inner membrane-bound Ni-Fe hydrogenase (HydB)	61	75	2.2e-195
SO3920 (HydA)	*Thermotoga maritima* NADP-reducing hydrogenase, D subunit (putative)	44	61	1.5e-72

3.2 Tc(VII) Reduction Pathways in Bacteria are Electron Donor-Specific

The enzymatic reduction of Tc(VII) is electron donor specific. Hydrogen serves as electron donor in all known Tc(VII)-reducing organisms [13, 41, 91], while the ability to couple the oxidation of other carbon sources to the reduction of Tc(VII) occurs in only a small subset of organisms. Unlike *G. sulfurreducens* and *D. fructosovorans* (which have an exclusive requirement for hydrogen as electron donor for Tc(VII) reduction and *E.coli* which is limited to formate and hydrogen as electron donor), *S. oneidensis* MR-1 couples formate, lactate and hydrogen oxidation to Tc(VII) reduction [72, 91].

As summarized above, Tc(VII) reduction by *E.coli* proceeds via the action of a bi-directional hydrogenase [4, 40]. Tc(VII) reduction by *S. oneidensis* MR-1 and *S. putrefaciens* CN32, on the other hand, appears to involve multiple components in highly branched electron transport pathways. The respiratory capabilities of Tc(VII) reduction-deficient point mutants of *S. oneidensis* MR-1

suggest that the Tc(VII) reduction pathways are electron donor-specific [72]. H_2 and lactate-dependent Tc(VII) reduction was severely impaired in one set of mutants, while formate-dependent Tc(VII) reduction was not affected. This finding is similar to results obtained with *S. putrefaciens* CN32: the end products of Tc(VII) reduction depend on the electron donor oxidized. Amorphous Tc(IV) oxides are formed during H_2-dependent Tc(VII) reduction, while hydrous Tc(IV) oxides are formed during lactate-dependent Tc(VII) reduction [91]. TEM images of *S. putrefaciens* CN32 indicate that the subcellular location of the end products is also electron donor-specific: amorphous Tc(IV) oxides resulting from H_2 oxidation are found in both the periplasmic space and associated with the OM, while hydrous Tc(IV) oxides resulting from lactate oxidation are presumably in the extracellular milieu since they are not detectable within the periplasm by TEM imaging [91].

The first genetic studies on Tc(VII) reduction have been carried out in *S. oneidensis* MR-1 [72]. *S. oneidensis* MR-1 provides an attractive model for studying the molecular basis of Tc(VII) reduction as genetic manipulations may be carried out under aerobic conditions and its genome has recently been sequenced [29]. *S. oneidensis* MR-1 displays remarkable respiratory versatility as it is able to respire a wide variety of compounds as alternate electron acceptor including oxygen (O_2), nitrate (NO_3^-), nitrite (NO_2^-), Mn(III,IV), Fe(III), trimethylamine-N-oxide (TMAO), sulfite (SO_3^{2-}), thiosulfate ($S_2O_3^{2-}$), S(0), fumarate, U(VI), Tc(VII) and potentially several others [16, 53]. A genetic screen for identifying Tc(VII) reduction-deficient mutants of *S. oneidensis* MR-1 was developed based on the observation that microaerobically grown colonies plated on Tc(VII)-amended agar produce a precipitate on their colony surface during microaerobic growth [72]. Tc(VII) reduction-deficient mutants were generated in MR-1 by treating wild-type cells with ethyl methane sulfonate (EMS) and transferring them to Tc(VII)-amended agar. Colonies arising on the Tc(VII) amended agar plates were screened for the inability to produce black precipitate (i.e., Tc(IV)).

Potential Tc(VII) reduction-deficient mutants identified via the genetic screen were subsequently tested for Tc(VII) reduction activity in anaerobic liquid medium. The liquid reduction assay was performed in Tc(VII)-supplemented carbonate-bicarbonate buffer that permitted spectrophotometric determination of different ^{99}Tc species [69]. Complexation of Tc(IV) with bicarbonate produces a pink-colored complex that absorbs light at 512 nm [33]. Tc(VII) reduction was subsequently measured as the accumulation of Tc(IV)-bicarbonate at 512 nm.

Tc(VII) reduction-deficient (Tcr) mutants were tested for the ability to respire a set of electron acceptors. A large majority of the Tcr mutants displayed multiple respiratory deficiencies, an indication that the mutation resides in shared electron transport chain components and not in the terminal reductase

itself [8, 16, 84, 89]. Several mutants, however, retained the ability to respire all alternate electron acceptors except Tc(VII). In one specific mutant, Tc(VII) reduction was severely impaired with either lactate or H_2 as electron donor, yet was not affected with formate as electron donor [72].

The similarities in Tc(VII) reduction between *S. oneidensis* MR-1 and *S. putrefaciens* CN32 indicate that the H_2- and lactate-dependent Tc(VII) reduction pathways may share electron transport chain components, although the Tc(VII) terminal reductases are different.

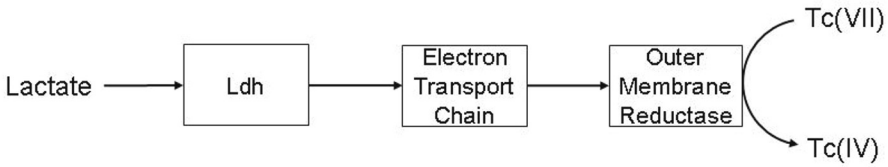

Figure 6. Working model for lactate-dependent Tc(VII) reduction pathway in S. oneidensis.

The different forms of Tc(IV) oxides are deposited according to the location of the terminal reductase within the cell (Figs. 6 and 7). The lactate-dependent Tc(VII) reduction pathway is predicted to terminate with a Tc(VII) reductase located in the OM and the presence of hydrous Tc(IV) oxides in the surrounding media (Fig. 6). H_2-dependent Tc(VII) reduction is predicted to be linked to both a periplasmic- and OM-associated reductase accounting for accumulation of amorphous Tc(IV) oxides at both locations in H_2-oxidizing cells (Fig. 7) [91]. Neither the Tc(VII) reduction end product nor the subcellular location of these products have been determined in the case of formate-dependent Tc(VII) reduction. Formate-dependent Tc(VII) reduction appears to proceed through a unique pathway sharing few components with either the H_2- or lactate-dependent Tc(VII) reduction pathways [72].

4. CONCLUSIONS

Metal-reducing gram-negative bacteria such as *Shewanella* are presented with a unique physiological challenge: they are required to respire anaerobically on terminal electron acceptors which are either highly insoluble (e.g., Fe(III)- and Mn(IV)-oxides) and reduced to soluble end-products or highly soluble (e.g., U(VI) and Tc(VII)) and reduced to insoluble end-products. To overcome physiological problems associated with metal solubility, metal-respiring *Shewanella* have been found to localize terminal reductase complexes to the outer membrane, deliver electrons to extracellular electron acceptors via exogenous or endogenous electron shuttles or produce metal-chelating compounds that dramatically increase the solubility of solid terminal electron acceptors. Further research on the molecular mechanism of metal reduction by *Shewanella*

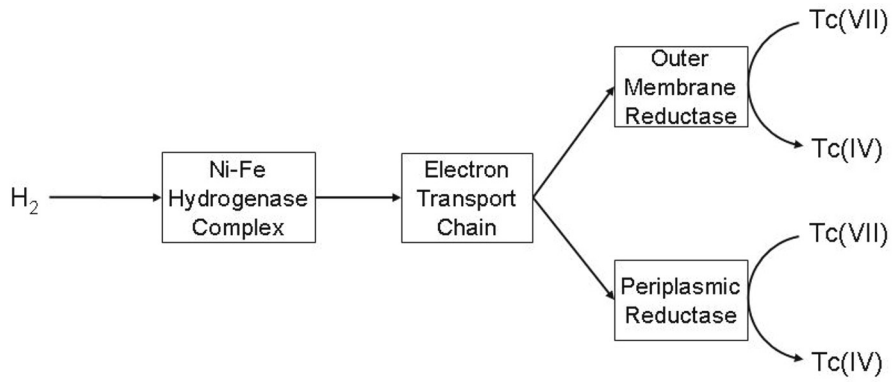

Figure 7. Working model for H_2-dependent Tc(VII) reduction pathway in S. oneidensis.

is required to identify the individual components of the metal-specific terminal reductase complexes.

Acknowledgements

This work was supported by grants from the National Science Foundation and the Department of Energy.

References

[1] Aller R.C. Bioturbation and Manganese Cycling in Hemipelagic Sediments. Philos T Roy Soc A 1990;331:51-68.

[2] Arnold R.G., DiChristina T.J. and Hoffmann M.R. Reductive dissolution of iron-oxides by *Pseudomonas sp.* 200. Biotech and Bioeng 1988;32:1081-96.

[3] Aubert C., Brugna M., Dolla A., Bruschi M. and Giudici-Orticoni M.T. A sequential electron transfer from hydrogenases to cytochromes in sulfate-reducing bacteria. Bba-Protein Struct M 2000;1476(1):85-92.

[4] Bagramyan K. and Trchounian A. Structural and functional features of formate hydrogen lyase, an enzyme of mixed-acid fermentation from *Escherichia coli*. Biochemistry-Moscow 2003;68(11):1159-70.

[5] Beliaev A.S. and Saffarini D.A. *Shewanella putrefaciens* mtrB encodes an outer membrane protein required for Fe(III) and Mn(IV) reduction. J Bacteriol 1998;180(23):6292-(9)7.

[6] Brettar I., Moore E.R.B. and Hofle M.G. Phylogeny and abundance of novel denitrifying bacteria isolated from the water column of the central Baltic Sea. Microbial Ecol 2001;42(3):295-305.

[7] Brooks S.C., Fredrickson J.K., Carroll S.L., Kennedy D.W., Zachara J.M., Plymale A.E., Kelly S.D., Kemner K.M. and Fendorf S. Inhibition of bacterial U(VI) reduction by calcium. Environm Sci Technol 2003;37(9):1850-58.

[8] Burnes B.S., Mulberry M.J. and DiChristina T.J. Design and application of two rapid Screening techniques for isolation of Mn(IV) reduction-deficient Mutants of *Shewanella putrefaciens*. Appl Environ Microbiol 1998;64(7):2716-20.

[9] Caccavo F., Blakemore R.P. and Lovley D.R. A Hydrogen-oxidizing, Fe(III)-reducing microorganism from the Great Bay Estuary, New-Hampshire. Appl Environ Microb 1992;58(10):3211-16.

[10] Coates J.D., Cole K.A., Chakraborty R., O'Connor S.M. and Achenbach L.A. Diversity and ubiquity of bacteria capable of utilizing humic substances as electron donors for anaerobic respiration. Appl Environ Microbiol 2002;68(5):2445-52.

[11] Coates J.D., Ellis D.J., Blunt-Harris E.L., Gaw C.V., Roden E.E. and Lovley D.R. Recovery of humic-reducing bacteria from a diversity of environments. Appl Environ Microbiol 1998;64(4):1504-09.

[12] Cochran J.K., Carey A.E., Sholkovitz E.R. and Suprenant L.D. The geochemistry of uranium and thorium in coastal marine sediments and sediment pore waters. Geochim Cosmochim Ac 1986;50(5):663-80.

[13] De Luca G., De Philip P., Dermoun Z., Rousset M. and Vermeglio A. Reduction of technetium(VII) by *Desulfovibrio fructosovorans* is mediated by the nickel-iron hydrogenase. Appl Environ Microb 2001;67(10):4583-87.

[14] Derby H.A. and Hammer B.W. Bacteriology of Butter IV. Bacteriological Studies of surface taint butter. Iowa Agricultural Experimental Station Research Bulletin 1931;145:387-416.

[15] DiChristina T.J. and DeLong E.F. Design and application of rRNA-targeted oligonucleotide probes for the dissimilatory iron- and manganese-reducing bacterium *Shewanella putrefaciens*. Appl Environ Microbiol 1993;59(12):4152-60.

[16] DiChristina T.J. and DeLong E.F. Isolation of anaerobic respiratory mutants of *Shewanella putrefaciens* and genetic analysis of mutants deficient in anaerobic growth on Fe^{3+}. J Bacteriol 1994;176(5):1468-74.

[17] DiChristina T.J., Moore C.M. and Haller C.A. Dissimilatory Fe(III) and Mn(IV) reduction by *Shewanella putrefaciens* requires ferE, a homolog of the pulE (gspE) type II protein secretion gene. J Bacteriol 2002;184(1):142-51.

[18] DiChristina T.J., Adiga M., Bates D. and Haller C.A. *Shewanella oneidensis* MR-1 requires the secretion homolog of Type II protein secretion (gspD) for anaerobic respiration on solid but not Soluble forms of iron and manganese. Appl Environ Microbiol 2004; Submitted.

[19] Ehrlich H.L. *Geomicrobiology*. 3rd ed. New York: Marcel Dekker, 1996.

[20] Eriksen T.E., Ndalamba P., Bruno J. and Caceci M. The Solubility of $T_cO_2 \cdot H_2O$ in neutral to alkaline-solutions under constant pCO_2. Radiochimica Acta 1992;58-9:67-70.

[21] Finneran K.T., Housewright M.E. and Lovley D.R. Multiple influences of nitrate on uranium solubility during bioremediation of uranium-contaminated subsurface sediments. Environ Microbiol 2002;4(9):510-16.

[22] Francis A.J., Dodge C.J., Lu F.L., Halada G.P. and Clayton C.R. Xps and Xanes Studies of Uranium Reduction by Clostridium sp. Environ Sci Technol 1994;28(4):636-39.

[23] Fredrickson J.K., Zachara J.M., Kennedy D.W., Duff M.C., Gorby Y.A., Li S.M.W. and Krupka K.M. Reduction of U(VI) in goethite (α-FeOOH) suspensions by a dissimilatory metal-reducing bacterium. Geochim Cosmochim Ac 2000;64(18):3085-98.

[24] Fredrickson J.K., Zachara J.M., Kennedy D.W., Liu C.X., Duff M.C., Hunter D.B. and Dohnalkova A. Influence of Mn oxides on the reduction of uranium(VI) by the metal-reducing bacterium *Shewanella putrefaciens*. Geochim Cosmochim Ac 2002;66(18):3247-62.

[25] Ganesh R., Robinson K.G., Reed G.D. and Sayler G.S. Reduction of hexavalent uranium from organic complexes by sulfate- and iron-reducing bacteria. Appl Environ Microb 1997;63(11):4385-91.

[26] Haas J.R. and DiChristina T.J. Effects of Fe(III) chemical speciation on dissimilatory Fe(III) reduction by *Shewanella putrefaciens*. Environ Sci Technol 2002;36(3):373-80.

[27] Haines R.I., Owen D.G. and Vandergraaf T.F. Technetium-iron oxide reactions under anaerobic conditions: a Fourier transform infrared, FTIR study. Nuclear Journal of Canada 1987;1:32-37.

[28] Harada E., Kumagai J., Ozawa K., Imabayashi S., Tsapin A.S., Nealson K.H., Meyer T.E., Cusanovich M.A. and Akutsu H. A directional electron transfer regulator based on heme-chain architecture in the small tetraheme cytochrome c from *Shewanella oneidensis*. FEBS Lett 2002;532(3):333-37.

[29] Heidelberg J.F., Paulsen I.T., Nelson K.E., Gaidos E.J., Nelson W.C., Read T.D., Eisen J.A., Seshadri R., Ward N., Methe B., Clayton R.A., Meyer T., Tsapin A., Scott J., Beanan M., Brinkac L., Daugherty S., DeBoy R.T., Dodson R.J., Durkin A.S., Haft D.H., Kolonay J.F., Madupu R., Peterson J.D., Umayam L.A., White O., Wolf A.M., Vamathevan J., Weidman J., Impraim M., Lee K., Berry K., Lee C., Mueller J., Khouri H., Gill J., Utterback T.R., McDonald L.A., Feldblyum T.V., Smith H.O., Venter J.C., Nealson K.H. and Fraser C.M. Genome sequence of the dissimilatory metal ion-reducing bacterium *Shewanella oneidensis*. Nat Biotechnol 2002;20(11):1118-23.

[30] Hernandez M.E., Kappler A. and Newman D.K. Phenazines and other redox-active antibiotics promote microbial mineral reduction. Appl Environ Microbiol 2004;70(2):921-28.

[31] Hussain H., Grove J., Griffiths L., Busby S. and Cole J. A 7-Gene operon essential for formate-dependent Nitrite reduction to ammonia by enteric bacteria. Mol Microbiol 1994;12(1):153-63.

[32] Kashefi K. and Lovley D.R. Reduction of Fe(III), Mn(IV), and toxic metals at 100 degrees C by *Pyrobaculum islandicum*. Appl Environ Microb 2000;66(3):1050-56.

[33] Khijniak T.V., Medvedeva-Lyalikova N.N. and Simonoff M. Reduction of pertechnetate by haloalkaliphilic strains of *Halomonas*. FEMS Microbiol Ecol 2003;44(1):109-15.

[34] Kieft T.L., Fredrickson J.K., Onstott T.C., Gorby Y.A., Kostandarithes H.M., Bailey T.J., Kennedy D.W., Li S.W., Plymale A.E., Spadoni C.M. and Gray M.S. Dissimilatory reduction of Fe(III) and other electron acceptors by a Thermus isolate. Appl Environ Microb 1999;65(3):1214-21.

[35] Korenevsky A.A., Vinogradov E., Gorby Y. and Beveridge T.J. Characterization of the lipopolysaccharides and capsules of *Shewanella spp.* Appl Environ Microbiol 2002;68(9):4653-57.

[36] Langmuir D. *Aqueous environmental geochemistry.* Vol. 42., Upper Saddle River, New Jersey: Prentice Hall, 1997.

[37] Lengeler J.W., Drews G. and Schlegel H.G. *Biology of the Prokaryotes.* Stuttgart, Germany: Georg Thieme Verlag, 1999.

[38] Liu C.X., Gorby Y.A., Zachara J.M., Fredrickson J.K. and Brown C.F. Reduction kinetics of Fe(III), Co(III), U(VI) Cr(VI) and Tc(VII) in cultures of dissimilatory metal-reducing bacteria. Biotechnol Bioeng 2002;80(6):637-49.

[39] Liu C.X., Zachara J.M., Fredrickson J.K., Kennedy D.W. and Dohnalkova A. Modeling the inhibition of the bacterial reduction of U(VI) by β-$MnO_{2(s)}$(g). Environ Sci Technol 2002;36(7):1452-59.

[40] Lloyd J.R., Cole J.A. and Macaskie L.E. Reduction and removal of heptavalent technetium from solution by *Escherichia coli.* J Bacteriol 1997;179(6):2014-21.

[41] Lloyd J.R., Sole V.A., Van Praagh C.V.G. and Lovley D.R. Direct and Fe(II)-mediated reduction of technetium by Fe(III)-reducing bacteria. Appl Environ Microb 2000;66(9):3743-49.

[42] Lloyd J.R. Microbial reduction of metals and radionuclides. FEMS Microbiol Rev 2003;27(2-3):411-25.

[43] Lovley D.R. Dissimilatory Fe(III) and Mn(IV) reduction. Microbiol Rev 1991;55(2):259-87.

[44] Lovley D.R., Phillips E.J.P., Gorby Y.A. and Landa E.R. Microbial reduction of uranium. Nature 1991;350(6317):413-16.

[45] Lovley D.R., Widman P.K., Woodward J.C. and Phillips E.J.P. Reduction of uranium by Cytochrome-C_3 of Desulfovibrio-Vulgaris. Appl Environ Microb 1993;59(11):3572-76.

[46] Lovley D.R., Coates J.D., BluntHarris E.L., Phillips E.J.P. and Woodward J.C. Humic substances as electron acceptors for microbial respiration. Nature 1996;382(6590):445-48.

[47] Lovley D.R. and Woodward J.C. Mechanisms for chelator stimulation of microbial Fe(III)-oxide reduction. Chem Geol 1996;132(1-4):19-24.

[48] Lovley D.R., Coates J.D., Saffarini D. and Lonergan D.J. Dissimilatory Fe(III) reduction, in transition metals in microbial metabolism, G. Winkelman and C.J. Carrano, Editors. 1997, Harwood Academic Publishers: Amesteldjik, The Netherlands.

[49] Lower S.K., Hochella M.F., Jr., and Beveridge T.J. Bacterial recognition of mineral surfaces: nanoscale interactions between *Shewanella* and α-FeOOH. Science 2001; 292(5520):1360-63.

[50] Lyalikova N.N. and Khizhnyak T.V. Reduction of heptavalent technetium by acidophilic bacteria of the genus *Thiobacillus*. Microbiology 1996; 65(4):468-73.

[51] Madigan M.T., Martinko J.M., Parker J. and Brock T.D. Biology of microorganisms. 10th ed. 2003, Upper Saddle River, NJ: Prentice Hall/Pearson Education. 1 v. (various pagings).

[52] Moura I. and Moura J.J.G. Structural aspects of denitrifying enzymes. Curr Opin Chem Biol 2001; 5(2):168-75.

[53] Myers C.R. and Nealson K.H. Bacterial manganese reduction and growth with manganese oxide as the sole electron-acceptor. Science 1988; 240(4857):1319-21.

[54] Myers C.R. and Nealson K.H. Respiration-linked proton translocation coupled to anaerobic reduction of manganese(IV) and iron(III) in *Shewanella putrefaciens* MR-1. J Bacteriol 1990; 172(11):6232-38.

[55] Meyer R.E., Arnold W.D., Case F.I. and O'Kelley G.D. Solubilities of Tc(IV)-oxides. Radiochim Acta 1991; 55:11-18.

[56] Myers C.R. and Myers J.M. Localization of cytochromes to the outer membrane of anaerobically grown *Shewanella putrefaciens* MR-1. J Bacteriol 1992; 174(11):3429-38.

[57] Myers C.R. and Myers J.M. Ferric Reductase is associated with the membranes of anaerobically grown *Shewanella Putrefaciens* Mr-1. FEMS Microbiol Lett 1993; 108(1):15-22.

[58] Myers C.R. and Myers J.M. Role of Menaquinone in the Reduction of Fumarate, Nitrate, Iron(Iii) and Manganese(Iv) by Shewanella-Putrefaciens Mr-1. FEMS Microbiol Lett 1993; 114(2):215-22.

[59] Myers C.R. and Myers J.M. Cloning and sequence of cymA a gene encoding a tetraheme cytochrome c required for reduction of iron(III), fumarate, and nitrate by *Shewanella putrefaciens* MR-1. J Bacteriol 1997; 179(4):1143-52.

[60] Myers J.M. and Myers C.R. Role of the tetraheme cytochrome CymA in anaerobic electron transport in cells of *Shewanella putrefaciens* MR-1 with normal levels of menaquinone. J Bacteriol 2000; 182(1):67-75.

[61] Myers J.M. and Myers C.R. Role for outer membrane cytochromes OmcA and OmcB of *Shewanella putrefaciens* MR-1 in reduction of manganese dioxide. Appl Environ Microbiol 2001; 67(1):260-69.

[62] Myers C.R. and Myers J.M. MtrB is required for proper incorporation of the cytochromes OmcA and OmcB into the outer membrane of *Shewanella putrefaciens* MR-1. Appl Environ Microbiol 2002; 68(11):5585-94.

[63] Myers J.M. and Myers C.R. Overlapping role of the outer membrane cytochromes of *Shewanella oneidensis* MR-1 in the reduction of manganese(IV) oxide. Lett Appl Microbiol 2003; 37(1):21-5.

[64] Nealson K.H., Myers C.R. and Wimpee B.B., Isolation and identification of manganese-Reducing bacteria and estimates of microbial Mn(Iv)-Reducing Potential in the Black-Sea. Deep-Sea Res 1991; 38:907-20.

[65] Nealson K.H. and Myers C.R. Microbial reduction of manganese and iron: new approaches to carbon cycling. Appl Environ Microbiol 1992; 58(2):439-43.

[66] Nealson K.H. and Saffarini D. Iron and manganese in anaerobic respiration: environmental significance, physiology, and regulation. Annu Rev Microbiol 1994; 48:311-43.

[67] Nevin K.P. and Lovley D.R. Mechanisms for accessing insoluble Fe(III) oxide during dissimilatory Fe(III) reduction by *Geothrix fermentans*. Appl Environ Microbiol 2002; 68(5):2294-99.

[68] Newman D.K. and Kolter R. A role for excreted quinones in extracellular electron transfer. Nature 2000; 405(6782):94-97.

[69] Paquette J. and Lawrence W.E. A Spectroelectrochemical Study of the Technetium(IV/Technetium(III) Couple in bicarbonate solutions. Can J Chem 1985; 63(9):2369-73.

[70] Pasilis S.P. and Pemberton J.E. Speciation and coordination chemistry of uranyl(VI)-citrate complexes in aqueous solution. Abstr Pap Am Chem S 2003; 225:U807-U807.

[71] Payne R.B., Gentry D.A., Rapp-Giles B.J., Casalot L. and Wall J.D. Uranium reduction by *Desulfovibrio desulfuricans* strain G20 and a cytochrome c3 mutant. Appl Environ Microb 2002; 68(6):3129-32.

[72] Payne A.N. and Dichristina T.J. H_2 and lactate-dependent Tc(VII) reduction-deficient mutants of *Shewanella oneidensis* MR-1 retain formate-dependent Tc(VII) reduction activity, 2004.

[73] Pitts K.E., Dobbin P.S., Reyes-Ramirez F., Thomson A.J., Richardson D.J. and Seward H.E. Characterization of the *Shewanella oneidensis* MR-1 decaheme cytochrome MtrA: expression in *Escherichia coli* confers the ability to reduce soluble Fe(III) chelates. J Biol Chem 2003; 278(30):27758-65.

[74] Rai D., Felmy A.R., and Ryan J.L. Uranium(Iv) hydrolysis constants and solubility product of $UO_2 \cdot H_2O$ (am). Inorganic Chemistry 1990; 29(2):260-64.

[75] Rard J.A. Critical review of the chemistry and thermodynamics of technetium and some of its inorganic compounds and aqueous species. UCRL-53440, ed. Livermore, California: L.L.N. Laboratory, 1983.

[76] Saffarini D.A., Blumerman S.L. and Mansoorabadi K.J. Role of menaquinones in Fe(III) reduction by membrane fractions of *Shewanella putrefaciens*. J Bacteriol 2002; 184(3):846-48.

[77] Schwalb C., Chapman S.K. and Reid G.A. The tetraheme cytochrome CymA is required for anaerobic respiration with dimethyl sulfoxide and nitrite in *Shewanella oneidensis*. Biochemistry 2003; 42(31):9491-97.

[78] Shewan J.M., Hobbs G. and Hodgkiss W. A determinative scheme for the identification of certain genera of gram-negative bacteria with special reference to *Pseudomonadaceae*. J Appl Bacteriol 1960; 23:379-90.

[79] Shyu J.B., Lies D.P. and Newman D.K. Protective role of tolC in efflux of the electron shuttle anthraquinone-2,6-disulfonate. J Bacteriol 2002; 184(6):1806-10.

[80] Simon J., Gross R., Einsle O., Kroneck P.M.H., Kroger A. and Klimmek O. A NapC/NirT-type cytochrome c (NrfH) is the mediator between the quinone pool and the cytochrome c nitrite reductase of Wolinella succinogenes. Mol Microbiol 2000; 35(3):686-96.

[81] Simon J. Enzymology and bioenergetics of respiratory nitrite ammonification. FEMS Microbiol Rev 2002; 26(3):285-309.

[82] Suzuki Y., Kelly S.D., Kemner K.M. and Banfield J.F. Radionuclide contamination - Nanometer-size products of uranium bioreduction. Nature 2002; 419(6903):134-134.

[83] Taillefert M., Lau D., Burns J. and DiChristina T.J. Non-reductive dissolution of solid Fe(III) oxides by Fe(III)-respiring *Shewanella*. Manuscript in preparation, 2004.

[84] Taratus E.M., Eubanks S.G. and DiChristina T.J. Design and application of a rapid screening technique for isolation of selenite reduction-deficient mutants of *Shewanella putrefaciens*. Microbiol Res 2000; 155(2):79-85.

[85] Thamdrup B., Rossello-Mora R. and Amann R. Microbial manganese and sulfate reduction in Black Sea shelf sediments. Appl Environ Microbiol 2000; 66(7):2888-97.

[86] Turick C.E., Tisa L.S. and Caccavo F. Jr. Melanin production and use as a soluble electron shuttle for Fe(III) oxide reduction and as a terminal electron acceptor by *Shewanella algae* BrY. Appl Environ Microbiol 2002; 68(5):2436-44.

[87] Venkateswaran K., Moser D.P., Dollhopf M.E., Lies D.P., Saffarini D.A., MacGregor B.J., Ringelberg D.B., White D.C., Nishijima M., Sano H., Burghardt J., Stackebrandt E. and Nealson K.H. Polyphasic taxonomy of the genus *Shewanella* and description of *Shewanella oneidensis* sp. nov. Int J Syst Bacteriol 1999; 49 Pt 2:705-24.

[88] Venter J.C., Remington K., Heidelberg J.F., Halpern A.L., Rusch D., Eisen J.A., Wu D.Y., Paulsen I., Nelson K.E., Nelson W., Fouts D.E., Levy S., Knap A.H., Lomas M.W., Nealson K., White O., Peterson J., Hoffman J., Parsons R., Baden-Tillson H., Pfannkoch C., Rogers Y.H. and Smith H.O. Environmental genome shotgun sequencing of the Sargasso Sea. Science 2004; 304(5667):66-74.

[89] Wade R. and DiChristina T.J. Isolation of U(VI) reduction-deficient mutants of *Shewanella putrefaciens*. FEMS Microbiol Lett 2000; 184(2):143-48.

[90] Wielinga B., Bostick B., Hansel C.M., Rosenzweig R.F. and Fendorf S. Inhibition of bacterially promoted uranium reduction: Ferric (hydr)oxides as competitive electron acceptors. Environ Sci Technol 2000; 34(11):2190-95.

[91] Wildung R.E., Gorby Y.A., Krupka K.M., Hess N.J., Li S.W., Plymale A.E., McKinley J.P. and Fredrickson J.K. Effect of electron donor and solution chemistry on products of dissimilatory reduction of technetium by *Shewanella putrefaciens*. Appl Environ Microb 2000; 66(6):2451-60.

V

MICROBIAL ECOLOGY OF THE OXIC/ANOXIC INTERFACE

MICROBIAL ECOLOGY OF THE CARIACO BASIN'S REDOXCLINE: THE U.S.-VENEZUELA CARIACO TIMES SERIES PROGRAM

Gordon T. Taylor[1], Maria Iabichella-Armas[2], Ramon Varela[3], Frank Müller-Karger[4], Xueju Lin[1] and Mary I. Scranton[1]

[1] *Stony Brook University, Marine Sciences Research Center, Stony Brook NY 11794-5000, USA*

[2] *Universidad de Oriente, Instituto Oceanográfico de Venezuela, Cumaná, Venezuela*

[3] *Fundación la Salle de Ciencias Naturales, Estaćion de Investigaciónes Mariñas de Margarita, Nueva Esparta, Venezuela*

[4] *University of South Florida, Department of Marine Sciences, 140 7th Avenue South, St. Petersburg 33701 USA*

Abstract The cooperative U.S.-Venezuela CARIACO program (CArbon Retention In A Colored Ocean) has begun to elucidate the microbial ecology of the Cariaco Basin's redoxcline. This anoxic water column supports highly stratified microbial assemblages of prokaryotes, protozoa and viruses, exhibiting abundance and activity maxima near the O_2/H_2S interface. In the oxic layer, abundance and activity of microheterotrophs vary annually to the same extent (16 to 20-fold) as primary producers in the upper 75-100 m, but out of phase. In the redoxcline and anoxic layer, relationships of these same variables to surface production are not readily apparent. Heterotrophic carbon demands within the redoxcline exceed local delivery of sinking organic matter from the mixed layer. The Cariaco's redoxcline appears to be inhabited by microaerophilic and anaerobic chemoautotrophs, such as ε-proteobacteria, whose metabolism is controlled by inorganic chemical gradients and transport. Time series data demonstrate that distribution and activity profiles of prokaryotes, protozoa and viruses vary in response to one another and to fluctuations in the interface's position. Rapid turnover of prokaryotic biomass in the redoxcline is deduced from the perennial presence of bacterivorous protozoan and viral communities. Chemoautotrophic production is sufficient to support heterotrophic demand for reduced carbon within the redoxcline and yields reasonable specific growth rates for total prokaryotic communities, averaging between 0.4 and 0.6 d^{-1}. However, reconciliation of microbial demand for energy and oxidants with supply is not possible applying the classic 1-D vertical model to the Cariaco and remains one of the greatest challenges to understanding the microbial ecology of anoxic water columns in general.

L. N. Neretin (ed.), Past and Present Water Column Anoxia, 473–499.

Keywords: prokaryotes, protozoa, viruses, chemoautotrophs, redoxcline, anaerobes, productivity

1. INTRODUCTION

The Cariaco Basin is a tectonically-formed depression on Venezuela's northern continental margin, reaching depths of nearly 1400 m and enclosing an approximate volume of 5.2 x 10^{12} m^3 below the 180 m isobath [40]. The Basin is surrounded by a sill (90-150 m in depth) and its bathymetry confines lateral water exchange primarily to the surface 100 m, although sporadic intrusions of oxygenated Caribbean surface waters to depths of $\geq$ 310 m have been documented recently [2]. While sulfide concentrations in bottom waters are known to vary over decadal time scales [43], the Cariaco Basin has been euxinic almost continuously for the past 12.6 - 14.6 ky [25,38].

Stratified anoxic water columns have long been known to support multiple layers of biological activity, variously fueled by oxygenic photosynthesis, anoxygenic photosynthesis, chemolithoautotrophy and heterotrophy [18,20,-21,28,49,50]. While somewhat of a simplification, for the purposes of this study we will divide the Cariaco system into three major layers, oxic (< 250 m), redoxcline (250-450 m) and anoxic (>450 m). The oxic layer is made up of an aphotic sublayer, which is supplied with organic matter from the shallow euphotic zone (usually < 75 m). The oxic layer may be comprised of more than one water mass and is structurally and functionally similar to other upwelling-prone coastal seas in the tropics and subtropics. The redoxcline is the depth interval over which the chemical redox potential undergoes its largest change and where the transition from oxic to sulfidic state occurs. Its precise position and thickness vary, but generally it falls between 250 and 450 m in the Cariaco. As in the Black Sea and other anoxic water columns, the Cariaco's redoxcline supports enriched inventories of prokaryotes, microbial ATP, protozoa, enhanced cycling of redox-sensitive elements and chemoautotrophic production [4,13,14,15,23,24,30,49,56]. The anoxic layer is characterized by increasing concentrations of H_2S, CH_4, PO_4^{3-} and NH_4^+ and diminishing microbial activity with depth [14,42,56]. Linkages between processes in the upper 250 m and underlying waters in this system are poorly understood.

The present communication explores basic aspects of the microbial ecology of the redoxcline of the Cariaco Basin and their relationship to surface processes. Results are derived from monthly hydrographic/ productivity cruises and seasonal process cruises staged by the cooperative US-Venezuelan CARIACO program (CArbon Retention In A Colored Ocean).

2. MATERIALS AND METHODS

2.1 Study Site and Sampling

All results presented are from the CARIACO time series station (10.50°N, 64.67°W) located in the eastern sub-basin of the Cariaco system. Sampling was conducted aboard the B/O Hermano Gines, operated by Estaćion de Investigaciónes Mariñas (EDIMAR), Fundación La Salle de Ciencias Naturales located on Margarita Island, Venezuela. Water samples were collected at 15-18 depths with a Sea-Bird rosette accommodating 12 teflon-lined, 8-L Niskin bottles. For hydrographic profiling, the rosette included a Sea-Bird CTD, YSI oxygen probe, Chelsea Instruments fluorometer for chlorophyll-a estimates and Sea Tec c-beam transmissometer (660 nm).

Peaks in the transmissometer's beam attenuation have been found to be reliable proxies for bacterial maxima near the interface in the Cariaco Basin, and sampling depths were adjusted accordingly to resolve these features as well as time and manpower permitted. Samples were withdrawn from Niskin bottles under N_2 atmosphere to prevent oxygenation of samples. All samples used for biological rate measurements were transferred from Niskin bottles to HCl-washed 1-L teflon-stoppered glass bottles and sealed without headspace after overflowing ~ 1 volume. Samples for all biological incubations were then dispensed from these 1-L bottles under N_2 pressure into acid-washed, 40-ml septa vials (laminated teflon-butyl rubber septa; Pierce Inc.) or into 40-ml glass-stoppered bottles and sealed without headspace after overflowing. Further details are presented in [56].

2.2 Phytoplankton Dynamics

Chlorophyll *a* concentrations were measured in methanol-extracted samples routinely collected monthly from 1, 7, 15, 25, 35, 55, 75 and 100 m before dawn. Primary production was measured from these same depths by standard ^{14}C-bicarbonate protocols in samples [62]. For each depth, 1 dark and 3 clear polycarbonate bottles were spiked with ~3.5 μCi of ^{14}C-bicarbonate and returned to their collection depth on a buoyed array for 4-h exposures to ambient light fields, representing ~33% of total daily irradiance at this latitude. After recovery, samples were filtered through Whatman GF/F filters, rinsed with 0.25 ml of 0.48N HCl, placed in scintillation vials and radioassayed. Data were corrected for isotopic fractionation (x 1.06) and dark assimilation. Daily photosynthetic rates were estimated from measured hourly rates, photoperiod and DIC concentrations [62]. Net primary production was seldom detectable below 75 m, so 100 m integrations captured the entire photic zone. Details appear in [32].

2.3 Bulk Organic Carbon

Particulate organic carbon and nitrogen (POC, PON) concentrations were routinely measured on materials retained on GF/F filters from samples collected at 15 depths over the entire water column (see [32]). Aliquots of the GF/F-filtrate were acidified and stored at 5°C in precombusted 40 ml EPA bottles with acid-washed Teflon-lined caps until analysis for DOC. DOC was measured using a Shimadzu TOC-5000 Total Organic Carbon Analyzer [47].

2.4 Microbial Dynamics

Prokaryotes and flagellated protozoa were enumerated in DAPI-stained samples from 15-18 depths as described in [56]. Viral-like particles (VLP) were enumerated in the same preserved samples by epifluorescence microscopy at 1000x magnification according to [36]. VLP from 0.3 to 2-ml subsamples retained on 0.02 μm Al_2O_3 Anodisk 25-mm membranes (Whatman International Ltd.) were stained for 15 min with SYBR Green I fluorochrome (Molecular Probes, Inc.) [see ref. 57 for details]. Ciliated protozoa were enumerated by a similar technique differing only in that cells from 150-ml samples were captured on 2.0 μm Nuclepore membranes and stained with acridine orange. Based on size and gross morphological features, ciliates were enumerated separately to the class or sub-order taxonomic levels.

Prokaryotic biomass was estimated from 200 randomly selected cells in each sample by visually sorting into eight size classes based on their linear dimensions, approximated with an ocular micrometer at 1000x magnification. Cellular carbon biomass (C) was estimated from biovolume (V) using an allometric carbon to volume extrapolation function, $C = 0.12\ V^{0.72}$ [37]. Cell carbon content estimates varied from 25 to 79 fg C $cell^{-1}$ ($\bar{x} \pm 1$ SD = 47 ± 10, n = 37) within oxic layer samples. Heterotrophic bacterial net production (BNP), acetate turnover and chemoautotrophic production were determined throughout the water column by ^{3}H-leucine, ^{14}C-acetate and ^{14}C-bicarbonate assimilation, respectively, as described in [14] and [56]. All rate measurements were obtained from samples incubated under in situ redox and temperature conditions by immersing vials sealed without a headspace (described above) in water baths. Inhibition and stimulation experiments were performed by adding inhibitor (N-Serve) or putative stimulants (S_2O_3, S^0, NO_3^-, MnO_2, Fe_2O_3) to replicate ^{14}C-bicarbonate assimilation sample bottles, then incubating and processing in parallel with the chemoautotrophy assay [56].

3. RESULTS AND DISCUSSION

3.1 Surface Production

Waters overlying the Cariaco Basin are subject to strong seasonal oscillations in productivity driven by upwelling [32]. More than eight years of monthly CARIACO observations have revealed that phytoplankton standing stocks usually remain low from June through December (<1.0 μg chlorophyll *a* (Chl *a*) L^{-1} in upper 100 m) and reach concentrations as high as 8 μg Chl *a* L^{-1} in January through May. Annually integrated Chl *a* inventories in the oxic layer vary up to 18-fold, from approximately 12 to 220 mg Chl *a* m^{-2} (Fig. 1a). In the upper 100 m, variance in Chl *a,* NPP, POC and PON are all significantly correlated with one another (Table 1), suggesting that accumulation of particulate organic matter is driven principally by local primary production. DOC concentrations in the surface layer, however, do not covary with any other measured variable (Table 1).

Standing stocks of the most numerous category of planktonic organisms – prokaryotes (Bacteria and Archaea) - exhibit annual variations similar to Chl *a*. Inventories integrated over the surface oxic layer (<250 m) vary by as much as 16-fold over an annual cycle (Fig. 1b). While most prokaryotes in this oxic layer are presumed to be heterotrophic and reliant upon organic matter derived from primary production in the upper 100 m [7], prokaryotic inventories do not correlate ($p>0.05$) with Chl *a,* NPP, POC, PON nor DOC (Fig. 1, Table 1). Results are the same whether depth integrations are confined to the upper 100m or extended to 250 m. Furthermore, bacterial net production and abundances of viruses and flagellated protozoa do not covary with phytoplankton production or organic matter pools in any layer (Table 1). The poor temporal coherence observed between organic matter pools (production) and microheterotrophic variables (consumption) probably signifies that our monthly sampling is too infrequent to capture lagged responses of the microbial communities to variations in organic matter pools.

3.2 Unique Depth Distributions

In most aquatic systems, fluxes of sinking particulate organic matter (POM) decrease exponentially with depth and the POM changes in composition, becoming less labile and supporting ever-diminishing bacterial abundances [7,65]. Only about 6-9% of net primary production sinks to the redoxcline's upper boundary as biogenic debris at Station CARIACO and is collected by its shallowest sediment traps at ~265-275 m [58]. The proportion of surface production exported to this depth is similar to that seen in many open ocean systems. However, prokaryotic abundances and activities in the Cariaco's redoxcline (250-450 m) are significantly enriched relative to the overlying 50-100 m

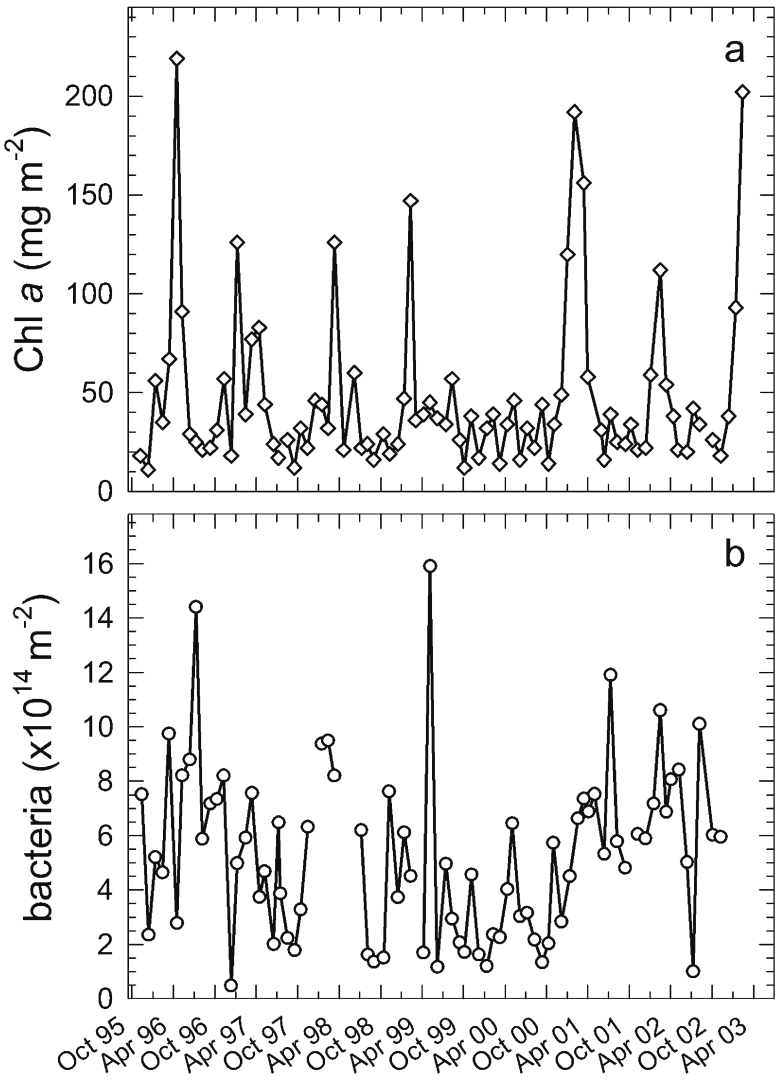

Figure 1. Monthly variation in chlorophyll a (a) and prokaryotic inventories (b) within Station CARIACO's oxic layer, integrated over upper 250 m of the water column. Breaks in curves represent 1-2 month gaps in data records.

(Fig. 2), which is inconsistent with the general trend of diminishing POM delivery and quality. Peaks in abundances of prokaryotes and rates of heterotrophic BNP, acetate turnover and dark assimilation of dissolved inorganic carbon (DIC) have been consistently positioned near the O_2/H_2S interface throughout the CARIACO time series. Plausible mechanisms to support enriched micro-

Table 1. Pearson product-moment correlation matrix of organic matter pools, sources and sinks within the Cariaco Basin; oxic layer (<250 m), redoxcline (250-450 m) and anoxic waters (>450 m). NPP = net primary production, POC = particulate organic carbon, PON = particulate organic nitrogen, DOC = dissolved organic carbon and Microbial Variables = abundances of prokaryotes, flagellates and viruses as well as BNP and dark DIC assimilation (all calculated separately). Numbers in parentheses = minimum number of variates compared (n).

	NPP	**POC**	**PON**	**DOC**	**Microbial variables**
Chlorophyll a[1]					
<250 m	0.62***	0.61***	0.59***	ns	ns
250-450 m	na	ns	ns	ns	ns
>450 m	na	ns	ns	ns	ns
	(91)	(74)	(77)	(46)	(6-79)[2]
NPP[1]					
<250 m		0.39***	0.42***	ns	ns
250-450 m		ns	ns	ns	ns
>450 m		ns	ns	0.47**	ns
		(73)	(76)	(45)	(8-78)
POC					
<250 m			0.82***	ns	ns
250-450 m			0.62***	ns	ns
>450 m			0.72***	ns	ns
			(71)	(40)	(6-73)
PON					
<250 m				ns	ns
250-450 m				ns	ns
>450 m				ns	ns
				(43)	(7-71)
DOC					
<250 m					ns
250-450 m					ns
>450 m					ns
					(6-42)

1 – measured in upper 100 m only
2 – range in sample size (n) for abundances of prokaryotes, flagellates and viruses as well as BNP and dark DIC assimilation
na = not applicable
ns = not significant ($p > 0.05$); *=$p < 0.05$; **=$p < 0.01$; *** = $p < 0.001$)

bial communities in this layer are explored below and include; accumulation of particle-bound cells on water density surfaces within a pycnocline, particle translocation by migrating animals, lateral transport of organic-rich waters at depth, lower prokaryotic mortality rates and in situ production of organic matter.

The Cariaco Basin's pycnocline typically is found between 30 and 200 m, where σ_θ increases from ~24.890 to 26.390 kg m^{-3}. Water densities below

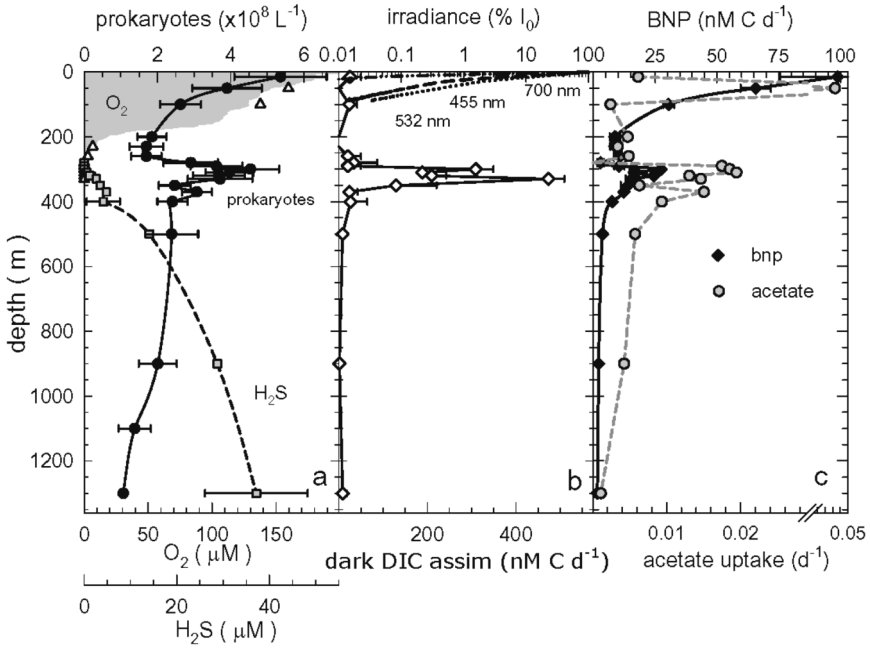

Figure 2. Vertical profiles of prokaryotic abundances and activity obtained on 16 Jan 02 at Station CARIACO (CAR-74). (a) solid circles and error bars = mean ± SE of total prokaryotes (hetero- and autotrophic Bacteria and Archaea); shaded area defines dissolved O_2 profile determined by polarographic electrode on rosette: triangles = dissolved O_2 determined in discrete samples by Winkler titration; squares = H_2 S concentrations determined in discrete samples (see [44] for chemistry protocols). (b) open diamonds = mean ± 1 SD of dark DIC assimilation in triplicate samples; broken lines = % of surface irradiance determined at three wavelengths by spectral radiometer, wavelengths are listed in order of extinction (532 nm deepest). (c) solid diamonds and error bars = mean ± 1 SD of bacterial net production in triplicate samples; shaded circles = specific rates of ^{14} C-acetate turnover determined in time course experiments (see [14]).

this are relatively homogenous with σ_θ only increasing by 0.060 kg m^{-3} from 200 to 450 m and by 0.024 kg m^{-3} between 450 m and the seafloor (Fig. 3a). Therefore, accumulation of prokaryotic cells along density surfaces between 250 and 450 m based on buoyancy is highly improbable. Warm deepwater temperature (≥ 17.2°C at 1380 m) is another unique feature of the Basin which contributes to its weak stratification and undoubtedly accelerates chemical and biological reactions.

Fluorescence profiles confirm that phytoplankton standing stocks are largely confined to the upper 50-100 m of the Cariaco and rapidly diminish with depth (Fig. 3b). Vertical profiles of light scattering (beam attenuation coefficient) suggest that bulk particle distributions are far less uniform than live phyto-

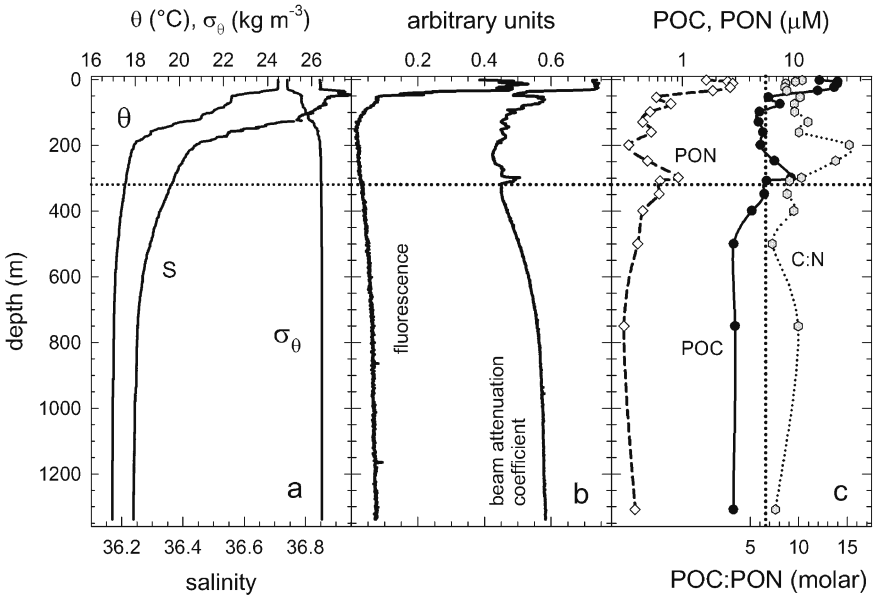

Figure 3. Vertical profiles of hydrographic and optical properties and particle distributions during CAR-74 (16 Jan 02). (a) potential temperature, θ, salinity, S, and density, σ_θ; (b) chlorophyll fluorescence and light scattering presented as beam attenuation coefficient; (c) suspended particulate organic carbon and nitrogen (POC, PON) and particle's elemental ratio (C:N). Broken horizontal line denotes O_2/H_2S interface. Dotted vertical line represents Redfield C:N ratio (6.6).

plankton cells. Light scattering is uniformly high in the mixed layer, attenuates rapidly with depth, but typically exhibits several subsurface peaks, such as those between 50 and 100 m, at 140-160 m and 270-315 m observed on 16 Jan 02 (Fig. 3b). Without exception, light scattering layers have been found within the redoxcline, very close to the O_2/H_2S interface, and they seem to coincide with prokaryotic abundance peak(s) (n = 17 of 17 cruises). Unlike deep light scattering layers in the Black Sea [39,8], these do not appear to be attributable to anoxygenic photoautotrophs. The Cariaco's redoxcline is at least 150 m deeper than the Black Sea's and downwelling irradiance attenuates dramatically, with the 0.01% I_0 isolume typically positioned at $\leq$ 100 m (Fig. 2b). Turbidity-driven light scattering below 450 m is typically uniformly low, but may increase towards the seafloor, suggesting increasing abundances of fine, suspended particles.

In the open ocean, concentrations of suspended organic matter (POC/PON) typically attenuate more or less as a power function of depth and primary production, reflecting depth-dependent consumption, solubilization, remineralization and transport of surface-produced organic matter [7,41,65]. Vertical

distributions of POC/PON in the Cariaco almost never conform to this model and frequently exhibit mid-water maxima within the redoxcline. For example, the shallowest POC/PON maximum during CAR-74 coincided with the subsurface fluorescence peak and the deeper POC/PON maxima coincide with light scattering peaks (Fig. 3c). These midwater peaks can account for significant fractions of total suspended matter inventories in the Basin. Median inventories of POC and PON integrated over the redoxcline (250-450 m) are 66±21 and 61±28% of inventories residing in the upper 250 m (Table 2). By comparison, at Station ALOHA in the North Pacific Central Gyre, median POC and PON inventories within the shallow mesopelagic zone (250-450 m) equal 27±5% and 25%+6% ($\bar{x}$ ± 1 S.D.) of the POC/PON measured in the upper 250 m (n = 55 cruises), respectively (`http://hahana.soest.hawaii.edu/hot/hot_jgofs.html`). This comparison clearly indicates that the Cariaco's redoxcline is significantly enriched in POC relative to shallow mesopelagic zones elsewhere in the world's ocean. The potential sources of these midwater enrichments are explored below.

Table 2. Integrated inventories of organic pools and microorganisms and activities within the redoxcline (250-450 m) compared to the surface layer (0-250 m). Expressed as ratio of redoxcline: surface layer.

	n[1]	Minimum	Maximum	Mean	Median
POC	80	0.26	1.35	0.67	0.66
PON	79	0.30	2.02	0.68	0.61
DOC	47	0.19	3.02	0.83	0.75
Prokaryotes	82	0.26	3.29	0.94	0.74
Flagellates	29	0.29	11.11	2.78	2.19
Viruses	8	0.05	0.75	0.41	0.47
BNP	21	0.02	0.87	0.19	0.16
DCA	13	0.38	8.94	4.01	3.37

[1] n = number of cruises included in statistics. Profiles from each cruise include 15-18 depths.
[2] DCA = dark DIC assimilation.

3.3 Potential Sources of Midwater Enrichments

Profiles in the Cariaco suggest that particulate organic matter might be introduced to the redoxcline through active translocation by migrating animals. Acoustic scattering layers migrating from surface waters through the redoxcline on a diel basis have been documented repeatedly (R. Varela, unpubl.). Furthermore, codlet fish have been recovered from deep (≤ 800 m) night-time net tows in the Basin [3]. The behavior and physiology of these migrators are poorly known. However, it seems improbable that they would forage a large

fraction of surface production and defecate primarily at the oxygen/sulfide interface. Future studies will help resolve this issue.

Another possibility is that the maxima represent horizontal transport of organic carbon from shallow areas. Temporally variable east-west gradients in primary production are evident across the northern continental margin of Venezuela (`http://seawifs.gsfc.nasa.gov/SEAWIFS.html`). Waters east of the CARIACO station tend to be more productive [32,33]. Some intrusions of water into the Basin appear to originate in less productive Caribbean regions to the northwest of Isla Margarita and are forced through the Canal de la Tortuga (135 m) by mesoscale eddy circulation, although other (unknown) processes also appear to cause intrusion events [2]. Therefore, lateral transport at depth of significant amounts of relatively labile organic matter to the CARIACO station is inconsistent with existing observations.

Major elemental composition of suspended organic matter may provide clues to its provenance. This material becomes nitrogen-depleted in the upper 200 m, where C:N molar ratios increase from 8.6 in the surface to 15 above the redoxcline (Fig. 3c). This is consistent with open ocean observations, where C:N ratios in the epipelagic zone are lower than in the mesopelagic. At Station ALOHA, for example, the median C:N ratio above 200 m is 6.4 (n = 533) which is significantly lower ($p<0.0001$; Mann-Whitney Rank Sum test) than between 201 and 1044 m (7.0; n = 223), (`http://hahana.soest.hawaii.edu/hot/hot_jgofs.html`). Apparently N is preferentially remineralized and retained in surface waters and particulate organic matter's nutritional quality diminishes rapidly with depth [23,55,65]. In the Cariaco, however, ratios return to near Redfield values at depths below 250 m (Fig. 3c). This trend suggests that POM in the redoxcline is comprised of higher proportions of living cells or fresher detritus than material in the overlying 100 m. In fact, estimates of prokaryotic carbon biomass within the redoxcline accounted for 9-54% ($\bar{x}$ = 26%) of the POC inventory during 14 cruises. Furthermore, the redoxcline supports inventories of prokaryotes that vary from 26 to 329% of those in the oxic layer ($\bar{x}$ = 94%; Table 2). Estimates of the C:N ratio in prokaryotes vary between 3.8 and 6.7 [12], so significant contributions from microbial biomass to organic carbon inventories can offset high C:N ratios of nitrogen-depleted organic matter in bulk measurements. Unlike Station ALOHA, particulate organic C:N ratios in the oxic layer and underlying waters were not statistically different during 79 CARIACO cruises ($p>0.05$; Mann-Whitney Rank Sum test); median C:N ratios were 8.5 (n = 908) and 8.9 (n = 604), respectively. Elemental ratio profiles suggest that particles below 250 m are on average no more N-depleted than particles in oxic waters and are probably comprised of redoxcline-derived microorganisms and byproducts (low C:N) along with surface-derived debris (high C:N). The high median C:N ratios within the Cariaco Basin oxic layer

probably reflect the limited vertical extent of the photic zone that produces low C:N particles compared to the relatively broad remineralization zone.

3.4 Trophic Structure in the Redoxcline

Suboxia and anoxia are known to exclude most animals and to support relatively simple food webs with fewer trophic levels than oxic systems [9,10,64]. Therefore, enriched prokaryotic inventories in the redoxcline might be hypothesized to result from reduced grazing in oxygen-depleted waters. Mortality rates have not been measured for prokaryotes within Cariaco's redoxcline. Nonetheless, variance in distributions of the primary bacterivores (flagellated and some ciliated protozoa) imply significant grazing pressure on prokaryotes. Flagellate cell size varied between 2 and 6 μm in diameter, typical of marine bacterivores. Their abundance profiles are quite variable, sometimes exhibiting maxima in the photic zone, coinciding with elevated prokaryotic numbers (e.g., Figs. 4a, 4b), but often not. Over the course of 29 cruises, flagellate abundances in the oxic layer have covaried with BNP, but not with prokaryotic abundances (Table 3). We interpret depauperate inventories in surface waters as manifestations of grazing pressure on the flagellates themselves. Multiple peaks in flagellate abundance are frequently evident through the redoxcline and abundances usually diminish below 500 m (Fig 4b). In fact, flagellate inventories in the redoxcline vary from 29 to 1111% ($\bar{x}$ = 278%) of those integrated for the oxic layer (Table 2) and are positively correlated with abundances of prokaryotes (Table 3).

The CARIACO database for ciliated protozoan distributions is more limited than for other members of the microbial food web. As was the case for flagellates, ciliate depth distributions and abundances are variable, presumably responding to bottom-up and top-down controls (Fig. 5). At least one peak in total ciliate abundance is commonly observed in the vicinity of the O_2/H_2S interface, sizable standing stocks exist in the redoxcline and ciliate numbers approach detection limits below 500 m. Based on gross morphological characteristics, composition of ciliate communities appears to vary widely with depth. For example in samples from CAR-5, tintinnids, known herbivores, were confined to the oxic layer (Fig. 6). Hypotrichs, known to be particle-associated (thigmotactic), exhibited a strong maximum through the redoxcline and a small peak in the photic zone. In contrast, depth profiles of aloricate oligotrichs and peritrichs exhibited peaks within the redoxcline, but standing stocks were smaller than in the photic zone. Ciliate cell size within the redoxcline varied between 15 and 50 μm in length, so the community appeared to be populated by bacterivores and nanoplanktivores. Sizable anaerobic ciliate inventories and similar stratified distributions have been reported for the Black and Baltic Seas as well [46,67].

Table 3. Pearson product-moment correlation matrix of microbiological variables within the Cariaco Basin; oxic layer (<250 m), redoxcline (250-450 m) and anoxic layer (>450 m). BNP = bacterial net production and DCA = dark carbon (CO_2) assimilation. Numbers in parentheses are minimum number of samples compared (n).

	Flagellates	**Viruses**	**BNP**	**DCA**
Prokaryotes				
<250 m	ns	ns	ns	ns
250-450 m	0.44*	ns	ns	ns
>450 m	ns	ns	ns	ns
	(28)	(8)	(19)	(10)
Flagellates				
<250 m		ns	0.62**	ns
250-450 m		0.82*	ns	ns
>450 m		0.74*	ns	ns
		(8)	(16)	(7)
Viruses				
<250 m			ns	ns
250-450 m			0.84*	ns
>450 m			ns	ns
			(7)	(5)
BNP				
<250 m				0.75**
250-450 m				ns
>450 m				ns
				(12)

ns = not significant ($p > 0.05$); *=$p < 0.05$; **=$p < 0.01$)

Phylogenetic analyses (18S rDNA libraries) from the Cariaco redoxcline and anoxic layer have revealed both novel and familiar anaerobic protistan lineages [52]. Novel lineages include new clades at the highest taxonomic level, branching near the base of the eukaryotic evolutionary tree. Several Cariaco phylotypes have high phylogenetic affinities with well-studied microaerophilic and anaerobic ciliates, some of whom host archaean and bacterial symbionts that may carry out geochemically important reactions (sulfate reduction; methanogenesis) [9]. Thus, at least three trophic levels (prokaryotes → flagellates → ciliates) appear to thrive in the Cariaco's redoxcline.

Viral lysis is the other potential source of prokaryotic mortality. Most recent evidence suggests that marine virioplankton communities are primarily comprised of bacteriophages [5,11,51]. As elsewhere, VLP in surface waters of the Cariaco Basin are abundant, sometimes exceeding 6×10^{10} VLP L^{-1} [57]. Vertical distributions are similar to those of prokaryotes, with peaks near the O_2/H_2S interface (Fig. 4c). However, VLP peaks are typically offset from prokaryote peaks by one depth interval, consistent with the fact that bacteriophages are produced at the expense of their prokaryotic hosts. Over the course of 8 cruises,

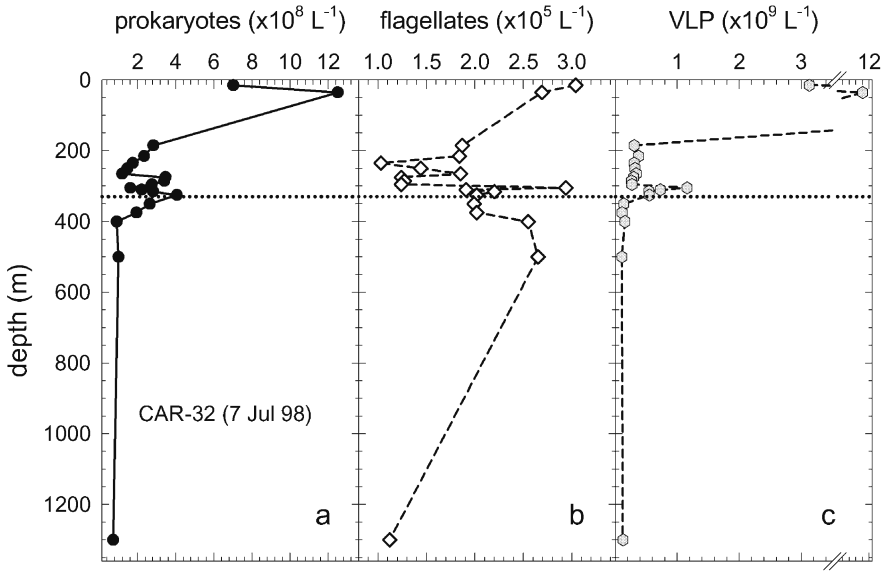

Figure 4. Vertical distributions of (a) total prokaryotes, (b) flagellated protozoa and (c) viral-like particles determined by epifluorescence microscopy in samples collected on 7 Jul 98 (CAR-32). Only means presented for clarity's sake. Relative standard error at any given depth is typically <20% of the mean. Broken horizontal line denotes O_2/H_2S interface.

variations in viral inventories corresponded most closely with flagellate abundance and BNP in the redoxcline (Table 3), while varying independently of all other measured variables throughout the water column (Tables 1 and 3). These trends support the interpretation that rates of free virus and flagellate production are controlled by prokaryotic production, or in other words, that parasites and bacterivores proliferate when hosts/prey actively grow.

3.5 Biological Production in the Redoxcline

While depth distributions of BNP always exhibit peaks within the redoxcline (Fig. 2c), this production typically amounts to a minor fraction ($\bar{x}$ = 19%) of surface BNP (Table 2), and this production is insufficient to support the enriched inventories of prokaryotes, protozoa and viruses within the redoxcline. Marine redoxclines are known to support elevated levels of dark DIC assimilation, attributable to chemoautotrophy [19,21,31,49,50,56,60,61]. In the Cariaco, depth of the 80-100 m thick chemoautotrophic layer varies in response to the interface's position and most DIC assimilation occurs where O_2 is undetectable (Fig. 7). Like photoautotrophic production in the surface layer, chemoautotrophic production within the redoxcline has varied about 20-fold over our observation period (0.16 to 3.33 g C m^{-2} d^{-1}; n = 16 cruises).

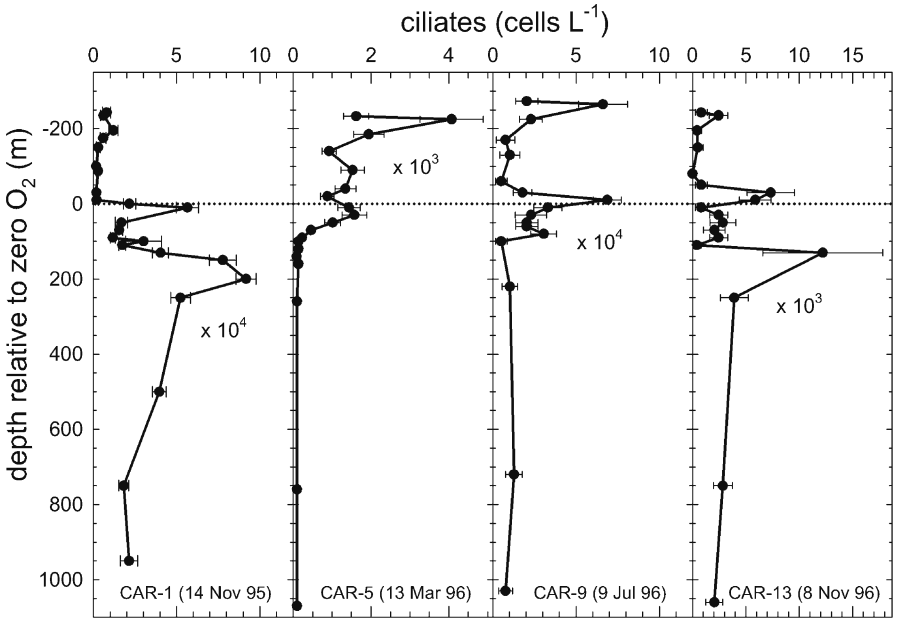

Figure 5. Vertical distributions of total ciliated protozoan communities relative to first depth of undetectable O_2 at Station CARIACO on four dates. Scaling factors presented in each panel.

One important question is whether these levels of production are sufficient to support observed prokaryotic inventories. Specific growth rates calculated by dividing the sum of dark DIC assimilation and BNP rates by microbial biomass for the 11 cruises in which all were measured, yields a range of cell division rates of 0.02 – 3.02 d^{-1} and a median value of 0.38 d^{-1} ($\bar{x}$ = 0.60 d^{-1}; n = 77). Sixty four of 77 observations yield growth rates below 1.0 d^{-1} and only 13% yield rates >1.5 d^{-1}. Comparable growth rates (0.07 – 2.3 d^{-1}) have been observed in surface waters of the oligotrophic Sargasso Sea [6]. Therefore, growth rates are not unreasonable for microaerophiles and anaerobes in productive coastal waters with temperatures consistently >17°C. Moreover, measured prokaryotic production rates (chemoautotrophy + BNP) are sufficient to support the microbial communities observed in the Cariaco's redoxcline.

On average, chemoautotrophy represents about 70% (median) of local primary production in surface waters at Station CARIACO (Fig. 8). Similarly high proportions have been reported previously for the Cariaco Basin and Black Sea [21,35,56,61]. All existing evidence suggests that this production is fueled by remineralization of export production from surface waters. However, a semi-enclosed ecosystem in steady-state can not sustain such high energy recoveries because less than 10% of local surface production (in C units) sinks to the

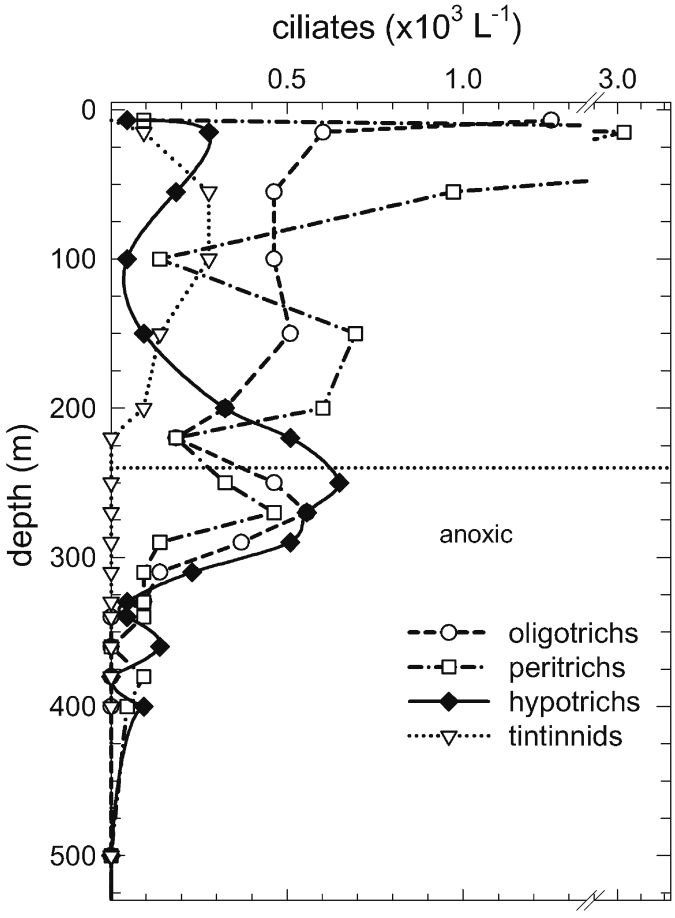

Figure 6. Vertical profiles of four major groups of ciliates, identified by size and gross morphology for 12 Mar 96 (CAR-5). Broken horizontal line denotes O_2/H_2S interface.

redoxcline. Temporal and spatial variability in physical, chemical and biological processes are likely to be important in creating the perceived imbalance [16,43,66]. Better assessments of horizontal gradients in productivity and remineralization, advective transport and temporal variability are all essential to attain closure of the Basin's energy budget, which will be addressed in our future studies.

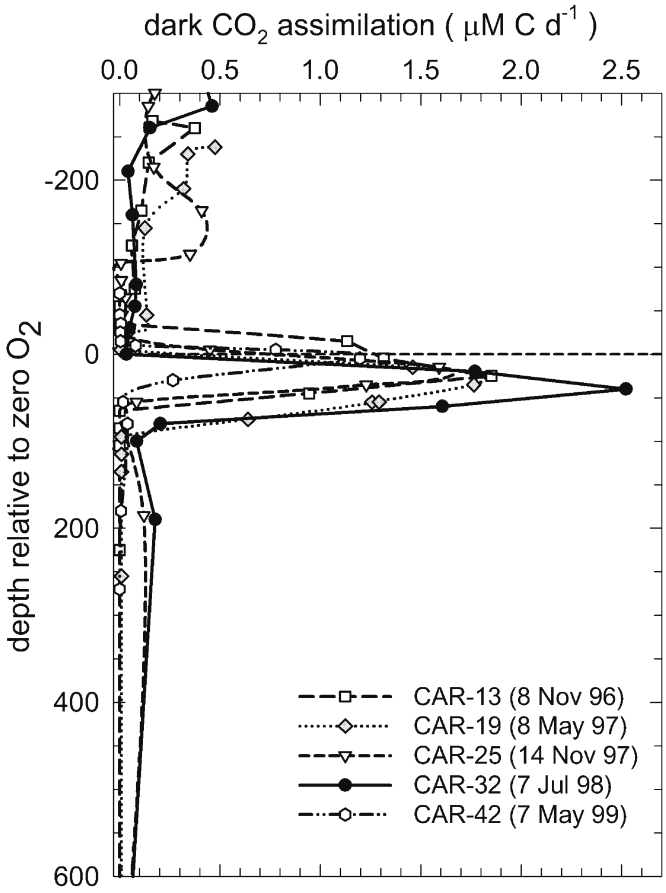

Figure 7. Vertical distribution of dark DIC assimilation relative to first depth of undetectable O_2 on five dates.

3.6 Redoxcline's Chemoautotrophic Communities

The organisms responsible for chemoautotrophic carbon fixation are poorly known. A portion of the observed DIC assimilation can be attributed to anaplerotic reactions that occur within all organisms [50] During 14 CARIACO cruises, these reactions potentially amount to ~7% (median; n = 32) of total carbon production (NPP + BNP) in the upper 100m. However, in the redoxcline only 1% of dark DIC assimilation can be derived anaplerotically (n = 137), assuming that it accounts for as much as 10% of observed BNP. Furthermore, addition of Hg^{2+}, formaldehyde or NaN_3 to incubations completely shuts down dark ^{14}C particle production (not presented). Clearly, biological assimilation

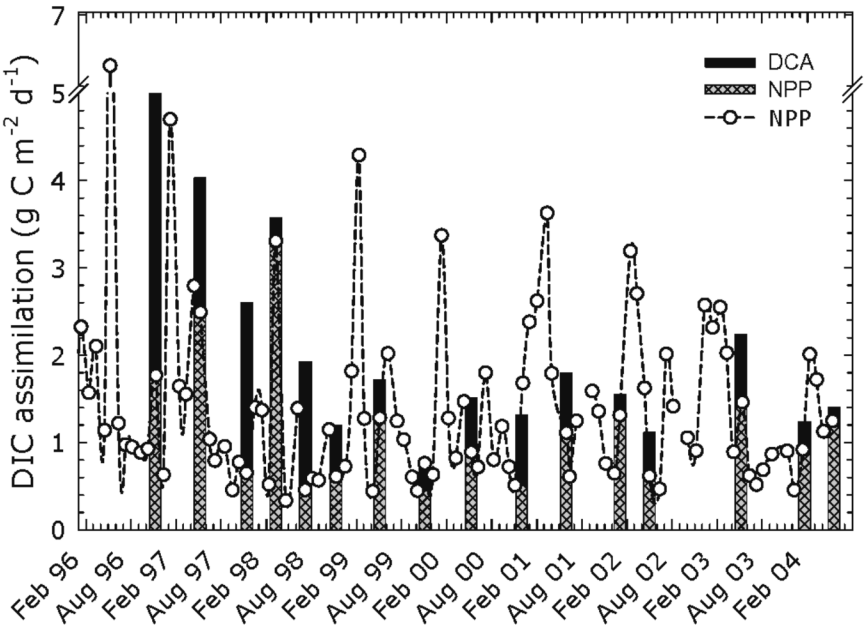

Figure 8. Monthly variation in net primary production (NPP) and seasonal variation in dark DIC assimilation (DCA), integrated over 0-100 m and 250-450 m intervals, respectively. Total bar height is sum of photoautotrophic production (hatched portion) and dark DIC assimilation (solid portion).

of DIC through one or more chemoautotrophic process is operative in the redoxcline. Inhibition experiments strongly suggest that most DIC assimilation immediately above the O_2/H_2S interface is performed by nitrifying bacteria. Addition of a specific nitrification inhibitor, N-Serve (nitrapyrin), dramatically reduced DIC assimilation in samples 10 and 25 m above the interface while having no inhibitory effect on samples in sulfidic waters (Fig. 9a). A NO_2^- peak in the redoxcline and ^{15}N isotopic signatures are additional evidence for a nitrifying layer residing immediately above the O_2/H_2S interface [45,56,59].

Experiments in which replicate samples were amended with likely electron donors or acceptors were performed on six cruises and produced mixed results (Fig. 9b,c). On different occasions, amendments of H_2S, S_2O_3 and S^0 stimulated dark DIC assimilation 2 to 30-fold, had no effect or became inhibitory with no apparent depth trend. Ammonium amendments only produced 2 to 3-fold stimulations in sulfidic waters and appeared to exert no effect or inhibit activity in shallower waters. Below the interface, NO_3^-, MnO_2 and Fe_2O_3 amendments induced 2 to 30-fold stimulations in dark DIC assimilation or exhibited no effect (Fig. 9c). Introduction of air (headspace) seldom stimulated, and often

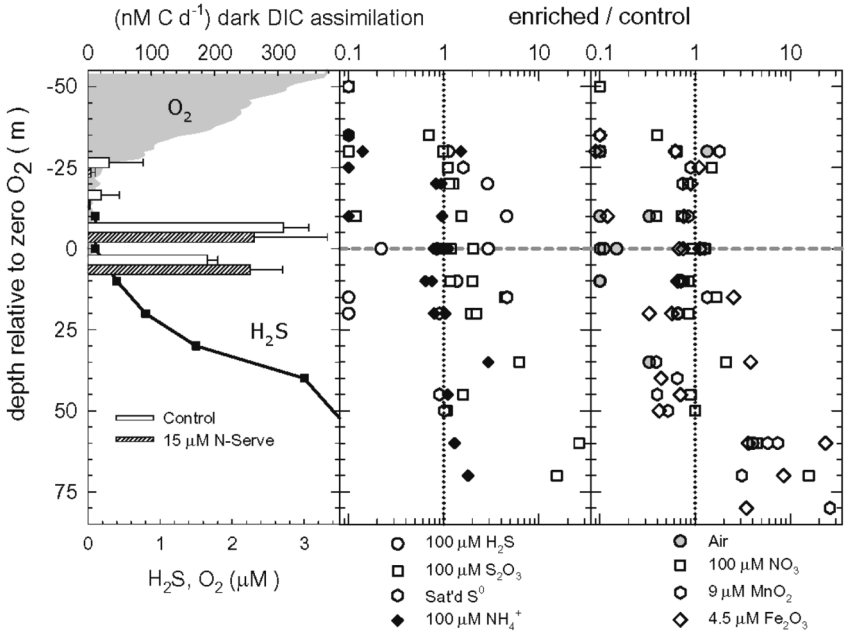

Figure 9. Effects of N-Serve (nitrapyrin), the nitrification-specific inhibitor and alternate electron donors and acceptors on dark DIC assimilation across the redoxcline. (a) N-Serve inhibition experiment from CAR-74 (16 Jan 02). (b) ratio of dark DIC assimilated in samples amended with potential electron donors divided by assimilation in unamended controls during CAR-32 (7 Jul 98), CAR-36 (7 Nov 98), CAR-42 (7 Apr 99), CAR-54 (3 May 00), CAR-60 (30 Oct 00) and CAR-96 (20 Jan 04). (c) same as (b) except potential electron acceptors substituted. Ratio of 1.0 = no effect.

inhibited, apparent activity. This may have resulted from chemical oxidation of reductants, essentially in competition with biological consumption. Negative results in stimulant amendment experiments may have been due to other nutrient limitations, chemical interactions or poor sampling resolution of highly stratified microbial communities.

Preliminary molecular studies (16S rDNA libraries) have shown that the redoxclines of both the Cariaco and Black Sea are highly enriched with ϵ-proteobacteria that have strong phylogenetic affinities to organisms with known sulfur and hydrogen metabolisms, many of whom are microaerophiles or nitrate-reducers [27,63]. Unlike the Cariaco, a portion of autotrophic production in the Black Sea's shallower redoxcline appears to be driven by anoxygenic phototrophic S-bacteria [4,8,39]. To date, enrichment cultures from the Cariaco have yielded microaerophilic thiosulfate-oxidizers, sulfur and thiosulfate-disproportionaters, thiosulfate-oxidizing manganese-reducers and denitrifying thiosulfate-oxidizers [26, X. Lin unpubl. data]. Results from stimulation/inhi-

bition experiments, 16S rDNA libraries, and enrichment cultures all support the assertion that the redoxcline is inhabited by highly stratified guilds of diverse chemoautotrophs that organize in response to resource availability. They appear to largely rely on energy from S in reduced and intermediate oxidation states, which are potentially oxidized by a variety of chemical species (O_2, NO_3^-, Mn^{4+}, Fe^{3+}).

A growing culture collection of chemoautotrophic ϵ-proteobacteria, capable of oxidizing H_2, H_2S, S^0, S_2O_3 at the expense of O_2, S^0 and NO_3^- is emerging from deep-sea hydrothermal field exploration [1,17,29,53,54]. These newly described isolates closely cluster with phylotypes present in Cariaco and Black Sea 16S rDNA libraries. However in the case of the Cariaco, O_2 and NO_3^- are undetectable where peak chemoautotrophy is observed (Fig. 7 in [56]) and S^0 concentrations are presently unknown. Alternate electron acceptors, such as metals and sulfur intermediates, must be invoked to explain observed activity distributions. While anaerobic, manganese-reducing chemo-organotrophs are well-known (e.g., *Shewanella* sp.), strict chemoautotrophs that use metals as final electron acceptors are yet to be described. Moreover, the relative importance of specific reductants and oxidants, including NH_4^+, H_2S, S^0, S_2O_3, SO_3, H_2, CH_4, Mn^{4+} and Fe^{3+}, in supporting microbial community growth remains unresolved for anoxic basins.

4. CONCLUSIONS

As summarized in Fig. 10, information amassed from the Cariaco Basin, Black Sea and other anoxic water columns all show that redoxclines support active microbial food webs with multiple trophic levels but appear to be less complex than food webs in oxic waters [4,9,56,57,67]. Heterotrophic production directly fueled by passively sinking biogenic debris can only support a small fraction of this food web. Rather this food web appears to be supported primarily by chemoautotrophic prokaryotes, potentially dividing at rates of about 0.4 - 0.6 d^{-1}. However, determining actual fluxes of inorganic ions driving this production, defining efficiency of their biological utilization and describing community composition of these prokaryotes are among the largest challenges facing researchers of these systems.

The hypothesis that large prokaryotic inventories observed in redoxclines of anoxic water columns result from diminished mortality rates and slow growth rates is contrary to our observations. Large and variable communities of anaerobic flagellates and ciliates have been observed repeatedly in the Cariaco Basin. While protozoan grazing and growth rate measurements are unavailable, flagellates and many taxa of ciliates are bacterivorous and can only proliferate if coexisting with actively growing prey. These organisms represent the second trophic level. Preliminary phylogenetic information suggests that anaerobic cil-

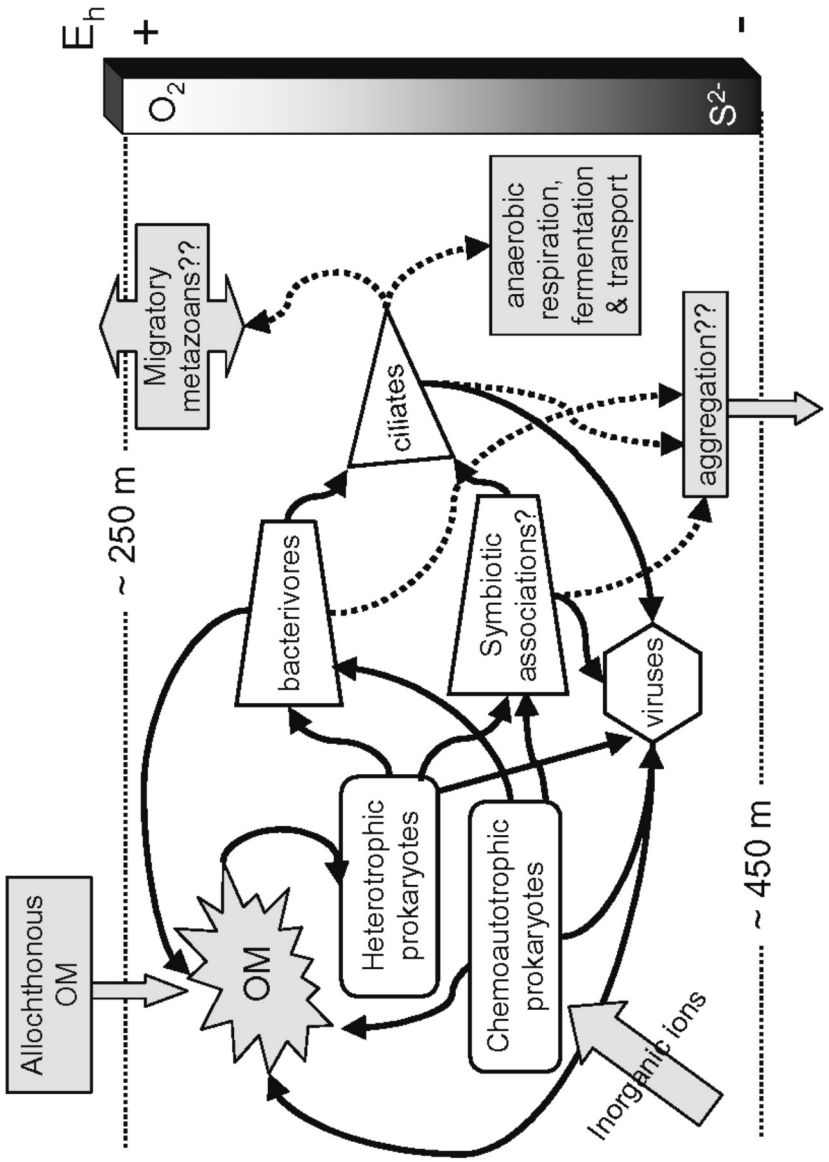

Figure 10. Conceptual model of the microaerophilic/suboxic/anaerobic microbial food web in the Cariaco Basin's redoxcline. Vertical bar represents the gradient in redox potential (E_h) from the shallow micro-oxic to deep sulfidic conditions, residing between 250 m and 450 m. For clarity, not all pathways are presented, e.g., from bacterivores to viruses.

iate communities are diverse, and may include hosts to prokaryotic symbionts and larger taxa that prey upon flagellates and other ciliates (third trophic level) [4,9,46,52,67]. Typical of many food webs, our biomass estimates within the redoxcline diminish by an order of magnitude between ascending trophic levels, from prokaryotes to flagellates to ciliates.

The fates of top predators and ungrazed production in the chemoautotrophic layer are intriguing unknowns. Are larger protozoans culled by migratory suspension feeders? Do predators die off during periods of low prey availability or viral epidemics, permitting the redoxcline community to simply recycle nutrients fueled by fluxes of reductants and oxidants from below and above as proposed by Ho et al. [15]? Does a portion of the redoxcline's production sink into the anoxic layer and eventually to the seabed? We have observed that in more than 20% of Cariaco's sediment trap collections, POC flux to 455 m exceeded fluxes to 265 m [56]. However, there is currently no direct evidence of the redoxcline's contribution to sedimentation (Thunell, pers. comm.). The largest predators (ciliates) in this web produce uncompacted feces of incompletely digested cells with no appreciable sinking velocity. Nevertheless, various microbes are known to stimulate particle aggregation by exuding polymeric material (reviewed in [48]). Perhaps this aggregation process contributes to the sedimenting flux (Fig. 10).

Viral infection is dependent on susceptible host population densities and proliferation is dependent on host growth rates, irrespective of whether hosts are aerobic or anaerobic [11,57]. Hence bacteriophages most likely dominate viral communities in the redoxcline, because prokaryotes are the most abundant hosts. We speculate that viral attack on abundant protozoan populations in the redoxcline community is also possible (Fig. 10). Therefore, viruses may represent competitors to grazer populations at two or more trophic levels. Viral lysis effectively returns high-quality organic matter to non-living pools, thereby stimulating heterotrophic activity and elemental cycling [34]. Waters supporting high population densities and low diversity are more prone to viral epidemics than species-rich communities [11]. Therefore, the relative importance of viral lysis to prokaryotic mortality, elemental cycling and energy flow within the redoxcline are likely to depend on productivity and host diversity.

Full understanding of how redoxclines sustain the high standing stocks and productivity presented above awaits further study and new approaches. Improved descriptions of water circulation and horizontal structure, inferences provided by stable isotopes, phylogenetic and physiological studies and investigations of symbioses will all be useful in solving this fascinating problem. Detailed phylogenetic and biogeochemical studies of prokaryotes and protists residing in the Cariaco's redoxcline are currently underway.

Acknowledgements

The authors are grateful to the captain and crew of the B/O Hermano Gines and the staff of the Estación de Investigaciones Marinas de Margarita (Fundación La Salle de Ciencias Naturales, Punta de Piedras, Isla de Margarita, Venezuela) for their field assistance in this study. We are indebted to Y. Astor, A. Modanesi, L. Li, C. Gomes and M.A. Rizzo for O_2 data, laboratory assistance, acetate turnover measurements, flagellate enumeration and for ciliate enumeration, respectively. This research has been supported since 1994 by a series of U.S. NSF grants to M.I.S. ,G.T.T and F. M-K. and by Proyecto Cariaco grant from FONACIT (Fondo Nacional de Ciencia, Tecnologia e Innovacion) #96280221 and #2000001702 (to R. Varela et al.). Marine Sciences Research Center contribution no. 1300.

References

[1] Alain K., Querellou J., Lesongeur F., Pignet P., Crassous P., Raguénès G., Cueff V. and Cambon-Bonavita M.-A. *Camnibacter hydrogeniphilus* gen. Nov., sp. Nov., a novel thermophilic, hydrogen-oxidizing bacterium isolated from an East Pacific Rise hydrothermal vent. Int J Syst Evol Microbiol 2002; 52:1317-23.

[2] Astor Y., Muller-Karger F. and Scranton M.I. Seasonal and interannual variation in the hydrography of the Cariaco Basin: implications for basin ventilation. Contin Shelf Res 2003; 125-44.

[3] Baird R.C., Wilson D.F. and Milliken D.M. Observations on *Bregmaceros all nectabanus* Whitley in the anoxic, sulfurous water of the Cariaco Trench. Deep-Sea Res 1973; 20:503-04.

[4] Bird D.F. and Karl D.M. Microbial biomass and population diversity in the upper water column of the Black Sea. Deep-Sea Res 1991; 38:1069-82.

[5] Breitbart M., Salamon P., Andersen B., Mahaffy J.M., Segall A.M., Mead D., Azam F. and Rohwer F. Genomic analysis of uncultured marine viral communities. Proc Natl Acad Sci 2002; 99:14250-55.

[6] Carlson C.A. and Ducklow H.W. Growth of bacterioplankton and consumption of dissolved organic carbon in the Sargasso Sea. Aquat Microb Ecol 1996; 10:69-85.

[7] Cho B.C. and Azam F. Major role of bacteria in biogeochemical fluxes in the ocean's interior. Nature 1988; 441-43.

[8] Coble P.G., Gagosian R.B., Codispoti L.A., Friedrich G.E. and Christensen J.P. Vertical distribution of dissolved and particulate fluorescence in the Black Sea. Deep-Sea Res 1991; 38:985-1001.

[9] Fenchel T. and Finlay B.J. The evolution of life without oxygen. Amer Sci 1994; 82:22-29.

[10] Fenchel T., Kristensen L.D. and Rasmussen L. Water column anoxia: vertical zonation of planktonic protozoa. Mar Ecol Prog Ser 1990; 62:1-10.

[11] Fuhrman J.A. and Suttle C.A. Viruses in marine planktonic systems. Oceanography 1993; 6:51-63.

[12] Gundersen K., Heldal M., Norland S., Purdie D.A. and Knap A.H. Elemental C, N, and P cell content of individual bacteria collected at the Bermuda Atlantic Time-series Study (BATS) site. Limnol Oceanogr 2002; 47:1525-30.

[13] Hastings D. and Emerson S. Sulfate reduction in the presence of low oxygen levels in the water column of the Cariaco Trench. Limnol Oceanogr 1988; 33:391-96.

[14] Ho T.-Y., Scranton M.I., Taylor G.T., Thunell R.C., Varela R. and Muller-Karger F. Acetate cycling in the water column of the Cariaco Basin: Seasonal and vertical variability and implication for carbon cycling. Limnol Oceanogr 2002; 47:1119-28.

[15] Ho T.-Y., Taylor G.T., Astor Y., Varela R., Muller-Karger F. and Scranton M.I. Vertical and temporal variability of redox zonation in the water column of the Cariaco Basin: implications for organic oxidation pathways. Mar Chem 2004; 86:89-104.

[16] Holmen K.J. and Rooth C.G.H. Ventilation of the Cariaco Trench, a case of multiple source competition. Deep-Sea Res 1990; 37:203-25.

[17] Inagaki F., Takai K., Kobayashi H., Nealson K.H. and Horikoshi K. *Sulfurimonas autotrophica* gen nov., sp. Nov., a novel sulfur-oxidizing ϵ-proteobacterium isolated from hydrothermal sediments in the Mis-Okinawa Trough. Int J Syst Evol Microbiol 2003; 53:1801-05.

[18] Indrebø G., Pengerud B. and Dunsa I. Microbial activities in a permanently stratified estuary: I. Primary production and sulfate reduction. Mar Biol 1979; 51:295-304.

[19] Jannasch H.W., Wirsen C.O. and Molyneaux S.J. Chemoautotrophic sulfur-oxidizing bacteria from the Black Sea. Deep-Sea Res 1991; 38:1105-20.

[20] Jørgensen B.B., Kuenen J.G. and Cohen Y. Microbial transformations of sulfur compounds in a stratified lake (Solar Lake, Sinai). Limnol Oceanogr 1979; 24:799-822.

[21] Jørgensen B.B., Fossing H., Wirsen C.O. and Jannasch H.W. Sulfide oxidation in the anoxic Black Sea redoxcline. Deep-Sea Res 1991; 38:1083-1103.

[22] Karl D.M. Distributions, abundance, and metabolic states of microorganisms in the water column and sediments of the Black Sea. Limnol Oceanogr 1978; 23:936-49.

[23] Karl D.M. Nutrient dynamics in the deep blue sea. Trends Microbiol 2002; 10:410-18.

[24] Karl D.M., LaRock P.A. and Schultz D.J. Adenosine triphosphate and organic carbon in the Cariaco Trench. Deep-Sea Res 1977; 24:105-13.

[25] Lyons T.W., Werne J.P., Hollander D.J. and Murray R.W. Contrasting sulfur geochemistry and Fe/Al and Mo/Al ratios across the last oxic-to-anoxic transition in the Cariaco Basin, Venezuela. Chem Geology 2003; 195:131-57.

[26] Madrid V. Characterization of the Bacterial communities in the anoxic zone of the Cariaco Basin, M.S. Thesis, SUNY Stony Brook, 2000.

[27] Madrid V.M., Taylor G.T., Scranton M.I. and Chistoserdov A.Y. Phylogenetic diversity of Bacterial and Archaeal communities in the anoxic zone of the Cariaco Basin. Appl Environ Microbiol 2001; 67:1663-74.

[28] McDonough R.J., Sanders R.W., Porter K.G. and Kirchman D.L. Depth distribution of bacterial production in a stratified lake with an anoxic hypolimnion. Appl Environ Microbiol 1986; 52:992-1000.

[29] Miroshnichenko M.L., Kostrikina N.A., L'Hairdon S., Jeanthon C., Hippe H., Stackebrandt E. and Bonch-Osmolovskaya E.A. *Nautilia lithotrophica* gen nov., sp. Nov., a thermophilic sulfur-reducing ε-proteobacterium isolated from deep-sea hydrothermal vent. Int J Syst Evol Microbiol 2002; 52:1299-1304.

[30] Mopper K. and Kieber D.J. Distribution and biological turnover of dissolved organic compounds in the water column of the Black Sea. Deep-Sea Res 1991; 38:1021-47.

[31] Morris I., Glover H.E., Kaplan W.A., Kelly D.P. and Weightman A.L. Microbial activity in the Cariaco Trench. Microbios 1985; 42:133-44.

[32] Muller-Karger F., Varela R., Thunell R., Scranton M., Bohrer R., Taylor G., Capelo J., Astor Y., Tappa E., Ho T.-Y. and Walsh J.J. Annual cycle of primary production in the Cariaco Basin: Response to upwelling and implications for vertical export. J Geophys Res 2001; 106:4527-42.

[33] Muller-Karger F., Varela R., Thunell R., Astor Y., Zhang H., Luerssen R. and Hu C. Processes of coastal upwelling and carbon flux in the Cariaco Basin. Deep-Sea Res (pt. II) 2004; 51:927-43.

[34] Murray A.G. and Eldridge P. Marine viral ecology: incorporation of bacteriophage into the microbial planktonic food web paradigm. J Plankton Res 1994; 16:627-41.

[35] Murray J.W., Codispoti L.A. and Friedrich G.E. "Oxidation-reduction environments: The suboxic zone in the Black Sea." In: *Aquatic Chemistry: Interfacial and Interspecies Processes*, Huang C.P., O'Melia C.R., Morgan J.J. eds., ACS Adv Chem Series, 1995.

[36] Noble R.T. and Fuhrman J.A. Use of SYBR Green I for rapid epifluorescence counts of marine viruses and bacteria. Aquat Microb Ecol 1998; 14:113-18.

[37] Norland S. "The relationship between biomass and volume of bacteria." In: *Handbook of Methods in Aquatic Microbial Ecology*, Kemp P.F., Sherr B.F., Sherr E.B., Cole J.J. eds., Boca Raton, FL: Lewis Publishing, 1993.

[38] Peterson L.C., Overpeck J.T., Kipp N.G. and Imbrie J. A high-resolution late Quaternary upwelling record from the anoxic Cariaco Basin, Venezuela. Paleoceanography 1991; 6:99-119.

[39] Repeta D.J., Simpson D.J., Jørgensen B.B. and Jannasch, H.W. Evidence for anoxygenic photosynthesis from the distribution of bacteriochlorophylls in the Black Sea. Nature 1989; 342:69-72.

[40] Richards F.A. The Cariaco Basin (Trench). Oceanogr Mar Biol Annu Rev 1975; 13:11-67.

[41] Romankevich E.A. *Geochemistry of Organic Matter in the Ocean.* Berlin: Springer-Verlag, 1984.

[42] Scranton M.I. Temporal variations in the methane content of the Cariaco Trench. Deep-Sea Res 1988; 35:1511-23.

[43] Scranton M.I., Sayles F.L., Bacon M.P. and Brewer P.G. Temporal changes in the hydrography and chemistry of the Cariaco Trench. Deep-Sea Res 1987; 34:945-63.

[44] Scranton M.I., Astor Y., Bohrer R., Ho T.-Y. and Muller-Karger F. Controls on temporal variability of the geochemistry of the deep Cariaco Basin. Deep-Sea Res 2001; 48:1605-25.

[45] Scranton M.I., McIntyre M., Taylor G.T. Muller-Karger F., Fanning K. and Astor Y. "Temporal variability in the nutrient chemistry of the Cariaco Basin." In: *Past and Present Water Column Anoxia*, L.N. Neretin ed. Dordrecht: Springer, 2006.

[46] Setälä O. Ciliates in the anoxic water layer of the Baltic. Arch Hydrobiol 1991; 4:483-92.

[47] Sharp J.H., Benner R., Bennett L., Carlson C.A., Fitzwater S.E., Peltzer E.T. and Tupas L.M. Analyses of dissolved organic carbon in seawater – the JGOFS EQPAC methods comparison. Mar Chem 1995; 48:91-108.

[48] Simon M., Grossart H.-P., Schweitzer B. and Ploug H. Microbial ecology of organic aggregates in aquatic ecosystems. Aquat Microb Ecol 2002; 28:175-211.

[49] Sorokin Y.I. The bacterial population and the process of hydrogen sulphide oxidation in the Black Sea. J Cons int Explor Mer 1972; 34:423-55.

[50] Sorokin Y.I., P. Sorokin Y., Avdeev V.A., Sorokin D. Y. and Ilchenko S.V. Biomass, production and activity of bacteria in the Black Sea, with special reference to chemosynthesis and the sulfur cycle. Hydrobiologia 1995; 308:61-76.

[51] Steward G.F., Montiel J.L. and Azam F. Genome size distributions indicate variability and similarities among marine viral assemblages from diverse environments. Limnol Oceanogr 2000; 45: 1697-1706.

[52] Stoeck T., Taylor G.T. and Epstein S. Novel eukaryotes from a permanently anoxic Cariaco Basin (Caribbean Sea). Appl Environ Microbiol 2003; 69:5656-63.

[53] Takai K., Inagaki F., Nakagawa S., Hirayama H., Nunoura T., Sako Y., Nealson K.H. and Horikoshi K. Isolation and phylogenetic diversity of members of previously uncultivated ϵ-Proteobacteria in deep-sea hydrothermal fields. FEMS Microbiol Letters 2003; 218:167-74.

[54] Takai K., Nealson K.H. and Horikoshi K. *Hydrogenimonas thermophile* gen. nov., sp. nov., a novel thermophilic, hydrogen–oxidizing Chemolithoautotroph within the ϵ-*Proteobacteria*, isolated from a black smoker in a Central Indian Ridge hydrothermal field. Int J Syst Evol Microbiol 2004; 54:25-32.

[55] Taylor G.T., Karl D.M. and Pace M.L. Impact of bacteria and zooflagellates on the composition of sinking particles: An in situ experiment. Mar Ecol Prog Ser 1986; 29:141-55.

[56] Taylor G.T., Scranton M.I., Iabichella M., Ho T.-Y., Thunell R.C., Muller-Karger F. and Varela R. Chemoautotrophy in the redox transition zone of the Cariaco Basin: A significant midwater source of organic carbon production. Limnol Oceanogr 2001; 46:148-63.

[57] Taylor G.T., Hein C. and Iabichella M. Temporal variations in viral distributions in the anoxic Cariaco Basin. Aquat Microb Ecol 2003; 30:103-16.

[58] Thunell R., Varela R., Llano M., Collister J., Muller-Karger F. and Bohrer R. Organic carbon fluxes and regeneration rates in an anoxic water column: sediment trap results from the Cariaco Basin. Limnol Oceanogr 2000; 45:300-08.

[59] Thunell R.C., Sigman D.M., Muller-Karger F., Astor Y. and Varela R. Nitrogen isotope dynamics of the Cariaco Basin, Venezuela. Global Biogeochem Cycles 2004; 18:GB3001, doi:10.1029/2003GB002185.

[60] Tuttle J.H. and Jannasch H.W. Sulfide and thiosulfate-oxidizing bacteria in anoxic marine basins. Mar Biol 1973; 20:64-70.

[61] Tuttle J.H. and Jannasch H.W. Microbial dark assimilation of CO_2 in the Cariaco Trench. Limnol Oceanogr 1979; 24:746-53.

[62] UNESCO. Protocols for the Joint Global Ocean flux Study (JGOFS) Core measurements Intergovernmental Oceanographic Commission. Manual and Guides 1994; 29:128-34.

[63] Vetriani C., Tran H.V. and Kerkhof L.J. Fingerprinting microbial assemblages from the oxic/anoxic chemocline of the Black Sea. Appl Environ Microbiol 2003; 69:6481-88.

[64] Vinogradov M.E., Flint M.V. and Shushkina E.A. Vertical distribution of mesoplankton in the open area of the Black Sea. Mar Biol 1985; 89:95-107.

[65] Wakeham S.G., Lee C., Hedges J.I., Hernes P.J. and Peterson M.L. Molecular indicators of diagenetic status in marine organic matter. Geochim Cosmochim Acta 1997; 61:5363-69.

[66] Zhang J.-Z. and Millero F.J. The chemistry of the anoxic waters in the Cariaco Trench. Deep-Sea Res 1993; 40:1023-41.

[67] Zubkov M.V., Sazhin A.F. and Flint. M.V. The microplankton organisms at the oxic-anoxic interface in the pelagial of the Black Sea. FEMS Microbiol Ecol 1992; 101:245-50.

COMPOSITION AND ACTIVITIES OF MICROBIAL COMMUNITIES INVOLVED IN CARBON, SULFUR, NITROGEN AND MANGANESE CYCLING IN THE OXIC/ANOXIC INTERFACE OF THE BLACK SEA

Nikolay V. Pimenov[1] and Lev N. Neretin[2,3]

[1] *Winogradsky Institute of Microbiology of Russian Academy of Sciences, 60-letiya Oktyabrya Prosp., 7-2, 117811 Moscow, Russia*

[2] *Max Planck Institute for Marine Microbiology, Biogeochemistry Department, Celsiusstrasse 1, 28359 Bremen, Germany*

[3] *Federal Institute for Geosciences and Natural Resources, Section Geomicrobiology, Stilleweg 2, 30655 Hannover, Germany*

Abstract Own and literature data on the structure and functional activities of microbial communities in the Black Sea chemocline are reviewed. Bacterial numbers in the oxic/anoxic interface increase by an order of magnitude compared to above-lying waters. The dark carbon dioxide fixation rate increases too and often does not correspond to the maximum in total cell numbers. Carbon isotope measurements of particulate organic carbon indicate that bacterial chemosynthesis (rates are between 9.6 and 25 mmol C m^{-2} d^{-1}) is the main source of organic matter in the Black Sea chemocline and accounts for 20-50% of total primary production. The increased dark CO_2 fixation rates in the chemocline reflect a mixed signal derived from CO_2 fixation of a number of lithoautotrophic bacteria involved in sulfide oxidation, but also with methanotrophs, methanogens and with sulfate reducers. Chemolithoautotrophic bacteria related to *Thiobacillus* and *Thiomicrospira* and heterotrophic sulfur oxidizing *Rhizobiaceae* strains are probably the main sulfide oxidizing bacteria. *Shewanella* species using Mn (Fe) oxyhydroxides as an alternative electron acceptor to dissolved oxygen may play a role in sulfide oxidation too. Anoxygenic photosynthesis mediated by green sulfur bacteria related to *Chlorobium* accounts for not more than 13% of the total sulfide flux [Overmann and Manske, this volume]. 'Anammox' bacteria together with denitrifiers may be mainly responsible for the inorganic nitrogen loss in the interface. Below the interface, sulfate reduction, methane oxidation and methanogenesis co-occur. Highest sulfate reduction rates are observed below the interface down to 300 m; however this process is detected throughout the entire water column. Several lines of evidence (isolates, rate measurements, molecular fingerprinting and biomarkers) suggest that both, aerobic and anaerobic methane oxidation occur at the Black Sea oxic/anoxic interface and in anoxic waters. ANME-1 and

L. N. Neretin (ed.), Past and Present Water Column Anoxia, 501–521.

ANME-2 groups of *Archaea* in association with δ-Proteobacteria are possible candidates mediating anaerobic methane oxidation in the water column. However neither consortia present in marine sediments nor direct rates of anaerobic methane oxidation in the water column are known. Literature data suggest a presence of an abundant community of protozoa, mostly ciliates, in the Black Sea redox zone. Many of these microorganisms harbor bacteria as ecto- or endosymbionts. A protozoa-bacteria food web can play an important role in the organic matter transfer between the oxic and anoxic waters and can also have a significant impact on functional characteristics of bacterial communities.

Keywords: Black Sea, oxic/anoxic interface, water column, chemosynthesis, microbial community, microbial activity

1. INTRODUCTION

The Black Sea has been known as a meromictic basin for more than a century since the first Andrusov's expedition [2]. In the central part of the sea, the water column is aerobic from the surface to the depth of 90-100 m; at the continental slope, dissolved oxygen disappears deeper, at depths of 130-180 m. Hydrogen sulfide appears below the oxic zone and its concentration gradually increases to the bottom and approaches 370 μM at 2200 m water depth [48].

The contact zone between oxygen- and sulfide-containing waters in the Black Sea is of special biogeochemical interest. This zone is characterized by heterogeneous distributions of hydrochemical parameters. The zonation is regulated by a change of the redox potential over depth. For a long time dissolved oxygen was believed to be the main oxidant for hydrogen sulfide and other reduced compounds diffusing up from the anaerobic water. The zone, where oxygen and sulfide co-exist (so called, redox-zone or C-layer) in the Black Sea was considered to be 10-30 m thick [3, 51, 53]. During a US-Turkish expedition in 1988, the co-existence of oxygen and sulfide in the interface between oxic and anoxic waters was challenged. Measurements demonstrated that oxygen concentrations are in the range 5-7 μM and sulfide is below the detection limit in this zone [16, 29]. These data were later confirmed with a modified Winkler method [62] and with oxygen sensor measurements [54]. The results were of crucial importance for understanding the redox processes at the oxic/anoxic interface and have initiated a number of studies to investigate alternative electron acceptors to dissolved oxygen involved in sulfide oxidation. Many chemists now believe that Mn(III,IV) oxyhydroxides and less important Fe(III) oxyhydroxides are responsible for hydrogen sulfide oxidation [22, 45]. A model for cycling of suspended and dissolved Mn and Fe in the Black Sea redox zone has been developed and attempts have been made to relate cycling of these elements to cycling of other elements undergoing redox transformations at the interface such as nitrogen (NH_4^+, NO_2^-, NO_3^-) and sulfur (H_2S, S^0,

$S_2O_3^{2-}$, SO_4^{2-}) species. Microbial processes were only formally taken into account in most of the models developed [61].

Most of the processes occurring in the redox zone are mediated by microorganisms of different physiological groups. However, the information about the physiology, diversity and biogeochemical role of bacteria inhabiting the oxic/anoxic interface in the Black Sea is still limited. Microorganisms in the interface zone serve as a "biogeochemical filter" between oxic and anoxic waters. They directly or indirectly mediate all oxidation-reduction processes that occur there, particularly those related to carbon, sulfur, nitrogen and metal cycling. Furthermore, bacteria of the redox zone represent an important source of chemosynthetically-produced organic matter that feeds microbial communities in the anoxic zone and sediments. Bacteria associated with protozoa link the two distinct food chains of the oxic and anoxic zones. Here we summarize the existing data about different physiological groups of microorganisms in the interface zone between oxic and anoxic waters of the Black Sea and discuss the specific activities and biogeochemical roles these microorganisms play in carbon, sulfur, nitrogen, and manganese (iron) cycling.

2. GENERAL STRUCTURE OF THE REDOX ZONE

Depth distributions of hydrochemical parameters in the Black Sea water column correlate strongly with density, which allows using density distributions instead of depth distributions to make the Black Sea water column spatial data comparable [27, 59].

The following layers in the redox zone are distinguished based on the distribution of major nutrients [28, 62]:

1. The upper part of the redox (suboxic) zone is located in the density interval σ_t=15.5-15.7 (70-100 m depth in the central Black Sea). The oxygen content in this zone decreases to 15-20 μM. Dissolved oxygen and nitrate are the main electron acceptors.

2. In the middle part of the redox zone (σ_t=15.9-16.0; 100-120 m) dissolved oxygen and nitrate disappear and reductants such as ammonium, soluble manganese and iron, elemental sulfur, thiosulfate, and methane appear.

3. Hydrogen sulfide and particulate Mn and Fe are present in the lower redox zone (σ_t=16.1-16.5; 120-160 m). The upper H_2S boundary corresponds to σ_t=16.15-16.25.

Recent more accurate measurements have shown that dissolved oxygen concentrations are in the range from 0 to 5 μM at the hydrogen sulfide boundary [Murray and Yakushev, this volume].

Table 1. Total number of bacteria (N, 10^6 cells ml^{-1}), their average volume (V, μm^3), biomass (B, mgC m^{-3}), and production (mgC m^{-3} d^{-1}) in the open Black Sea. UML is Upper Mixed Layer (0-25 m), CIL is Cold Intermediate Layer (40-100 m), and RZ is a redox-zone (120-200 m) (modified from [53]).

	Zone	*N, range*	*V*	*B, range (average)*	*P, range (average)*
Western Black Sea	UML	0.90 - 1.63	0.16	12 - 40 (22)	4.0 - 12.8 (7.4)
	CIL	0.24 - 0.43	0.10	5 - 11 (8)	0.6 - 1.8 (1.4)
	RZ	0.35 - 0.51	0.21	14 - 19 (16)	2.0 - 3.2 (2.6)
Eastern Black Sea	UML	0.85 - 1.05	0.15	12 - 24 (21)	4.0 - 4.9 (4.2)
	CIL	0.25 - 0.34	0.08	6 - 11 (8)	1.2 - 1.4 (1.3)
	RZ	0.40 - 0.48	0.25	12 - 19 (16)	2.8 - 4.6 (3.9)

3. DISTRIBUTION AND BIOMASS OF BACTERIOPLANKTON

First measurements of bacterial numbers and biomass in the Black Sea water column were obtained using a direct microscopic counting on membrane filters stained with erythrosine [19]. More exact epifluorescent methods using dyes such as fluorescamine, acridine orange and DAPI are currently in use [4, 21, 26, 39, 53]. The total number of bacteria, their biomass and productivity in the open sea are summarized in Table 1. The upper mixed layer is characterized by maximums of bacterial biomass and productivity. Bacterioplankton numbers in the Cold Intermediate Layer (CIL) located at depths between 40 and 100 m below a seasonal thermocline are usually low. This may be explained by the transient origin of CIL, which is formed either by downwelling of the upper mixed layer waters during winter convection in the central Black Sea or(and) by downwelling of the NW Black Sea shelf surface waters that spread along the sea area. Microbial density and biomass increase below the CIL and reach higher values in the redox zone (120-200 m). The mean volume of microorganisms that inhabit the oxic/anoxic interface increases also (Table 1). Bacterioplankton in the oxic zone is represented by small coccoid cells of 0.4-0.6 μm in diameter with some yeast-like and filamentous forms. Observed morphological types of bacteria in the oxic zone of the Black Sea are typical forms of aerobic marine heterotrophs [4, 53]. About one-third of bacteria in the oxic zone form bacterial aggregates of 3-10 μm in size. Below the thermocline and CIL these aggregates tend to form larger particles of 'marine snow' 1-3 cm in size [52].

A typical depth distribution of the total number of microorganisms counted using DAPI staining in the open sea is presented in Fig. 1. The vertical distribution of bacterioplankton in the water column is characterized by two maxima. The upper one is located in the upper oxic part at the depths of 0-50 m; cell densities are up to 10^6 cells ml^{-1}. Cell densities in the CIL are below 10^5

cells ml^{-1} and increase to $(1.5\text{-}5.5)\times10^5$ at the oxic/anoxic interface [25, 39, 53]. Bird and Karl [4] direct microscopic and total ATP measurements made in spring during R/V Knorr cruise in 1998 gave much lower values than all previous measurements. No local maximum of bacterial cell densities at or below the interface was observed. We suppose that the number and biomass of bacteria in the Black Sea redox zone are subjected to seasonal variability controlled by phytoplankton production in the oxic zone and CIL formation (replenishment) by convective mixing during winter and early spring, when Bird and Karl performed their studies. The total number of bacterioplankton at depths below 250-300 m is in the range of $(1.0\text{-}1.5)\times10^5$ cells ml^{-1} [52].

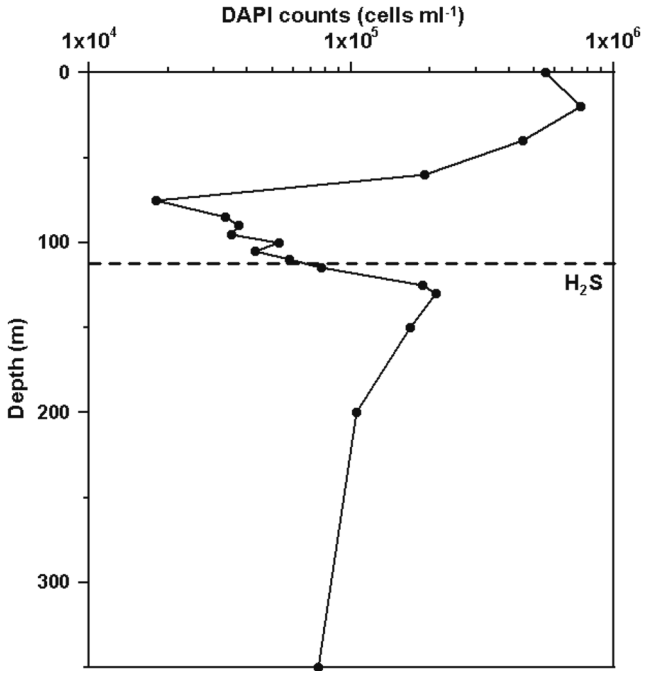

Figure 1. Typical distribution of total number of bacteria in the open Black Sea. Here and in the following figures the horizontal dashed line shows the upper sulfide boundary (Station position 44°20.23'N, 32°09.54'E, depth 1998 m; average data are from cruises in May 1998, in May 1997, and in August 1995).

4. DARK CO_2 FIXATION RATES AS AN INDICATOR OF MICROBIAL ACTIVITY

A radioisotopic technique with ^{14}C-bicarbonate was used for studying the activity of the microbial community at the oxic/anoxic interface. Many studies demonstrated a sharp increase in the rate of dark carbon dioxide fixation in the

interface between oxic and anoxic waters [10, 16, 39, 51, 53]. The presence of the CO_2 fixation maximum in the chemocline is a typical feature of other freshwater and marine euxinic environments such as the Cariaco Basin [Taylor et al., this volume] and Framvaren Fjord [63]. In the Black Sea several peaks of dark CO_2-fixation rates were observed in the density range of σ_t=16.20-16.45. The upper peak usually corresponded to the depth of sulfide appearance, while lower peaks occurred 10-50 m below (Fig. 2). The dark carbon dioxide fixation rate is an ambiguous indicator for the autotrophic bacterial production. Heterotrophic microorganisms are also able to fix up to 10% of CO_2 for the biomass synthesis [44]. The problem of distinguishing between autotrophic and heterotrophic fixation rates using existing radioisotopic method remains obscure. Given unspecific reaction of commonly used inhibitors such as N-serve, chlorate, picolinic acid, and aside their application in mixed microbial communities provides unreliable results. They can not be used to distinguish carbon dioxide fixation from different groups of microorganisms [34, 38].

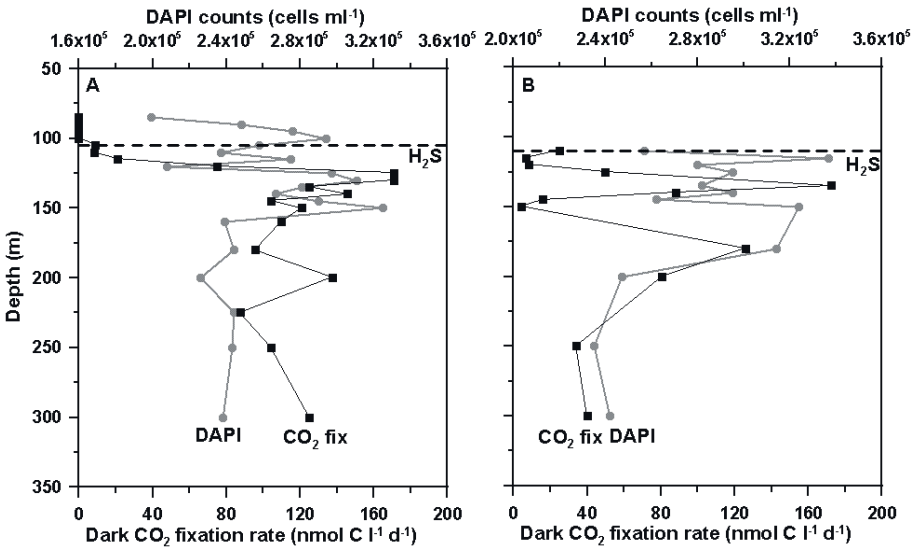

Figure 2. Combined depth profiles of dark $^{14}CO_2$ fixation rates (CO_2 fix) and bacterial cell numbers (DAPI) at two open-sea stations in May 1998 (panel A: Station 5; 43°15.22'N, 33°59.92'E, depth 2172 m; panel B – Station 6; 43°59.91'N, 37°30.06'E, depth 2123 m).

There is a range of microorganisms, which may potentially be responsible for observed peaks of CO_2 fixation rates below the oxic/anoxic interface. Most probable candidates are sulfate-reducing bacteria, which can fix CO_2 during autotrophic growth with hydrogen such as those related to *Desulfovibrio*, *Desulfobacterium*, *Desulfobacter*, *Desulfosarcina* species or those using external CO_2 as an additional to organic carbon source by the pyruvate synthase

reaction [40]. At least one phylotype retrieved from a 217 m water depth in the Black Sea water column was closely related to *Desulfobacterium* species [58]. Autotrophic CO_2 fixation was reported at least in aerobic methanotrophs possessing ribulose-biphosphate carboxylase (*Methylococcus* species as representative) [23]. Type II aerobic methanotrophs that belong to α-Proteobacteria employ the serine pathway for formaldehyde assimilation, in which CO_2 is assimilated too. These bacteria can potentially use the external pool of CO_2 and contribute to the measured fixation rates. Finally, autotrophic methanogens which activity was detected (see discussion below) and related phylotypes retrieved [58] may also be responsible for CO_2 fixation rates measured well below the oxic/anoxic interface. The simultaneous rate measurements of the processes mentioned above and dark CO_2 fixation rates at and below the interface suggest that the latter represent a mixed signal.

The isotopic composition of POC in the redox zone indicates that organic matter production there is mostly due to CO_2 fixation, or chemosynthetic production. POC had the carbon isotopic composition of -28.5 to -26.5‰ in the redox zone at σ_t=16.15-16.50 (100-250 m), where the maximum dark CO_2 fixation rates were observed (Fig. 3) [14, 18]. Bacterial chemosynthesis generally results in greater utilization of the lighter isotope and as a result, chemosynthetically produced carbon has a more negative isotopic composition than carbon of photosynthetic origin [11]. Depleted in ^{13}C POC at the oxic/anoxic interface originates from chemosynthetic bacteria. Below the zone of active chemosynthesis (σ_t =16.3-16.5) the "lighter" isotopic composition of particulate organic carbon is probably due to the preferential consumption of chemosynthetically produced bacterial biomass by anaerobic heterotrophs, primarily sulfate-reducing bacteria [14].

We have obtained integral chemosynthetic production rates in the range between 9.6 and 17.3 mmol C m^{-2} day^{-1} in spring in the open sea [39]. Sorokin et al. [53] estimated that the integral microbial production in the Black Sea water column during summer and fall was in the range of 25.0-66.7 mmol C m^{-2} day^{-1} and accounted for 50-80% of primary production. Chemosynthesis was responsible for 85-90% of the total microbial production in the chemocline and for 20-40% of total microbial production in the water column. Other data show that chemosynthesis in the Black Sea usually accounts for 20% and in some cases up to 50% of the total primary production [39]. These values are surprisingly high; they however resemble those obtained in the Cariaco Basin redoxcline, where chemoautotrophic production accounted on average for 70% of the overall primary production [Taylor et al., this volume]. Since about 10% of the organic carbon originated in the oxic zone from primary producers reach the chemocline [48], an additional carbon source is needed to fuel such high chemosynthetic production rate. The data suggest that chemosynthetic production is driven by the CO_2 sources other than those originated in the photic zone

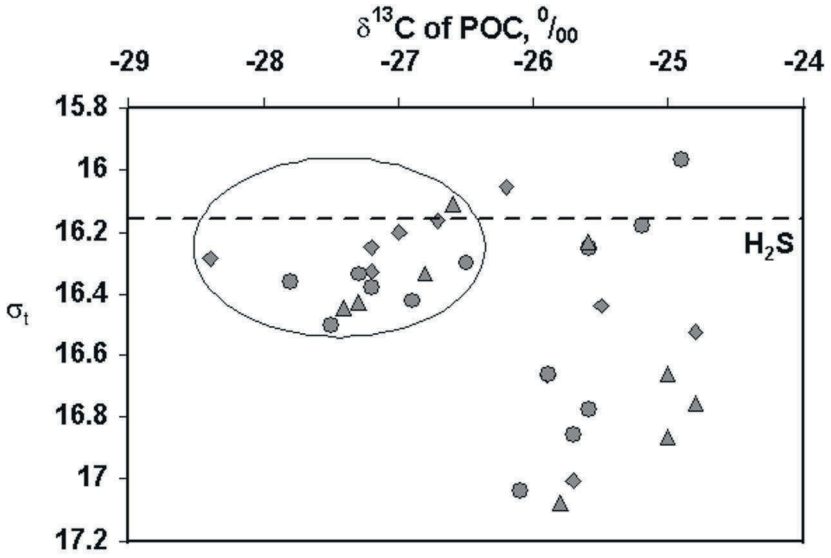

Figure 3. The carbon isotopic composition (δ^{13}C) of particulate organic carbon (POC) vs. relative density σ_t in the open Black Sea. Filled circles are data from Station 5 (43˚14.92'N, 34˚00.11'E, depth 2172 m), filled triangles are data from Station 6 (43˚00.20'N, 34˚30.25'E depth 2123 m), and filled diamonds are data from Station 4 (44˚20.23'N, 32˚09.54'E depth 1998 m) (modified from [14]).

at the same localities. Both, in the Cariaco Basin and in the Black Sea, lateral transport processes may be largely responsible for this discrepancy, but quantitatively their role in supplying allochtonous CO_2 available for chemosynthesis was not so far studied and should be addressed by future studies.

5. COMPOSITION AND ACTIVITY OF DIFFERENT BACTERIOPLANKTON GROUPS IN THE REDOX-ZONE

Bacteria of the Oxidative Part of the Sulfur Cycle. Bacteria of the oxic/anoxic interface usually consist of large rod-shaped *Achromatium* type bacteria with densities of 100-300 cells ml^{-1} and filamentous (chain-forming) bacteria are related probably to thiobacilli. The latter represent over 60% of the total bacterioplankton in the redox zone and their numbers can reach (1-5)×10^5 cells ml^{-1} [52, 53]. In the Black Sea chemocline Zubkov et al. [64] observed high cell densities (more than 10^3 cells ml^{-1}) of large strongly motile, spherical bacteria of 5-20 μm in diameter, which resembled gradient-type, colorless, sulfur bacteria of the genus *Thiovulum*. This was the first report on the presence of these 'sediment' bacteria in pelagic waters. Ten heterotrophic strains related to the *Rhizobiaceae* family were isolated from the Black Sea chemocline and were able to oxidize sulfide, elemental sulfur and thiosulfate

to sulfate using CO_2 fixation via pyruvate carboxylation [50]. Two strains of sulfite-oxidizing bacteria were described as a new species of a new genus, named *Sulfitobacter pontiacus* [49]. MPN counts demonstrated that density of the thiosulfate-oxidizing bacteria in the Black Sea interface zone may be as high as 10^1-10^4 cells ml^{-1} [53]. Obligately chemolithoautotrophic bacteria related to the genus *Thiomicrospira sp*. were also isolated from the Black Sea chemocline. Recent molecular data confirmed that *Thiomicrospira denitrificans* related microorganisms belonging to ε-Proteobacteria are an abundant group of microorganisms inhabiting oxic/anoxic interface [58]. This group can be a candidate for biologically-mediated sulfide oxidation.

Which group(s) of microorganisms is mainly responsible for hydrogen sulfide oxidation in the Black Sea is debated and a highly controversial issue among microbiologists. Sorokin was among the first who suggested that chemolithoautotrophic sulfide-oxidizing *Thiobacillus* are the main oxidation agents. Using MPN technique he estimated that the density of these microorganisms in the redox zone can reach 10^5 cells ml^{-1} [51]. Studies on chlorophorm-poisoned samples showed that the initial step of hydrogen sulfide oxidation is mediated chemically. Bacteria were responsible for the subsequent elemental sulfur and thiosulfate oxidation to sulfate. Jannasch and coworkers [15] isolated from the Black Sea chemocline obligately chemolithoautotrophic sulfur-oxidizing bacteria related to two genera, *Thiobacillus* and *Thiomicrospira.* These bacteria were able to oxidize hydrogen sulfide, elemental sulfur and tetrathionate up to sulfate and did not use nitrate or Mn and Fe oxides as alternative to oxygen electron acceptors. In experimental studies these authors showed that these organisms may potentially compete with chemically mediated sulfide oxidation if present in cell densities higher than 10^4 cells ml^{-1} [15].

The occurrence of photosynthetic bacteria in the Black Sea water column at the depth of 500 m was first reported by Kriss [20]. Based on morphological features these bacteria were later identified along the southern coasts at Kiloys and Trabson at 160-200 m depths and referred to the phototrophic *Thiocapsa roseopersicina* [6]. The possibility of anoxygenic photosynthesis at these depths was not considered during that time. The presence of *Thiocapsa* type phototropic bacteria in the western and southern Black Sea was explained by oxygen intrusions in the anoxic part with modified Mediterranean waters or by transport to the open sea from surface shelf sediments exposed to favorable light conditions.

The presence of bacteriochlorophyll *e* and carotenoids in the Black Sea oxic/anoxic interface was interpreted as direct evidence that anoxygenic photosynthesis occurs and may be an important factor for sulfide oxidation [42, 43]. The presence of these pigments is a diagnostic feature of phototrophic bacteria *Chlorobium* that are able to survive at low light intensities in stratified water columns. Phototrophic bacteria related to *Chlorobium phaeobacteroides*

were enriched from the Black Sea chemocline at depths of 77-83 m by Overmann [36]. Black Sea *Chlorobium sp.* strain BS-1 is the only known green sulfur bacteria, which is able to grow at extremely low light intensities of 0.25 μEinst m^{-2} sec^{-2}. At these light intensities, each bacteriochlorophyll molecule adsorbs only 1 photon every 8 hours. The Black Sea strain required for growth the presence of sulfide and a strongly reduced environment (Eh=-560 mV).

In May 1998 Gorlenko et al. [9] attempted to detect the activity and abundance of phototrophic bacteria in the Black Sea chemocline. They were unable to either isolate anoxygenic phototrophic bacteria on specific media or to measure the presence of bacteriochlorophyll *e* in the chemocline. Gorlenko and colleagues, however, succeeded with isolation of two strains of green sulfur bacteria from the surface 0-1 cm of deep-sea Black Sea sediment. Pigment composition and morphological characteristics of these strains were used to assign these isolates to earlier described green sulfur bacteria *Chlorobium sp.* [9, 39]. Furthermore pure cultures of green *Chlorobium sp.,* purple *Chromatium sp.* and *Thiocapsa sp.* were isolated from the Black Sea northwestern shelf surface sediments. These data suggest that anoxygenic photosynthesis in Black Sea waters may be a transient feature with spatial and temporal variability. Light penetration depth varies between the continental slope and the open sea as well as seasonally and may be the main factor regulating the abundance and activity of phototrophs in the chemocline. The hypothesis is partially supported by recent data of Overmann and Manske (this volume), who calculated that anoxygenic photosynthesis accounted for 4 to 13% in summer and for 0.002 to 0.01% in winter to the total sulfide flux in the Black Sea chemocline.

Bacteria of the Reductive Part of the Sulfur Cycle. Sulfate reducing bacteria are present in the entire anoxic water column as confirmed by direct MPN counts and measurements of sulfate reduction rates using $^{35}SO_4^{2-}$ [1, 31, 52]. The highest rates of up to 1569 nmol l^{-1} d^{-1} were observed in the upper anoxic water below the zone of active chemosynthesis down to 250-300 m (Fig. 4). Vertical profiles of sulfate reduction rates show a significant variability, possibly due to activity changes associated with seasonal and spatial variable organic detritus fluxes. MPN counts of sulfate-reducing bacteria give very low numbers in the range between 30 and 600 cells L^{-1}, which was explained by the low efficiency of the MPN method for estimating the abundance of sulfate reducers [3]. Quantification of the *dsrA* gene of sulfate-reducing bacteria by quantitative polymerase chain reaction in the Black Sea water column in winter 2001 showed that their numbers increased at the interface and were rather uniform throughout the anoxic water column with cell densities of 10^2-10^3 cells ml^{-1}. Sulfate-reducers accounted for less than 1.5% of total bacteria in the anoxic zone (Neretin et al., unpublished data). δ-Proteobacteria (most of them are sulfate-reducers) were detected both, at the oxic/anoxic interface and in the

anoxic zone. Phylotypes were related to members of hydrocarbon-degrading consortia, SAR406 cluster, and to *Desulfobacterium anilini* [58]. Perry et al. [37] isolated *Shewanella putrefaciens* from the Black Sea water column, a respiratory facultative anaerobe that can reduce quantitatively thiosulfate, sulfite, and elemental sulfur to sulfide. *Shewanella* species were accounted for 20 to 50% of the total bacterial counts in the suboxic zone (10^5 cells ml^{-1}) [30]. Several authors speculated that due to their respiratory versatility, *Shewanella* may play a significant role in both, metal and sulfur cycling.

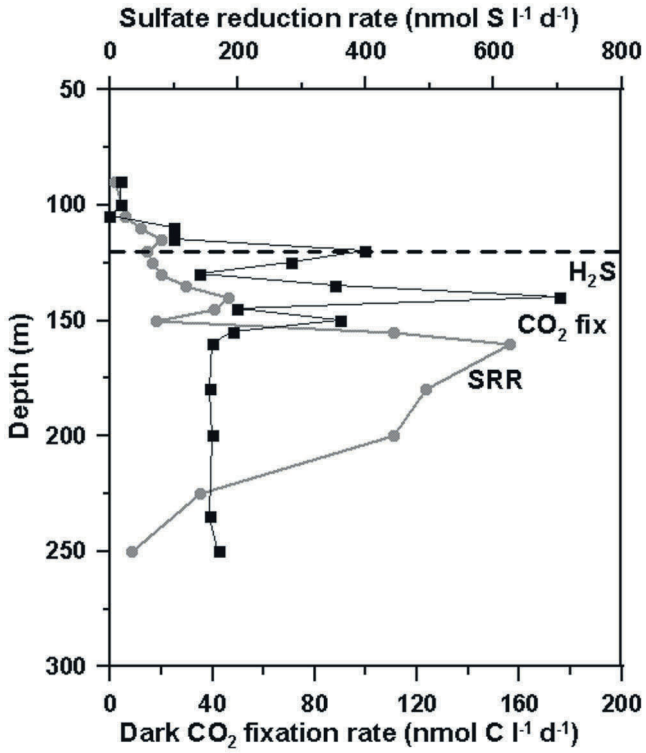

Figure 4. Combined depth profiles of sulfate reduction rates (SRR) and dark $^{14}CO_2$ fixation rates (CO_2 fix) in the open Black Sea at Station 4 in May 1988; 44˚20.23'N, 32˚09.54'E, depth 1998 m.

Bacteria of the Nitrogen Cycling. A brief overview of different bacterial groups related to the sulfur cycling present in the Black Sea chemocline shows that autotrophic and chemolithotrophic thiobacilli of *Thiobacillus* and *Thiomicrospira* genera play an important role in the chemosynthesis and sulfide oxidation in the chemocline. Some of these strains may use nitrate as an electron acceptor in oxidizing sulfide [52, 56, 57], but the depth distribution of

nitrate that usually disappears above the sulfide onset suggests that nitrate is of minor importance in oxidizing sulfide. A high density of nitrifying bacteria of up to 10^4 cells ml^{-1} was observed in the oxycline and nitrifiers were suggested to account for over 50% of the Black Sea chemosynthesis [33]. Sorokin [52] however argued that the CO_2-fixation rate by nitrifiers may contribute to not more than 1% of the chemosynthesis by thiobacilli at the oxic/anoxic interface. Recently Kuypers et al. [21] reported the occurrence of 'anammox' bacteria in the Black Sea chemocline capable of oxidizing ammonium with nitrite/nitrate under anaerobic conditions. Using fluorescence in situ hybridization (FISH) analyses the authors estimated the highest density of these bacteria at the nitrite peak of 1.9 ($\pm$0.8)$\times 10^3$ cells ml^{-1} or about 0.75% of the total number of bacteria detectable with DAPI [21, Kuypers et al., this volume]. Calculations showed that microorganisms oxidizing ammonium together with denitrifiers may play an important role in the loss of fixed inorganic nitrogen; however given their low cell numbers and biomass, they are unlikely to have any notable effect on the carbon cycle of the Black Sea.

Mn(II)-Oxidizing and Mn(IV)-Reducing Bacteria. Mn(II) oxidation is microbiologically mediated process and its maximum rates between 1 and 68 nM Mn(II) oxidized per hour have been measured in the Black Sea suboxic zone [46, 55]. These studies unambiguously showed that anaerobic Mn(II) oxidation with nitrate, nitrite, or iodate in the Black Sea water column hypothesized in earlier geochemical studies is absent and dissolved oxygen is the only possible electron acceptor for Mn(II) oxidation. Furthermore Schippers et al. [46] argued that lateral intrusions of oxygen in the western Black Sea were responsible for ventilation of the suboxic zone and could explain the observed Mn(II) oxidation rates in the chemocline. Morphologies of Mn(IV) aggregates found in lakes and usually associated with several Mn(II)-oxidizing genera such as *Metallogenium, Siderococcus, and Siderocapsa* were found in the Black Sea water column, but pure cultures of these bacteria were not isolated. Mn(II)-oxidizing and Mn(IV)-reducing bacteria are mostly probably associated with those Mn(III,IV)-rich aggregates. Nealson et al. [30] isolated several groups of Mn(IV)-reducing microorganisms related to *Shewanella, Pseudomonas, Bacillus,* and some unidentified Gram-negative rods and coccobacilli. These strains were capable to reduce Fe(III) in addition to Mn(IV).

Bacteria and Archaea Involved in Methane Cycling. The presence of ether-linked isoprenoids suggested that Archaea are widely distributed throughout the Black Sea water column. The analyses suggested that a number of psychrophilic Archaea, representing both, methanogens and thermophilic-type Archaea are common groups [13, 17]. ^{13}C depleted archaeal biphytanes (up to -58‰) occurring in the anoxic Black Sea suggested the presence of a methane oxidizing archaeal community [47, 60].

For methane-oxidizing bacteria methane is both, the energy and cellular carbon source. Methane oxidation rates increased below the oxic/anoxic interface and, on average, up to 40% of the oxidized CH_4 carbon was incorporated into the organic matter [8, 39, 41, 53, Ivanov and Lein, this volume]. The highest rates using $^{14}CH_4$ were measured in the upper 100 m of the anoxic zone. The zone of increased methane oxidation rates often but not always corresponded to the increased rate of carbon dioxide fixation (Fig.5A). Maximum CH_4 oxidation rate at this station was about 0.9 nM d^{-1}, but was as high as 8 nM d^{-1} in the central western part of the sea. Reeburgh et al. [41] have used both, $^{14}CH_4$ and C^3H_4 labeled methane, to obtain rates in the range between 1 and 10^3 nM d^{-1}. The water column rates were higher below 300 m. Our data obtained in the upper anoxic zone are comparable with Reeburgh et al.' data. The abundance and taxonomic composition of methane oxidizing bacteria inhabited the chemocline were analyzed using MPN and direct immunofluorescence methods. Density of methane oxidizing bacteria at the oxic/anoxic interface was up to 10^4 cells ml^{-1} and they were represented by several genera such as *Methylomonas, Methylobacter, Methylococcus, Methylosinus,* and *Methylocystis* [8].

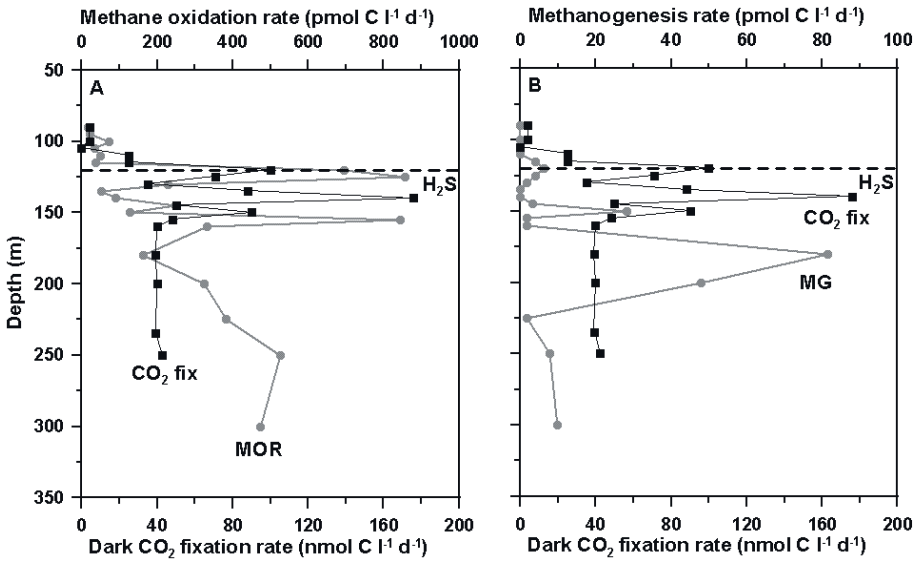

Figure 5. Combined depth profiles of methane oxidation rates, $^{14}CH_4$, (MOR; panel A), total ($^{14}CO_2$-lithotrophic and ^{14}C-aceate acetoclastic) methanogenesis rates (MG; panel B), and dark $^{14}CO_2$ fixation rates (CO_2 fix) in the open Black Sea at Station 4 in May 1988; 44°20.23'N, 32°09.54'E, depth 1998 m.

The presence of aerobic methane-oxidizing bacteria was detected down to 400-500 m using immunofluorescence method [8]. Rate measurements, however, suggest that methanotrophs may exist in the water column down to the

bottom. High methane oxidation rates were observed at and well below the sulfide appearance where dissolved oxygen is absent. These data suggest that methane in the Black Sea redox zone can be oxidized both aerobically and anaerobically. Galchenko et al [8] isolated strains of methanotrophs being all strict aerobes. They most probably dominate at the oxic/anoxic interface where traces of oxygen may exist. Vetriani et al. [58] retrieved closely related to *Methylobacter psychrophilus* phylotype from the Black Sea chemocline and amplified *pmoA* genes indicative of aerobic methane oxidation.

Below the H_2S upper boundary the presence of active aerobic methanotrophs is hardly possible. Molecular fingerprinting revealed that Archaea that belong to ANME 2 cluster potentially responsible for anaerobic methane oxidation are present in the Black Sea anoxic zone at the 305 m depth. Most recent FISH data by Schubert et al. (this volume) confirmed the presence of ANME-1 and ANME-2 groups in the Black Sea water column. Consortia consisting of sulfate-reducing bacteria and ANME 1 as well as ANME 2 groups were found to be responsible for anaerobic methane oxidation in a number of sedimentary environments [5, 35] and in microbial mats around Black Sea methane seeps [24]. Vetriani et al. [58] have found several clones of δ-Proteobacteria related to members of hydrocarbon-degrading consortia, the SAR406 cluster and to *Desulfobacterium anilini* in the anoxic water column including the oxic/anoxic interface. The phylogenetic association of these δ-Proteobacteria was considered indicative for the presence of anaerobic methane oxidation in the Black Sea water column. Yet 'typical' consortia of sulfate-reducers and methanogens have not been found so far in the water column [for details on the anaerobic methane oxidation see Ivanov and Lein, this volume; Schubert et al., this volume]. *Methanobacteriales* and *Methanosarcinales* related archaea are most probable groups involved in methanogenesis in the Black Sea water column [58].

We have measured lithotrophic (using $^{14}CO_2$) and acetoclastic (using ^{14}C-acetate), methanogenesis. Acetoclastic methanogenesis was usually responsible for less than 5% of the total methanogenesis rate in the Black Sea water column [Ivanov and Lein, this volume]. According to the classical model of redox zonation, methanogenesis can occur only when sulfate reduction is ceased (e.g. [12]). The Black Sea water column data however provide contradictory evidence. Active sulfate reduction was observed together with high rates of litotrophic methanogenesis up to 80 pmol l^{-1} d^{-1} measured using ^{14}C-bicarbonate at the station in western halistase (Fig. 5B). Methane oxidation rates were at least one order of magnitude higher than methanogenesis rate in the redox zone at this station. Therefore we observed co-existence of sulfate reduction, supposedly anaerobic methane oxidation and methanogenesis at the same depths in the Black Sea anoxic zone. There are two possible explanations for this controversy. (1) Methanogenic archaea can co-exist with sulfate-reducing bacteria if

they do not compete for substrates. For example, methylamines are common substrates for methanogens, whereas they are not used by sulfate-reducers. (2) Another mechanism facilitating co-existence between two groups could be spatial separation. Detritus particles can provide niches for active methanogenesis and separate them from a direct substrate competition and/or interaction with sulfate-reducers.

6. PROTOZOA IN THE BLACK SEA REDOX-ZONE

The analysis of microbial communities in the Black Sea chemocline would not be complete without considering the role of protozoa. Protists of the redox zone represent a diverse and vertically structured community. In spring 1988 suboxic waters are populated by the ciliate *Pleuronema marinum* (up to 30 cells L^{-1}) as well as by the ciliate's families *Tracheliidae, Holophryidae,* and *Amphileptidae* (up to 130 cells L^{-1}) [64]. The same authors reported that most of these ciliates were fed on *Thiovulum* cells. Other communities dominated by a ciliate *Askenasia sp.* populated the lower part of the redox zone and upper layers of the hydrogen sulfide zone. *Scuticociliatida* and heterotrophic flagellates were associated with the upper anoxic layers down to 300 m. Most of these scuticocilliates beared bacteria as ecto- and/or endosymbionts. Sulfide-oxidizing or sulfate-reducing bacteria were proposed as possible candidates. Several studies in stratified fresh and marine environments such as e.g., in Mariager Fjord [7] and Cariaco Basin [Taylor et al., this volume] clearly demonstrated that protist communities play an important role in utilization and controlling chemosynthetic production. Sorokin [52] proposed that in the Black Sea transfer of chemosynthetic bacterial production to higher trophic levels occurs via ciliates of the redox zone that are grazed by migrating zooplankton at the base of the oxycline. Systematics and occurrence of the Black Sea protozoa is well documented (reviewed in [52]). However, we know very little about physiology and in situ activity of this group of microorganisms in the Black Sea water column. Without this information, our understanding of the role of bacterial communities in the food web and overall biogeochemical carbon cycle in the sea will be unsatisfactory.

7. CONCLUSIONS AND DIRECTIONS FOR FUTURE RESEARCH

The Black Sea redox-zone harbors a diverse microbial community, which composition and activities were the subject of this chapter. Total number of microorganisms increases by an order of magnitude within the redox zone and bacterial chemosynthesis estimated using dark CO_2 fixation rates is the main source of newly synthesized organic matter as supported by rate and carbon isotopic composition measurements. This process accounts for 20-50% of total primary production in the oxic zone. The surprisingly high value suggests that

in addition to vertical transport, lateral processes are an additional source of nutrients in the redox zone. Dissolved oxygen as energetically most favorable electron acceptor in addition to a vertical diffusion mechanism is probably transported laterally as has been demonstrated for microbial Mn(II) oxidation. Mn(Fe) oxyhydroxides are other possible candidate electron acceptors that cause increased oxidation rates of hydrogen sulfide in the interface. Their vertical flux however is not sufficient to account for the major part of sulfide oxidation (e.g., [27]). Future research should concentrate more on lateral mechanisms that influence composition and production of microbial communities in the redox zone.

Existing data show a diverse population of bacteria involved in sulfur cycling, particularly in sulfide and sulfur intermediates (elemental sulfur, sulfite and thiosulfate) oxidation. They are represented by autotrophic *Thiobacillus* and *Thiomicrospira* and heterotrophic bacteria related to *Rhizobiaceae*. Some evidence suggests that some of these bacteria can use Mn(III,IV) oxyhydroxides as electron acceptor in addition to oxygen and by doing so provide a link between sulfur and manganese cycling. Marine aggregates with encrusted Mn oxyhydroxides provide high nutrient-rich niches for bacteria and may serve as an active transport shuttle between the oxic and anoxic zones as has been demonstrated in the redox zone of the Gotland Deep, Baltic Sea [32]. Sulfide oxidation via anoxygenic photosynthesis mediated by green sulfur bacteria *Chlorobium* usually plays a minor role, but favorable light conditions occurring in summer in the central Black Sea may cause their increased activity. Recently discovered in the Black Sea chemocline 'anammox' bacteria oxidizing ammonium with nitrite/nitrate may play in important role in the total loss of inorganic nitrogen from nutrient-rich anoxic waters. Their relationship with nitrifying and denitrifying bacteria and specific role in the nitrogen cycling of the redox zone deserves further studies. Maximum activity of sulfate reducing bacteria is observed below the zone of active chemosynthesis. Sulfate reduction may be enhanced due to the supply of labile organic matter primarily of chemosynthetic origin; however sulfate-reducers occur throughout the entire water column and are the main source of hydrogen sulfide in the basin. The most intriguing questions of the Black Sea microbial ecology are related to bacteria of the methane cycling. Rate measurements of their activities using labeled compounds provided evidence that both processes of methane generation and consumption occur simultaneously at the same depth in the upper anoxic column and both are often measurable in the lower anoxic zone [41, Ivanov and Lein, this volume]. Strictly aerobic methanotrophs isolated from the Black Sea chemocline may be responsible for CH_4 oxidation rates measured at or several meters below the upper anoxic boundary, where oxygen flux can be supported by lateral diffusion/advection processes. Methane oxidation rates in the deeper anoxic layers are probably related to anaerobic processes mediated by ANME-1

and ANME-2 Archaea in consortia with sulfate reducers or without them. Future research combining FISH, quantitative gene expression studies, protein isolation and sequencing, and biogeochemical rate measurements could help to resolve one of the largest Black Sea scientific mysteries related to methane cycling – simultaneous co-existence of methane oxidation, production and sulfate reduction.

Acknowledgements

This work was supported by the grant of Russian President for supporting scientific schools 2068.2003.04 and by the Russian Academy of Sciences (grant MCB RAS) to N. Pimenov and by the DFG grant SCHI535.

References

[1] Albert D.B., Taylor C. and Martens C.S. Sulfate reduction rates and low molecular weight fatty acid concentrations in the water column and surface sediments of the Black Sea. Deep-Sea Res 1995; 42(7):1239-60.

[2] Andrusov N.I. Preliminary report on the Black Sea expedition. Izv. Imp. Russ. Geograf. Obshch. 1890; 26(5):398-409. (In Russian)

[3] Bezborodov A.A. Eremeev V.N. Black Sea: the oxic-anoxic interface. Marine Hydrophys. Institute, Sevastopol, 1993. (In Russian)

[4] Bird D.F. and Karl D.M. Microbial biomass and population diversity in the upper water column of the Black Sea. Deep-Sea Res 1991; 38(2):1069-82.

[5] Boetius A., Ravenschlag K., Schubert C.J., Rickert D., Widdel F., Gieseke A., Amann R., Jorgensen B.B., Witte U. and Pfannkuche O. A marine microbial consortium apparently mediating anaerobic oxidation of methane. Nature 2000; 407:623-26.

[6] Dickman M. and Artuz I. Mass mortality of photosynthetic bacteria as a mechanism for dark lamina formation in sediments of the Black Sea. Nature 1978; 275(5677):191-95.

[7] Fenchel T., Bernard C., Esteban G., Finlay B.J., Hansen P.J. and Iversen N. Microbial diversity and activity in a Danish Fjord with anoxic deep water. Ophelia 1995; 43(1):45-100.

[8] Galchenko V.F., Abramochtchkina F.N. and Besrukova L.V.. Taxonomy of aerobic methanotrophic bacteria in the Black Sea. Microbiologiya 1988; 57:305-11. (In Russian)

[9] Gorlenko V.M., Micheev P.V., Rusanov I.I., Pimenov N.V. and Ivanov M.V. Ecophysiological properties of phototrophic bacteria from the Black Sea chemocline. Microbiologiya 2005; 74(2):239-47. (In Russian)

[10] Gulin M.B.. Study of bacterial processes of sulfate reduction and chemosynthesis in waters of the Black Sea. Thesis candidate of science1991, Sevastopol. 20 pp. (In Russian)

[11] Hayes J.M. Fractionation of carbon and hydrogen isotopes in biosynthetic processes. (J.W.Valley, D.R. Cole, eds.) Stable isotope geochemistry. Rev Mineral Geochem 2001; 43:225-78.

[12] Hoehler, T.M., Alperin M.J., Albert D.B. and Martens C.S. Field and laboratory studies of methane oxidation in an anoxic marine sediment: Evidence for a methanogen-sulfate reducer consortium. Global Biogeochem Cycl 1994; 8(4):451-64.

[13] Hoefs M.J.L., Schouten S., deLeeuw W., King L.L., Wakeham S.G., Sinninghe Damste J.S. Ether lipids of planktonic archaea in the marine water column. Appl Environ Microbiol 1997; 63(8):3090-95.

[14] Ivanov M.V., Lein A.Yu., Miller Yu.M., Yusupov S.K., Pimenov N.V., Wehrli B., Rusanov I.I. and Zehnder A. The effect of microorganisms and seasonal factors on the isotopic composition of particulate organic carbon from the Black Sea. Microbiology 2000; 69(4): 449-59. Translated from Microbiologiya 2000, 69(4):541-52.

[15] Jannasch H.W., Wirsen C.O. and Molyneaux S.J. Chemoautotrophic sulfur-oxidizing bacteria from the Black Sea. Deep-Sea Res 1991; 38(2):1105-20.

[16] Jørgensen B.B., Fossing H., Wirsen C.O. and Jannasch H.W. Sulfide oxidation in the anoxic Black Sea chemocline. Deep-Sea Res II 1991; 38(2):1083-103.

[17] King L.L., Pease T.K. and Wakeham S.G. Archaea in Black Sea water column particulate matter and sediments-evidence from ether lipid derivatives. Organic Geochemistry 1998; 28:677-88.

[18] Kodina L.A., Bogacheva M.P. and Luzarev S.V. Particulate organic carbon in the Black Sea: isotopic composition and nature. Geokhimiya 1996; 9:884-90. (In Russian)

[19] Kriss A.E. and Lebedeva M.A. Distribution of numerical density and biomass of microorganisms in the deep Black Sea regions. Doklady of Acad. Sci. USSR 1953; 89:633-36. (In Russian)

[20] Kriss, A.E. "Purple sulfur bacteria in hydrogen sulfide deeps of Black Sea." In:*Marine microbiology (Deep Sea)*, Kriss A.E. ed., Academija Nauk SSSR, Moscow,1959. (In Russian)

[21] Kuypers M.M.M., Sliekers A.O., Lavik G., Schmid M., Jorgensen B.B., Kuenen J.G., Damste J.S.S., Strous M. and Jetten M.S. Anaerobic ammonium oxidation by anammox bacteria in the Black Sea. Nature 2003; 422:608-11.

[22] Lewis B.L. and Landing W.M. The biogeochemistry of manganese and iron in the Black Sea. Deep-Sea Res 1991; 38(2A):773-803.

[23] Lidstrom M. "Aerobic methylotrophic prokaryotes." In: *The Prokaryotes*, Dworkin M., Falkow S., Rosenberg E., Schleifer K.-H. and Stackebrandt E. eds., Release 3.7, electronic edition. Springer-Verlag, New-York, 2005.

[24] Michaelis W., Siefert R., Nauhaus K., Treude T., Thiel V., Blumenberg M., Knittel K., Gieseke A., Peterknecht K., Pape T., Boetius A., Amann R., Jørgenesen B.B., Widdel F., Peckmann J.R., Pimenov N.V. and Gulin M.B. Microbial reefs in the Black Sea fueled by anaerobic oxidation of methane. Science 2002; 297:1013-15.

[25] Mitskevich I.N. The total number and biomass of microorganisms in deep waters of the Black Sea. Microbiologiya. 1979; 68(3):552-57. (In Russian)

[26] Mitskevich I.N. and Sazhin A.F. "Comparative measurement of numerical density of bacterioplankton with the use of Rasumov's method and the epifluorescence microscopy." In: *Structure and production of planktonic communities in the Black Sea*, Vinogradov M.E. and Flint M.V. eds, Nauka. Moscow, 1989. (In Russian)

[27] Murray J.W., Codispoti L.A. and Friederich G.E. "Oxidation-reduction environments: The suboxic zone of the Black Sea." In: *Aquatic Chemistry: Interfacial and interspecies processes.* Huang C.P., O'Melia C.R. and Morgan J.J. eds., ACS Advances in Chemistry Ser. 1995.

[28] Murray J.W., Lee B., Bullister J. and Luther G.W. The suboxic zone of the Black Sea. Environmental degradation of the Black Sea: Challenges and remedies. Dordrecht: Kluwer, 1999.

[29] Murray J.W., Jannasch H.W., Honjo S., Reeburgh W.S., Friederich G.E., Godispoti L.A., Anderson R.F., Top Z. and Izdar E. Unexpected changes in the oxic/anoxic interface in the Black Sea. Nature 1989; 338:411-13.

[30] Nealson K.H., Myers C.R. and Wimpee B.B. Isolation and identification of manganese-reducing bacteria and estimates of microbial Mn(IV)-reducing potential in the Black Sea. Deep-Sea Res 1991; 38(2):907-20.

[31] Neretin L.N., Volkov I.I., Böttcher M.E and Grinenko V.A. A sulfur budget for the Black Sea anoxic zone. Deep Sea Res I 2001; 48:2569-93.

[32] Neretin L.N., Pohl C., Jost G., Leipe T. and Pollehne F. Manganese cycling in the Gotland Deep, Baltic Sea. Mar Chem 2003; 82:125-43.

[33] Nesterov A.I., Namsaraev B.B. and Borzenkov I.A. "Bacterial chemosynthesis in western halistase of the Black Sea." In: *Variability of the Black Sea ecosystems*, Vinogradov M.E. ed., Nauka, 1991. (In Russian)

[34] Oremland R.S. and Capone D.G. Use of "specific" inhibitors in biogeochemistry and microbial ecology. Adv Microb Ecol 1988; 10:285-383.

[35] Orphan V.J., Hinrichs K.U., Ussler W., Paull C.K., Taylor L.T., Sylva S.P., Hayes J.M and DeLong E.F. Comparative analysis of methane-oxidizing archaea and sulfate-reducing bacteria in anoxic marine sediments. Appl Environ Microbiol 2001; 67:1922-34.

[36] Overmann J., Cypionka H. and Pfennig N. An extremely low-light-adapted phototrophic sulfur bacterium from the Black See. Limnol Oceanogr 1992; 37(1):150-55.

[37] Perry K.A., Kostka J.E., Luther III G.W. and Nealson K.H. Mediation of sulfur speciation by a Black Sea facultative anaerobe. Nature 1993; 259:801-03.

[38] Pimenov N.V., Nesterov A.I., Galchenko V.F. and Sokolova E.N. Effect of inhibitors on carbon dioxide assimilation by different microorganisms. Microbiologiya 1990; 59 (1):26-34. (In Russian)

[39] Pimenov N.V., Rusanov I.I., Yusupov S.K., Fridrich J., Lein A.Yu., Wehrli B. and Ivanov M.V. Microbial processes at the aerobic-anaerobic interface in the deep-water zone of the Black Sea. Microbiology 2000; 69(4):436-48. Translated from Microbiologiya 2000; 69(4):527-40.

[40] Rabus R., Hansen T. and Widdel F. "Dissimilatory sulfate- and sulfur- reducing prokaryotes." In: *The Prokaryotes.* Dworkin M., Falkow S., Rosenberg E., Schleifer K.-H. and Stackebrandt E. eds., Release 3.3, electronic edition. Springer-Verlag, New-York, 2005.

[41] Reeburgh W.S., Bess B.W., Whalen S.C., Sandbeck K.A. and Kilpatrick K.A. Black Sea methane geochemistry. Deep-Sea Res 1991; 38(2):1189-210.

[42] Repeta D.J. and Simpson D.J. The distribution and recycling of chlorophyll, bacteriochlorophyll and carotenoids in the Black Sea. Deep-Sea Res 1991; 38:969-84.

[43] Repeta D.J., Simpson D.J. and Jannasch H.W. Evidence for anoxygenic photosynthesis from the distribution of bacteriochlorophylls in Black Sea. Nature 1989; 342:69-72.

[44] Romanenko V.I. Heterotrophic assimilation of CO_2 by bacterial flora of water. Microbiologiya 1964; 33:679-83. (In Russian)

[45] Rozanov A.G. and Volkov I.I. "Manganese in the Black Sea. Modern notion of redox zone vertical hydrochemical structure in the Black Sea." In:*Multidisciplinary investigations of the northeast part of the Black Sea*, Zatsepin A.G. and Flint M.V. eds., Nauka, Moscow, 2002.

[46] Schippers A., Neretin L.N., Lavik G., Leipe T. and Pollehne F. Manganese (II) oxidation driven by lateral oxygen intrusions in the western Black Sea. Geochim Cosmochim Ac 2005; 69(9):2241-52.

[47] Schouten S., Wakeham S.G. and Damste J.S. Evidence for anaerobic methane oxidation by archaea in euxinic waters of the Black Sea. Organic Geochemistry 2001; 32:1277-81.

[48] Skopintsev B.A. Formation of the modern chemical composition of the Black Sea. Leningrad, Gidrometeoizdat, 1975. (In Russian)

[49] Sorokin D.Yu. *Sulfitobacter pontiacus* gen. nov. sp. nov. – A new heterotrophic bacterium from the Black Sea, specialized on sulfite oxidation. Mikrobiologiya 1995; 64(3):354-65. (In Russian)

[50] Sorokin D.Yu. and Lysenko A.M. Characterization of heterotrophic bacteria from the Black Sea oxidizing reduced sulphur compounds to sulphate. Microbiologiya 1993; 62:1018-31. (In Russian)

[51] Sorokin Yu.I. On the primary production and bacterial activity in the Black Sea. J. du Council Explor. Mer. 1964; 29:41-60.

[52] Sorokin Yu.I. The Black Sea ecology and oceanography. Backhuys Publishers, Leiden, The Netherlands, 2002.

[53] Sorokin Yu.I, Sorokin P.Y., Avdeev V.A., Sorokin D.Y. and Il'chenko S.V. Biomass, production and activity of bacteria in the Black Sea, with special reference to chemosynthesis and sulfur cycle. Hydrobiology 1995; 308:61-76.

[54] Stunzhas P.A. "Fine structure of vertical oxygen distribution in the Black Sea. Modern notion of redox zone vertical hydrochemical structure in the Black Sea." In: *Multidisciplinary investigations of the northeast part of the Black Sea*, Zatsepin A.G. and Flint M.V. eds., Nauka, Moscow, 2002.

[55] Tebo B.M. Manganese oxidation in the suboxic zone of the Black Sea. Deep Sea Res 1991; 38(2):883-905.

[56] Tuttle J.H. and Jannasch H.W. Occurrence and types of Thiobacillus-like bacteria in the sea. Limnology and Oceanography 1972; 17:532-43.

[57] Tuttle J.H. and Jannasch H.W. Sulfide and thiosulfate-oxidizing bacteria in anoxic marine basins. Marine Biology 1973; 20:64-70.

[58] Vetriani C., Tran H.V. and Lee J.K. Fingerprinting microbial assemblages from the oxic/anoxic chemocline of the Black Sea. Appl Environ Microbiol 2003; 69(11):6481-88.

[59] Vinogradov M.E. and Nalbandov Yu.P. Effect of changes in water density on the profiles of physical, chemical and biological characteristics in the pelagic ecosystems of the Black Sea. Oceanology (Moscow) 1990; 30:567-73. (In Russian)

[60] Wakeham S.G., Lewis C.M., Hopmans E.C., Schouten S. and Sinninghe Damsté J.S. Archaea mediate anaerobic oxidation of methane in deep sea euxinic waters of the Black Sea. Geochim Cosmochim Ac 2003; 67:1359-74.

[61] Yakushev E.V. and Debolskaya E.I. Particulate manganese as a main factor of oxidation of hydrogen sulfide in redox zone of the Black Sea. Oceanic fronts and related phenomena: Konstantin Fedorov memorial symp.: Proc. IOC Workshop Rep. No. 159. Moscow, GEOS 2000:592-597.

[62] Yakushev E.V., Lukashev Yu.F., Chasovnikov V.K. and Chzhu V.P. "Modern notion of redox zone vertical hydrochemical structure in the Black Sea." In: *Multidisciplinary investigations of the northeast part of the Black Sea.* Zatsepin A.G. and Flint M.V. eds., Nauka, Moscow, 2002.

[63] Zopfi J., Ferdelman T.G., Jørgensen B.B., Teske A. and Thamdrup B. Influence of water column dynamics on sulfide oxidation and other biogeochemical processes in the chemocline of Mariager Fjord (Denmark). Mar Chem 2001; 74:29-51.

[64] Zubkov M.V., Sazhin A.F. and Flint M.V. The microplankton organisms at the oxic-anoxic interface in the pelagial of the Black Sea. FEMS Microbiol Ecol 1992; 101:245-50.

ANOXYGENIC PHOTOTROPHIC BACTERIA IN THE BLACK SEA CHEMOCLINE

Jörg Overmann and Ann K. Manske

University of Munich, Institute for Genetics and Microbiology, Department Biology I, Maria-Ward-Str. 1a, Munich, Germany

Abstract Currently, the Black Sea is the largest anoxic water body on the planet and represents the closest contemporary analogue to past sulfidic oceans. For the understanding of such oxic/anoxic environments, green sulfur bacteria are significant, since they [1] can substantially alter the carbon and sulfur cycles and [2] may be used as indicator organisms for the reconstruction of past photic zone anoxia. In the chemocline of the Black Sea, brown-colored green sulfur bacteria form an extremely dilute, but detectable population. Based on analysis of their 16S rRNA gene sequences, these bacteria represent a single and novel phylotype. Measurements of light intensities in the chemocline and experiments with laboratory cultures revealed that the strain from the Black Sea is extraordinarily low-light adapted and grows with doubling times of several years. Fossil 16S rRNA gene sequences of the chemocline green sulfur bacterium have been detected in different sediment layers, indicating past photic zone anoxia during which the chemocline must have been positioned at a depth of up to 150 m. Although not significant in the carbon and sulfur cycles of the Black Sea, the particular type of green sulfur bacterium present in the chemocline thus represents a valuable indicator organism for the reconstruction of the paleoenvironmental conditions of the Black Sea.

Keywords: Chemocline, green sulfur bacteria, 16S rRNA, low-light adaptation, primary productivity, photic zone, paleomicrobiology

1. INTRODUCTION

In the present day ocean, anoxic sediments cover ~0.3% of the seafloor [44], corresponding to ~0.22% of the surface of the earth. An even smaller area of the planet is covered by sulfidic water bodies like the Black Sea (0.083%), the Cariaco Basin as the second largest basin (~0.0022%) [62], the Gotland Basin of the Baltic Sea, some smaller anoxic fjords, and numerous coastal lagoons [8]. Since 87-92% of the water body of the Black Sea is permanently anoxic [11, 38, 69], the latter currently contains the largest volume of anoxic water on the planet.

L. N. Neretin (ed.), Past and Present Water Column Anoxia, 523–541.

In contrast to the present situation, the entire Proterozoic ocean may have consisted of sulfidic deep water covered by a possibly 100 m-thick oxygenated surface layer. This has been inferred from the S isotopic composition of sedimentary sulfides, the fraction of reactive iron and the degree of pyritization, the evidence for decreased organic carbon burial, and a limited abundance and diversity of protists [1]. The sulfidic pelagial of the Proterozoic ocean may have persisted over 1000 million years. Extended water column anoxia may have occurred also during the Phanerozoic. Derivatives of bacteriochlorophylls and carotenoids of the obligately anoxygenic phototrophic green sulfur bacteria have been detected in sediments deposited throughout this period [40], starting with late Ordovician marine black shales, and including Upper Devonian [24], Permian and Mid-Triassic shales [21] and Messinian Marl [37] sediments. From the presence and the distinct carbon isotopic composition of these bacterial biomarkers, it has been deduced that the anoxic layers in paleoceans frequently extended into the photic zone. These findings have sparked a considerable interest in the structure and function of such large oceanic oxic/anoxic environments. The Black Sea may represent the largest and closest contemporary analogue to past sulfidic oceans [15], and hence constitutes a valuable model system for the study of the biogeochemical cycles and the (micro)organisms which become relevant in these environments.

Anoxygenic phototrophic bacteria typically occur where light reaches sulfidic water layers. Among the anoxygenic phototrophic bacteria, green sulfur bacteria are especially well adapted to low-light habitats due to their large photosynthetic antennae, their lower maintenance energy requirements and higher sulfide tolerance [56]. Green sulfur bacteria are significant for the understanding of oxic/anoxic oceans in two respects. Firstly, like other phototrophic sulfur bacteria, they may substantially alter the carbon and sulfur cycles by reoxidizing a major portion of the biogenic sulfide, thereby efficiently recycling electrons and feeding additional organic carbon into the pelagic carbon cycle [51]. In order to be able to assess the role of green sulfur bacteria in anoxic oceans, however, the regulation of photosynthetic activity by environmental factors like light, sulfide and temperature first needs to be quantified for those types which are typical for euxinic water bodies. Secondly, green sulfur bacteria have been used as indicator organisms for past photic zone anoxia when reconstructing oceanic paleoenvironments [40] (Coolen, this volume). Green sulfur bacteria are especially well suited for this purpose since their photosynthetic pigments are well preserved in anoxic sediments and since the origin even of pigment derivatives can be verified by their distinct carbon isotopic signatures [37]. Still, a correct interpretation of fossil green sulfur bacterial biomarkers and a detailed reconstruction of environmental conditions in ancient oceans require a better knowledge of the physiology of green sulfur bacteria typical for the marine oxic/anoxic pelagial. From a more general perspective, green sulfur bacteria

represent excellent model systems for the study of low-light adaptation and of mechanisms of adaptation towards extreme energy-limited environments in general. As outlined below, the green sulfur bacteria recovered from the Black Sea chemocline represent a particularly well suited model system for the investigation of these basic scientific questions.

2. ANOXYGENIC PHOTOTROPHIC BACTERIA IN THE BLACK SEA

The first report on the occurrence of phototrophic sulfur bacteria in the Black Sea dates back to 1953, when Kriss and Rukina [41] described the enrichment of purple sulfur bacteria from the dark water layers between 500 and 2000 m depths. These findings were corroborated by microscopic observations of cells resembling *Thiocapsa roseopersicina* which occurred in water samples from 160 and 200 m depth [16]. Similar reports were made by others [79], and it was suggested that these bacteria may be major primary producers in the Black Sea [66].

However, the presence of anoxygenic phototrophic bacteria in the water column could not be confirmed in two parallel studies in which pure cultures of *Chromatium warmingii* and *Thiocapsa roseopersicina* and enrichment cultures of *Chlorobium phaeovibrioides* were obtained exclusively from 660 m and 2240 m-deep sediment layers, but not from 129 different pelagic water samples [25, 30]. Because of the low salt requirements for growth of these strains, and because of the absence of light and the presence of high amounts of organic carbon in the deep sediments it was proposed that the cells of phototrophic sulfur bacteria in sediments originate in coastal lagoons of the Black Sea and survive by means of a fermentative metabolism [25]. Active proliferation still seems unlikely due to extremely low turnover rates at deep sea hydrostatic pressures [29, 31]. The presence of large spherical cells below the chemocline observed by Dickman and Artuz [16] was confirmed more recently [4, 69]. These cells constituted 5-10% of the total living biomass, but resemble *Achromatium* and thus most likely are not phototrophic.

More specific evidence for the presence of phototrophic sulfur bacteria became available more than a decade ago. Bacterial cells exhibiting autofluorescence were observed at the oxic/anoxic interface [5]. Since cells of green sulfur bacteria become red fluorescent upon treatment with fixative due to the formation of free bacteriopheophytins [73], the bacterial cells accumulated in the chemocline most likely contained bacteriochlorophylls and consequently were identified as green sulfur bacteria. These cells were reported to account for 10% of the total bacterial cell number [5]. Traces of different bacteriochlorophyll *e* homologues were directly detected by the U.S.-Turkish expedition on the RV *Knorr* in May 1988 [60]. These pigments are characteristic for the obligate anaerobic photolithotrophic green sulfur bacteria *Chlorobium*

phaeobacteroides and *Chl. phaeovibrioides*. Pigment concentrations reached 940 ng BChl*e* l^{-1} at a depth of 74 m in the central western basin [60].

From water samples obtained during the same U.S.-Turkish expedition on the RV *Knorr*, the first successful enrichment of green sulfur bacteria could be established in 1989 (strain MN1; [54]). The inoculum was retrieved in the central western basin from a water depth of 80 m where oxygen and hydrogen sulfide concentrations were below detection limit. A very similar green sulfur bacterial strain (BS-1) was isolated again from chemocline water samples recovered in 2001 from a depth of 95 m in the central western basin [45].

In a recent survey of 16S rRNA genes of chemocline bacteria, no green sulfur bacteria-like sequences could be detected [75] despite the presence of the specific pigment biomarkers. This discrepancy may be attributed to the clonal bias in the *E. coli* library used for 16S rRNA gene analyses and, together with the very low concentrations of green sulfur bacterial pigments, indicates that specific detection methods need to be employed for a molecular identification of the green sulfur bacteria present in the Black Sea. Primers specific for 16S rRNA gene sequences of green sulfur bacteria have become available [55] and permit a highly selective PCR amplification of 550 bp-gene fragments from as little as 100 cells [19]. Employing these specific primers and separation of the PCR products by denaturing gradient gel electrophoresis yielded a single and novel type of 16S rRNA gene sequence from the 2001 chemocline water samples, phylogenetically clustering with the other marine strains of green sulfur bacteria (Fig. 1). This sequence was identical to that from strains MN1 and BS-1, indicating that the *in situ* population exclusively consists of this type of green sulfur bacterium which persisted at least over a time period of 13 years. The successful isolation of the green sulfur bacterium permits detailed laboratory investigations of the physiological adaptations to the specific environmental conditions in the Black Sea chemocline.

3. ENVIRONMENTAL CONDITIONS IN THE BLACK SEA CHEMOCLINE

Within the chemocline of the Black Sea, salinity values of 20 - 21 ‰ and temperatures of 8 - 9 °C have been measured. Chemical analysis of samples from 70 to 100 m showed suboxic concentrations of molecular oxygen (0 - 3.8 μM), concentrations of nitrate of up to 8 μM, of nitrite < 0.3 μM, of ammonia between 0.2 and 8.8 μM, and of phosphate between 1 and 7 μM. Sulfide concentrations reach 15 μM and elemental sulfur 0.2 μM in the chemocline [12, 32, 33, 49, 60].

Whereas the above environmental factors correspond to those in other oxic-/anoxic habitats, the Black Sea chemocline is characterized by a very extreme light climate. The chemocline is positioned much deeper in the water column than in other environments of phototrophic sulfur bacteria described so far.

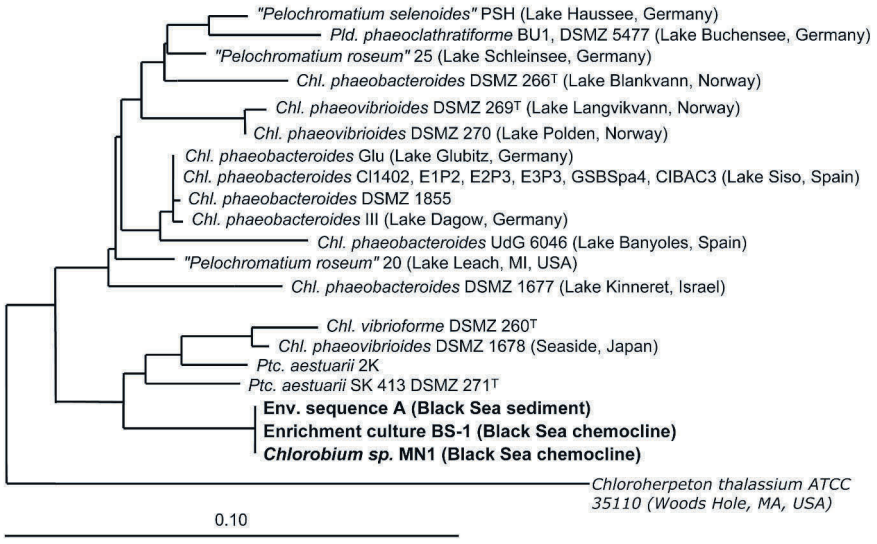

Figure 1. Phylogenetic position of the strain BS-1, isolated from the Black Sea chemocline, within other brown colored green sulfur bacteria. The partial sequence obtained from the sediment at 109 cm below sea floor (*Env. sequence A*) is identical to that from the chemocline. *Bar* represents 0.1 fixed nucleotide exchanges.

Typically, accumulations of phototrophic sulfur bacteria have been observed between 2 and 20 m, rarely up to 30 m depth [74]. In such environments, values for the light transmission to populations of phototrophic sulfur bacteria range from 0.015 to 10% [57, 74]. Due to the lower position of the chemocline, the *in situ* light intensities in the Black Sea were expected to be significantly lower and consequently represent the limiting factor for the growth of the green sulfur bacteria [60, 61].

A first estimate for the light transmission to the top of the population of green sulfur bacteria at 78 m depth was based on Secchi disk measurements and arrived at a value of 0.2% of surface light intensity [5]. Another estimate, similarly derived from Secchi depth readings amounted to 0.0006% of total incident solar radiation, corresponding to 0.012 μmol Quanta m^{-2} s^{-1} [12]. Based on a more detailed calculation which took into consideration the chlorophyll-specific attenuation coefficient [52], the light transmission reported by Repeta et al. [60] and data from irradiance measurements at Odessa [54], the underwater irradiance available for photosynthesis in the Black Sea chemocline was estimated to be 0.003 μmol Quanta m^{-2} s^{-1} (max. in June 0.01 μmol Quanta m^{-2} s^{-1}). This corresponds to 0.0005 % (0.002 %) of the surface irradiance (600 μmol Quanta m^{-2} s^{-1} in winter) [54].

However, the actual values of the light intensities available to the green sulfur bacteria present in the Black Sea chemocline remained obscure until 2001, when the first direct measurement of light intensities in the Black Sea chemocline, then positioned between 90 and 110 m depth, was made with an integrating quantum meter [45]. According to these recent measurements, *in situ* light intensities during winter reach 0.001 μmol Quanta m^{-2} s^{-1} in the chemocline, corresponding to 0.0007% of surface light intensity. These measurements hence confirm the earlier estimates.

4. SPECIFIC LOW-LIGHT ADAPTATION OF GREEN SULFUR BACTERIA

Previous to the discovery of green sulfur bacteria in the Black Sea chemocline, the deepest populations of green sulfur bacteria were detected at depths of 25 - 30 m in some freshwater lakes [20, 23, 48, 74]. So far, all attempts to discover photosynthetic activity in natural samples from the Black Sea chemocline have failed [5, 33, 68] with only one possible exception where light-dependent $^{14}CO_2$-incorporation was observed once and at intensities above *in situ* values [12]. It has therefore been questioned whether the green sulfur bacteria in this environment are at all photosynthetically active [69]. As an independent line of evidence, modeling of sulfide fluxes revealed that direct and indirect oxidation by molecular oxygen accounts for most, if not all of the sulfide removal in and beneath the Black Sea chemocline [38, 39]. In accordance with these results, a stimulation of sulfide oxidation by light could not be detected in natural water samples [60]. As a consequence, anoxygenic photosynthesis most likely does not represent a biogeochemically important process in this system (see below). Furthermore, a large portion of microorganisms present in water layers below 50 m depth may be moribund or dead based on their low specific ATP content [5].

However, oxygenic coralline red algae have been observed at a depth of 268 m in the Caribbean where *in situ* light intensities reach only as little as 0.007-0.025 μmol Quanta$\cdot m^{-2}\cdot s^{-1}$ (0.0005% of the surface light intensity) [42]. These values are comparable to those determined for the Black Sea chemocline (see above). Since they strictly depend on sulfide-containing environments and are obligately phototrophic, at least some green sulfur bacterial lineages would be expected to have experienced a high selection pressure towards low-light adaptation. The fact that fluorescence measurements of pigment extracts demonstrated the presence of intact bacteriochlorophyll *e* pigments, together with the very low abundance of bacteriopheophytins [12, 60] contradicts the assumption that green sulfur bacterial cells in the Black Sea chemocline are in a moribund state. Further indirect evidence for a light dependence of anoxygenic photosynthetic bacteria comes from the variation of their population densities with depth of the chemocline. Whereas pigment concentrations of 940 ng

BChl*e* l^{-1} were determined at 74 m at a central station in the western basin, much lower concentrations of bacteriochlorophyll *e* (214 ng l^{-1}) were found closer to the Turkish coast, where the chemocline was located at a greater depth of 100 m depth [60]. This pronounced decrease in the chemocline bacteriochlorophyll *e* concentrations towards the coastal sampling stations was fully confirmed by the recent comparison of the population densities of green sulfur bacteria at 100 m and 150 m depths [45].

Direct evidence for a specific adaptation of green sulfur bacteria dwelling in the chemocline of the Black Sea comes from the study of five strains of brown-colored green sulfur bacteria which were isolated from chemocline water samples during the U.S.-Turkish expedition with the RV *Knorr* in May 1988 [54]. All strains contained bacteriochlorophyll *e* as the main photosynthetic pigment and revealed an extreme low-light adaptation compared to 12 other green and purple sulfur bacterial strains. One isolate was chosen for a detailed study of this low-light adaptation. Under severely limiting light intensities ≤ 1 μmol Quanta·m^{-2}·s^{-1}, the Black Sea isolates grew significantly faster than related green sulfur bacteria. In contrast, growth rates at light saturation were lower than in other phototrophic sulfur bacteria.

Most notably, the Black Sea bacterium is capable of growing at 0.25 μmol Quanta·m^{-2}·s^{-1} of daylight fluorescent tubes (0.04 % of surface irradiance), which is too low to support growth of most other anoxygenic phototrophic bacteria. Only two strains of the brown-colored *Chlorobium phaeovibrioides* could also grow at this low quantum flux, albeit at much slower rate than the Black Sea strain. Since not only the growth rate, but also the sulfide oxidation rates of whole cells were significantly higher under light limitation [54], the photosynthetic reaction itself must be more efficient in the Black Sea strain, which has been attributed to an increase in light-harvesting pigments by a factor of ~2 as compared to other green sulfur bacteria. This might also be an explanation for the high concentrations of bacteriochlorophyll compared to rather low amounts of biomass detected in this water depth [5, 60]. Green sulfur bacteria employ specialized intracellular structures, so-called chlorosomes, for photosynthetic light-harvesting [56]. As demonstrated by ultrathin sectioning, the Black Sea strain MN1 produced two-fold larger chlorosomes than another *Chlorobium phaeobacteroides* strain (DSMZ 266^T) [18]. The number of chlorosomes per cell was found to be constant and independent of light intensity. Changes in chlorosome volume, hence cellular pigment content, are due to changes in chlorosome length, but not width [18]. A second unusual feature of the Black Sea green sulfur bacterium is its extraordinarily low maintenance energy requirement which is commensurate with the extremely low doubling time of 2.8 years calculated for green sulfur bacterial cells under *in situ* conditions [54]. Recent assimilation experiments with ^{14}C-labeled bicarbonate revealed that the green sulfur bacteria from the Black Sea are capable of anoxygenic

photosynthesis even at light intensities as low as 0.015 - 0.08 μmol Quanta m^{-2} s^{-1} depending on the light adaptation state of the culture [45].

However, growth of the green sulfur bacteria under the extremely low light intensities *in situ* may also be supported by the assimilation of organic carbon compounds. Under suboptimal light conditions, organic carbon substrates strongly influence the phototrophic growth of different green sulfur bacteria [2, 3]. Green sulfur bacteria are capable of incorporating acetate into cellular components in the CO_2-dependent reaction of pyruvate synthase [64]. This reaction requires reduced ferredoxin and hence depends on light for the regeneration of reducing power. While the photosynthetic rate is decreased in the presence of organic substrates, the lowest light intensity supporting growth of a brown-colored *Chlorobium phaeobacteroides* isolated from Lake Kinneret is decreased from 1.0 μmol Quanta$\cdot m^{-2}\cdot s^{-1}$ in the absence to 0.3 μmol Quanta$\cdot m^{-2}\cdot s^{-1}$ in the presence of acetate [2]. The hypolimnion of Lake Kinneret contains acetate at concentrations of 3.3 μM [2]. At present, the concentrations and types of low molecular weight organic compounds in the chemocline of the Black Sea have not been investigated.

From the *in situ* data mentioned in the preceding section, it can be calculated that each bacteriochlorophyll *e* molecule present in the chemocline layer absorbs one photon every 8 hours. The ecological situation of phototrophic organisms in the Black Sea chemocline is comparable to that of growing plants at a distance of 50 m from a little candle in an otherwise pitch black glass house. The evidence accumulated to date indicates that the particular strain of green sulfur bacteria dwelling in the Black Sea chemocline is indeed capable of exploiting this minute light intensity. The green sulfur bacterium dwelling in the Black Sea chemocline so far represents the most extreme case of low-light adaptation. It therefore represents a valuable model system for the study of the molecular basis of low light adaptation. Comparison of its 16S rRNA gene sequence with all known sequences in the databases revealed that the Black Sea bacterium so far is unique and has not been discovered in any other system (Fig. 1).

5. BIOGEOCHEMICAL SIGNIFICANCE OF ANOXYGENIC PHOTOSYNTHESIS

Karl and Knauer [34] determined a total rate of oxic primary productivity in the photic zone of 575 mg C m^{-2} day^{-1}. Because the total amount of bacteriochlorophyll *e* determined in the chemocline of the Black Sea surpasses the amount of chlorophyll *a* in the overlying oxygenated water layers, it has been argued that anoxygenic photosynthesis has become a significant process in the Black Sea carbon cycle [60, 61]. In many oxic/anoxic aquatic ecosystems, anoxygenic phototrophic bacteria reoxidize a major fraction of the sulfide

produced in the chemocline or in deeper water layers [74]. Since the electrons from sulfide oxidation are almost completely transferred onto CO_2, anoxygenic photosynthesis couples the carbon and sulfur cycles much more efficiently than chemolithotrophic sulfide oxidation. Phototrophic sulfur bacteria hence may substantially alter the pelagic carbon and sulfur cycles [51], for example via the accumulation of a high microbial biomass which may enter the aerobic pelagic food web.

One attempt to determine the ecological significance of green sulfur bacteria in the Black Sea was made by Repeta et al. [60]. They tried to translate the measured bacteriochlorophyll values into biomass with POC data (particulate organic matter) and estimated a total photosynthetic bacterial biomass of 0.5 $g \cdot m^{-2}$ in the chemocline compared to a total phytoplankton biomass in the upper water layers of 0.9 $g \cdot m^{-2}$. They also detected the highest rates of H_2S oxidation *in situ* at the base of the bacteriochlorophyll maximum which shows a correlation to anoxygenic photosynthetic bacteria. However, a significant light induced increase in bacterial photosynthesis rates *in situ* could not be shown.

The light intensity determined *in situ* was 0.001 μmol Quanta m^{-2} s^{-1} in winter (Section 3). Based on the very slow growth, the lowest light intensity which could be employed in growth experiments with laboratory cultures was 0.25 μmol Quanta m^{-2} s^{-1} [54] and hence far higher than the *in situ* light intensity values. Therefore, $^{14}CO_2$ assimilation rates were recently assessed at much decreased intensities of as low as 0.006 μmol Quanta$\cdot m^{-2} \cdot s^{-1}$, and then used to calculate photosynthesis rates and sulfide oxidation rates (see below) in the chemocline of the Black Sea [45]. These calculations yielded a rate of anaerobic primary production of 211 ngC m^{-2} day^{-1} under *in situ* conditions. Considering the integrated biomass of green sulfur bacteria in the chemocline of 798 μg *BChle* m^{-2} (Fig. 3), equal to 2.89 mgC m^{-2}, this primary production corresponds to an average growth rate of $7.31 \cdot 10^{-5}$ d^{-1} and a doubling time of 26 years. Although experimental conditions in the laboratory cultures may be suboptimal, and anoxygenic photosynthesis will be higher during summertime, green sulfur bacteria in the chemocline of the Black Sea clearly form the least dense and slowest growing population known to date as revealed by a cross-system comparison of stratified aquatic ecosystems (Figs. 2, 3). Specific adaptations, like the assimilation of organic carbon substrates generated by accompanying bacteria could theoretically result in a higher growth rate as calculated from CO_2-incorporation alone. Auxiliary metabolic reactions and the role of interactions with accompanying bacteria should therefore be the focus of future investigations of bacterial physiology in the Black Sea chemocline.

From the very low growth rates calculated for green sulfur bacteria in the chemocline, it also has to be concluded that losses of these bacteria must be extraordinarily small in order to explain the persistence of these bacteria even in winter. Indeed, ciliates of the order Scuticociliatida and isokont flagellates

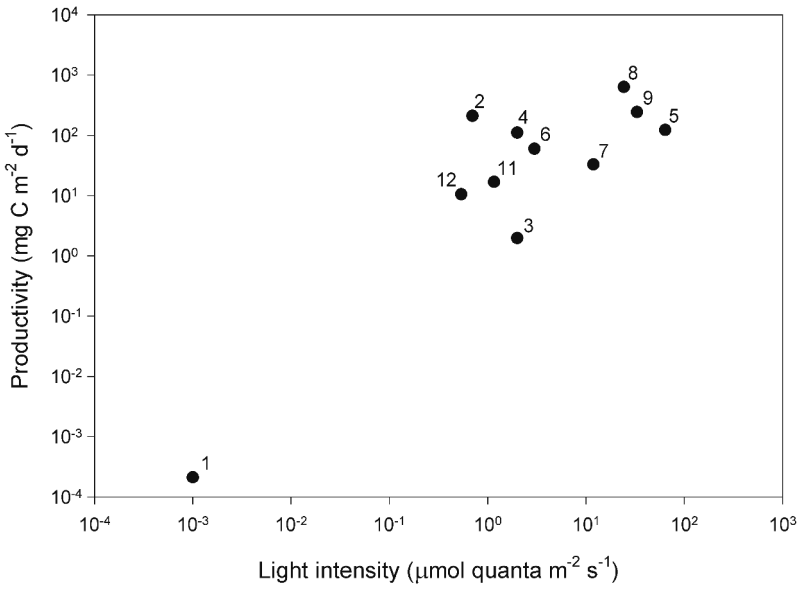

Figure 2. Relation between productivity and available light intensities (determined directly above the bacterial layer) in different anoxygenic photosynthetic communities. *1* Black Sea [45]; *2* Big Soda Lake [10]; *3* Mary [6, 57]; *4* Knaack Lake [58]; *5* Mahoney Lake [50]; *6* Mirror Lake [6, 57]; *7* Rose Lake [6, 57], *8* Lake Cisó [22]; *9* Lake Vilar [22]; *11* Paul [6, 57]; *12* Peter [6, 57].

are confined to the upper layers of the H_2S-containing zone [80]. Since their population densities are rather low (maximum of 2 cells per ml], it appears unlikely that they cause significant losses of the bacterial population by grazing. Similarly, losses by sedimentation appear to be very low, since no biomarkers of green sulfur bacteria could be detected in sediment traps incubated below the chemocline of the Black Sea (see Section 6 below).

Besides CO_2-fixation, green sulfur bacteria could theoretically be significant for sulfide oxidation in the Black Sea chemocline. Jørgensen et al. [33] observed a peak maximum of H_2S oxidation in a depth of 85 m at the top of the sulfide zone. It was accompanied by a similarly sharp maximum of dark CO_2 fixation and of total bacterial numbers. Sulfide oxidation experiments with $H_2{}^{35}S$ with samples from that depth showed maximum rates of up to 1.4 mmol m^{-2} h^{-1} [33] which confirmed previous data [67]. Chemical oxidation of sulfide by oxidized metals such as iron and manganese could only account for <0.1% of the measured H_2S oxidation rates as calculated from the iron fluxes into the chemocline.

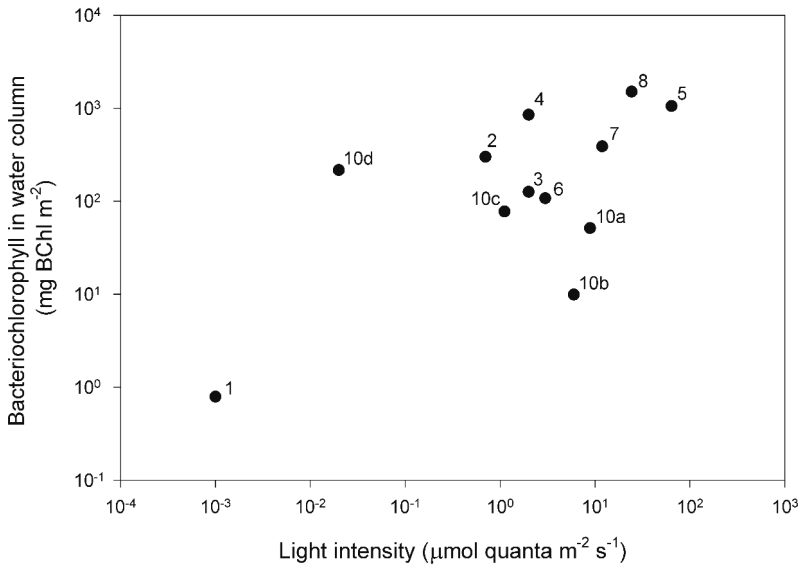

Figure 3. Relation between bacteriochlorophyll amount in the water column and light intensity reaching the bacterial plate for different anoxygenic phototrophic communities. *1* Black Sea [45]; *2* Big Soda Lake [10]; *3* Mary Lake [57]; *4* Knaack Lake [58]; *5* Mahoney Lake [50]; *6* Mirror Lake [57]; *7* Rose Lake [57]; *8* Lake Cisó [22, 47]; *10a* Banyoles, BChl *a* plate (August); *10b* Banyoles, BChl *a* plate (May); *10c* Banyoles, BChl *e* plate (August); *10d* Banyoles, BChl *e* plate (May) [7].

Field and laboratory data can be used to infer the significance of anoxygenic photosynthesis for sulfide turnover in the Black Sea chemocline. Based on the vertical profiles of sulfide concentrations determined at two stations in the western basin of the Black Sea [45], and employing a coefficient for turbulent diffusivity of $1.0 \cdot 10^{-5}$ $m^2 \cdot s^{-1}$ (at 100 m depth) [38], the sulfide flux into the layer of green sulfur bacteria amounts to 0.37 – 0.53 mmol m^{-2} d^{-1}. This value is very similar to that estimated earlier for a depth of 150 m (0.421 mmol m^{-2} d^{-1}) [38]. The results of modeling the upward fluxes of sulfide suggest that sulfide is actually consumed within the anoxic zone between the chemocline and 150 m depth, but not within the chemocline [38]. Most likely molecular oxygen enters the anoxic zone by massive lateral injections of oxygen-enriched Mediterranean waters through the Bosporus plume, and leads to the formation and sedimentation of particulate MnO_2 in the chemocline which in turn serves as the oxidant of ~70% of the sulfide diffusing upwards [39]. Together with molecular diffusion of O_2 from upper water layers (accounting for ~10% of the sulfide oxidation) [38], the fluxes of molecular oxygen thus are sufficient to

explain most of the sulfide oxidation in the Black Sea. This indirect evidence suggests that anoxygenic photosynthesis is of little importance for the sulfur cycle in the Black Sea. Presently it is unknown, whether the intrusion of oxygen has direct effects on the physiological activity of green sulfur bacteria in the chemocline of the Black Sea.

Support for this conclusion comes from specific sulfide oxidation rates which were determined in laboratory cultures of the green sulfur bacterium from the chemocline of the Black Sea [54]. An extrapolation from data obtained at higher light intensities to *in situ* light levels yielded sulfide oxidation rates of anoxygenic photosynthesis which could account for not more than 4 to 13% of total sulfide oxidation in the chemocline during summer [54]. Using the most recent data for the rate of anoxygenic photosynthesis (211 ngC m^{-2} day^{-1}, or 17.6 nmol m^{-2} day^{-1}, see above) a sulfide oxidation rate of 8.8 – 35.2 nmolH_2S m^{-2} day^{-1} can be inferred depending on the oxidation product formed (sulfate or elemental sulfur, respectively). This range of predicted oxidation rates accounts for 0.002 - 0.01% of total sulfide oxidation in the Black Sea chemocline during winter.

Nevertheless, the significance of anoxygenic photosynthesis in the carbon and sulfur cycles may actually be higher due to a vertical displacement of the chemocline caused by internal waves [35]. Such short-term exposure of green sulfur bacteria to higher quantum fluxes can significantly enhance their contribution to photosynthetic carbon assimilation [2].

6. MOLECULAR FOSSILS OF GREEN SULFUR BACTERIA AND THEIR IMPLICATIONS FOR THE RECONSTRUCTION OF THE PALEOENVIRONMENT

Caused by the postglacial sea-level rise, the Black Sea was first inundated with Mediterranean water about 9000 yr BP, leading to the deposition of a sequence of sediment horizons [9], which indicates a conversion of the fresh-water lake to an anoxic marine basin [65]. Most of the paleoceanographic data obtained to date cover the last 7000 – 8000 years (radiocarbon dating) of Black Sea history [69]. Only few excursions yielded sediment cores long enough to document earlier periods. Two of them were the Glomar challenger deep sea drilling operation [63] and the recent excursion of the french research vessel *Marion Dufresne* in May 2004.

In the Black Sea, oxic freshwater conditions started 22,000 years BP and lasted for a period of over 13,000 years [14]. After deposition of this sediment Unit III, a microlaminated sapropel layer formed at about 8200 yr BP [59] (or 7500, or 5000 yr BP depending on the dating method, see [77]), probably indicating the onset of euxinic conditions in the center of the basin. Unit II is an organic rich (12 – 15% organic matter, [77]) sapropel and was deposited during

an early stage as the Black Sea and Mediterranean Sea were reconnected. In sediments on the slope, deposition of this sapropel started significantly later. The rise of the O_2-H_2S-interface from the bottom at 2200 m depth to a water depth of 500 m has been calculated from the rate of sedimentation of organic matter and on the chemical characteristics of contemporaneous sediment layers at the two depths, and probably lasted between 2300 to 3000 years [15]. The bottom part of Unit II (Unit IIb) has a higher organic carbon content and was deposited during a period of higher productivity, whereas the layers above (Unit IIa) contain a higher fraction of terrigenous material deposited under a period of lower primary productivity and stronger terrestrial inputs due to an intensified erosion of the Eurasian continent [26, 27]. During the deposition of Unit IIa, however, the water column was probably largely oxic [65].

Increasing salinity allowed the final invasion of the marine coccolithophorid *Emiliania huxleyi* between 3500 and 1600 yr BP (depending on the dating method). This event initiated the deposition of finely laminated coccolith ooze, defined as Unit I. These microlamina are thought to represent varves [63] of annual events like spring blooms [28]. The sediments contain 3-5% organic carbon, with the white laminae consisting mainly of coccoliths (over 90 weight %) deposited during spring and fall blooms. The intervening dark laminae are enriched in terrigenous material. These laminated layers are separated from an earlier invasion (at the very beginning of Unit I; [65]) by a several cm-thick transition sapropel which consists largely of terrigenous material and contains 9% TOC. The transition sapropel was deposited over a time interval of 400-1000 years.

Independent evidence for the vertical extent of the anoxic zone may come from fossil biomarkers of green sulfur bacteria. Diaromatic carotenoids and their sulfur-linked derivatives have been used as indicators of the presence of green sulfur bacteria in various past depositional environments, even those which are now located on land like the Messinian Vena del Gesso basin (Northern Apennines, Italy) [36]. Similarly, isorenieratene [59] and sulfurized isorenieratane [65, 77] have been detected in the analyses of organic sulfur fractions from Black Sea sediments. In Unit IIb, free isorenieratene was found [17, 65, 72] as well as farnesane with $\delta^{13}C$ values typical for green sulfur bacteria which use the reverse TCA cycle for CO_2 fixation. Isorenieratene reaches ranges between 2-72 μg/gdw in Unit I and up to 1.4 μg/gdw in Unit IIb [59]. Compared to free isorenieratene, sulfurized isorenieratane reached lower concentrations in Unit I (8.3 – 13.0 $\mu g \cdot (g \text{ dry weight})^{-1}$) but higher concentrations in Unit IIb (50.0 $\mu g \cdot (g \text{ dry weight})^{-1}$) [65, 77]. Taken together, these data indicate that photic zone anoxia, hence a large anoxic water body, developed during the deposition of Unit IIb and Unit I.

Recently, the 16S rRNA gene sequences of *Chlorobium* sp. BS-1 have been detected in sediment layers of the Black Sea by PCR employing specific primers

[46]. The occurrence of fossil 16S rRNA gene sequences of the extremely low-light adapted green sulfur bacterium may now be used as a more specific biomarker to infer photic zone anoxia and hence the vertical extent of the oxic zone more specifically.

Currently, the vertical position of the anoxic interface in the Black Sea is positioned between ~60 and 200 m depending on sampling location, and also varies over time [9]. The chemocline is bent towards the shelf edges similar to the situation during the deposition of Unit I and II [70, 71]. If the maximum penetration of light in the marine environment is considered [42] green sulfur bacteria could theoretically colonize water layers down to 250 m depth. Since the vertical attenuation is usually higher in oxic/anoxic environments, populations of green sulfur bacteria would be expected to occur in shallower depths. In the Black Sea, a depth of 121 m has been considered the maximum depth for photoautotrophic growth [59]. The compensation depth for the extremely low-light adapted green sulfur bacteria in the Black Sea may actually be even lower, since bacteriochlorophyll *e* has recently been detected even at a sampling location where the chemocline was positioned at 150 m [45]. In the Cariaco Basin, where lipids and pigments of anoxygenic phototrophic bacteria are entirely absent, the oxic/anoxic interface is positioned at 275-300 m depth [43, 76]. In conclusion, the presence of specific 16S rRNA gene sequence biomarkers of the low-light adapted green sulfur bacterium in a potentially oxic/anoxic marine environment most likely indicates photic zone anoxia down to a maximum of 150 m depth.

However, a more detailed analysis of the fossil DNA sequences of green sulfur bacteria present in the Black Sea sediments suggests that molecular markers have to be interpreted with caution. Firstly, in contrast to other oxic/anoxic environments with accumulations of phototrophic sulfur bacteria [53], the vertical concentration profile of bacterial pigments showed an unusually sharp drop below the chemocline, where BChl *e* concentrations declined below the detection limit at a depth of 120 m [60, 61]. Secondly, chlorophyll *a*, but no pigments of green sulfur bacteria were detected in the sedimenting matter (at 87.5 hours deployment of sediment traps) [61] although the total amount of bacteriochlorophyll *e* determined in the chemocline of the Black Sea surpasses the total chlorophyll a in the overlying oxygenated water layers [60]. Both observations indicate that only a very small fraction of the green sulfur bacteria present in the Black Sea chemocline actually reach the deep-sea sediments. Similarly, biomarkers of archaea involved in anaerobic methane oxidation could not be detected in sinking particulate matter and even not in underlying sediments [78], indicating that important bacterial or archaeal biomarkers may be entirely absent or underrepresented in Black Sea sediments. On the opposite, 16S rRNA gene sequences have been detected in sediments from the Eastern Mediterranean as old as 240,000 years [13]. All the Mediter-

ranean sequences, however, show identity or strong similarity to sequences from freshwater strains and therefore may not represent indigenous low-light indicators for photic zone anoxia. In comparison to aromatic carotenoids, fossil DNA sequences with their significantly larger information content thus permit a more differentiated view of past environmental conditions. It is also in this respect that the Black Sea serves as the most important contemporary model system for photic zone anoxia in the past.

References

[1] Anbar A.D. and Knoll A.H. Proterozoic ocean chemistry and evolution: a bioinorganic bridge? Science 2002; 297:1137-42.

[2] Bergstein T., Henis Y. and Cavari B.Z. Investigations on the photosynthetic sulfur bacterium *Chlorobium phaeobacteroides* causing seasonal blooms in Lake Kinneret. Can J Microbiol 1979; 25:999-1007.

[3] Bergstein T., Henis Y. and Cavari B.Z. Uptake and metabolism of organic compounds by *Chlorobium phaeobacteroides* isolated from Lake Kinneret. Can J Microbiol 1981; 27:1087-91.

[4] Bird D.F. and Karl D.M. Microbial stratification within oxygenated, suboxic and sulfidic zones of the Black Sea. EOS 1988; 69:1241.

[5] Bird D.F. and Karl D.M. Microbial biomass and population diversity in the upper water column of the Black Sea. Deep-Sea Res 1991; 38 (Suppl 2):1069-82.

[6] Borrego C.M., Garcia-Gil J., Cristina X.P., Vila X. and Abella C.A. Occurrence of new bacteriochlorophyll *d* forms in natural populations of green photosynthetic sulfur bacteria. FEMS Microbiol Ecol 1998; 26:257-67.

[7] Borrego C.M., Bañeras L. and Garcia-Gil J. Temporal variability of *Chlorobium phaeobacteroides* antenna pigments in a meromictic karstic lake. Aquat Microb Ecol 1999; 17:121-29.

[8] Burnett W.C., Landing W.M., Lyons W.B. and Orem W. Jellyfish Lake, Palau: A model anoxic environment for geochemical studies. EOS 1989; 70:777-79.

[9] Canfield D.E., Lyons T.W. and Ralswell R. A model for iron deposition to euxinic Black Sea sediments. Am J Sci 1996; 296:818-34.

[10] Cloern J.E., Cole B.E. and R.S. Oremland. Autotrophic processes in meromictic Big Soda Lake, Nevada. Limnol. Oceanogr. 1983; 28:1049-61.

[11] Codispoti L.A., Friederich G.E., Murray J.W. and Sakamoto C.M. Chemical variability in the Black Sea: implications of continuous vertical profiles that penetrated the oxic/anoxic interface. Deep Sea Res 1991; 38 (suppl.2):691-710.

[12] Coble P.A., Gagosian R.B., Codispoti L.A., Friedrich G.E. and Christensen J.P. Vertical distribution of dissolved and particulate fluorescence in the Black Sea. Deep-Sea Res 1991; 38 (Suppl. 2):985-1001.

[13] Coolen M.J.L. and Overmann J. 240'000 year-old DNA sequences indicate different origins of green sulfur bacteria in mediterranean sapropels.(submitted)

[14] Degens E.T. and Ross D.A. Chronology of the Black Sea over the last 25,000 years. Chem Geol 1972; 10:1-16.

[15] Degens E.T. and Stoffers P. Stratified waters as a key to the past. Nature 1976; 263:22-27.

[16] Dickman M. and Artuz I. Mass mortality of photosynthetic bacteria as a mechanism for dark lamina formation in sediments of the Black Sea. Nature 1978; 275:191-95.

[17] Freeman K.H., Wakeham S.G. and Hayes J.M. Predictive isotopic biogeochemistry: hydrocarbons from anoxic marine basins. Org Geochem 1994; 21:629-44.

[18] Fuhrmann S., Overmann J., Pfennig N. and Fischer U. Influence of vitamin B_{12} and light on the formation of chlorosomes in green- and brown-colored *Chlorobium* species. Arch Microbiol 1993; 16:193-98.

[19] Glaeser J. and Overmann J. Biogeography, evolution and diversity of the epibionts in phototrophic consortia. Appl Environ Microbiol 2004; 70:4821-30.

[20] Gorlenko V.M. "Ecological niches of green sulfur and gliding bacteria." In: *Green photosynthetic bacteria.* Olson J.M., Ormerod J.G., Amesz J., Stackebrandt E., Trüper H.G. eds., New York, London: Plenum Press, 1988.

[21] Grice K., Gibbison R., Atkinson J.E., Schwark L., Eckhardt C.B. and Maxwell J.R. Maleimides (1*H*-pyrrole-2,5-diones) as molecular indicators of anoxygenic photosynthesis in ancient water columns. Geochim Cosmochim Acta 1996; 60:3913-24.

[22] Guerrero R., Montesinos E., Pedrós-Alió C., Esteve I., Mas J., Van Gemerden H., Hofman P.A.G. and Bakker J.F. Phototrophic sulfur bacteria in two Spanish lakes: Vertical distribution and limiting factors. Limnol Oceanogr 1985; 30:919-31.

[23] Guerrero R., Pedrós-Alió C., Esteve I. and Mas J. Communities of phototrophic bacteria in lakes of the Spanish Mediterranean region. Acta Acad Aboensis 1987; 47:125-51.

[24] Hartgers W.A., Sinninghe Damsté J.S., Requejo A.G., Allan J., Hayes J.M. and de Leeuw J.W. Evidence for only minor contributions from bacteria to sedimentary organic carbon. Nature 1994; 369:224-27.

[25] Hashwa F.A. and Trüper H.G. Viable phototrophic sulfur bacteria from the Black-Sea bottom. Helgoländer wiss Meeresunters 1978; 31:249-53.

[26] Hay B.I. Sediment accumulation in the central western Black Sea over the past 5100 years. Paleoceanogr 1988; 3:491-508.

[27] Hay B.I. and Arthur M.A. Sediment deposition in the Holocene Black Sea. Deep-Sea Res 1991; 38 (suppl 2):1211-35.

[28] Hay B.I., Honjo S. and Kempe S. Interannual variability in the particle flux in SW Black Sea. Deep-Sea Res 1990; 37 (6A):911-28.

[29] Jannasch H.W., Eimhjellen K., Wirsen C.O. and Farmanfamaian A. Microbial degradation of organic matter in the deep sea. Science 1971; 171:672-75.

[30] Jannasch H.W, Trüper H.G., Tuttle J.H. "Microbial sulfur cycle in Black Sea." In: *The Black Sea – Geology, Chemistry, and Biology*, Degens E.T. and Ross D.A. eds., Tulsa, Oklahoma: Am. Ass. Petroleum Geologists, 1974.

[31] Jannasch H.W., Wirsen C.O., Taylor C.D. Undecompressed microbial populations from the deep sea. Appl environ Microbiol 1976; 32:360-67.

[32] Jørgensen B.B. and Fossing H. Black Sea Cruise, Knorr-88-2. Preliminary data report, 1990.

[33] Jørgensen B.B., Fossing H., Wirsen C.O., Jannasch H.W. Sulfide oxidation in the Black Sea chemocline. Deep-Sea Res 1991; 38 (Suppl):1083-1103.

[34] Karl D.M. and Knauer G.A. Microbial production and particle flux in the upper 350 m of the Black Sea. Deep-Sea Res 1991; 38 (Suppl):921-42.

[35] Kempe S., Liebezeit G., Dierks A.-R. and Asper V. Water balance in the Black Sea. Nature 1990; 346:419.

[36] Kohnen M.E.L., Sinninghe Damsté J.S., DeLeeuw J.W. Biases from natural sulphurization in palaeoenvironmental reconstruction based on hydrocarbon biomarker distribution. Nature 1991; 349:775-78.

[37] Kohnen M.E.L., Schouten S., Sinninghe Damsté J.S., DeLeeuw J.W., Merritt D.A. and Hayes J.M. Recognition of paleochemicals by a combined molecular sulfur and isotope geochemical approach. Science 1992; 256:358-62.

[38] Konovalov S.K., Ivanov L.I., Samodurov A.S. Fluxes and budgets of sulphide and ammonia in the Black Sea anoxic layer. J Mar Syst 2001; 31:203-16.

[39] Konovalov S.K., Luther G.W., Friederich G.E., Nuzzio D.B., Tebo B.M., Murray J.W., Oguz T., Glazer B., Trouwborst R.E., Clement B., Murray K.J. and Romanov A.S. Lateral injection of oxygen with the Bosporus plume – fingers of oxidizing potential in the Black Sea. Limnol Oceanogr 2003; 48:2369-76.

[40] Koopmans M.P., Köster J., van Kaam-Peters H.M.E., Kenig F., Schouten S., Hartgers W.A., de Leeuw J.W. and Sinninghe Damsté J.S. Diagenetic and catagenic products of isorenieratene: Molecular indicators for photic zone anoxia. Geochim Cosmochim Acta 1996; 60:4467-96.

[41] Kriss A.E. and Rukina E.A. Purple sulfur bacteria in deep sulfureous water of the Black Sea. Dokl Akad Nauk SSSR 1953; 93:1107-10.

[42] Littler M.M., Littler D.S., Blair S.M., Norris J.N. Deepest known plant life discovered on an uncharted seamount. Science 1985; 227:57-59.

[43] Lyons T.W., Werne J.P., Hollander D.J., Murray R.W. Contrasting sulfur geochemistry and Fe/Al and Mo/Al ratios across the last oxic-to-anoxic transition in the Cariaco Basin, Venezuela. Chem Geol 2003; 195:131-57.

[44] Manheim F.T. "Molybdenum." In: *Handbook of Geochemistry*, Wedepohl K.H. ed., Springer-Verlag, 1974.

[45] Manske A.K., Glaeser J. and Overmann J. Phylogenetic identification and low light limits of green sulfur bacteria from the Black Sea chemocline, 2005a. (submitted)

[46] Manske A.K. and Overmann J. Reconstruction of paleoceanography of the Black Sea based on subfossil DNA of green sulfur bacteria, 2005b. (submitted)

[47] Mas J., Pedrós-Alió C., Guerrero R. *In situ* specific loss and growth rates of purple sulfur bacteria in Lake Cisó. FEMS Microbiol Ecol 1990; 73:271-81.

[48] Montesinos E., Guerrero R., Abella C., Esteve I. Ecology and physiology of the competition for light between *Chlorobium limicola* and *Chlorobium phaeobacteroides* in natural habitats. Appl Environ Microbiol 1983; 46:1007-16.

[49] Murray J.W., Jannasch H.W., Honjo S., Anderson R.F., Reeburgh W.S., Top Z., Friederich G.E., Codispoti L.A., Izdar E. Unexpected changes in the oxic/anoxic interface in the Black Sea. Nature 1989; 338:411-13.

[50] Overmann J. Standortspezifische Anpassung bei phototrophen Schwefelbakterien. Dissertation der Universität Konstanz, 1991. ISBN 3-89191-494-6.

[51] Overmann J. Mahoney Lake: a case study of the ecological significance of phototrophic sulfur bacteria. Adv Microbial Ecol 1997; 15:251-88.

[52] Overmann J. and Tilzer M.M. Control of primary productivity and the significance of photosynthetic bacteria in a meromictic kettle lake (Mittlerer Buchensee, West Germany). Aquat Scie 1989; 51:261-78.

[53] Overmann J., Beatty J.T., Hall K.J., Pfennig N. and Northcote T.G. Characterization of a dense, purple sulfur bacterial layer in a meromictic salt lake. Limnol Oceanogr 1991; 36:846-59.

[54] Overmann J., Cypionka H., Pfennig N. An extremely low-light-adapted phototrophic sulfur bacterium from the Black Sea. Limnol Oceanogr 1992; 37:150-55.

[55] Overmann J., Coolen M.J.L. and Tuschak C. Specific detection of different phylogenetic groups of chemocline bacteria based on PCR and denaturing gradient gel electrophoresis of 16S rRNA gene fragments. Arch Microbiol 1999; 172:83-94.

[56] Overmann J. and Garcia-Pichel F. "The Phototrophic Way of Life." In: *The Prokaryotes: An Evolving Electronic Resource for the Microbiological Community*, Dworkin M. et al. eds., 3rd edition, Springer, New York, 2000. (`http://ep.springer-ny.com:6336/contents/`.

[57] Parkin T.B. and Brock T.D. Photosynthetic bacterial production in lakes: the effects of light intensity. Limnol Oceanogr 1980; 25:711-18.

[58] Parkin T.B. and Brock T.D. Photosynthetic bacterial production and carbon mineralization in a meromictic lake. Arch Hydrobiol 1981; 91:366-82.

[59] Repeta D.J. A high resolution historical record of Holocene anoxygenic primary production in the Black Sea. Geochim Cosmochim Acta 1993; 57:4337-42.

[60] Repeta D.J., Simpson D.J., Jørgensen B.B., Jannasch H.W. Evidence for anoxygenic photosynthesis from the distribution of bacteriochlorophylls in the Black Sea. Nature 1989; 342:69-72.

[61] Repeta D.J. and Simpson D.J. The distribution and recycling of chlorophyll, bacteriochlorophyll and carotenoids in the Black Sea. Deep-Sea Res 1991; 38 (Suppl. 2):969-84.

[62] Richards F.A. The Cariaco Basin (Trench). Oceanogr Mar Biol Ann Rev 1975; 13:11-67.

[63] Ross D.A. and Degens E.T. The Black Sea – Geology, Chemistry and Biology (eds Degens E. and Ross D.) 183-199. (Memoir No. 20. Am Ass. Petrol. Geol., Tulsa, Oklahoma), 1974.

[64] Sadler W.R. and Stanier R.Y. The function of acetate in photosynthesis by green bacteria. Proc Natl Acad Sci USA 1960; 46:1328-34.

[65] Sinninghe Damsté J.S., Wakeham S.G., Kohnen M.E.L., Hayes J.M., de Leeuw J.W. A 6000-year sedimentary record of chemocline excursions in the Black Sea. Nature 1993; 362:827-29.

[66] Sorokin Yu. I. On primary production and microbial activity in the Black Sea. Journ du Cons Expl Mer 1964; 29:41-54.

[67] Sorokin Yu. I. The bacterial population and the processes of hydrogen sulphide oxidation in the Black Sea. J du Conseil Int pour l'exploitation de la Mer 1972; 34:423-54.

[68] Sorokin Yu. I. The Black Sea: nature and resources. Nauka Moscow 1982.

[69] Sorokin Yu. I. *The Black Sea. Ecology and oceanography.* Leiden, The Netherlands: Backhuys Publishers, 2002.

[70] Spencer D. W. and Brewer P. G. Redox potential as control on the vertical distribution of Mn in waters of the Black Sea. J geophys Res 1971; 76:5877-92.

[71] Spencer D. W., Brewer P. G. and Sachs P. L. Aspects of the distribution and trace element composition of suspended matter in the Black Sea. Geochim cosmochim Acta 1972; 36:71-86.

[72] Summons R.E. and Powell T.G. Identification of aryl isoprenoids in source rocks and crude oils: biological markers for the green sulfur bacteria. Geochim Cosmochim Acta 1987; 59:521-33.

[73] Tuschak C., Glaeser J., Overmann J. Specific detection of green sulfur bacteria by in situ-hybridization with a fluorescently labeled oligonucleotide probe. Arch Microbiol 1999; 171:265-72.

[74] van Gemerden H. and Mas. J. "Ecology of purple sulfur bacteria." In: *Anoxygenic Photosynthetic Bacteria*, Blankenship RE, Madigan MT, Bauer CE eds., Kluwer Academic Publishers, 1995.

[75] Vetriani C., Tran H.V. and Kerkhof L.J. Fingerprinting microbial assemblages from the oxic/anoxic chemocline of the Black Sea. Appl Environ Microbiol 2003; 69:6481-88.

[76] Wakeham S.G. Lipid biomarkers for heterotrophic alteration of suspended particulate organic matter in oxygenated and anoxic water columns of the ocean. Deep-Sea Res 1995; 42:1749-71.

[77] Wakeham S.G., Sinnighe Damsté J.S., Kohnen M.E.L. and DeLeeuw J.W. Organic sulfur compounds formed during early diagenesis in Black Sea sediments. Geochim Cosmochim Acta 1995; 59:521-33.

[78] Wakeham S.G., Lewis C.M., Hopmans E.C., Schouten S., Sinninghe Damste J.S. Archaea mediate anaerobic oxidation of methane in deep euxinic waters of the Black Sea. Geochim Cosmochim Acta 2003; 67:1359-74.

[79] Zenkewitch L. *Biology of the Seas of the U.S.S.R.* London: Allen and Unwin, 1963.

[80] Zubkov M.V., Sazhin A.F. and Flint M.V. The microplankton organisms at the oxic-anoxic interface in the pelagial of the Black Sea. FEMS Microbiol Ecol 1992; 101:245-50.